Indian Journal of Natural Sciences *www.tnsroindia.org.in ©IJONS*

Vol.15 / Issue 83 / Apr / 2024 *International Bimonthly (Print) – Open Access* *ISSN: 0976 – 0997*

RESEARCH ARTICLE

Application of MCDM using PROMETHEE II Techniques in the Case of Fertilizer Selection for Agriculture

A.Rajkumar[1], A.Ezhilarasi[2]* and J.Sharmila Jessie Ignatia[2]

[1]Assistant Professor, PG and Research Department of Mathematics, Annai Vailankanni Arts and Science College, Thanjavur (Affiliated to Bharathidasan University, Tiruchirappalli), Tamil Nadu, India.
[2]Research Scholar, PG and Research Department of Mathematics, Annai Vailankanni Arts and Science College, Thanjavur (Affiliated to Bharathidasan University, Tiruchirappalli), Tamil Nadu, India.

Received: 13 Oct 2023 Revised: 12 Jan 2024 Accepted: 25 Mar 2024

***Address for Correspondence**
A.Ezhilarasi
Research Scholar,
PG and Research Department of Mathematics,
Annai Vailankanni Arts and Science College, Thanjavur
(Affiliated to Bharathidasan University, Tiruchirappalli),
Tamil Nadu, India.
Email: ezhilselvi99@gmail.com

ABSTRACT

If we want to make the best decision in a complex situation, MCDM is the way to go. This paper provides an overview of the use of MCDM in determining the best fertilizer selection. The Promethee method is a significant method for providing a brisk solution to problems. Data were gathered through in-person communication with decision makers and the use of a likert scale. In multicriteriaanalysis, the PROMETHEE method is a new class of outranking method. On a finite set of feasible actions, a partial preorder (PROMETHEE I) or a complete preorder (PROMETHEE II) can be obtained.

Keywords: PROMETHEE II, MCDM, Fertilizer, Likert scale.

INTRODUCTION

Multi criteria decision making (MCDM) method is referred as a method used for scoring and ranking a finite number of alternatives. MCDM concern with evaluating and selecting alternatives that fit with the goals and necessity. PROMTHEE is one of the many MCDM methods that are listed in the literature, which includes many other MCDM techniques. Preference Ranking Organization Method for Enrichment Evaluation is referred to as the PROMETHEE. In comparison to many other MCDM methods, this ranking method is regarded as being straightforward in both idea and computation. The first PROMETHEE implementation was made by Bertrand Mareschal on the ULB mainframe computer in FORTRAN around 1984. It was very different from today's software. And it was very

difficult to adapt programs to different computers. The University of Split was a pioneer: they got a stack of punched cards and had the software running on their Vax system in a matter of days. Later the software was ported to the IBM PC. It was the basis for PromCalc.

Fertilizers enhance the growth of plants. This goal is met in two ways, the traditional one being additive that provide nutrients. The second way that certain fertilisers work is to improve the soil's productivity by altering its water retention and aeration. Fertilizers are one of the major inputs of agriculture. The average fertilizer consumption (per hectare) was very meager amounting to 2kg in 1950.It increased to 128 kg in 2012-13 due to the development of technology. About 90% of fertilizers are applied as solids. The most widely used solids inorganic fertilizer are urea, Diammonium phosphate and potassium chloride. The three macronutrients are Nitrogen (N) –leaf growth, Phosphorus (P) - development of roots, flowers seeds, fruits and potassium (k) - strong stem growth, movement of water in plants, promotion of flowering and fruiting. The secondary macronutrients are calcium (Ca), magnesium (Mg) and sulfur(S) and the next one is micronutrients, like copper(Cu),iron(Fe), manganese(Mn), molybdenum(Mo),Zinc(Zn),Boron(B) of occasional significance are silicon(Si) cobalt(Co),Vanadium(v).

Types of generalized criterion functions:		**Preference function value for various types of criterion functions**
1. Usual criterion		$H(d_j) = \begin{bmatrix} 0 if d_j = 0 \\ 1 if d_j > 0 \end{bmatrix}$
2. Quasi criterion		$H(d_j) = \begin{bmatrix} 0 if d_j \leq q_j \\ 1 if d_j > q_j \end{bmatrix}$
3. Criterion with linear preference and no indifference area		$H(d_j) = \begin{bmatrix} \frac{d_j}{p_j} if d_j = 0 \\ 1 \end{bmatrix}$
4. Level criterion		$H(d_j) = \begin{bmatrix} 0 & if & d_j \leq q_j \\ 0.5 & if & q_j < d_j \leq p_j \\ 1 & if & d_j > p_j \end{bmatrix}$
5. Criterion with linear preference and indifference area		$H(d_j) = \begin{bmatrix} 0 & if & d_j \leq q_j \\ \frac{(d_j - q_j)}{(p_j - q_j)} & if & q_j < d_j \leq p_j \\ 1 & if & d_j > p_j \end{bmatrix}$
6. Gaussian criterion		$H(d_j) = \left[1 - e^{\frac{-d^2 j}{2\sigma' j2}} \right]$

Multicriteria preference index $\pi(a,b)$ a weighted average of the preference functions $P_j(a,b)$ for the entire criterion is defined as:

Algorithm:

Step1. Enter the no. of alternatives, criteria, payoff matrix, and weight of each criterion
Step 2: Compute pair wise difference between values of alternative for each criterion (dj).
Step 3: Compute preference function matrix for each criterion based on dj and type of chosen criterion function.
Step 4: Compute the entering flow and leaving flow for each alternative.
Step 5: Compute the net ϕ value for each alternative and corresponding rank.
Step 6: Select the best suitable alternative having highest ϕ value.

METHODOLOGY

Step 1: Normalize the evaluation matrix (Decision matrix)

$$r_{ij} = \frac{[a_{ij} - \min(a_{ij})]}{[\max\{a_{ij} - \min(a_{ij})]} \ldots\ldots\ldots\ldots\ldots (1)\text{Beneficial}$$

$$r_{ij} = \frac{[\max(a_{ij}) - a_{ij}]}{[\max(a_{ij}) - \min(a_{ij})]} \ldots\ldots\ldots\ldots\ldots (2)\text{Non Beneficial}$$

Step 2: **Calculation the preference function**

$p_{j(a,b)} = 0\ if\ r_{aj} \leq r_{bj} \rightarrow D(S_a - S_b) \leq 0$…… (3)

$p_{j(a,b)} = (r_{aj} - r_{bj}) if\ r_{aj} > r_{bj} \rightarrow D(S_a - S_b) > 0 \ldots\ldots\ldots\ldots$(4)

Step 3: **Calculate aggregated preference aggregated preference function $\Pi(a, b)$**

$= \sum_{j=1}^{n} wjpj(a,b) / \sum_{j=1}^{n} wj$…… (5)

Sum of the weight is 1 (unity)

Step 4: **Calculate the entering flow and leaving flow for ath alternative Φ^{+}**

Leaving (positive) Flow

$= {}^{1}/_{S-1} \sum_{b=1}^{s} \pi(a,b)(a \neq b)$…… (6)

Entering (Outranking) Flow

$= {}^{1}/_{S-1} \sum_{b=1}^{m} \pi(a,b) \quad (a \neq b)$ …… (7)

Step 5: **Calculate Net Flow**

$\phi(i) = \phi^{+}(i) - \phi^{-}(i)$ …… (8)

NUMERICAL EXAMPLE:

The results of the tests in evaluating fertilizer selection for cultivation show that the PROMETHEE Based on analytical evidence, the approach will aid in determining land potential. The first step is to define the alternatives as well as the parameters that will be used**.**

Here are the five crop production criteria and four alternatives. In this case, alternative indicates the amount of fertilizer in kilograms, and criteria indicate the five types of crops**.** Once alternate principles and parameters have been defined, the next step is to classify them based on each criterion's dominance. The meaning of the current path is then calculated using the outflow value outline to achieve a better or alternate rating.

As shown in Table 3, Alternative 3 has the highest rating in the assessment table of fertilizer production using the PROMETHEE method, indicating that the measure is the most significant alternative in evaluating the suitability of fertilizer selection.

RESULT AND DISCUSSION

The PROMETHEE rankings

There are two PROMETHEE rankings that are computed:

- The PROMETHEE I Partial ranking is based on the computation of two preference flows(Phi+ and Phi-).It allows for incomparability between actions when both Phi+ and Phi- preference flows give conflicting rankings.
- The PROMETHEE II complete ranking is based on the net preference flow (Phi).

While the **PROMETHEE II** complete ranking is easier to explain it is also less informative as the differencesbetween Phi+ and Phi- scores are not visible anymore. Incomparability in the **PROMETHEE I** ranking isinteresting because it emphasizes actions that are difficult to compare and thus helps the decision-maker tofocus on these difficult cases.

PROMETHEE Diamond

The PROMETHEE Diamond is an alternative two dimensional joint representatio of both PROMETHEE I and II rankings.The square corresponds to the (Phi+, Phi-) plane where each action is represented by a point. The plane isangled 45° so that the vertical dimension gives the Phi net flow. Phi+ scores increase from the left to the topcorner and Phi- scores increase from the left to the bottom corner.

For each action, a cone is drawn from the action position in the plane.

PROMETHEE Network

In the PROMETHEE Network display each action is represented as a node and preferences are represented by arrows. The nodes are located in relative positions corresponding to the PROMETHEE Diamond so that the proximities between flow values appear clearly.

PROMETHEE II rainbow

For each action a bar is drawn. The different slices of each bar are colored according to the criteria. Eachslice is proportional to the contribution of one criterion (flow value times the weight of the criterion) to the Phi net flow score of the action. Positive (upward) slices correspond to good features while negative (downward) slices correspond to weaknesses. This way, the balance between positive and negative slices is equal to the Phi score. Actions are ranked from left to right according to the PROMETHEE II Complete Ranking.

PROMETHEE GAIA

The GAIA plane is a descriptive complement to the PROMETHEE rankings.

WALKING WEIGHTS

The Walking Weights window allows you to change the weights of the criteria and see the impact on the Visual PROMETHEE analysis.

CONCLUSION

Fertilizer selection is one of the necessary parts of agriculture, and this article gives the conclusion of the best fertilizer for your field and crop production.In this case, we select the four types of fertilizer for five crops, and among them, we select the one that is best for each crop using this PROMETHEE method. This paper assumes that one of the most important aspects of agriculture is fertilizer selection, and in this study, we examine the four types of fertilizer to determine which is best for agricultural purposes. Finally, using the Prometheus II method, we can see that the manure has the highest rank.In this paper, the author explores the use of Extended PROMETHEE II method in solving the problem of determining the best fertilizer and generates more efficient decisions.

CONFLICT OF INTEREST:

There is no conflict of interest by authors

REFERENCES

1. Dr.A. Rajkumar,A.Ezhilarasi,J.Sharmila Jessie Ignatia (“Analysis of MCDM using Promethee II Techniques in the Case of River Water Quality Monitoring”)-Indian Journal Of Natural Science.Vol.14/Issue 79/Aug/2023. ISSN:0976-0997.

2. Muhammet Gul, Erkan celik, Alev Taskin Gumus, Ali Fuat Guneri ("A fuzzy logic based PROMETHEE method for material selection problem")- Benni-suef University Journal of Basic and Applied Science 7(2018)68-79
3. Albadvi, A., Chaharsooghi, S., Esfahan pour, A., 2007. Decision making in stock trading: an application of PROMETHEE. Eur.J.Oper, Res.177, 673-683.
4. Bilsel, R.U., Buyikozjan, G., Runa, D., 2006. A fuzzsy preference ranking model for a quality evaluation of hospital web sites.Int.J.syswt.21, 1181-1197.
5. S. Kusumadewi,S. Hartati, A. Harjoka, and r. Wardoyo, fuzzy multi Attribute Decision Making (Fuzzy MADM). Yogyakarta: Graha Ilmu,2006.
6. Risawandi And R.Rahim, "Study of the simple Multi Attribute Rating Techniques for Decision support", IJSRST, vol, no.6, pp.491-494, 2016.
7. World Health Organization. (2020). Corona virus disease 2019(COVID -19): Situation Report, 59.
8. Ghasemi P, Talebi E. An integrated FAHP-PROMETHEE approach for selecting the best Flexible Manufacturing system. EUR Online J Nat soc sci. 2014:3:1137-1150.
9. Dagdeviren, M.: Decision making in equipment selection: an integrated approach with AHP and PROMETHEE. J. Intel. Manuf. 19(4), 397–406 (2008).
10. Macharis, C., Springael, J., de Brucker, K., Verbeke, A.: PROMETHEE and AHP: the design of operational synergies in multicriteria analysis. Stengthening PROMETHEE with ideas of AHP. Eur. J. Oper. Res. 153(2), 307–317 (2004).
11. Cude, 2001b. Oregon Water Quality Index: a tool for evaluating water quality management effectiveness. J. Am. Water Resour. Assoc. 37 (1),125–137.
12. ICMR (Council of Medical Research), 1975. Manual of Standards of Quality for Drinking Water Supplies, Indian. Special Report No. 44., pp. 27.
13. Verma, R.K., Murthy, S., Tiwary, R.K., Verma, S., 2019. Development of simplified WQIs for assessment of spatial and temporal variations of surface water quality in upper Damodar river basin , eastern India. Appl. Water Sci. 0–15 https://doi.org/10.1007/ s13201-019-0893-0.
14. Wu, Z., Wang, X., Chen, Y., Cai, Y., Deng, J., 2018. Assessing river water quality using water quality index in Lake Taihu Basin, China. Sci. Total Environ. https://doi.org/ 10.1016/j.scitotenv.2017.08.293.
15. W. Bengal, W. Bengal, and W. Bengal, "A comparative study of preference dominance-based approaches for selection of industrial robots," *Adv. Prod. Eng. Manag.*, vol. 9, no. 1, pp. 5–20, 2014.
16. P. Chatterjee and S. Chakraborty, "Flexible manufacturing system selection using preference ranking methods:A comparative study," *Int. J. Ind. Eng. Comput.*, vol. 5, no. 2, pp. 315–338, 2014.
17. S. Kusumadewi, S. Hartati, A. Harjoko, and R. Wardoyo, *Fuzzy Multi-Attribute Decision Making (FuzzyMADM)*. Yogyakarta: GrahaIlmu, 2006.
18. Risawandi and R. Rahim, "Study of the Simple Multi-Attribute Rating Technique For Decision Support," *IJSRST*, vol. 2, no. 6, pp. 491–494, 2016.
19. Jasri, D. Siregar, and R. Rahim, "Decision Support System Best Employee Assessments with Technique forOrder of Preference by Similarity to Ideal Solution," *Int. J. Recent TRENDS Eng. Res.*, vol. 3, no. 3, pp. 6–17, 2017.
20.] Mesran, G. Ginting, Suginam, and R. Rahim, "Implementation of Elimination and Choice Expressing Reality (ELECTRE) Method in Selecting the Best Lecturer (Case Study STMIK BUDI DARMA)," *Int. J. Eng. Res. Technol.(IJERT*, vol. 6, no. 2, pp. 141–144, 2017.
21. M. Iswan, W. Fitriani, N. Mayasari, and A. P. U. Siahaan, "Tuition Reduction Determination Using Fuzzy Tsukamoto," *Int. J. Eng. Sci. Invent.*, vol. 5, no. 9, pp. 68–72, 2016.

Table 1: criteria and alternatives for fertilizer selection

Alternative/Criteria	Pulses(C1)	Gingelly (C2)	Groundnut(C3)	Paddy(C4)	Sugarcane(C5)
Nitrogen(A1)	78	86	73	70	77
Phosphorous(A2)	44	23	25	28	11
Manure(A3)	16	47	27	24	36
Potassium(A4)	90	89	94	88	92

Table 2: Value range of min and max value of criteria

Alternative/Criteria	Pulses(C1)	Gingelly (C2)	Groundnut(C3)	Paddy(C4)	Sugarcane(C5)
Nitrogen(A1)	78	86	73	70	77
Phosphorous(A2)	44	23	25	28	11
Manure(A3)	16	47	27	24	36
Potassium(A4)	90	89	94	88	92
Max	90	89	94	88	92
Min	16	23	25	28	11
Max-min	74	66	69	60	81

Table 3: PROMETHEE Flow Table

Alternative	Phi	Phi+	Phi-	Rank
Alternative 3	0,6295	0,7233	0,0939	1
Alternative 2	0,4772	0,6472	0,1700	2
Alternative 1	-0,3550	0,1983	0,5533	3
Alternative 4	-0,7517	0,0000	0,7517	4

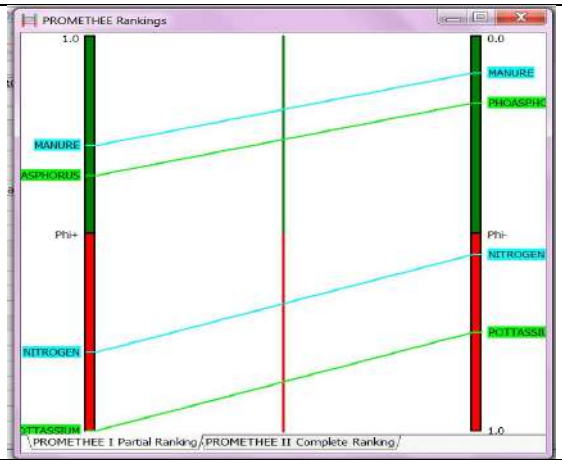

Fig 1:PROMETHEE I Partial ranking

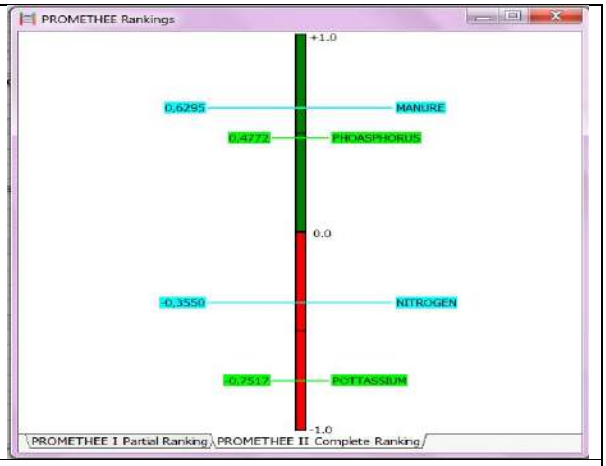

Fig 2:PROMETHEE II complete ranking

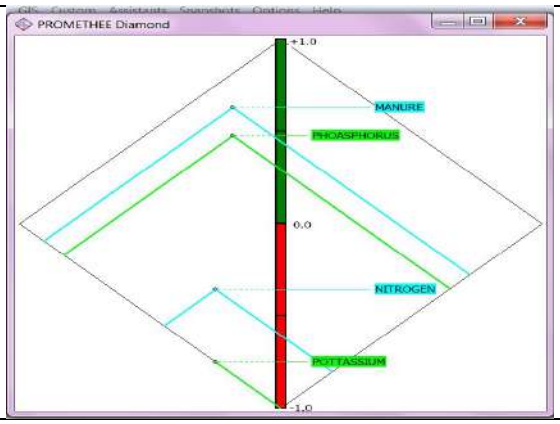

Fig 3:PROMETHEE diamond

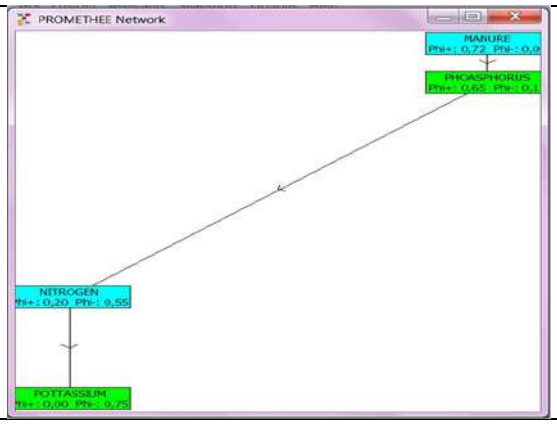

Fig 4:PROMETHEE Network

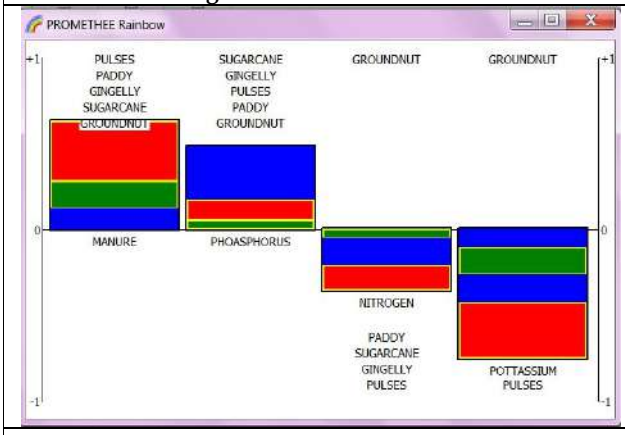

Fig 5:PROMETHEE Rainbow

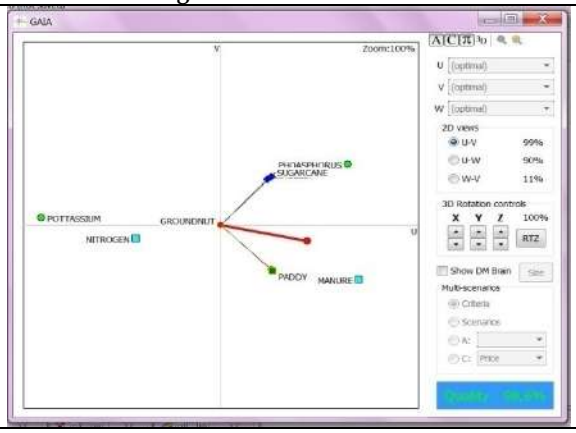

Fig 6:PROMETHEE GAIA

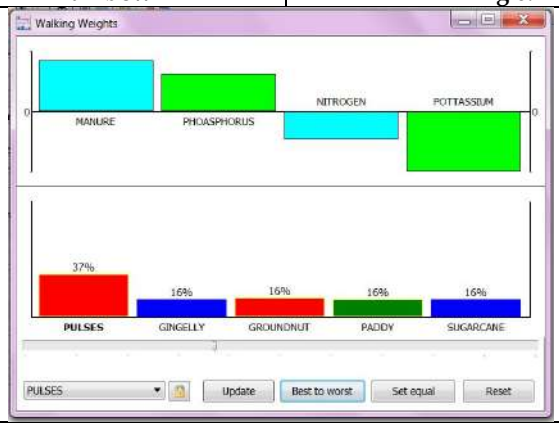

Fig 7:Walking Weights

Indian Journal of Natural Sciences *www.tnsroindia.org.in ©IJONS*

Vol.15 / Issue 83 / Apr / 2024 *International Bimonthly (Print) – Open Access* *ISSN: 0976 – 0997*

RESEARCH ARTICLE

Separation and Higher Separation Axioms in Topological Bispace

K.Karpagam[1]*, G.Ramesh[2] and N. Anbarasi[3]

[1]Research Scholar, Department of Mathematics, Government Arts College (Autonomous), Kumbakonam, (Affiliated to Bharathidasan University) Tiruchirappalli, Tamil Nadu, India.
[2]Associate Professor, Department of Mathematics, Government Arts College (Autonomous), Kumbakonam, (Affiliated to Bharathidasan University) Tiruchirappalli, Tamil Nadu, India.
[3]Assistant Professor, Department of Mathematics, Agurchand Manmull Jain college, Meenambakkam, (Affiliated to University of Madras) Chennai, Tamil Nadu, India.

Received: 24 Dec 2023 Revised: 09 Jan 2024 Accepted: 10 Apr 2024

***Address for Correspondence**
K.Karpagam
Research Scholar,
Department of Mathematics,
Government Arts College (Autonomous), Kumbakonam,
(Affiliated to Bharathidasan University)
Tiruchirappalli, Tamil Nadu, India.
Email: karpagamjagan06@gmail.com

ABSTRACT

In this paper, we introduce and study some new lower separation axioms and higher separation axioms in topological bispace.

AMS Subject Classification: 54C08, 54E35, 15A18, 54D15.
Keywords: Topological bispace, hausdroff and locally hausdroffbispace, regular, locally regular and normal bispace.

INTRODUCTION

Topology is an important branch of mathematics. Separation axioms in topology are among the most beautiful and interesting concepts. Various generalization of separation axioms have been studied for generalized topological spaces. Several forms of higher separation axioms exist in the topology literature in which closed sets generalized closed sets are separated by open sets. These forms of generalized open sets such as semi-open sets, alpha-open sets, pre-open sets etc. have been introduced and utilized to study general topology in the past. It is evident from Smyth (1995) that topological structures that are more general than the usual topology are worthy of study because they can provide a suitable framework for various approaches to digital topology. Cech(1966) introduced cech closure operator which are obtaine from the kuratowski ones by omitting the requirement of idempotency.

In this paper, we introduced some new higher separation axioms including normal bispaces and it is observed that this class of space is independent of the class of normal topological bispace. Throught the present paper K-normal space contains the class of normal bispaces which is independent of normality.

Preliminaries

As the preliminary information, which is necessary to study [6], [7] , give some definitions.

Definition 2.1

[8] A topology [5] on a biset $X_B$is a collection τ of subsets of a bisetA_B *having the following properties*

i. $\emptyset$ *and* X_B are in τ *that is* $\emptyset$ *and* X_1 are in τ and $\emptyset$ *and* X_2 are in τ.
ii. The union of the elements of any sub collection of each components of τ is in τ.
iii. The intersection of the elements of any finite sub collection of each components of τ is in τ.

Example 2.2

Let $X_B = X_1 \cup X_2 = \{a, b\} \cup \{2,3\}$

Let $\tau = \{\{\emptyset, \{a\}, \{a\} \cup \{2,3\}, \{b\} \cup \{2,3\}, \{X_B\}\}$

Then τ satisfies the following properties

i. $\emptyset$ *and* X_B are in τ *that is* $\emptyset$ *and* X_1 are in τ and $\emptyset$ *and* X_2 are in τ.
ii. The union of the elements of any sub collection of each components of τ is in τ.
iii. The intersection of the elements of any finite sub collection of each components of τ is in τ.

Hence (X_B, τ) is topological bispace.

Definition 2.3 [8] A bisetX_B for which a topology τ is called a topological bispace and it is denoted by (X_B, τ).

Definition 2.4 [8]Let $X_B = X_1 \cup X_2$ is a biset. A basis for a topology onbispaceX_B is a collection of subbisets of $B_B$of $X_B$such that,

i. for each $x_1 \in X_1$and$x_2 \in X_2$there is atleast one basis element in the components B_1containing $x_1$and in the components B_2containing x_2.

ii. if x_1 belongs to the intersection of two basis elements $B_1^1$and B_1^2 and x_2 belongs tothe intersection of two basis elements $B_2^1$and B_2^2 then there exits basis elements B_1^3 and B_2^3containing $x_1$and $x_2$respectively such that $B_1^3 \subset B_1^1 \cap B_1^2andB_2^3 \subset B_2^1 \cap B_2^2$

Definition 2.5[8] A subset of $U_B$of $X_B$is said to be to open biset in X_B [that is, to be an element of τ] if for each $x_B \in U_B$,there is a basis elements $x_B \in U_B$such that $x_B \in B_B$and $B_B \in U_B$.

Definition 2.6 [8] A subbisets $A_B$of a topological bispaceτ,the interior of $A_B$is defined as the union of all open Bisets contained in A_B.

The interior of $A_B$is denoted by $IntA_B$or rA_Bandthe closure of A_B is denoted ClA_B or$\bar{A}_B$.

Obviously, A_B is an open biset and $\bar{A}_B$ is a closed biset.

Furthermore, $IntA_B \subset A_B \subset \bar{A}_B$which implies that $IntA_1 \subset A_1 \subset \bar{A}_1andIntA_2 \subset A_2 \subset \bar{A}_2$.

If $A_B$open biset which implies that $A_B = IntA_B$ while if $A_B$is closedbiset which that $A_B = \bar{A}_B$.pair

Definition 2.7 [8] let X_B be a subspace of topological bispaceτ. Then $x_B = x_1 \cup x_2$is a limit point of $X_B$if every neighbourhood of $x_1$intersects X_1 in some parts other than $x_1$and every neighbourhood of $x_2$intersects X_2in some points other x_2.

Definition 2.8 [8] A Topological bispaceX_B is called hausdroff bispace if for each pair x_1^1 ,$x_1^2$of distinct points of X_1, there exists neighbourhoodsU_1^1 and $U_1^2$of $x_1^1$and x_1^2respectively, that are disjoint, and for each x_2^1 ,$x_2^2$of distinct points of X_2, there exists neighbourhoodsU_2^1 and $U_2^2$of $x_2^1$and x_2^2respectively, that are disjoint.

Definition 2.9 A Topological bispace is said to be locally hausdroff if every pair ofpoint has an open bi se tneighbourhood, that is a hausdroff bispace.

Definition 2.10 A topological bispace is said to be regular bispace if given a closedbiset$\mathcal{C}_B$ in the topological bispace and a pair of point $a_B \notin \mathcal{C}_B$, there are open bisets $U_B^1$and U_B^2such that $\mathcal{C}_B \subseteq U_B^1, a_B \in U_B^2$and $U_B^1 \cap U_B^2 = \emptyset$.
Definition 2.11 A Topological bispace is said to be locally regular if every pair of point has an open neighbourhood that is a regular bispace in the subbispace topology.

Definition 2.12 A Topological bispace is said to be normal if given pair of two disjoint closed bisets in it, there are disjoint open bisets containing the closed bisets.

That, is a topological bispaceX_B is normal if whenever u_B and v_B are closed bisets in $X_B$with no intersection, there are open bisets $U_B$and $V_B$with $u_B \subseteq U_B$ and $v_B \subseteq V_B$ and $U_B \cap V_B$is empty.

Separation Axioms

In this section separation axioms are developed and also investigated some of theirtheorems.

i. (T_0)bispace:

A bispace$X_B$is a T_0bispaceiff it satisfies the T_0axioms, that is, for $a_B, b_B \in X_B$such that$a_B \neq b_B$ there is an open biset$U_B \subseteq X_B$so that $U_B$contains one of a_B and b_B but not the other.

In the otherword, a topological bispaceX_B is called T_0 if given any two pair of points a_B and b_B there is either an open biset containing a_B but not b_B, or an open biset containing b_B but not a_B.

ii. T_1bispace:

A bispace$X_B$is a T_1bispace or frechetiff it satisfies the T_1axioms, that is, for $x_B, y_B \in X_B$such that$x_B \neq y_B$ there is an open biset$U_B \subseteq X_B$so that $x_B \in X_B$but $y_B \notin U_B$.

Note: Every T_1 is bispace T_0.

iii. T_2bispace :

A bispace$X_B$is a T_2bispace or hausdroff spaceiff it satisfies the T_2axioms, that is, for $x_B, y_B \in X_B$such that$x_B \neq y_B$ there is an open biset$U_B, V_B \subset X_B$so that$x_B \in U_B, y_B \in V_B$ and $U_B \cap V_B = \emptyset$.

Note: Every T_2bispace isT_1 .

iv. T_3bispace :

A bispace$X_B$is regular iff for each $x_B \in X_B$ and each closed biset $c_B \subset X_B$such that$x_B \notin c_B$ there is an open biset$U_B, V_B \subset X_B$so that$x_B \in U_B, c_B \subset V_B$ and $U_B \cap V_B = \emptyset$.

Note: A regular T_1bispace is called T_3bispace.

Every T_3bispace isT_2 .

v. T_4bispace :

A bispace$X_B$is normal iff for each pair $A_B, B_B$of disjoint closed subbisets of X_B,there is a pair $U_B, V_B$of disjoints open subbisets of $X_B$so that $A_B \subset U_B, B_B \subset V_B$ and $U_B \cap V_B = \emptyset$.

Note: A normal T_1bispace is called T_4bispace.

Theorem 3.1 The intersection of finite collection of open biset is open.
Proof: Let (X_B, τ)be a topological bispace and $(X_B^1, X_B^2, \ldots, X_B^n)$be open bisets of (X_B, τ).
then,$\cup X_B^i$is also open bisets of (X_B, τ).that is, the intersection of any two elements of τ is an elements of τ and $X_B$is itself an elements of τ.
Hence the intersection of any finite collection of open bisets is open.

Theorem 3.2 Prove that a product of two hausdroffbispace is hausdroff.

Proof: let $X_B$and Y_B be two hausdroff bispaces.
To prove that $X_B XY_B$is a hausdroff.
Since, $(a_B^1, b_B^1)$and (a_B^2, b_B^2)be a pair of points, that are distinct.
That is, $a_B^1 \neq a_B^2$or $b_B^1 \neq b_B^2$.
If $a_B^1 \neq a_B^2$,we first separate$a_B^1$and a_B^2inX_B. That is, let disjoint open bisets in X_B; U_B^1containinga_B^1andU_B^2containinga_B^2.

Clearly$U_B^1XY_B$ and $U_B^2XY_B$ are disjoint open bisets containing $(a_B^1, b_B^1)$and (a_B^2, b_B^2)respectively. Hence $a_B^1 \neq a_B^2$is succeeded.
If $b_B^1 \neq b_B^2$, we separate$b_B^1$and b_B^2in$Y_B$and disjoints open bisetsV_B^1andV_B^2.
Then $Y_BXV_B^1$and$Y_BXV_B^2$are disjoint open bisets containinga_B^1, b_B^1anda_B^2 , b_B^2.
Hence $X_BXY_B$is hausdroffbispaces.

Theorem 3.3: Every subbispaceE_B of a hausdorff bispace X_B is a hausdorff bispace.

Proof: Let a_B, b_B be any two distinct pair of points in E_B.
Since X_B is Hausdorff bispace, there exists open bisets U_B in X_B such that $a_B \in U_B, b_B \in V_B$ and $U_B \cap V_B = \emptyset$.
Let $U_B^* = E_B \cap U_B$ and $V_B^* = E_B \cap V_B$.
Then U_B^* and V_B^* are open bisets of the subbispace E_B.
Since $a_B \in U_B^*, b_B \in V_B^*$ and $U_B^* \cap V_B^* = \emptyset$, it follows that $E_B$is aHausdorff bispace.

Theorem 3.4: The topological sum X_B of any pair of disjoint collection $\{X_B^\mu \backslash \mu \in M\}$ of hausdorff bispace is a hausdorff bispace.

Proof: Let a_B, b_B be any two distinct points in X_B. Then there exists $\mu, \gamma \in M$ such that $a_B \in X_B^\mu$ and $b_B \in X_B^\gamma$. If $\neq \gamma$, then take $U_B = X_B^\mu$ and $V_B = X_B^\gamma$.
If $\mu = \gamma$, then a_B and b_B are two distinct pair of points in a hausdorff bispace X_B^μ and hence there are open bisets U_B and V_B in X_B^μ such that $a_B \in U_B, b_B \in V_B$ and $U_B \cap V_B = \emptyset$.
In both cases U_B and V_B are open bisets of the topological sum X_B. This implies that X_B is ahausdorff bispace.

Theorem 3.5: Every regular Frechetbispace is a hausdorffbispace.
Proof: Let X_B be a regular Frechet bispace and a_B, b_B be any two distinct points in X_B.
Since X_B is a Frechet bispace, $X_B \backslash b_B$ is an open bisets of X_B. From the regularity of X_B at the point a_B, there follows the existence of a closed biset neighbourhood N_B of a_B with $N_B \subset X_B \backslash b_B$.
Let $U_B = Int\,(N_B), V_B = X_B \backslash N_B$. Then U_B and V_B are open bisets X_B such that $a_B \in U_B, b_B \in V_B$ and $U_B \cap V_B = \emptyset$.

HIGHER SEPARATION AXIOMS

Definition 4.1: A topological bispaceX_B is K-normal if whenever u_B and v_B are disjoint canonical closed subbisets of X_B there exists disjoint open subbisets of X_B, U_B and V_B, such that $u_B \subset U_B$ and $v_B \subset V_B$. That is, a topological bispace is said to be K-normal if given pair of two disjoint closed bisets in it, there are disjoint open bisets containing the closed bisets.

Definition 4.2: A topological bispaceX_B is said to be strongly normal bispace if every pair of disjoint pre closed biset can be separated by disjoint open bisets.

Definition 4.3: A topological bispaceX_B is said to be weakly normal bispace if every pair of disjoint closed biset whose interior is non-empty can be separated by disjoint open biset.

Remark 4.4: A bispaceX_B is completely normal bispace if every pair of separated biset can be separated by disjoint open biset and a bispace X_B is K-normal bispace if every pair of disjoint regularly closed biset can be separated by disjoint open biset.

Lemma 4.5: A topological bispaceX_B is normal bispace iff for every closed biset F_B contained in a open biset U_B there exists an open biset V_B such that $F_B \subset V_B \subset \bar{V}_B \subset U_B$.
Proof: Assume that X_B is normal bispace.

To prove that for every closed bisetF_B contained in an open biset U_B there exists an open biset V_B such that $F_B \subset V_B \subset \bar{V}_B \subset U_B$. We have every pair of components of disjoint closed biset can be separated by disjoint open biset. Since every regularly closed biset is closed biset $F_B \subset V_B \subset \bar{V}_B \subset U_B$.
Conversely, let F_B contained in a open biset such that every pair of components of disjoint closed biset can be separated by disjoint open biset. Hence is normal bispace.

Lemma 4.6: A topological bispace is strongly normal bispace iff for every pre closed biset contained in a pre-open biset there exists an open biset such that $F_B \subseteq V_B \subseteq \bar{V}_B \subseteq U_B$.

Proof: Let F_B be pre-closed biset in X_B and U_B be a pre-open biset containing F_B.
Then F_B and $X_B - U_B$ are disjoint pre-closed biset in X_B and so by strong normality bispace of X_B, there exist two disjoint open bisets V_B and W_B such tat $F_B \subseteq V_B$ and $X_B - U_B \subseteq W_B$. Now $V_B \cap W_B = \emptyset$.
Thus, $F_B \subseteq V_B \subseteq X_B - W_B \subseteq U_B$ which implies $F_B \subseteq V_B \subseteq \bar{V}_B \subseteq U_B$.

Conversely, let F_B and H_B be two disjoint pre-closed bisets in X_B. Since $X_B - H_B$ is pre-open in X_B and $F_B \subseteq X_B - H_B = U_B$, by hypothesis there exists an open biset W_B' such that $F_B \subseteq W_B' \subseteq \bar{W}_B' \subseteq U_B$. Here W_B' and $X_B - \bar{W}_B'$ are two disjoint open bisets in X_B containing F_B and H_B respectively. Thus the bispace is strongly normal bispace.

Lemma 4.7: A topological bispaceX_B is weakly normal bispace iff for every closed biset F_B with a non-empty interior contained in an open biset U_B satisfying $\bar{U}_B \neq X_B$, there exists an open biset V_B such that $F_B \subseteq V_B \subseteq \bar{V}_B \subseteq U_B$.

Proof: Let X_B be a weakly normal bispace and F_B be a closed biset with in $F_B \neq \emptyset$ and U_B be an open biset containing F_B satisfying $\bar{U}_B \neq X_B$.

Here F_B and $H_B = X_B - U_B$ are two disjoint closed bisets whose interiors are non-empty. Since $X_B - \bar{U}_B \subseteq X_B - U_B = H_B$. Similar way, by weakly normality bispace of X_B there exists two disjoint open bisects V_B and W_B such that $F_B \subseteq V_B$ and $X_B - U_B \subseteq W_B$.

Now $V_B \cap W_B = \emptyset$. Thus, $F_B \subseteq V_B \subseteq X_B - W_B \subseteq U_B$ which implies $F_B \subseteq V_B \subseteq \bar{V}_B \subseteq U_B$.

Conversely, assume that every closed bisetF_B with a non-empty interior contained in an open biset U_B satisfying $\bar{U}_B \neq X_B$, there exists an open biset V_B such that, $F_B \subseteq V_B \subseteq \bar{V}_B \subseteq U_B$. Since U_B be an open biset containing F_B satisfying $\bar{U}_B \neq X_B$.

Here F_B and H_B are two disjoint closed bisets whose interior are non-empty and $F_B \subseteq V_B, H_B \subseteq W_B$ which implies $X_B - \bar{U}_B \subseteq W_B$. Thus $V_B \cap W_B = \emptyset$, so every pair of components of disjoint closed biset can be separated by disjoint open biset. Hence X_B is weakly normal bispace.

CONCLUSION

In the present work, we investigate more properties of separation and some new higher separation axioms including normal bispac$X_B$es and it is observed that this class of space is independent of the class of normal topological bispace.

REFERENCES

1. Herstein IN, Topics in Algebra, John wiley, 1975.
2. Lipschutz, Seymour, Schaum's outline of General topology, Mc Graw-Hill, first edition, June 1, 1968, ISBN 0-07-037988-2.
3. Kuratowski K, Topology, I. Warzawa, 1933.
4. Munkers, Topology, edition-2, PHI learning pvt. Ltd., New Delhi, 2010.
5. Munkers J.R, Topology, A first course prientice Hill, New Jersey, 1975.
6. Munkers J.R., Topology, Prentice Hall Inc., New Jersey, 2000.

7. Ramesh G, Karpagam K., A Study on Bisets, International Journal of Mathematics Trends and Technology, 68.1(2022), 94-100.
8. Ramesh G., Karpagam K., A Study on Topological Bispace, (Submitted).
9. Stoll, Robert R(1979); Set theory and Logic, Mineola, N.Y; Dover Publications, ISBN 0-486-63829-4.
10. Thomas H. Cormen; Charles E Leiserson; Ronald L Rivest; Clifford stein(2001), Introduction to Algorithms, MIT press. p. 1070, ISBN 978-0-262-03293-3.
11. Vasanthakandasamy W.B., Bialgebraic structures and SmarandacheBialgebraic structures, Amercian research press, Rehoboth, 2003.
12. Velleman, Daniel, How to prove it: A structured approach, Cambridge University Press, (2006), ISBN 0-521-67599-5.
13. Voyevodin V. V., Linear Algebra, Mir Publishers, 1983.
14. Zelinksy D., A First Course in Linear Algebra, Academic Press, 1973.

Indian Journal of Natural Sciences *www.tnsroindia.org.in ©IJONS*

Vol.15 / Issue 83 / Apr / 2024 *International Bimonthly (Print) – Open Access* *ISSN: 0976 – 0997*

RESEARCH ARTICLE

Importance of Starch Modification in the Ruminant Nutrition

Lalu.K[1]*, George Sherin .K[2] , Dipu .M. T[2] and Rejeesh .R[3]

[1]Associate Professor, Department of Dairy Husbandry, College of Dairy Science and Technology, Thiruvananthapuram (Affiliated to Kerala Veterinary and Animal Sciences University (KVASU), Kerala, India

[2]Associate Professor, Department of Animal Nutrition, College of Veterinary and Animal Sciences, Mannuthy, Thrissur (Affiliated to Kerala Veterinary and Animal Sciences University (KVASU), Kerala, India

[3]Assistant Professor, Department of Dairy Microbiology , College of Dairy Science and Technology, Thiruvananthapuram (Affiliated to Kerala Veterinary and Animal Sciences University (KVASU)) Kerala, India

Received: 17 Oct 2023 Revised: 13 Jan 2024 Accepted: 06 Mar 2024

***Address for Correspondence**
Lalu.K,
Associate Professor,
Department of Dairy Husbandry,
College of Dairy Science and Technology,
Thiruvananthapuram (Affiliated to Kerala Veterinary and Animal Sciences University (KVASU),
Kerala, India

ABSTRACT

Starch is one of the important energy sources for ruminant nutrition. Starch granule is arranged in concentric layers of crystalline and amorphous lamellae. Microbial and digestive enzymes areinvolved in starch digestion, generating products which can positively or negatively affect animal performance and health, depending on the starch contents of the diet. A number of factors affect starch digestibility, including granule size, amylose-amylopectin ratio, nature of endosperm, presence of starch-lipid and starch-protein complexes, and physico-chemical processing of the feed. Ingestion of large amounts of starch can trigger ruminal acidosis. However, its rational use in the diet has positive effects on methane emissions, rumen papillae development and in milk yield and composition. Development of rumen resistant starch whichcan bypass rumen can be adapted to counter the development of acidosis.

Keywords: Starch structure, digestion, acidosis, rumen resistant starch.

INTRODUCTION

Starch is a major energy-yielding component of cereal grains, which are important diet components used for intensive milk and beef production.. It is important to understand the structural characteristics of starch, its ruminal and post-ruminal digestion and the factors affecting its digestibility in order to improve performance and profit of livestock systems. Development of rumen resistant starch which bypass rumen can be adapted to counter the development of acidosis.A number of factors affect starch digestibility, including granule size, amylose/amylopectin ratio, proportion of farinaceous and vitreous endosperm, presence of starch-lipid and starch-protein complexes, and physical-chemical processing of the feed.Ingestion of large amounts of starch can trigger ruminal acidosis (Plaizier *et al*., 2009). However, its rational use in the diet has positive effects on methane emissions and in milk yield and composition.

COMPOSITION AND STRUCTURE OF STARCH

Starch is composed of two different glucan chains, amylose and amylopectin. Amylose is a linear polymer of a-D-glucose molecules linked by α-1,4 glycosidic linkages. Amylopectinis a branched polymer of a-D-glucose units linked by α-1,4 & α-1,6 glycosidic bonds. These 2molecules represent the 98-99% of dry weight of starch. They have the same basic structure but differ in their length and degree of branching, which ultimately affects their physicochemical properties. Amylose has a molecular weight of around 100 kDa, amylopectin has a much higher molecular weight in the order 104–106 kDa. They are held together by hydrogen bonding in the starch granule.
Starch granules are formed by concentrically growing layers alternating semi- crystalline and amorphous films. The semi-crystalline region is more abundant in amylopectin and is more impervious to enzymatic attack because of its resistance to entry of water. The amorphous region is rich in amylose and has lower density than the crystalline area, which facilitates water flow and enzyme attack; however, it isabundant in hydrogen bonds (Perez *et al*., 2009).

RUMINAL AND POST-RUMINAL DIGESTION OF STARCH

Although protozoa and fungi participate in ruminal digestive processes, the bulkof the fermentation is performed by ruminal bacteria. Several species of ruminal bacteria are able to digest starch. Amylolytic organisms are found in larger percentages of the total microbial population when rations high in starch are fed. Important species that have been enumerated in cattle fed high grain diets are *Bacteroides amylophilus, Butyrivibrio fibrisolvens,Bacteroides ruminocola, Selenomona lactylitica, Streptococcus bovis, Prevotella ruminocola, Eubacterium ruminantium, Ruminobacter amylophilus, Ruminococcus bromii, Succinimonas amylolytica* and Lactobacillus sp. The α-1-4 and α-1-6 endo and exoamylases produced by rumen microorganisms have the ability to hydrolyze amylose and amylopectin glycosidic linkages, releasing different oligosaccharides.

The glucose produced from the hydrolysis of starch in the rumen is rarely detectable due to its rapid uptake and metabolism by the ruminal microorganisms. Pyruvate is subsequently produced as a result of glycolysis. Several chemical pathways are then available for the conversion of pyruvate to the volatile fatty acids (VFA) which can be absorbed by the cow from the rumen. It is the phosphorylation of ADP to ATP during the production of the VFAs which creates an energy supply for the microbes and allows microbial growth, provided an adequate supply of amino acids, ammonia and other minerals are present. Methane, carbon-dioxide and hydrogen are produced in addition to the VFA from the fermentation of starch.

In ruminants, the site of starch digestion affects the substrates absorbed. Ruminal digestion generates volatile fatty acids (VFA) for absorption and provides energy for microbialprotein synthesis (Huhtanen and Sveinbjörnsson, 2006)
The post-ruminal process of starch degradation begins with pancreatic α-amylase secretion, which hydrolyzes amylose and amylopectin into dextrins and linear oligosaccharides with two to three glucose units. The process is

completed by the action of oligosaccharidases (maltase and iso-maltase) secreted in the intestinal membrane (Ortega and Mendoza, 2003). Digestion of starch in the small intestine digestion provides glucose for absorption. Increased starch digestion in the small intestine has suggested enhancing milk protein production, perhaps by sparing amino acids from being used for gluconeogenesis in the liver (Nocek and Tamminga,1991). The efficiency of energy utilization for absorbed glucose in the small intestine is assumed to be greater than for starch digested in the rumen (Owens *et al*., 1986) due to reduced methane and fermentation heat losses and higher efficiency of metabolizable energy (ME) utilization.

FACTORS AFFECTING STARCH DIGESTIBILITY IN RUMINANTS

Granule Size

Size of the starch granule also may affect digestibility, as the relationship between surface area and starch volume, and thus contact between substrate and enzyme, decreases as size of the granule increases. This is a limiting factor in starch digestion because the relationship between starch volume and surface area, and thus substrate-enzyme contact, decreases as granule size increases (Svihus *et al*., 2005). Franco *et al*. (1992), separated starch granules from cassava and maize into different sizes and studied breakdown in the presence of amylase and amylo-glucosidase.

Grain processing

Grain processing using temperature, humidity and pressure facilitate binding of bacteria to starch granules, increasing its digestibility (Huntington *et al*., 2006). The grain processing methods can be broadly classified into dry and wet processing methods. Grinding, dry rolling, popping, extruding, pelleting, roasting, micronizing, dehulling etc. are the major dry processing methods whereas soaking, steam rolling, steam flaking, pressure cooking, exploding, reconstitution, ensiling at high moisture are the main wet processing methods used in feed processing units. All these processes aim to break grain barriers such as the pericarp and the protein-starch matrix, allowing access of microorganisms to starch granules. These processes also reduce the particle size, and increase surface area and microbial colonization (Giuberti *et al*., 2014).

Starch-protein complex

The proteinaceous matrix surrounding starch granules affects starch digestibility. Digestibility is negatively associated with the presence of prolamins. Prolamins are storage proteins that receive a different name for each cereal, namely zein (corn), kafirins (sorghum), gliadin (wheat), hordeins (barley), secalins (rice), and avenines (oats). Usually, wheat, oats, rice and barley have fewer prolamins than corn and sorghum (Giuberti *et al*., 2014). The proteins act as a barrier which reduce the surface accessibility of starch to enzyme and/or ruminal bacteria by blocking the absorption sites or by influencing enzyme binding.

STARCH AND RUMINAL ACIDOSIS

Starch fermentation increases volatile fatty acids (VFA) and lactate production, which can reduce ruminal pH and kill cellulolytic microorganisms, to decreased fiber digestibility and dry matter (DM) intake. Additionally, it can cause metabolic disorders such as acute and sub- acute ruminal acidosis, rumenitis, laminitis, liver abscesses and polioencephalomalacia (Plaizier *et* al., 2009). Plaizier *et al*. (2009) conducted SARA challenge in 8 lactating cows and found that the average rumen pH is declining during SARA induction and the average time of pH being less than 5.6 had increased to 279 minutes. They also studied the level of lipopolysaccharide (LPS) in rumen as well plasma. It showed increase in the amount for both in case of SARA challenge. A continuous presence of a low amount of LPS in peripheral plasma of SARA induced cows could result in a metabolic endotoxemia that triggers a low-grade inflammation compared with acute disorders such as septicemia. The presence of lipopolysaccharide binding protein (LBP) in plasma also denote the translocation of rumen LPS into plasma and further.

RUMEN RESISTANT STARCH

High-producing ruminants are fed high amounts of cereal grains, at the expense of dietary fiber, to meet their high energy demands. Grains consist mainly of starch, which is easily degraded in the rumen by microbial glycosidases, providing energy for rapid growth ofrumen microbes and short-chain fatty acids (SCFA) as the main energy source for the host. Yet, low dietary fiber contents and the rapid accumulation of SCFA lead to rumen disorders in cattle. The processing of grains has become increasingly important to confer their starch resistances against rumen microbial glycosidases, hence generating ruminally resistant starch (RRS). In ruminants, unlike monogastric species, the strategy of enhancing resistant starch is useful, notonly in lowering the amount of carbohydrate substrates available for digestion in the upper gutsections, but also in enhancing the net hepatic glucose supply, which can be utilized by the hostmore efficiently than the hepatic gluconeogenesis of SCFA (Deckardt *et al*.,2013)

Different treatments are employed for the development of RRS. Sodium hydroxide, formaldehyde, ammonia were used earlier. They are not preferred now because they can causehealth issues and treatments using them are very laborious (Dehghan-Banadaky *et al*., 2007). Lactic acid treatment and treatment of grains using organic acids are the latest chemical processing methods used for production of RRS. Gelatinization and coolingfor an extended period of time is good physical processing method to improve resistant starchlevel in substrate. The study by Iqbal *et al*(2011) showed that unlike the control group, the ruminal pH value of the lactic acid-treatment group was above SARA values indicating a slower degradation of barley starch in the rumen because of the treatment with lactic acid. Milk fat and protein level also increased in cows fed with lactic acid barley grains.

CONCLUSION

Starch is the main energy component used in ruminants feed to modulate ruminal fermentation and promote sync with the nitrogen sources. More research is required to evaluatethe effect of using one or more sources of starch — with different degrees of degradability and processing— on protein use efficiency, milk yield and compositional quality. Studies should focus on addition levels and nutrient composition of the forage base according with the stage of lactation and energy requirements of the animal. Further studies regarding whether development of rumen resistant starch helps to mitigate acidosis in cattle are to be conducted.

REFERENCES

1. Deckardt, K., Khol-Parisini, A. and Zebeli, Q. 2013. Peculiarities of enhancing resistant starchin ruminants using chemical methods: opportunities and challenges. *Nutr.*, 5(6): 1970-1988.
2. Dehghan-Banadaky, M., Corbett, R. and Oba, M. 2007. Effects of barley grain processing on productivity of cattle. *Anim. Feed Sci. and Tech*. 137: 1-24.
3. Franco, C.M., do Rio Preto, S.J. and Ciacco, C.F. 1992. Factors that affect the enzymatic degradation of natural starch granules-effect of the size of the granules. *Starch-Stärke*, 44(11):422-426.
4. Giuberti, G., Gallo, A., Masoero, F., Ferraretto, L.F., Hoffman, P.C. and Shaver, R.D. 2014. Factors affecting starch utilization in large animal food production system: A review. *Starch- Stärke*, 66(1-2): 72-90.
5. Huhtanen, P. and Sveinbjörnsson, J. 2006. Evaluation of methods for estimating starchdigestibility and digestion kinetics in ruminants. Anim. Feed Sci. and Tech. 130(1-2): 95-113.
6. Huntington, G.B., Harmon, D.L. and Richards, C.J. 2006. Sites, rates, and limits of starch digestion and glucose metabolism in growing cattle. *J. of Anim. Sci*. 84: 14-24.
7. Iqbal, S.; Zebeli, Q.; Mazzolari, A.; Bertoni, G.; Dunn, S.M.; Yang, W.Z.; Ametaj, B.N. 2009.Feeding barley grain steeped in lactic acid modulates rumen fermentation patterns and increases milk fat content in dairy cows. *J. Dairy Sci*.92: 6023–6032.

8. Nocek, J.E. and Tamminga, S. 1991. Site of digestion of starch in the gastrointestinal tract of dairy cows and its effect on milk yield and composition. J. of Dairy Sci. 74(10): 3598-3629.
9. Ortega, M.E., Mendoza, G. 2009. Starch digestion and glucose metabolism in the ruminant: a review. *Interciencia.* 28: 380-386.
10. Owens, F., Zinn, R.A. and Kim, Y.K. 1986. Limits to starch digestion in the ruminant small intestine. J. of Anim. Sci. 63(5): 1634-1648.
11. Perez, S., Baldwin, P.M., Gallant, D.J. 2009. Structural features of starch granules. *Starch: Chemistry and Technology. 3th ed. Academic Press USA*. 149-192p.
12. Plaizier, J.C., Krause, D.O., Gozho, G.N. and McBride, B.W. 2008. Subacute ruminal acidosis in dairy cows: The physiological causes, incidence and consequences. *The Vet. J.* 176(1): 21- 31.
13. Svihus, B., Uhlen, A.K. and Harstad, O.M. 2005. Effect of starch granule structure, associated components and processing on nutritive value of cereal starch: A review. Anim. Feed Sci. and Tech. 122(3-4): 303-320.

Indian Journal of Natural Sciences *www.tnsroindia.org.in ©IJONS*

Vol.15 / Issue 83 / Apr / 2024 *International Bimonthly (Print) – Open Access* *ISSN: 0976 – 0997*

RESEARCH ARTICLE

On Symmetric Circulant Neutrosophic Fuzzy Matrices

N. Premalatha and V.Revathi*

Assistant Professor, Jai Shriram Engineering College, Tiruppur (Affiliated to Anna University, Chennai) Tamil Nadu, India

Received: 18 Oct 2023 Revised: 10 Jan 2024 Accepted: 06 Mar 2024

***Address for Correspondence**
V.Revathi
Assistant Professor,
Jai Shriram Engineering College, Tiruppur
(Affiliated to Anna University, Chennai)
Tamil Nadu, India.
Email: revathiperiasamy14@gmail.com

ABSTRACT

In this paper, we introduced the concept of k- symmetric circulant and s-symmetric circulant Neutrosophic Fuzzy Matrices (NFM) as a generalization of symmetric circulant fuzzy Matrices. The basic concepts, theorems and properties of k-symmetric circulant Neutrosophic Fuzzy Matrix and s- symmetric circulant Neutrosophic Fuzzy Matrix are discussed with examples.

Keywords: Circulant Fuzzy Matrix, Neutrosophic Fuzzy Matrix, Symmetric Circulant Fuzzy Matrix, S-symmetric circulant fuzzy matrix, k-symmetric circulant fuzzy matrix,,

INTRODUCTION

Academics in economics, sociology, medical science, industrial, atmosphere science and many other numerous fields agree with the vague, imprecise and infrequently lacking information of exhibiting inexact data. As a result, fuzzy set theory was introduced by L. A. Zadeh [14]. Then, the intuitionistic fuzzy sets was developed by K. A. Atanassov [1, 2]. Estimation of non-membership values is also not constantly possible for the identical reason as in case of membership values and so, there exists an indeterministic part upon which hesitation persists. As a result, Smarandache et al. [5, 11, 12] has introduced the concept of Neutrosophic Set (NS) which is a generalization of conventional sets, fuzzy set, intuitionistic fuzzy set etc.

The problems concerning various types of hesitations cannot solved by the classical matrix theory. That type of problems are solved by using fuzzy matrix [4, 6, 7]. Fuzzy matrix deals with only membership values. These matrices cannot deal non membership values. Intuitionistic fuzzy matrices (IFMs)

introduced first time by Khan, Shyamal and Pal [8]. A square matrix A is Symmetric if$A=A^T$and k-symmetric if $A=KAK^T$[2,3,4,5,11]. Any matrix with entries in [0, 1] and matrix operator defined by fuzzy logical operators are called fuzzy matrix [1, 14]. In [10], Rajesh and et al. defined the concept of Symmetric, k-symmetric circulants-Symmetric in the year 2016. Throughout in this paper all matrices considered over a fuzzy algebra F with support [0, 1] under the concept of S-symmetric matrices k-symmetric matrices was introduced in [1, 4]. In [9], Poongodi and et al. have presented the notation on regular neutrosophic fuzzy matrices. In this paper, k-symmetric circulant Neutrosophic Fuzzy Matrices and s-symmetric circulant Neutrosophic Fuzzy Matrices are discussed.

Preliminaries

In this section, some basic definitions and results needed are given. Let N_n denotes the set of all n×n Neutrosophic Fuzzy Matrices.

Definition 2.1

A fuzzy matrix(FM) of order mxn is defined as A=(aij), where aij⍟[0,1]. Let F_{mn} denote the set of all fuzzy matrices of order mxn.

Definition 2.2

A matrix A ∈ $F_{n\times n}$ is said to be symmetric if $A = A^T$.

Definition 2.3

Let A=(aij) and B=(bij) ∈F_{mn}. We write A ≤ B if aij≤ bij for all i, j and we say that A is dominated by B (or) B dominates A. A and B are said to be comparable if either A ≤ B (or) B ≤ A

For any A∈F_{nxn} is a fuzzy circulant matrix then A^T, A^S are transpose, secondary transpose respectively. Let k be a fixed product of disjoint transposition in Sn and K be the permutation matrix associated with k, V is a permutation matrix with units in the secondary diagonal. Clearly K^2= I, K^T=K, V^2=I, V^T=V.

Definition 2.4

For any given a0, a1 ,…. an-1 F, Then the Fuzzy circulant matrix A=(aij)nxn is defined by (aij)= (^{a}j-1(mod n))

$$A=\begin{bmatrix} a_0 & a_1 & a_2 & \dots & a_{n-1} \\ a_{n-1} & a_0 & a_1 & \dots & a_{n-2} \\ a_{n-2} & a_{n-1} & a_0 & \dots & a_{n-3} \\ \vdots & \vdots & \vdots & \dots & \vdots \\ a_1 & a_2 & a_3 & \dots & a_0 \end{bmatrix}$$

Definition 2.5

A matrix A Fnxn is circulant and it is said to be symmetric circulant fuzzy matrix if A = A^T ⭾

For Example,
$$A=\begin{bmatrix} 0.1 & 0.3 & 0.3 \\ 0.3 & 0.1 & 0.3 \\ 0.3 & 0.3 & 0.1 \end{bmatrix}, \quad A^T=\begin{bmatrix} 0.1 & 0.3 & 0.3 \\ 0.3 & 0.1 & 0.3 \\ 0.3 & 0.3 & 0.1 \end{bmatrix}$$

Here A F_{nxn} is circulant as well as $A=A^T$. Hence A is symmetric circulant fuzzy matrix.

Definition 2.6

A matrix A∈F^{nxn} is said to be k - symmetric circulant fuzzy matrix if $A = KA^TK$, where K be the permutation associated with k.

Example:
$$A=\begin{bmatrix} 0.3 & 0.5 & 0.5 \\ 0.5 & 0.3 & 0.5 \\ 0.5 & 0.5 & 0.3 \end{bmatrix}, \text{then } KA^TK=\begin{bmatrix} 0.3 & 0.5 & 0.5 \\ 0.5 & 0.3 & 0.5 \\ 0.5 & 0.5 & 0.3 \end{bmatrix}$$

Here A F_{nxn} is circulant as well as A= KA^TK. Hence A is k- symmetric circulant fuzzy matrix.

Definition 2.7

An neutrosophic fuzzy matrix (NFM) A of order m × n is defined as A= $[X_{ij}, <a_{ij\mu}, a_{ij\lambda}, a_{ij\nu}>]_{mxn}$, where $a_{ij\mu}$, $a_{ij\gamma}$, $a_{ij\nu}$ are called truth, indeterminacy and falsity of X_{ij} in A, which maintaining the condition $0 \leq a_{ij\mu} + a_{ij\lambda} + a_{ij\nu} \leq 3$. For simplicity, we write A = $[X_{ij}, a_{ij}]_{mxn}$ or simply $[a_{ij}]_{mxn}$ where $a_{ij} = < a_{ij\mu}, a_{ij\lambda}, a_{ij\nu} >$.

Lemma 2.8

For A = $[A_\mu, A_\gamma, A_\nu] \circledcirc N_{mn}$ and B = $[B_\mu, B_\gamma, B_\nu] \circledcirc N_{np}$, the following hold.

$A^T = [A_\mu^T, A_\gamma^T, A_\nu^T]$

i. AB = $[A_\mu B_\mu, A_\gamma B_\gamma, A_\nu B_\nu]$

k-Symmetric Circulant Neutrosophic Fuzzy Matrices.

In this section, we define k-symmetric circulant Neutrosophic Fuzzy Matrices and the basic concepts, theorems and properties of k-symmetric circulant NFMs is discussed.

Definition 3.1

A matrix $A \in N_{nxn}$ is said to be k - symmetric circulant NFM if $A = KA^TK$, where K be the permutation associated with k.

Theorem 3.2

If A and B are k-symmetric circulant NFMs then A+B is also k-symmetric circulant NFM.

Proof: Since A and B are k- symmetric circulant NFMs, then $A = KA^TK$ and $B = KB^TK$

To prove A+B is k - symmetric circulant NFM IVFM. $A+B = KA^TK + KB^TK$

$A+B = K [A^T+B^T] K$ $A+B = K [A+B]^TK$

Hence A+B is also k-symmetric circulant NFM.

Theorem 3.3

If A and B are k-symmetric circulant NFMs then AB is also k-symmetric circulant NFM.

Proof: Since A and B are k-symmetric circulant NFMs then $A = KA^TK$ and $B = KB^TK$

To prove AB is k - symmetric circulant NFM. $AB=(KA^TK)(KB^TK)$

$= (KA^T)K^2(B^TK)$

$= KA^TB^TK$

$= K (BA)^TK$ AB

$= K (AB)^T K$

Hence AB is also k-symmetric circulant NFM.

Theorem 3.4

Let A $\in N_{nxn}$ be k-symmetric circulant NFM and K is the permutation matrix then KA is also k-symmetric circulant NFM.

Proof: Since A and A^T are k-symmetric circulant NFMs then, $A=KA^TK$, $A^T=KAK$

To Prove KA is k - symmetric circulant NFM.

$KA= K(KA^TK)$

$=KK^TA^TK$

$=K (AK)^TK$ $KA =K(KA)^TK$

Hence KA is also k-symmetric circulant NFM.

Theorem 3.5

Let A $\in N_{nxn}$ be k-symmetric circulant NFM and K is the permutation matrix then AK is also k-Symmetric circulant NFM.

Proof: Since A and A^T are k-symmetric circulant NFMs then $A=KA^TK$, $A^T=KAK$
To Prove AK is k - symmetric circulant NFM.

$AK = (KA^TK)\ K$
$= KA^TK^TK$
$=K\ (KA)^TK$ $AK=K\ (AK)^TK$
Hence AK is also k-symmetric circulant NFM.

Theorem 3.6

If A $\in N_{nxn}$ be k-symmetric circulant NFM then AA^T and A^TA is also k-symmetric circulant NFM.
Proof: Since A and A^T are k - symmetric circulant NFMs then $A = KA^TK$, $A^T = KAK$.
To Prove AA^T is k-symmetric circulant NFM
$AA^T = (KA^TK)\ (KAK)$
$= K\ (A^TA)\ K$ $AA^T = K\ (AA^T)^TK$
Similarly we will prove A^TA is also k - symmetric circulant NFM.

Theorem 3.7

If A$\in N_{nxn}$ be k - symmetric circulant NFM then $A+A^T$ is also k – symmetric circulant NFM.

Proof: Since A and A^T are k-symmetric circulant NFMs then, $A=KA^TK$, $A^T=KAK$.
To Prove $A+A^T$ is k-symmetric circulant NFM
$A+A^T = KA^TK+ KAK$
$= K\ (A^T+A)\ K$ $A+A^T = K(A+A^T)^TK$
Hence $A+A^T$ is also k-symmetric circulant NFM.

Theorem 3.8
If A and B are k-symmetric circulant NFMs then AB+BA is also k-symmetric circulant NFM.
Proof: Given A and B are k - symmetric NFMs then $A = KA^TK$ and $B = KB^TK$
To prove AB+BA is k-symmetric circulant NFM. $AB+BA=(KA^TK)(KB^TK) + (KB^TK)(KA^TK)$
$= (KA^T)K^2(B^TK) + (KB^T)\ K^2(A^TB)$
$= K\ A^TB^T\ K + K\ B^TA^T\ K$
$= K\ (BA)^TK + K\ (AB)^T\ K$
$= K\ (AB+ BA)^T\ K$
Hence AB+BA is also k-symmetric circulant NFM.

Theorem 3.9
Let A is k-symmetric circulant NFM and if α, $\beta \geq 0$ are scalar Fuzzy and $\alpha+\beta=1$ then $\alpha A+\beta B$ is also k-symmetric circulant NFM.
Proof: Since A and B are k-symmetric circulant NFM then $A = KA^TK$ and $B =KB^TK$
To prove $\alpha A+\beta B = \alpha\ KA^TK + \beta\ KB^TK$

$= K\ [\alpha\ A^T + \beta\ B^T]\ K$

$= K\ [\alpha\ A + \beta\ B]^TK$
Hence $\alpha A+\beta B$ is also k-symmetric circulant NFM.

Remarks: If $\alpha, \beta \geq 0$ and $\alpha+\beta= 1$ with $\alpha A+\beta B$ are symmetric circulant NFM so the set of all symmetric circulant NFMs over the permutation k is a convex set.

s – Symmetric Circulant Neutrosophic Fuzzy Matrices.

In this section, we define s-symmetric circulant Neutrosophic Fuzzy Matrices and the basic concepts, theorems and properties of s-symmetric circulant NFMs is discussed.

Theorem 4.1

A matrix $A \in N_{nxn}$ be s - symmetric circulant NFM then A^T is also s - symmetric circulant NFM.

Proof: Since A is s - symmetric circulant NFM then $A=A^S=VA^TV$

To prove A^T is s - symmetric circulant NFM. $A = A^S$

$A^T = (VA^TV)^T$

$= V (A^T)^T V$

$= V A V A^T= VA^SV$

Hence A^T is also s-symmetric circulant NFM.

Theorem 4.2

If A and B are s - symmetric circulant NFMs then (A+B) is also s - symmetric circulant NFM.

Proof: Since A and B are s - symmetric circulant NFMs then $A=A^S=VA^TV$ and $B=B^S=VB^TV$

To prove (A+B) is s - symmetric circulant NFM. $(A+B)^S$

$= (VA^TV +VB^TV)^S$

$= V (A^T)^S V + V (B^T)^S V$

$= V [(A^S)^T + (B^S)^T] V$

$= V [A^T+B^T] V$ $(A+B)^S= V [A+B]^T V = A+B$

Hence (A+B) is also s-symmetric circulant NFM.

Theorem 4.3

If A and B are s - symmetric circulant NFMs then (AB) is also s - symmetric circulant NFM.

Proof: Since A and B are s - symmetric circulant NFMs then $A=A^S=VA^TV$ and $B=B^S=VB^TV$.

To prove (AB) is s - symmetric circulant NFM. $(AB)^S = (VA^TV\ VB^TV)^S$

$= [VA^T V^2B^T V]^S$

$= [VA^T B^T V]^S$

$= [V (AB)^T V]^S$

$= V [(AB)^T]^S V$

$= V [(AB)^S]^T V$

$= V (AB)^T V$

Hence (AB) is also s-symmetric circulant NFM.

Theorem 4.4

A matrix $A \in N_{nxn}$ be s - symmetric circulant NFM and V is a permutation matrix with units in the secondary diagonal then VA and AV also s - symmetric circulant NFM.

Proof: Since A is s - symmetric circulant NFM then $A=A^S=VA^TV$

To prove VA is s - symmetric circulant NFM. $VA = VA^S$

$= V (VA^TV)$

$= V A^T V V$

$= V A^T V^T V$

$= V (VA)^T V$
Similarly we will prove AV is s - symmetric circulant NFM.

Theorem 4.5

If $A \in N_{nxn}$ be s - symmetric circulant NFM then AA^T and $A^T A$ are also s - symmetric circulant NFM.
Proof: A matrix A is said to be s - symmetric circulant NFM then $A=A^S=VA^TV$.
Since A^T is s - symmetric circulant NFM then $A=A^T=VA^S V$
To prove AA^T is s - symmetric circulant NFM,
$AA^T = (AA^T)^S$
$= (A^T)^S A^S$
$= (A^S)^T A^S$
$= (VA^TV)^T (VA^TV)$
$= (V (A^T)^TV)(VA^TV)$
$= V AA^T V$
$= V (A^TA)^T VA$
$AA^T= (AA^T) S = V (AA^T)^TV$
Similarly we will prove $A^TA = V (A^TA)^TV$

Theorem 4.6

If $A \in N_{nxn}$ be s - symmetric circulant NFM then $A+A^T$ is also s - symmetric circulant NFM.
Proof: A matrix A is said to be s - symmetric circulant neutrosophic fuzzy matrix then $A=A^S=VA^TV$.
To Prove $A + A^T = (A + A^T)^S$
$= A^S+ (A^S)^T$
$= VA^TV + (VA^TV)^T$
$= VA^TV + V (A^T)^TV$
$= VA^TV + VAV$
$=V[A^T + A]V$
$= V[A+A^T]V$

Theorem 4.7
If A and B are s - symmetric circulant NFMs then AB + BA is also s - symmetric circulant NFM.
Proof: A matrix A is said to be s - symmetric circulant NFMs then $A=A^S=VA^TV$.
To prove $(AB+BA)^S = [(VA^TV) (VB^TV) + (VB^TV) (VA^TV)]^S$
$= [V (A^TB^T) V+V (B^TA^T) V]^S$
$= [V (BA)^TV+V (AB)^TV]^S$
$= [V (BA)^TV]^S+ [V (AB)^TV]^S$
$= V \{[(BA)^S]^T + [(AB)^S]^T\} V$
$= V [(AB)^T+ (BA)^T] V$
$= V (AB +BA)^T V$

Theorem 4.8
Let A is s-symmetric circulant NFM and if $\alpha, \beta \geq 0$ are scalar Fuzzy and $\alpha+\beta= 1$ then $\alpha A+\beta B$ is also s-symmetric circulant NFM.
Proof: Since A and B are s-symmetric circulant NFMs then $A=A^S= VA^TV$ and $B=B^S= VB^TV$
To prove $(\alpha A+ \beta B)^S = \alpha (VA^TV) + \beta (VB^TV)$
$= V [\alpha A^T + \beta B^T] V$
$= V [\alpha A + \beta B]^T$

REFERENCES

1. K. Atanassov, Intuitionistic fuzzy sets, Fuzzy Sets and Systems 20 (1986), 87-96.
2. K. Atanassov, Operations over interval-valued intuitionistic fuzzy sets, Fuzzy Sets and Systems 64 (1994), 159-174.
3. Cho, H.H., (1999), Regular Fuzzy matrices and Fuzzy equations, Fuzzy sets and systems 105, 445 – 451.
4. Kim, K.H., (1982), Boolean Matrix Theory and applications Marcel Dekker.Inc.New York
5. Kim, K.H., and Roush, F.W., (1980), Generalized Fuzzy Matrices, Fuzzy sets and systems, 4, 293 – 315.
6. Mamouni Dhar, Said Broumi, and Florentin Smarandache, A Note on Square Neutrosophic Fuzzy Matrices, Neutrosophic Sets and Systems, Vol. 3, 2014.
7. Meenakshi, AR.., (2008), Fuzzy Matrix, theory and applications, MJP. Publishers, Chennai.
8. M. Pal, S. K. Khan and A. K. Shyamal, Intuitionistic fuzzy matrices, Notes on Intuitionistic Fuzzy Sets 8(2) (2002), 51-62.
9. P.Poongodi, S.Princy Christinal Esther and M.M.Shanmugapriya, On Regular Neutrosophic Fuzzy Matrices, , Indian Journal of Natural Sciences, 13(71), pp:40932 – 40938, 2022.
10. K. Rajesh kannan and N. Elumalai, "k- symmetric circulant, s- symmetric circulant and s-k symmetric circulant matrices", Journal of ultra-scientist of physical sciences, Vol. 28, no.6, (2016) pp. 322-327.
11. Rakhal Das, Florentin, Smarandache, Binod Chandra Tripathy, Neutrosophic Fuzzy Matrices and Some Algebraic Operations, Neutrosophic sets and systems, Vol 32, pp:401- 409, 2020 .
12. F. Smarandache, Neutrosophic set, A generalization of the intuitionistic fuzzy sets, Inter. J. Pure Appl. Math. 24 (2005), 287-297.
13. Thomason, M.G., (1977), Convergence of powers of Fuzzy Matrix, J.Math Anal Appl. 57, 476 – 480.
14. Zadeh, L.A. (1965). *Fuzzy sets, Information and Control*, 8: 338 – 353.

Indian Journal of Natural Sciences *www.tnsroindia.org.in ©IJONS*

Vol.15 / Issue 83 / Apr / 2024 *International Bimonthly (Print) – Open Access* *ISSN: 0976 – 0997*

RESEARCH ARTICLE

Optimization of Process Parameters for TIG Welding of Aluminium Alloy 3000 using RSM Technique

Manjeet Bohat[1]* and Rahul Modgil[2]*

[1]Assistant Professor, Department of Mechanical, UIET, Kurukshetra University, Kurukshetra, Haryana, India.
[2]M.Tech Scholar, Department of Mechanical, UIET, Kurukshetra University, Kurukshetra , Haryana, India.

Received: 02 Nov 2023 Revised: 09 Jan 2024 Accepted: 07 Mar 2024

***Address for Correspondence**
Manjeet Bohat
Assistant Professor,
Department of Mechanical,
UIET, Kurukshetra University,
Kurukshetra, Haryana, India.
Email: msbohat2015@kuk.ac.in

ABSTRACT

To improve welding quality of aluminium alloy 3000 grade plate on tig welding system. Aluminium alloy is selected because of its unique properties of light weight and corrosion resistance, welding is performed for aluminium alloy plate by changing different welding parameter. Effect of gas flow, angle and welding current on welding joint has been investigated for the experiment, hardness value of the welded zone has been measured to understand the change in mechanical property and RSM is also used.
Key word: Tig welding, Hardness, RSM

Keywords: TIG, RSM, Optimization, Aluminium alloy 3000, Hardness.

INTRODUCTION

Welding is the process of joining two or more than two similar and dissimilar materials. Welding joint is formed when two materials are in molten state due to intense heat provided by external source. They are of many types, Gas welding, Resistance welding, Energy beam welding, Arc welding, Shielded metal arc welding, Gas metal arc welding, and Gas tungsten arc welding (TIG) etc., developed in different past decades. Welding has many applications in the sheet metal industry, aerospace industry, automobile industry and construction industry. So it is imperative to study the different properties like tensile strength, resistant to corrosion and porosity of the welded joint used in modern industries. Many researchers have studied the effect of different parameters like voltage,

current, speed, gas flow, arc gap and filler wire etc. on welded joint properties like strength of weld, porosity and hardness etc. For example ,**Pradhan and Punyankanti**(2019) investigated the effect of gas flow rate and welding current on the hardness and tensile strength on aluminium alloy 7075 sheet, size of 300 x 200 mm, thickness 6 mm. experimentally they inferred that in both cases higher gas flow and lower gas flow produces weaker welded joint**[1].Mohan ()** adopted automated TIG welding by varying the current and speed of welding to investigate the hardness and tensile strength of welded joint. In first phase welding is accomplished on one face and in second phase welding is accomplished on another phase. He observed that tensile strength is enhanced by increasing the intensity of current. Further, he claimed that better result of welding is obtained with low speed.**[2]**.Al 5052, is known for its nonmagnetic property, low ignition point and light weight, has many applications in sheet metal industry, heat exchanger and pressure vessel etc. Sharma et al (2020) chosen Al 5052 specimen for welding with different varying input parameters, current, speed, root gap and gas flow, to predict the microstructure and strength of welded specimen. RSM is utilised to obtain the optimised results. They come with results speed and current both effect the weld strength [**3**].Ravinder et al used AI 5052 alloy, size 100 x 2.5 x 50 mm, with 4043 grade filler wire by varying welding speed and gas flow at constant voltage (20 volt) and constant current (210 ampere) for welding.

They opined that depth of penetration is linearly increase with the increase in welding speed until optimized values achieved (welding speed 147.78 and depth of penetration 2.02 mm) [**4**].Soni and Dwivedi performed experiment on aluminium sheet, size 120 x 50 x 3 mm, in the range of current 100 to 140 A, speed 3.5 to 4 mm/s, gas flow rate 8 to 10 liter/min at constant 50 votl and weld centre tip distance 3 mm. They come upwith the conclusion that uniform welding of aluminium is possible when elasticity of the welded joint increases with the increase of current. They also assessed that toughness of the welded joint is almost same to base material when welding performed on both side **[5].**Gou and Wang performed TIG welding on aluminium alloy 5052 at varying current 100 to 120 A to investigate welded microstructure, tensile strength and corrosion resistance. They found that higher tensile strength 212.1 MPa, 90.8% of the base metal, is obtained at 115 A current. It is observed that corrosion resistance is 168h when welding current is in between 100 to 110A **[6].** Author performed pulsed tungsten inert gas welding (PTIGW) with varying pulsed current 100 to 300A and gas flow rate 7 and 15 litre/min on 6 mm thick aluminium plate. It is observed that maximum shear strength and refined grain structure is obtained at base current 200 A, pulse current 250 A and flow of gas 15 litre/min**[7]**.27 experiments, TIG welding, were performed on steel structural plate of 8 mm thickness with a range of welding current 55-95 A, welding speed 15-45 mm/sec and arc length 2-3 mmwith three levels factor control to predict the shape profile characteristics and shape of heat affected zone (HAZ). A fuzzy logic model is built from 27 experimental data to predict the response by changing the control factors **[8]**.Raveendraet. al conducted experiment to determine how pulsed current affected the properties of GTAW weldments. Welding current of 80-83 A and arc travel speed of 700-1230 mm/min. are used to weld 304 stainless steel of 3 mm thick.

The non-pulsed current weldment has higher tensile strength. It was found that non pulsed current weldment has higher ultimate tensile strength and yield strength value than parent metal**[9]**.SUS304L and SUS316L material is largely used for hydrogen storage super tank and storage tank. Welding is performed by varying the voltage 8 to 10 volt, current 120 to 210 A and at constant welding speed of 80 mm/min. tensile strength and yield strength are measured after welding. It is observed that base material has long fatigue life as comparison to welded materials in low cycle fatigue case. The ratio of fatigue strength to tensile strength of the welded material range between 0.35 to 0.7 and lesser than that of base materials in case of high cycle fatigue test **[10]**.Kumar and sundarrajan conducted experiment on aluminium alloyAA5456 thickness 2014mm. They performed pulsed TIG welding with different range of parameters i.e. welding speed 210-230 mm/min., welding current 40-90 A. Taguchi method was used to optimize the parameters to obtain optimised responses. It is noted that mechanical properties are enhanced by 10 to 15% after planishing that reduce the internal stress of the welded material **[11]**.Wang used Al Alloys SA12, range of parameters are current 60 to 100 A and welding speed 800 to 1400 mm/sec and thickness of the work piece is 6 to 25 mm for TIG welding. Residual distortion out of plane may be of three types bowling distortion, bukling and arch. Dynamic process and residual distortion out of plane are greatly influenced by welding heat input and thickness of plate **[12]**.AA5052 H32 is well known for its high strength, corrosion resistance and light weight and having applications in automobile industry. Author adopted four input parameters i.e. welding current, arc voltage, gas

flow and welding speed with two responses yield strength and tensile strength. Researchers claimed that welding current and gas flow rate influence the welding **[13].**Norman et al investigated the microstructure of autogenous TIG welding using Al-Mg-Cu-Mn alloy at different parametric setting viz: welding speed 7 to 25 mm/sec and current 100 to 190 A. The weld's center showed a fine microstructure because of a faster cooling rate than the surrounding areas. Moreover, it is found that the rate of weld center cooling rises, when speed of welding increases**[14]**.Wang et al studied the effect of TIG arc welding process parameters on Ni based super alloy in terms of microstructure, tensile properties, and fracture. Process parameters are in range of, current 55-90 A, speed 2100-2900 mm/sec and width 1.2-1.5 mm. As indicated by the exploratory discoveries, welding current increments with diminishing welding speed as intensity input increments**[15]**. Literature review reveals that different types of metals and alloys are used for various types of welding, TIG, MIG and arc etc., with numerous parameters like current, speed, voltage and thickness of plate etc. to optimise and investigate the microstructure, hardness, tensile strength and yield strength etc. A few work is reported on TIG welding of aluminium alloy 3000 with different parameters as current, gas flow and angle to investigate the hardness.

MATERIALS AND EXPERIMENTAL SETUP

Aluminium alloy 3000 grade have excellent strength, good hardness, resistance to chemical agent and atmospheric agents, used in kitchen equipment and hardware to heat exchangers. The aluminium alloy 3000 grade, size 600 x 145 x 3 mm, is used as a work piece for this study. It is a high aluminium material, the percentage of aluminium is about 96.8% to 99%, copper 0.5% to 0.20%, Iron 0.7% maximum and manganese 1% to 1.5%. The welding experiments were carried out in Happy Industries, located at Industrial area phase-2, Tribune chowk, Chandigarh, India using Tungsten Inert Gas Welding (TIG) as shown in fig 1(a). From the literature review, three parameter are selected namely welding current (range 110 to 200 A), gas flow (range 8 to 180cc/min)and angle of welding (range 30 to 60°) with level of process parameters are depicted in table 1. Fifteen specimens are prepared, suggested by RSM (Design Expert), and one of them is shown in fig 1 (b). Rockwell Hardness machine (Specifications) used to measure the response (hardness) and is shown in fig 1(c).

RESULTS AND DISCUSSION

Hardness of the each specimen is testedon Brinell Hardness Machine, as depicted in table 2. Executing all data, as mentioned in table 2, adequate model selection, sequential model sum of square and lack of fit is observed. Regression model is generated from the relevant model. The choice of sufficient model depends on three unique tests for example successive model amount of squares, model outline measurable and absence of fit test which is to be performed for the reaction hardness. The table3 shows various tests to choose suitable model to fit different reactions. Consecutive model amount of squares zero on choosing the most elevated request polynomial where the extra terms are huge and model isn't associated. Model outline measurements tested zero in on the model boosting the Changed R2and anticipated R2. The absence of fit test zero on choosing a model having unimportant absence of fit. Quadratic model is suggested as shown in fig. 3. It is observed that when welding current increases from 123 to 187 A, hardness increases at constant gas flow rate 9cc/min. At constant welding current at 123 A, hardness decreases while gas flow increases from 9 to 17cc/min. In another instance, when both welding current and gas flow increases from 123 to 187 A and 9 to 17 cc/min respectively, results increase in hardness as depicted in fig. 2 (a). It is observed that when welding current increases from 123 to 187 A, hardness increases at constant angle of welding 34°. At constant welding current at 123 A, hardness increases while angle of welding increases from 34 to 56°. In another instance, when both welding current and angle of welding increases from 123 to 187 A and 34 to 56°respectively, results increase in hardness as depicted in fig. 2 (b). It is observed that when gas flow increases from 9 to 17cc/min, hardness increases at constant angle of welding 34°. At constant gas flow at 9cc/min, hardness increases while angle of welding increases from 34 to 56°. In another instance, when both gas flow and angle of welding increases from 123

to 187 A and 34 to 56°respectively, results increase in hardness as depicted in fig. 2 (c). Errors between actual hardness and predicted from RSM is less evident as all points lies in the straight line shown in 2(d).

ANOVA

P value of the model is less than 0.0001 with high F value 919.97 suggests that model is significant. F value of the welding current, angle of welding and gas flow is 2290.4, 892.95 and 21.80 respectively in decreasing order. It can be inferred that hardness is significantly influenced by welding current followed by angle of welding and gas flow rate depending on the value of F and evident from the perturbation diagram fig. 4. Parameter A (welding current) has maximum slope followed by C (angle of welding) and B (gas flow).The difference between the Predicted R^2 of 0.9976 and the Adjusted R^2 of 0.9983 is less than 0.2, which is considered to be a reasonable agreement. Adeq Precision of 120.244 is signal to noise ratio, preferred at least 4, and shows a strong enough signal. The Hardness in actual factor equation is given as equation (1).

Hardness =-121.81677+0.39719 * A-5.92383 * B+6.60831 * C+0.083359 * A * B – 027214* A * C-0.15104 * B * C.

CONCLUSIONS

It is observed from the present study that welding current, gas flow and angle of welding has influence on the hardness of welded specimen, as discussed below.

1. Hardness increases by increasing welding current during welding due to increase in internal stress of the welded piece by raising heat.
2. Hardness of the welded piece is low at extremely low and high gas flow.
3. Hardness increases when angle of welding increases.

REFERENCES

1. prradhan, P. k., &punyankanti, S. (n.d.). Study the Effect of Welding Parameters during TIG Welding of Aluminum Plate and its Optimization. International Journal of Engineering and Management Research.
2. Mohan., P. (n.d.). STUDY THE EFFECTS OF WELDING PARAMETERS ON TIG WELDING OF ALUMINIUM PLATE. 30.
3. sharma, L. k., tiwari, a., &vasnani, h. (03, MARCH 2020). "Optimization Of Tig Welding Parameters And Their Effect On Aluminium 5052 Plate''. INTERNATIONAL JOURNAL OF SCIENTIFIC & TECHNOLOGY RESEARCH VOLUME 9,, 14.
4. Raveendra, A., kumar, D. B., kumar, D. A., & Santhosh, N. (3, March 2014). Effect of welding parameters on 5052 aluminium alloy weldments Using TIG welding. International Journal of Innovative Research in Science,Engineering and Technology.
5. Soni, H., &Dwivedi, A. (October/2019). Study of Effect of TIG Welding Process Parameters for Welding of Aluminium Plate. IAETSD JOURNAL FOR ADVANCED RESEARCH IN APPLIED SCIENCES.
6. Gou, W., & Wang, L. (n.d.). Effects of Welding Currents on Microstructure and Properties of 5052 Aluminum Alloy TIG Welded Joint. IOP Conference Series: Materials Science and Engineering.
7. Kumar, S.(2010) Experimental investigation on pulsed TIG welding of aluminium plate. Advanced Engineering Technology.1(2), 200-211.
8. Narang, H. K., Singh, U. P., Mahapatra, M. M., &Jha, P. K. (2011). Prediction of the weld pool geometry of TIG arc welding by using fuzzy logic controller. International Journal of Engineering, Science and Technology, 3(9), 77-85.
9. Kumar, B. R.(2013). Experimental study on Pulsed and NonPulsed Current TIG Welding of Stainless Steel sheet (SS304). International Journal of Innovative Research in Science, Engineering and Technology, 2(6).
10. Yuri,T., Ogata, T.,Saito.M.,&Hirayama,Y.(2000). Effect of welding structure and δ- ferrite on fatigue properties for TIG welded austenitic stainless steels at cryogenic temperatures. Cryogenics, 40, 251-259.

11. kumar, A., &Sundarrajan, S. (2009). Optimization of pulsed TIG welding process parameters on mechanical properties of AA 5456 Aluminum alloy weldments. Materials & Design, 30(4), 1288-1297.
12. Rui, W., Zhenxin, L., &Jianxun, Z. (2008). Experimental Investigation on Out-ofPlane Distortion of Aluminum Alloy 5A12 in TIG Welding. Rare Metal Materials and Engineering, 37(7), 1264-1268. 33
13. Shanavas, & J, E. R. (2016). Weldability of AA 5052 H32 aluminium alloy by TIG welding and FSW process – A comparative study . IOP Conference Series: Materials Science and Engineering.
14. Norman, A. F., Drazhner, V., &Prangnell, P. B. (1999). Effect of welding parameters on the solidification microstructure of autogenous TIG welds in an Al– Cu–Mg–Mn alloy. Materials Science and Engineering: A, 259(1), 53-64.
15. Wang, Q., Sun, D. L., Na, Y., Zhou, Y., Han, X. L., & Wang, J. (2011). Effects of TIG Welding Parameters on Morphology and Mechanical Properties of Welded Joint of Ni-base Superalloy. Procedia Engineering, 10, 37-41.

Table 1. Levels of Parameters

Coded factor	Real factor	Input parameter	Levels				
			-2	-1	0	1	2
A	Welding current	Welding current	110	123	155	187	200
B	Gas flow	Gas flow	8	9	13	17	18
C	Angle of welding	Angle of welding	30	34	45	56	60

Table 2. Experimental data

Std	Run	Welding current (A)	Gas flow (Cc/min)	Angle (°)	Hardness (HRB)
	1	110	13	45	41.5
	2	155	13	45	49.5
	3	155	13	45	50
	4	187	17	34	58.6
	5	155	8	45	43.8
	6	155	13	45	49.8
	7	155	13	30	40.2
	8	155	13	60	53
	9	200	13	45	62
	10	155	13	45	49.4
	11	155	18	45	45.8
	12	187	9	56	52
	13	123	17	56	43.6
	14	123	9	34	32.2
	15	155	13	45	50.2

Table 3 a. (Sequential Model Sum of Squares)

Source	Sum of Square	Df	Mean Square	F- value	P - value	
Mean vs Total	34713.77	1	34713.77			
Linear vs Mean	628.46	3	209.49	17.51	0.0002	
2FI vs Linear	55.11	3	18.37	1.92	0.2047	
Quadratic vs 2FI	**76.03**	**3**	**25.34**	**276.23**	**< 0.0001**	**Suggested**
Cubic vs Quadratic	0.0107	1	0.0107	0.0956	0.7726	Aliased

Residual	0.4480	4	0.1120			
Total	35473.82	15	2364.92			

Table 3 b. (Model Summary Statistics)

Source	Std. dev.	R^2	Adjusted R^2	Predicted R^2	Press	
Linear	3.46	0.8269	0.7796	0.5967	306.52	
2FI	3.09	0.8994	0.8239	0.2517	568.75	
Quadratic	**0.3029**	**0.9994**	**0.9983**	**0.9976**	**1.83**	**Suggested**
Cubic	0.3347	0.9994	0.9979		*	Aliased

Table 3 c. (Lack of Fit Tests)

Source	Sum of square	df	Mean square	F- value	P- value	
Linear	131.14	7	18.73	167.28	< 0.0001	
2FI	76.04	4	19.01	169.72	0.0001	
Quadratic	**0.0107**	**1**	**0.0107**	**0.0956**	**0.7726**	**Suggested**
Cubic	0.0000	0				Aliased
Pure Error	0.4480	4	0.1120			

Table 4 ANOVA for Hardness

Sources	Sum of square	df	Mean square	F-value	P-value	
Model	**759.59**	**9**	**84.40**	**919.97**	**< 0.0001**	**significant**
A-Welding Current	210.13	1	210.13	2290.4	< 0.0001	
B-Gas Flow	2.00	1	2.00	21.80	0.0055	
C-Angle of welding	81.92	1	81.92	892.95	< 0.0001	
AB	22.12	1	22.12	241.09	< 0.0001	
AC	28.77	1	28.77	313.62	< 0.0001	
BC	4.22	1	4.22	45.97	0.0011	
A^2	7.15	1	7.15	77.97	0.0003	
B^2	48.68	1	48.68	530.62	< 0.0001	
C^2	20.05	1	20.05	218.52	< 0.0001	
R^2 = 0.9994			**Adjusted R^2** = 0.9983			
Predicted R^2 = 0.9976			**Adeq Precision** = 120.2437			

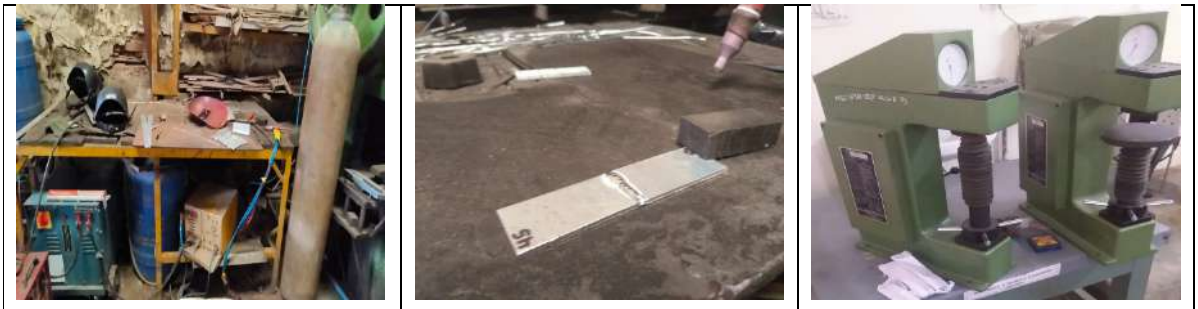

a (Welding setup) **b (Specimen)** **c (Testing machine)**

Fig. 1 Experimental Setup

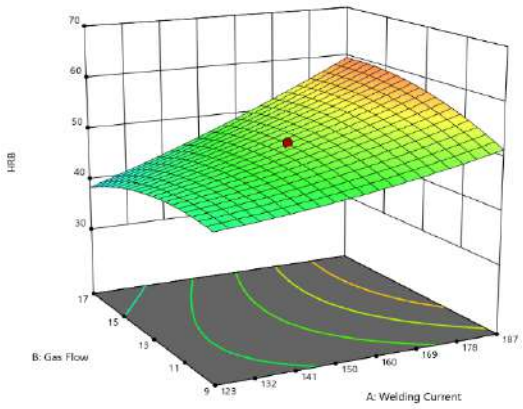

Fig. 2 a(Effect of welding current and gas flow on hardness)

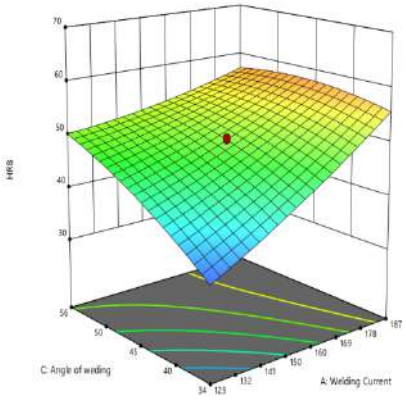

Fig. 2 b (Effect of welding current and angle of welding on hardness)

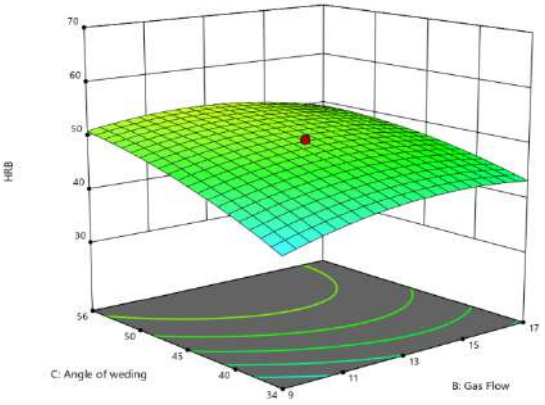

Fig. 2 c (Effect of gas flow and angle of welding on hardness)

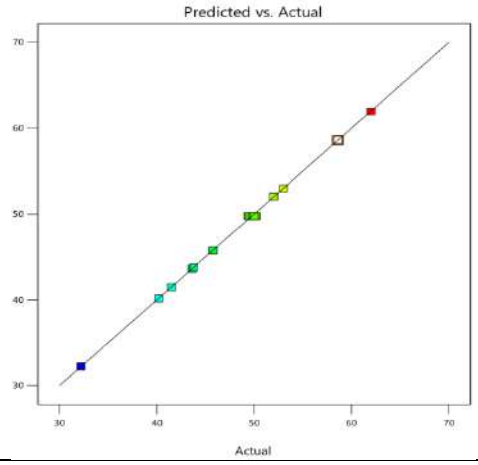

Fig. 2 d (Predicted vs Actual graph)

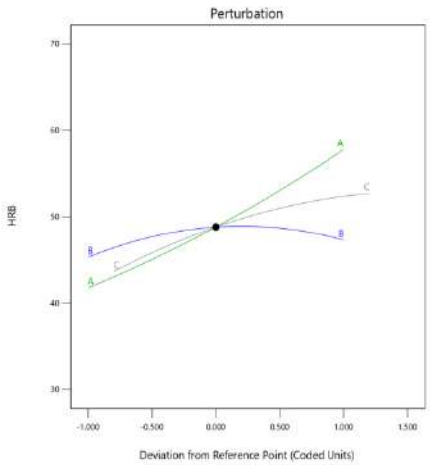

Fig.3 Perturbation Diagram

Indian Journal of Natural Sciences *www.tnsroindia.org.in ©IJONS*

Vol.15 / Issue 83 / Apr / 2024 *International Bimonthly (Print) – Open Access* *ISSN: 0976 – 0997*

RESEARCH ARTICLE

Evaluating Milk Adulteration in Bangalore: A Preliminary Study

Umme Salma Razak[1], Fathima Zohra[1], Mithra Thomas[1], Himani Sharma[2]*

[1]Postgraduate Student, Department of Forensic Science, Kristu Jayanti College (Autonomous), (Affiliated to Bengaluru North University) Bangalore, India.
[2]Assistant Professor, Department of Forensic Science, Faculty of Kristu Jayanti College (Autonomous), (Affiliated to Bengaluru North University) Bangalore, India.

Received: 30 Dec 2023 Revised: 09 Jan 2024 Accepted: 27 Mar 2024

***Address for Correspondence**
Himani Sharma
Assistant Professor,
Department of Forensic Science,
Faculty of Kristu Jayanti College (Autonomous),
(Affiliated to Bengaluru North University) Bangalore, India.
Email: himani.s@kristujayanti.com

ABSTRACT

Given the vital role milk plays in our diets, the issue of milk adulteration reduces the quality of milk and hence, is a matter of utmost concern. This study was conducted to identify most prevalent adulterants in branded and unbranded milk samples across various areas of Bangalore. A sum of 20 milk samples were gathered including 10 branded milk packets and 10 unbranded milk samples from local milk men. The results obtained in our study emphasize that among the 9 tested adulterants, detergent (60%) and sugar (90%) were the most prevalent in branded milk samples while urea (20%) and sodium chloride (50%) were the most prevalent in unbranded milk samples. These unbranded samples were further examined for water content which was found to be positive in 80% of the samples.Lastly, none of milk samples indicated the presence of 5 adulterants namely neutralizer, hydrogen peroxide, starch, formaldehyde and nitrate nitrogen. This is valuable data for the regulatory authorities to improve milk quality and safety in Bangalore. Furthermore, it can raise consumer awareness, enabling them to make well-informed choices.

Keywords: Milk adulteration, Bangalore, adulterants, urea, detergent, sugar, sodium chloride.

INTRODUCTION

Milk, a pale white fluid produced by mammals primarily to nourish their offspring, consists of abundant essential nutrients necessary for bodily growth and development. It is also known for its easy digestibility and high absorbability, making it an ideal wholesome food. The composition of cow milk includes carbohydrates, lactose (4.8%), fat (4%), minerals like calcium, potassium, iodine (0.8%), protein (3.5%)with an energy supply of 66 kcal/100g [1]. The increasing consumption of milk across various age groups, spanning from infancy to old age, makes the issue of milk adulteration a major concern. Milk adulteration is the deliberate act of reducing the quality of milk, achieved either by the removal of valuable components or substitution with inferior substances[2,5]. Common adulterants like water, skimmed milk powder, sugar, starch, salt, melamine, detergents, neutralizers, urea, hydrogen peroxide, formaldehyde etc., are added for various reasons like an increase in profit margin, or to create an illusion of better milk quality or to reduce the perishable nature of milk[1, 3, 4].Unfortunately, some of these adulterants result in severe health issues. For instance, detergents and peroxides in milk can lead to gastritis and intestinal inflammation while urea in milk can place a heavy load on the kidneys to eliminate urea content from the body[4].

Previously, studies have explored the presence of different milk adulterants in various parts of India, however, a comparative study on milk adulteration using branded and unbranded milk samples in Bangalore is absent. This study was therefore conducted to detect nine common adulterants which include urea, neutralizers, detergents, hydrogen peroxide, sodium chloride, starch, formaldehyde, nitrate nitrogen, sugar etc., in branded and unbranded milk samples collected from various regions of Bangalore. The primary objectives were as follows:

- To identify the most prevalent adulterants found in branded and unbranded milk samples.
- To create awareness among consumers about the risks associated with milk adulteration and promote informed choices.
- To contribute valuable data to the regulatory authorities for improving milk quality and safety in Bangalore.

MATERIALS AND METHODS

Procurement of Milk Samples

A sum of 20 milk samples were gathered from different regions of Bangalore (table 1). This collection included 10 branded milk samples, sourced from local retail stores, as well as 10 unbranded samples (250 ml each), sourced from local milkmen. The unbranded milk samples were collected in sterile, clean and dry bottles. Subsequently, these bottles or branded milk packets were transported to the laboratory in an ice filled box.All the necessary precautions and protocols were adhered to during the collection and laboratory processing of the milk samples. The analysis of these milk samples was conducted within one hour of their arrival.

For Detection of Adulterants and Preservatives

A standardized milk adulteration testing kit was used which was manufactured by NICE CHEMICAL Pvt Ltd., Kochi, India. The milk samples were analysed for nine common adulterants including urea, neutralisers detergent, hydrogen peroxide, sodium chloride, starch, formaldehyde, nitrate nitrogen, sugar. All the tests were conductedin accordance with the manufacturer's guidelines and procedures as outlined in the manual. The presence of different adulterants and preservatives was decided based on the colour changes (table 2). Further, the 10 unbranded milk samples were analysed for water content using the glass-plate method as per FSSAI standards.

RESULTS AND DISCUSSION

The milk samples were analysed at room temperature and were tested in triplicates. The 20 milk samples (branded and unbranded) were analysed for the presence of nine different adulterants (Fig 1). Further, 10 unbranded milk samples were analysed for water content (Fig 2). The results observed are presented in Table 3.

Urea

Urea is naturally found in raw milk and 70mg/100ml is the permissible threshold set by PFA Rules, 1955 and FSSAI Act, 2006.Urea is introduced to milk for enhancing its colour, improving consistency, and balancing the Solid-Not-Fat (SNF) content [2]. In our study, three (15%) milk samples were tested positive for urea, of which two were unbranded, and one was a branded milk sample. As per the survey report by FSSAI (2019), 2 samples out of 6,432 milk samples were tested positive for urea [13]. The studies done by Mane et al [9], Arun Kumar et al [5],Bharham et al [8], Swetha et al [6] found that urea was present in 3.33%, 60%,10%, 1.09%, of the tested samples respectively. However, the study done by Rajarajan [7] showed that urea was not present (0%) in the tested samples. An excess of urea in milk can strain the kidneys, potentially leading to renal failure. Additionally, it can also cause vision impairment, unwanted facial hair growth, swollen limbs and irregular heartbeats[2].

Neutralizers: This is added to conceal the pH and acidity levels of milk that had not been preserved well, to give an appearance of freshness [5].They may result in interfering with hormones responsible for development and reproduction [15]. In our study, none of the milk samples indicated the presence of neutralizers. The study done by Sapkal [14] reported that only 1 sample indicated the presence of neutralizers while studies done by Rajarajan [7], Arun Kumar et al [5], Swetha et al [6] found that neutralizer was present in 32.73%, 28%,8.7% of the tested samples respectively.

Detergent- Thisis added to create the desired frothy, white appearance of milk by emulsifying and dissolving the oil in water[2] or can be accidentally introduced if the utensils are not rinsed properly after being washed with detergent[7]. In our study, nine (45%) milk samples were tested positive for detergent, of which three were unbranded and six were branded milk samples. As per survey report done by FSSAI (2019), 3 samples out of 6,432 milk samples contained detergents [13]. Similarly, other studies done byRajarajan [7],Mane et al [9],Arun Kumar et al [5], Bharham et al [8],Swetha et al [6], found that detergent was present in 19.09%, 3.33%, 44%, 32%, 14.13% of the tested samples respectively. However, the study done by Abbas [10] found that detergent was not present (0%) in the tested samples. Detergents in milk can lead to gastritis and intestinal inflammation[4].

Hydrogen Peroxide- It is used as a preservative to reduce the perishable nature of milk and inhibit the growth of microorganisms that spoil it. It can cause increased heart rate, irregular heart rhythms, gastritis and intestinal inflammation. It's impact onantioxidants in the body can weaken the immune system and accelerate the aging process[16]. In our study, none of the milk samples indicated the presence of hydrogen peroxide. This is similar to the results of studies conducted by Sapkal [14], Mane et al [9], Arif et al [11]. However, studies done byRajarajan [7], Arun Kumar et al [5],Bharham et al [8],Swetha et al [6]found that hydrogen peroxide was present in 2.73%, 36%, 13%,3.3% of the tested samples respectively. As per survey report done by FSSAI (2019), 6 samples out of 6,432 milk samples were tested positive for hydrogen peroxide [13].

Sodium Chloride

Salt is incorporated to enhance the density of milk in order to hide the excess water content[6]. In our study, nine (45%) milk samples were tested positive for sodium chloride, of which five were unbranded and four were branded milk samples. The studies done by Rajarajan [7],Mane et al [9], Arun Kumar et al [5], Swetha et al [6] found that sodium chloride was present in 30%, 22.5%, 80% , 28.26% of the tested samples respectively. However, the study done by Arif et al [11] reported that only 1.66% of tested samples contained sodium chloride. It can inflict permanent harm on individuals who have a prior history of high blood pressure and kidney issues[1,6].

Starch It is incorporated to enhance the consistency of milk after diluting with water and to also prevent curdling of milk[4].Excess amount of starch can lead to diarrhoea due to undigested starch in colon. It can be harmful for individuals with diabetes when accumulated in the body[15]. In our study, none of the milk samples indicated the presence of starch.This is similar to the results of studies conducted byMane et al [9],Sapkal [14], Swetha et al [6]. However, studies done by Bharham et al [8], Arun Kumar et al [5], Rajarajan[7] found that starch was present in 12%, 20% , 1.82 %of the tested samples respectively.

Formaldehyde

It is used as a preservative to reduce the perishable nature of milk and even at low concentration can inhibit the growth of microorganisms that spoil it.Even in small amounts, it is highly toxic to humans. When ingested with milk, it can lead to acute poisoning, causing irritation, dermatitis, headaches, and allergic asthma development[16].

In this study, none of the milk samples indicated the presence of this preservative. Similarly, studies done by Sapkal [14], Mane et al [9] tested the milk samples for formalin and found that none of the samples had its presence. However,Arif et al [11], Arun Kumar et al [5],Bharham et al [8], Swetha et al [6] reported that formalin was present in 3.3%, 30%, 11%, 2.20% of the tested samples respectively.

Nitrate Nitrogen

Using nitrate-contaminated water for milk dilution can result decreased milk quality.Excessive nitrate consumption from milk could lead to nitrate poisoning, which lowers the blood's ability to carry oxygen, especially in infants and young children. In our study none of the milk samples indicated the presence of nitrate nitrogen. Previously, studies conducted by Mane et al [9], Rajarajan [7] tested the milk samples for nitrates and found its presence in 0.83%, 18.18% of the tested samples respectively.

Sugar- It is typically added to enhance the milk density (Solid-Not-Fat content)in order to hide the presence of excess water content [7]. In our study, sixteen (80%) milk samples were tested positive for sugar, of which seven were unbranded and nine were branded milk samples.The studies done byArif et al [11],Rajarajan [7],Arun Kumar et al [5], Bharham et al [8]found that urea was present in 4.16%, 40.91%, 24%,22% of the tested samples respectively. However, the studies done by Mane et al [9] andSwetha et al [6]showed that sugar was not present (0%) in the tested samples. Excessive amount of sugar in milk can be harmful for diabetic patients [1].

Water

It is the most prevalent adulterant in milk, added to increase its quantity [1].

In this study, eight (80%) samples of the 10 unbranded milk samples were found to contain water. Similar results were obtained by Bari et al [12] and Bharham et al [8]wherein water was present in 93.33% and 73% of the tested samples respectively. Water polluted with pesticides and heavy metals not only degrades the quality of milk but also increases health hazards for consumers [1].

Overall, it was found that the same adulterants namely urea, detergent, sodium chloride and sugar, were present in both branded and unbranded milk samples. However, the positive percentage varied between both the types of milk samples (fig 3). Urea (20%) and sodium chloride (50%) were found to be more prevalent in unbranded milk samples, while detergent (60%) and sugar (90%) were found to be more prevalent in branded milk samples.

CONCLUSION

Milk being a crucial dietary component, its adulteration is a significant cause for concern. The results of this study emphasize that a considerable number of milk samples contain adulterants, some of which pose serious health risks when consumed. These findings canraise consumer awareness about the dangers associated with milk adulteration and encourage individuals to make informed choices. Additionally, this data is a valuable resource for regulatory authorities for improving milk quality and safety in Bangalore, ultimately safeguarding public health. A simpler

solution is to include a small, cheap, portable milk testing kit with milk packets, offering consumers the means to understand the quality of the milk they are consuming. As this was a pilot study, the sample size was limited, and only nine adulterants were examined. Also, the tests conducted could only determine the presence or absence of adulterants but were unable to confirm their concentrations. This study can serve as a basis for providing preliminary findings for future analysis on milk adulteration. The study can also be broadened using a larger milk sample size from diverse sources to evaluate additional types of adulterants. Advanced Techniques can also be employed for detection or quantification of adulterants such as NIR or MIR spectroscopy, MALDI-TOF MS, fluorescence spectroscopy, Raman spectroscopy etc[1].

ACKNOWLEDGEMENTS

We would like to express our deep and sincere gratitude to the Management of Kristu Jayanti College for providing us with an excellent environment to carry out our research work.

REFERENCES

1. C. Paramasivam, "Milk adulteration: An overview on adulterants, detection tests and effects on human health," *Advances in Applied Research*, vol. 13, pp. 63–68, Jan. 2021.
2. S. D. Kandpal, A. Srivastava, and K. Negi, "Estimation of quality of raw milk (Open & branded) by milk adulteration testing kit," *Indian Journal of Community Health*, vol. 24, pp. 188–192, Jul. 2012.
3. R. Chugh and G. Kaur, "A Study on Milk Adulteration and methods of detection of various Chemical Adulterants qualitatively," *IOP Conference Series: Materials Science and Engineering*, vol. 1225, p. 012046, Feb. 2022.
4. T. Azad and S. Ahmed, "Common milk adulteration and their detection techniques," *International Journal of Food Contamination*, vol. 3, Dec. 2016.
5. A. Kumar, S. GOYAL, R. Pradhan, and R. Goyal, "A Study on Status of Milk Adulterants using in Milk of District Varanasi," *South Asian J. Food Technol. Environ.*, vol. 1, pp. 140–143, Jun. 2015.
6. C. Swetha, B. Sukumar, and S. Sudhanthirakodi, "The Study on Detection of Adulteration in Milk Samples Supplied by Local Vendors in Tirupathi Region, India," *SHANLAX INTERNATIONAL JOURNAL OF VETERINARY SCIENCE*, vol. 2, pp. 4–11, Oct. 2014.
7. R. G., "Assessment of market milk adulteration in Tiruchirapalli city of Tamil Nadu," *Indian Journal of Dairy Science*, vol. 74, pp. 232–237, Aug. 2021.
8. G. Barham, M. Khaskheli, A. H. Soomro, and Z. Nizamani, "Extent of extraneous water and detection of various adulterants in market milk at Mirpurkhas, Pakistan," *IIOSR Journal of Agriculture and Veterinary Science*, vol. 7, pp. 83–89, Apr. 2014.
9. B. Mane, A. Sharma, S. Thakur, D. Thakur, and S. Khurana, "Evaluation of Milk Quality and Level of Adulteration in Kangra Valley of Himachal Pradesh," vol. 4, pp. 1–03, May 2020.
10. M. Abbas, B. Khattak, A. Sajid, T. Islam, Q. Jamal, and S. Munir, "Biochemical and bacteriological analysis of cows' milk samples collected from District Peshawar," *International Journal of Pharmaceutical Sciences Review and Research*, vol. 21, pp. 221–226, Jul. 2013.
11. H. Arif *et al.*, "Milk Adulterants in Quetta: A Threat to Public Health," *Pak-Euro Journal of Medical and Life Sciences*, vol. 5, pp. 435–442, Jun. 2022.
12. L. Bari, M. Hoque, S. Reza, M. Hossain, and A. Islam, "Adulteration of Raw Milk in Selected Regions of Tangail District of Bangladesh," *Journal of Environmental Science & Natural Resources*, vol. 8, pp. 41–44, Sep. 2015.
13. FSSAI, "Food Safety and Standards Authority of India Survey: Your Milk is Largely Safe," *Press release on National Milk Safety and Quality Survey 2018*, New Delhi, pp 1-7, 2019.
14. H. Sapkal, "Assessment of adulteration found in different milk samples collected from Akola city," *Indian Journal of Applied Research*, vol. 10, June. 2020.

15. T. Rideout, P. Wood, and M. Fan, "Nutrient utilisation and intestinal fermentation are differentially affected by the consumption of resistant starch varieties and conventional fibres in pigs," *The British journal of nutrition*, vol. 99, pp. 984–92, May 2008.
16. P. Singh and N. Gandhi, "Milk Preservatives and Adulterants: Processing, Regulatory and Safety Issues," *Food Reviews International*, vol. 31, p. 150203005056007, Feb. 2015.

Indian Journal of Natural Sciences *www.tnsroindia.org.in ©IJONS*

Vol.15 / Issue 83 / Apr / 2024 *International Bimonthly (Print) – Open Access* *ISSN: 0976 – 0997*

RESEARCH ARTICLE

Evaluation of *Trichoderma* spp. from Rhizospheric Soil against *Colletotrichum truncatum* (Syn. *C.capsici*) Causing Fruit rot of Chilli (*Capsicum annum* L.)

R. Karthikeyan[1]* and C. Kannan[2]

[1]Research Scholar, Department of Plant Pathology, Faculty of Agriculture, Annamalai University, Chidambaram, Tamil Nadu, India.
[2]Assistant Professor, Department of Plant Pathology, Faculty of Agriculture, Annamalai University, Chidambaram, Tamil Nadu, India.

Received: 30 Dec 2023 Revised: 09 Jan 2024 Accepted: 27 Mar 2024

***Address for Correspondence**
R. Karthikeyan
Research Scholar,
Department of Plant Pathology,
Faculty of Agriculture,
Annamalai University,
Chidambaram, Tamil Nadu, India.
Email: karthi22297@gmail.com

ABSTRACT

Chilli (*Capsicum annuum L.)* is an important spice crop grown in tropical and subtropical areas of India. The chilli crop suffers from several diseases, in which fruit rot of the chilli plant is one of the most significant diseases that affect the chilli crop. It is caused by *Colletotrichum truncatum*(syn. *C. capsici*).Management of the fruit rot was found to be difficult, uneconomical and harmful for the environment. Keeping in view of the residual nature of fungicides on the environment, the idea of biocontrol was undertaken. Biological control is a great renaissance of interest and research in microbiological balance to control plant pathogens and leads to the development of a better farming system. One of the best bioagents for biological control is the genus Trichoderma, which is proven to be efficient against a variety of infections. Trichoderma is a filamentous fungus that lives in soil and is a member of the Ascomycota division.In this study, an experiment was conducted to evaluate the native *Trichoderma* isolates against fruit rot of chilli**.** Ten isolates of *Trichoderma*spp., were isolated from the rhizosphere soil of chilli field. Among these different isolates, Tr-3 isolate reported maximum percent inhibition of 89.33%, whereas least inhibition was noticed in the isolate Tr-10 with 64.11% inhibition when compared over control.

Keywords: Chilli, fruitrot, *Colletotrichum truncatum*, bio-control, *Trichoderma*

INTRODUCTION

Chilli is one of the most important and widely cultivated spice crops across India and it alone contributes nearly 25% of the total chilli production in the world. Chilli is rich in vitamins A, E and C and is also a good source of potassium, folic acid and low in sodium and cholesterol (Marin *et al*., 2004). It also contains a wide range of compounds, such as fatty oils, volatile oils, carotenoids, capsaicinoids, vitamins, fibers, protein, and mineral components. India has enormous potential for producing and exporting different kinds of chillies to a wide range of international markets. At various phases of crop development, the chilli crop is susceptible to a number of diseases brought on by nematodes, bacteria, viruses, fungus, and physiological issues. These are mainly fruit rot, damping off, powdery mildew, bacterial leaf spot, cercospora leaf spot and dry root rot. Among the major diseases of chilli, fruit rot of chilli caused by Colletotrichum truncatumis one of the most destructive diseases of chilli in India. Fruit rot mainly becomes problematic when it attacks mature fruits, causing both pre and post-harvest fruit decay, causing severe economic losses (Bosland and Votava, 2003) .The disease tends to be seed and soil borne as well as air borne and affects seed germination and vigor to a greater extent . The pathogen *Colletotrichum truncatum* is seed transmitted in chilli in the form of acervuli and micro sclerotia (Perenzny *et al.*, 2003) and can also survive on other solanaceous or leguminious crops, plant debris and rotten chilli fruits in the field. This disease affects all the aerial parts of the plant and mainly it produces fruit rot to both green and ripe fruits which is having major economic importance. However, the prevalence of the disease is more on the ripen fruits when compared to the green fruits, hence the name ripe fruit rot of chilli (Lokhande *et al.*, 2019). India leads first in producing, consuming, and exporting of chillies. Tamil Nadu ranks eighth place in India with 1.15 percent of the country's total production of chillies, while Andhra Pradesh leads the country with 37.35%. In India, 15.78 lakh tonnes of chillies are produced on 8.52 lakh hectares of land. During 2021–2022, Tamil Nadu produced 0.24 lakh tonnes of chilli from 0.54 lakh hectares. Chilli is grown sparingly in practically all other districts, but primarily in the districts of Virudhunagar, Thoothukudi, Ramanathapuram, and Tirunelveli. (TNAU Price Forecast, 2023).

Symptomatology

The characteristic symptom of this disease appears as multiple sunken circulars or angular lesions which often coalesce to form severe fruit rot. These lesions are characterized by the presence of black-colored spots in concentric rings. These masses are called acervuli containing setae entrapping conidia. The symptom also appears on stems and leaves which results in defoliation. The infection of the growing tip results in necrosis of branches which proceeds backward and killing it (Die backstage) and it may kill the whole plant (Gupta *et al.*, 2017). Presence of a small lesion on the fruits will drastically reduce the marketability of the produce (Ahila Devi and Prakasam, 2016). However, in India, a yield loss of 10 – 54.91% has been reported due to fruit rot disease (Mishra *et al*., 2018). Traditionally, chemical fungicides were used for controlling the disease under field conditions. There are numerous reports of using chemical fungicides which affects the human health and toxic contamination to the environment due to their long-lasting residual nature, particularly in developing countries (Voorrips *et al*., 2004). Thus, emphasis should be given for using bioagents for the management of the plant disease which is not only cost effective but also environment friendly. Fungi of the genus *Trichoderma* are potential biocontrol agents of several phytopathogens (Hassan *et al*., 2014). Moreover, all *Trichoderma* isolates exhibited inhibition to the mycelial growth of various pathogens. This might result from the synthesis of diffusible substances, like lytic enzymes or metabolites that are soluble in water (Anees et al., 2010). Free-living fungi called Trichoderma strains are frequently found in soil and root environments. In the ecosystems of roots, soil, and leaves, they are quite interacting. A range of chemicals that cause plants to develop systemic or localized resistance responses are produced or released by them. According to Rekha et al. (2012), Trichoderma spp. have the ability to manufacture antibiotics on agar and their culture filtrates can also be utilized to restrict the growth of fungal colonies. The aim of the current investigation was to examine the antagonistic potential of different *Trichoderma* species for bio control of *Colletotrichum truncatum* .

MATERIALS AND METHODS

ISOLATION

The infected plant samples collected are taken to the laboratory and are washed thoroughly in tap water for removing all the debris present in it. A small portion of the infected tissue along with a healthy portion of the tissue was exercised by using a sterile scalpel (2×2 mm). Then these bits are surface sterilized in 70% alcohol for 20 seconds followed by 1% sodium hypochlorite for 1 min. Then they are rinsed thrice with sterile distilled water to get rid of the surface sterilizing agents and dried on a sterile filter paper in the air of the laminar airflow chamber. After drying, the bits were aseptically transferred to Petri-plates containing potato dextrose agar medium (PDA) in such a way that each of the plate containing three bits towards the periphery of the plates. These plates are now incubated in biological oxygen demand (BOD) incubator at28 ± 2^0C for 3 days. Purification is done by the single spore isolation method (Dhingra and Sinclair, 2017) and the pure cultures thus obtained are maintained on PDA slants and stored in the refrigerator at 4^0C for carrying out further studies. The same procedure is adopted forall the isolates of the pathogen collected from different Chilli growing areas of Tamil Nadu.

Cultural and Morphological characterization

Nine mm discs of the 15 days old culture of pathogen were placed at the center of Petri plates containing 20 ml of PDA aseptically and incubated at 28 ± 2^0C for 20 days in BOD incubator. The mycelial and morphological characters like mycelial growth, color, conidial shape, and a number of septa per setae of isolates were observed.

Isolation of fungal antagonistic culture

Using Trichoderma selective medium (TSM) (Elad and Chet, 1983), ten Trichoderma spp. were isolated from several chilli growing sites using the soil dilution plate technique (Dhingra and Sinclair, 1995). After using the single hyphal tip procedure to purify the isolates, the culture was kept for later research at 4°C in test tube slants. The assessment of hyphal diameter, conidiophore and conidia size, as well as the physical and cultural features of the colonies, were the only methods used to identify opposing strains (Rifaee, 1969).

Efficacy of antagonistic *Trichoderma* spp. against *Colletotrichum truncatum*

In vitro antagonistic potential of *Trichoderma* spp. was evaluated against the virulent Colletotrichum truncatum isolate through dual culture technique (Dennis and Webster, 1971). Seven-day old cultures of both pathogenic and antagonistic fungi were inoculated on PDA plates at periphery. In control plate only pathogenic fungi were inoculated. Three replications were maintained in each treatment. Plates were incubated at 28 ± 2°c. Observations of colony growth were recorded. Diameter of colony was measured in cm and percent inhibition was calculated by using following formula suggested by Pandey *et al*., (2000).

Percent inhibition (I) = C-T/C × 100

Where,

I = Per cent inhibition in growth of test pathogen

C = Radial growth in control

T = Radial growth in treatment

Preparation of the culture filtrates of *Trichoderma* spp.

The chosen Trichoderma isolates were cultured in Erlenmeyer flasks with 50 ml of sterile potato dextrose broth for 15 days at room temperature (28 ± 2°C). The cultures were then vacuum-filtered using a bacteriological filter, and the resulting filtrates were utilized in the investigations.

Effect of antagonistic culture filtrates on the mycelial growth of *Colletotrichum truncatum* (Poisoned food technique) (Groover and Moore, 1962)

Using a sterile pipette, the antagonist culture filtrates were individually added to sterile PDA melting media at concentrations of 5, 10, 15, and 20 percent. The modified media were divided into individual, sterile Petri plates, with 15 ml in each plate, and left to solidify. As a control, PDA media was used without the culture filtrate. Each plate was inoculated at the centre with a five days old PDA culture disc of *Colletotrichum truncatum.* Three replications were maintained for each treatment. The diameter of the mycelial growth (mm) of *C. truncatum* was measured after 5 days of incubation. The per cent inhibition of the test fungi was calculated by the formula suggested by Pandey *et al*., (2000).

Percent inhibition (I) = C-T/C × 100

Where,

I = Per cent inhibition in growth of test pathogen

C = Radial growth in control

T = Radial growth in treatment

Experimental Design and Results

The experiments were conducted following the Completely Randomized Design (CRD) with three replications. The significant difference, if any, among the means was compared by Duncan's Multiple Range Test (DMRT). Whenever necessary, the data are transformed before statistical analysis following appropriate methods.

RESULT AND DISCUSSION

A field survey was conducted in major chilli growing areas of Tamil Nadu to collect the 25 different fruit rot infected samples. To evaluate the virulence among 25 isolates, pathogenicity test was conducted in pots and C_{10} recorded the highest disease incidence. Based on the morphological and molecular characters, C_{10} isolate was identified as *Colletotrichum truncatum* (OR642780).

Cultural characteristics of different *Trichoderma* spp. isolates

Ten different *Trichoderma* isolates were isolated from different locations and the growth patterns of the different isolates were determined by the colony growth, colony color, conidiophore, conidial color, conidia shape, conidial breadth and length. The Petri plates were fully occupied with the mycelial growth of the *Trichoderma* spp. within five days and colonies were observed on whitish green, dull green, light green, dark green, pale white and pale yellow in color with compact or floccose in mycelial form (Table 1). Conidial characters were observed and recorded on the Table 2. Conidiophores are highly branched with regular or irregular manner and some of the species were noticed on moderately branched conidiophores. Shape of the conidia observed in globose, ellipsoidal and obovoid in nature with dark or dull green in color. Conidial length and breadth were measured in the range of 2.11-3.72(µ) and 1.63-4.18(µ) respectively. Conidiophores of *Trichoderma virens* were smoothly bent gather and not spread to top. Conidia broadly rounded to obovoid, both ends broadly rounded or with the base narrower (Shah *et al*., 2012). 6 *Trichoderma* isolates were exhibited hyaline conidiophores arising in clusters from aerial mycelium, branching toward the tip, each branch terminating in a penicillus of 3-6 closely appressed and divergently branched phialides towards the apex, with a sterile stipe (Sharma and Singh, 2012). Different *Trichoderma* isolates colony showed dark green to dark bluish green sporulation, colony reverse was amber or uncolored. Conidiophore usually long, infrequently branched, verticillate conidiophores. Phialides are frequently paired, lageniform convergent or divergent. Conidial shape was globose to ellipsoidal (Chandra sekar *et al*., 2017).

In vitro* efficacy of *Trichoderma* spp. against *Colletotrichum truncatum

Ten *Trichoderma* isolates were collected from different Chilli growing areas of Tamil Nadu, and are tested against the pathogenic culture of *Colletotrichum truncatum by* dual culture technique (Table 3). Among the ten isolates, the isolate Tr-3 recorded the maximum percent inhibition of 73.55% followed by Tr-4 which recorded 69.00 % inhibition,

whereas least inhibition was noticed in the isolate Tr-10 with 43.00% inhibition over control. There are many studies that have revealed broad antagonistic activity of *Trichoderma against Colletotrichum* disease in many plants. Kannan C *et al*., 2020 reported that *T. asperellum* recorded the maximum inhibition zone over the test pathogen. Similar research findings were also given by Yelleti and Sunil, 2022.

Efficacy of Non- Volatile compounds produced by *Trichoderma* spp. against *Colletotrichum truncatum*

The *Trichoderma* spp. was selected to study the antagonistic potential against pathogenic culture of *Colletotrichum truncatum by* poison food technique. The results represented in the table 4 showed that all the five isolates were significantly inhibited the mycelial growth of *C. capsici* when compared to control Among the five isolates were tested, the isolate Tr-3 recorded least mycelial growth of 0.96cm at 30% concentration of the culture filtrate with mycelial inhibition of 89.33%. Based on the morphological and molecular characters, Tr-3 isolate was identified as *Trichoderma asperellum.* The culture Sequence was deposited in NCBI GenBank with accession no (OR681494). Hirpara *et al*., 2017 stated that the mycoparasitism is one of the main mechanisms used by *Trichoderma* isolates and also, they can produce chitinase and β-1, 3-glucanase, which are involved in mycoparasitism. Sunpapao, 2020 also reported that *Trichoderma* spp. restricts the invasion, penetration and proliferation of fungal phytopathogens by emitting volatile compounds (antibiosis), competing for nutrient utilization and mycoparasitism.

CONCLUSION

In summary, the significance of chili as a versatile spice crop with various applications has been highlighted. The presence of *Colletotrichum truncatum*, causing anthracnose disease, poses a major challenge to chili production, resulting in extensive crop damage and economic losses. Over-reliance on chemical treatments is not sustainable due to their negative environmental and health impacts. Therefore, there is a critical need for biological management strategies to combat this pathogen effectively. The early detection and identification of the pathogen through conventional and molecular methods play a vital role in minimizing yield losses under field conditions. The present study reveals the important role of *Trichoderma* spp has a very effective antagonistic activity against *Colletotrichum truncatum* as compeer to fungicide. Therefore, it could be strongly suggested the potential of *Trichoderma spp* used as a Bio-control agent for the management of fruit rot of chilli without effecting the environment serving to reduce soil salinity and increase the fertility.

REFERENCES

1. Ahila Devi P and Prakasam V, 2016. Characterization and management of *Colletotrichum capsici* causing anthracnose in chilli. Indian Phytopathology, 69(2): 155-161. http://epubs.icar.org.in/ejournal/index.php.
2. Anees M, Tronsmo A, Hermann V, Hjeljord LG, Heraud C, Steinberg C. Characterization of field strains of *Trichoderma* antagonistic against *Rhizoctonia solani*.Fungal Biology,2010:114:691-701.
3. Bosland, P. W., E. J. Votava, and E. M. Votava. "Peppers: vegetable and spice capsicums. CAB International." (2003).
4. Chandra Sekhar Y, Khayum Ahammed S, Prasad TNVKV, Sarada Jayalakshmi Devi R. Identification of *Trichoderma* species based on morphological characters isolated from rhizosphere of groundnut (*Arachis hypogaea* L.) International Journal of Science,Environment and Technology, 2017:6(3):2056-2063.
5. Choudhary, C. S., et al. "Efficacy of different fungicides, biocides and botanical extract seed treatment for controlling seed borne *Colletotrichum sp*. in chilli (*Capsicum annuum* L.)." *The Bioscan* 8.1 (2013): 123-126.
6. Dennis C, Webster J. Antagonists properties of species groups of *Trichoderma* Production of non-volatile antibiotics. T. Brit. Mycol. Soc,1971:57:25-39.
7. Dhingra OP, Sinclair JB. Basics Plant Pathologymethods, 2ndedn. CRC press, Bocca Raton, America, 1995.
8. Dhingra, Onkar D, James B Sinclair. Basic Plant Pathology Methods. CRC press, 2017.
9. Elad Y, Chet I. Improved selective media for isolation of *Trichoderma* spp and *Fusarium* spp.

Phytoparasit,1983:11:55-58.

10. Groover RF, Moore RD (1962) Resistance inducing chemicals and disease resistance in plants. Phytopathology 52: 876-880.
11. Gupta, Veerendra, et al. "Comparative studies on isolation, identification and purification of *Colletotrichum capsici* causing anthracnose disease of chilli." *Inter. J of Chemical Studies* 5.6 (2017): 744-747.
12. Hassan MM, Gaber A, El-Hallous EI. Molecular and Morphological Characterization of *Trichoderma harzianum* from different Egyptian Soils. Wulfenia Journal,2014:21:80-96.
13. Hirpara DG, Gajera HP, Hirpara HZ, Golakiya BA. Antipathy of *Trichoderma* against *Sclerotium rolfsii* Sacc. Evaluation of cell wall-degrading enzymatic activities and molecular diversity analysis of antagonists.J.Mol.Microbiol.Biotechnol,2017:27(1):22-28.
14. Jayawardena, R. S., Hyde, K. D., Jeewon, R., Li, X. H., Liu, M., & Yan, J. Y. (2016).
15. Kannan C, Praveen A, Jaiganesh V, Senthil Murugan S. Evaluation of fungal and bacterial antagonist against *sclerotium rolfsii* in groundnut. Plant Archives,2020:20(2):5087-5090.
16. Lokhande RD, Tiwari S, Patil RV (2019) Eco-friendly management of anthracnose ofchilli (*Capsicum annuum* L.), caused by *Colletotrichum capsici*. Journal of Current Microbiology & Applied Science 8(2): 1045-1052.
17. Marín, Alicia, et al. "Characterization and quantitation of antioxidant constituents of sweet pepper (Capsicum annuum L.)." *Journal of agricultural and food chemistry* 52.12 (2004): 3861-3869.
18. Mishra, A.; Ratan, V.; Trivedi, S.; Dabbas, M.R.; Shankar, K.; Singh, A.K.; Srivastava, Y. Survey of anthracnose and wilt of chilli: A potential threat to chilli crop in central Uttar Pradesh. *Int. J. Pharmacognosy. Phytochem.* 2018, *7*, 1970–1976.
19. Pandey KK, Upadhayay JP (2000) Microbial population from rhizosphere and non- rhizosphere soil of pigeon pea: screening for resistant antagonist and mode of mycoparasitism. Journal of Mycology and Plant Pathology 30: 7-10
20. Perenzny K, Roberts P D, Murphy J F & Goldberg N P 2003 Compendium of pepper diseases. APS Press, St. Paul, Minnesota, UAS, pp.73
21. Rekha D, Patil MB, Shridhar S, Swamy P, Rajini K, Gamanagatti B. In vitro screening of native *Trichoderma* isolates against *Sclerotium rolfsii* causing collar rot of ground nut. Pak. J. Bot,2012:34:117-120.
22. Rifaee MA (1969) A revision of the genus *Trichoderma*. CommonwealthMycological Institute 116-156
23. Shah S, Nasreen S, Sheikh PA. Cultural and morphological characterization of *Trichoderma* spp. associated with green mold disease of *Pleurotus* spp. in Kashmir. Research Journal of Microbiology,2012:7:139-144.
24. Sharma KK, Singh US. Cultural and morphological characterization of rhizospheric isolates of fungalantagonist *Trichoderma*. Journal of Applied and Natural Science,2014:6(2):451-456.
25. Sunpapao, A. 2020. Antagonistic Microorganisms: Current Research and Innovations. LAP LAMBERT Academic Publishing.
26. TNAU Price Forecast for Red Chilli - Eng.pdf.
27. Voorrips RE, Finkers R, Sanjaya L, Groenwold R. QTLmapping of anthracnose (*Colletotrichum* spp.) resistance in a cross between *Capsicum annuum* and *C. chinense*. Theoretical and Applied Genetics,2004:109(6):1275-1282

Table 1.Morphological and cultural characteristics of different *Trichoderma* spp

Isolates	Locality	Mycelial characters(5 DAI)		
		Growth rate (cm)	Colony color	Mycelial form
Tr-1	Sivapuri	9	Light Green to bright green	Floccose
Tr-2	Radhapuram	9	Dark green	Floccose
Tr-3	Kovilpatti	9	Yellow to green	Arachnoid
Tr-4	Palur	9	Pale yellow green	Scattered
Tr-5	Omalur	9	Light Green to	Floccose to

			bright green	Arachnoid
Tr-6	Kulithalai	9	Pale white to dull green	Compact colony
Tr-7	Melur	9	Whitish green to dull green	Floccose to Arachnoid
Tr-8	Thandrampet	9	Whitish green to dull green	Compact and cottony
Tr-9	Vengikkal	9	Dark green to whitish green	Compact and cottony
Tr-10	Paramakudi	9	Whitish green to dull green	Floccose

Table 2.Morphological and cultural characteristics of different *Trichoderma* spp

Isolates	Locality	Conidial characters				
		Conidiophore	Conidial shape	Conidial color	Conidial length(µ)	Conidial breadth(µ)
Tr-1	Sivapuri	Few lateral branches at apex,Irregular	Globose	Dark green	2.11-3.08	1.67-3.26
Tr-2	Radhapuram	Highly branched, Irregular	Sub globose to obovoid	Dark green	2.84-3.72	2.53-3.18
Tr-3	Kovilpatti	Branched regular	Ellipsoidal	Dull green	2.37-3.62	2.34-3.63
Tr-4	Palur	Few lateral branches at apex,Irregular	Globose	Dull green	2.11-3.13	2.32-3.16
Tr-5	Omalur	Rarely branched, Regular	Ellipsoidal	Green	2.58-3.33	2.53-4.18
Tr-6	Kulithalai	Moderately branched, Regular	Globose	Light green	2.86-3.51	1.63-3.06
Tr-7	Melur	Highly branched, Regular	Globose to ellipsoidal	Green	2.68-3.64	2.22-3.52
Tr-8	Thandrampet	Highly branched	Narrow ellipsoidal	Dark green	2.41-3.62	2.03-2.74
Tr-9	Vengikkal	Moderately branched, Regular	Globose	Dark green	2.56-3.39	2.92-3.01
Tr-10	Paramakudi	Branched regular	Obovoid	Dull green	2.38-3.21	2.38-3.32

Table 3.In vitro efficacy of *Trichoderma* spp. against *Colletotrichum truncatum*

S. No	Isolates	Mycelia growth (cm)		Percent inhibition over control
		Trichoderma spp.	*Colletotrichum truncatum*	
1	Tr-1	5.16	3.84	57.33^{de}(49.21)
2	Tr-2	5.63	3.37	62.55^{c}(52.27)
3	Tr-3	6.62	2.38	73.55^{a}(59.05)
4	Tr-4	6.21	2.79	69.00^{b}(56.17)
5	Tr-5	5.32	3.68	59.11^{d}(50.25)
6	Tr-6	4.89	4.11	54.33^{e}(47.48)
7	Tr-7	4.53	4.47	50.33^{f}(45.19)
8	Tr-8	4.09	4.91	45.44^{fg}(42.38)
9	Tr-9	6.08	2.92	67.55^{bc}(55.27)
10	Tr-10	3.87	5.13	43.00^{g}(40.98)
11	Control	-	9.00	-

Mean of three replications

Values in the column followed by common letters do not differ significantly at 5% level by Duncan's multiple range tes (DMRT)

Table 4. Efficacy of Non-Volatile compounds produced by Trichoderma spp. against *Colletotrichum truncatum*

Sl. No	Isolates	Mycelial growth (cm) (5DAI)							
		5%	Percent inhibition over control	10%	Percent inhibition over control	15%	Percent inhibition overcontrol	20%	Percent inhibition over control
1	Tr-1	4.58e(12.35)	49.11d(44.49)	3.84e(11.30)	57.33cd(49.21)	3.26e(10.40)	63.77e(52.99)	2.17e(8.47)	75.88de(60.58)
2	Tr-2	5.40g(13.43)	40.00f(39.23)	3.62d(10.96)	59.77c(50.63)	2.74c(9.52)	69.55c(56.50)	1.63c(7.33)	81.88c(64.80)
3	Tr-3	3.32a(10.50)	63.11a(52.60)	2.53a(9.14)	71.88a(57.97)	1.81a(7.72)	79.88a(63.34)	0.96a(5.62)	89.33a(70.93)
4	Tr-4	4.03d(11.57)	55.22c(47.99)	3.01c(9.98)	66.55bc(54.66)	4.01i(11.55)	55.44g(48.12)	2.40f(8.91)	73.33e(58.90)
5	Tr-5	4.86f(12.73)	46.00de(42.70)	3.91ef(11.40)	56.55d(48.76)	2.86cd(9.73)	68.22d(55.68)	1.98d(8.08)	78.00d(62.02)
6	Tr-6	3.78b(11.21)	58.00b(49.60)	2.78b(9.60)	69.11ab(56.23)	3.78g(11.21)	58.00f(49.60)	3.01h(9.99)	66.55f(54.96)
7	Tr-7	5.05fg(12.98)	43.88e(41.48)	4.29f(11.95)	52.33d(46.33)	3.58f(10.89)	60.22ef(50.89)	3.09i10.12)	65.66fg(54.12)
8	Tr-8	3.93bc(11.43)	56.33bc(48.63)	4.58g(12.36)	49.11e(44.49)	2.13b(8.38)	76.33b(60.88)	2.67g(9.40)	70.33ef(56.99)
9	Tr-9	5.89h(14.03)	34.55gh(36.00)	2.89bc(9.78)	67.88b(55.47)	2.92d(9.83)	67.55cd(55.27)	1.33b(6.62)	85.22b(67.39)
10	Tr-10	5.67gh(13.75)	37.00g(37.46)	4.89h(12.75)	45.66ef(42.51)	3.90gh(11.37)	56.67fg(48.83)	3.23j(10.33)	64.11h(53.19)
11	Contro l	9.00							

Mean of three replications

Values in the column followed by common letters do not differ significantly at 5% level by Duncan's multiplerange test (DMRT)

Indian Journal of Natural Sciences *www.tnsroindia.org.in ©IJONS*

Vol.15 / Issue 83 / Apr / 2024 *International Bimonthly (Print) – Open Access* *ISSN: 0976 – 0997*

RESEARCH ARTICLE

A Comparative Clinical Trial of "Yogam Therapy" and "*Asuwathi Chooranam*" (Internal) in the Management of "*Athithoolam*" (Obesity)

M.Vanitha[1]*, P. Sugasini[2], P.Samundeswari[3] and N.J.Muthu Kumar[4]

[1]Associate Professor, Department of Udal Koorugal (Anatomy), Santhigiri Siddha Medical College, Kerala, India.
[2]Ph.D Scholar, Department Sirappu Maruthuvam, National Institute of Siddha, Chennai, Tamil Nadu, India
[3]Assistant Professor, Department of Varmam Maruthuvam, National Institute of Siddha, Chennai, Tamil Nadu, India.
[4]Professor, Department of Varmam Maruthuvam, National Institute of Siddha, Chennai, Tamil Nadu, India.

Received: 20 Oct 2023 Revised: 10 Dec 2023 Accepted: 11 Mar 2024

***Address for Correspondence**
M.Vanitha
Associate Professor,
Department of Udal Koorugal (Anatomy),
Santhigiri Siddha Medical College,
Kerala, India.
E mail: drvanithapooncholai@gmail.com

ABSTRACT

Obesity*(Athithoolam)* is one of the most common non-communicable diseases in the world, leading to various systemic illnesses. This study aims to compare clinical trials of *Yogam* therapy with and without intervention in the management of *Athithoolam*(Obesity). Objectives are to bring about a reduction of body weight, reduction of waist-to-hip line, Mid arm circumference(both sides) and improvement in their quality of life. 40 samples of obese patients, aged 20 to 50 years, who were willing to participate in the study, were included. Those suffering from any comorbidity and mental disorders were excluded. Their Body Mass Index, Waist-Hip ratios, and Mid arm circumference (both sides) were measured. The trial drug *Aswathi Chooranam* was given for 3 months and *Siddhar Yogam* practice (Standard Operating Procedure) was taught and advised to practice daily for 45 minutes. They were instructed to practice daily (morning and evening) Reassessment was done once in seven days. *Siddhar Yogam* Therapy for 3 months resulted in a significant reduction in all body weight measures such as a decrease in Body Mass Index (0.001), Waist hip ratio(0.001), Mid-arm-circumference(0.001),(P values < 0.001) with mild variations and differences less appreciable. So,it accepts the null hypothesis. Hence this study reveals patients treated with the trial drugs *SiddharYogam* therapy along with rejuvenating internal medicine may provide promising outcomes as a way to assist in maintaining body weight and in the management of obesity.

Keywords: Obesity, *SiddharYogam* therapy, Weight,BMI(Body mass index), Waist-hip ratio,Mid arm circumference, Quality of life.

INTRODUCTION

Siddha system of medicine is one of the traditional Indian system of medicine and is said to be ancient as the Tamil language itself. *Siddha* system of medicine has a distinctive approach to the management and treatment care of specific ailments and also to build up the immune system of the person being treated against all diseases. In the *Siddha* system of medicine, diseases are classified into 4448 types [1]. In the text,*T.V.Sambasivam pillai's Siddha* medical dictionary,the term *Athithoolam* means excessive accumulation of fat in the system-obesity [2]. Many diseases are emerging as a result of lifestyle modifications due to stress, sedentary lifestyle and food habits [3]. One among them is *Athithoolam* which may be correlated with Obesity. Obesity has reached epidemic proportions in India in the 21st century, with morbid obesity affecting 5% of the country's population [4]. Obesity is a major risk factor for cardiovascular disease and NGOs such as the Indian Heart Association have been raising awareness about this issue [5]. Urbanization and modernization have been associated with obesity [6]. *Athithoolam*is an abnormal accumulation of body fat, usually 20% or more over an individual's body weight. It is associated with an increased risk of illness and disability. The symptoms of *Athithoolam* are weight gain, increased abdominal girth, excessive hunger, feeling of tiredness and excessive [9].

BMI (Body mass index) is considered a measure of obesity, it was observed that for Asian Indians BMI cut-off points are to be considered much lesser than the WHO standards for categorizing obesity. Nowadays according to WHO, a BMI of 25kg/m^2 or above is considered obese. Furthermore, obesity is due to physical inactivity, improper diet and a sedentary lifestyle [10. 11] *Siddhar Yogam* is a mind and body practice with historical origins in ancient Indian philosophy. Like other meditative movements practices used for health purposes, various styles of *yoga typically* combine physical postures, breathing techniques and meditation or relaxation. *Siddhar Yogam* is a form of mind-body fitness that involves a combination of muscular activity and an internally directed mindful focus on awareness of the self, the breath, and energy.

Most of the research suggests that practicing *SiddharYogam* might improve quality of life, reduce stress, lowers heart rate and blood pressure, helps to relieve anxiety and depression and improve overall physical fitness, strength and flexibility. Nowadays, Obesity is very common in society due to a lack of physical activity and lifestyle changes. The number of *Athithoolam* patients attending the APH of the National Institute of Siddha Hospital is increasing day by day. So, the need of the hour is to search for an effective drug and *Yogam* therapy to treat obesity with less or no adverse effects. Hence an attempt had been made to validate the trial drug and *SiddharYogam* therapy –specific yoga postures for the management of *Athithoolam*. Therefore,I have chosen this polyherbal formulation "*ASUWATHI CHOORANAM*" [12]. All ingredients of the trial drug have anti-Obesity, anti-hyperlipidemic and antioxidant activity.

MATERIALS AND METHODS

Athithoolam patients satisfying the inclusion and exclusion criteria are admitted to the trial. Informed consent was obtained from the patients. Investigations have been carried out before and at the end of the trial. l00 samples underwent screening through screening proforma. Among 100 samples, 40 patients were selected for trial from OPD of Ayothidoss Pandithar Hospital, under prescribed proforma. Among 40 patients, 20 patients were treated with the trial drug *Asuvathichooranam* & *Siddharyogam* therapy- specific yoga postures and the remaining 20 patients were treated with *Siddharyogam* therapy - specific *yoga* postures only for 3 months.OPD Patients visit the hospital once in 7 days. At each visit clinical assessment was done and prognosis noted.

The Laboratory investigations were done on the 1st day and the 91st day of the trial. At the end of the treatment, the patients were advised to visit the OPD for further 3 months for follow-up. Patients were advised to practice asanas on empty stomach for 45-60 minutes every morning after evacuation of urine and motion. Patients were taught yogic

postures in 1st day of the trial and the trial drug has been advised to take daily for 90 days in morning and evening . Patients were motivated to practice asanas regularly for their well-being even after the study.

YOGAM THERAPY [14,15,16,21]

ASANAM
(i). LOOSENING ASANAM:
Surya vanakkam
(ii). STANDING POSTURE:
Arthachakkrasanam
Arthakattichakkarasanam
Trikonasanam 10 minutes
Padahastasanam
Relaxation: *Shanthisanam*
(iii). SITTING POSTURE:
Vakkrasanam
Arthamatyendrasanam
Relaxation :*Tandasanam*

(iv). LYING POSTURE:
Ysthikasanam
Jadaraparivarthini
Bavanamuktasanam
Pujangasanam
Vilasanam
Relaxation :*Shanthiasanam*

PRANAYAMAM
Thirumoolarvasipayirchi.

P*RATHIYAGARAM*
Thirumoolar way of Prathiyagaram.

DHARANAI
Thirumoolar way of Dharanai.

DYANAM
Thirumoolar way of Dhyanam.

RESULTS

Statistical Analysis
All collected data were entered into MS excel software using different columns variables and rows as patients. SPSS software was used to perform statistical analysis. Basic descriptive statistics include frequency distributions and cross –tabulations were performed. The quantity variables were expressed as Mean ±standard Deviation and qualitative data as percentage .A probability value of <0.05 was considered to indicate statistical significance. Paired "t" test was performed for determining the significance between before and after treatment.

Inference

Group -A (Trial Medicine with *Siddhar Yogam* Therapy):

The mean BMI before treatment is 32.8600, after treatment is reduced to 30.8200, Waist Hip –ratio before treatment is.9355, after treatment is reduced to.8805, and Mid arm circumference before treatment is 34.0000, after treatment it is reduced to 31.6000. On comparing statistically before and after treatment reveals BMI (Body mass index), WHR (Waist hip ratio), MAC (Mid arm circumference) with mild variations and differences less appreciable. So, it accept null hypothesis. Hence there is a very slight statistical significant.

Group –B (*Siddhar Yogam* Therapy Only)

The Mean BMI (Body mass index) before treatment is 32.0250, after treatment is reduced to30.7900, Waist -hip ratio before treatment is.9280, after treatment is reduced to.8875s, mid –arm circumference before treatment is 33.3500, after treatment is reduced to 31.9000. On comparing statistically before and after treatment reveals BMI (Body mass index), WHR (Waist –hip ratio), MAC (Mid-arm circumference) with mild variations and differences less appreciable. So, it accept null hypothesis. Hence there is a very slight statistical significant. Hence this study reveals patients treated with trial drug and *SiddharYogam* therapy- specific yoga postures and *Siddhar yogam* therapy alone showed mild effective in reducing bodyweight and other associated symptoms, Statistical analysis showed very slight significance.

DISCUSSION

The retrospective review of the diseases Athithoolam mentioned in *Siddha* parameters begins with the correlation of signs and symptoms of obesity. The drug which possess anti –hyperlipidemic property which is mentioned in *Siddha* Literature agasthiyar vaithiya kaviyam-1500 .40 patients of both genders were recruited for this study. The treatment was aimed to normalise the deranged humours and gradual reduction of body weight. Before treatment the patients were advised to take *Meganathakuligai*(130 mgs) – 2 with warm water in empty stomach at early morning for purgation. The patients were advised to take rest diet with intake of gruel and regular monitoring of blood pressure,pulse rate, heart rate had found to be normal. The patients were treated with trial drug *Asuwathi chooranam* twice a day in a dosage of 1.5 gm with honey, and *yogam* therapy-specific yoga postures for 90 days. Patients were instructed to take medicines and do yoga regularly, advised to follow the standard dietary regimen. Out patients were asked to visit the hospital once in 7 days. For out- patients trial drug along with *SiddharYogam* therapy-specific yogic postures, and *SiddharYogam* therapy-specific yoga postures alone were given for 90 days and the clinical assessment was done under the supervision of faculty on 1st day,8th day,15th day, 22nd day,29th day,36th day, 43rd day,50th day,57th day,64th day, 71st day, 78th day ,85th day and 91st day. Regarding gender distribution, the present study showed that a maximum of 82.5 % of patients were female and only 17.5% were male. According to various studies[18], Overweight was more prevalent in the females 20-29 years of age as compared to men, but the 30-49 years females had a higher prevalence of overweight.

Regarding age, 37% of affected patients come under the age group between 31-40 years, 33% of them are between 21-30 years, and the remaining 30% of the patients come under the age group of 41-50 years. According to various studies[19],Overweight was more prevalent in females 20-29 years of age as compared to men, but the 30-49 years male had a higher prevalence of overweight. Male and female >50 years had almost an equal prevalence of overweight. Dietary habits of the reported patients reveals that 90% of patients were nonvegetarians and remaining 10% of patients were vegetarians. According to various studies[20] an inverse association between a prudent/healthy dietary pattern and overweight/obesity risk and a positive association between a western/unhealthy dietary pattern and overweight/obesity. Occupation status has a great impact on obesity. Among 40 patients, 48.5% were housewife, 30% were tailor, store work and coolie, 15% were students, and 7.5% were security. Laboratory investigations of blood and urine were done for all 40 cases, there were no significant changes in blood and urine parameters before and after treatment. Clinically, no adverse effects were reported during the trial

CONCLUSION

This study reveals that patients treated with the trial drug and *SiddharYogam* therapy- (specific yoga postures) showed mild therapeutic effectiveness in reducing bodyweight and other associated symptoms. Statistical analysis done for BMI (Body mass index), WHR (Waist hip ratio), MAC (Mid arm circumference) and score shows that the trial drug with *SiddharYogam* therapy-specific yoga postures is effective and significant ($p<0.001$).
The mechanism underlying *Yogam's* effectiveness in the reduction of weight remains unclear. *SiddharYogam* therapy may prove its effectiveness through high energy expenditure, heightening mindfulness, improving mood, and reducing stress which may help to reduce food intake. Hence, I conclude large sample size in the future including *SiddharYogam* therapy along with rejuvenating internal medicine may provide promising outcomes as a way to assist in maintaining body weight and in the management of obesity

REFERENCES

1. Kaliyaperumal, Karunamoorthi & Jegajeevanram, Kaliyaperumal & X, Jerome & Vijayalakshmi, Jayaraman & Melita, Luke. (2012). Tamil Traditional Medicinal System – Siddha: An Indigenous Health Practice in the International Perspectives. International Journal of Genuine Traditional Medicine (TANG). 2. 1-11. 10.5667/tang.2012.0006.
2. *T.V.Sambasivam pillai, Siddha* medical dictionary, Research Institute of Siddhar's Science, 1931, Volume - 1, Page no.135
3. Farhud DD. Impact of Lifestyle on Health. Iran J Public Health. 2015 Nov;44(11):1442-4. PMID: 26744700; PMCID: PMC4703222.
4. Ahirwar R, Mondal PR. Prevalence of obesity in India: A systematic review. Diabetes MetabSyndr. 2019 Jan-Feb;13(1):318-321. doi: 10.1016/j.dsx.2018.08.032. Epub 2018 Sep 21. PMID: 30641719.
5. Akil L, Ahmad HA. Relationships between obesity and cardiovascular diseases in four southern states and Colorado. J Health Care Poor Underserved. 2011;22(4 Suppl):61-72. doi: 10.1353/hpu.2011.0166.
6. Congdon P. Obesity and Urban Environments. Int J Environ Res Public Health. 2019 Feb 5;16(3):464. doi: 10.3390/ijerph16030464. PMID: 30764541; PMCID: PMC6388392.
7. Yadav, K. and Krishnan, A. (2008), Changing patterns of diet, physical activity and obesity among urban, rural and slum populations in north India. Obesity Reviews, 9: 400-408.
8. Anekwe CV, Jarrell AR, Townsend MJ, Gaudier GI, Hiserodt JM, Stanford FC. Socioeconomics of Obesity. CurrObes Rep. 2020 Sep;9(3):272-279.
9. Vij VA, Joshi AS. Effect of excessive water intake on body weight, body mass index, body fat, and appetite of overweight female participants. J Nat Sci Biol Med. 2014 Jul;5(2):340-4.
10. Misra A. Ethnic-Specific Criteria for Classification of Body Mass Index: A Perspective for Asian Indians and American Diabetes Association Position Statement. Diabetes Technol Ther. 2015 Sep;17(9):667-71.
11. Hall KD, Kahan S. Maintenance of Lost Weight and Long-Term Management of Obesity. Med Clin North Am. 2018 Jan;102(1):183-197.
12. MunaivarV.R.Madhavan, *Agathiyarvaithiya kaviyam-1500,* First edition, Year of Publication : 1994, Page no. 713-715
13. R.Alagapan, Manual of Practical Medicine, Page no. Sixth Edition-2018.
14. Asana andiappan,*Thirumoolar'sAstanga yoga*– paperback –tarot, January 1, 2004.
15. Dr.R.Thiyagarajan,L.I.M Siddha MaruthuvamSirappu, Publisher-Commissionerate of Indian Medicine &Homoeopathy,Arumbakkam,Chennai-600 106,First edition-1985.
16. G.Manikavasakan,*Thirumoolarthirumanthiram - MoolamumVilakaUraiyum,* Tenth edition, Year of Publication : 2016, Page no : 408 - 413
17. Aanaivaarianantha n,*Sarakkusuthiseimuraigal,* Department of Indian medicine and homeopathy, Chennai, 1st edithion, 2008.

18. Vahratian A. Prevalence of overweight and obesity among women of childbearing age: results from the 2002 National Survey of Family Growth. Matern Child Health J. 2009 Mar;13(2):268-73.
19. Luhar S, Timæus IM, Jones R, Cunningham S, Patel SA, Kinra S, Clarke L, Houben R. Forecasting the prevalence of overweight and obesity in India to 2040. PLoS One. 2020 Feb 24;15(2):e0229438.
20. Mu M, Xu LF, Hu D, Wu J, Bai MJ. Dietary Patterns and Overweight/Obesity: A Review Article. Iran J Public Health. 2017 Jul;46(7):869-876.
21. Yogacharyasundaram.*Anantharagasyam*– 30thedition,January 2014, Page no : 35-50.

Table-2. Comparison Of BMI, WHR & Mac Before And After Treatment Of Group A(Trial Medicine With *Siddhar Yogam* therapy) By Using Paired Samples Statistics:

Sl. No	Treatment Status	Mean ± Std. Deviation	Significance
1.	BMI -BT	32.8600±1.24326	t=23.482,p<0.001
	BMI-AT	30.8200±1.25009	
2.	WHR -BT	0.9355±.03561	t = 15.013, p<0.001
	WHR -AT	0.8805±.03649	
3.	MAC-BT	34.0000±2.31699	t = 21.354, p<0.001
	MAC-AT	31.6000±2.50053	

Table-3. Comparison Of BMI, WHR & Mac Before And After Treatment Of Group B (*Siddhar Yogam* Therapy Only) By Using Paired Samples Statistics:

Sl. No	Treatment Status	Mean ± Std. Deviation	Significance
1.	BMI -BT	32.0250±1.41379	t=15.270, p<0.001
	BMI-AT	30.7900±1.49628	
2.	WHR -BT	0.9280±.03968	t=11.776, p<0.001
	WHR -AT	0.8875±.03851	
3.	MAC-BT	33.3500±1.38697	t=8.542, p<0.001
	MAC-AT	31.9000±1.48324	

Indian Journal of Natural Sciences *www.tnsroindia.org.in ©IJONS*

Vol.15 / Issue 83 / Apr / 2024 *International Bimonthly (Print) – Open Access* *ISSN: 0976 – 0997*

RESEARCH ARTICLE

Simultaneous Spectrophotometric Analysis of Multicomponent Pharmaceutical Mixtures: Validation and Method Comparison

Karthick.S[1], K.Vinod Kumar[2], V.Charani[3], H.Tanveer[3], R.Aparna[3], P.Vamshi[3], K.Divya[3] and Shaik Nuzhath[4*]

[1]Student, Department of Pharmaceutical Analysis, *Jawaharlal Nehru Technological University, Anantapur,* Andhra Pradesh, India.
[2]Professor, Department of Pharmaceutical Analysis, Raghavendra Institute of Pharmaceutical Education and Research, (Affiliated to *Jawaharlal Nehru Technological University), Anantapur,* Andhra Pradesh, India.
[3]Student, Department of Pharmaceutical Analysis, Raghavendra Institute of Pharmaceutical Education and Research, (Affiliated to *Jawaharlal Nehru Technological University), Anantapur,* Andhra Pradesh, India.
[4]Assistant Professor, Department of Pharmaceutical Analysis, Raghavendra Institute of Pharmaceutical Education and Research, (Affiliated to *Jawaharlal Nehru Technological University), Anantapur,* Andhra Pradesh, India.

Received: 30 Dec 2023 Revised: 09 Jan 2024 Accepted: 27 Mar 2024

***Address for Correspondence**
Shaik Nuzhath
Assistant Professor,
Department of Pharmaceutical Analysis,
Raghavendra Institute of Pharmaceutical Education and Research,
(Affiliated to *Jawaharlal Nehru Technological University),*
Anantapur, Andhra Pradesh, India.
Email: nuzhathpharma@gmail.com

ABSTRACT

This comprehensive review explores simultaneous spectrophotometric analysis in the context of multicomponent pharmaceutical mixtures, focusing on validation and method comparison. Its purpose is to assess the reliability of these methods in pharmaceutical analysis and compare their performance to other techniques. The review examines principles, techniques, and instrumentation used in pharmaceutical mixture analysis. It emphasizes validation parameters essential for accuracy and precision, following guidelines like those from the International Council for Harmonisation (ICH). The review also evaluates studies comparing simultaneous spectrophotometric methods with alternative approaches, highlighting their strengths and limitations. It include an understanding of the method's principles, its advantages, and challenges. It underscores the importance of validation parameters (accuracy, precision, linearity, specificity, robustness) for method reliability. Comparative studies reveal scenarios where simultaneous spectrophotometric analysis excels and where complementary techniques like chromatography or titration may enhance results. This review illuminates the role of simultaneous

spectrophotometric analysis in pharmaceuticals, offering accurate solutions for complex mixtures. It emphasizes the significance of validation and method comparison in ensuring analytical reliability. This comprehensive review article explores the critical realm of simultaneous spectrophotometric analysis in the context of multicomponent pharmaceutical mixtures, with a primary focus on validation and method comparison. The review's purpose is to assess the reliability and effectiveness of simultaneous spectrophotometric methods in pharmaceutical analysis and to evaluate their performance relative to other analytical techniques.

Keywords: Simultaneous spectrophotometric analysis, Pharmaceutical mixtures, Validation, Method comparison, Analytical reliability and Multicomponent analysis

INTRODUCTION

Pharmaceutical research and development constitute a complex and multifaceted endeavor with the ultimate goal of delivering safe, effective, and high-quality therapeutic agents to patients(1). At the heart of this process lies the need for precise and reliable analytical techniques that can unravel the intricate compositions of pharmaceutical formulations(2). One such technique that has gained prominence in recent years is simultaneous spectrophotometric analysis(3). This analytical approach plays a pivotal role in pharmaceutical research, offering insights into the composition, stability, and quality of multicomponent pharmaceutical mixtures(4).

Complexity in Pharmaceutical Formulations

Pharmaceutical formulations have evolved significantly over time, mirroring advances in drug discovery, patient needs, and therapeutic goals(5). Traditionally, pharmaceuticals often consisted of single-component drug products(6). However, the modern pharmaceutical landscape is characterized by the prevalence of multicomponent formulations, which encompass a diverse array of products, including combination therapies, fixed-dose combinations, extended-release formulations, and complex drug delivery systems(7).

The complexities inherent in these modern pharmaceutical formulations arise from several factors

Combination Therapies: In the quest for improved therapeutic outcomes, combination therapies have gained popularity(8). These therapies involve the concurrent administration of multiple drugs, often targeting different aspects of a medical condition(9). Analyzing these formulations demands the quantification of multiple active pharmaceutical ingredients (APIs) simultaneously(10).Polypills and Fixed-Dose Combinations: Polypills and fixed-dose combinations are designed to simplify drug regimens, enhance patient compliance, and optimize therapeutic effects(11). They contain multiple APIs in a single dosage form, necessitating comprehensive analytical techniques(12).Excipients and Additives: Pharmaceutical formulations frequently incorporate a range of excipients, including binders, fillers, disintegrants, and stabilizers, which are essential for product formulation and performance(13). However, these excipients can complicate the analysis by potentially interfering with the quantification of APIs.Stability and Degradation: Understanding the stability of pharmaceuticals is of paramount importance(14). Factors such as temperature, humidity, and light exposure can impact the stability of drugs and excipients within a formulation(15). Therefore, analyzing the degradation kinetics of multiple components is essential to ascertain product quality and shelf-life(16).

The Significance of Pharmaceutical Analysis

In the realm of pharmaceutical research and development, analytical chemistry plays a central role(17). Pharmaceutical analysis is the linchpin that connects drug discovery, formulation development, manufacturing, and quality control(18). The importance of analytical techniques in pharmaceutical research is multifaceted:

Drug Discovery

During the early stages of drug discovery, analytical methods are employed to identify potential drug candidates, assess their purity, and elucidate their chemical properties(19). Reliable analytical techniques are essential for selecting promising compounds with the desired pharmacological properties(20).

Formulation Development

Formulation scientists rely on analytical methods to design drug formulations that exhibit specific release profiles, stability characteristics, and bioavailability(21). Analytical data guides the selection of excipients and helps optimize the final product(22).

Quality Control

In pharmaceutical manufacturing, rigorous quality control measures are imperative to ensure that products meet predefined specifications and comply with regulatory standards(23). Analytical methods are deployed to assess batch-to-batch consistency and product uniformity(24).

Stability Studies

Pharmaceuticals are subject to various environmental factors that can affect their stability over time(25). Analytical techniques are used to monitor the stability of drugs and drug products during storage, aiding in the determination of shelf-life(26).

Regulatory Compliance

Regulatory agencies, such as the U.S. Food and Drug Administration (FDA) in the United States and the European Medicines Agency (EMA) in Europe, require extensive analytical data as part of the drug approval process(27). Regulatory submissions must include comprehensive analytical data to demonstrate the safety, efficacy, and quality of pharmaceutical products(28).

Patient Safety

The precision of analytical methods is crucial in ensuring patient safety. Impurities, contaminants, and incorrect dosages in pharmaceutical products can lead to adverse events(29). Precise analytical methods are necessary to detect and quantify such issues(30). Given the pivotal role of pharmaceutical analysis, it is imperative to develop and validate analytical methods capable of deciphering the intricate compositions of multicomponent pharmaceutical mixtures(31).

Spectrophotometry in Pharmaceutical Analysis

Spectrophotometry, a fundamental analytical technique, has been integral to pharmaceutical analysis for decades(32). It relies on the interaction of light with matter to provide insights into the chemical composition and concentration of substances(33). Spectrophotometric techniques encompass various methodologies, including ultraviolet-visible (UV-Vis) spectroscopy, infrared (IR) spectroscopy, and nuclear magnetic resonance (NMR) spectroscopy, each offering unique perspectives on pharmaceutical analysis(34).Spectrophotometry offers several attributes that render it indispensable in pharmaceutical research

Versatility

Spectrophotometric techniques cover a broad spectrum of applications, allowing researchers to choose the most suitable method for their specific analytical needs(35).

Non-destructive Nature: Many spectrophotometric analyses are non-destructive, allowing samples to be reanalysed or used for further testing(36). This characteristic is particularly valuable when working with limited quantities of valuable(37)

Literature search

Conducting a comprehensive literature search on simultaneous spectrophotometric analysis, validation, and method comparison in pharmaceutical mixtures involves exploring a range of academic databases, journals, and reputable sources(45). Below is a summary of the key findings from recent research articles, reviews, and relevant guidelines in this domain(46). The methodology for the literature search and article selection process in the review on "Simultaneous Spectrophotometric Analysis of Multicomponent Pharmaceutical Mixtures: Validation and Method Comparison" involved a systematic approach to identify relevant research articles, reviews, and guidelines. Here's a detailed description of the methodology used

METHODOLOGY

Simultaneous spectrophotometric analysis Multicomponent pharmaceutical mixtures Validation Method comparison Pharmaceutical analysis Spectrophotometry Pharmaceutical formulations Quality control Analytical methods
These terms were combined using Boolean operators (AND, OR) to construct comprehensive search queries(47).
Databases Several academic databases and search engines were utilized to access a wide range of academic and scientific publications. The primary databases included

PubMed

This database was used for accessing biomedical and pharmaceutical research articles, reviews, and guidelines.

Web of Science

Web of Science offers a broad spectrum of research literature, including multidisciplinary and pharmaceutical journals.

Scopus

Scopus provides access to a vast collection of scientific articles and conference papers, making it an essential resource for comprehensive literature searches.

Google Scholar

Google Scholar was used to identify additional sources, including gray literature and conference proceedings.

ScienceDirect

ScienceDirect contains a wealth of peer-reviewed research articles and journals relevant to pharmaceutical analysis.

Inclusion Criteria

To select relevant articles for the review, the following inclusion criteria were applied(48):
Articles published in reputable peer-reviewed journals. Articles written in English. Articles published from 2010 to 2023, ensuring that the review includes recent research and developments. Articles focusing on simultaneous spectrophotometric analysis in the context of multicomponent pharmaceutical mixtures. Articles discussing the validation aspects of simultaneous spectrophotometric methods. Articles that explore the comparison of simultaneous spectrophotometry with alternative analytical techniques in pharmaceutical mixtures(49). Guidelines from regulatory bodies such as the ICH and national pharmacopeias relevant to validation and pharmaceutical analysis.

Exclusion Criteria

Articles that did not meet the inclusion criteria were excluded from the review. Exclusion criteria included:
Articles published in languages other than English. Articles outside the specified publication date range.

Articles unrelated to simultaneous spectrophotometric analysis, validation, or method comparison in pharmaceutical mixtures(50). Articles that lacked relevance to pharmaceutical analysis. that were not available in full text or were inaccessible.

Article Selection Process

The article selection process involved several steps:

Initial Search

A preliminary search was conducted using the identified search terms and databases. This generated a large pool of potential articles and resources.

Screening of Titles and Abstracts

Titles and abstracts of the retrieved articles were screened to assess their relevance to the review's objectives and inclusion criteria.

Full-Text Assessment

Full texts of articles that passed the initial screening were assessed thoroughly to determine their suitability for inclusion in the review.

Critical Evaluation

The selected articles underwent critical evaluation to ensure their quality and relevance to the review's focus on simultaneous spectrophotometric analysis, validation, and method comparison in pharmaceutical mixtures.

Data Extraction

Relevant information, key findings, and important references were extracted from the selected articles and used to construct the review.

Incorporation of Guidelines

Relevant guidelines and regulatory documents were included to provide a comprehensive overview of validation standards in pharmaceutical analysis(51). The article selection process aimed to ensure that only high-quality, recent, and pertinent literature was included in the review. The systematic approach helped identify and select articles that contributed meaningfully to the understanding of simultaneous spectrophotometric analysis in the context of pharmaceutical mixtures, its validation, and its comparison with alternative analytical techniques.

Simultaneous Spectrophotometric Analysis in Pharmaceutical Mixtures

Simultaneous spectrophotometric analysis is a powerful analytical technique employed in pharmaceutical research to determine the concentration of multiple components in a mixture simultaneously. This method relies on the principles of spectrophotometry, which involve measuring the absorbance or transmittance of light by a sample at various wavelengths. In the context of pharmaceutical mixtures, simultaneous spectrophotometry offers several advantages but also presents certain challenges that researchers must address.

Principles of Simultaneous Spectrophotometric Analysis

Beer-Lambert Law: The fundamental principle underlying spectrophotometry is the Beer-Lambert Law, which establishes a linear relationship between the concentration of an analyte and the absorbance of light at a specific wavelength. This law is expressed as $A = \varepsilon cl$, where A is the absorbance, ε is the molar absorptivity (extinction coefficient), c is the analyte concentration, and l is the path length of the sample.Multi-Wavelength Analysis: Simultaneous spectrophotometry extends the Beer-Lambert Law to multiple wavelengths, allowing the quantification of multiple analytes in a single sample. By measuring absorbance at various wavelengths, the concentrations of different components can be determined simultaneousl(40)y.

Techniques and Instrumentation

UV-Visible Spectrophotometry: UV-Visible spectrophotometry is the most common technique used in simultaneous analysis. It covers the ultraviolet and visible regions of the electromagnetic spectrum. UV-Visible spectrophotometers are equipped with a light source, a monochromator to select specific wavelengths, a sample compartment, and a detector(52). The absorbance of light by the sample is measured at selected wavelengths.Diode Array Spectrophotometry (DAD): DAD spectrophotometers are equipped with an array of photodiodes, allowing them to

simultaneously scan a wide range of wavelengths. This technology enables rapid multi-wavelength analysis and is particularly suitable for complex mixtures.

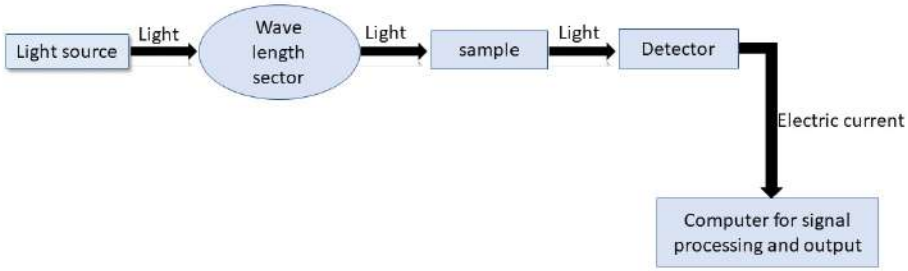

Advantages of Simultaneous Spectrophotometric Analysis

Time Efficiency: Simultaneous spectrophotometry significantly reduces analysis time by measuring multiple components in a single run. This is particularly advantageous in high-throughput environments, such as pharmaceutical quality control laboratories.Sample Conservation: Analyzing a single sample for multiple components minimizes sample consumption and reduces the need for sample preparation, preserving valuable or limited quantities of substances.Cost-Effective: Simultaneous analysis offers cost savings in terms of reduced reagent and solvent usage, decreased analysis time, and lower operational costs compared to sequential analysis methods.Real-Time Monitoring: Simultaneous spectrophotometry provides real-time data on the composition of mixtures, facilitating immediate decision-making in pharmaceutical manufacturing or research processes.Reduced Operator Error: By reducing the number of handling steps and simplifying the analysis process, simultaneous spectrophotometry minimizes the potential for operator errors and contamination(52).

Challenges of Simultaneous Spectrophotometric Analysis

Overlapping Spectra: In complex mixtures, the spectra of different components may overlap, making it challenging to deconvolute and quantify individual analytes accurately. Advanced data analysis techniques, such as chemometric methods, are often necessary to address this issue.

Interference

Excipients and other components in pharmaceutical formulations can interfere with the analysis, leading to inaccurate results(53). Methods to mitigate interference, such as sample pretreatment or selective derivatization, may be required.

Sensitivity

Simultaneous spectrophotometry may have limitations in terms of sensitivity, especially when low concentrations of analytes need to be quantified. In such cases, more sensitive techniques like high-performance liquid chromatography (HPLC) may be preferred.

Instrumentation

The choice of spectrophotometric instrumentation can impact the method's sensitivity and accuracy. Advances in instrument design and technology are continually improving the performance of simultaneous spectrophotometric methods.

Validation

Ensuring the reliability of simultaneous spectrophotometric methods through rigorous validation is essential(54). Validation parameters, such as accuracy, precision, linearity, specificity, and robustness, must be systematically evaluated. Simultaneous spectrophotometric analysis is a valuable tool in pharmaceutical research for quantifying multiple components in complex mixtures. Its time efficiency, sample conservation, and cost-effectiveness make it an attractive option for pharmaceutical laboratories. However, researchers must be aware of the challenges associated

with overlapping spectra, interference, and sensitivity and implement robust validation protocols to ensure the accuracy and reliability of simultaneous spectrophotometric methods. When applied judiciously, this technique contributes to the advancement of pharmaceutical analysis, formulation development, and quality control.

Validation Parameters for Simultaneous Spectrophotometric Methods

Validation is a critical process in pharmaceutical analysis to ensure the reliability and accuracy of analytical methods, including simultaneous spectrophotometric methods(55). Several key validation parameters are essential for assessing the performance of these methods

Accuracy

Accuracy measures how close the measured values are to the true or reference values. In simultaneous spectrophotometric analysis, accuracy is determined by comparing the calculated concentrations of analytes with known reference values or by analyzing spiked samples.

Precision

Precision evaluates the repeatability and reproducibility of measurements. It includes two components: repeatability (intra-day precision) and intermediate precision (inter-day precision). Precision is typically assessed by analyzing multiple replicate samples.

Linearity

Linearity assesses the method's ability to provide results that are directly proportional to the analyte's concentration over a specified range. A linear calibration curve should be established by analyzing standard solutions of known concentrations.

Specificity

Specificity measures the method's ability to accurately measure the analyte of interest in the presence of potential interferences, such as excipients or other components in the pharmaceutical formulation. It ensures that the method is selective for the target analyte.

Robustness

Robustness evaluates the method's capacity to remain unaffected by small variations in experimental conditions, such as changes in pH, temperature, or mobile phase composition. Robustness studies help identify the method's tolerance to minor variations.

Common Validation Guidelines for Pharmaceutical Analysis

Several regulatory authorities and organizations provide guidelines for the validation of analytical methods in the pharmaceutical industry(56). These guidelines offer a structured framework to ensure that analytical methods meet rigorous standards for reliability and accuracy. Some of the most widely recognized validation guidelines include

ICH (International Council for Harmonisation) Guidelines

ICH Q2(R1): Validation of Analytical Procedures: This guideline outlines the principles and methodology for the validation of analytical methods. It covers parameters such as accuracy, precision, linearity, specificity, and robustness. ICH Q2(R1) is a globally accepted standard for method validation in pharmaceutical analysis.

USP (United States Pharmacopeia)

USP General Chapter <1225>: Validation of Compendial Procedures: This chapter provides guidance on the validation of analytical procedures, including spectrophotometric methods. It aligns with ICH principles and is essential for ensuring the quality and reliability of pharmaceutical analyses.

EP (European Pharmacopoeia)

EP Chapter 2.2.46: Validation of Analytical Procedures: This chapter in the European Pharmacopoeia offers guidelines for method validation, emphasizing parameters such as specificity, accuracy, and precision. It is widely referenced in Europe.

FDA (U.S. Food and Drug Administration)

The FDA provides guidance documents on various aspects of pharmaceutical analysis, including method validation(57). These documents offer insights into regulatory expectations for method validation in the context of drug development and approval.

Pharmacopoeias

National pharmacopoeias, such as the British Pharmacopoeia (BP) and Japanese Pharmacopoeia (JP), often include specific chapters or monographs related to analytical method validation. These pharmacopoeias are essential references for pharmaceutical analysis in their respective regions. Pharmaceutical companies are required to adhere to these guidelines when developing and validating analytical methods for drug products. The validation parameters outlined in these guidelines, including accuracy, precision, linearity, specificity, and robustness, serve as the foundation for ensuring the quality and reliability of simultaneous spectrophotometric methods and other analytical techniques used in pharmaceutical analysis. Compliance with these guidelines is crucial for regulatory approval and ensuring patient safety.

Comparison of Simultaneous Spectrophotometric Methods with Alternative Analytical Techniques

Several studies have compared simultaneous spectrophotometric methods with alternative analytical techniques, such as High-Performance Liquid Chromatography (HPLC), titration, and chromatography, in pharmaceutical analysis. These comparative studies offer insights into the strengths and limitations of simultaneous spectrophotometric analysis relative to alternative methods.

Strengths of Simultaneous Spectrophotometric Analysis

Cost-Effectiveness: Simultaneous spectrophotometric analysis is often more cost-effective than techniques like HPLC. It requires less expensive equipment, minimal sample preparation, and reduced consumption of solvents and reagents, making it an attractive option for routine pharmaceutical analysis.

High Throughput

Simultaneous spectrophotometric methods excel in high-throughput scenarios. They can analyze multiple components in a single run, significantly reducing analysis time compared to sequential techniques like HPLC.

Non-Destructive

Simultaneous spectrophotometric analysis is generally non-destructive, allowing samples to be reanalyzed or used for further testing(58). In contrast, HPLC consumes the entire sample during analysis.

Real-Time Monitoring

Simultaneous spectrophotometric methods provide real-time data on multiple components in a mixture, enabling immediate decision-making in pharmaceutical manufacturing or quality control.

Ease of Use: These methods are relatively easy to implement, making them accessible to a broader range of analysts. The instrumentation is user-friendly, and the analysis process is straightforward.

Limitations of Simultaneous Spectrophotometric Analysis

Overlapping Spectra: In complex mixtures, the spectra of different components may overlap, making it challenging to deconvolute and quantify individual analytes accurately. This limitation requires advanced data analysis techniques, such as chemometric methods, to address.

Interference

Excipients and other components in pharmaceutical formulations can interfere with simultaneous spectrophotometric analysis, leading to inaccurate results. Methods to mitigate interference, such as sample pretreatment or selective derivatization, may be necessary.

Sensitivity

Simultaneous spectrophotometric methods may have limitations in terms of sensitivity, especially when low concentrations of analytes need to be quantified. HPLC or other specialized techniques may be preferred for trace-level analysis.

Specificity

While simultaneous spectrophotometric methods offer specificity for the analytes of interest, they may lack the selectivity of HPLC(59). Chromatographic techniques can provide higher selectivity by separating analytes based on their chemical properties.

Sample Complexity

The suitability of simultaneous spectrophotometric analysis depends on the complexity of the sample matrix. For highly complex matrices, HPLC may offer better separation and accuracy.

Comparative Studies

Comparing Simultaneous Spectrophotometry and HPLC: A study comparing simultaneous spectrophotometry with HPLC for the analysis of a multicomponent pharmaceutical formulation found that both methods provided comparable results in terms of accuracy and precision. Simultaneous spectrophotometry offered advantages in terms of cost and speed, making it suitable for routine quality control, but HPLC was preferred for trace impurity analysis.

Titration vs. Simultaneous Spectrophotometry

In a comparative study, titration and simultaneous spectrophotometric methods were evaluated for the determination of an active ingredient in a tablet formulation. Simultaneous spectrophotometry exhibited faster analysis times and lower consumable costs compared to titration, making it a practical choice for routine analysis(60).

Chromatography vs. Simultaneous Spectrophotometry

A study comparing chromatography and simultaneous spectrophotometry for the analysis of complex herbal formulations found that while chromatography offered superior selectivity and sensitivity, simultaneous spectrophotometry was a valuable preliminary screening tool, allowing for rapid identification of major components. simultaneous spectrophotometric analysis offers several strengths, including cost-effectiveness, high throughput, and ease of use, making it a valuable tool in pharmaceutical analysis. However, its limitations, such as spectral overlap and interference, must be considered in the context of the sample matrix and analyte concentrations. Comparative studies indicate that while simultaneous spectrophotometric methods may not always replace techniques like HPLC or chromatography, they complement these methods, offering practical solutions for routine pharmaceutical analysis and rapid screening. Researchers must carefully evaluate the suitability of simultaneous spectrophotometry based on the specific analytical requirements and sample complexity.

Case and applications

Case Studies in Simultaneous Spectrophotometric Analysis in Pharmaceutical Analysis:Simultaneous spectrophotometric analysis has been applied in various practical scenarios in pharmaceutical analysis, offering solutions to complex problems and providing valuable insights. Below are two case studies highlighting the outcomes and lessons learned from these applications:

Case Study 1

Determination of Multicomponent Antibiotics in Pharmaceutical Formulations

Problem: A pharmaceutical manufacturer needed a rapid and cost-effective method to simultaneously quantify three different antibiotics (A, B, and C) in a complex tablet formulation. Traditional analysis methods were time-consuming and required extensive sample preparation.

Solution

Simultaneous spectrophotometric analysis was chosen as a potential solution. A UV-Visible spectrophotometer was used to measure the absorbance of the tablet dissolution solution at three distinct wavelengths corresponding to the maximum absorbance of each antibiotic.

Outcome

Accuracy and Precision

The simultaneous spectrophotometric method demonstrated high accuracy and precision compared to reference HPLC analysis(61). The results were consistent with the labeled amounts of antibiotics in the tablets.

Time and Cost Savings

The simultaneous method significantly reduced the analysis time, as multiple analytes were quantified in a single run. Additionally, it required fewer reagents and solvents, leading to cost savings.

Robustness

The method was found to be robust against minor variations in experimental conditions, such as changes in pH or temperature.

Lessons Learned

This case study illustrates that simultaneous spectrophotometric analysis can be a practical choice for the rapid quantification of multiple components in pharmaceutical formulations. It offers advantages in terms of accuracy, cost-effectiveness, and reduced analysis time. However, careful method development and validation are essential to ensure reliable results.

Case Study 2

Monitoring Dissolution Profiles of Immediate-Release Tablets

Problem: A pharmaceutical company needed a method to monitor the dissolution profiles of immediate-release tablets containing several active pharmaceutical ingredients (APIs). Traditional HPLC analysis was time-consuming and resource-intensive.

Solution

Simultaneous spectrophotometric analysis was considered for its ability to provide real-time data on dissolution profiles(62). A UV-Visible spectrophotometer equipped with a dissolution cell was employed to simultaneously measure the absorbance of multiple APIs at different time points during dissolution.

Outcome

Real-Time Monitoring

Simultaneous spectrophotometric analysis enabled real-time monitoring of the dissolution profiles of multiple APIs in the tablet formulation. This provided insights into the release kinetics of each API.

Quality Control

The method was integrated into the pharmaceutical manufacturing process for routine quality control, ensuring that dissolution profiles met the predefined specifications.

Efficiency

The simultaneous analysis reduced the analysis time and resource requirements, making it a cost-effective choice for monitoring dissolution profiles.

Lessons Learned

This case study demonstrates the practical utility of simultaneous spectrophotometric analysis for monitoring dissolution profiles in pharmaceutical manufacturing. It offers real-time insights into the release kinetics of multiple APIs, aiding in quality control and process optimization. Implementation of such methods in manufacturing processes can improve efficiency and reduce costs. In both case studies, simultaneous spectrophotometric analysis proved to be a valuable tool in pharmaceutical analysis, addressing specific analytical challenges and offering practical solutions. These applications highlight the importance of method development and validation to ensure

accurate and reliable results. Simultaneous spectrophotometry is particularly advantageous in scenarios where time efficiency, cost-effectiveness, and real-time monitoring are crucial. However, it is essential to recognize its limitations, such as spectral overlap and interference, and carefully consider its suitability for specific analytical requirements and sample matrices. Overall, these case studies underscore the versatility and effectiveness of simultaneous spectrophotometric analysis in pharmaceutical research and quality control.

Challenges and Future Directions

While simultaneous spectrophotometric analysis offers numerous advantages in pharmaceutical research and quality control, it is not without its challenges and limitations(63). Recognizing and addressing these limitations is essential for maximizing the effectiveness of this analytical technique:

Spectral Overlap

One of the primary challenges of simultaneous spectrophotometric analysis is dealing with overlapping spectra in complex mixtures. When multiple components absorb light at similar wavelengths, it becomes challenging to deconvolute the spectra and accurately quantify individual analytes. Advanced data analysis techniques, such as chemometrics and multivariate calibration, are often necessary to address this issue.

Interference from Excipients

Pharmaceutical formulations typically contain excipients and additives, which can interfere with the analysis by contributing to the absorbance at certain wavelengths. This interference can lead to inaccurate results if not properly accounted for. Sample pretreatment or selective derivatization may be required to mitigate interference

Sensitivity

The sensitivity of simultaneous spectrophotometric methods may be limited, especially when low concentrations of analytes need to be quantified. In cases where trace-level analysis is required, more sensitive techniques like High-Performance Liquid Chromatography (HPLC) or Mass Spectrometry (MS) may be preferred.

Specificity

While simultaneous spectrophotometric methods offer specificity for the analytes of interest, they may lack the selectivity of chromatographic techniques like HPLC. Chromatography can provide higher selectivity by separating analytes based on their chemical properties.

Sample Complexity

The suitability of simultaneous spectrophotometric analysis depends on the complexity of the sample matrix. For highly complex matrices with numerous components, such as natural products or herbal extracts, chromatographic techniques may be more appropriate.

Future Developments and Advancements

To address the challenges and limitations associated with simultaneous spectrophotometric analysis in pharmaceutical mixtures, several potential future developments can be anticipated:

Advancements in Instrumentation

Ongoing advancements in spectrophotometric instrumentation are expected to enhance the capabilities of simultaneous analysis. This includes improvements in the resolution of diode array detectors (DADs) and the development of new spectrophotometric techniques with higher sensitivity(64).

Multimodal Spectrophotometry

Future developments may incorporate other spectroscopic techniques, such as fluorescence or Raman spectroscopy, into simultaneous analysis. Combining multiple spectroscopic modalities can provide complementary information and improve the specificity and sensitivity of the analysis.

Machine Learning and AI

Machine learning and artificial intelligence (AI) algorithms are increasingly being used in data analysis for simultaneous spectrophotometric methods. These techniques can help deconvolute complex spectra and improve the accuracy of quantification, even in the presence of spectral overlap.

Miniaturization and Portable Devices

The development of miniaturized and portable spectrophotometric devices may enable on-site and real-time analysis of pharmaceutical samples. This can be particularly valuable for field applications and point-of-care testing.

Chemometric Models

Chemometric models for data analysis will continue to evolve, allowing for more accurate quantification of analytes in complex mixtures. Advanced chemometric techniques will be tailored to the specific challenges of simultaneous spectrophotometric analysis.

Customized Analytical Software

Customized software packages for simultaneous spectrophotometric analysis will become more user-friendly and powerful(65). These software tools will streamline method development, data processing, and validation. while simultaneous spectrophotometric analysis has its challenges and limitations, ongoing developments in instrumentation, data analysis techniques, and software tools are expected to address many of these issues. As the pharmaceutical industry continues to demand rapid, cost-effective, and reliable analytical methods, simultaneous spectrophotometry will play an increasingly important role, especially in scenarios where time efficiency and cost-effectiveness are critical. Researchers and analysts should stay informed about these advancements to harness the full potential of simultaneous spectrophotometric analysis in pharmaceutical research and quality control.

CONCLUSION

The review on "Simultaneous Spectrophotometric Analysis of Multicomponent Pharmaceutical Mixtures: Validation and Method Comparison" highlights the significance of simultaneous spectrophotometric analysis as a valuable analytical tool in pharmaceutical research and quality control. This technique offers several advantages, including cost-effectiveness, high throughput, and real-time monitoring, making it well-suited for various pharmaceutical applications.However, the review also emphasizes the importance of addressing challenges and limitations associated with simultaneous spectrophotometric analysis, such as spectral overlap and interference from excipients. Advanced data analysis techniques and ongoing advancements in instrumentation are crucial for mitigating these challenges.Validation and method comparison emerge as critical pillars in ensuring the accuracy and reliability of simultaneous spectrophotometric analysis. Rigorous validation parameters, including accuracy, precision, linearity, specificity, and robustness, are essential to demonstrate the method's suitability for its intended purpose. Furthermore, comparative studies with alternative analytical techniques, such as HPLC or titration, provide insights into the strengths and limitations of simultaneous spectrophotometric analysis.In the context of pharmaceutical analysis, where the safety and efficacy of medications are paramount, validation and method comparison ensure that simultaneous spectrophotometric methods meet the highest standards of quality control and regulatory compliance. Therefore, these processes remain indispensable for harnessing the full potential of simultaneous spectrophotometric analysis in pharmaceutical mixtures and advancing drug development and manufacturing with confidence and precision.

REFERENCES

1. van der Greef J, McBurney RN. Rescuing drug discovery: in vivo systems pathology and systems pharmacology. Nature Reviews Drug Discovery. 2005;4(12):961-7.

2. Ndioumabia O. Unveiling the Power of Pharmaceutical Sciences from Molecules to Medicines. Journal Wetenskap Health. 2022;3(2):11-20.
3. Peris-Pastor G, Alonso-Rodríguez S, Benedé JL, Chisvert A. High-throughput determination of oxidative stress biomarkers in saliva by solvent-assisted dispersive solid-phase extraction for clinical analysis. Advances in Sample Preparation. 2023;6:100067.
4. Li M, Xu W, Su Y. Solid-state NMR spectroscopy in pharmaceutical sciences. TrAC Trends in Analytical Chemistry. 2021;135:116152.
5. LaPlante SR, Fader LD, Fandrick KR, Fandrick DR, Hucke O, Kemper R, et al. Assessing atropisomer axial chirality in drug discovery and development. Journal of medicinal chemistry. 2011;54(20):7005-22.
6. Kale DP, Zode SS, Bansal AK. Challenges in translational development of pharmaceutical cocrystals. Journal of pharmaceutical sciences. 2017;106(2):457-70.
7. Griffin JP, Posner J, Barker GR. The textbook of pharmaceutical medicine: John Wiley & Sons; 2013.
8. Mokhtari RB, Homayouni TS, Baluch N, Morgatskaya E, Kumar S, Das B, et al. Combination therapy in combating cancer. Oncotarget. 2017;8(23):38022.
9. Li C, Jia W-w, Yang J-l, Cheng C, Olaleye OE. Multi-compound and drug-combination pharmacokinetic research on Chinese herbal medicines. Acta Pharmacologica Sinica. 2022;43(12):3080-95.
10. Chrisikou I, Orkoula M, Kontoyannis C. FT-IR/ATR solid film formation: Qualitative and quantitative analysis of a piperacillin-tazobactam formulation. Molecules. 2020;25(24):6051.
11. Kim D-W, Weon KY. Pharmaceutical application and development of fixed-dose combination: Dosage form review. Journal of Pharmaceutical Investigation. 2021;51:555-70.
12. Edinger M, Jacobsen J, Bar-Shalom D, Rantanen J, Genina N. Analytical aspects of printed oral dosage forms. International Journal of Pharmaceutics. 2018;553(1-2):97-108.
13. Zarmpi P, Flanagan T, Meehan E, Mann J, Fotaki N. Biopharmaceutical aspects and implications of excipient variability in drug product performance. European Journal of Pharmaceutics and Biopharmaceutics. 2017;111:1-15.
14. Chaudhary A. Application of HPLC-CAD in Pharmaceutical Analysis.
15. Serajuddin AT, Thakur AB, Ghoshal RN, Fakes MG, Ranadive SA, Morris KR, et al. Selection of solid dosage form composition through drug–excipient compatibility testing. Journal of pharmaceutical sciences. 1999;88(7):696-704.
16. Taoukis PS, Labuza TP, Saguy IS. Kinetics of food deterioration and shelf-life prediction. The Editors. 1997;30.
17. Balandrin MF, Klocke JA, Wurtele ES, Bollinger WH. Natural plant chemicals: sources of industrial and medicinal materials. Science. 1985;228(4704):1154-60.
18. Chackalamannil S, Rotella D, Ward S. Comprehensive medicinal chemistry III: Elsevier; 2017.
19. Steinmetz KL, Spack EG. The basics of preclinical drug development for neurodegenerative disease indications. BMC neurology. 2009;9(1):1-13.
20. Bajorath J. Integration of virtual and high-throughput screening. Nature Reviews Drug Discovery. 2002;1(11):882-94.
21. Bannigan P, Aldeghi M, Bao Z, Häse F, Aspuru-Guzik A, Allen C. Machine learning directed drug formulation development. Advanced Drug Delivery Reviews. 2021;175:113806.
22. Dave VS, Saoji SD, Raut NA, Haware RV. Excipient variability and its impact on dosage form functionality. Journal of pharmaceutical sciences. 2015;104(3):906-15.
23. Patil AS, Pethe AM. Quality by Design (QbD): A new concept for development of quality pharmaceuticals. International journal of pharmaceutical quality assurance. 2013;4(2):13-9.
24. Munson J, Freeman Stanfield C, Gujral B. A review of process analytical technology (PAT) in the US pharmaceutical industry. Current Pharmaceutical Analysis. 2006;2(4):405-14.
25. Pokharana M, Vaishnav R, Goyal A, Shrivastava A. Stability testing guidelines of pharmaceutical products. Journal of Drug Delivery and Therapeutics. 2018;8(2):169-75.
26. Ambhore JP, Adhao VS, Cheke RS, Popat RR, Gandhi SJ. Futuristic review on progress in force degradation studies and stability indicating assay method for some antiviral drugs. GSC Biological and Pharmaceutical Sciences. 2021;16(1):133-49.

27. Baumfeld Andre E, Reynolds R, Caubel P, Azoulay L, Dreyer NA. Trial designs using real-world data: the changing landscape of the regulatory approval process. Pharmacoepidemiology and drug safety. 2020;29(10):1201-12.
28. Macdonald JC, Isom DC, Evans DD, Page KJ. Digital innovation in medicinal product regulatory submission, review, and approvals to create a dynamic regulatory ecosystem—are we ready for a revolution? Frontiers in Medicine. 2021;8:660808.
29. Lin ID, Hertig JB. Risk control drives risk assessment and risk review: A cause and effect model of pharmaceutical drug recall on patient safety. The Journal of Medicine Access. 2023;7:27550834231170075.
30. Bressolle F, Bromet-Petit M, Audran M. Validation of liquid chromatographic and gas chromatographic methods Applications to pharmacokinetics. Journal of Chromatography B: Biomedical Sciences and Applications. 1996;686(1):3-10.
31. Durão P, Fauteux-Lefebvre C, Guay J-M, Simard J-S, Abatzoglou N, Gosselin R. Specificity of process analytical tools in the monitoring of multicomponent pharmaceutical powders. Pharmaceutical Development and Technology. 2019;24(3):380-9.
32. Paudel A, Raijada D, Rantanen J. Raman spectroscopy in pharmaceutical product design. Advanced drug delivery reviews. 2015;89:3-20.
33. Izadi P, Izadi P, Eldyasti A. Holistic insights into extracellular polymeric substance (EPS) in anammosx bacterial matrix and the potential sustainable biopolymer recovery: A review. Chemosphere. 2021;274:129703.
34. Luykx DM, Van Ruth SM. An overview of analytical methods for determining the geographical origin of food products. Food chemistry. 2008;107(2):897-911.
35. Ammann AA. Inductively coupled plasma mass spectrometry (ICP MS): a versatile tool. Journal of mass spectrometry. 2007;42(4):419-27.
36. Jones GT, Bailey DG, Beck C. Source provenance of andesite artefacts using non-destructive XRF analysis. Journal of Archaeological Science. 1997;24(10):929-43.
37. Whitesides GM. The origins and the future of microfluidics. nature. 2006;442(7101):368-73.
38. Gupta D, Bhardwaj S, Sethi S, Pramanik S, Das DK, Kumar R, et al. Simultaneous spectrophotometric determination of drug components from their dosage formulations. Spectrochimica Acta Part A: Molecular and Biomolecular Spectroscopy. 2022;270:120819.
39. Mahrouse MA, Elkady EF. Validated spectrophotometric methods for the simultaneous determination of ciprofloxacin hydrochloride and metronidazole in tablets. Chemical and Pharmaceutical Bulletin. 2011;59(12):1485-93.
40. Kamal AH, El-Malla SF, Hammad SF. A review on UV spectrophotometric methods for simultaneous multicomponent analysis. Eur J Pharm Med Res. 2016;3(2):348-60.
41. Bonfilio R, De Araujo MB, Salgado HRN. Recent applications of analytical techniques for quantitative pharmaceutical analysis: a review. WSEAS Trans Biol Biomed. 2010;7(4):316-38.
42. Guideline IHT. Validation of analytical procedures: text and methodology. Q2 (R1). 2005;1(20):05.
43. Weitzel MJ. The estimation and use of measurement uncertainty for a drug substance test procedure validated according to USP< 1225>. Accreditation and Quality Assurance. 2012;17(2):139-46.
44. Scheer F, Krämer I. A liquid chromatography assay for the simultaneous quantification of piperacillin and ciprofloxacin in human plasma and dialysate in critically ill patients undergoing continuous renal replacement therapy. International Journal of Analytical Mass Spectrometry and Chromatography. 2014;2(02):43.
45. Smith NF, Raynaud FI, Workman P. The application of cassette dosing for pharmacokinetic screening in small-molecule cancer drug discovery. Molecular Cancer Therapeutics. 2007;6(2):428-40.
46. Elston K, Draper J, editors. A review of meeting planner site selection criteria research. Journal of Convention & Event Tourism; 2012: Taylor & Francis.
47. Aromataris E, Riitano D. Constructing a search strategy and searching for evidence. Am J Nurs. 2014;114(5):49-56.
48. Van Spall HG, Toren A, Kiss A, Fowler RA. Eligibility criteria of randomized controlled trials published in high-impact general medical journals: a systematic sampling review. Jama. 2007;297(11):1233-40.

49. Khoshayand M, Abdollahi H, Shariatpanahi M, Saadatfard A, Mohammadi A. Simultaneous spectrophotometric determination of paracetamol, ibuprofen and caffeine in pharmaceuticals by chemometric methods. Spectrochimica Acta Part A: Molecular and Biomolecular Spectroscopy. 2008;70(3):491-9.
50. Korany MA, Abdine HH, Ragab MA, Aboras SI. Application of derivative spectrophotometry under orthogonal polynomial at unequal intervals: determination of metronidazole and nystatin in their pharmaceutical mixture. Spectrochimica Acta Part A: Molecular and Biomolecular Spectroscopy. 2015;143:281-7.
51. Ramesh B, Jarke M. Toward reference models for requirements traceability. IEEE transactions on software engineering. 2001;27(1):58-93.
52. Østergaard J. UV/VIS spectrophotometry and UV imaging. Analytical Techniques in the Pharmaceutical Sciences. 2016:3-27.
53. Chadha R, Bhandari S. Drug–excipient compatibility screening—role of thermoanalytical and spectroscopic techniques. Journal of pharmaceutical and biomedical analysis. 2014;87:82-97.
54. Riedl J, Esslinger S, Fauhl-Hassek C. Review of validation and reporting of non-targeted fingerprinting approaches for food authentication. Analytica Chimica Acta. 2015;885:17-32.
55. Tome T, Zigart N, Časar Z, Obreza A. Development and optimization of liquid chromatography analytical methods by using AQbD principles: Overview and recent advances. Organic process research & development. 2019;23(9):1784-802.
56. Swartz ME, Krull IS. Handbook of analytical validation: CRC Press; 2012.
57. Breaux J, Jones K, Boulas P. Analytical methods development and validation. Pharm Technol. 2003;1:6-13.
58. Adriaens A. Non-destructive analysis and testing of museum objects: An overview of 5 years of research. Spectrochimica Acta Part B: Atomic Spectroscopy. 2005;60(12):1503-16.
59. Bakhtiar R, Majumdar TK. Tracking problems and possible solutions in the quantitative determination of small molecule drugs and metabolites in biological fluids using liquid chromatography–mass spectrometry. Journal of pharmacological and toxicological methods. 2007;55(3):227-43.
60. Cerdá V, Ferrer L, Avivar J, Cerdá A. Flow analysis: a practical guide: Newnes; 2014.
61. Erk N. Analysis of binary mixtures of losartan potassium and hydrochlorothiazide by using high performance liquid chromatography, ratio derivative spectrophotometric and compensation technique. Journal of Pharmaceutical and Biomedical Analysis. 2001;24(4):603-11.
62. Nir I, Lu X. In situ UV fiber optics for dissolution testing-what, why, and where we are after 30 years. Dissolut Technol. 2018;25:70-7.
63. KLUPCZY—SKA A, DEREZI—SKI P, Kokot ZJ. Metabolomics in medical sciences ń trends, challenges and perspectives. Acta poloniae pharmaceutica. 2015:629.
64. Ramirez-Ambrosi M, Abad-Garcia B, Viloria-Bernal M, Garmon-Lobato S, Berrueta L, Gallo B. A new ultrahigh performance liquid chromatography with diode array detection coupled to electrospray ionization and quadrupole time-of-flight mass spectrometry analytical strategy for fast analysis and improved characterization of phenolic compounds in apple products. Journal of Chromatography A. 2013;1316:78-91.
65. Decosterd LA, Widmer N, André P, Aouri M, Buclin T. The emerging role of multiplex tandem mass spectrometry analysis for therapeutic drug monitoring and personalized medicine. TrAC Trends in Analytical Chemistry. 2016;84:5-13.

Table 1: Literature search

Title	Year	Conclusion	Reference
Recent Research Articles: Application of Simultaneous Spectrophotometric Analysis in Multicomponent Pharmaceutical Mixtures	2023	This study explores the practical application of simultaneous spectrophotometric analysis in quantifying multiple active pharmaceutical ingredients (APIs) in complex pharmaceutical formulations. The researchers discuss the advantages and challenges of this method and provide case studies demonstrating its effectiveness.	**(38)**

Validation of Simultaneous Spectrophotometric Methods for Pharmaceutical Mixtures	2022	This research article focuses on the validation aspects of simultaneous spectrophotometric methods. It discusses the validation parameters, such as accuracy, precision, linearity, specificity, and robustness, and provides detailed validation protocols for pharmaceutical mixture analysis.	**(39)**
Comparative Study of Simultaneous Spectrophotometry vs. HPLC for Multicomponent Pharmaceutical Analysis	2021	This comparative study investigates the performance of simultaneous spectrophotometric analysis against high-performance liquid chromatography (HPLC) in analyzing multicomponent pharmaceutical mixtures. The findings highlight scenarios where spectrophotometry offers advantages in terms of speed and cost-effectiveness.	**(40)**
Reviews: Spectrophotometric Techniques in Pharmaceutical Analysis: A Comprehensive Review	2022	This comprehensive review discusses various spectrophotometric techniques, including simultaneous spectrophotometry, in pharmaceutical analysis. It provides an overview of principles, instrumentation, and applications, emphasizing the role of validation in ensuring reliable results.	**(41)**
Recent Advances in Spectrophotometric Methods for Pharmaceutical Mixture Analysis	2020	This review focuses on recent advances in spectrophotometric methods, with a particular emphasis on simultaneous analysis of multicomponent pharmaceutical mixtures. It covers the evolution of instrumentation, data analysis techniques, and validation strategies.	**(40)**
Relevant Guidelines: "ICH Harmonized Tripartite Guideline: Validation of Analytical Procedures: Text and Methodology Q2(R1)"	2021	The International Council for Harmonisation (ICH) guideline Q2(R1) outlines the principles and methodology for the validation of analytical procedures, including spectrophotometric methods. It provides a structured framework for conducting method validation to ensure accuracy, precision, and reliability.	**(42)**
"USP General Chapter <1225>: Validation of Compendial Procedures"	2019	The United States Pharmacopeia (USP) General Chapter <1225> provides guidelines on the validation of analytical procedures, including spectrophotometric methods. It offers recommendations for demonstrating the suitability of analytical methods for their intended applications	**(43)**
"EMA Guideline on Validation of Bioanalytical Methods"	2020	The European Medicines Agency (EMA) guideline on the validation of bioanalytical methods is relevant to spectrophotometric analysis in pharmaceutical research. It provides guidance on method validation in the context of bioanalysis, which includes pharmaceutical mixture analysis.Therecent research articles, reviews, and relevant guidelines in the field of simultaneous spectrophotometric analysis, validation, and method comparison in pharmaceutical mixtures provide valuable insights into the practical application of this analytical technique. These sources emphasize the importance of validation, precision, and	**(44)**

		reliability in pharmaceutical analysis, offering researchers and professionals a comprehensive understanding of the challenges and opportunities in this critical area of pharmaceutical research.	

Indian Journal of Natural Sciences *www.tnsroindia.org.in ©IJONS*

Vol.15 / Issue 83 / Apr / 2024 *International Bimonthly (Print) – Open Access* *ISSN: 0976 – 0997*

RESEARCH ARTICLE

Designing Single Sampling Plans Integrated with Supply Chain Contract - A Simulation Study Based on Weibull Distribution and Gamma Distribution

S.Ravi Sankar[1] and J. Sinthiya[2]*

[1]Associate Professor, Department of Statistics, Government Arts College, (Affiliated to *Bharathiar University)* Coimbatore, Tamil Nadu, India
[2]Assistant Professor, Department of Mathematics, Sri Ramakrishna College of Arts & Science, (Affiliated to *Bharathiar University*) Coimbatore, Tamil Nadu, India

Received: 16 Nov 2023 Revised: 12 Jan 2024 Accepted: 16 Mar 2024

***Address for Correspondence**
J. Sinthiya
Assistant Professor,
Department of Mathematics,
Sri Ramakrishna College of Arts & Science,
(Affiliated to *Bharathiar University*)
Coimbatore, Tamil Nadu, India
Email: sinthiya@srcas.ac.in

ABSTRACT

Supply Chain Contract (SCC) is relatively a new method which introduces a new mechanism for managing uncertainties in the projects. In this paper, single sampling plans for the supply chain contract are constructed using the simulation software (GoldSim 14.0). The Gamma distribution and the Weibull distribution are considered for the single sampling plans. The optimal parameters are determined with the minimum sample size. Extensive tables are provided for the selection of single sampling plan parameters according to the desired proportion defective. Examples are also provided to illustrate the selection of the single sampling plans.

Keywords: Supply Chain Contract, Single Sampling Plan, Simulation, Gamma distribution, Weibull distribution

INTRODUCTION

Acceptance sampling has become important field of Statistical Quality Control and it was popularized by Dodge and Romig. Many types of life testing and acceptance sampling plans are being used to investigate whether the quality level of items meets the consumers' requirement such as the minimum lifetime or reliability. Acceptance sampling is

one of the major areas in statistical quality control. An acceptance sampling plan deals with the decision to accept or reject a lot based on the inspection of samples taken from the lot. Acceptance sampling plans are classified into sampling plans by attributes and sampling plans by variables. The main purpose of using an acceptance sampling plan is to reduce the cost of inspection and to provide protection to the producer as well as the consumer. The single acceptance sampling plan is very popular among industrial engineers due to its simplicity. Deros *et al*. [1] discussed the application of acceptance sampling plans in manufacturing electronic products. Many authors developed the single sampling plans based on certain distributions: Epstein [2] for exponential distribution, Goode and Kao [3] for Weibull distribution, Gupta and Groll [4] for Gamma distributions, Gupta [5] for normal and log–normal distributions, Tsai and Wu [6] for a generalized Rayleigh distribution, Rosaiah *et al*. [7] for the exponentiated log–logistic distributions, Balakrishnan *et al*. [8] for the generalized Birnbaum–Saunders distribution and so on.

Contract Model for Acceptance Sampling Plan

Supply Chain Contracts (SCC) are two or more persons linked by flow of men, machine, material, and money etc., However, any work has been done on the relationships of those supply chain contract models. SSC have been studied extensively in management, marketing and economics.

The figure 1 shows the basic transaction between manufacturer and customer. The customer places an order with a manufacturer and the manufacturer provides the same quantity of products in the expected quality. At this stage, the retailer can apply the sampling inspection to confirm the incoming lot quality. Then the customer makes a decision whether to accept or reject the lot. If the incoming lot is rejected, the manufacturer should replace the defective products. Hence, the contract required that the retailer be given an incentive to increase his order. Supply chain contracting has brought a broad appreciation for economic modelling in production research with information updating. Supply chain contracts include wholesale-price contracts, revenue sharing contracts, return contracts, two-part tariff contracts, service commitment contracts, quantity flexibility contracts, etc. (Cachon 2003; Tsay and Agrawal 2004). Pricing contracts can be categorised into single-price contracts (e.g. wholesale price contract, fixed-fee contract) and two-price contracts (e.g. two-part tariff). The different types of supply chain contracts with price have been studied by various authors. Choi (9) considers the fixed-fee contract, Keser and Paleologo (10) and Loch and Wu (11) study wholesale price contracts. Anandasivam Gopal and Sivaramakrishnan (12) observe the difference between the fixed price and time materials contracts in their projects. Starbird (13) examines the effect of rewards, penalties and inspection policies on the behaviour of an expected cost-minimizing supplier. RaviSankar and Sinthiya (15) constructed a simulation model for a double sampling plan integrated with a supply chain contract through the Weibull distribution.

The notations used in this study are:

c : *Acceptance Number*
C : *Total Cost*
n : *Sample Size*
N : *Optimum Lot Size*
$t(q)$: *Target Quality*
$m(q)$: *Mean Quality*
R_i : *Reward*
D_i : *Demand*
P_i : *Penalty*

Research Methodology

A simulation software (GoldSim14.0) is used to design a simulation model for a single sampling plan used in supply chain contracts, in order to find out the economic order quantity. RaviSankar and Sinthiya (15) designed the simulation model for SCC using Goldsim (14.0) software. In this paper, the simulation model is developed for SSP integrated with SCC through the Gamma distribution using mean lifetime as the quality parameter. The acceptance numbers, sample sizes, lot size and total cost are obtained using the simulation models given in Figure 2 and Figure 3 by minimizing the total cost as well as the sample size.

Single Sampling Plan (SSP) and its Probability of Acceptance

The procedure for SSP(n, c) consists of the following steps:

i) Draw a random sample of size *n* from the lot of size *N* received from the supplier.

ii) Count the number of defective units (*d*) found in the sample.

iii) If d ≤ c, the acceptance number, the lot is accepted.

iv) If d >c, the lot is rejected and go for 100% inspection.

The parameters *n* and *c* are the design parameters of the single sampling plan. The probability of acceptance for SSP is calculated using the Poisson distribution and is given in equation 2.1.

$$P_a(p) = \sum_{k=0}^{c} \frac{e^{-np}(np)^k}{k!} \quad \text{..... (2.1)}$$

where p = F(t) is the probability of defective observed through the time *t*. For various combinations of target quality and mean quality, the producer wishes that his product should not be rejected and the consumer wants to reject the product of poor quality level.

The script used in the GoldSim software to calculate probability of acceptance P_a (p) for various 'p' values is given in Figure 1.

The simulation model presented in Figure-2 for supply chain contracts is developed using the GoldSim Software.

Designing a Simulation Model for Integrating SSP with SCC based on Weibull Distribution

Suppose that the lifetime of a product follows the Weibull distribution with the probability density function (pdf)

$$f(x, \alpha,\beta)= \frac{\beta}{\alpha}\left(\frac{x}{\alpha}\right)^{\beta-1} e^{-\left(\frac{x}{\alpha}\right)^{\beta}} \text{ , } x \geq 0 \text{ and } \alpha, \beta > 0 \quad \text{..... (2.2)}$$

where α is the unknown scale parameter and β is the known shape parameter.

Its cumulative distribution function (cdf) is given by

$$F(t; \alpha,\beta) = 1- e^{-(\frac{t}{\alpha})^{\beta}} \quad \text{.....(2.3)}$$

which is taken as the proportion defective (p) of an item discussed in the equation (2.1).

ie., $p = F(t; \alpha,\beta) = 1-e^{-(\frac{t}{\alpha})^{\beta}}$ ..... (2.4)

A simulation model for Integrating SSP (based on Weibull Distribution) with SCC
Is developed using the GoldSim Software and is presented in figure 3.

Designing a Simulation Model for Integrating SSP (based on Gamma Distribution) with SCC

In this section, it is assumed that the lifetime of a product follows the Gamma distribution and that the shape parameter β is known. The probability density function of the Gamma distribution is given by

$$f(x, \alpha,\beta)= \frac{\alpha^{\beta}}{\Gamma_{\beta}}(x)^{\beta-1}e^{-\alpha x} \text{ , } x\geq 0 \text{ and } \alpha,\beta>0 \quad \text{..... (2.5)}$$

where α is the rate parameter and β is the known as the shape parameter.

The cumulative distribution function (cdf) of the Gamma distribution is given by

$$F(t; \alpha,\beta) =\frac{1}{\Gamma_{\beta}}\gamma(\alpha,\beta x) \quad \text{..... (2.6)}$$

The Reliability at time 't', is defined as

$$R(t) = 1- F(t; \alpha,\beta) =1- \frac{1}{\Gamma_{\beta}}\gamma(\alpha,\beta x) \quad \text{..... (2.7)}$$

A simulation model for Integrating SSP (based on Gamma distribution) with SCC
is developed using the GoldSim Software and is presented in the figure 4.

In the model given in the Figure 3 and the Figure 4, the input parameters mean quality (m(q)), target quality (t(q)) and the known shape parameter (β) are initialized with certain initial values. With these input values, the proportion

defectives *(p)* value is calculated using the Weibull distribution and using Gamma distribution. The probability of acceptance $P_a(p)$ values for SSP using the Poisson distribution are calculated with the help of the script given in the Figure 1. While inspecting the lot using SSP, if the lot is rejected, the defective items are replaced with good ones by applying 100% inspection.

Construction of SSP(n, c) with Optimum of Lot Size (N) and Total Cost (C)

In this section, it is assumed that the reward (R_i) is Rs.0.5 and the penalty (P_i) is Rs.250. For various combinations of t(q) and m(q), the SSP(n, c) plans with optimum lot size (N) and the total cost (C) have been constructed based on the Weibull distribution and the Gamma distribution separately and are presented in Table 1, Table 2 and Table 3, for the demand values as 500 , 700 and 1000 respectively.

Comparing SSP(n,c) Plans based on the Weibull distribution and the Gamma distribution

Generally, the Gamma distribution led to a lower sample size than the Weibull distribution when other parameters are the same. In this section, the comparison is made between the SSPs based on the Weibull Distribution and the Gamma distribution both integrated with SCC in terms of the sample size. From the Figure 5, Figure 6, and Figure 7, it is found that the Gamma distribution yields the single sampling plans integrated with SCC having smaller sample size than that of the Weibull Distribution.

Example -1:

Suppose a manufacturer has put a contract with his retailer that he receives the reward of Rs.0.5 / unit for better quality and the penalty of Rs.250 / unit for the failure. It is also decided to run this contract for the target quality t(q)=100, mean quality m(q) =120 and demand (d) = 500. Further, it is observed that the lifetime of the product follows the Weibull distribution with shape parameter (β) 1. From the Table 1, the optimal single sampling plan is obtained as SSP(162,6) and the total cost (C) is ₹ 1,96,31,800.

Example -2:

Suppose another manufacturer has put a contract with his retailer that he receives the reward of Rs.0.5 / unit for better quality and the penalty of Rs.250 / unit for the failure. It is also decided to run this contract for the target quality t(q) =100, mean quality m(q) =120 and demand (d) = 500. Further, it is observed that the lifetime of the product follows the Gamma distribution with shape parameter (β) 1. From the Table 1, the optimal single sampling plan is obtained as SSP(139,1) and the total cost (C) is ₹ 1,96,31,500.

CONCLUSION

In this study, the constructed Single Sampling Plans integrated with SCC which are listed in the tables may be applied for the products whose lifetime follows either the Gamma distribution or the Weibull distribution. According to the present comparative study, it is found that the Gamma distribution yields more efficient SSPs integrated with SCC than that of the Weibull distribution by means of lesser sample size. It is found that if Gamma distribution is used to construct the SSP for integrating with SCC, the time, cost and efforts will be reduced considerably based on the sample size reduction in SSPs while comparing with that of the Weibull distribution. The extensive tables may be used for industrial purpose. The same study may be extended for other sampling plans as further studies.

REFERENCES

1. Deros BM, Peng CY, AbRahman MN, Ismail AR, Sulong AB. Assessing acceptance sampling application in manufacturing electrical and electronic products. J Achievements Mater Manuf Eng. 2008;31(2):622–628.
2. B. Epstein, Truncated life tests in the exponential case. Ann. Math. Stat. 25:3 (1954), pp. 555–564.

3. H.P. Goode and J.H.K. Kao, Sampling plans based on the Weibull distribution, Proceedings of the Seventh National Symposium on Reliability and Quality Control, Philadelphia, 1961, pp. 24–40.
4. S.S. Gupta and P.A. Groll, Gamma distribution in acceptance sampling based on life tests. J. Am. Stat. Assoc. 56 (1961), pp. 942–970.
5. S.S. Gupta, Life test sampling plans for normal and lognormal distributions. Technometrics, 4:2 (1962), pp. 151–175.
6. T.-R. Tsai and S.-J. Wu. Acceptance sampling based on truncated life tests for generalized Rayleigh distribution, J. Appl. Stat. 33:6 (2006), pp. 595–600.
7. K. Rosaiah, R.R.L. Kantam, and Ch. Santosh Kumar, Reliability of test plans for exponentiated log-logistic distribution, *Econ. Qual. Control, 21(2) (2006),* 165–175.
8. N. Balakrishnan,V. Leiva, and J. Lopez,Acceptance sampling plans from truncated life tests based on the generalized Birnbaum–Saunders distribution, *Commun. Stat. Simul. Comput. 36* (2007), 643–656.
9. Choi, T. M. 2016. "Inventory Service Target in Quick Response Fashion Retail Supply Chains." Service Science 8 (4): 406–419.
10. Keser, C., &Paleologo, G. (2004). Experimental investigation of retailer-supplier contracts: The wholesale price contract. *Working paper, IBM TJ Watson Research Center, Yorktown Heights, NY*.
11. Loch, C. H., & Wu, Y. (2008). Social preferences and supply chain performance: An experimental study. *Management Science*, *54*(11), 1835-1849.
12. Gopal, A., &Sivaramakrishnan, K. (2008). Research note—On vendor preferences for contract types in offshore software projects: The case of fixed price vs. time and materials contracts. *Information Systems Research*, *19*(2), 202-220.
13. Starbird, S. A. (2001). Penalties, rewards, and inspection: provisions for quality in supply chain contracts. *Journal of the Operational Research Society*, *52*(1), 109-115.
14. Starbird, S. A. (2003). Effect of coordinated replenishment policies on quality. *Journal of the Operational Research Society*, *54*(1), 32-39.
15. RaviSankar, S. &Sinthiya, J. (2023). Construction of Double Sampling Plans Integrated with Supply Chain Contracts through Weibull Distribution - A Simulation Study With Quality Related Costs Optimization. *Advances and Applications in Statistics*, *88*(2), 159-174.
16. https://www.goldsim.com/Web/Customers/Downloads/

Table 1: SSP(n, c) with (N, C) for Demand = 500

S.No	t(q)	m(q)	N	SSP(n,c) for Weibull			SSP(n,c) for Gamma		
				n	c	C	n	c	C
1	100	120	1999	162	6	₹ 1,96,31,800	139	1	1,96,31,500
2	130	120	1999	109	5	₹ 1,96,32,800	51	1	1,96,32,000
3	140	125	2166	111	6	₹ 2,06,27,200	51	6	1,96,32,000
4	120	120	2166	155	1	₹ 2,06,30,600	92	7	1,96,32,000
5	130	130	1999	175	9	₹ 1,96,31,800	81	9	1,96,31,000
6	120	140	1999	90	2	₹ 1,96,32,000	87	4	1,96,32,000
7	150	130	1999	119	10	₹ 1,96,32,000	101	7	1,96,32,000
8	120	130	2164	104	3	₹ 2,07,82,300	104	4	1,96,32,000
9	125	135	2200	151	4	₹ 2,08,10,100	70	10	1,97,38,800
10	135	125	1999	165	10	₹ 1,96,32,000	38	7	1,96,32,000
11	125	130	1999	173	10	₹ 1,96,31,800	122	7	1,96,31,700
12	100	105	1999	113	3	₹ 1,96,32,000	108	1	1,96,31,900
13	100	110	1999	64	1	₹ 1,96,32,000	60	7	1,96,32,000
14	105	100	2166	157	4	₹ 2,06,27,200	152	6	1,99,02,200
15	110	100	2166	122	7	₹ 2,06,30,500	88	1	1,96,31,800

16	120	125	1999	144	5	₹ 1,96,31,800	127	2	1,96,31,700
17	125	120	2123	83	5	₹ 2,08,10,400	72	3	1,96,32,000
18	130	135	2000	61	7	₹ 1,96,32,000	39	0	1,96,32,000
19	135	130	1999	200	10	₹ 1,96,32,800	58	6	1,96,32,000
20	130	140	1999	176	5	₹ 1,96,32,900	71	9	1,96,32,100

Table 2: SSP(n, c) with (N, C) for Demand = 700

S.No	t(q)	m(q)		SSP(n,c) for Weibull			SSP(n,c) for Gamma		
			N	n	c	C	n	c	C
1	100	120	2799	92	6	₹ 2,91,64,600	87	8	₹ 2,91,63,800
2	130	120	2799	97	3	₹ 2,91,63,500	80	3	₹ 2,91,63,500
3	140	125	2799	132	10	₹ 2,91,64,400	125	8	₹ 2,91,63,500
4	120	120	2799	106	8	₹ 2,91,64,500	82	2	₹ 2,91,63,600
5	130	130	2799	94	2	₹ 2,91,64,500	54	7	₹ 2,91,63,700
6	120	140	2799	70	2	₹ 3,05,54,200	78	7	₹ 2,91,63,700
7	150	130	2799	66	2	₹ 2,91,63,400	64	2	₹ 2,91,63,400
8	120	130	2799	98	4	₹ 2,91,63,500	56	9	₹ 2,91,63,400
9	125	135	2799	120	4	₹ 2,91,64,500	123	0	₹ 2,91,63,700
10	135	125	2799	50	3	₹ 3,05,54,100	48	10	₹ 2,91,63,500
11	125	130	2799	163	8	₹ 2,91,63,800	125	4	₹ 2,91,63,600
12	100	105	2799	88	5	₹ 2,91,63,800	83	2	₹ 2,91,63,600
13	100	110	2799	84	8	29579300.00	43	5	₹ 2,91,69,000
14	105	100	2799	117	7	₹ 2,91,63,500	134	1	₹ 2,91,63,500
15	110	100	2799	108	9	29163500.00	65	3	₹ 2,91,63,500
16	120	125	2799	136	4	₹ 2,91,63,800	58	4	₹ 2,91,63,600
17	125	120	2799	168	9	29163500.00	143	5	₹ 2,91,63,500
18	130	135	2799	125	3	₹ 2,91,63,800	99	9	₹ 2,91,63,600
19	135	130	2799	94	9	₹ 2,91,63,500	72	5	₹ 2,91,63,500
20	130	140	2799	197	9	₹ 2,91,64,500	101	2	₹ 2,91,63,700

Table 3: SSP(n, c) with (N, C) for Demand = 1000

S.No	t(q)	m(q)	N	SSP(n,c) for Weibull			SSP(n,c) for Gamma		
				n	c	C	n	c	C
1	100	120	3999	197	4	₹ 4,34,55,000	67	5	₹ 4,34,50,400
2	130	120	3999	146	4	₹ 4,54,80,100	85	9	₹ 4,34,49,800
3	140	125	3999	136	2	₹ 4,34,49,900	107	6	₹ 4,34,49,800
4	120	120	3999	152	3	₹ 4,34,49,800	79	0	₹ 4,34,49,800
5	130	130	4333	198	7	₹ 4,54,80,100	116	3	₹ 4,34,50,000
6	120	140	3999	196	6	₹ 4,34,51,000	105	8	₹ 4,34,50,300
7	150	130	3999	112	0	₹ 4,34,49,700	95	0	₹ 4,34,49,700
8	120	130	4193	200	10	₹ 4,56,40,000	97	6	₹ 4,34,50,100
9	125	135	3999	146	8	₹ 4,34,50,900	105	8	₹ 4,34,50,100
10	135	125	3999	69	0	₹ 4,55,74,500	67	4	₹ 4,54,80,200
11	125	130	3999	179	7	₹ 4,34,50,900	118	1	₹ 4,34,50,100
12	100	105	3999	110	4	₹ 4,34,50,900	61	9	₹ 4,34,50,500
13	100	110	3999	192	7	₹ 4,34,50,900	87	9	₹ 4,34,50,200
14	105	100	4333	151	6	₹ 4,54,75,600	97	7	₹ 4,34,49,900
15	110	100	4334	67	5	₹ 4,56,77,000	63	5	₹ 4,54,80,100

16	120	125	4193	151	5	₹ 4,56,40,000	100	1	₹ 4,34,50,100
17	125	120	3999	151	4	₹ 4,34,50,800	114	2	₹ 4,34,49,900
18	130	135	3999	139	5	₹ 4,34,50,800	116	5	₹ 4,34,49,900
19	135	130	3999	95	4	₹ 4,34,50,800	44	3	₹ 4,34,49,900
20	130	140	4333	158	3	₹ 4,54,75,500	85	2	₹ 4,34,50,100

Figure 1 : Basic Transaction Model

```
Script:
-------

VALUE PROB = 0.0
VALUE pr1 = 1.0
FOR (j = c1+1; ~j <= c2; j = ~j + 1)
   VALUE fact = 1
   FOR (k = 1; ~k <= ~j; k = ~k + 1)
      fact = ~fact*~k
   END FOR // k
   pr1 = (n*p)^~j/~fact
   VALUE pr2 = 0
   FOR (i = 0; ~i <= c2-~j; i = ~i + 1)
      fact = 1
      FOR (k = 1; ~k <= ~i; k = ~k + 1)
         fact = ~fact*~k
      END FOR // k
      pr2 = (2*n*p)^~i/~fact+~pr2
   END FOR // i
   PROB = ~pr1*~pr2+~PROB
END FOR // j
Result = ~PROB*exp(-3*n*p)
```

Figure 2: Script

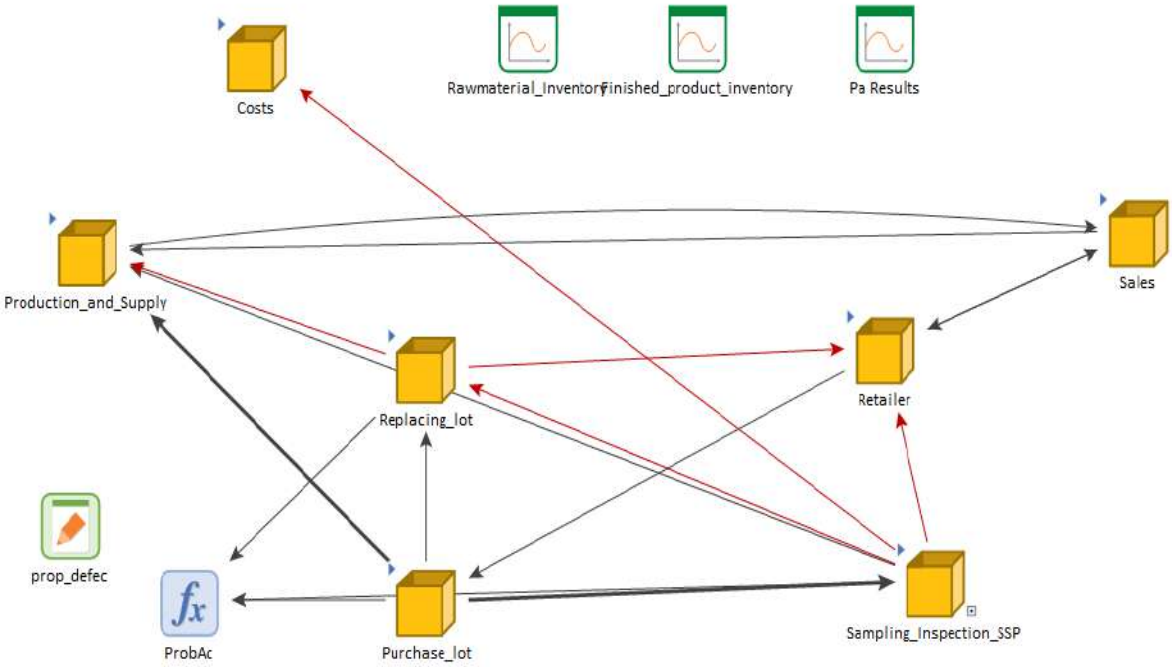

Figure .3: Simulation Model for Integrating SSP

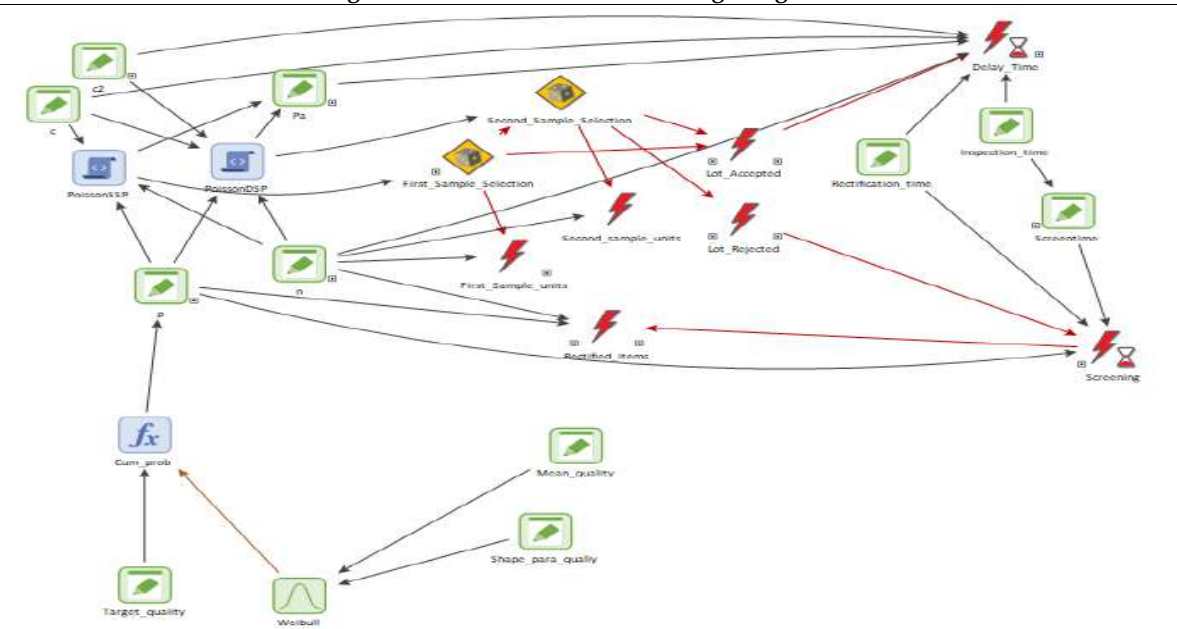

Figure 4: Simulation Model for Integrating SSP (based on Weibull Distribution) with SCC

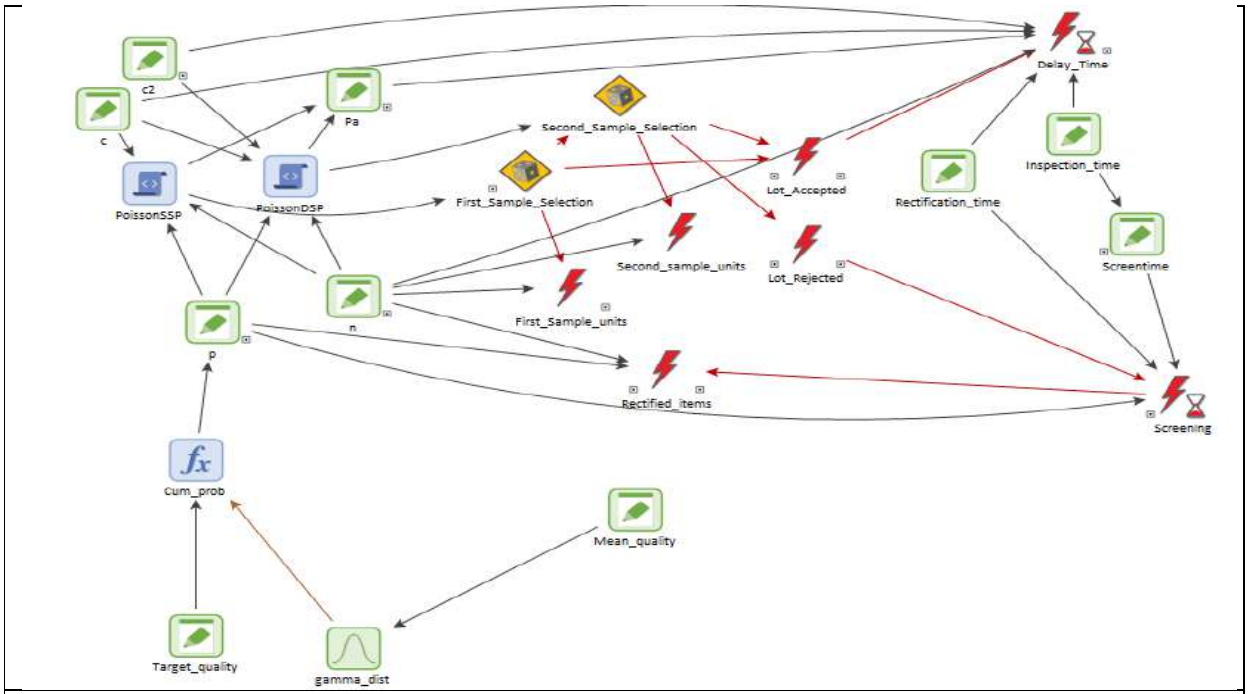

Figure 5: Simulation Model for Integrating SSP with SCC under Gamma

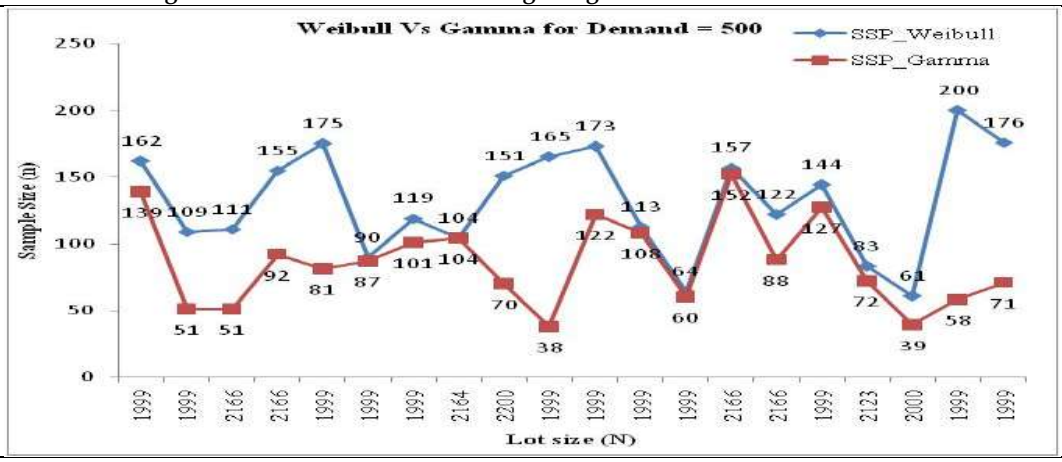

Figure 6: Sample Sizes by Weibull and Gamma for Demand = 500

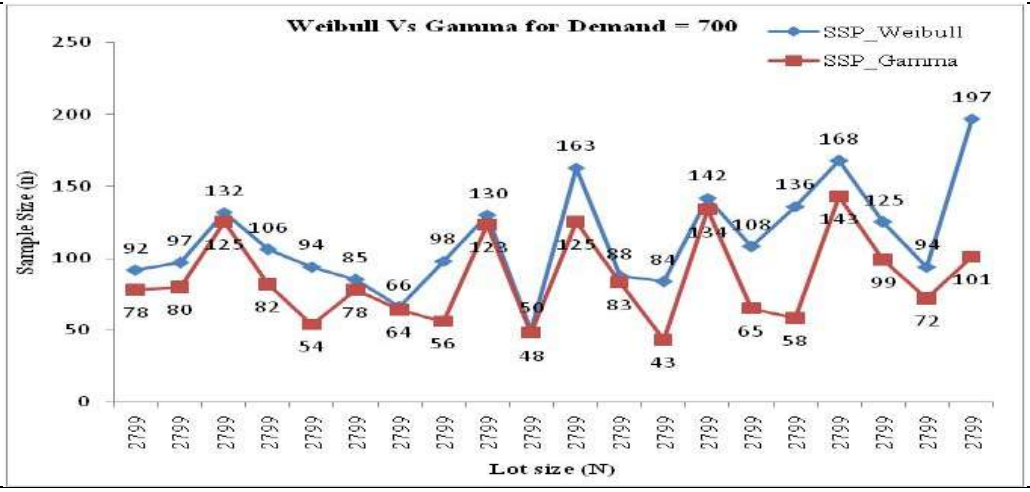

Figure 7: Sample Sizes by Weibull and Gamma for Demand = 700

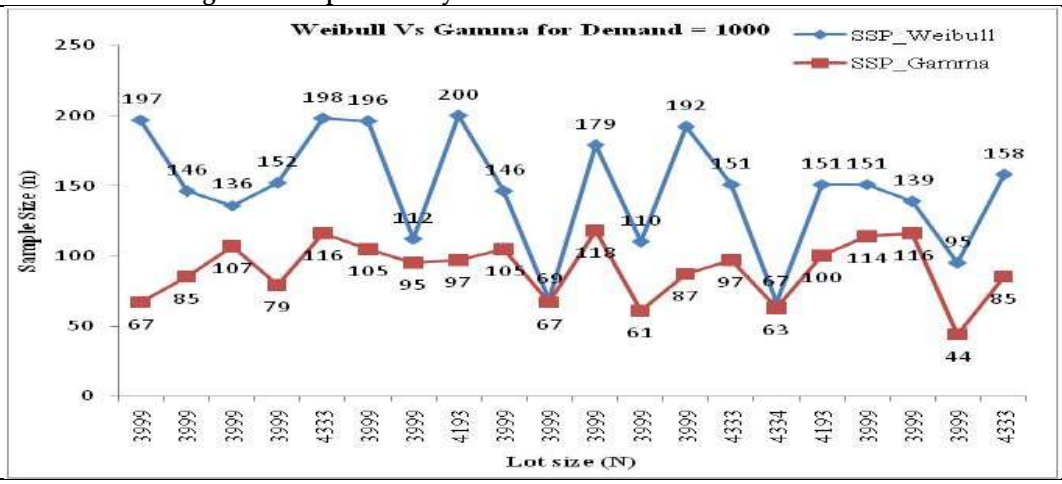

Figure 8: Sample Sizes by Weibull and Gamma for Demand = 1000

Indian Journal of Natural Sciences *www.tnsroindia.org.in ©IJONS*

Vol.15 / Issue 83 / Apr / 2024 *International Bimonthly (Print) – Open Access* *ISSN: 0976 – 0997*

RESEARCH ARTICLE

Some Basic Concepts of Circulant m – Polar Fuzzy Matrices

G.Punithavalli[1]* and M.Rajeswari[2]

[1]Assistant Professor, Department of Mathematics, Annamalai University, Tamil Nadu, India.
[2]Research Scholar, Department of Mathematics, Annamalai University, Tamil Nadu, India.

Received: 17 Oct 2023 Revised: 25 Dec 2023 Accepted: 16 Mar 2024

***Address for Correspondence**
G.Punithavalli
Assistant Professor,
Department of Mathematics,
Annamalai University,
Tamil Nadu, India.
Email: punithavarman78@gmail.com.

ABSTRACT

In this article, It introduces the idea of Circulant m – polar fuzzy matrix . A Circulant matrix is a square matrix whose rows are obtained by cyclically rotating by its first rows. In m - polar fuzzy matrix, each element represents the membership value of an element. We define some operations on circulant m-polar fuzzy matrices .Also we discuss the idea of reflexive, symmetric, antisymmetric, permanent of circulant m - polar fuzzy matrices based on this definitions.

Keywords: Fuzzy Matrices,m -Polar fuzzy matrices(m – PFM), Circulant matrices , Circulant m-polar fuzzy matrices(CmPFM) .

INTRODUCTION

The concept of fuzzy set was introduced by Zadeh in 1965, Which is an extension of the classical notion of the ordinary sets. In a Matrix, the elements which belongs to the interval [0,1]is called fuzzy matrix.When the elements of fuzzy matrices are subintervals of the unit interval [0,1], then the fuzzy matrix is known as Interval - valued Fuzzy Matrix(IVFM). Thomason [13] defined fuzzy Matrices for the first time and discussed the convergence of their powers. A number of findings regarding the convergence of the power sequence of fuzzy matrices were presented by a number of authors .Some properties of the min-max composition of fuzzy matrices were introduced by Ragab and Emam [10]. The idea of Interval-valued fuzzy matrices with Interval-valued fuzzy rows and columns was first proposed by Pal [7]. Shyamal and Pal [11] introduced two new operators and applications of fuzzy matrices. Bhowmik and Pal [1] introduced the concept of circulant triangular fuzzy number matrices (TFNMs) and discussed

some results onTNFMs. The max-min iterates of fuzzy CirculantMatrices were investigated by Hemasinha, Pal and Bezdek [8]. Some of the properties based on the concept of Circulant interval valued fuzzy matrices were outlined by Loganathan and Pushpalatha also the determinant, some binary operations on Circulant interval valued fuzzy matrices are defined. Some results on intuistionstic circulant fuzzy matrix, generalized intuistionistic fuzzy matrix, and IFMs were presented by Bhowmik and Pal [2]. Shyamal and Pal [12] defined the distance between IFMs and hence defined a metric on IFMs. They also cited few applications of IFMs. The m - polar fuzzy set is investigated in many other areas such as m -polar fuzzy graph theory [4].In [5] the$m$ - polar fuzzy matrix is introduced.Pal [9] introduced the new concepts of fuzzy matrix with fuzzy rows and fuzzy columns. In this fuzzy matrix, we assumed that the rows and columns are uncertain. Loganathan C and Pushpalatha V the concept of Circulant Interval -valued fuzzy matrices (CIVFMs) are defined with some of its properties. In this article, the concept of Circulant m- polar fuzzy matrices are defined with some of its properties, some binary operations on Circulant m - polar fuzzy matrix are defined and some important theorems are proved with examples.

Preliminaries

Definition 2.1 [14]A m –polar fuzzy relation(m-PFR)between two mPFS and is defined as a m – PFS. In $r \times s$if R is a relation between r and s , $\alpha \in r$ and $\beta \in s$, if $\psi_1(\alpha,\beta), \psi_2(\alpha,\beta) \ldots . \psi_m(\alpha,\beta)$, are the membership value to which $\alpha$is in relation R with β, then $\psi = (\psi_1, \psi_2 \ldots \psi_m) \in R$

Definition 2.2 [14] Let $\alpha, \beta \in M_f$, where $\alpha = \langle \alpha_1, \alpha_2, \alpha_3, \ldots, \alpha_m \rangle$, $\beta = \langle \beta_1, \beta_2, \beta_3, \ldots, \beta_m \rangle$ then $\alpha \leq \beta$ iff $\alpha + \beta = \beta$.

Definition 2.3 [5] An m – polar fuzzy matrix X = $\langle x_{1_{lt}}, x_{2_{lt}}, x_{3_{lt}}, \ldots, x_{m_{lt}} \rangle$ is a matrix on fuzzy algebra.The zero matrices 0 is a square matrix of order s in which each element are $O_m = \langle 0,0,0, \ldots, 0 \rangle$ and I_s is an identity matrix of order s whose element of the diagonal are $I_m = \langle 1,0,1,0 \ldots 1,0 \rangle$ and the non – diagonal elements are $0_m = \langle 0,0,0, \ldots, 0 \rangle$.

The set $M_{st}$is the set of $s \times t$ rectangular m-PFMs and M_s, the set of $s \times s$ matrices. From the definition, we have if $\mathbb{Q} = [q_{lt}] \in M_{st}$, then $q_{lt} = \langle q_{1_{lt}}, q_{2_{lt}}, q_{3_{lt}}, \ldots, q_{m_{lt}} \rangle \in M_s$, where $\langle q_{1_{lt}}, q_{2_{lt}}, q_{3_{lt}}, \ldots, q_{m_{lt}} \rangle \in [0.1]$ are the m - membership value of the element q_{lt} respectively.

Definition 2.4 [5] If P = $[a_{ij}]_{r \times r}$ is a crisp matrix of order $r \times r$, then the permanent of P is denoted by $per(P)$ and defined as $per(P) = \sum_{\alpha \epsilon V_n} \prod_{i=1}^{n} a_{i\alpha(i)}$. (Where V_n is the symmetric group of order n) .

Definition 2.5 An $n \times n$ fuzzy matrix C is called circulant if and only if $((C^2)) \leq C, (or)$ more explicitly $C_{jk} C_{ki} \leq C_{ij}$ for every k = 1,2,3,…m.$\left(\left(C_1, C_2, C_3, \ldots, C_m \right)^2 \right)' \leq \left(C_1, C_2, C_3, \ldots, C_m \right)$

Result 2.6 An $n \times n$ fuzzy matrix C is circulant and reflexive iff it is similarity.

Proof Suppose that C is circulant and reflexive. Then$C_{ij} = C_{ij}\ C_{jj} \leq C_{ji}$, also $C_{ji} = C_{ji}\ C_{ii} \leq C_{ij}$.So $C_{ij} = C_{ji}$.Hence C is Symmetric. Also, we have $C_{ij} = C_{ij}\ C_{jj} \leq C_{ji}$. ie) C is transitive. Hence C is Similarity. Conversely, Suppose that C is Similarity Then $C_{ij}^{(2)} \leq C_{ij} = C_{ji}$. Hence C is circulant.

Some Basic Result for Circulant m- polar fuzzy matrix

Definition3.1 A m – PFM is said to be circulant m - polar fuzzy matrix(CmPFM), if all the elements of $\mathcal{A}$ can be determined completely by its first row. Suppose the first row of $\mathcal{A}$ is $(C_1', C_1'', C_1''', \ldots C_1^m)$, $(C_2', C_2'', C_2''', \ldots C_2^m)$,… $(C_n', C_n'', C_n''', \ldots C_n^m)$, then any element=($'$, $''$, $'''$,…), n = 1,2,3,…,m of can be determined (throughout the element of the first row) as $C_{ij} = C_{1(n-i+j+1)}$ with a $C_{i(j+k)} = C_{1k}$.A CmPFM of the form

$$\mathcal{A} = \begin{bmatrix} (C_1', C_1'', C_1''', \ldots C_1^m), & (C_2', C_2'', C_2''', \ldots C_2^m), \ldots . & , (C_n', C_n'', C_n''', \ldots C_n^m) \\ (C_n', C_n'', C_n''', \ldots C_n^m), & (C_1', C_1'', C_1''', \ldots C_1^m), \ldots & , (C_{n-1}', C_{n-1}'', C_{n-1}''', \ldots C_{n-1}^m) \\ (C_2', C_2'', C_2''', \ldots C_2^m), & (C_n', C_n'', C_n''', \ldots C_n^m), \ldots . & , (C_1', C_1'', C_1''', \ldots C_1^m) \end{bmatrix}$$

Remark 3.2 (i) It is noted that the matrix m – PFM iscirculant if and only if $C_{ij} = C_{(k \oplus i)(k \oplus j)}$ for every $i, j, k \in$ {1,2,3,....n}, where $\oplus$ is sum module n . Here the entire diagonal elements are equal.

(ii) For a CmPFM $\mathcal{A}$, we notice that $C_{in} = C_{1(j \oplus 1)}$ for every $i, j \in$ {1,2,3,....n}.

(iii) For a CmPFM $\mathcal{A}$, we notice that $C_{i \oplus (n-1)j} = C_{i(j \oplus 1)}$ for every $i, j \in$ {1,2,3,....n}.

Theorem3.3 An $n \times nm$ – PFM$\mathcal{A}$ is circulant if and only if $\mathcal{A}\chi_n = \chi_n \mathcal{A}$, where χ_n is the permutation matrix of m – PFM,where

$\chi_n = \begin{bmatrix} (0,0,0,\dots,0),(0,0,0,\dots,0),\dots(1,1,1,\dots,1) \\ (1,1,1,\dots,1),(0,0,0,\dots,0),\dots(0,0,0\dots,0) \\ \dots\dots. \\ (0,0,0,\dots,0),(0,0,0,\dots,0),\dots(1,1,1,\dots,1) \\ (0,0,0,\dots,0),\dots,(1,1,1,\dots,1)(0,0,0,\dots,0) \end{bmatrix}$.

Proof Let$\mathcal{A}$ be an $m-$ PFM and $\mathcal{X} = \mathcal{A}\chi_n$ then $\mathcal{X}_{ij} = \sum \tilde{a}_{ij}\chi_{kj}$.

In the first row, only χ_{1n} is (1,1,1,…1) and all the other elements are (0,0,0,...0).Therefore we get $\mathcal{X}_{ij} = \tilde{a}_{1(j+1)}$.Let $\mathcal{Y}=\chi_n\mathcal{A}$, Then $\mathcal{Y}_{ij} = \sum C_{ik}\tilde{a}_{kj} = \tilde{a}_{(i+(n-1)j}$.By Remark(iii), $\mathcal{X}_{ij} = \mathcal{Y}_{ij}$for 1,2,3,…). Hence $\mathcal{A}\mathcal{X}_n = \mathcal{X}_n\mathcal{A}$.Therefore we get $\mathcal{A}$ *is* CmPFM.

Example 3.4 Let $\mathcal{X}$ are any two CmPFM of order 3×3, where

$\mathcal{X} = \begin{pmatrix} (0.3,0.5,0.8) & (0.1,0.2,0.4) & (0.2,0.4,0.6) \\ (0.2,0.4,0.6) & (0.3,0.5,0.8) & (0.1,0.2,0.4) \\ (0.1,0.2,0.4\,) & (0.2,0.4,0.6) & (0.3,0.5,0.8) \end{pmatrix}$ and C $= \begin{pmatrix} (0,0,0) & (0,0,0) & (1,1,1) \\ (1,1,1) & (0,0,0) & (0,0,0) \\ (0,0,0) & (1,1,1) & (0,0,0) \end{pmatrix}$

$\mathcal{X}$C = max (0,0.1,0),max(0, 0.2, 0), max (0,0.4,0)= (0.1,0.2,0.3)

= max (0,0,0.2), max(0,0,0.4), max(0,0,0.6)= (0.2,0.4,0.6)

= max (0.3,0,0), max(0.5,0,0), max(0.8,0,0)= (0.3,0.5,0.8)

= max (0,0.3,0), max(0,0.5,0), max(0,0.8,0) = (0.3,0.5,0.8)

= max(0,0,0.1), max(0,0,0.2), max(0,0,0.4) = (0.1,0.2,0.3)

= max (0,0.2,0), max(0,0.4,0), max(0,0.6,0)= (0.2,0.4,0.6)

we get $\mathcal{X}$C $= \begin{pmatrix} (0.1,0.2,0.4) & (0.2,0.4,0.6) & (0.3,0.5,0.8) \\ (0.3,0.5,0.8) & (0.1,0.2,0.4) & (0.2,0.4,0.6) \\ (0.2,0.4,0.6) & (0.3,0.5,0.8) & (0.1,0.2,0.4) \end{pmatrix}$ and

C$\mathcal{X}$= $\begin{pmatrix} (0.1,0.2,0.4) & (0.2,0.4,0.6) & (0.3,0.5,0.8) \\ (0.3,0.5,0.8) & (0.1,0.2,0.4) & (0.2,0.4,0.6) \\ (0.2,0.4,0.6) & (0.3,0.5,0.8) & (0.1,0.2,0.4) \end{pmatrix}$. Therefore $\mathcal{X}$C = C$\mathcal{X}$.

Theorem 3.5 Let $\mathcal{X}$and $\mathcal{Y}$ be any two Circulant m- Polar fuzzy matrices, then it satisfies the following properties (i)$\mathcal{X}+\mathcal{Y}$ is a CmPFM (ii)$\mathcal{X}'$ is a CmPFM (iii) $\mathcal{X}\mathcal{Y}$ is a CmPFM.

ProofIn Particular X^k is also a CmPFM.(i) By definition, the Proof is obvious.

(ii) Since X$\mathcal{X}$ is CmPFM, then $\mathcal{X}$ commutes with χ_n.Therefore we get $\mathcal{X}\chi_n = \chi_n\mathcal{X}$.

Take the transpose on both sides, we get $X'\chi_n{}' = \chi_n{}'X'$.

Pre multiplying by χ_n, we get $\chi_n\,\chi_n{}'X' = \chi_n\,X'\chi_n{}' \Longrightarrow X' = \chi_n X'\chi_n{}'$.

Post multiplying by χ_n, we get $X'\chi_n = \chi_n\,X'\chi_n{}'\chi_n = \chi_n\,X'$. Hence $X'\chi_n = \chi_n\,X'$

(By the Theorem 3.4) A is Circulant $\Leftrightarrow$A$\chi_n = \chi_n$A.

(iii) Since X and Y are CmPFM, each of X and Y commutes with χ_n.Hence XY commutes with χ_n.

(By Remark 3.4(iii)) and by the above theorem, we get XY is CmPFM.

Theorem 3.6 A CmPFM $\mathcal{A}$ is symmetric iff $C_{1i} = C_{1(n-i+2)}$for every $i, j \in$ {1,2,3,....n}.

Proof Let$\mathcal{A}$ *be* symmetric, then $C_{1i} = C_{(1+k)}C_{(i+k)} = C_{i1} = C_{(i+k)}C_{(1+k)}$for every $i, j \in$ {1,2,3,....n}.

Taking $K = n - i$, then

$C_{(1+(n-i))}C_{(i+(n-i))} = C_{(i+(n-i))}C_{(l+(n-i))}$

$= C_{n(n-i+1)} = C_{1(n-i+2)}$(by remark3.4(ii)).

Conversely,Suppose $C_{1i} = C_{1(n-i+2)}$ for every $i \in$ {1,2,3,....n}.Then $C_{1i} = C_{(i+k)}C_{(l+k)}$ for every $i, k \in$ {1,2,3,....n}.Taking $K = n - i$, we get $C_{i1} = C_{n(n-i+1)} = (C+1)_{(n-i+2)} = C_{1i}$.But since $\mathcal{A}$is circulant and $C_{1i} = C_{i1}$.We have $C_{ij} = C_{ji}$ for every $i, k \in$ {1,2,3,....n} and $\tilde{A}$ is symmetric.

Operators on CmPFM

Definition 4.1 Let $\mathcal{A} = (C_{ij})_{n\times n} = (C_1, C_2, C_3, \dots C_m)$ and $\mathcal{B} = (D_{ij})_{n\times n} = (D_1, D_2, D_3, \dots D_m)$

$\mathcal{A} \vee \mathcal{B} = (C_{ij}) \vee (D_{ij}) = (C_1, C_2, C_3, \dots C_m) \vee (D_1, D_2, D_3, \dots D_m) = (C_1 \vee D_1, C_2 \vee D_2, C_3 \vee D_3, \dots, C_m \vee D_m)$

Theorem 4.2 If$\mathcal{A}$and $\mathcal{B}$are two CmPFM then $\mathcal{A} \vee \mathcal{B}$ is also CmPFM.

ProofBy definition above, it is clear that $\mathcal{A}$ and $\mathcal{B}$ are circulant. $\mathcal{A} \vee \mathcal{B}$ is also circulant.

Definition 4.2 The $\wedge$ operation is similar to $\vee$ operation.Let $\mathcal{A} = (C_{ij})_{n\times n} = (C_1, C_2, C_3, \dots C_m)$ and $\mathcal{B} = (D_{ij})_{n\times n} = (D_1, D_2, D_3, \dots D_m)$.$\mathcal{A} \vee \mathcal{B} = (C_{ij}) \wedge (D_{ij}) = (C_1, C_2, C_3, \dots C_m) \wedge (D_1, D_2, D_3, \dots D_m) = (C_1 \wedge D_1, C_2 \wedge D_2, C_3 \wedge D_3, \dots, C_m \wedge D_m)$.

Example 4.3 Consider the 3× 3 circulant m – polar fuzzy matrix

$\mathcal{A}=\begin{pmatrix}(0.2,0.4,0.6) & (0.3,0.5,0.7) & (0.5,0.7,0.9)\\ (0.5,0.7,0.9) & (0.2,0.4,0.6) & (0.3,0.5,0.7)\\ (0.3,0.5,0.7) & (0.5,0.7,0.9) & (0.2,0.4,0.6)\end{pmatrix}$ and

$\mathcal{B}=\begin{pmatrix}(0.3,0.4,0.5) & (0.8,0.9,0.2) & (0.4,0.5,0.6)\\ (0.4,0.5,0.6) & (0.3,0.4,0.5) & (0.8,0.9,0.2)\\ (0.8,0.9,0.2) & (0.4,0.5,0.6) & (0.3,0.4,0.5)\end{pmatrix}$ then

$\mathcal{A}\vee\mathcal{B}=\begin{pmatrix}(0.3,0.4,0.6) & (0.8,0.9,0.7) & (0.5,0.7,0.6)\\ (0.5,0.7,0.6) & (0.3,0.4,0.6) & (0.8,0.9,0.7)\\ (0.8,0.9,0.7) & (0.5,0.7,0.6) & (0.3,0.4,0.6)\end{pmatrix}$ and

$\mathcal{A}\wedge\mathcal{B}=\begin{pmatrix}(0.2,0.4,0.5) & (0.3,0.5,0.2) & (0.4,0.5,0.6)\\ (0.4,0.5,0.6) & (0.2,0.4,0.5) & (0.3,0.5,0.2)\\ (0.3,0.5,0.2) & (0.4,0.5,0.6) & (0.2,0.4,0.5)\end{pmatrix}$

Theorem 4.4 Let $\mathcal{A}=(C_{ij})_{n\times n}=(C_1, C_2, C_3, \dots C_m)$ and $\mathcal{B}=(D_{ij})_{n\times n}=(D_1, D_2, D_3, \dots D_m)$ are two CmPFM.Then (i) $(\mathcal{A}\vee\mathcal{B})^C=\mathcal{A}^C\wedge\mathcal{B}^C$ (ii) $(\mathcal{A}\wedge\mathcal{B})^C=\mathcal{A}^C\vee\mathcal{B}^C$.

Proof Let P = $\mathcal{A}\vee\mathcal{B}$then $\mathcal{P}_{ij}=[C_{ij}\vee D_{ij}]$

$=(C_1, C_2, C_3, \dots, C_m)\vee(D_1, D_2, D_3, \dots, D_m)$

$=[C_1\vee D_1, C_2\vee D_2, C_3\vee D_3, \dots, C_m\vee D_m]$

Let $\mathcal{Q}=P^C$, Then $\mathcal{Q}_{ij}=1-\mathcal{P}_{ij}=[1-C_{ij}\vee D_{ij}]=(1,1,1,\dots,m)-C_{ij}\vee D_{ij}$

$=(1,1,1,\dots m)-(C_1, C_2, C_3, \dots, C_m)\vee(D_1, D_2, D_3, \dots, D_m)$

$=(1-C_1\vee D_1, 1-C_2\vee D_2, 1-C_3\vee D_3, \dots, 1-C_m\vee D_m)$

Let $\mathcal{R}=\mathcal{A}^C\wedge\mathcal{B}^C$, then $\mathcal{R}_{ij}=(1-C_{ij})\wedge(1-D_{ij})$

$=[(1,1,1,\dots,1)-(C_1, C_2, C_3, \dots, C_m)]\wedge[(1,1,1,\dots 1)-(D_1, D_2, D_3, \dots D_m)]=1-C_{ij}\vee D_{ij}$

Hence $(\mathcal{A}\vee\mathcal{B})^C=\mathcal{A}^C\wedge\mathcal{B}^C$

Example 4.5 Let$\mathcal{A}=\begin{pmatrix}(0.2,0.4,0.6) & (0.2,0.3,0.4)\\ (0.2,0.3,0.4) & (0.2,0.4,0.6)\end{pmatrix}$ and$\mathcal{B}=\begin{pmatrix}(0.7,0.6,0.5) & (0.5,0.6,0.7)\\ (0.5,0.6,0.7) & (0.7,0.6,0.5)\end{pmatrix}$ be 2× 2 CmPFM, then$\mathcal{A}\vee\mathcal{B}=\begin{pmatrix}(0.7,0.6,0.6) & (0.5,0.6,0.7)\\ (0.5,0.6,0.7) & (0.7,0.6,0.6)\end{pmatrix}$

$(\mathcal{A}\vee\mathcal{B})^{CC}=1-(\mathcal{A}\vee\mathcal{B})=\begin{pmatrix}(0.3,0.4,0.4) & (0.5,0.4,0.3)\\ (0.5,0.4,0.3) & (0.3,0.4,0.4)\end{pmatrix}$

$\mathcal{A}^C=\begin{pmatrix}(0.8,0.6,0.4) & (0.8,0.7,0.6)\\ (0.8,0.7,0.6) & (0.8,0.6,0.4)\end{pmatrix}$ and $\mathcal{B}^C=\begin{pmatrix}(0.3,0.4,0.5) & (0.5,0.4,0.3)\\ (0.5,0.4,0.3) & (0.3,0.4,0.5)\end{pmatrix}$

$\mathcal{A}^C\wedge\mathcal{B}=\begin{pmatrix}(0.3,0.4,0.4) & (0.5,0.4,0.3)\\ (0.5,0.4,0.3) & (0.3,0.4,0.4)\end{pmatrix}$. Hence $(\mathcal{A}\vee\mathcal{B})^C=\mathcal{A}^C\wedge\mathcal{B}^C$

Definition 4.6 A matrix $\mathcal{A}$ is said to be symmetric Circulant m-polar fuzzy matrix if $\mathcal{A}=\mathcal{A}'$.

Example 4.7

Consider the 3× 3CmPFM$\mathcal{A}=\begin{pmatrix}(0.3,0.2,0.3) & (0.2,0.1,0.2) & (0.2,0.1,0.2)\\ (0.2,0.1,0.2) & (0.3,0.2,0.3) & (0.2,0.1,0.2)\\ (0.2,0.1,0.2) & (0.2,0.1,0.2) & (0.3,0.2,0.3)\end{pmatrix}$ and

$\mathcal{A}'=\begin{pmatrix}(0.3,0.2,0.3) & (0.2,0.1,0.2) & (0.2,0.1,0.2)\\ (0.2,0.1,0.2) & (0.3,0.2,0.3) & (0.2,0.1,0.2)\\ (0.2,0.1,0.2) & (0.2,0.1,0.2) & (0.3,0.2,0.3)\end{pmatrix}$

Definition 4.8 A matrix $\mathcal{A}\in F^{n\times n}$ is said to be K – Symmetric Circulant m - polar fuzzy matrix if K$\mathcal{A}^TK=\mathcal{A}$.The following examples shows the antisymmetriccirculant m – polar fuzzy matrix

Let 3×3 CmPFM$\mathcal{A}=\begin{pmatrix}(0.3,0.2,0.3) & (0.2,0.1,0.2) & (0.2,0.1,0.2)\\ (0.2,0.1,0.2) & (0.3,0.2,0.3) & (0.2,0.1,0.2)\\ (0.2,0.1,0.2) & (0.2,0.1,0.2) & (0.3,0.2,0.3)\end{pmatrix}$ and

K$=\begin{pmatrix}(0,0,0) & (0,0,0) & (1,1,1)\\ (1,1,1) & (0,0,0) & (0,0,0)\\ (0,0,0) & (1,1,1) & (0,0,0)\end{pmatrix}$ then K$\mathcal{A}^TK=\begin{pmatrix}(0.2,0.1,0.2) & (0.2,0.1,0.2) & (0.3,0.2,0.3)\\ (0.3,0.2,0.3) & (0.2,0.1,0.2) & (0.2,0.1,0.2)\\ (0.2,0.1,0.2) & (0.3,0.2,0.3) & (0.2,0.1,0.2)\end{pmatrix}\neq\mathcal{A}$. Therefore K –anti symmetric CmPFM.

Permanent Circulant m - polar fuzzy Matrix(CmPFM)

Definition 5.1 Let $\mathcal{A} = [a_{rs}]_{x\times y}$ be a Circulant m –polar fuzzy matrix , where $a_{rs} = (a_{1s}^{(1)}, a_{1s}^{(2)}, \dots\dots a_{1s}^{(m)})$, and $0\leq a_{rs}^{(m)} \leq 1$, for all k. Then the permanent of $\mathcal{A}$is denoted by $\mathcal{P}$ert($\mathcal{A}$) and defined as $\mathcal{P}\text{ert}(\mathcal{A}) = \sum_{\alpha\epsilon V_n} \prod_{i=1}^{n} a_{i\alpha(i),}$ for $x \leq y$.(where V is the set of all one to one mapping from {1,2,3,…,x}to {1,2,3,…,y}) and $\mathcal{P}ert(\mathcal{A}) = \sum_{\alpha\epsilon V_n} \prod_{i=1}^{n} a_{i\alpha(i).}$ for $x > y$.

Remark 5.2 Two expressions are written for the permanent of matrix, for $x > y$, there are one – one mapping from {1,2,3,…,y}to {1,2,3,…,x}. But the one – one mapping is not possible from {1,2,3,…,x}to {1,2,3,…,y}.

Example 5.3 Let 3×3 CmPFM $\mathcal{A}$= $\begin{pmatrix} (0.2,0.4,0.6) & (0.3,0.6,0.5) & (0.5,0.6,0.7) \\ (0.5,0.6,0.7) & (0.2,0.4,0.6) & (0.3,0.6,0.5) \\ (0.3,0.6,0.5) & (0.5,0.6,0.7) & (0.2,0.4,0.6) \end{pmatrix}$ then

$\mathcal{P}ert(\mathcal{A})$=max(min(0.2,0.4,0.6)(0.2,0.4,0.6)(0.2,0.4,0.6), min(0.3,0.6,0.5)(0.3,0.6,0.5)(0.3,0.6,0.5),
min(0.5,0.6,0.7)(0.5,0.6,0.7)(0.5,0.6,0.7) , min(0.5,0.6,0.7)(0.2,0.4,0.6)(0.3,0.6,0.5),
min(0.3,0.6,0.5)(0.5,0.6,0.7)(0.2,0.4,0.6), min(0.2,0.4,0.6)(0.3,0.6,0.5)(0.5,0.6,0.7)) .
= max((0.2,0.4,0.6)(0.3,0.6,0.5)(0.5,0.6,0.7)(0.2,0.4,0.5)(0.2,0.4,0.5)(0.2,0.4,0.5).
= (0.5,0.6,0.7)

Note 5.4 Some properties of permanent CmPFMs.

(i)For any triangular or diagonal CmPFM $\mathcal{A}$. per ($\mathcal{A}$) = min of its diagonal entries.

(ii)For any row CmPFM such that both $\mathcal{AB}$ and $\mathcal{BA}$ are defined, then $per(\mathcal{AB}) \neq per(\mathcal{BA})$.

(iii)For any row CmPFM or column CmPFM $\mathcal{A}$, per($\mathcal{A}$) =max of the entries.

Example 5.5

Let $\mathcal{A} = \begin{pmatrix} (0.1,0.2,0.3) & (0,0,0) & (0,0,0) \\ (0,0,0) & (0.1,0.2,0.3) & (0,0,0) \\ (0,0,0) & (0,0,0) & (0.1,0.2,0.3) \end{pmatrix}$

$\mathcal{A}$=max(min(0.1,0.2,0.3)(0.1,0.2,0.3)(0.1,0.2,0.3)
min(0,0,0)(0,0,0)(0,0,0) min(0,0,0)(0,0,0)(0,0,0)).
=max (0.1,0.2,0.3) = (0.1,0.2,0.3).

REFERENCES

1. Bhowmik M, Pal M and Pal A "Circulant triangular fuzzy number matrices", *Journal of physical Sciences*, 12 (2008) 141-154.
2. Bhowmik M and Pal M, Some results on intuitionistic fuzzy matrices and circulant intuitionistic fuzzy matrices, *International Journal of Mathematical Sciences*, 7(1-2) (2008) 81-96.
3. Loganathan C and Pushpalatha V, Circulant Interval valued Fuzzy Matrices, *Annals of pure and Applied Mathematics*, (2018) 313-322.
4. Ghorai G and Pal M, Some properties of m-polar fuzzy graphs, Pacific Science Review A: Natural Science and Engineering, 18 (1) (2016) 38-46.
5. GoirikaSaha, Convergence, Permanent and g-inverse of m-polar Fuzzy Matrix, Progress in Nonlinear Dynamic and Chaos,(2020) 41 -51.
6. Hashimoto H, Convergence of power of a fuzzy transitive matrix, *Fuzzy Sets and Systems*, 9 (1983) 153-160.
7. Hemasinha R, Pal N. R, and Bezdek J C, Iterates of fuzzy circulant matrices *Fuzzy Sets and Systems*, 60 (1993) 199-206.
8. Pal M, Interval-valued fuzzy matrices with fuzzy rows and columns, *Fuzzy Information and Engineering*, 7(3) (2015) 335-368.
9. Pal M, Fuzzy matrices with fuzzy rows and fuzzy columns, *Journal of Intelligent and Fuzzy Systems*, 30(1) (2015) 561-573.
10. Ragab M Z and Emam E G, On the min-max composition of fuzzy matrices, *Fuzzy Sets and Systems*, 75 (1995) 83-92.

11. Shyamal A K and Pal M, Two new operations on fuzzy matrices, *Journal of Applied Mathematics and Computing*, 15 (2004) 91-107.
12. Shyamal A K and Pal M, Triangular fuzzy matrices, *Iranian Journal of Fuzzy Systems*, 4 (1) (2007) 75-87.
13. Thomason M G, Convergence of powers of a fuzzy matrix, *J. Math Anal. Appl*., 57 (1977) 476-480.
14. Tan Y J, Eigenvalues and eigenvectors for matrices over distributive lattice, Linear Algebra Appl., 283 (1998) 257-272.
15. Ramakrishna MankenaTEigenvalues and Eigenvectors of an m-Polar Fuzzy Matrix, International Journal of Future Generation Communication and Networking Vol. 13, No. 3, (2020), pp. 3685–3698

Indian Journal of Natural Sciences *www.tnsroindia.org.in ©IJONS*

Vol.15 / Issue 83 / Apr / 2024 *International Bimonthly (Print) – Open Access* *ISSN: 0976 – 0997*

RESEARCH ARTICLE

Semi Closed Sets in Interval Valued Neutrosophic Topological Spaces

S.Sathiya[1]* and A.Puspalatha[2]

[1]Research Scholar, Department of Mathematics, Government Arts College, Udumalpet, Tiruppur (Affiliated to Bharathiar University, Coimbatore), Tamil Nadu, India.
[2]Associate Professor, Department of Mathematics, Government Arts and Science College, Pollachi, (Affiliated to Bharathiar University), Coimbatore, Tamil Nadu, India.

Received: 24 Nov 2023 Revised: 09 Jan 2024 Accepted: 16 Mar 2024

***Address for Correspondence**
S.Sathiya
Research Scholar, Department of Mathematics,
Government Arts College, Udumalpet, Tiruppur
(Affiliated to Bharathiar University, Coimbatore),
Tamil Nadu, India.
Email: sathiyasanthg6@gmail.com

ABSTRACT

The intention of this paper is to introduce a new concept in interval valued neutrosophic topological spaces called interval valued neutrosophic semi open sets. Further, we study the properties of interval valued neutrosophic semi closed sets, which is the complements of interval valued neutrosophic semi open sets.

Keywords: Interval valued neutrosophic set, Interval valued neutrosophic topology, Interval valued neutrosophic semi closed set, Interval valued neutrosophic semi open set.

INTRODUCTION

Fuzzy set theory, which Zadeh developed in 1965[16], characterizes fuzzy sets as membership functions that allocate a degree of membership between zero and one to each article.In 1983, Atanassov introduced the intuitionistic fuzzy set[2], a generalization of fuzzy sets with membership functions and non-membership functions between zero and one. Smarandache introduced the neutrophobic set[10], three separate membership functions—truth, indeterminacy, and falsity-that range from zero to one make up this idea.The neutrosophic set is a mathematical technique that is used for dealing with problems comprising inconsistent, imprecise, and indeterminate data.Wang, Smarandache, Zhang, and Sunderraman introduced the interval valued neutrosophic set [15] and discussed the characteristics of it. Recently, Interval valued neutrosophic topology [7]introduced and studied its properties by Nandhini. T and Puspalatha. A. In this paper, we introduce new sets called Interval valued neutrosophic semi open set and semi closed set and also to discuss its properties in interval valued neutrosophic topological spaces.

Preliminaries:

Defintion 2.1 [15] Let $\widetilde{X}$ be space of points(objects), with a element in $\widetilde{X}$ denoted by y. An interval valued netrosophic set (IVNS in short) G in $\widetilde{X}$ is characterized by truth-membership function I_G, indeterminacy-membership function I_G and false- membership function F_G. For each point y in X, $T_E(y), I_E(y), F_E(y) \subseteq [0,1]$.

Definition 2.2[15] (containment) . Let$\wedge$ denotes infimum of any interval between[0,1]. Let$\vee$ denotes supremum of any interval between[0,1].An IVNSG is contained in the other IVNSH, $G \subseteq H$, if and only if

$\wedge T_G(y) \leq \wedge T_H(y), \vee T_G(y) \leq \vee T_H(y)$

$\wedge I_G(y) \geq \wedge I_H(y), \vee I_G(y) \geq \vee I_H(y)$

$\wedge F_G(y) \geq \wedge F_H(y), \vee F_G(y) \geq \vee F_H(y)$ for all y in $\widetilde{X}$.

Definition2.3 [15] Two IVNSsG and H are equal, written as $G = H$, if and only if $G \subseteq H$ and $H \subseteq G$. Let $0_N = \langle [0,0],[1,1],[1,1] \rangle$, $1_N = \langle [1,1],[0,0],[0,0] \rangle$.

Definition 2.4[15] (Complement) The complement of an IVNSG is denoted by $\overline{G}$ and is defined by $T_{\overline{G}}(y) = F_G(y)$; $\inf I_{\overline{G}}(y) = 1 - \sup I_G(y)$; $\sup I_{\overline{G}}(y) = 1 - \inf I_G(y)$; $F_{\overline{G}}(y) = T_G(y)$ for all y in $\widetilde{X}$ and $\overline{\overline{G}} = G$.

Definition 2.5[15] (Intersection) The intersection of two IVNSsG and H is an IVNSI, written as $I = G \cap H$, whose truth- membership function, indeterminacy-membership function and false-membership function are related to those of G and H by

(i) $\wedge T_I(y) = \min(\wedge T_G(x), \wedge T_H(x))$

$\vee T_I(x) = \min(\vee T_G(x), \vee T_H(x))$

(ii) $\wedge I_I(x) = \max(\wedge I_G(x), \wedge I_H(x))$

$\vee I_I(x) = \max(\vee I_G(x), \vee I_H(x))$

(iii) $\wedge F_I(x) = \max(\wedge F_G(x), \wedge F_H(x))$

$\vee F_I(x) = \max(\vee F_G(x), \vee F_H(x))$ for all y in $\widetilde{X}$.

Theorem 2.6[15]$I = G \cap H$ is largest IVNS contained in both G and H .

Definition2.7 [15](Union) The union of two IVNSsG and His an IVNSI, written as I = GUH, whose truth – membership function, indeterminacy – membership function and false membership function are related to those of G and H by

(i) $\wedge T_I(y) = \max(\wedge T_G(y), \wedge T_H(y))$,

$\vee T_I(y) = \max(\vee T_G(y), \vee T_H(y))$

(ii) $\wedge I_I(x) = \min(\wedge I_G(y), \wedge I_H(y))$,

$\vee I_I(x) = \min(\vee I_G(y), \vee I_H(y))$

(iii) $\wedge F_I(x) = \min(\wedge F_G(y), \wedge F_H(y))$,

$\vee F_I(x) = \min(\vee F_G(y), \vee F_H(y))$ for all y in $\widetilde{X}$.

Theorem 2.9[15] I = GUH is smallest IVNS containing both GandH.

Definition2.10[5] An interval valued neutrosophic topological space(IVN topological space in short) of IVNS is a pair $(\widetilde{X}, \tau_{IVN})$ where $\widetilde{X}$ is a nonempty set and τ_{IVN} is a family of IVNSs on $\widetilde{X}$ satisfying the following axioms:

(i) $0_N, 1_N \in \tau_{IVN}$

(ii) $G, H \in \tau_{IVN} \Rightarrow G \cap H \in \tau_{IVN}$

(iii) $G_i \in \tau_{IVN}, i \in I \Rightarrow \cup_{i \in I} G_i \in \tau_{IVN}$

τ_{IVN}Members are called interval valued neutrosophic open sets (IVNOS in short). A Interval valued neutrosophic set F is called interval valued neutrosophic closed set (IVNCS in short) if and only if the complement of Fis IVNOS.

Theorem 2.11 [5] Let $(\widetilde{X}, \tau_{IVN})$ be a IVN topological space and $G, H \in IVNSs(\widetilde{X})$ then the following properties holds:

(i)IVÑInt(G)$\subseteq$G

(ii)$G \subseteq H \Rightarrow$IVÑInt(G)$\subseteq$IVÑInt(H)

(iii)$IV\tilde{N}Int(G) \in \tau_{IVN}$
(iv)$G \in \tau_{IVN}$ iff $IV\tilde{N}Int(G) = G$
(v)$IV\tilde{N}Int\left(IV\tilde{N}Int(G)\right) = IV\tilde{N}Int\,(G)$
(vi)$IV\tilde{N}Int(0_N) = 0_N, IV\tilde{N}Int(1_N) = 1_N$

Theorem 2.12[5]Let $(\tilde{X}, \tau_{IVN})$ be a IVN topological space and $G, H \in IVNSs(\tilde{X})$ then the following properties holds:
(i)$G \subseteq IV\tilde{N}Cl(H)$
(ii)$G \subseteq H \Rightarrow IV\tilde{N}Cl(G) \subseteq IVNCl(H)$
(iii)$(IV\tilde{N}Cl(G))^c \in \tau_{IVN}$
(iv) $G^c \in \tau_{IVN}$ iff $IV\tilde{N}Cl(G) = G$
(v)$IV\tilde{N}Cl\left(IV\tilde{N}Cl(A)\right) = IV\tilde{N}Cl(A)$
(vi)$IV\tilde{N}Cl(0_N) = 0_N, IV\tilde{N}Cl(1_N) = 1_N$

Theorem 2.13[5]Let$(\tilde{X}, \tau_{IVN})$be*IVN*topological space and $G, H \in IVNSs(\tilde{X})$thenholdthefollowingproperties:
(i)$IV\tilde{N}Int(G \cap H) = IV\tilde{N}Int(G) \cap IV\tilde{N}Int(H)$
(ii)$IV\tilde{N}Int(G \cup H) \supseteq IV\tilde{N}Int(G) \cup IV\tilde{N}Int(H)$

(iii)$IVN\tilde{N}Cl(G \cup H) = IV\tilde{N}Cl(G) \cup IV\tilde{N}Int(H)$
(iv)$IV\tilde{N}Cl(G \cap H) = IV\tilde{N}Cl(G) \cap IV\tilde{N}Int(H)$
(v)$(IV\tilde{N}Int(G))^C = IV\tilde{N}Cl(G^C)$
(vi)$(IV\tilde{N}Cl(G))^C = IV\tilde{N}Int(G^C)$

Interval Valued Neutrosophic Semi Open Sets:
we present new concept called Interval valued neutrosophic semi open set (IVNSOS in short) in IVN topology and also analyse its characterizations.
Definition3.1 Let Gbe IVNSof a IVN topological space (X, τ_{IVN}). Then G is said to an IVNSOS of $\tilde{X}$ if there exist an IVNOS such that $IV\tilde{N}OS(G) \subseteq G \subseteq IV\tilde{N}Cl(IVNOS(G))$.
Theorem 3.2 An IVNS G in a IVN topological space $(\tilde{X}, \tau_{IVN})$ is an IVNSOS if and only if $G \subseteq IV\tilde{N}Cl\left(IV\tilde{N}Int(G)\right)$.
Proof: Sufficiency: Consider $G \subseteq IV\tilde{N}Cl\left(IV\tilde{N}Int(G)\right)$.
Then for$IVNOS(G) = IV\tilde{N}Int(G)$, we have,$IVNOS(G) \subseteq G \subseteq IV\tilde{N}Cl(IVNOS(G))$.
Necessity: Let G be a IVNSOS in $\tilde{X}$. Then $IVNOS(G) \subseteq G \subseteq IV\tilde{N}Cl(IVNOS(G))$ for some IVNOS G. But $IVNOS(G) \subseteq IV\tilde{N}Int(G)$ and therefore $IV\tilde{N}Cl(IVNOS(G)) \subseteq IV\tilde{N}Cl\left(IV\tilde{N}Int(G)\right)$. Hence $G \subseteq IV\tilde{N}Cl(IVNOS(G)) \subseteq IV\tilde{N}Cl\left(IV\tilde{N}Int\,(G)\right)$.
Theorem:3.3 Let $(\tilde{X}, \tau_{IVN})$ be a IVN Topological space. Then the union of two IVNSOSs is an IVNSOS in a IVN Topological space $(\tilde{X}, \tau_{IVN})$.
Proof: Assume G and H be IVNSOSs in$(\tilde{X}, \tau_{IVN})$, then $G \subseteq IV\tilde{N}Cl\left(IV\tilde{N}Int(A)\right)$ and $H \subseteq IV\tilde{N}Cl\left(IV\tilde{N}Int(H)\right)$.Therefore $G \cup H \subseteq IV\tilde{N}Cl\left(IV\tilde{N}Int(G)\right) \cup IV\tilde{N}Cl\left(IV\tilde{N}Int(H)\right) \subseteq$
$IV\tilde{N}Cl\left(\left(IV\tilde{N}Int\,(G)\right) \cup \left(IV\tilde{N}Int(H)\right)\right) \subseteq IV\tilde{N}Cl(\left(IV\tilde{N}Int(G \cup H)\right))$, by theorem 2.13. Hence $G \cup H$ is a IVNSOS in $\tilde{X}$.

Theorem:3.4 Let $(\tilde{X}, \tau_{IVN})$ be an IVN topological space. If $\{G_i\}_{i \in \Delta}$ is a collection of IVNSOSs in an IVNSs in $\tilde{X}$. Then $\cup_{i \in \Delta} G_i$ is IVNSOS in$\tilde{X}$.
Proof : For each $i \in \Delta$, there exists a $IVNOSG_i$such that$IVNOS(G_i) \subseteq G_i \subseteq IV\tilde{N}Cl(IVNOS\,(G_i))$. Then $\cup_{i \in \Delta} IVNOS(G_i) \subseteq \cup_{i \in \Delta} G_i \subseteq \cup_{i \in \Delta} IV\tilde{N}Cl(IVNOS(A_i)) \subseteq IV\tilde{N}Cl(\cup_{i \in \Delta} IVNOS\,(G_i))$. Let $IVNOS(G) = \cup_{i \in \Delta} IVNOS(G_i)$. Hence $IVNOS(G) \subseteq \cup_{i \in \Delta} G_i \subseteq IV\tilde{N}Cl(IVNOS(G))$. Hence the proof.
Remark:3.5 As the following example illustrates, the intersection of any two IVNSOSs need not be an IVNSOS in $\tilde{X}$.
Example:3.6 Consider$\tilde{X} = \{f, g\}$ and IVNSs are
$0_N = \langle [0,0], [1,1], [1,1] \rangle$, $1_N = \langle [1,1], [0,0], [0,0] \rangle$,

$A = \langle \frac{([0.1,0.4],[0.2,0.7],[0.4,0.6])}{f}, \frac{([0.6,0.8],[0.2,0.3],[0.2,0.3])}{g} \rangle$

$B = \langle \frac{([0.1,0.3],[0.3,0.8],[0.5,0.8])}{f}, \frac{([0.2,0.7],[0.4,0.8],[0.3,0.7])}{g} \rangle$

Then $\tau_{IVN} = \{0_N, A, B, 1_N\}$ is IVN topological space on $\tilde{X}$.

Consider IVNS C as follows

$$C = \langle \frac{([0.2,0.3],[0.1,0.2],[0.2,0.3])}{f}, \frac{([0.6,0.9],[0.2,0.3],[0.1,0.2])}{g} \rangle$$

Now IVNSs A and C are IVNSOSs. But its intersection,

$A \cap C = \langle \frac{([0.1,0.3],[0.2,0.7],[0.4,0.6])}{f}, \frac{([0.6,0.8],[0.2,0.3],[0.2,0.3])}{g} \rangle$

is not an IVNSOS in IVN topological space $\tilde{X}$.

Theorem: 3.7 Let G be IVNSOS in IVN topological space,$G \subseteq H \subseteq IV\tilde{N}Cl(G)$. Then H is also an IVNSOS in $\tilde{X}$.

Proof: Since G is an IVNSOS, there exists IVNOS'G' such that $IVNOS(G) \subseteq G \subseteq IV\tilde{N}Cl(IVNOS(G))$. Since $G \subseteq H$then $IVNOS(G) \subseteq H$ and $IV\tilde{N}Cl(G) \subseteq IV\tilde{N}Cl(IVNOS(G))$ and therefore $G \subseteq IV\tilde{N}Cl(IVNOS(G))$. Hence $IVNOS(H) \subseteq H \subseteq IV\tilde{N}Cl\,(IVNOS(H))$ and hence His an IVNSOS in $\tilde{X}$.

Theorem 3.8 Every IVNOS G in the IVN Topological space $(\tilde{X}, \tau_{IVN})$ is IVNSOS in $\tilde{X}$.

Proof: Let G be an IVNOS in IVN topological space $\tilde{X}$. Then we have $G = IV\tilde{N}Int(G)$. Also $IV\tilde{N}Int(G) \subseteq IV\tilde{N}Cl\left(IV\tilde{N}Int(G)\right)$. Therefore $G \subseteq IV\tilde{N}Cl\left(IV\tilde{N}Int(G)\right)$. Hence by theorem 3.2, G is a IVNSOS in $\tilde{X}$.

Remark 3.9: The following example indicates that the converse of the mentioned above theorem may not be true.

Example 3.10: Let $X = \{f, g\}$and IVNSs are

$0_N = \langle [0,0],[1,1],[1,1] \rangle$, $1_N = \langle [1,1],[0,0],[0,0] \rangle$,

$A = \langle \frac{([0.1,0.4],[0.2,0.7],[0.4,0.6])}{f}, \frac{([0.6,0.8],[0.2,0.3],[0.2,0.3])}{g} \rangle$

$B = \langle \frac{([0.1,0.3],[0.1,0.6],[0.5,0.8])}{f}, \frac{([0.2,0.7],[0.1,0.2],[0.3,0.7])}{g} \rangle$

$\tau_{IVN} = \{0_N, A, B, 1_N\}$is IVN topology in the IVN topological space $(\tilde{X}, \tau_{IVN})$.Considerthe IVNS 'C' as

$C = \langle \frac{([0.2,0.5],[0.3,0.8],[0.3,0.5])}{f}, \frac{([0.8,0.9],[0.2,0.4],[0.1,0.2])}{g} \rangle$

C is IVNSOS but not IVNOS in IVN topological space$(\tilde{X}, \tau_{IVN})$.

Interval Valued Neutrosophic Semi Closed Sets:

Definition4.1 Let G be IVNS of a IVN topological space $\tilde{X}$. Then H is said to be an interval valued neutrosophic semi closed set (IVNSCS in short) of $\tilde{X}$ if there exist an IVNCS'G' such that $IV\tilde{N}Int(IVNCS(G)) \subseteq G \subseteq IVNCS(G)$.

Theorem:4.2 A IVNSG in an IVN topological space $\tilde{X}$ is IVNSCS if and only if $IV\tilde{N}Int\left(IV\tilde{N}Cl(G)\right) \subseteq G$.

Proof: Sufficiency: Let $IV\tilde{N}Int\left(IV\tilde{N}Cl(G)\right) \subseteq G$. Then for $IVNCS(G) = IV\tilde{N}Cl(G)$, we have $IV\tilde{N}Int(IVNCS(G)) \subseteq A \subseteq (IVNCS(G))$.

Necessity: Let G be an IVNSCS in $(\tilde{X}, \tau_{IVN})$. Then $IV\tilde{N}Int(IVNCS(G)) \subseteq G \subseteq IV\tilde{N}CS(G)$ for some IVNCS 'G'. But $IV\tilde{N}Cl(G) \subseteq IVNCS(G)$ and thus $IV\tilde{N}Int\left(IV\tilde{N}Cl(G)\right) \subseteq IV\tilde{N}Int(IVNCS(G))$.

Hence $IV\tilde{N}Int\left(IV\tilde{N}Cl(G)\right) \subseteq IV\tilde{N}Int(IVNCS(G)) \subseteq G$.

Theorem : 4.3 Let $(\tilde{X}, \tau_{IVN})$ be a IVN topological space and G be a IVNS of X. Then A is an IVNSCS if and only if $\overline{G}$ is IVNSOS in $\tilde{X}$.

Proof: Necessity: Take G be a IVNSCS of $\tilde{X}$. Then by theorem 4.2,$IV\tilde{N}Int\left(IV\tilde{N}Cl(G)\right) \subseteq G$. Both sides taking complement, $\overline{G} \subseteq \overline{IV\tilde{N}Int(IV\tilde{N}Cl(G))} = IV\tilde{N}Cl(\overline{IV\tilde{N}Cl(G)})$. This implies $\overline{G} \subseteq IV\tilde{N}Cl(IV\tilde{N}Int(\overline{G}))$. By theorem 3.2, $\overline{G}$ is IVNSOS.

Sufficiency: Let $\overline{G}$ isan IVNSOS in $\widetilde{X}$. This implies $\overline{G} \subseteq IV\tilde{N}Cl(IV\tilde{N}Int(\overline{G}))$. Both sides taking complement, $G \supseteq \overline{(IV\tilde{N}Cl(IV\tilde{N}Int\,\overline{G}))} = IV\tilde{N}Int(\overline{IV\tilde{N}Int\overline{G}})$. This implies $G \supseteq IV\tilde{N}Int\left(IV\tilde{N}Cl(G)\right)$. By theorem 4.2, G is IVNSCS in $\widetilde{X}$.

Theorem:4.4 Let $(\widetilde{X}, \tau_{IVN})$ be an IVN topological space$(\widetilde{X}, \tau_{IVN})$. Then the intersection of two IVNSCSs is a IVNSCS in IVN topological space $(\widetilde{X}, \tau_{IVN})$.

Proof : Let G and H be IVNSCSs in $\widetilde{X}$. Then $IV\tilde{N}Int\left(IV\tilde{N}Cl(G)\right) \subseteq G$, and $IV\tilde{N}Int\left(IV\tilde{N}Cl(H)\right) \subseteq H$. We have $G \cap H \supseteq IV\tilde{N}Int\left(IV\tilde{N}Cl(G)\right) \cap IV\tilde{N}Int\left(IV\tilde{N}Cl(H)\right) = IV\tilde{N}Int\left(IV\tilde{N}Cl(G) \cap IV\tilde{N}Cl(H)\right) = IV\tilde{N}Int(IV\tilde{N}Cl(G \cap H)$.

By theorem 4.2, $G \cap H$ is a IVNSCS in $\widetilde{X}$.

Theorem:4.5 Let $(\widetilde{X}, \tau_{IVN})$ be a IVN topological space. If $\{G_i\}_{i\in\Delta}$ is a collection of IVNSCSs in a IVNSs in $\widetilde{X}$. Then $\bigcap_{i\in\Delta} G_i$ is IVNSOSs in $\widetilde{X}$.

Proof : For each $i \in \Delta$, there exist a IVNCS G_i such that $IV\tilde{N}Int(IVNCS(G_i)) \subseteq G_i \subseteq (IVNCS(G_i))$. Then $IV\tilde{N}Int(\bigcap_{i\in\Delta}(IVNCS(G_i)) \subseteq \bigcap_{i\in\Delta} IV\tilde{N}Int((IVNCS(G_i)) \subseteq \bigcap_{i\in\Delta} G_i \subseteq \bigcap_{i\in\Delta}(IVNCS(G_i))$. let $IVNCS(G) = \bigcap_{i\in\Delta}(IVNCS(G_i))$. Hence the proof.

Remark:4.6 The union of any two IVNSCSs need not be an IVNSCS in $\widetilde{X}$ as seen from the following example.

Example:4.7

Let $\widetilde{X} = \{f, g\}$and IVNSs are

$0_N = \langle [0,0], [1,1], [1,1] \rangle$, $1_N = \langle [1,1], [0,0], [0,0] \rangle$,

$A = \langle \frac{([0.1,0.4], [0.2,0.7], [0.4,0.6])}{f}, \frac{([0.6,0.8], [0.2,0.3], [0.2,0.3])}{g} \rangle$

$B = \langle \frac{([0.1,0.3], [0.3,0.8], [0.5,0.8])}{f}, \frac{([0.2,0.7], [0.4,0.8], [0.3,0.7])}{g} \rangle$

Then $\tau_{IVN} = \{0_N, A, B, 1_N\}$ is IVN topological space.Consider an IVNSCS 'C' as follows

$C = \langle \frac{([0.2,0.3], [0.1,0.2], [0.2,0.3])}{f}, \frac{([0.6,0.9], [0.2,0.3], [0.1,0.2])}{g} \rangle$

Here C and B are IVNSCSs. But its intersection

$A \cap C = \langle \frac{([0.1,0.3], [0.2,0.7], [0.4,0.6])}{f}, \frac{([0.6,0.8], [0.2,0.3], [0.2,0.3])}{g} \rangle$

is not an IVNSCSin $\widetilde{X}$.

Theorem:4.8 Let G be IVNSCS in IVN topological space $(\widetilde{X}, \tau_{IVN})$ and suppose that $IV\tilde{N}Int(G) \subseteq H \subseteq G$. Then G is an IVNSCS in $\widetilde{X}$.

Proof: Let A be IVNSCS in $(\widetilde{X}, \tau_{IVN})$. There exists a IVNCS 'G' such that $IV\tilde{N}Int(IVNCS(G)) \subseteq G \subseteq IVNCS(G)$. Now $IV\tilde{N}Int\left(IV\tilde{N}Cl(G)\right) \subseteq IV\tilde{N}Int(G)$ and hence $IV\tilde{N}Int(IVNCS(G)) \subseteq H$. Hence$IV\tilde{N}Int(IVNCS(H)) \subseteq H \subseteq IVNCS(H)$. Hence H is an IVNSCS in $\widetilde{X}$.

Theorem:4.9 Every IVNCS in the IVN topological space$\widetilde{X}$ is IVNSCS in $\widetilde{X}$.

Proof: Let G be IVN closed set in IVN topological space $\widetilde{X}$. Then $G = IV\tilde{N}Cl(G)$. Also $IV\tilde{N}Int\left(IV\tilde{N}Cl(G)\right) \subseteq IV\tilde{N}Cl(G)$. This implies that $IV\tilde{N}Int\left(IV\tilde{N}Cl(G)\right) \subseteq G$. By theorem 4.2, G is IVNSCS in $\widetilde{X}$.

Remark: 4.10 The converse of the preceding theorem does not need to be true, as demonstrated by the following example.

Example: 4.11 Let $X = \{f, g\}$and IVNSs are

$0_N = \langle [0,0], [1,1], [1,1] \rangle$, $1_N = \langle [1,1], [0,0], [0,0] \rangle$,

$A = \langle \frac{([0.5,0.6], [0.3,0.6], [0.2,0.8])}{f}, \frac{([0.2,0.7], [0.1,0.2], [0.4,0.5])}{g} \rangle$

$B = \langle \frac{([0.3,0.4],[0.4,0.7],[0.3,0.9])}{f}, \frac{([0.1,0.5],[0.3,0.5],[0.6,0.7])}{g} \rangle$

$C = \langle \frac{([0.5,0.6],[0.3,0.5],[0.2,0.8])}{f}, \frac{([0.2,0.8],[0.1,0.2],[0.3,0.4])}{g} \rangle$

$D = \langle \frac{([0.3,0.5],[0.3,0.7],[0.2,0.9])}{f}, \frac{([0.2,0.5],[0.1,0.5],[0.4,0.5])}{g} \rangle$

Then $\tau_{IVN} = \{0_N, A, B, C, D, 1_N\}$ is IVN topological space on $\tilde{X}$.

Consider

$E = \langle \frac{([0.4,0.6],[0.2,0.6],[0.1,0.8])}{f}, \frac{([0.3,0.6],[0.1,0.4],[0.3,0.4])}{g} \rangle$

E is an IVNSCS but not an IVNCS in $\tilde{X}$.

Semi-interior in IVN Topological Space

Definition 5.1: Let $(\tilde{X}, \tau_{IVN})$ be a IVN topological space. Then for a IVNSG of X, the interval valued neutrosophic semi interior of A [IVNŠInt(A)in short] is the union of all IVNSOSs of X contained in G. That is, IVNŠInt(G) = ∪{L: L is a IVNSOSs in $\tilde{X}$ and L ⊆G}.

Proposition 5.2: Let $(\tilde{X}, \tau_{IVN})$ be an IVN topological space. Then for any IVNSsG and H of an IVNS $\tilde{X}$ we have

i) IVNŠInt(G)⊆ H

ii) G is IVNSOS set in X ⇔ IVNŠInt(G) = G

iii) $\text{IVNŠInt}\left(\text{IVNŠInt(G)}\right) = \text{IVNŠInt(G)}$

iv) If G⊆H then IVNŠInt(G)⊆IVNŠInt(H)

Proof:

(i) follows from definition 5.1.

(ii) Let G be IVNSOS in $\tilde{X}$. Then G⊆ IVNŠInt(G). By using (i) we get that IVNŠInt(G) = G. Conversely assume thatIVNŠInt(G) = G. By definition 5.1, G is an IVNSOS in $\tilde{X}$. Hence (ii).

(iii) $\text{IVNŠInt}\left(\text{IVNŠInt(G)}\right) = \text{IVNŠInt(G)}$, by using (ii). Hence (iii).

(iv) Given G⊆H , using (i), IVNŠInt(G)⊆G ⊆H⇒IVNŠInt(G)⊆H and $\text{IVNŠInt}\left(\text{IVNŠInt(G)}\right) \subseteq \text{IVNŠInt(H)}$. By (iii) we have IVNŠInt(G)⊆ IVNŠInt(H). Hence (iv).

Theorem :5.3 Let $(\tilde{X}, \tau_{IVN})$ be a IVN topological space. Then for any IVNSsG and H of an IVN topological space$\tilde{X}$, we have

(i)IVNŠInt(G∩H) = IVNŠInt(G)∩ IVNŠInt(H)

(ii)IVNŠInt(G∪H)⊇IVNŠInt(G)∪IVNŠInt(H)

Proof: (i) For any IVNSsG and H we have G∩H⊆G and G∩H⊆H , using proposition 5.2(iv), IVNŠInt(G∩H)⊆IVNŠInt(G) and IVNŠInt(G∩H)⊆IVNŠInt(H). Therefore IVNŠInt(G∩H)⊆IVNSŠInt(G)∩ IVNŠInt(H) ----------(1).

By proposition 5.2(i), IVNŠInt(G)⊆G and IVNŠInt(H)⊆ H⇒IVNŠInt(G)∩IVNŠInt(H)⊆G∩H. By using Proposition 5.2 (iv), $\text{IVNŠInt}\left(\text{IVNŠInt(G)}\cap\text{IVNŠInt(H)}\right) \subseteq \text{IVNŠInt(G}\cap\text{H)}$.

By applying(1), $\text{IVNŠInt}\left(\text{IVNŠInt(G))}\cap\text{IVNŠInt(IVNŠInt(H)}\right) \subseteq \text{IVNŠInt(G}\cap\text{H)}$. By applying 5.2 (iii) IVNŠInt(G)∩ IVNŠInt(H)⊆ IVNŠInt(G∩H)----------(2).

From (1) and (2) IVNŠInt(G∩H) = IVNŠInt(G)∩ IVNŠInt(H). Hence (i).

(ii) For any IVNSsG and H we have G⊆G∪H and G⊆G∪H, by applying proposition 5.2 (iv)IVNŠIntG⊆ IVNŠInt(G∪H) and IVNŠIntH ⊆ IVNŠInt(G∪H)⇒IVNŠIntG ∪ IVNŠIntH ⊆IVNŠInt(G∪H). This implies (ii).

In Theorem 5.3 (ii), the equality need not be hold as seen from the below example.

Example:5.4 Let $\widetilde{X} = \{f, g\}$ and IVNSs are
$0_N = \langle [0,0], [1,1], [1,1] \rangle$, $1_N = \langle [1,1], [0,0], [0,0] \rangle$,
$A = \langle \frac{([0.1,0.5], [0.2,0.6], [0.4,0.8])}{f}, \frac{([0.6,0.9], [0.2,0.5], [0.2,0.4])}{g} \rangle$
$B = \langle \frac{([0.1,0.2], [0.3,0.8], [0.5,0.8])}{f}, \frac{([0.2,0.7], [0.4,0.7], [0.3,0.7])}{g} \rangle$
Now, $\tau_{IVN} = \{0_N, A, B, 1_N\}$is IVN topological space.Consider the IVNSs C and D are
$C = \langle \frac{([0.1,0.5], [0.3,0.6], [0.5,0.8])}{f}, \frac{([0.4,0.9], [0.2,0.5], [0.2,0.4])}{g} \rangle$
$D = \langle \frac{([0.1 ,0.3], [0.2,0.8], [0.4,0.9])}{f}, \frac{([0.6,0.7], [0.3,0.6], [0.2,0.5])}{g} \rangle$
Now, IVNŠIntC $= 0_N$ and IVNŠIntD $= 0_N$. This implies that IVNŠInt C∪IVNŠIntD $= 0_N$.Now, the union of IVNSs C and D is C∪D = A. IVNŠInt C∪D = A. Hence IVNŠInt(A∪B)⊄ IVNŠInt (A)∪IVNŠInt (B).

Semi-Closure in IVN Topological Spaces

Definition 6.1: Let $(\widetilde{X}, \tau_{IVN})$ be a IVN topological space. Then for a IVNS G of $\widetilde{X}$, the interval valued neutrosophic semi closure of G [IVNŠCl(G) in short] is the intersection of all IVNSCSs of $\widetilde{X}$ containingG.
That is, IVNŠCl(G) =∩ {M: M is a IVNSCS in X and M⊇G}.

Proposition 6.2: Let $(\widetilde{X}, \tau_{IVN})$ be a IVN topological space. Then for any IVNSG of $\widetilde{X}$,
(i)$\overline{\left(\text{IVNŠInt (G)}\right)} = \text{IVNŠCl}(\overline{G})$
(ii)$\overline{\left(\text{IVNŠCl(G)}\right)} = \text{IVNŠInt}(\overline{G})$.

Proof: By applying definition 5.1, IVNŠInt(G) = ∪ {L: L is a IVNSOSs in $\widetilde{X}$ and L⊆G }. Applying complement on both sides, We have$\overline{\left(\text{IVNŠInt(G)}\right)} = \overline{(\cup\{\text{L: L is a IVNSOS in X and L}\subseteq \text{G }\})} = \cap\{\overline{L}: \overline{L} \text{ is a IVNSCS in X and } \overline{G}\subseteq\overline{L}\}$. By replacing $\overline{L}$ by K, we get that $\overline{\left(\text{IVNŠInt(A)}\right)} = \cap\{K: K \text{ IVNSCS in } \widetilde{X} \text{and } \overline{G}\subseteq K\}$. By applying definition 6.1, $\overline{\left(\text{IVNŠInt(G)}\right)} = \text{IVNŠCl}(\overline{G})$. Hence (i).
By applying (i), $\overline{\left(\text{IVNŠInt}(\overline{G})\right)} = \text{IVNŠCl}(\overline{(\overline{G})}) = \text{IVNŠCl(G)}$. By applying complement on both sides, $\text{IVNŠInt}(\overline{G}) = \overline{\left(\text{IVNŠCl(G)}\right)}$. Hence (ii).

Proposition 6.3: Let $(\widetilde{X}, \tau_{IVN})$ be a IVN topological space. Then for any IVNSG and H of a IVN topological space$\widetilde{X}$. We have
(i) G⊆ IVNŠCl(G).
(ii) A is IVNSCS in $\widetilde{X} \Leftrightarrow$ IVNŠCl(G) = G
(iii) $\text{IVNŠCl}\left(\text{IVNŠCl(G)}\right) = \text{IVNŠCl(G)}$
(iv) If G⊆H then IVNŠCl(G)⊆IVNŠCl(H).

Proof: From the definition 6.1, (i) follows.
Let Gbe IVNSCS in $\widetilde{X}$. By applying theorem 4.3,$\overline{G}$is a IVNSOS in $\widetilde{X}$.
By proposition 5.2 (ii), $\text{IVNŠInt}\overline{G} = \overline{G} \Leftrightarrow \overline{\left(\text{IVNŠCl(G)}\right)} = \overline{G} \Leftrightarrow \text{IVNŠCl(G)} = \text{G}$. Hence (ii).
By applying (ii), $\text{IVNŠCl}\left(\text{IVNŠCl(G)}\right) = \text{IVNŠCl(G)}$. Hence (iii).
Given G⊆H, then $\overline{H}\subseteq\overline{G}$. By applying proposition 5.2 (iv), $\text{IVNŠInt}(\overline{H})\subseteq\text{IVNŠInt}(\overline{G})$. Applying complement on bothsides,$\overline{\left(\text{IVNŠInt}(\overline{H})\right)} \supseteq (\overline{\text{IVNŠInt}(\overline{G})})$. By proposition 6.2 (ii), IVNŠCl(G)⊆IVNŠCl(H). Hence (iv).

Proposition 6.4: Let G be a IVNS in IVN topological space$(\widetilde{X}, \tau_{IvN})$. Then IVNĬInt$(G)$⊆IVNŠInt(G)⊆G⊆IVNŠCl(G)⊆IVNĈl(G).

Proof: Proof follows from the corresponding definitions.

Proposition 6.5: Let (X, τ_{IVN}) be a IVN topological space. Then for any IVNSsG and H of a IVN topological space X. we have

(i)IVNŠCl(G∪H) = IVNŠCl(G)∪IVNŠCl(H)

(ii)IVNŠCl(G∩H)⊆IVNŠCl(G)∩IVNŠCl(H)

Proof: We know IVNŠCl (G∪H) = IVNŠCl$\left(\overline{\left(\left(\overline{G \cup H}\right)\right)}\right)$. By applying Proposition 6.2(i), IVNŠCl(G∪H) = $\overline{\text{IVNŠInt}\left(\overline{G \cup H}\right)}$ = $\overline{(\text{IVNŠInt}\left(\left(\overline{G} \cap \overline{H}\right)\right)}$.

By applying 5.3(i), IVNŠCl(G∪H) = $\overline{\left(\text{IVNŠInt}\left(\overline{G}\right) \cap \text{IVNŠInt}\left(\overline{H}\right)\right)}$ = $\left(\overline{\text{IVNŠInt}\left(\overline{G}\right)} \cup \overline{(\text{IVNŠInt}\left(\overline{H}\right)}\right)$.

By applying proposition 6.2(i), IVNŠCl(G∪H) = IVNŠCl($\overline{\overline{G}}$ ∪ IVNŠCl($\overline{\overline{H}}$) = IVNŠCl(G) ∪ IVNŠCl(H). Hence (i).

We know G∩H⊆G and G∩H⊆H, by using proposition 6.3(iv), IVNŠCl(G∩H)⊆IVNŠCl(G) and IVNŠCl(G∩H)⊆IVNŠCl(H).

⇒ IVNŠCl(G∩H)⊆IVNŠCl(G)∩IVNŠCl(H). Hence (ii).

In Theorem 6.3 (ii), the equality need not be hold as seen from the below given example.

Example:6.6

Let $\widetilde{X} = \{a, b\}$ and IVNSs are

$0_N = \langle [0,0], [1,1], [1,1] \rangle$, $1_N = \langle [1,1], [0,0], [0,0] \rangle$,

$A = \langle \frac{([0.2,0.6], [0.2,0.7], [0.5,0.9])}{f}, \frac{([0.7,0.9], [0.3,0.6], [0.3,0.5])}{g} \rangle$

$B = \langle \frac{([0.1,0.2], [0.2,0.9], [0.6,0.9])}{f}, \frac{([0.3,0.8], [0.5,0.8], [0.4,0.8])}{g} \rangle$

$\tau_{IVN} = \{0_N, A, B, 1_N\}$ is IVN topological space. Consider IVNSs C and D as follows

$C = \langle \frac{([0.6,0.7], [0.1,0.2], [0.2,0.9])}{f}, \frac{([0.4,0.6], [0.2,0.3], [0.1,0.5])}{g} \rangle$

$D = \langle \frac{([0.8,0.9], [0.1,0.9], [0.8,0.9])}{f}, \frac{([0.6,0.7], [0.1,0.6], [0.2,0.8])}{g} \rangle$

And their intersection is

$C \cap D = \langle \frac{([0.6,0.7], [0.2,0.9], [0.8,0.9])}{f}, \frac{([0.4,0.6], [0.2,0.6], [0.2,0.8])}{g} \rangle$

Now, IVNŠCl(C∩D) = H^c and IVNŠCl(C) = 1_N and IVNŠCl(D) = 1_N. We have IVNŠCl(C)∩ IVNŠCl(D) = 1_N Hence IVNŠCl(C)∩IVNŠCl(D)⊄ IVNŠCl(C∩D).

Theorem 6.7: Let $(\widetilde{X}, \tau_{IVN})$ be an IVN topological spaces. Then for any IVNSs G and H of an IVN topological space $\widetilde{X}$ we have,

(i) IVNŠCl(G)⊇G∪IVNŠCl(IVNŠInt(G))

(ii) IVNŠInt(G)⊆G∩IVNŠInt(IVNŠCl(G))

(iii) IVNĬInt$\left(\text{IVNŠCl(G)}\right)$ ⊆IVNĬInt$\left(\text{IVNĈl(G)}\right)$

(iv) IVNĬInt$\left(\text{IVNŠCl(G)}\right)$⊇ IVNĬInt(IVNŠCl(IVNŠInt(G)))

Proof:

By applying Proposition 6.3(i), G⊆IVNŠCl(G)----------(1)

By applying Proposition 5.2 (i), IVNŠInt(G)⊆G. Implies IVNŠCl$\left(\text{IVNŠInt(G)}\right)$⊆IVNŠCl(G). Hence(i).

By proposition 5.2(i), IVNŠInt(G)⊆G……(1). And by proposition 6.3(1), G⊆IVNŠCl(G).

Now, IVNŠInt(G)⊆ IVNŠInt(IVNŠCl(G))……..(2).

From (1) and (2) wegetIVNŠInt(G)⊆G∩IVNŠInt(IVNŠCl(G)). Hence (ii).

By proposition 6.4, $IVN\tilde{S}Cl(G) \subseteq IV\tilde{N}Cl(G)$. Wehave $IV\tilde{N}Int\left(IVN\tilde{S}Cl(G)\right) \subseteq IV\tilde{N}Int\left(IV\tilde{N}Cl(G)\right)$.This proves (iii).

By(i),$IVN\tilde{S}Cl(G) \supseteq G \cup IVN\tilde{S}Cl\left(IVN\tilde{S}Int(G)\right)$. Implies $IV\tilde{N}Int\left(IVN\tilde{S}Cl(G)\right) \supseteq IV\tilde{N}Int\left(G \cup IVN\tilde{S}Cl\left(IVN\tilde{S}Int(G)\right)\right)$.

We have $IV\tilde{N}Int(G \cup H) \supseteq IV\tilde{N}Int(G) \cup IV\tilde{N}Int(H)$.

Hence $IV\tilde{N}Int\left(IVN\tilde{S}Cl(G)\right) \supseteq IV\tilde{N}Int(G) \cup IV\tilde{N}\left(IVN\tilde{S}Cl\left(IVN\tilde{S}Int(G)\right)\right) \supseteq IV\tilde{N}(IVN\tilde{S}Cl\left(IVN\tilde{S}Int(G)\right)$

This proves (iv).

REFERENCES

1. Atanassov. K, Intuitionistic fuzzy sets. *In VII ITKR's Session;Publishing House:* Sofia, Bulgaria, (1983).
2. Atanassov.K, Intuitionistic fuzzy sets, *Fuzzy sets and systems* 20(1986), 87-96.
3. Chang.C.L, Fuzzy Topological spaces, *J.Math.Anal.Appl*.24 (1968), 182-190.
4. Dogan Coker, An introduction to intuitionistic fuzzy topological spaces, *Fuzzy Sets and System*, 88(1997), 81-89.
5. Floretin Smarandache, A unifying field in logics, neutrosophy : Neutrosophic probability set and logic, *American Research Press, Rehoboth*, (1999).
6. Floretin Smarandache, Neutrosophy and Neutrosophic Logic, *First International Conference* on Neutrosophy, Neutrosophic Logic, Set, Probability, and Statistics Unversity of New Mexico, Gallup, NM 87301, USA(2002), smarad@unm,edu.
7. Nanthini. T and Pushpalatha. A, Interval Valued Neutrosophic Topological space, *Neutrosophic Sets and Systems*, Vol. (32), (2020).
8. Salama. A.A and Alblowi.S.A, Neutrosophic sets and Neutrosophic topological space, *ISOR J. Mathematics*, Vol. (3), Issue (4), (2012).Pp-31-35.
9. Salama. A.A and Alblowi.S.A, Generalized Neutrosophic Set and Generalized Neutrosophic Topological Spaces, Journal computer Sci. Engineering, Vol. (2), (2012), No.(7).
10. Floretin Smaradache, Neutrosophic set – a generalization of intuitionistic fuzzy sets, in *J. Pure Appl. Math*.24 (2005), 287297.
11. Floretin Smaradache, Neutrosophic set – A generalization of intuitionisticfuzzy sets, *Journal of Defense Resourses Management*. 1(2010), 107-116.
12. Iswarya.P and Bageertthi. K, On Neutrosophic semi-open sets in Neutrosophic topological spaces, *International Jour. of Math, Trends and Tech*. (2016), 214-223.
13. Lupianez.F.G, Interval Neutrosophic Sets and Topology, Proceedings of 13th WSEAS, *International conference on Applied Mathematics(MATH'08)*Kybernetes,38(2009) 621-624.
14. Turksen. I, Interval valued fuzzy sets based on normal forms, *Fuzzy sets and systems 20*(1986), 191-210.
15. Wang.H, Smarandache.H, Zhang Y.Q, Sunderraman R., Interval Neutrosophic sets and logic: Theory and Applications in computing ,Hexis (2005)
16. Zadeh.L.A, Fuzzy sets, *Inform. And control* 8(1965), 338-353.

Indian Journal of Natural Sciences *www.tnsroindia.org.in ©IJONS*

Vol.15 / Issue 83 / Apr / 2024 *International Bimonthly (Print) – Open Access* *ISSN: 0976 – 0997*

RESEARCH ARTICLE

Isolation, Optimization and Purification of Alkaline Protease from Bacillus subtilis Isolated from Trash Fish Hydrolysate

R.Anburaj[1]*, G. Roseline Jebapriya[2] ,P.Sivaranjani[3], S.Vanmathi vidhyashini[1] ,K.Raja[4]

[1]AssociateProfessor, Department of Biotechnology and Microbiology, National College (Autonomous), (Affiliated to Bharathidasan University) Tiruchirapalli, Tamil Nadu, India.
[2]Scientist, Department of Marine Science, National College (Autonomous), (Affiliated to Bharathidasan University) Tiruchirapalli, Tamil Nadu, India
[3]Research Scholar, Department of Marine Biology, Annamalai University, Tamil Nadu, India.
[4]Assistant Professor, Department of Marine Biology, Annamalai University, Tamil Nadu, India.

Received: 16 Nov 2023 Revised: 17 Jan 2024 Accepted: 16 Jan 2024

***Address for Correspondence**
R.Anburaj
AssociateProfessor,
Department of Biotechnology and Microbiology,
National College (Autonomous), (Affiliated to Bharathidasan University)
Tiruchirapalli, Tamil Nadu, India.
Email: anbu_nanthu@rediffmail.com

ABSTRACT

Forty two bacterial strains were isolated from hydrolyzed trash fish wastes and qualitatively screened for alkaline protease activity. Of the screened bacterial strains, one promising isolate identified as *Bacillus subtilis* through morphological and biochemical characterization exhibited potent alkaline protease activity. The optimal pH and temperature for alkaline protease production was found to be pH 9, and 37ºC, respectively. Maximum alkaline protease activity was observed with glucose and peptone as carbon and nitrogen source, respectively. The protease enzyme was purified by acetone precipitation, DEAE (Diethylaminoethyl) sephadox A-50 ion exchange column chromatography. Purified protease enzyme showed specific activity of 169.08 U/mL of protein with purification fold of 7.59. The SDS (*Sodium dodecyl sulfate*) polyacrylamide gel electrophoresis analysis revealed that the protease enzyme has the relative molecular weight of 60 kDa.

Keywords: Trash fish waste; *Bacillus subtilis;* alkaline protease; column chromatography.

INTRODUCTION

Marine resources provide enormous benefits for human needs both in terms of food and economy, but in general the fishing activities produce large quantities of organic waste and it can accumulate on the pool as well as suspended in the water column near the coastal and its adjacent areas. The low economic value (adults and damaged) fishes that are discarded during the process of post harvesting by-catching, poor handling, storage, distribution and processing limit the utilization of a portion of the landed catches known as trash fish for direct human consumption. In India 10 to 20 % of trash fishes are landed in total fish catches [1]. Discarding of these trash fish creates enormous environmental problem. So far, only limited trash fish used for traditional products such as salted fish, fish crackers, fish sauce and fish meal [2] Apart from which fish wastes has many positive roles some of them are used as an animal feed, biodiesel/biogas, natural pigments, cosmetics, fertilizers, dietic applications, food packaging and enzyme isolation especially proteases. The enzyme isolated from these fish wastes has numerous economical values [3].

Protease refers to a group of enzymes whose catalytic function is to hydrolyze proteins. They are also called proteolytic enzymes or proteinases. Proteases are one of the most important groups of industrial enzymes, and commercial proteases account for nearly 60% of the total industrial enzyme market [4]. They are widely used in leather processing, detergent industry, food industries, bioremediation process, pharmaceutical, textile industry, waste processing companies, and in the film industry etc. [5,6]. Proteases are obtained from plants and animal organs. In recent years a number of studies have been conducted to characterize alkaline protease from different microorganisms. However, many of the alkaline proteases applied to industrial purposes face some limitations such as low stability towards surfactants and production of enzymes are very expensive [7]. It has been well demonstrated that, a large proportion of commercially available proteases are derived from *Bacillus* strains [8]. Proteases derived from *Bacillus* strains have wide applications in pharmaceutical, leather, laundry, food and waste processing industries (Pastor et al. 2001). In view of the commercial interest, microbes from varied habitants have been examined by many researchers for industrially suitable alkaline protease [9]. Instead of these cost effective growth medium for the production of alkaline proteases from an alkalophilic *Bacillus* sp. is especially important. Generally, the amount of enzyme produced greatly depends on strain and growth conditions. Therefore, there is a need to the search of new strains of bacteria that produce proteolytic enzymes with novel properties and the development of cost effective medium. The present investigation aimed to isolate, optimize enzyme production (submerged fermentation) and purification of alkaline protease from *Bacillus subtilis*.

MATERIALS AND METHODS

Isolation of Proteolytic Bacteria

The fish wastes were collected from Annankoil landing centre, Parangipettai. The fish wastes were then hydrolyzed for 21 days in closed container. At different time interval (0, 7, 14 and 21 days) 1 g sample was taken from hydrolyzed fish waste and transferred to a sterile conical flask (250 mL) containing 100 mL of sterile distilled water and serial dilutions (up to 10^{-6}) of suspensions were prepared. One hundred millilitre of aliquots was aseptically inoculated on medium containing 5 g of beef extract, 5 g of peptone, 5 g of glucose, 3 g of sodium chloride, 15 g of agar in 1000 mL of 50 % seawater at pH of 7.0 and incubated at 30°C for 24 to 48 h.

Screening and Identification of Proteolytic Bacteria

The purified bacterial isolates were streaked on skim milk agar plates containing 5 g of peptone, 10 g of glucose, 5 g of yeast extract, 0.1 g of casein hydrolysate, 15 g of agar in 1000 mL 50 % seawater at a pH of 7.0 and were incubated at 37ºC for 24 to 48 h. The isolates showing a clear zone of casein hydrolysis were identified as protease producers. Protease positive isolates were identified based on morphological and biochemical characterization according to Bergey's manual of determinative bacteriology [10].

Optimization for Alkaline Protease Production Under Submerged Fermentation

The optimization studies included the production of protease under different pH (6-10) and incubation temperature (25°C, 30°C, 35°C, 37ºC, 40°C) of the growth medium, supplementation of the growth medium with different carbon sources (10 g/L), such as lactose, maltose, dextrose, glucose and sucrose as well as different nitrogen sources (5 g/L), peptone, beef extract, yeast extract, ammonium sulphate, urea, sodium nitrate and tryptone, respectively.

Mass Production Of Alkaline Protease Under Submerged Fermentation

The culture media used for mass production of protease contains Glucose1 % (w/v), peptone 0.5 %, KH_2PO4 0.2 %, $MgSO4 \cdot 7H_2O$ 0.2 %, Casein 1 % and pH 9.0. It was maintained at 37°C for 48 h in a shaking incubator. Then 1 mL of enriched seed culture was inoculated into 250 mL flask containing 100 mL optimizing media. The culture was then incubated for 48 h under shaking condition at 140 rpm. At the end of incubation period, the whole culture broth was centrifuged at 10,000 rpm for 15 min, to remove the cellular debris and the clear supernatant was used for enzyme assay and purification.

Protease Assay

The proteolytic activity of cell free supernatant of PAB28 was determined by following the method of Olajuyigbe and Ajela [(10)]. The assay system consists of following ingredients such as 1.25 mL Tris buffer (pH 7.2), 0.5 mL of 1 % aqueous casein solution, and 0.25 mL culture supernatant. Approximate controls were also made by adding assay mixture without culture filtrate. The mixture was incubated for 30 min at 30ºC. After incubation, 3 mL of 5 % ice cold tricarboxylic acid (TCA) was added to this mixture, and the formed precipitate was placed at 4ºC for 10 min and centrifuged at 5000 rpm for 15 min. After centrifugation, the cell free supernatant was collected. To 0.5 mL of supernatant, 0.5 M sodium carbonate (2.5 mL) was added and the mixture incubated for 20 min. Five hundred milliliter of folin phenol reagent was added to the mixture and the absorbance was read at 660 nm using UV-Vis Spectrophotometer. The amount of protease produced was measured with the help of a tyrosine standard graph. The protease activity was expressed in micrograms of tyrosine released under standard assay conditions [11, 12,13]. Specific enzyme activity was expressed as units/mg of protein.

Protein Estimation

To determine the protease specific activity, the concentration of soluble protein in the cell free sample was estimated by the method described by Lowry et al.[14] by using bovine serum albumin as a standard.

Partial Purification and Gel Electrophoretic Characterization of Alkaline Protease

The supernatant were precipitated by adding two volumes of acetone and kept for 1 h at 4ºC to allow complete precipitation. The resulting precipitate was collected by centrifugation at 1000 rpm for 30 min and the pellet was air dried and resuspended in a minimal volume of 20 mM Tris HCl buffer (pH 7.2). Finally, the insoluble substances were removed by centrifugation at 1000 rpm for 30 min. The supernatant thus obtained was applied to ion exchange column chromatography of DEAE sephadex - A50 (2.5 to 3.0 cm), which had been equilibrated with 20 mM Tris Hcl (pH 7.2). After loading the sample, the column was washed with the same buffer until the optical density of the elution was zone at 280 nm. The bound proteins were then eluted with a linear gradient of sodium chloride in the range of 0.1 to 1 M in the equilibrating buffer. 4 mL of each fraction was collected at a flow rate of 40 mL/h. The enzyme activity and protein content of the each fraction were determined. Homogeneity of the protein was checked by SDS-PAGE, According to Laemmle's method (1970) to determine the molecular weight of partially purified protease. The molecular weight of the protease was determined from broad range molecular weight (10-250 kDa) protein standards.

Statistical Analysis

In all experiments, the measurements were carried out with duplicated parallel cultures. Test for significant difference was analyzed using one way analysis of variance (ANOVA) by SPSS 11.5 software.

RESULTS

Forty two bacterial strains were isolated from hydrolyzed fish wastes. Out of 42 bacterial strains, twenty five strains were exhibiting proteolytic activity. From the protease positive bacteria, one potential candidate PSR28 was selected for further studies based on the largest zone of casein hydrolysis greater than 10 mm in diameter which was highest as compared to other isolated strains. Based on the morphological and biochemical characterization, the isolate PAB28 was identified as *Bacillus subtilis*. The effect of pH on protease production was tested with different range from 6 to 10 and maximum activity of 188.97 U/mL at pH 9 and minimum activity of 79.88 U/mL at pH 6 was observed (Fig. 1). The influence of temperature on protease production was determined at different temperatures ranged from 25°C to 40°C. Maximum protease production of 216.48 U/mL was observed at 37ºC and the minimum enzyme production of 61.10 U/mL was recorded at temperature 25ºC. However, increase in temperature beyond 37°C led to decline in protease production (Fig. 2).

In continuation of assessment of effect of pH and temperature on protease enzyme production, further, a range of carbon and nitrogen sources were tested to maximize protease production. As shown in figure 3, of the five different carbon sources tested, glucose was the most effective sole carbon source resulting in the increased protease activity of 142.78 U/mL. Similarly, of the five different nitrogen sources tested, the maximum enzyme activity of 142.38 U/mL was observed in the presence of peptone added medium (Fig. 4). Whereas, ammonium sulphate shown minimum (27.65 U/mL) value of protease production. The summary of purification data is given in Table 1. Protease from the culture supernatant was purified by the combination of acetone precipitation followed by DEAE sephadox A-50 ion exchange column chromatography. Initially the crude enzyme was concentrated by acetone precipitation. Above fifty percent of purity was achieved with 2.2 fold purification. Following the acetone precipitation the resulted crude enzyme precipitate was applied to DEAE sephadex A-50 column. Purified protease enzyme showed specific activity of 169.08 U/mL of protein with purification fold of 7.59. The purified protease was analyzed by SDS- PAGE. The purified alkaline protease was resolved on a SDS-PAGE found to be a homogeneous protein as evident by single band corresponding to 60 kDa on SDS-PAGE relative to the standard molecular weight markers (Fig. 5).

DISCUSSION

Generally fish waste contains protease enzymes in gut and intestine and also contains proteolytic microbes. In the present study, alkaline protease producing *Bacillus* sp. was isolated from the hydrolyzed fish wastes. Several species of *Bacillus* sp. have been reported to be proteolytic and are commercially exploited [15,16]. Sudeepa et al. [17] isolated the proteolytic bacteria such as *Aeromonas, Bacillus* sp. and *Pseudomonas* sp. from fish processing waste and also found that among the *Bacillus* sp. they have tested *Bacillus proteolyticus* CFR3001 is a potential strain for production of alkaline protease. Esakkiraj et al. [(18)] reported a protease producing *Bacillus cereus* strain from gut of estuarine fish *Mugil cephalus* using tuna fish processing waste as a substrate. In the present investigation, protease producing *B. subtilis* were isolated from hydrolyzed trash fish wastes.

In the present investigation, the potential strain *B. subtilis* showed maximum protease activity in alkaline pH as shown in Fig.1. Similar results were obtained from *B. proteolyticus* CFR3001 isolated from fish processing waste [18] and *B. subtilis* isolated from mid gut of fresh water fish *Labeo rohita* [19]. Dunaevsky et al. [20] reported majority of microorganisms producing alkaline proteases shows growth and enzyme production under alkaline conditions. The present result coincide with Joo et al. [21] who reported that the protease production is maximum at pH 7 to 11 for *Bacillus* sp. strain S4 and *Pseudomonas* sp strain S22. The temperature was found to influence extracellular protease enzyme secretion; possibly changing the physical properties of the cell membrane [22]. In the present study the maximum enzyme activity was recorded at 37ºC and minimum enzyme production at 25ºC. The similar findings were observed in *B. proteolyticus* CFR3001 [17], whereas in another report by Fujiwara and Yamamoto [23], protease activity exhibited by *Bacillus* sp. was higher at 30°C. Few previous reports suggested the optimum temperature for protease production by *B. subtilis* and *Bacillus aquimaris* was found to be at 40 ºC [24,25,26,27]

Production of extracellular proteases has been to be sensitive to repression by different carbohydrate and nitrogen sources [28]. In the present work, glucose was considered the suitable carbon source as compared to other supplied carbon sources (Fig. 3). There are several reports showing that different carbon sources have different influence on enzyme production by different bacteria and fungi. In our findings, next to glucose other carbon sources like lactose and maltose also showed better protease production at 24 hrs but considerably reduced by 48 h of incubation. Similar findings were observed in *B. subtilis* isolated from fresh water fish (*Labeo rohita*) gut [19]. Malathi et al. [29] reported carbon sources such as lactose, maltose, sucrose and fructose as a best source for the maximal production of alkaline protease, while Githashree and Prasad [30] have reported the highest protease when dextrose used as a carbon source for optimization of enzyme production by *B. subtilis*. Mahendran et al. [24] found that sucrose is optimum carbon source for production of alkaline protease from *B. aquimaris*. The present work also derived the suitable nitrogen source for maximum protease activity by *B. subtilis*. (Fig. 4) among the nitrogen sources; peptone produced maximum protease 71.54 U/mL. Wang and Hsu [31] found that casein and peptone were better nitrogen sources for protease production by *Prevotella ruminicolo*. However, production medium enriched with natural sources (soya bean meal) also reported as best nitrogen source for protease production [32]. Githashree and Prasad [30] optimized protease production with peptone as nitrogen source; Kalaiarasi and Sunitha [33] reported that peptone was good source for alkaline protease production from *Pseudomonas fluorescens*. Uyar et al. [34] reported that skim milk was a suitable nitrogen source for production of alkaline protease from *B. cereus* strain CA15. In some earlier reports, it was found that different nitrogen sources such as soybean meal, casamino acid, and peptone were effective medium ingredients for the protease production by *Bacillus* sp. [8,9].

Ammonium sulphate is being commonly used for the enzyme purification for many years. But researchers have found much more efficient methodologies such as protein precipitation by ammonium sulphate, anion exchange chromatography, desalt/buffer exchange of protein, and gel filtration chromatography. In present study, during purification all the proteins other than protease were bound to the matrix. Totally eighteen fractions were observed and the fractions of protease were recovered in washing and the eight fractions had a highest enzyme activity that the enzyme was purified 7.59 fold with a yield of 6.74%. The specific activity was 169.08 U/mg of protein. Similar kind of behavior was also observed in the case of *Bacillus* sp. Protease [35] and *Pseudomonas* sp. protease [36]. Purified alkaline protease from *B. subtilis* migrated as single band with 60 kDa in SDS PAGE under reducing conditions, suggests that the purified protein was homogenous with high molecular weight. The relative molecular weight of protease enzyme was previously reported from *Beauveria bassiana* (Bals.) Vuil. [37]. The microbial proteases and their molecular masses ranged between 15 and 36 kDa with few exceptions of high molecular mass, such as 42 kDa from *Bacillus* sp. PS719 [38] and very high 90 kDa from *B. subtilis* [39]. In previous findings, the alkaline protease from *Bacillus* sp. was reported as a single band with molecular weight ranging from 16 to 32 kDa [40, 42] and other halophilc and alkaline proteases have molecular weight in range from 40 to 130 kDa [41, 43]. Most of the purified protease from *B. cereus* was found to have a molecular weight between 34 to 45 kDa [44,45]. Thus, the *Bacillus subtilis* isolated from the hydrolyzed fish waste is a potent species that can be used for the large scale industrial production of protease under the optimized environmental conditions.

Conflict of Interest: The authors have no conflicts of interest to declare.

REFERENCES

1. Jayaraman, R. (2004). Overview of status and trend of 'trash fish'from marine fisheries and their utilization, with special reference to aquaculture: India. *Mar. Fish. Inf. Ser. T&E. Ser*, *149*, 6.
2. Roos, N., Wahab, M. A., Hossain, M. A. R., & Thilsted, S. H. (2007). Linking human nutrition and fisheries: incorporating micronutrient-dense, small indigenous fish species in carp polyculture production in Bangladesh. *Food and nutrition bulletin*, *28*(2_suppl2), S280-S293.
3. Jebapriya, G. R., & Gnanadoss, J. J. (2001). Screening and molecular characterization of white rot fungi capable of laccase production and dye decolourization. *Life*, *50*, 12.

4. Kathiresan, K., Saravanakumar, K., Anburaj, R., Gomathi, V., Abirami, G., Sahu, S. K., & Anandhan, S. (2011). Microbial enzyme activity in decomposing leaves of mangroves. *Int J Adv Biotechnol Res*, *2*(3), 382-389.
5. Benluvankar, V., Jebapriya, G. R., & Gnanadoss, J. J. (2015). Protease production by Penicillium sp. LCJ228 under solid state fermentation using groundnut oilcake as substrate. *Life*, *50*, 12
6. Jebapriya, G. R., Gnanasalomi, V. D. V., & Gnanadoss, J. J. (2013). Application of mushroom fungi in solid waste management. *Int J Comput Algorithm*, *2*, 279-285.
7. Singh, J., Vohra, R. M., & Sahoo, D. K. (1999). Alkaline protease from a new obligate alkalophilic isolate of Bacillus sphaericus. *Biotechnology letters*, *21*, 921-924.
8. Joo, H. S., & Chang, C. S. (2005). Production of protease from a new alkalophilic Bacillus sp. I-312 grown on soybean meal: optimization and some properties. *Process Biochemistry*, *40*(3-4), 1263-1270.
9. Mehrotra, S., Pandey, P. K., Gaur, R., & Darmwal, N. S. (1999). The production of alkaline protease by a Bacillus species isolate. *Bioresource Technology*, *67*(2), 201-203.
10. Jebapriya, G. R., & Gnanadoss, J. J. (2013). Bioremediation of textile dye using white rot fungi: a review. *International Journal of Current Research and Review*, *5*(3), 1
11. Asmathunisha, N. Anburaj. R., & Kathiresan, K. (2018). Synthesis of silver and gold nanoparticles by mangrove-derived cyanobacteria. *J Advan Nanomater*, *3*(3), 1-7.
12. Gençkal, H., & Tari, C. (2006). Alkaline protease production from alkalophilic Bacillus sp. isolated from natural habitats. *Enzyme and Microbial Technology*, *39*(4), 703-710.
13. Annamalai, N., Kumar, A., Saravanakumar, A., Vijaylakshmi, S., & Balasubramanian, T. (2011). Characterization of protease from Alcaligens faecalis and its antibacterial activity on fish pathogens. *Journal of Environmental Biology*, *32*(6), 781.
14. Sethi, B. K., Rout, J. R., Das, R., Nanda, P. K., & Sahoo, S. L. (2013). Lipase production by Aspergillus terreus using mustard seed oil cake as a carbon source. *Annals of Microbiology*, *63*, 241-252.
15. Classics Lowry, O., Rosebrough, N., Farr, A., & Randall, R. (1951). Protein measurement with the Folin phenol reagent. *J biol Chem*, *193*(1), 265-75.
16. Saravanakumar, K., Anburaj, R., Gomathi, V., & Kathiresan, K. (2016). Ecology of soil microbes in a tropical mangrove forest of south east coast of India. *Biocatalysis and Agricultural Biotechnology*, *8*, 73-85.
17. Esakkiraj, P., Immanuel, G., Sowmya, S. M., Iyapparaj, P., & Palavesam, A. (2009). Evaluation of protease-producing ability of fish gut isolate Bacillus cereus for aqua feed. *Food and Bioprocess Technology*, *2*, 383-390.
18. Geethanjali, S., & Anitha, S. (2011). Optimization of protease production by Bacillus subtilis isolated from mid gut of fresh water fish Labeo rohita. *World Journal of Fish and Marine Sciences*, *3*(1), 88-95.
19. Joo, H. S., Kumar, C. G., Park, G. C., Kim, K. T., Paik, S. R., & Chang, C. S. (2002). Optimization of the production of an extracellular alkaline protease from Bacillus horikoshii. *Process Biochemistry*, *38*(2), 155-159.
20. Radhika, R., Jebapriya, G. R., & Gnanadoss, J. J. (2014). Decolourization of synthetic textile dyes using the edible mushroom fungi Pleurotus. *Pak. J. Biol. Sci*, *17*, 248-253.
21. Mahendran, S., Sankaralingam, S., Shankar, T., & Vijayabaskar, P. (2010). Alkalophilic protease enzyme production from estuarine Bacillus aquimaris. *World J. Fish and Marine Sci*, *2*(5), 436-443.
22. Anburaj R. 2005. Studies on antimicrobial properties of bivalves. M.Sc., Thesis. Annamalai Univarsity,Tamil Nadu, India. Pp.85.
23. Hariharan, A., Rajadurai, U. M., & Palanivel, I. (2019). Isolation, purification and mass production of protease from Bacillus subtilis. *Available at SSRN 3370124*.
24. Anburaj, R., Nabeel, M. A., Sivakumar, T., & Kathiresan, K. (2012). The role of rhizobacteria in salinity effects on biochemical constituents of the halophyte Sesuvium portulacastrum. *Russian Journal of Plant Physiology*, *59*, 115-119.
25. Anburaj R. (2011). Studies on marine cyanobacteria (chroococcales) isolated from mangrove biotope for their possible utility. Ph.D., Thesis. Annamalai Univarsity,Tamil Nadu, India. Pp.218.
26. Radhika, R., Jebapriya, G. R., & Gnanadoss, J. J. (2013). Production of cellulase and laccase using Pleurotus sp. under submerged and solid-state fermentation. *Int J Curr Sci*, *6*, 7-13.
27. Anburaj R, Roseline Jebapriya G, Nabeel MA, Kathiresan K, Arun K. (2023). Ecology and Biotechnological applications of Marine cyanobacteria: A review. Algal, Fungal and Microbial Research,1:255-265.

28. Sathya, TA., Anburaj, R., Angelina. (2023). Extraction of Bioactive Compounds from Niger Seed and The Detection Of Their Antimicrobial Activity Against The Pathogenic Microbes. *International Journal of Food and Nutritional Sciences*,11(12):8249-8259.
29. Anburaj, R., Jebapriya, G. R., Asmathunisha, N., & Kathiresan, K. (2020). Antibacterial Activity of Mangrove-Derived Marine Cyanobacteria. *International Journal of Scientific Research and Engineering Development*, *3*(2), 542-550.
30. Wang, H. T., & Hsu, J. T. (2005). Optimal protease production condition for Prevotella ruminicola 23 and characterization of its extracellular crude protease. *Anaerobe*, *11*(3), 155-162.
31. [31]. JebaPriya, G. R., Anburaj, R., Kanmani, M., & Singh, C. R. (2020). In vitro antimicrobial activity and phytochemical analysis of ethanolic leaf extract of Rosemarinus officinalis L. *International Journal of Innovative Engineering and Management Research*, *3*(09), 12.
32. Nabikhan, A., Kandasamy, K., Raj, A., & Alikunhi, N. M. (2010). Synthesis of antimicrobial silver nanoparticles by callus and leaf extracts from saltmarsh plant, Sesuvium portulacastrum L. *Colloids and surfaces B: Biointerfaces*, *79*(2), 488-493.
33. Anburaj R. (2009). Effect of rhizobacteria on salinity induced changes in Sesuvium portulacastrum L. M.Phil., Thesis. Annamalai Univarsity,Tamil Nadu, India. Pp.98.
34. Gnanadoss, J. J., Robert, R., & Jebapriya, R. (2011). Production of protease from Aspergillus niger and Mucor mucedo under submerged and solid state fermentation. *International Journal of Current Research*, *3*, 75-78.
35. Raj, A., Kandasamy, S., Venugopal, G., Jayabalan, Y., & Kandasamy, K. (2011). Calcium removal from aqueous solution by marine cyanobacterium, Gloeocapsa species: adsorption kinetics and equilibrium studies. *International Journal of Pharmaceutical Application*, *2*(3), 195-201.
36. Annamalai, N., Anburaj, R., Jayalakshmi, S., & Thavasi, R. (2007). Antibacterial activities of green mussel (Perna viridis) and edible oyster (Crassostrea madrasensis). *Res J Microbiol*, *2*(12), 978-982.
37. Somasundaram, R., Jebapriya, R., & Mir, R. A. (2021). Effect of Auxin derivatives on morphological and isoenzyme pattern of enzymatic Antioxidant peroxidase (POX) of "blinding eye mangrove" Excoecaria agallocha. L stem cuttings. *Iranian Journal of Plant Physiology*, *11*(2), 3571-3578.
38. Benluvankar, V., Jebapriya, G. R., & Gnanadoss, J. J. (2015). Protease production by Penicillium sp. LCJ228 under solid state fermentation using groundnut oilcake as substrate. *Life*, *50*, 12.
39. Olajuyigbe, F. M., & Ajele, J. O. (2005). Production dynamics of extracellular protease from Bacillus species. *African Journal of Biotechnology*, *4*(8), 776-779.
40. Abd Rahman, R. N. Z., Geok, L. P., Basri, M., & Salleh, A. B. (2005). Physical factors affecting the production of organic solvent-tolerant protease by Pseudomonas aeruginosa strain K. *Bioresource technology*, *96*(4), 429-436.
41. Kalaiarasi, K., & Sunitha, P. U. (2009). Optimization of alkaline protease production from Pseudomonas fluorescens isolated from meat waste contaminated soil. *African Journal of Biotechnology*, *8*(24).
42. Uyar, F., & Baysal, Z. (2004). Production and optimization of process parameters for alkaline protease production by a newly isolated Bacillus sp. under solid state fermentation. *Process Biochemistry*, *39*(12), 1893-1898.
43. Gupta, A., Roy, I., Khare, S. K., & Gupta, M. N. (2005). Purification and characterization of a solvent stable protease from Pseudomonas aeruginosa PseA. *Journal of Chromatography A*, *1069*(2), 155-161.
44. Adinarayana, K., Raju, K. B., & Ellaiah, P. (2004). Investigations on alkaline protease production with B. subtilis PE-11 immobilized in calcium alginate gel beads. *Process Biochemistry*, *39*(11), 1331-1339.
45. Rebeca, B. D., Pena-Vera, M. T., & Diaz-Castaneda, M. (1991). Production of fish protein hydrolysates with bacterial proteases; yield and nutritional value. *Journal of food Science*, *56*(2), 309-314.

Table 1: Purification summary of alkaline protease produced from *Bacillus subtilis* under optimum condition

S.No	Purification steps	Total volume (mL)	Total enzyme activity (U)	Total protein content (mg)	Specific activity (U/mg)	Purification fold	% yield
1	Crude enzyme	100	12400	180	69	1	100
2	Acetone precipitation	25	4850	24.9	202.08	2.2	39.11
3	DEAE-Sephadex-G-100	10	2384	8.4	284	7.59	19.2

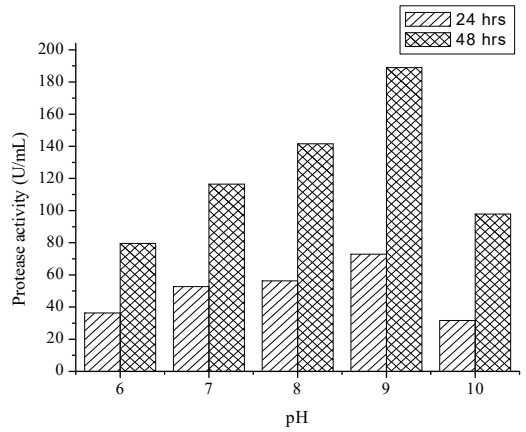

Figure 1: Effect of pH on production of alkaline protease by *Bacillus subtilis*

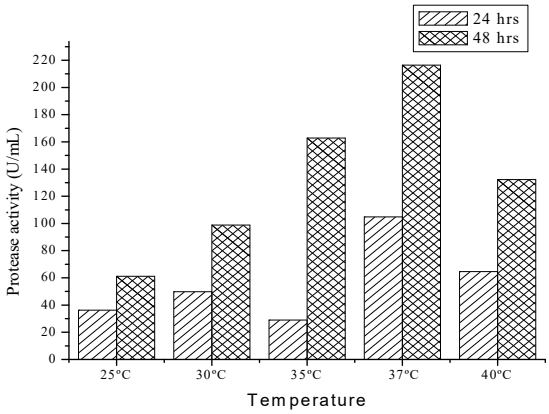

Figure 2: Effect of temperature on production of alkaline protease by *Bacillus subtilis*

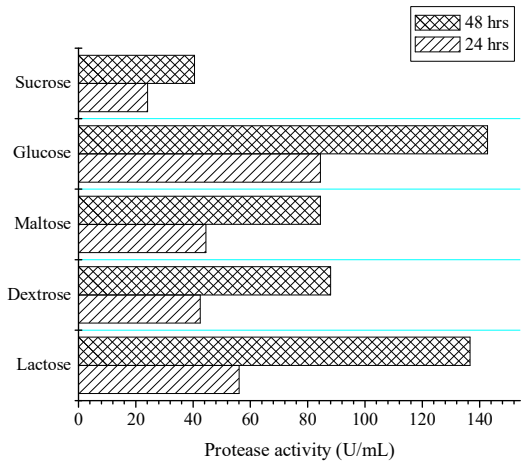

Figure 3: Effect of different carbon sources on production of alkaline protease by *Bacillus subtilis*

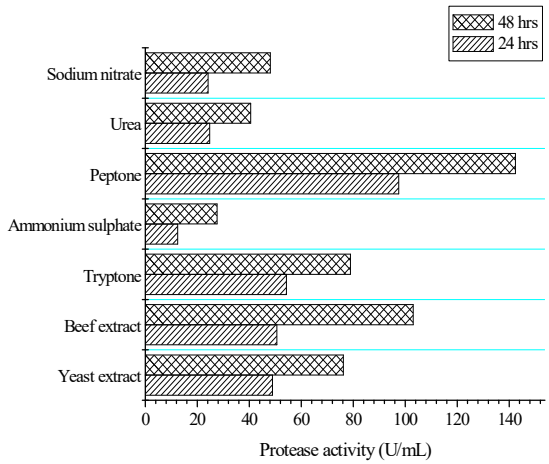

Figure 4: Effect of different nitrogen sources on production of alkaline protease by *Bacillus subtilis*

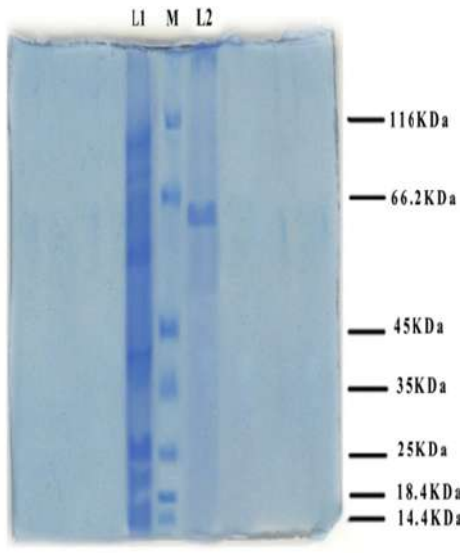

Figure 5: Molecular weight determination of purified alkaline protease by SDS-PAGE
(L1- Crude extract, M- Protein marker, L2- Purified alkaline protease)

Indian Journal of Natural Sciences *www.tnsroindia.org.in ©IJONS*

Vol.15 / Issue 83 / Apr / 2024 *International Bimonthly (Print) – Open Access* *ISSN: 0976 – 0997*

RESEARCH ARTICLE

Study of Serial Channels with various customers' behaviour linked with Non-Serial Service Channels showing balking behaviour

Sangeeta[1]*, Man Singh[2], Deepak Gupta[3]

[1*]Research Scholar, MMEC, MM(DU), Mullana
[2]Prof. of Mathematics (Retd.), CCS, H.A.U. Hisar Haryana, India
[3]Prof. & Head, Dept. of Mathematics, MMEC, MM(DU), Mullana,

Received: 30 Dec 2023 Revised: 09 Jan 2024 Accepted: 12 Jan 2024

***Address for Correspondence**
Sangeeta
Research Scholar,
MMEC, MM(DU), Mullana
Email: sangeetaturka999@gmail.com

ABSTRACT

In this work, the queuing model is formed consisting of Serial and non-serial service channels. Concepts such as feedback and reneging due to urgent call/message and impatient of the customers are studied in the serial queues. The Balking behaviour is included in both types of the queues. The customers arrive in Poisson stream from outside and may join any service channel of the queuing system directly. The units may leave the serial channels of queuing model with or without getting service. The service time distribution is negative exponential and arrival of customer is random. Marginal probabilities and mean length of the queue have been calculated for unlimited to measure the efficiency of the system.

Keywords: Service channels, Poisson, exponential, Urgent message, Impatient behavior, Queue discipline, Steady-state, Waiting space.

INTRODUCTION

Since last century, number of Mathematicians, Researchers and Statisticians have worked a lot in queuing theory namely O'Brien (1954), Jackson (1954) Hunt(1955) , Finch (1959), Singh (1984)and many more. Meenu et.al. (2018) studied the customers' behaviour in multi-channel finite queuing system. Deepak et.al.(2021) studied the concept of feedback and reneging because of important call and impatience behavior. Singh et.al. (2016) studied in his thesis about serial queues linked with non-serial queues with balking in both types of queues along with reneging and feedback in serial queues. Here, we study balking in non-serial queues and feedback is permitted from each serial service channel to all its previous serial service channels which is an extension of research discussed in reference no 21.Keeping in mind the given details, a realistic and more general queuing model has been constructed such that:

1. R service channels in series are linked with S non-serial Service channels .
2. The customers may join the system at any stage from outside directly and may leave the system at any stage after service.
3. The customers may not join the service channels in both series and non-series service channels due to large number of customers already present there and their joining rate depends upon the queue size.
4. Feedback is permitted from each service channel to all its previous service channels
5. There is reneging in serial queues either due to urgent call or due to impatient behaviour of the customers.
6. Arrival is Poisson distributed, service rate is negative exponential and queue follows SIRO pattern.
7. There is waiting space which is infinite.

FORMULATION OF QUEUING MODEL:

We studied the queuing model having serial service channels $Q_1, Q_2, Q_3, \ldots, Q_{R-1}, Q_R$ with respective servers $S_1, S_2, S_3, \ldots, S_{R-1}, S_R$. The last channel Q_R of the serial queues is connected with S Non-Serial service channels $Q_{11}, Q_{12}, Q_{13}, \ldots, Q_{1S-1}, Q_{1S}$ with respective server $S_{11}, S_{12}, S_{13}, \ldots, S_{1S-1}, S_{1S}$. The customers arrive for various services at the service channels from outside in Poisson stream with η_i at $Q_i\ (i = 1,2,3,\ldots\ldots,R)$ and η_{1j} at $Q_{1j}\ (j = 1,2,\ldots\ldots,S-1,S)$ but the fresh customers may not join the queue $Q_i\ (i = 1,2,3,\ldots\ldots,R)$ on seeing the long queue there then the Poisson input rate η_i becomes $\eta_i / a_i + 1$, a_i is the number of customers in the queue Q_i . Also , due to balking, the customer may not enter the non-serial queues $Q_{1j}\ (j = 1,2,\ldots\ldots,S-1,S)$ such that arrival rate would be $\frac{\eta_{1j}}{b_j + 1}$ instead of η_{1j} The service time distribution for the servers S_i (i=1,2,3,…,R) and S_{1j} (j=1,2,3,….,S) are mutually independent negative exponential distributions with parameters $\omega_i\ (i = 1,2,3,\ldots\ldots,R)$ and $\omega_{1j}\ (j = 1,2,3,\ldots\ldots,S)$ respectively. After completing service at S_i , the customer either leaves the i^{th} service channel with probability d_i or joins the next service channel with probability $\frac{p_i}{a_{i+1}+1}(i = 1,2,3,\ldots,R-1)$ or joins back for re-service any of its previous channels with probabilities $\frac{r_{il}}{a_l + 1}(l = 1,2,3,\ldots,i-1)$ such that $d_i + \frac{p_i}{a_{i+1}+1} + \sum_{l=1}^{i-1} \frac{r_{il}}{a_l + 1} = 1\ (i = 1,2,3,\ldots,R-1)$. After getting served at Q_R ,the customer either leaves the system with probability d_R or joins back for re service any of its previous service channels with probabilities $\frac{r_{Rl}}{a_l + 1}(l = 1,2,3,\ldots,R-1)$ or joins any non-serial queue Q_{1j}(j=1,2,3,…,S) with probability $\frac{t_{Rj}}{b_j + 1}$ such that $d_R + \sum_{l=1}^{R-1} \frac{r_{Rl}}{a_l + 1} + \sum_{j=1}^{S} \frac{t_{Rj}}{b_j + 1} = 1$ It is also seen that the customer shows impatience because of long queue and leaves the system without getting service. Even at times, the customer receives the urgent call/message when they wait in the queue and left the queue immediately even if there is no long queue. Under such situations, the average reneging rates of the customer in the i^{th} serial service channel have been taken α_i

due to urgent call/message(i=1,2,…,R) and C_{ia_i} due to impatient behaviour of the customer after a wait of certain time T_{0i} defined by $C_{ia_i} = \dfrac{\omega_i e^{\frac{-\omega_i T_{0i}}{a_i}}}{\left(1 - e^{\frac{-\omega_i T_{0i}}{a_i}}\right)}$ where ω_i is rate of getting served and a_i is the queue size

Such types of queuing modelsare commonly used in administrative setup of district administration.

$P\left(a_1, a_2, a_3, \ldots . a_R; b_1, b_2, b_3, \ldots b_S; t\right)$ is assumed as the probability that at a time 't' there are a_i units (which may balk or renege either due to urgent call or impatient behaviour or join the next channel or join back any of its previous service channel or leave the system after getting service) waiting in the i^{th} service channel before the server S_i(i=1,2,3,…,R-1) , a_R customers (which may leave the system or join back all its previous channels or join any non-serial service channels) waiting in R^{th} service channel before the server S_R ;b_j customers (which either balk or leave the system after getting service) waiting in Q_{1j} before the server S_{1j}(j=1,2,3,…,S)

Using the given operators, we formulate the system's equations in compact form.

Z_{i^-}, $Z_{\cdot i}$, *and* $Z_{\cdot i, i+1^-}$ on the vector $\tilde{a} = (a_1, a_2, a_3, \ldots\ldots, a_R)$ defined by

$Z_{i^-}\left(\tilde{a}\right) = (a_1, a_2, a_3, \ldots\ldots, a_i - 1, \ldots., a_R)$; $Z_{\cdot i}\left(\tilde{a}\right) = (a_1, a_2, a_3, \ldots\ldots, a_i + 1, \ldots., a_R)$;

$Z_{\cdot i, i+1^-}\left(\tilde{a}\right) = (a_1, a_2, a_3, \ldots\ldots, a_i + 1, a_{i+1} - 1, \ldots., a_R)$.

Differential-difference Equations: The differential-difference equations of the system are written as under:

$$\frac{d}{dt}P\left(\tilde{a}, \tilde{b}, t\right) = -\left[\sum_{i=1}^{R}\frac{\eta_i}{a_i + 1} + \sum_{j=1}^{S}\frac{\eta_{1j}}{b_j + 1} + \sum_{i=1}^{R}\delta(a_i)\left(\omega_i + \alpha_i + c_{ia_i}\right) + \sum_{j=1}^{S}\delta(b_j)\omega_{1j}\right]P\left(\tilde{a}, \tilde{b}, t\right)$$

$$+\sum_{i=1}^{R}\frac{\eta_i}{a_i}P\left(Z_{i^-}\left(\tilde{a}\right), \tilde{b}; t\right) + \sum_{j=1}^{S}\frac{\eta_{1j}}{b_j}P\left(\tilde{a}, Z_{j^-}\left(\tilde{b}\right); t\right) + \sum_{i=1}^{R-1}\frac{\omega_i p_i}{a_{i+1}}P\left(Z_{\cdot i, i+1^-}\left(\tilde{a}\right), \tilde{b}; t\right)$$

$$+\sum_{i=1}^{R}\left(\omega_i d_i + c_{ia_i + 1} + \alpha_i\right)P\left(Z_{\cdot i}\left(\tilde{a}\right), \tilde{b}; t\right)$$

$$+\sum_{i=2}^{R}\mu_i\sum_{l=1}^{i-1}\frac{r_{il}}{a_l}P\left((a_1, a_2, \ldots a_{l-1}, a_l - 1, a_{l+1}, .., a_i + 1, .., a_R), \tilde{b}; t\right)$$

$$+\sum_{j=1}^{S}\omega_R\frac{t_{Rj}}{b_j}P(a_1, a_2, \ldots., a_R + 1, Z_{j^-}(\tilde{b}); t) + \sum_{j=1}^{S}\omega_{1j}P(\tilde{a}; Z_j(\tilde{b}); t)$$

for $a_i \geq 0, b_j \geq 0; (i = 1, 2, 3, \ldots, R; j = 1, 2, 3, \ldots., S)$

where $\delta(a_i)=\begin{cases}1 & if \quad a_i \neq 0\\ 0 & if \quad a_i = 0\end{cases}$

$\delta(b_j)=\begin{cases}1 & if \quad b_j \neq 0\\ 0 & if \quad b_j = 0\end{cases}$ |

And $P\left(\tilde{a},\tilde{b};t\right)=\tilde{0}$ if any of the arguments is negative.

Steady–State Equations

The Steady-State equations obtained from (1) by equating the time derivative to zero in differential - difference Equation are as under

$$\left[\sum_{i=1}^{R}\frac{\eta_i}{a_i+1}+\sum_{j=1}^{S}\frac{\eta_{1j}}{b_j+1}+\sum_{i=1}^{R}\delta(a_i)\left(\omega_i+\alpha_i+c_{ia_i}\right)+\sum_{j=1}^{S}\delta(b_j)\omega_{1j}\right]P\left(\bar{a},\tilde{b}\right) =$$

$$\sum_{i=1}^{R}\frac{\eta_i}{a_i}P\left(Z_{i\cdot}(\tilde{a}),\tilde{b}\right)+\sum_{j=1}^{S}\frac{\eta_{1j}}{b_j}P\left(\tilde{a},Z_{j\cdot}\left(\tilde{b}\right)\right)+\sum_{i=1}^{R-1}\frac{\omega_i p_i}{a_{i+1}}P\left(Z_{\cdot i,i+1\cdot}(\tilde{a}),\tilde{b}\right)$$

$$+\sum_{i=1}^{R}\left(\omega_i d_i+c_{ia_i+1}+\alpha_i\right)P\left(Z_{\cdot i}\left(\tilde{a}\right),\tilde{b}\right)+\sum_{i=2}^{R}\omega_i\sum_{l=1}^{i-1}\frac{r_{il}}{b_l}P\left((a_1,a_2,\ldots a_{l-1},a_l-1,a_{l+1},\ldots,a_i+1,\ldots,a_R),\tilde{b}\right)$$

$$+\sum_{j=1}^{S}\omega_R\frac{t_{Rj}}{b_j}P\left(a_1,a_2,\ldots,a_R+1,Z_{j\cdot}(\tilde{b})\right)+\sum_{j=1}^{S}\omega_{1j}P\left(\tilde{a};Z_{\cdot j}(\tilde{b})\right) \quad (2)$$

for $a_i \geq 0, b_j \geq 0; (i=1,2,3,\ldots,R;\ j=1,2,3,\ldots,S)$

Steady-State Solutions:

The equations in steady form are satisfied by the following Steady-State solutions

$$P\left(\tilde{a},\tilde{b}\right)=P\left(\tilde{0},\tilde{0}\right)\left(\frac{1}{a_1!}\frac{\left(\eta_1+\sum_{i=2}^{R}\frac{\omega_i r_{i1}\rho_i}{(a_i+1)(\omega_i+\alpha_i+c_{ia_i+1})}\right)^{a_1}}{\prod_{i=1}^{a_1}(\omega_1+C_{1i}+\alpha_i)}\right)\left(\frac{1}{a_2!}\frac{\left(\eta_2+\frac{\omega_1 p_1\rho_1}{(a_1+1)(\omega_1+\alpha_1+c_{1a_1+1})}+\sum_{i=2}^{R}\frac{\omega_i r_{i2}\rho_i}{(a_i+1)(\omega_i+\alpha_i+c_{ia_i+1})}\right)^{a_2}}{\prod_{i=1}^{a_2}(\omega_2+\alpha_2+C_{2i})}\right)$$

$$\left(\frac{1}{a_3!}\frac{\left(\eta_3+\frac{\omega_2 p_2\rho_2}{(a_2+1)(\omega_2+\alpha_2+c_{2a_2+1})}+\sum_{i=4}^{R}\frac{\omega_i r_{i3}\rho_i}{(a_i+1)(\omega_i+\alpha_i+c_{ia_i+1})}\right)^{a_3}}{\prod_{i=1}^{m_3}(\omega_3+\alpha_3+C_{3i})}\right)\cdots$$

$$\cdot\left(\frac{1}{a_{R-1}!}\frac{\left(\eta_{R-1}+\frac{\omega_{R-2}p_{R-2}\rho_{R-2}}{(a_{R-2}+1)(\omega_{R-2}+\alpha_{R-2}+c_{R-2a_{R-2}+1})}+\frac{\omega_R r_{R,R-1}\rho_R}{(a_R+1)(\omega_R+\alpha_R+c_{R,a_R+1})}\right)^{a_{R-1}}}{\prod_{i=1}^{m_{R-1}}(\omega_{R-1}+C_{R-1,i}+\alpha_{R-1})}\right)$$

$$\cdot\left(\frac{1}{a_R!}\frac{\left(\eta_R+\frac{\omega_{R-1}p_{R-1}\rho_{R-1}}{(a_{R-1}+1)(\omega_{R-1}+\alpha_{R-1}+c_{R-1,a_{R-1}+1})}\right)^{a_R}}{\prod_{i=1}^{a_R}(\mu_R+C_{R,i}+\alpha_R)}\right)$$

$$\cdot\left[\frac{1}{b_1!}\left(\frac{\eta_{h1}+\frac{\omega_R t_{R1}\rho_R}{(b_R+1)(\omega_R+\alpha_R+C_{Rb_R+1})}}{\omega_{1_1}}\right)^{b_1}\right]\cdot\left[\frac{1}{b_2!}\left(\frac{\eta_{h2}+\frac{\omega_R t_{R2}\rho_R}{(b_R+1)(\omega_R+\alpha_R+C_{Rb_R+1})}}{\omega_{1_2}}\right)^{b_2}\right]\cdot$$

$$\left[\frac{1}{b_3!}\left(\frac{\eta_{h3}+\frac{\omega_R t_{R3}\rho_R}{(b_R+1)(\omega_R+\alpha_R+C_{Rb_R+1})}}{\omega_{1_3}}\right)^{b_3}\right]\cdots\cdots\left[\frac{1}{b_S!}\left(\frac{\eta_{hS}+\frac{\omega_R t_{RS}\rho_R}{(b_R+1)(\omega_R+\alpha_R+C_{Rb_R+1})}}{\omega_{1_S}}\right)^{b_S}\right]$$

$$\left.\begin{aligned}
&\rho_1=\eta_1+K_{21}\rho_2+K_{31}\rho_3+K_{41}\rho_4+\ldots+K_{R-2,1}\rho_{R-2}+K_{R-1,1}\rho_{R-1}+K_{R,1}\rho_R\\
&\rho_2=\eta_2+\frac{\omega_1 p_1\rho_1}{h_1}+K_{32}\rho_3+K_{42}\rho_4+\ldots+K_{R-2,2}\rho_{R-2}+K_{R-1,2}\rho_{R-1}+K_{R,2}\rho_R\\
&\rho_3=\eta_3+\frac{\omega_2 p_2\rho_2}{h_2}+K_{43}\rho_4+K_{53}\rho_5+\ldots+K_{R-2,3}\rho_{R-2}+K_{R-1,3}\rho_{R-1}+K_{R,3}\rho_R\\
&\ldots\\
&\ldots\\
&\rho_{R-2}=\eta_{R-2}+\frac{\omega_{R-3}p_{R-3}\rho_{R-3}}{h_{R-3}}+K_{R-1,R-2}\rho_{R-1}+K_{R,R-2}\rho_R\\
&\rho_{R-1}=\eta_{R-1}+\frac{\omega_{R-2}p_{R-2}\rho_{R-2}}{h_{R-2}}+K_{R,R-1}\rho_R\\
&\rho_R=\eta_R+\frac{\omega_{R-1}p_{R-1}\rho_{R-1}}{h_{R-1}}
\end{aligned}\right\}\text{5(R-equations)}$$

Here,

$$\rho_1=\eta_1+\sum_{i=2}^{R}\frac{\omega_i r_{i1}\rho_i}{(a_i+1)(\omega_i+\alpha_i+c_{ia_i+1})}$$

$$\rho_2=\eta_2+\frac{\omega_1 p_1\rho_1}{(a_1+1)(\omega_1+\alpha_1+c_{1a_1+1})}+\sum_{i=3}^{R}\frac{\omega_i r_{i2}\rho_i}{(a_i+1)(\omega_i+\alpha_i+c_{ia_i+1})}$$

$$\rho_3=\eta_3+\frac{\omega_2 p_2\rho_2}{(a_2+1)(\omega_2+\alpha_2+c_{2a_2+1})}+\sum_{i=4}^{R}\frac{\omega_i r_{i3}\rho_i}{(a_i+1)(\omega_i+\alpha_i+c_{ia_i+1})}$$

…

…

$$\rho_R = \eta_R + \frac{\omega_{R-1} p_{R-1} \rho_{R-1}}{(a_{R-1}+1)(\omega_{R-1} + \alpha_{R-1} + c_{R-1,a_{R-1}+1})}$$

For the sake of simplicity, we take

$$K_{ij} = \frac{\omega_i r_{ij}}{(a_i+1)\left(\omega_i + C_{ia_i+1} + \alpha_i\right)} (j = 1, 2, 3, \ldots, S-1)$$

$$h_i = (a_i+1)(\omega_i + \alpha_i + C_{ia_i+1}) (i = 1, 2, 3, \ldots, R)$$

These unknown parameters $\rho_1, \rho_2, \rho_3 \ldots\ldots \rho_{R-1}, \rho_R$ can be found out by using (5) R-equations. Solving these (5) R-equations for ρ_R by finding the values of determinants, we get

$$\rho_R = \begin{pmatrix} \eta_R \Delta_{R-1} + \frac{p_{R-1}\omega_{R-1}}{h_{R-1}} \eta_{R-1} \Delta_{R-2} + \frac{p_{R-1}\omega_{R-1}}{h_{R-1}} \cdot \frac{p_{R-2}\omega_{R-2}}{h_{R-2}} \eta_{R-2} \Delta_{R-3} + \ldots \\ + \left(\frac{p_{R-1}\omega_{R-1}}{h_{R-1}} \cdot \frac{p_{R-2}\omega_{R-2}}{h_{R-2}} \cdot \frac{p_{R-3}\omega_{R-3}}{h_{R-3}} \ldots \frac{p_3\omega_3}{h_3} \cdot \frac{p_2\omega_2}{h_2} \eta_2 \Delta_1 \right) \\ + \left(\frac{p_{R-1}\omega_{R-1}}{h_{R-1}} \cdot \frac{p_{R-2}\omega_{R-2}}{h_{R-2}} \cdot \frac{p_{R-3}\omega_{R-3}}{h_{R-3}} \ldots \frac{p_3\omega_3}{h_3} \cdot \frac{p_2\omega_2}{h_2} \cdot \frac{p_1\omega_1}{h_1} \eta_1 \right) \\ \hline \Delta_{R-1} - \frac{p_{R-1}\omega_{R-1}}{h_{R-1}} K_{R,R-1} \Delta_{R-2} - \frac{p_{R-1}\omega_{R-1}}{h_{R-1}} \cdot \frac{p_{R-2}\omega_{R-2}}{h_{R-2}} K_{R,R-2} \Delta_{R-3} - \\ \ldots - \left(\frac{p_{R-1}\omega_{R-1}}{h_{R-1}} \cdot \frac{p_{R-2}\omega_{R-2}}{h_{R-2}} \ldots \frac{p_2\omega_2}{h_2} K_{R,2} \Delta_1 \right) \\ - \left(\frac{p_{R-1}\omega_{R-1}}{h_{R-1}} \cdot \frac{p_{R-2}\omega_{R-2}}{h_{R-2}} \ldots \frac{p_2\omega_2}{h_2} \cdot \frac{p_1\omega_1}{h_1} K_{R,1} \right) \end{pmatrix} \quad (6)$$

Then

$$\Delta_{R-1} = \begin{vmatrix} 1 & -K_{2,1} & -K_{3,1} & \ldots & -K_{R-2,1} & -K_{R-1,1} \\ \frac{-p_1\omega_1}{h_1} & 1 & -K_{3,2} & \ldots & -K_{R-2,2} & -K_{R-1,2} \\ 0 & \frac{-p_2\omega_2}{h_2} & 1 & \ldots & -K_{R-2,3} & -K_{R-1,3} \\ 0 & 0 & \frac{-p_3\omega_3}{h_3} & \ldots & -K_{R-2,4} & -K_{R-1,4} \\ . & . & . & . & . & . \\ . & . & . & . & . & . \\ . & . & . & . & . & . \\ 0 & 0 & 0 & \ldots & -K_{R-2,R-3} & -K_{R-1,R-3} \\ 0 & 0 & 0 & \ldots & 1 & -K_{R-1,R-2} \\ 0 & 0 & 0 & \ldots & \frac{-p_{R-2}\omega_{R-2}}{h_{R-2}} & 1 \end{vmatrix}$$

Continuing in this way

$$\Delta_3 = \begin{vmatrix} 1 & -K_{2,1} & -K_{3,1} \\ \frac{-p_1\omega_1}{h_1} & 1 & -K_{3,2} \\ 0 & \frac{-p_2\omega_2}{h_2} & 1 \end{vmatrix}, \quad \Delta_2 = \begin{vmatrix} 1 & -K_{2,1} \\ \frac{-p_1\omega_1}{h_1} & 1 \end{vmatrix}, \quad \Delta_1 = |1| = 1$$

Since ρ_R has been calculated, so we get ρ_{R-1} by putting the value of ρ_R in the last (5)R-equations, ρ_{R-2} by putting the values of ρ_{R-1} and ρ_R in the last but one equation of (5)R-equations, continuing like this, we get the values of $\rho_{R-3}, \rho_{R-4}, ---, \rho_3, \rho_2,$ and ρ_1.

All the parameters $\rho_1, \rho_2, \rho_3, ---, \rho_{R-1}, \rho_R$ have been calculated except $P\left(\tilde{0}, \tilde{0}\right)$ which can be determined by normalizing condition

$\sum_{\substack{\tilde{a}=\tilde{0} \\ \tilde{b}=\tilde{0}}}^{\infty} P\left(\tilde{a}, \tilde{b}\right) = 1$ and with the limitation that each service channel in the system has a lower than a unified traffic intensity

$$P(\tilde{a},\tilde{b}) = P(\tilde{0},\tilde{0}) \left(\frac{1}{a_1!} \left(\frac{(\rho_1)^{a_1}}{\prod_{i=1}^{a_1} (\mu_1 + C_{1i} + \alpha_1)} \right) \right) \cdot \left(\frac{1}{a_2!} \left(\frac{(\rho_2)^{a_2}}{\prod_{i=1}^{a_2} (\mu_2 + C_{2i} + \alpha_2)} \right) \right)$$

$$\cdot \left(\frac{1}{a_3!} \left(\frac{(\rho_3)^{a_3}}{\prod_{i=1}^{a_3} (\omega_3 + C_{3i} + \alpha_3)} \right) \right) \cdots \left(\frac{1}{a_{R-1}!} \left(\frac{(\rho_{R-1})^{a_{R-1}}}{\prod_{i=1}^{a_{R-1}} (\omega_{R-1} + C_{R-1,i} + \alpha_{R-1})} \right) \right)$$

$$\left(\frac{1}{a_R!} \left(\frac{(\rho_R)^{a_R}}{\prod_{i=1}^{\infty} (\omega_R + C_{Ri} + \alpha_R)} \right) \right) \cdots \left[\frac{1}{b_1!} \left(\frac{\eta_{11} + \frac{\omega_R f_{R1} \rho_R}{(b_R+1)(\omega_R + \alpha_R + C_{Ra_R+1})}}{\omega_{11}} \right) \right]^{b_1} \cdot$$

$$\left[\frac{1}{b_2!} \left(\frac{\eta_{12} + \frac{\omega_R f_{R2} \rho_R}{(b_R+1)(\omega_R + \alpha_R + C_{Ra_R+1})}}{\omega_{12}} \right) \right]^{b_2} \cdot \left[\frac{1}{b_3!} \left(\frac{\eta_{13} + \frac{\omega_R f_{R3} \rho_R}{(b_R+1)(\omega_R + \alpha_R + C_{Ra_R+1})}}{\omega_{13}} \right) \right]^{b_3} \cdots\cdots$$

$$\left[\frac{1}{b_S!} \left(\frac{\eta_{1S} + \frac{\omega_R f_{RS} \rho_R}{(b_R+1)(\omega_R + \alpha_R + C_{Ra_R+1})}}{\omega_{1S}} \right) \right]^{b_S}$$

Thus,(7) $a_i \geq 0, b_j \geq 0; (i = 1,2,3,...,R;\ j = 1,2,3,....,S)$ has been determined completely.

Further, since the present queuing model is being discussed in steady state conditions and derivative of $P\left(\tilde{a}, \tilde{b}\right)$ does not depend upon any specific queue discipline so in the long run, the reneging due to impatient behaviour of the customers of the system becomes constant and reneging rate C_{ia_i} would be $C_i \left(i = 1,2,3,...,R\right)$. Putting $C_{ia_i} = C_i$ in the difference-differential equations (1), in the equations (2) and in the solutions (3) and (7), we get steady-state solutions as under

$$P(\tilde{a},\tilde{b}) = P\left(\tilde{0},\tilde{0}\right) \left(\frac{1}{a_1!} \left(\frac{\rho_1}{(\omega_1 + C_1 + \alpha_1)} \right)^{a_1} \right) \cdot$$

$$\left(\frac{1}{a_2!} \left(\frac{\rho_2}{(\omega_2 + C_2 + \alpha_2)} \right)^{a_2} \right)$$

$$\left(\frac{1}{a_3!} \left(\frac{\rho_3}{(\omega_3 + C_3 + \alpha_3)} \right)^{a_3} \right) \cdots \left(\frac{1}{a_{R-1}!} \left(\frac{\rho_{R-1}}{\omega_{R-1} + C_{R-1} + \alpha_{R-1})} \right)^{a_{R-1}} \right)$$

$$\left(\frac{1}{a_R!} \left(\frac{\rho_R}{(\omega_R + C_R + \alpha_R)} \right)^{a_R} \right) \cdot \left[\frac{1}{b_1!} \left(\frac{\eta_1 + \frac{\omega_R f_{R1} \rho_R}{(b_R+1)(\omega_R + \alpha_R + C_{Ra_R+1})}}{\omega_1} \right) \right]^{b_1} \cdot$$

$$\left[\frac{1}{b_2!} \left(\frac{\eta_2 + \frac{\omega_R f_{R2} \rho_R}{(b_R+1)(\omega_R + \alpha_R + C_{Ra_R+1})}}{\omega_2} \right) \right]^{b_2} \cdot \left[\frac{1}{b_3!} \left(\frac{\eta_3 + \frac{\omega_R f_{R3} \rho_R}{(b_R+1)(\omega_R + \alpha_R + C_{Ra_R+1})}}{\omega_3} \right) \right]^{b_3} \cdots\cdots$$

$$\left[\frac{1}{b_S!} \left(\frac{\eta_S + \frac{\omega_R f_{RS} \rho_R}{(b_R+1)(\omega_R + \alpha_R + C_{Ra_R+1})}}{\omega_S} \right) \right]^{b_S}$$

$$a_i \geq 0, b_j \geq 0; (i = 1,2,3,...,R;\ j = 1,2,3,....,S) \tag{8}$$

Where,

$$\rho_1 = \eta_1 + K_{21}\rho_2 + K_{31}\rho_3 + K_{41}\rho_4 + ... + K_{R-2,1}\rho_{R-2} + K_{R-1,1}\rho_{R-1} + K_{R,1}\rho_R$$

$$\rho_2 = \eta_2 + \frac{\omega_1 p_1 \rho_1}{h_1} + K_{32}\rho_3 + K_{42}\rho_4 + ... + K_{R-2,2}\rho_{R-2} + K_{R-1,2}\rho_{R-1} + K_{R,2}\rho_R$$

$$\rho_3 = \eta_3 + \frac{\omega_2 p_2 \rho_2}{h_2} + K_{43}\rho_4 + K_{53}\rho_5 + ... + K_{R-2,3}\rho_{R-2} + K_{R-1,3}\rho_{R-1} + K_{R,3}\rho_R$$

...

…

$$\rho_{R-2} = \eta_{R-2} + \frac{\omega_{R-3} p_{R-3} \rho_{R-3}}{h_{R-3}} + K_{R-1,R-2}\rho_{R-1} + K_{R,R-2}\rho_R$$

$$\rho_{R-1} = \eta_{R-1} + \frac{\omega_{R-2} p_{R-2} \rho_{R-2}}{h_{R-2}} + K_{R,R-1}\rho_R$$

$$\rho_R = \eta_R + \frac{\omega_{R-1} p_{R-1} \rho_{R-1}}{h_{R-1}}$$

As discussed earlier, we can find ρ_R from R-equations given above with the help of determinants or ρ_R can be derived easily directly by taking $K_{ij} = \frac{p_{ij}\omega_i}{(a_i+1)(\omega_i + C_i + \alpha_i)} (j = 1,2,3,....,R-1)$ and $h_i = (b_i+1)(\omega_i + C_i + \alpha_i)(i = 1,2,3,..,S)$ in results (6) and (7) and in the values of $\Delta_{R-1},....,\Delta_3,\Delta_2$.

Using the normalizing condition, $P(\tilde{0},\tilde{0})$ can be calculated from result (8) as under

$$P(\tilde{a},\tilde{b}) = P(\tilde{0},\tilde{0})\left(\frac{1}{a_1!}\left(\frac{\rho_1}{(\omega_1 + C_1 + \alpha_1)}\right)^{a_1}\right).$$

$$\left(\frac{1}{a_2!}\left(\frac{\rho_2}{(\omega_2 + C_2 + \alpha_2)}\right)^{a_2}\right)$$

$$\left(\frac{1}{a_3!}\left(\frac{\rho_3}{(\omega_3 + C_3 + \alpha_3)}\right)^{a_3}\right)...\left(\frac{1}{a_{R-1}!}\left(\frac{\rho_{R-1}}{\omega_{R-1} + C_{R-1} + \alpha_{R-1})}\right)^{a_{R-1}}\right)$$

$$\left(\frac{1}{a_R!}\left(\frac{\rho_R}{(\omega_R + C_R + \alpha_R)}\right)^{a_R}\right).\left[\frac{1}{b_1!}\left(\frac{\eta_{11} + \frac{\omega_R t_{R1}\rho_R}{(b_R+1)(\omega_R + \alpha_R + C_{R\alpha_R+1})}}{\omega_{11}}\right)^{b_1}\right].$$

$$\left[\frac{1}{b_2!}\left(\frac{\eta_{12} + \frac{\omega_R t_{R2}\rho_R}{(b_R+1)(\omega_R + \alpha_R + C_{R\alpha_R+1})}}{\omega_{12}}\right)^{b_2}\right].\left[\frac{1}{b_3!}\left(\frac{\eta_{13} + \frac{\omega_R t_{R3}\rho_R}{(b_R+1)(\omega_R + \alpha_R + C_{R\alpha_R+1})}}{\omega_{13}}\right)^{b_3}\right].....$$

$$\left[\frac{1}{b_S!}\left(\frac{\eta_{1S} + \frac{\omega_R t_{RS}\rho_R}{(b_R+1)(\omega_R + \alpha_R + C_{R\alpha_R+1})}}{\omega_{1S}}\right)^{b_S}\right]$$

$$a_i \geq 0, b_j \geq 0; (i = 1,2,3,...,R; j = 1,2,3,....,S) \quad (8)$$

Where,

$$\rho_1 = \eta_1 + K_{21}\rho_2 + K_{31}\rho_3 + K_{41}\rho_4 + ... + K_{R-2,1}\rho_{R-2} + K_{R-1,1}\rho_{R-1} + K_{R,1}\rho_R$$

$$\rho_2 = \eta_2 + \frac{\omega_1 p_1 \rho_1}{h_1} + K_{32}\rho_3 + K_{42}\rho_4 + ... + K_{R-2,2}\rho_{R-2} + K_{R-1,2}\rho_{R-1} + K_{R,2}\rho_R$$

$$\rho_3 = \eta_3 + \frac{\omega_2 p_2 \rho_2}{h_2} + K_{43}\rho_4 + K_{53}\rho_5 + ... + K_{R-2,3}\rho_{R-2} + K_{R-1,3}\rho_{R-1} + K_{R,3}\rho_R$$

...

…

$$\rho_{R-2} = \eta_{R-2} + \frac{\omega_{R-3} p_{R-3} \rho_{R-3}}{h_{R-3}} + K_{R-1,R-2}\rho_{R-1} + K_{R,R-2}\rho_R$$

$$\rho_{R-1} = \eta_{R-1} + \frac{\omega_{R-2} p_{R-2} \rho_{R-2}}{h_{R-2}} + K_{R,R-1}\rho_R$$

$$\cdot\ \rho_R = \eta_R + \frac{\omega_{R-1} p_{R-1} \rho_{R-1}}{h_{R-1}}$$

As discussed earlier, we can find ρ_R from R-equations given above with the help of determinants or ρ_R can be derived easily directly by taking $K_{ij} = \frac{p_{ij}\omega_i}{(a_i+1)(\omega_i + C_i + \alpha_i)} (j = 1,2,3,....,R-1)$ and $h_i = (b_i+1)(\omega_i + C_i + \alpha_i)(i = 1,2,3,..,S)$ in results (6) and (7) and in the values of $\Delta_{R-1},....,\Delta_3,\Delta_2$.

Using the normalizing condition, $P(\tilde{0},\tilde{0})$ can be calculated from result (8) as under

$$1 = \sum_{\substack{\tilde{a}=\tilde{0} \\ \tilde{b}=\tilde{0}}}^{\infty} P(\tilde{a},\tilde{b}) = P\left(\tilde{0},\tilde{0}\right)\left(\sum_{a_1=0}^{\infty}\frac{1}{a_1!}\left(\frac{\rho_1}{\omega_1 + C_1 + \alpha_1}\right)^{a_1}\right).$$

$$\left(\sum_{a_2=0}^{\infty}\frac{1}{a_2!}\left(\frac{\rho_2}{\omega_2 + C_2 + \alpha_2}\right)^{a_2}\right)\cdot\left(\sum_{a_3=0}^{\infty}\frac{1}{a_3!}\left(\frac{\rho_3}{\omega_3 + C_3 + \alpha_3}\right)^{a_3}\right)\cdots\cdot\left(\sum_{a_{R-1}=0}^{\infty}\frac{1}{a_{R-1}!}\left(\frac{\rho_{R-1}}{\omega_{R-1} + C_{R-1} + \alpha_R}\right)^{a_{R-1}}\right).$$

$$\left(\sum_{b_R=0}^{\infty}\frac{1}{b_R!}\left(\frac{\rho_R}{\mu_R + C_R + \alpha_R}\right)^{n_R}\right)\cdot\sum_{b_1=0}^{\infty}\frac{1}{b_1!}\left(\frac{\rho_{11}}{\omega_{11}}\right)^{b_1}\cdot\sum_{b_2=0}^{\infty}\frac{1}{b_2!}\left(\frac{\rho_{12}}{\omega_{12}}\right)^{b_2}\cdot\sum_{b_3=0}^{\infty}\frac{1}{b_3!}\left(\frac{\rho_{13}}{\omega_{13}}\right)^{b_3}\cdots\sum_{b_S=0}^{\infty}\frac{1}{b_S!}\left(\frac{\rho_{1S}}{\omega_{1S}}\right)^{b_S}$$

where,

$$\rho_{1j} = \eta_{1j} + \frac{\omega_R \rho_R r_{Rj}}{(a_R + 1)(\omega_R + \alpha_R + C_R)}, j = 1, 2, 3...., S$$

Therefore,

$$1 = P\left(\tilde{0}, \tilde{0}\right)\left(\prod_{i=1}^{R} e^{\left(\frac{\rho_i}{(\omega_i + C_i + \alpha_i)}\right)}\right)\left(\prod_{j=1}^{S} e^{\frac{\rho_{1j}}{\omega_{1j}}}\right)$$

Thus,

$$P\left(\tilde{0}, \tilde{0}\right)^{-1} = \left(\prod_{i=1}^{R} e^{\left(\frac{\rho_i}{(\omega_i + C_i + \alpha_i)}\right)}\right)\left(\prod_{j=1}^{S} e^{\frac{\rho_{1j}}{\omega_{1j}}}\right)$$

Thus $P\left(\tilde{a}, \tilde{b}\right)$ has been calculated completely.

Marginal Probabilities in Steady-state

The steady-state marginal probability of the service channel Q_1 having a_1 customers waiting for service before the server S_1 denoted by $P\left(b_1\right)$, is determined by using (8) and above result as under

$$P\left(a_1\right) = \sum_{\substack{a_2=0=a_3,...,=a_R \\ \tilde{b}=0}}^{\infty} P\left(\tilde{a}, \tilde{b}\right) = \frac{\frac{1}{a_1!}\left(\frac{\rho_1}{\omega_1 + C_1 + \alpha_1}\right)^{a_1}}{e^{\left(\frac{\rho_1}{\omega_1 + C_1 + \alpha_1}\right)}}$$

$$P\left(a_i\right) = \frac{\frac{1}{a_i!}\left(\frac{\rho_i}{\omega_i + C_i + \alpha_i}\right)^{a_i}}{e^{\left(\frac{\rho_i}{\omega_i + C_i + \alpha_i}\right)}} \; for \; i = 2, 3, 4, ..., R-1, R$$

Mean Queue Length

Marginal mean queue length before the server S_1 is derived by

$$L_1=\sum_{a_1=0}^{\infty}a_1P(a_1)=\sum_{a_1=0}^{\infty}\frac{\frac{a_1}{a_1!}\left(\frac{\rho_1}{\omega_1+C_1+\alpha_1}\right)^{a_1}}{e^{\left(\frac{\rho_1}{\omega_1+C_1+\alpha_1}\right)}}=\frac{\rho_1}{\omega_1+C_1+\alpha_1}$$

Similarly

$$L_i=\frac{\rho_i}{\omega_i+C_i+\alpha_i};i=1,2,3,...,R$$

$$L_{1j}=\frac{p_{1j}}{\omega_{1j}};j=1,2,3,...,S$$

Therefore, Mean queue length of the system =

$$L=\sum_{i=1}^{R}L_i+\sum_{j=1}^{S}L_{1j}=\sum_{i=1}^{R}\frac{\rho_i}{\omega_i+C_i+\alpha_i}+\sum_{j=1}^{S}\frac{\rho_{1j}}{\omega_{1j}}$$

Behaviour of Marginal Mean Queue Length of the Model with Arrival Rate taking varying reneging rate
Keeping various parameters fixed by taking some constant value:

1. Probability of joining the next server i.e. p_i = 0.5
2. Probability of joining back the previous server i.e. r_{Rl} = 0.02
3. Number of customers before serial server i.e. a_i = 10
4. Arrival rate before serial server i.e. η_i =25
5. Number of customers before non-serial servers i.e. b_j =12
6. Arrival rate before non-serial server i.e. η_{1j} = 10
7. Probability of joining the non-serial servers i.e. T_{Rj} = 0.02
8. Service rate before non-serial server i.e. ω_{1j} = 15

The given graph indicates the following results:

- With the increase in service rate, the mean queue length of the system falls down gradually for various values of reneging rate.It means by providing services quickly the person stops reneging and also the length of the queue decreases .
- Also with the increase in service rate, the system becomes independent of reneging rate .
- Marginal mean queue length has higher values for lower value of reneging rate irrespective of the service rate though the gap becomes lesser with the increase in the value of ω_i

CONCLUDING REMARKS

1. The important concept of balking and reneging are studied deeply in the present work because both the concepts have a bearing effects on the direct as well as indirect cost of the business.
2. If the current model simply allows feedback from each service channel to its prior service channel, the outcomes would be similar to those of the queuing model stated in reference no. 21.

REFERENCES

1. Barrer, D.Y. (1955): A Waiting line problem characterized by impatient customers and indifferent clerk. Journal of Operation Research Society of America.Vol. 3, 360 .
2. Finch, P.D (1959):Cyclic queues with feedback. Journal of Royal Statistical Society B-21, 153-157.
3. Gupta,Deepak, Singh,Man and Sangeeta (2021):Queuing System with Feedback and Reneging due to Impatient Customers and Urgent Call. Turkish Online Journal Of Qualitative Enquiry,12(8),3937-3954.
4. 4.Gupta, Meenu, Singh,Man and Gupta, Deepak (2018).Study of customers' behaviour multi-channel finite queuing systems. LAP LAMBERT AcademicPub lishing, Mauritius.
5. 5.Gupta, Meenu, Singh,Man and Gupta,Deepak (2020) .Solutions for network of multi-channel Mixed Queues. LAP LAMBERT Academic Publishing, Mauritius.
6. 6.Gupta, Meenu, Singh,Man and Gupta,Deepak(2020).The time independent analysis of finite waiting space
7. generalized multi-channel mixed queuing system with balking and reneging due to long queue and some
8. message. Journal of computational and theoretical Nanoscience ,17(11), 5057-5061.
9. 7.Gupta; S.M.(1994):Inter relationship between queuing models with balking and reneging and machine repair problem with warm spares. Microelectronics and Reliability. Vol. 34, No. 2, 201-209.
10. 8.Gupta,Meenu, Singh,Man and Tonk, Manju (2020).Analysis of a queue process with balking , reneging
11. and pre-emptive priority. Mathematical sciences- Repositories of logical thoughts and analytical tools,
12. CCSHAU - Hisar.
9. Gupta,Renu and Gupta,Deepak (2020).Analysis of steady state behaviour of biserial and parallel queue
13. network model with batch arrival. Journal ofComputational and Theoretical Nano Science 17(11),5032
14. -5036.
10. Hunt, G.C. (1955): Sequential arrays of waiting lines. opps. Res. Vol. 4, 674-683
15. 11.Jackson, R.R.P(1954):Queuing system with phase type service. operat. Res. Quart.Vol.5, No. 2. 109-120.
16. 12.Kelly, F.P (1979):Reversibility and stochastic networks. John Willy and pons Inc. New York.
17. 13. O'Brien, G.G. (1954):The solution of some queuing problems. J. Soc. Ind. Appl. Math.
18. Vol. 2, 132-142.
19. 14. Singh. M.(1984):Steady-state behaviour of serial queuing processes with impatient customers. Math. operations forsch, U.statist. Ser. Statist. Vol. 15.No 2, 289-298.
20. 15. Singh, M and Singh, Umed (1994): Network of serial and non-serial queuing processeswith impatient customers. JISSOR Vol. 15, (1-4), 81-96.
21. 16. Singh, Satyabir and Singh, Man (2012). The Steady-State Solution of Serial Queuing Processes with Feedback and reneging. Journal of Contemporary Applied Mathematics ,2(1), 32-38.
22. 17. Singh,Satyabir ;Singh, Man (2016).Study of some serial and non-serial queuing processes with various types of customers' behaviour. Ph.D Thesis.

Service rate μi for server Si	Servers in Series Si	reneging rate before the serial server			ρi			Marginal Mean queue length before the server			Marginal mean queue length before non-serial server			Mean queue length of the system		
10	1	1	8	11	30.82222	29.89509	29.88978	2.37094	1.494754	1.286619	10.045623	10.04145	10.03988	12.41656	11.5362	11.3265
20	2	1	8	11	32.21363	30.71474	31.1914	1.400593	1.023825	0.917681	10.045623	10.04145	10.03988	11.44622	11.06527	10.95756
25	3	1	8	11	30.58672	29.68903	29.69214	1.092383	0.848258	0.773644	10.045623	10.04145	10.03988	11.13801	10.8897	10.81352
30	4	1	8	11	29.81557	29.12644	29.06199	0.903502	0.728161	0.671943	10.045623	10.04145	10.03988	10.94912	10.76961	10.71182
45	5	1	8	11	29.06318	28.51908	28.45245	0.605483	0.518529	0.48847	10.045623	10.04145	10.03988	10.65111	10.55997	10.52835
50	6	1	8	11	28.34045	27.9515	27.83985	0.534725	0.465858	0.441462	10.045623	10.04145	10.03988	10.58035	10.5073	10.48134
60	7	1	8	11	27.60035	27.3112	27.22664	0.438101	0.39016	0.372691	10.045623	10.04145	10.03988	10.48372	10.43161	10.41257
65	8	1	8	11	26.87916	26.68575	26.6154	0.395282	0.35581	0.341213	10.045623	10.04145	10.03988	10.4409	10.39726	10.38109
70	9	1	8	11	26.16788	26.05126	26.00816	0.358464	0.325641	0.313351	10.045623	10.04145	10.03988	10.40409	10.36709	10.35323

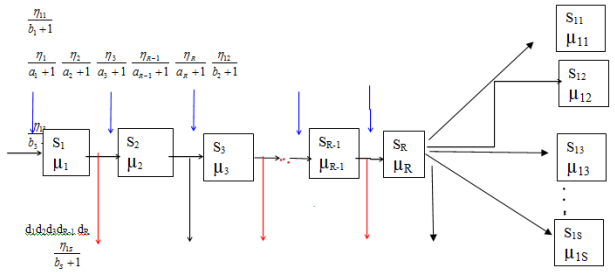

Fig.(i) Serial with non-serial service channel Queuing Model

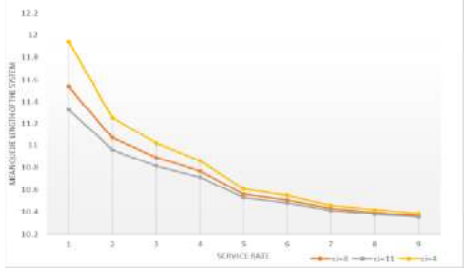

Graph

Indian Journal of Natural Sciences *www.tnsroindia.org.in ©IJONS*

Vol.15 / Issue 83 / Apr / 2024 *International Bimonthly (Print) – Open Access* *ISSN: 0976 – 0997*

RESEARCH ARTICLE

Fuzzy Analysis of Priority Queuing Model by using Two Different Approach

Aarti Saini[1]*, Vandana Saini[2] and Deepak Gupta[3]

[1]Govt. College for Women, Shahzadpur (Ambala), India.
[2]Govt. P. G. College, Naraingarh (Ambala), India
[3]Mathematics Department, Maharishi Markandeshwar (deemed to be University), Mullana (Ambala), Haryana, India.

Received: 30 Dec 2023 Revised: 09 Jan 2024 Accepted: 12 Jan 2024

***Address for Correspondence**
Aarti Saini
Govt. College for Women,
Shahzadpur (Ambala), India.
Email: aartisaini195@gmail.com

ABSTRACT

This study compares the performance of a parallel and biserial priority queue system in fuzzy environments. In this paper, we investigate fuzzy behavior of purposed model by applying two different approach α-cut and L-R. The model consists biserial subsystems with priority discipline and parallel subsystems assuming general arrival connected with common server. Numerical behavior of queue Parameters are well explained by both methods.

Keywords: fuzzy, Priority, Parallel, L-R method, Biserial, α-cut

INTRODUCTION

Priority queues are extremely important in queuing theory for offering various customer classes high-quality service. However, the input data for the priority queuing model is unpredictable, and fuzzy logics have been employed to eliminate this ambiguity. When compared to crisp values, fuzzy concepts produce solutions that are more acceptable. Numerous scholars developed queueing models in a fuzzy setting using various methodologies and fuzzy numbers. Li and Lee [1], Gupta [2,3], Singh T. P. [4], Mittal [5], Sharma [6], J. Devraj [7], B. Kalpana and N. Anusheela [8,9] used Zadeh Principle based α-cut approach. Saini A., Gupta D and A. K. Tripathi [10] analyzed queue system with heterogeneous server and bi-tandem queues in fuzzy by the use of α-cut. Ritha and Menon [11], W. Ritha and S. Josephine Vinnarasi [12], Mukeba [13,14], Saini V, Gupta D and Tripathi A. K. [15] discussed the queue models in fuzzy by applying feedback and triangular fuzzy numbers through the L-R method. Gupta D, Saini A and Tripathi A. K [16] discussed queue characteristics of priority queue model consisting bi-serial and parallel

servers in stochastic environment. The present paper is fuzzy representation of existing study by using two different approaches in fuzzy environment.

Definitions

Fuzzy Set If the results of a membership function of a function $\tilde{G}$ defined on the universal set X is either $\mu_{\tilde{G}}(x) = 1; x \in X \text{ or } \mu_{\tilde{G}}(x) = 0; x \notin X$, then the function is said to be fuzzy.

α – cut approach

A fuzzy set $\tilde{L}\ defined\ on\ X\ as\ \tilde{L}: X \to [0,1]\ and$ for any $\alpha \in [0,1]$, then the $\alpha - cut\ \alpha_L = \{x \in X, \mu_{\tilde{L}}(X) \geq \alpha\}$ for $\tilde{L}$is a crisp set.

Strong $\alpha - cuts: \alpha +_L = \{x \in X, \mu_L(X) > \alpha\}\ whenever\ \alpha\ lies\ between\ 0\ \&\ 1$

Weak $\alpha - cuts$: $\alpha_L = \{x \in X, \mu_L(X) \geq \alpha\} whenever\ \alpha\ lies\ between\ 0\ \&\ 1$ As all members of a fuzzy set must be greater than or equal to α, it is important to view fuzzy sets as crisp sets.

Fuzzy Triangular Number

A number $\tilde{L} = (l_1, m_1, l_2)$ is a fuzzy triangular number, if the membership function $\mu_{\tilde{L}}(x)\ of\ \tilde{L}$ is defined as

$$\mu_{\tilde{L}}(X) = \begin{cases} \dfrac{x - l_1}{m_1 - l_1}, & l_1 \leq x \leq m_1 \\ \dfrac{l_2 - x}{l_2 - m_1}, & m_1 \leq x \leq l_2 \\ 0, otherwise \end{cases}$$

Fuzzy L-R Number (J. P. Mukeba et al 2015,2016)

A number $\tilde{H} = (h_1,\ m_1, h_2)$ is said to be fuzzy L-R $\Leftrightarrow$ three real numbers $m_1,\ h_1,\ h_2 > 0$, as well as two continuous, positive and decreasing functions L and R, exist from R to [0,1], and satisfying the following conditions as such that

L (0) = 1, L (1) = 0, L (x) > 0, $\lim_{x\to\infty}$ L (x) = 0

R (0) = 1, R (1) = 0, R (x) > 0, $\lim_{x\to\infty}$ R (x) = 0

$$\mu_{\tilde{H}}(X) = \begin{cases} L\left(\dfrac{m_1 - x}{h_1}\right), & x \in [m_1 - h_1, m_1] \\ R\left(\dfrac{x - m_1}{h_2}\right), & x \in [m_1, m_1 + h_2] \\ 0, otherwise \end{cases}$$

A fuzzy number $\tilde{G}$ is represented in L-R form as its L-R representation is of the form $\tilde{H} = (\ m_1, h_1, h_2)_{LR}$, where m_1, h_1, h_2 are used as modal value, left and right spread of $\tilde{H}$ respectively.

Supp $(\tilde{H})$ = ($m_1 - h_1,\ m_1 + h_2$)

L-R fuzzy Arithmetic (J. P. Mukeba et al 2015, 2016)

L-R fuzzy Arithmetic operations on two L-R fuzzy numbers $\tilde{G} = (\ m_1, g_1, g_2)_{LR}$ &$\tilde{H} = (\ l_1, h_1, h_2)_{LR}$ are define as

$$\tilde{G} + \tilde{H} = (m_1 + l_1, g_1 + h_1, g_2 + h_2)_{LR}$$

$$\tilde{G} - \tilde{H} = (m_1 - l_1, g_1 + h_2, g_2 + h_1)_{LR}$$

$$\tilde{G}.\tilde{H} = (m_1 l_1, m_1 h_1 + l_1 g_1 - g_1 h_1, m_1 h_2 + l_1 g_2 + g_2 h_2)_{LR}$$

$$\frac{\tilde{G}}{\tilde{H}} = \left(\frac{m_1}{l_1}, \frac{m_1 h_2}{l_1(l_1 + h_2)} + \frac{g_1}{l_1} - \frac{g_1 h_2}{l_1(l_1 + h_2)}, \frac{m_1 h_1}{l_1(l_1 - h_1)} + \frac{g_2}{l_1} + \frac{g_2 h_1}{l_1(l_1 - h_1)}\right)_{LR}$$

Defuzzification

A triangular fuzzy number $\tilde{G}$ = (g_1, g_2, g_3) fuzzified into crisp number G = $\frac{g1+2\ g2+\ g3}{4}$ by using Yager's formula.

Model Description

The purposed model consists three subsystems C_1, C_2, C_3. The Subsystem C_1 has two biserial servers C_{11}& C_{12} and subsystem C_2 has parallel server C_{21} & C_{22}. Both C_1&C_2 are linked to C_3. Both type of low and high priority customer

enters into the system either from biserial or parallel server. After being served the customer move to next server for availing the service of next phase.

Notations

$\widetilde{m_{ij}}$ = fuzzy low and high priority arriving customer, i = 1,2 & j = L, H
$\widetilde{\lambda_{ij}}$ = fuzzy Priority input rate, i = 1,2 & j = L, H
$\widetilde{\lambda_i'}$ = fuzzy general arrivals, i = 1,2
$\widetilde{\mu_{ij}}$ = fuzzy cost of service for low and high priority visitors, i = 1,2 & j = L, H
$\widetilde{\mu_i'}$ = fuzzy service rate at parallel subsystem
$\widetilde{\alpha_{ij}}$ = fuzzy probabilities from i'th server to j'th server
$\tilde{L}$ = The system's fuzzy queue length

Mathematical Approach

The utilization factors at different servers, based on the mathematical characterization of stochastic processes of the work Saini A., Gupta D. and A. K. Tripathi (2023) are as -

$$\gamma_1 = \frac{\lambda_{1H} + \lambda_{2H}\alpha_{21}}{\mu_{1H}(1-\alpha_{12}\alpha_{21})}$$

$$\gamma_2 = \frac{\lambda_{2H} + \lambda_{1H}\alpha_{12}}{\mu_{2H}(1-\alpha_{12}\alpha_{21})}$$

$$\gamma_3 = \frac{\lambda_1'}{\mu_1'\alpha_{35}}$$

$$\gamma_4 = \frac{\lambda_2'}{\mu_2'\alpha_{45}}$$

$$\gamma_5 = \frac{\begin{matrix}(\lambda_1' + \lambda_2')(1-\alpha_{12}\alpha_{21}) + \alpha_{15}[(\lambda_{1H} + \lambda_{2H}\alpha_{21}) + (\lambda_{1L} + \lambda_{2L}\alpha_{21})] \\ +\alpha_{25}[(\lambda_{2H} + \lambda_{1H}\alpha_{12}) + (\lambda_{2L} + \lambda_{1L}\alpha_{12})]\end{matrix}}{\mu_3(1-\alpha_{12}\alpha_{21})}$$

$$\gamma_6 = \frac{\mu_{1L}(\lambda_{1H} + \lambda_{2H}\alpha_{21}) + \mu_{1H}(\lambda_{1L} + \lambda_{2L}\alpha_{21})}{\mu_{1L}\mu_{1H}(1-\alpha_{12}\alpha_{21})}$$

$$\gamma_7 = \frac{\mu_{2L}(\lambda_{2H} + \lambda_{1H}\alpha_{12}) + \mu_{2H}(\lambda_{2L} + \lambda_{1L}\alpha_{12})}{\mu_{2L}\mu_{2H}(1-\alpha_{12}\alpha_{21})}$$

Solution of the model

$$P_{m_{1L},m_{1H},m_{2L},m_{2H},m_2,m_{3,m_5}} = = \gamma_1^{m_{1H}}\gamma_2^{m_{2H}}\gamma_3^{m_2}\gamma_4^{m_3}\gamma_5^{m_5}\gamma_6^{m_{1L}}\gamma_7^{m_{2L}} (1-\gamma_1)(1-\gamma_2)(1-\gamma_3)(1-\gamma_4)(1-\gamma_5)(1-\gamma_6)(1-\gamma_7)$$

occur if $\gamma_1, \gamma_2, \gamma_3, \gamma_4, \gamma_5, \gamma_6, \gamma_7 \leq 1$

Fuzzy representation of queue parameters and server utilizations are as follows-

$$\widetilde{\gamma_1} = \frac{\widetilde{\lambda_{1H}} + \widetilde{\lambda_{2H}}\widetilde{\alpha_{21}}}{\widetilde{\mu_{1H}}(1-\widetilde{\alpha_{12}}\widetilde{\alpha_{21}})}$$

$$\widetilde{\gamma_2} = \frac{\widetilde{\lambda_{2H}} + \widetilde{\lambda_{1H}}\widetilde{\alpha_{12}}}{\widetilde{\mu_{2H}}(1-\widetilde{\alpha_{12}}\widetilde{\alpha_{21}})}$$

$$\widetilde{\gamma_3} = \frac{\widetilde{\lambda_1'}}{\widetilde{\mu_1'}\widetilde{\alpha_{35}}}$$

$$\widetilde{\gamma_4} = \frac{\widetilde{\lambda_2'}}{\widetilde{\mu_2'}\widetilde{\alpha_{45}}}$$

$$\widetilde{\gamma_5} = \frac{\widetilde{\lambda_1'} + \widetilde{\lambda_2'}}{\widetilde{\mu_3}} + \frac{\widetilde{\alpha_{15}}[(\widetilde{\lambda_{1H}} + \widetilde{\lambda_{2H}}\widetilde{\alpha_{21}}) + (\widetilde{\lambda_{1L}} + \widetilde{\lambda_{2L}}\widetilde{\alpha_{21}})] + \widetilde{\alpha_{25}}[(\widetilde{\lambda_{2H}} + \widetilde{\lambda_{1H}}\widetilde{\alpha_{12}}) + (\widetilde{\lambda_{2L}} + \widetilde{\lambda_{1L}}\widetilde{\alpha_{12}})]}{\widetilde{\mu_3}(1-\widetilde{\alpha_{12}}\widetilde{\alpha_{21}})}$$

$$\widetilde{\gamma_6} = \frac{\widetilde{\mu_{1L}}(\widetilde{\lambda_{1H}} + \widetilde{\lambda_{2H}}\widetilde{\alpha_{21}}) + \widetilde{\mu_{1H}}(\widetilde{\lambda_{1L}} + \widetilde{\lambda_{2L}}\widetilde{\alpha_{21}})}{\widetilde{\mu_{1L}}\widetilde{\mu_{1H}}(1-\widetilde{\alpha_{12}}\widetilde{\alpha_{21}})}$$

$\widetilde{\gamma_7} = \frac{\widetilde{\mu_{2L}}(\widetilde{\lambda_{2H}}+\widetilde{\lambda_{1H}}\widetilde{\alpha_{12}})+\widetilde{\mu_{2H}}(\widetilde{\lambda_{2L}}+\widetilde{\lambda_{1L}}\widetilde{\alpha_{12}})}{\widetilde{\mu_{2L}}\widetilde{\mu_{2H}}(1-\widetilde{\alpha_{12}}\widetilde{\alpha_{21}})}$

Fuzzy Lengths of queues

$$\widetilde{L_1} = \frac{\widetilde{\gamma_i}}{1-\widetilde{\gamma_i}}, i = 1,2,3,4,5,6,7$$

$$\tilde{L} = \widetilde{L_1} + \widetilde{L_2} + \widetilde{L_3} + \widetilde{L_4} + \widetilde{L_5} + \widetilde{L_6} + \widetilde{L_7}$$

Average Waiting Time

$E(\widetilde{w}) = \frac{\tilde{L}}{\tilde{\lambda}}$, $\tilde{\lambda} = \widetilde{\lambda_{1L}} + \widetilde{\lambda_{1H}} + \widetilde{\lambda_{2L}} + \widetilde{\lambda_{2H}} + \widetilde{\lambda_1'} + \widetilde{\lambda_2'}$

Fuzzy Evaluation of Queue Parameters

Evaluation using L-R Method

Numerical Illustration

We get, L-R representations of utilization factor with the help of above numerical values

$\widetilde{\gamma_1} = (.3906,.2402,.4365)_{LR}$

$\widetilde{\gamma_2} = (.4167,.2395,.4550)_{LR}$

$\widetilde{\gamma_3} = (.5555,.2876,.6943)_{LR}$

$\widetilde{\gamma_4} = (.4,.316,.8821)_{LR}$

$\widetilde{\gamma_5} = (.6087,.3934,.8171)_{LR}$

$\widetilde{\gamma_6} = (.6260,.4199,.9269)_{LR}$

$\widetilde{\gamma_7} = (.7045,.435,.9731)_{LR}$

Modal values of $\widetilde{\gamma_1}, \widetilde{\gamma_2}, \widetilde{\gamma_3}, \widetilde{\gamma_4}, \widetilde{\gamma_5}, \widetilde{\gamma_6}, \widetilde{\gamma_7}$ are as follows-

$\widetilde{\gamma_1}$ =.3906

$\widetilde{\gamma_2}$ =.4167

$\widetilde{\gamma_3}$ =.5555

$\widetilde{\gamma_4}$ = .4

$\widetilde{\gamma_5}$ =.6087

$\widetilde{\gamma_6}$ = .6260

$\widetilde{\gamma_7}$ =.7045

and for $\widetilde{L_1}, \widetilde{L_2}, \widetilde{L_3}, \widetilde{L_4}, \widetilde{L_5}, \widetilde{L_6}, \widetilde{L_7}$ are .6410, .7144, 1.2497, .6, 3.4984, 1.6738, 2.3841 respectively.

Supp $(\widetilde{\gamma_1})$ = (.3906 − .2402, .3906 + .4365) = (.1504, .8271)

Supp $(\widetilde{\gamma_2})$ = (.4167 − .2395, .4167 + .4550) = (.1772, .8717)

Supp $(\widetilde{\gamma_3})$ = (.5555 − .2876, .5555 + .6943) = (.2679, 1.2498)

Supp $(\widetilde{\gamma_4})$ = (.4 − .316, .4 + .8821) = (.084, 1.2821)

Supp $(\widetilde{\gamma_5})$ = (.6087 − .3934, .6087 + .8171) = (.2153, 1.4258)

Supp $(\widetilde{\gamma_6})$ = (.6260 − .4199, .6260 + .9269) = (.2061, 1.5529)

Supp $(\widetilde{\gamma_7})$ = (.7045 − .435, .7045 + .9731) = (.2695, 1.6776)

Evaluation by α-cut method

As the Methodology adopted by Sameer et al [6], fuzzy parameters are represented as

$$\widetilde{\lambda_{ij}} = (\lambda_{ij}^1, \lambda_{ij}^2, \lambda_{ij}^3),$$
$$\widetilde{\mu_{ij}} = (\mu_{ij}^1, \mu_{ij}^2, \mu_{ij}^3),$$
$$\widetilde{\alpha_{ij}} = (\alpha_{ij}^1, \alpha_{ij}^2, \alpha_{ij}^3),$$
$$\widetilde{\mu_i'} = (\mu_i'^1, \mu_i'^2, \mu_i'^3),$$
$$\widetilde{\lambda_i'} = (\lambda_i'^1, \lambda_i'^2, \lambda_i'^3) \quad \forall\, i \,\&\, j$$

Now, fuzzy utilization factors are defined as

$$\widetilde{\gamma_1} = \left\{\frac{\lambda_{1H}^1 + \alpha_{21}^1\lambda_{2H}^1}{\mu_{1H}^3(1-\alpha_{12}^3\alpha_{21}^3)}, \frac{\lambda_{1H}^2 + \alpha_{21}^2\lambda_{2H}^2}{\mu_{1H}^2(1-\alpha_{21}^2\alpha_{12}^2)}, \frac{\lambda_{1H}^3 + \alpha_{21}^3\lambda_{2H}^3}{\mu_{1H}^1(1-\alpha_{21}^1\alpha_{12}^1)}\right\}$$

$$\widetilde{\gamma_2} = \left\{\frac{\lambda_{2H}^1 + \alpha_{12}^1\lambda_{1H}^1}{\mu_{2H}^3(1-\alpha_{12}^3\alpha_{21}^3)}, \frac{\lambda_{2H}^2 + \alpha_{12}^2\lambda_{1H}^2}{\mu_{2H}^2(1-\alpha_{21}^2\alpha_{12}^2)}, \frac{\lambda_{2H}^3 + \alpha_{12}^3\lambda_{1H}^3}{\mu_{2H}^1(1-\alpha_{21}^1\alpha_{12}^1)}\right\}$$

$$\widetilde{\gamma_3} = \left\{\frac{\lambda_1^{'1}}{\alpha_{35}^3\mu_1^{'3}}, \frac{\lambda_1^{'2}}{\alpha_{35}^2\mu_1^{'2}}, \frac{\lambda_1^{'3}}{\alpha_{35}^1\mu_1^{'1}}\right\}$$

$$\widetilde{\gamma_4} = \left\{\frac{\lambda_2^{'1}}{\alpha_{45}^3\mu_2^{'3}}, \frac{\lambda_2^{'2}}{\alpha_{45}^2\mu_2^{'2}}, \frac{\lambda_2^{'3}}{\alpha_{45}^1\mu_2^{'1}}\right\}$$

$$\widetilde{\gamma_5} = \left\{\begin{array}{l} \frac{\lambda_1^{'1}+\lambda_2^{'1}}{\mu_3^3} + \frac{\alpha_{15}^1[(\lambda_{1H}^1 + \alpha_{21}^1\lambda_{2H}^1) + (\lambda_{1L}^1 + \alpha_{21}^1\lambda_{2L}^1)] + \alpha_{25}^1[(\lambda_{2H}^1 + \alpha_{12}^1\lambda_{1H}^1) + (\lambda_{2L}^1 + \alpha_{12}^1\lambda_{1L}^1)]}{\mu_3^3(1-\alpha_{12}^3\alpha_{21}^3)}, \\ \frac{\lambda_1^{'2}+\lambda_2^{'2}}{\mu_3^2} + \frac{\alpha_{15}^2[(\lambda_{1H}^2 + \alpha_{21}^2\lambda_{2H}^2) + (\lambda_{1L}^2 + \alpha_{21}^2\lambda_{2L}^2)] + \alpha_{25}^2[(\lambda_{2H}^2 + \alpha_{12}^2\lambda_{1H}^2) + (\lambda_{2L}^2 + \alpha_{12}^2\lambda_{1L}^2)]}{\mu_3^2(1-\alpha_{12}^2\alpha_{21}^2)}, \\ \frac{\lambda_1^{'3}+\lambda_2^{'3}}{\mu_3^1} + \frac{\alpha_{15}^3[(\lambda_{1H}^3 + \alpha_{21}^3\lambda_{2H}^3) + (\lambda_{1L}^3 + \alpha_{21}^3\lambda_{2L}^3)] + \alpha_{25}^3[(\lambda_{2H}^3 + \alpha_{12}^3\lambda_{1H}^3) + (\lambda_{2L}^3 + \alpha_{12}^3\lambda_{1L}^3)]}{\mu_3^1(1-\alpha_{12}^1\alpha_{21}^1)} \end{array}\right\},$$

$$\widetilde{\gamma_6} = \left\{\begin{array}{l} \frac{\mu_{1L}^1(\lambda_{1H}^1 + \alpha_{21}^1\lambda_{2H}^1) + \mu_{1H}^1(\lambda_{1L}^1 + \alpha_{21}^1\lambda_{2L}^1)}{\mu_{1L}^3\mu_{1H}^3(1-\alpha_{12}^3\alpha_{21}^3)}, \\ \frac{\mu_{1L}^2(\lambda_{1H}^2 + \alpha_{21}^2\lambda_{2H}^2) + \mu_{1H}^2(\lambda_{1L}^2 + \alpha_{21}^2\lambda_{2L}^2)}{\mu_{1L}^2\mu_{1H}^2(1-\alpha_{21}^2\alpha_{12}^2)}, \\ \frac{\mu_{1L}^3(\lambda_{1H}^3 + \alpha_{21}^3\lambda_{2H}^3) + \mu_{1H}^3(\lambda_{1L}^3 + \alpha_{21}^3\lambda_{2L}^3)}{\mu_{1L}^3\mu_{1H}^1(1-\alpha_{21}^1\alpha_{12}^1)} \end{array}\right\},$$

$$\widetilde{\gamma_7} = \left\{\begin{array}{l} \frac{\mu_{2L}^1(\lambda_{2H}^1 + \alpha_{12}^1\lambda_{1H}^1) + \mu_{2H}^1(\lambda_{2L}^1 + \alpha_{12}^1\lambda_{1L}^1)}{\mu_{2L}^3\mu_{2H}^3(1-\alpha_{12}^3\alpha_{21}^3)}, \\ \frac{\mu_{2L}^2(\lambda_{2H}^2 + \alpha_{12}^2\lambda_{1H}^2) + \mu_{2H}^2(\lambda_{2L}^2 + \alpha_{12}^2\lambda_{1L}^2)}{\mu_{2L}^2\mu_{2H}^2(1-\alpha_{21}^2\alpha_{12}^2)}, \\ \frac{\mu_{2L}^3(\lambda_{2H}^3 + \alpha_{12}^3\lambda_{1H}^3) + \mu_{2H}^3(\lambda_{2L}^3 + \alpha_{12}^3\lambda_{1L}^3)}{\mu_{2L}^3\mu_{2H}^1(1-\alpha_{21}^1\alpha_{12}^1)} \end{array}\right\},$$

From Table3, we get utilization factor

$$\widetilde{\gamma_1} = (\gamma_1^1, \gamma_1^2, \gamma_1^3) = (.2053, .3906, .5844)$$
$$\widetilde{\gamma_2} = (\gamma_2^1, \gamma_2^2, \gamma_2^3) = (.4456, .4167, .2983)$$
$$\widetilde{\gamma_3} = (\gamma_3^1, \gamma_3^2, \gamma_3^3) = (.375, .5555, .8928)$$
$$\widetilde{\gamma_4} = (\gamma_4^1, \gamma_4^2, \gamma_4^3) = (.5495, .4, .1961)$$
$$\widetilde{\gamma_5} = (\gamma_5^1, \gamma_5^2, \gamma_5^3) = (.7640, .7778, .7937)$$
$$\widetilde{\gamma_6} = (\gamma_6^1, \gamma_6^2, \gamma_6^3) = (.4580, .6260, .7597)$$
$$\widetilde{\gamma_7} = (\gamma_7^1, \gamma_7^2, \gamma_7^3) = (.7453, .7045, .6339)$$

and queue lengths

$$\widetilde{L_1} = \frac{\widetilde{\gamma_1}}{1-\widetilde{\gamma_1}} = (.3393, .6410, .9657)$$
$$\widetilde{L_2} = \frac{\widetilde{\gamma_2}}{1-\widetilde{\gamma_2}} = (.7095, .7144, .4750)$$
$$\widetilde{L_3} = \frac{\widetilde{\gamma_3}}{1-\widetilde{\gamma_3}} = (1.0243, 1.2497, 2.4387)$$
$$\widetilde{L_4} = \frac{\widetilde{\gamma_4}}{1-\widetilde{\gamma_4}} = (.8761, .6667, .3126)$$
$$\widetilde{L_5} = \frac{\widetilde{\gamma_5}}{1-\widetilde{\gamma_5}} = (3.4539, 3.5005, 3.5882)$$
$$\widetilde{L_6} = \frac{\widetilde{\gamma_6}}{1-\widetilde{\gamma_6}} = (1.1708, 1.6738, 1.9420)$$
$$\widetilde{L_7} = \frac{\widetilde{\gamma_7}}{1-\widetilde{\gamma_7}} = (2.4011, 2.3841, 2.0422)$$

De fuzzified values of utilization factors and length of queues by Yager's formula are

$$\widetilde{\gamma_1} = .3927, \quad \widetilde{\gamma_2} = .3943, \quad \widetilde{\gamma_3} = .5947, \quad \widetilde{\gamma_4} = .3864, \quad \widetilde{\gamma_5} = .7783, \quad \widetilde{\gamma_6} = .6174, \quad \widetilde{\gamma_7} = .6971$$

$$\widetilde{L_1} = .6468, \widetilde{L_2} = .6533, \widetilde{L_3} = 1.4906, \widetilde{L_4} = .6305, \quad \widetilde{L_5} = 3.5108, \widetilde{L_6} = 1.6151, \quad \widetilde{L_7} = 2.3029$$

The most possible value of utilization factors and length of queues, are as -

$$\widetilde{\gamma_1} = .3906, \quad \widetilde{\gamma_2} = .4167, \quad \widetilde{\gamma_3} = .5555, \quad \widetilde{\gamma_4} = .4, \quad \widetilde{\gamma_5} = .7778, \quad \widetilde{\gamma_6} = .6260, \quad \widetilde{\gamma_7} = .7045$$

$\widetilde{L_1} = .6410, \widetilde{L_2} = .7144, \widetilde{L_3} = 1.2497, \widetilde{L_4} = .6667, \widetilde{L_5} = 3.5005, \widetilde{L_6} = 1.6738, \widetilde{L_7} = 2.3841$

RESULTS

Comparing the numerical values obtained by α-cut and L-R approach on same data,

1. Utilization factors and mean length of queue modal values are $\widetilde{\gamma_1} = .3906, \widetilde{\gamma_2} = .4167, \widetilde{\gamma_3} = .5555, \widetilde{\gamma_4} = .4, \widetilde{\gamma_5} = .6087, \widetilde{\gamma_6} = .6260, \widetilde{\gamma_7} = .7045$ and $\widetilde{L_1} = .6410, \widetilde{L_2} = .7144, \widetilde{L_3} = 1.2497, \widetilde{L_4} = .6, \widetilde{L_5} = 3.4984, \widetilde{L_6} = 1.6738, \widetilde{L_7} = 2.3841$ respectively.
2. The most prevalent queue lengths and utilization parameters are $\widetilde{L_1} = .6410, \widetilde{L_2} = .7144, \widetilde{L_3} = 1.2497, \widetilde{L_4} = .6667, \widetilde{L_5} = 3.5005, \widetilde{L_6} = 1.6738, \widetilde{L_7} = 2.3841$ *and* $\widetilde{\gamma_1} = .3906, \widetilde{\gamma_2} = .4167, \widetilde{\gamma_3} = .5555, \widetilde{\gamma_4} = .4, \widetilde{\gamma_5} = .7778, \widetilde{\gamma_6} = .6260, \widetilde{\gamma_7} = .7045$.

Thus, the values of utilization factor and queue length by α-cut are higher than the values by L-R method at common server.

CONCLUSION

In this research paper, we have used two different methods α-cut and L- R on approximate same data to analyze the queue behavior of priority queue network of biserial and parallel server in fuzzy environment. From comparative analysis of these two methods, we cannot say which method gives more accurate results than the other because values of queue characteristics obtained by both methods are almost same on all servers except the common server. But we can observe that while calculating numeric values of queue parameters, the L-R technique is shorter, more concise, versatile, and practical as compared to α-cut method. Comparative analysis of these two methods can be applied on more complex models for more accuracy.

REFERENCES

1. Li R.J. and Lee E.S., Analysis of fuzzy queues. Computers and Mathematics with Applications, 17:1143–1147, 1989. http://dx.doi.org/10.1016/0898-1221(89)90044-8.
2. Seema, Gupta D., and Sharma S., Analysis of Biserial Servers Linked to a Common Server in Fuzzy Environment, International Journal of computing science and Mathematics, 68(6): 26-32, 2013. [CrossRef] [Google Scholar]
3. Sharma S., Gupta D., and Seema, Network Analysis of Fuzzy Bi-serial and Parallel Servers with a Multistage Flow Shop Model, 21st International Congress on Modelling and Simulation, Gold Coast, Australia, 697-703, 2015. [Google Scholar]
4. Singh T.P., Mittal M., and Gupta D., Modelling of a Bulk Queue System in Triangular Fuzzy Numbers using α-cut, International Journal of IT and Engineering, 4(9): 72-79, 2016. [Google Scholar]
5. Mittal M., Singh T.P., and Gupta D., Threshold Effect on a Fuzzy Queue Model with Batch Arrival, Aryabhatta Journal of Mathematics & Informatics, 7(1): 109-118, 2015. [Google Scholar] [Publisher Link]
6. Sharma S., Fuzzy Analysis of Synergistic Collaboration of Biserial and Parallel Servers with a Common Server, Advances in Fuzzy Mathematics, 12 (2): 283-296, 2017.
7. Devaraj J. and Jayalakshmi D., A Fuzzy Approach to Priority Queues, International Journal of Fuzzy Mathematics and Systems, 2 (4): 479-488, 2012.
8. Kalpana B., Dr. N. Anusheela, Analysis of Fuzzy Non-Preemptive Priority Queue using Non-Linear Programming, International Journal of Mathematics Trends and Technology (IJMTT), 56(1): 71-80, 2018.
9. Kalpana B., Evaluation of Performance Measures of Fuzzy Queues with Preemptive Priority using Different Fuzzy Numbers, Advances and Applications in Mathematical Sciences, 20(11): 2975-2985, 2021.

10. Saini A., Gupta D and Tripathi A. K., Analysis of Fuzzy Priority Queuing System with Heterogeneous Servers,Aryabhatta Journal of Mathematics and Informatics (AJMI), 15(1): 111-120, 2023.
11. Ritha W. and Menon S.B.), Fuzzy n policy queues with infinite capacity. Journal of Physical Sciences, 15:73–82, 2011.
12. Ritha W. and Vinnarasi Josephine S.), Analysis of Priority Queuing Models: L - R Method, Annals of Pure and Applied Mathematics, 15(2): 271-276, 2017.
13. Mukeba J. P., Mabela R. & Ulungu B., Computing Fuzzy Queuing Performance Measures by L-R Method, Journal of Fuzzy Sets Valued Analysis, 1:157-67, 2015. [CrossRef] [Google Scholar]
14. Mukeba J.P., Application of L-R Method to Single Server Fuzzy Retrial Queue with Patient Customers, Journal of Pure and Applied Mathematics: Advances and Applications, 16(1): 43-59, 2016. [CrossRef] [Google Scholar]
15. Saini V., Gupta D., and Tripathi A.K., Comparative Analysis of Heterogeneous Feedback Queue Model in Fuzzy Environment using L-R method and α-cut method, International Journal of Mathematics Trends and Technology, 69(3): 31-38, 2023.
16. Saini A., Gupta D. and Tripathi A.K., Analysis of Bi-Tandem Priority Queue System in Stochastic Environment, International Journal of Mathematics Trends and Technology, 69(5): 54-69, 2023.

Table 1. Fuzzy Particular Values

Customers in queue	Arrival times	Service costs	Probabilities
$m_{1L} = (2,3,4)$	$\widetilde{\lambda_{1L}} = (1,2,3)$	$\widetilde{\mu_{1L}} = (13,14,15)$	$\widetilde{\alpha_{12}} = (.6,.4,.2)$
$m_{1H} = (3,4,5)$	$\widetilde{\lambda_{1H}} = (2,4,6)$	$\widetilde{\mu_{1H}} = (14,16,18)$	$\widetilde{\alpha_{15}} = (.4,.6,.8)$
$m_{2L} = (3,2,1)$	$\widetilde{\lambda_{2L}} = (2,3,4)$	$\widetilde{\mu_{2L}} = (14,15,16)$	$\widetilde{\alpha_{21}} = (.2,.3,.4)$
$m_{2H} = (4,5,6)$	$\widetilde{\lambda_{2H}} = (3,5,7)$	$\widetilde{\mu_{2H}} = (16,18,20)$	$\widetilde{\alpha_{25}} = (.8,.7,.6)$
$m_2 = (1,3,5)$	$\widetilde{\lambda_1'} = (3,4,5)$	$\widetilde{\mu_1'} = (10,12,14)$	$\widetilde{\alpha_{35}} = (.4,.6,.8)$
$m_3 = (5,4,3)$	$\widetilde{\lambda_2'} = (1,3,5)$	$\widetilde{\mu_2'} = (13,15,17)$	$\widetilde{\alpha_{45}} = (.3,.5,.7)$
		$\widetilde{\mu_3} = (26,27,28)$	

Table 2. Fuzzy L-R Values

Arrival times	Service costs	Probabilities
$\widetilde{\lambda_{1L}} = (2,1,1)$	$\widetilde{\mu_{1L}} = (14,1,1)$	$\widetilde{\alpha_{12}} = (.4,.2,.2)$
$\widetilde{\lambda_{1H}} = (4,2,2)$	$\widetilde{\mu_{1H}} = (16,2,2)$	$\widetilde{\alpha_{15}} = (.6,.2,.2)$
$\widetilde{\lambda_{2L}} = (3,1,1)$	$\widetilde{\mu_{2L}} = (15,1,1)$	$\widetilde{\alpha_{21}} = (.3,.1,.1)$
$\widetilde{\lambda_{2H}} = (5,2,2)$	$\widetilde{\mu_{2H}} = (18,2,2)$	$\widetilde{\alpha_{25}} = (.7,.1,.1)$
$\widetilde{\lambda_1'} = (4,1,1)$	$\widetilde{\mu_1'} = (12,2,2)$	$\widetilde{\alpha_{35}} = (.6,.2,.2)$
$\widetilde{\lambda_2'} = (3,2,2)$	$\widetilde{\mu_2'} = (15,2,2)$	$\widetilde{\alpha_{45}} = (.5,.2,.2)$
	$\widetilde{\mu_3} = (27,1,1)$	

Table 3. fuzzy particular values

Customers in queue	**Arrival times**	**Service costs**	**Probabilities**
$m_{1L} = (2,3,4)$	$\widetilde{\lambda_{1L}} = (3,2,1)$	$\widetilde{\mu_{1L}} = (15,14,13)$	$\widetilde{\alpha_{12}} = (.6,.4,.2)$
$m_{1H} = (3,4,5)$	$\widetilde{\lambda_{1H}} = (2,4,6)$	$\widetilde{\mu_{1H}} = (14,16,18)$	$\widetilde{\alpha_{15}} = (.4,.6,.8)$
$m_{2L} = (3,2,1)$	$\widetilde{\lambda_{2L}} = (2,3,4)$	$\widetilde{\mu_{2L}} = (16,15,14)$	$\widetilde{\alpha_{21}} = (.2,.3,.4)$
$m_{2H} = (4,5,6)$	$\widetilde{\lambda_{2H}} = (7,5,3)$	$\widetilde{\mu_{2H}} = (16,18,20)$	$\widetilde{\alpha_{25}} = (.8,.7,.6)$
$m_2 = (1,3,5)$	$\widetilde{\lambda_1'} = (3,4,5)$	$\widetilde{\mu_1'} = (14,12,10)$	$\widetilde{\alpha_{35}} = (.4,.6,.8)$
$m_3 = (5,4,3)$	$\widetilde{\lambda_2'} = (5,3,1)$	$\widetilde{\mu_2'} = (17,15,13)$	$\widetilde{\alpha_{45}} = (.3,.5,.7)$
		$\widetilde{\mu_3} = (26,27,28)$	

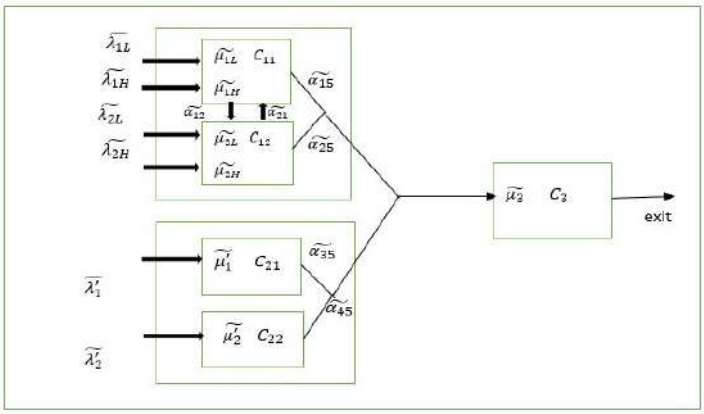

Figure 1. Fuzzy Priority Biserial and Parallel Queuing System

Indian Journal of Natural Sciences *www.tnsroindia.org.in ©IJONS*

Vol.15 / Issue 83 / Apr / 2024 *International Bimonthly (Print) – Open Access* *ISSN: 0976 – 0997*

RESEARCH ARTICLE

Electroactive Metals Salts Inorganic Solvents, a Novel Electrolyte Material for Designing Super capacitors with Enhanced Energy Density and Overall Performance

Vivek Chaudhry* and Joginder Singh

Department of Chemistry, Maharishi Markandeshwar (Deemed to be University), Mullana, Ambala, 133203, Haryana, India.

Received: 30 Dec 2023 Revised: 09 Jan 2024 Accepted: 12 Jan 2024

***Address for Correspondence**
Joginder Singh
Department of Chemistry,
Maharishi Markandeshwar (Deemed to be University),
Mullana, Ambala,
133203, Haryana, India.
Email: joginderchem@mmumullana.org

ABSTRACT

Super capacitors, the high-power energy storage devices, have gained significant attention because of their rapid charge and discharge capabilities along with a longer life cycle. However, to further advance their application in various domains like electric vehicles, renewable energy systems, and portable electronic devices, there is a pressing need to develop advanced electrolytes that can enhance their energy density, power density, and overall performance. This article presents a novel electrolyte formulation (Lithium chloride in ethylene glycol & Magnesium acetate in methanol), designed to address these challenges and improve the efficiency of the super capacitors. The enhanced specific capacitance (Csp= 582 F/g &Csp= 360 F/g), Specific energy (SE= 323Wh/Kg & SE= 200 Wh/Kg) and Specific power (SP=11628 W/Kg & SP=7200 W/Kg) offered by Lithium Chloride and Magnesium acetate electrolyte material respectively open new avenues for efficient and sustainable energy storage solutions in an increasingly electrified world. Further research and development in this direction are expected to unlock the full potential of super capacitors, contributing to a cleaner and more energy-efficient future.

Keywords: Super capacitors, enhanced energy density, power density, and cycling stability, organic electrolytes

INTRODUCTION

In an era characterized by burgeoning energy demands and a growing emphasis on sustainable technology, the development of higher performance energy storage devices has become paramount [1]. Among these, super capacitors stand out as promising candidates due to their ability to deliver rapid bursts of energy, longevity, and environmental friendliness. They have gained significant attention in recent years because of their unique ability to reduce the differences between traditional capacitors and batteries [1,2]. They offer high power density, rapid charge-discharge cycles, and a long operational lifespan, making them a promising candidate for a variety of applications, from mobile electronics to electric powered vehicles and renewable energy systems [3]. The fundamental component of any super capacitor is the electrolyte, which plays a major role in the determination of the device's performance characteristics. The electrolyte serves as a medium for ion transport between the two electrodes, enabling the storage and rapid release of energy [1,3]. Conventional super capacitors predominantly use aqueous or organic electrolytes, each with its own set of advantages and limitations [4,5]. To advance the capabilities of super capacitors and meet the growing demands of emerging technologies, researchers and engineers have been actively exploring novel electrolyte materials and designs [4,5]. These innovations aim to overcome existing challenges such as limited energy density, voltage stability, and temperature range. In brief, this article will outline the design and synthesis of newer organic electrolytes to be used in super capacitor for enhanced performance, safety, and environmental sustainability. This endeavour holds the promise of unlocking new horizons for super capacitors, enabling their integration into a broader range of applications and accelerating the transition to a sustainable energy future[5].

MATERIAL AND METHODS

Materials

All the required chemicals viz.; Amorphous carbon (AC)with particle size 40-100 microns, N-methyl pyrrolidone (NMP), Polyvinylidene fluoride (PVDF) with molecular weight about 280,000, Magnesium acetate ($Mg(OOCCH_3)_2$), Lithium chloride (LiCl), Methyl alcohol (CH_3OH) and ethylene glycol ($C_2H_6O_2$) were sourced from Sigma- Aldrich, India and were used without any further sanitization. Twice distilled water was taken from deionizer and was used where required.

Preparation of stainless-steel electrodes

The stainless steel electrodes (SSE) were prepared by cutting a stainless-steel strip into 1 cm x 1 cm square with provisions to attach it to the potentiostat with crocodile clips. The outer surfaces of the electrodes were cleaned using conc. HCl (12 N) and then rinsed with de ionized water and ethanol. Finally, they were kept in an oven maintained at 70^{o}C for 2 hours[5-6].

Deposition of amorphous carbon on SSEs surface

The 18mg amorphous carbon, 2mg PVDF used for binding in the ratio of 9:1 by mass was mixed with 0.4 ml of solvent NMP. The mixture was homogenized using ultra sonicator to form a slurry. Then this slurry was deposited onto the surface of SSEsusing a fine surgical blade covering surface area 1cm^2 and finally dried at 50^{o}C for 10 hrs [6,7] as shown in Figure 1. The active mass loaded on the SSE was determined by use of a microgram scale electronic balance and was found to be 7.5mg/cm^2 per electrode.

Assembling of the super capacitor

The two electrodes as prepared above were taken and a What man filter paper soaked in electrolyte gel and polyvinyl alcohol was inserted between the electrodes, and was wrapped in butter paper. Finally, the insulation tape was wrapped around it as shown in Figure 2, to prevent dislocation during the further working and testing[8,9].

Electro-chemical measurements

The electro-chemical features of the prepared electrodes were determined by Cyclic- Voltammetry curves (CV), Galvano static charge &discharge (GCD) measurement and Electrochemical impedance spectroscopy (EIS) using 1 M $Mg(OOCCH_3)_2$, 1M LiCl electro active salts in methyl alcohol (CH_3OH) and ethylene glycol ($C_2H_6O_2$) solvents respectively.

Cyclic voltammetry

Cyclic Voltammetry technique (CV) is a widely used electrochemical method that provides information about the redox behaviour of a system. It is involved with applying a potential sweep to an electrochemical cell and measurement of the observed current. The potential sweep is applied linearly as function of time, and the resulting current is recorded, creating a cyclic voltammo gram. This voltamm ogram provides us information related to electro analytical properties of the analyte in the solution or molecule that is adsorbed onto the electrode[9-10]. The value of specific capacitance (Csp)in F/g was determined on the basis of the values collected from the CV measurement by using the equation (1) and (3)

$$\mathrm{Csp} = \frac{\mathrm{A}}{2\mathrm{km}\Delta\mathrm{V}} \quad (1)$$

$$\mathrm{Csp} = \frac{\mathrm{I}}{\mathrm{m}}\frac{\Delta\mathrm{t}}{\Delta\mathrm{V}} \quad (2)$$

$$\mathrm{Csp} = \frac{\mathrm{Q}}{\mathrm{m}\Delta\mathrm{V}} \quad (3)$$

where area under the CV curve is represented by A, k is the scan rate, m (g) is the active mass of material, ΔV (V) is the voltage window, I (A) is the current during discharge, Δt (s) is the time of discharge, and Q is the stored charge in coulomb which is equal to half of the integrated area of the CV curve [11]. The specific power (SP), measured as W/Kg and specific energy (SE), measured as Wh/Kg were calculated according to equation (3) and (4), respectively.

$$\mathrm{SE} = \mathrm{Csp}(\Delta\mathrm{V})^2\mathrm{X}\frac{1000}{7200} \quad (4)$$

$$\mathrm{SP} = \frac{\mathrm{SE}}{\mathrm{td}}\ \mathrm{X}\ 3600 \quad (5)$$

where td is discharging time[12,13,14].

Galvanostatic charge discharge (GCD) analysis and Electrochemical impedance spectroscopy (EIS)

Along with CV the GCD is also used to calculate Csp, specific energy (energy density) Wh/kg and Specific power (Power density) W/kg using the equation (2), (4) and (5)[7,11,12].Further the EIS is also a useful technique to study electrode/electrolyte interactions. The EIS parameters were derived using the Palmsem4.0 software.

RESULT AND DISCUSSIONS

CV measurement and analysis

The CV plots of Li & Mg ions were obtained and are as shown in Figure 3 &4 and the area under the curve were used to calculate the specific capacitance Csp (F/g) of the designed super capacitor [17, 18, 19, 20] using equation 1. The curves display capacitive performance of electrical double layer (EDLC) capacitor at various scan rates with distortion free quasi rectangular curve for symmetric super capacitor which is preserved even with increase in voltage of upto 2 V. This curve hardly shows any change in shape which points towards a good reversible nature and high speed behaviour of prepared super capacitor cell [25, 26]. The plots between Csp and scan rate (mV) were drawn and are shown in Figure (4) and 5. The CV values were detected at scan rates of 10 to 100 mV/s. If the scan rate is low the electrolytes have time available to get into the pores of the electrode material, while if the scan rate is high it only accumulates on the outsidearea of the surface so any increase in scan rate causes a decline in the specific

capacitance as detailed in Table 1. Further the Csp was higher for Lithium ions as compared to Magnesium ions at 100 scan rate making Lithium ions a better electrolytic material.

Galvanostatic charge discharge and EIS measurements

The Figure 6 and 7 display the GCD curves obtained. They were quite similar with those reported in literature for supercapacitor[15,16]. The GCD curves were obtained at specific current of 1.0 mA with a voltage window range of 1.0 V for 2 to 5 charge discharge cycles. The td value obtained from Figure7was 100s. The longer charge-discharge time indicates the involvement of electrolyte in increased ionic conductivity which leads to higher energy storage.

The Csp, SE & SP obtained from GCD technique are as shown in Table 2 which shows an improvement in electrochemical properties of the AC electrodes. The values of specific capacitance (F/g), Specific Power SP (W/kg) and Specific Energy SE (Wh/kg) are in favourable agreement with those reported in literature.

EIS measurement

EIS is avery important tool to study impedance of supercapacitor through Ny quist plot to study electrode-electrolyte interactions. The plot obtained are shown in Figure 9-11.The semicircle represents the ESR, equivalent series resistance value which contains the electrode surface layer resistance which indicates the porous nature of the electrodes. It is followed by a straight line area called Warburg region which indicates the development of electrical double layer on the surface of electrode, where a charge transfer process between electrode and electrolyte interface takes place. The EIS measurement were evaluated with the range of frequency between 0.1 to 10^5 Hz at sinusoidal amplitude potential of 1mA and 100μA at room temperature. The shape of the curve i.e. semicircle and a straight line are atypical of supercapacitor. The equivalent series resistance (R_{ESR}) value at the starting intercept of the semicircle at the real impedance axis side of higher frequency are 47ohm for Li and 11ohm for Mg, the diameter of the semicircle can be used to calculate Rct, 103 ohm for Li and 59 ohm for Mg which indicates that the electrolytes have lower internal resistance and high ion transfer and conductivity.

CONCLUSION

In conclusion, the development of novel electrolytes composed of electro-active metal salts and organic solvents represents a promising avenue for designing supercapacitors with enhanced performance and activity. This innovative approach addresses several key challenges in the area of storage of energy and offers a range of advantages. First and foremost, the use of electro-active metal salts introduces a new dimension to supercapacitor design. These salts, often derived from alkaline earth metals, provide higher energy density and improved charge storage capabilities compared to traditional electrolytes. This enhancement in energy storage capacity is critical for meeting the growing demands of modern electronics and renewable energy systems. Furthermore, the incorporation of organic solvents in these novel electrolytes offers several advantages. Organic solvents, when chosen appropriately, can enhance the overall ionic conductivity of the electrolyte, facilitating faster charge and discharge rates. Additionally, organic solvents can improve the thermal stability of the super capacitor, reducing the risk of overheating and enhancing its long-term durability. The combination of electro-active metal salts and organic solvents in the novel electrolyte formulation leads to super capacitors with superior performance characteristics. These super capacitors can deliver much larger power densities, reduced charging times, and long cycle lifetimes, making them ideal for applications of a wider range like electric vehicles, portable electronic gadgets and energy storage in grid.

REFERENCES

1. C. Liu, F. Li, M. Lai-Peng, H.M. Cheng, Advanced materials for energy storage, Adv. Mater. 22 (2010) 28–62, https://doi.org/10.1002/adma.200903328.

2. S. Ould Amrouche, D. Rekioua, T. Rekioua, S. Bacha, Overview of energy storage in renewable energy systems, Int. J. Hydrogen Energy. 41 (2016) 20914–20927, https://doi.org/10.1016/j.ijhydene.2016.06.243.
3. Yu, M., and Feng, X. (2019). Thin-film electrode based supercapacitors. Joule 3, 338–360
4. Senthilkumar ST, Selvan RK, Lee YS, Melo JS. Electric double layer capacitor and its improved specific capacitance using redox additive electrolyte. J Mater Chem 2013;1(4):1086e95
5. Activated carbon electrode with promising specific capacitance based on potassium bromide redox additive electrolyte for supercapacitor application Mahmoud Maher a , Sameh Hassan b,* , Kamel Shoueirc,d,**, Bedir Yousif e,f , Mohy Eldin A. Abo-Elsoud
6. Dielectric-electrolyte supercapacitors Shian Dong,1 Weihang Gao,2 Kunming Shi,1 Qi Kang,1 Zhenli Xu,2 Jinkai Yuan,3 Yingke Zhu,1
7. Enhancing capacitance of super capacitor with both organic electrolyte and ionic liquid electrolyte on a biomass-derived carbon† XuehangWang,‡aYahaoLi,‡aFengliuLou,a Marthe Emelie MelandsøBuan,a Edel Sheridanb and De Chen
8. Importance of Electrode Preparation Methodologies in Super capacitor Applications Arunkumar M. and Amit Paul.
9. Electrolyte selection for supercapacitive devices: a critical review Bhupender Pal,aShengyuan Yang, b Subramaniam Ramesh,c Venkataraman Thangadurai d and Rajan Jose
10. A review of electrolyte materials and compositions for electrochemical super capacitors Cheng Zhong,a Yida Deng,b Wenbin Hu,*ab JinliQiao,c Lei Zhangd and JiujunZhangd
11. Revisiting Cyclic Voltammetry and Electrochemical Impedance Spectroscopy Analysis for Capacitance Measurements Oumaïma Gharbi*, Mai T.T. Tran, Bernard Tribollet, Mireille Turmine and Vincent Vivier
12. A Brief Study of Cyclic Voltammetry and Electrochemical Analysis * 1 Joshi P.S., 2Sutrave D.S.
13. Spray Deposition of Supercapacitor Electrodes using Environmentally Friendly Aqueous Activated Graphene and Activated Carbon Dispersions for Industrial Implementation Nicolas Boulanger,[a] Vasyl Skrypnychuk,[a] Andreas Nordenström.
14. New types of hybrid electrolytes for supercapacitors Wuquan Ye, Haiyan Wang, Jiqiang Ning, Yijun Zhong, Yong Hu
15. AnUltra-High-EnergyDensitySupercapacitor;FabricationBasedonThiol-functionalizedGrapheneOxideScrollsJanardhanan.R.Rani1,†,RanjithThangavel2,†,Se-IOh1,YunSungLee2and Jae-HyungJang1,3,
16. Supercapacitor and electrochemical techniques: A brief review Swati Sharma * , Prakash Chand * Department of Physics, National Institute of Technology, Kurukshetra 136119, India
17. A.G. Pandolfo, A.F. Hollenkamp, Carbon properties and their role in supercapacitors, J. Power Sources. 157 (2006) 11–27, https://doi.org/10.1016/j. jpowsour.2006.02.065.
18. G.A. Mabbott, An introduction to cyclic voltammetry, J. Chem. Educ. 60 (1983) 697–702, https://doi.org/10.1021/ed060p697
19. M.D. Stoller, R.S. Ruoff, Best practice methods for determining an electrode material's performance for ultracapacitors, Energy Environ. Sci. 3 (2010) 1294–1301, https://doi.org/10.1039/c0ee00074d.
20. Noori, M.F. El-Kady, M.S. Rahmanifar, R.B. Kaner, M.F. Mousavi, Towards establishing standard performance metrics for batteries, supercapacitors and beyond, Chem. Soc. Rev. 48 (2019) 1272–1341, https://doi.org/10.1039/ c8cs00581h
21. B.A. Mei, O. Munteshari, J. Lau, B. Dunn, L. Pilon, Physical interpretations of Nyquist plots for EDLC electrodes and devices, J. Phys. Chem. C. 122 (2018) 194–206, https://doi.org/10.1021/acs.jpcc.7b10582.
22. universite de sherbrooke) Lasis, andrzej (departement de chimie, Electrochemical Impedance Spectroscopy and its applications.pdf, Electrochem. Impedance Spectrosc. Its Appl. Mod. Asp. Electrochem. (1999) 143–248.
23. N. Nishi, Electrochemical impedance, Rev. Polarogr. 65 (2019) 87–88, https:// doi.org/10.5189 /revpolarography.65.87.
24. El Sharkawy HM, Dhmees AS, Tamman AR, El Sabagh SM, Aboushahba RM, Allam NK. N-doped carbon quantum dots boost the electrochemical supercapacitive performance and cyclic stability of MoS2. Journal of Energy Storage 2020;27:101078.

25. Jyothibasu JP, Lee R-H. Green synthesis of polypyrrole tubes using curcumin template for excellent electrochemical performance in supercapacitors. J Mater Chem 2020;8(6):3186e202.
26. X. B. Liu, P. B. Shang, Y. B. Zhang, X. L. Wang, Z. M. Fan, B. X. Wang and Y. Y. Zheng, J. Mater. Chem. A, 2014, 2, 15273–15278.

Table 1: Specific Capacitance (F/g) at various scan rates

S.No.	Scan Rate (mV/s)	Li^+ SC Csp F/g	Mg^{2+} SC Csp F/g
1	10	1591	2821
2	20	1461	1355
3	50	624	664
4	100	582	360

Table: 2 Carbon based Symmetric SCs using organic electrolytes:

Electrolyte	Electrode material	Csp (F/g)	Specific Energy SE(Wh/kg)	Specific Power SP(W/kg)	Ref
Na_2SO_4/H_2O	AC	74.5	10.3	257.4	5,6
Na_2SO_4,KBr/H_2O	AC	957.8	133	859.6	5,6
1M H2SO4	AC fibres	280	-	-	10
1M H2SO4	PANI grafted rGO	1045		60000	27
1M $TEABF_4$/CAN	Biomass derived carbon	224	92	-	9
Ethylene glycol/NMP	Graphene	318	-	-	9,10
1M $LiClO_4$/PC	MoO3 nanosheets	540	-	-	7,8
0.5M $LiClO_4$/PC	PANI/Graphite	420	-	-	7,8
$EMIMBF_4$	Thiol functionalized graphene oxide	-	206	32000	15
1MLiCl/ethylene glycol	**AC**	**582**	**323**	**11628**	**This work**
1M $Mg(OAc)_2$/MeOH	**AC**	**360**	**200**	**7200**	**This work**

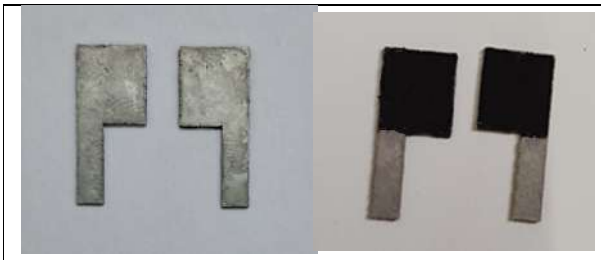

Figure 1: SSEs before and after coating with AC material

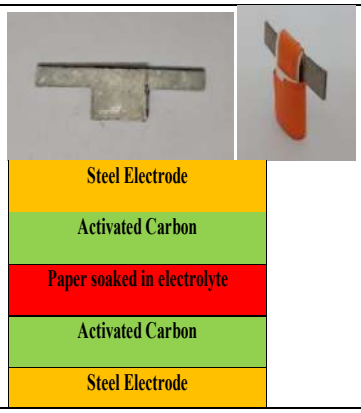

Figure 2: Assembling of the super capacitor

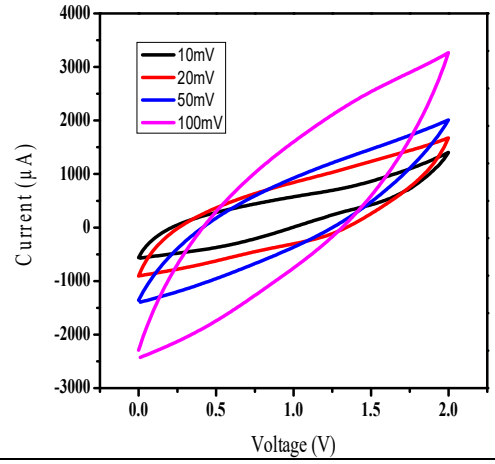

Figure 3: CV curve for Li ions

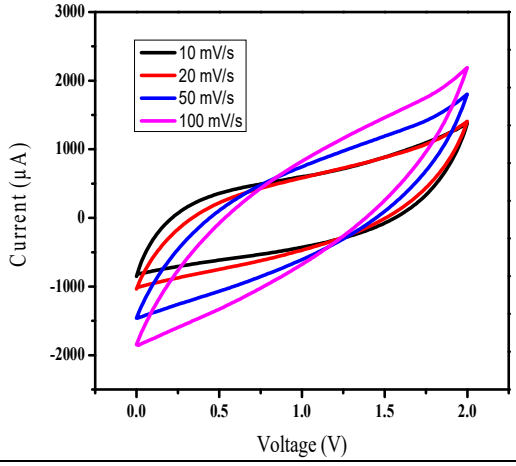

Figure 4: CV curve for Mg ions

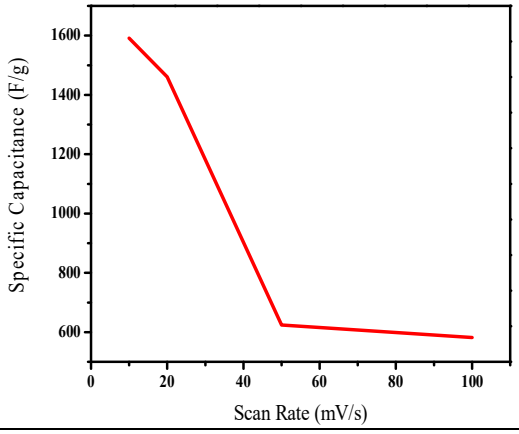

Figure 5: The plot between Specific capacitance (F/g) and Scan rate mV/s)

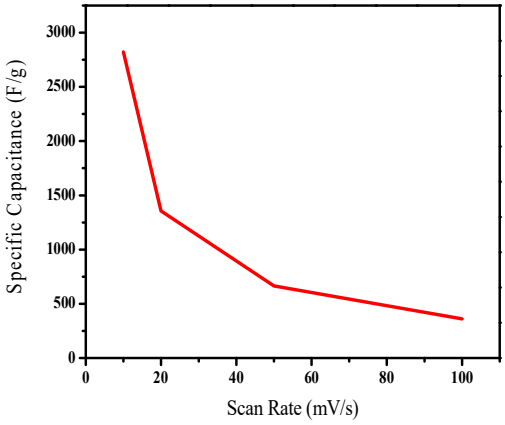

Figure 6. Mg ions

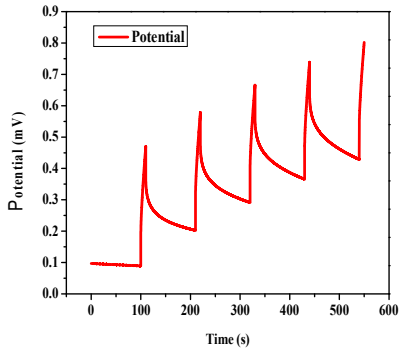

Figure 7: GCD curve of Li ions for five cycles

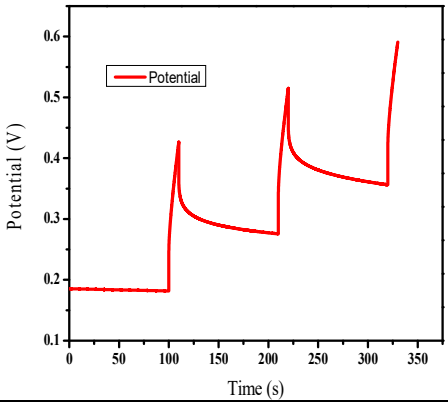

Figure: 8 GCD curve of Mg ions for three cycles

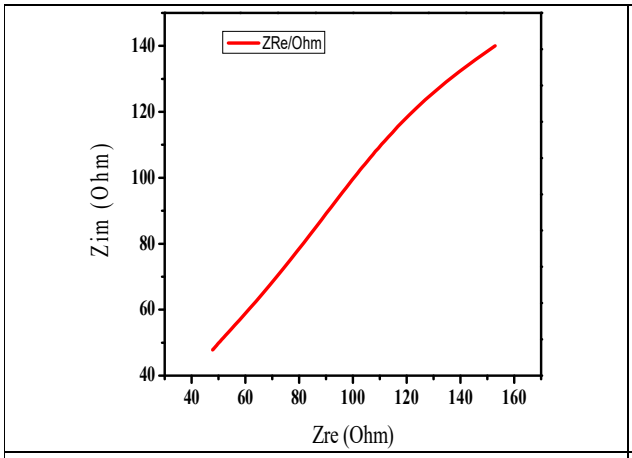

Figure 9: EIS curve Lions

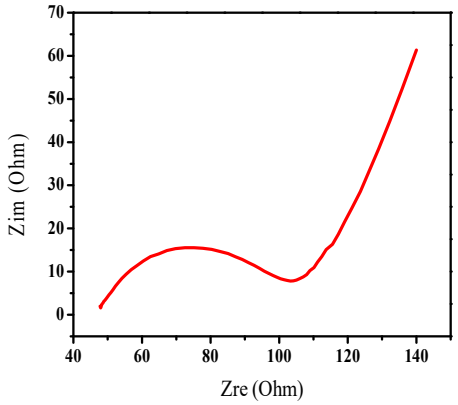

Figure 10: Nyquist Plot Li (high frequency)

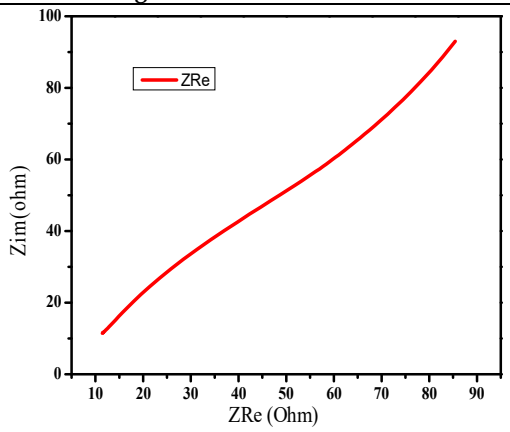

Figure 11: EIS curve Mg

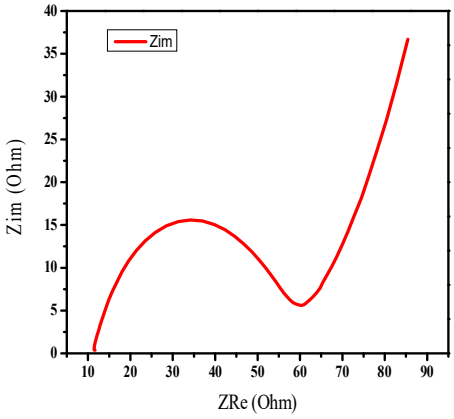

Figure 12: Nyquist Plot Mg (high frequency)

Indian Journal of Natural Sciences *www.tnsroindia.org.in ©IJONS*

Vol.15 / Issue 83 / Apr / 2024 *International Bimonthly (Print) – Open Access* *ISSN: 0976 – 0997*

RESEARCH ARTICLE

Z- Intuitionistic Fuzzy Relations and Their Properties

R.A.Latha Devi[1]* and G. Velammal[2]

[1]Part Time Research Scholar, Madurai Kamaraj University, Madurai, and Assistant Professor, Department of Mathematics, Sri Meenakshi Govt. Arts College for Women (A), (Affiliated to Madurai Kamaraj University), Madurai, Tamil Nadu, India.
[2]Associate Professor and Head (Retd), Department of Mathematics, Sri Meenakshi Govt. Arts College for Women (A), (Affiliated to Madurai Kamaraj University), Madurai, Tamil Nadu, India.

Received: 29 Dec 2023 Revised: 11 Jan 2024 Accepted: 19 Mar 2024

***Address for Correspondence**
R.A.Latha Devi
Part Time Research Scholar,
Madurai Kamaraj University, Madurai, and
Assistant Professor, Department of Mathematics,
Sri Meenakshi Govt. Arts College for Women (A),
(Affiliated to Madurai Kamaraj University),
Madurai, Tamil Nadu, India.
Email: lathadevira5791@gmail.com

ABSTRACT

In this paper some compositions of z- intuitionistic fuzzy relation have been defined and Some properties of z- intuitionistic fuzzy relation with respect to these compositions have been studied.

Keywords: Z-number, z-intuitionistic fuzzy relation, z-intuitionistic fuzzy relationship function, compositions of z- intuitionistic fuzzy Relations, ' L' level Reliable z- intuitionistic fuzzy Relation.

INTRODUCTION

In this paper, we are introducing the novel concept, Z- intuitionistic fuzzy relation (Z- IFR) which is a generalization of z-fuzzy relation. In our earlier paper, ''The properties of compositions of z-fuzzy relations' [3,4],, we have introduced the notion of compositions of z- fuzzy relations. Here we have extended this into some compositions of z-intuitionistic fuzzy relation and studied its properties with respect to these composition rules.

Preliminaries
Definition 2.1
An intuitionistic fuzzy set(IFS) A is a set of ordered triples,
$A = \{ x, \mu_A(x), \upsilon_A(x)\}$
where $\mu_A(x)$, $\upsilon_A(x)$ are functions mapping from X into [0, 1]. For each $x \in X$,

$\mu_A(x)$ represents the degree of membership of the element x to the subset A of X, and $\upsilon_A(x)\}$ gives the degree of non membership. For the function $\mu_A(x)$ and $\upsilon_A(x)$ mapping into [0, 1], the $0 \leq u_1(i,j) + u_2(i,j) \leq 1$holds. [1,9]

Definition 2.2

Z-number (Zadeh,2011). Z-number has two components Z = (A, B). The first component A , is a restriction on the values which a real-valued uncertain variable X is allowed to take. Second component B, is a measure of reliability of the first component. Typically, A and B are described in a natural language[8].

Definition 2.3

Z - Intuitionistic fuzzy relation

Let X and Y be arbitrary sets. A z- intuitionistic fuzzy relation R(X, Y) from X to Y can be described by specifying the z- intuitionistic fuzzy relationship function. A z- intuitionistic fuzzy relationship function f from X to Y must be in the following form.

For all x ∈X, y∈Y

f (x, y) = (A(x, y), B(x, y)) [4]

where $A(x,y) = (A_1(x,y), A_2(x,y))$ is an IFS with support in [0,1] and B (x, y) is a normal fuzzy set with support in [0,1]. Here A (x. y) gives an intuitionistic fuzzy estimate of the strength of relationship and B(x, y) refers to the reliability of the estimate (A(x, y)) of the strength of relationship [1,7].

Definition 2.4

Type 1 z- intuitionistic fuzzy relation

A z- intuitionistic fuzzy relationship function f from X to Y is said to be of Type 1 if for all x∈X, y∈Y, f(x, y) is a type1 z -number. In other words, $A_1(x,y), A_2(x,y))$ and B(x, y) are real numbers.

Example:2.5

Let $X = \{x_1, x_2\}$ and $Y = \{y_1, y_2, y_3\}$

Consider a z- intuitionistic fuzzy relationship function f is given in the matrix format $\left(f(x_i, y_j)\right) where f(x_i, y_j)$ is the element in i- th row, j-th column of the matrix .

$$\begin{pmatrix} ((.7,.2),1) & ((.6,.3),.9) & ((.9,0),.9) \\ ((.6,.2),.8) & ((.3,.6),1) & ((.2,.6),.9) \end{pmatrix}$$

For example, we note that, $f(x_1, y_2) = ((.6,.3),.9)$

So this means the strength of relationship between x_1 and y_2 is at least 0.6 and at most 1-0.3 =0,7 and the reliability of this information is .9.

Remark 2.6

For ease of notation we shall drop the bracket around $A_1(x,y), A_2(x,y))$. In rest of this paper, z- intuitionistic fuzzy relation will refer to type 1 z- intuitionistic fuzzy relation.

Compositions of z- Intuitionistic Fuzzy Relations

Let X, Y and W be arbitrary finite sets. Let P(X, Y) be a z- intuitionistic fuzzy relation from X to Y and Q (Y, Z) be z- intuitionistic fuzzy relation from Y to Z respectively. Let f, g be the z- intuitionistic fuzzy relationship functions of P and Q respectively. Let h be a z-intuitionistic fuzzy relationship function from X to W.

Suppose $X = \{x_1, x_2, x_3 \ldots x_l\}$, $Y = \{y_1, y_2, y_3 \ldots y_m\}$ $and W = \{w_1, w_2, \ldots w_n\}$. Let

$f(x_i, y_j) = (a_1(i,j), (a_2(i,j), b(i,j))$; $g(y_i, w_j) = (c_1(i,j), c_2(i,j), d(i,j))$ and $h(x_i, w_j) = (u_1(i,j), u_2(i,j), v(i,j))$

Then we can compose the relations of P and Q in several ways

Sup-min, Inf-max, Overall min Composition

The sup-min, Inf-min, Overall min composition of P and Q is given by the following z- intuitionistic fuzzy relationship function h.

$$h(x_i, w_j) = (u_1(i,j), u_2(i,j), v(i,j))$$

where $u_1(i,j) = Sup_k\{min(a_1(i,k), c_1(k,j))\}$

$u_2(i,j) = Inf_k\{max(a_2(i,k), c_2(k,j))\}$

The following result proves that $(u_1(i,j), u_2(i,j))$ is a valid IFS membership function,

Result :3.1.1

Result: $\mathbf{3.1.1}\ 0 \le u_1(i,j) + u_2(i,j) \le 1$

It is obvious that $u_1(i,j) \ge 0$ and $u_2(i,j)) \ge 0$

So only need to verify $u_1(i,j) + u_2(i,j) \le 1$

Suppose

$u_1(i,j) = Sup_k\{min(a_1(i,k), c_1(k,j))\}$

$= min(a_1(i,k_1), c_1(k_1,j))$ --------- (1)

and

$u_2(i,j) = Inf_k\{max(a_2(i,k), c_2(k,j))\}$

$= max(a_2(i,k_2), c_2(k_2,j))$ ---------- (2)

We know $a_1(l,m) + a_2(l,m) \le 1$ *and* $c_1(l,m) + c_2(l,m) \le 1$, since P, Q are Z- IFR relations.

From (1)

$u_1(i,j) = min(a_1(i,k_1), c_1(k_1,j))$

$\le a_1(i,k_1) = 1 - a_2(i,k_1)$ --------- (3)

By definition

$u_2(i,j) = Inf_k\{max(a_2(i,1), c_2(1,j)), \ldots (a_2(i,k_1), c_2(k_1,j) \ldots)\}$

$= max(a_2(i,k_1), c_2(k_1,j)) = M\,(say)$ ------- (4)

Case i: $M = a_2(i,k_1)$

Therefore

$u_2(i,j) \le a_2(i,k_1)$ -------- (5)

Adding (3) and (5) gives the required result.

Case ii: $M = c_2(k_1,j)$

Note $u_1(i,j) = min(a_1(i,k_1), c_1(k_1,j))$

$\le c_1(k,j)$ -------- (6)

Also from (4)

$u_2(i,j) \le c_2(k_1,j)$ --------- (7)

So (6) + (7) gives the result.

Example 3.1.2

Let Z- IFR of P, f (x_i, y_j) be given by

Let R(X, Y) *and* R(X) are

$$\begin{pmatrix} (.5,.5,.8) & (.9,.1,.9) & (.8,.2,.8) \\ (.4,.5,.9) & (.7,.2,.8) & (.6,.3,.9) \end{pmatrix} \text{and} \begin{pmatrix} (.2,.7,.9) & (.3,.7,.7) \\ (.3,.7,.9) & (.9,.1,1) \\ (.6,.2,.7) & (.3,.6,.9) \end{pmatrix}$$

After calculating $u_1(i,j)$, $u_2(i,j)$ and v(i, j) the composition of Z-IFR becomes

$$\begin{pmatrix} (.6,.2,.7) & (.9,.1,.7) \\ (.6,.3,.7) & (.7,.2,.7) \end{pmatrix}$$

Sup-min, Inf-max, Average min Composition 3.1.3

The (sup-min,Inf-max, Average min) composition of P and Q is given by the following z- intuitionistic fuzzy relationship function h.

$h(x_i, w_j) = (u_1(i,j), u_2(i,j), v(i,j))$

$$h(x_i, w_j) = (u_1(i,j), u_2(i,j), v(i,j))$$

$$where u_1(i,j) = Sup_k\{min\,(a_1(i,k), c_1(k,j))\}$$

$u_2(i\,,j) = Inf_k\{max(a_2(i,k), c_2(k,j))\} and$

v(i, j) = 1/m { min (b(i,1), d(1,j)) + min(b(i,2), d(2,j))+…+ min(b(i,m), d(m,j))}

Remark 3.1.4

In this composition also $u_1(i,j) + u_2(i\,,j) \leq 1$

In the above example

Calculating u_1(i, j), u_2(i , j) and v(i, j) the composition of Z-IFR becomes

$\begin{pmatrix}(.6,.2,.8) & (.9,.1,.8)\\ (.6,.3,.8) & (.7,.2,.8)\end{pmatrix}$

Properties of Compositions 3.4

Associativity

Theorem 3.4.1

The Inf-Max operation is associative.

$R_1: X \to Y \quad R_2: Y \to Z \quad R_3: Z \to W$

Proof

Let

$R_1: X \to Y \quad R_2: Y \to Z \quad R_3: Z \to W$

$((R_1 \circ R_2) \circ R_3)(x,w) = \min_z(\max(R_1 \circ R_2(x,z), R_3(z,w))$

$= \max(R_1 \circ R_2(x,z_k), R_3(z_k,w))$ (for some z_k)

$= \max\left(\min_y(\max(R_1(x,y), R_2(y,z_k))), R_3(z_k,w)\right)$

$= \max\left(\max(R_1(x,y_l), R_2(y_l\,,z_k)), R_3(z_k,w)\right)$ (for some y_l)

$= \max(R_1(x,y_l), R_2(y_l\,,z_k), R_3(z_k,w))$ … …. (1)

Similarly we can show

$(R_1 \circ (R_2 \circ R_3))(x,w) = \max(R_1(x,y_r), \max(R_2(y_r\,,z_s), R_3(z_s,w)))$

for some $y_r\,, z_s$

$= \max(R_1(x,y_r), R_2(y_r\,,z_s), R_3(z_s,w))$ … … … (2)

Since $((R_1 \circ R_2) \circ R_3)(x,w)$

$= \min_z(\max(R_1 \circ R_2(x,z), R_3(z,w))$it follows $((R_1 \circ R_2) \circ R_3)(x,w)$

$\leq \max(R_1 \circ R_2(x,z_s), R_3(z_s,w))$

$= \max\left(\min_y(\max(R_1(x,y), R_2(y,z_s))), R_3(z_s,w)\right)$

$\leq \max\left(\max(R_1(x,y_r), R_2(y_r,z_s)), R_3(z_s,w)\right)$

$= \max(R_1(x,y_r), R_2(y_r\,,z_s), R_3(z_s,w))$

$= (R_1 \circ (R_2 \circ R_3))(x,w)$

Thus we can shown

$((R_1 \circ R_2) \circ R_3)(x,w) \leq (R_1 \circ (R_2 \circ R_3))(x,w)$ … …. (3)

Similarly we can show

$((R_1 \circ R_2) \circ R_3)(x,w) \geq (R_1 \circ (R_2 \circ R_3))(x,w)$ … …. (4)

From (3) and(4)

$((R_1 \circ R_2) \circ R_3)(x,w) = (R_1 \circ (R_2 \circ R_3))(x,w)$

Hence the proof

Theorem 3.4.2
The Sup-Min, Inf-Max , overall Min composition is associative.
Proof:
Say $R_1 = (R_{11}, R_{12}, R_{13}) : X \to Y$
$R_2 = (R_{21}, R_{22}, R_{23}) : Y \to Z$
$R_3 = (R_{31}, R_{32}, R_{33}) : Z \to W$be IFS.
Then consider the composition $\circ$ = Sup-Min, Inf-Max, Overall Min
$* = \text{Sup} - \text{Min}$
$\blacksquare = \text{Inf} - \text{Max}$
$= \text{Overall Min}$
We note that
$R_1 \circ R_2 = (R_{11} * R_{21}, R_{12} \blacksquare R_{22}, R_{13} \cdot R_{23})$
$(R_1 \circ R_2) \circ R_3 = \big((R_{11} * R_{21}) * R_{31}, \quad (R_{12} \blacksquare R_{22}) \blacksquare R_{32}, \quad (R_{13} \cdot R_{23}) \cdot R_{33}\big) \ldots\ldots (1)$
$R_1 \circ (R_2 \circ R_3) = \big(R_{11} * (R_{21} * R_{31}), \quad R_{12} \blacksquare (R_{22} \blacksquare R_{32}), R_{13} \cdot (R_{23} \cdot R_{33})\big) \ldots\ldots (2)$
Since $*$, $\blacksquare$, $\cdot$ are associative it follows (1) and (2) are equal.

Reliability
Definition 3.5.1
Reliable z- intuitionistic fuzzy relations
A z- intuitionistic fuzzy relation from set X to set Y given by $R(x,y) = (R_1(xy), R_2(x,y), B(x,y))$ is said to be reliable if B(x, y) ≥ 0.5 for all (x, y) in X x Y.
Definition 3.5.2
'L' level reliable Z- intuitionistic fuzzy relation
A Z- intuitionistic fuzzy relations from set X to set Y given by $R(x,y) = (R_1(xy), R_2(x,y), B(x,y))$ is said to be 'L' level reliable if B(x, y) ≥ L for some $L \in [1/2, 1]$
Note: If L = 1, we say it is completely reliable.
Theorem 3.5.3
If P is L_P level reliable Z- IFR, Q is L_Q level reliable Z- IFR then the (Sup-min, Inf-max, Overall min) composition of P and Q is reliable at level of min (L_P, L_Q)
Theorem 3.5.4
If P is L_P level reliable Z- IFR, Q is L_Q level reliable Z- IFR then (Sup-min, Inf-max, Average-min) composition of P and Q is reliable at level of min (L_P, L_Q)

CONCLUSION

In this article the novel concept of Z-IFS has been introduced and some interesting results have been proved. This concept has potential for applications in areas of medical diagnosis[2,4],forecasting etc..

REFERENCES

1. Atanassov K, ' Intuitionistic Fuzzy Sets', Fuzzy sets and systems,pp 87-96,1986.
2. Kerre E.E A walk through fuzzy relations and their application to information retrieval, medical diagnosis and expert systems, seminar for Mathematical Analysis, State University of Gent,Belgium.1990
3. Latha Devi R.A Velammal G 'The concept of z fuzzy relation' *Utilitas Mathematica*, *120*, pp.1146–1154,2023.
4. Latha Devi R.A Velammal G 'The properties of compositions of z-fuzzy relations'*UtilitasMathematica*, 120,pp.1176 - 1183, 2023.
5. Sanchez, E. Medical Diagnosis and Composite Fuzzy Relation. In: Gupta, M.M., Ragade, R.K. and Yeager, R.R., Eds., Advances in Fuzzy Sets and Applications, North-Holland, New York, 437-447, 1979.

6. 6.Shahilabhanu.M.,Velammal.G.,'Operations on Zadeh's Z-number`, IOSR Journal of mathematics , 11 (3), pp. 88-94,2015.
7. Zadeh.L.A. Fuzzy sets, Information and Control,pp. 338-353, 1965.
8. Zadeh.L.A. A note on Z-number, information science 181, pp.2923-2932, 2011.
9. Zimmermann H J, Fuzzy set theory & its applications, fourth edition, Springer international edn.pp79, 2001.
10. Abdel-Basset, M., Mohamed, R., Zaied, A. E. N. H., Gamal, A., &Smarandache, F. (2020). Solving the supply chain problem using the best-worst method based on a novel Plithogenic model. In Optimization Theory Based on Neutrosophic and Plithogenic Sets (pp. 1-19). Academic Press.
11. Abdel-Basset, Mohamed, et al. "An integrated plithogenic MCDM approach for financial performance evaluation of manufacturing industries." Risk Management (2020): 1-27.
12. Abdel-Basst, M., Mohamed, R., &Elhoseny, M. (2020). A novel framework to evaluate innovation value proposition for smart product-service systems. Environmental Technology & Innovation, 101036.
13. Abdel-Basst, Mohamed, Rehab Mohamed, and Mohamed Elhoseny. "< covid19>A model for the effective COVID-19 identification in uncertainty environment using primary symptoms and CT scans." Health Informatics Journal (2020): 1460458220952918.
14. Atanassov.K, Neutrosophic sets, Fuzzy Sets and Systems 20,87-95. (1986)
15. Arokiarani.I, Dhavaseelan.R, Jafari.S, Parimala.M: On Some New Notions and Functions in Neutrosophic topological spaces , *Neutrosophic Sets and Systems*, Vol. 16 **(2017),** pp. 16-19. doi.org/10.5281/zenodo.831915.
16. Atkinswestley.AChandrasekar.S,Neutrosophic Weakly G^*-closed sets,Advances in Mathematics: Scientific Journal 9 (2020), no.5, 2853–2861.
17. Atkinswestley.AChandrasekar.S,, Neutrosophicϱ#S closed sets in Neutrosophic topological spaces,Malaya Journal of Matematik, Vol. 8, No. 4, 1786-1791, 2020
18. Atkinswestley.AChandrasekar.S,, Neutrosophicϱ*-Closed Sets and its maps,Neutrosophic Sets and Systems, Vol. 36, 2020,96-107
19. Banupriya.V,.Chandrasekar.S: Neutrosophic αgs Continuity and Neutrosophic αgs Irresolute Maps, *Neutrosophic Sets and Systems,* vol. 28, **2019,** pp. 162-170. DOI: 10.5281/zenodo.3382531
20. Banupriya.V,.Chandrasekar.Sand Suresh.M, Neutrosophic α-generalized semi homeomorphisms,Malaya Journal of Matematik, Vol. 8, No. 4, 1824-1829, 2020
21. Charles Le, Preamble to Neutrosophy and Neutrosophic Logic, Multiple-Valued Logic / An International Journal, Taylor & Francis, UK & USA, Vol. 8, No. 3, 285-295, June 2002.
22. R.Dhavaseelan, S.Jafari, and Hanifpage.md.:Neutrosophic generalized α-contra-continuity, *creat. math. inform.* 27, no.2, 133 - 139,(2018)
23. FlorentinSmarandache.:, Neutrosophic and NeutrosophicLogic, *First International Conference* On Neutrosophic, Neutrosophic Logic, Set, Probability, and Statistics University of New Mexico, Gallup, NM 87301, USA, *smarand@unm.edu*,(2002)
24. FloretinSmarandache.:,Neutrosophic Set: - A Generalization of Neutrosophic set, *Journal of Defense Resources Management*1,107-114,(2010).
25. Ishwarya.P, and Bageerathi..K, On Neutrosophicsemiopen sets in NTSs, *International Jour. Of Math. Trends and Tech.* , 214-223,(2016).
26. Jayanthi..DαGeneralized closed Sets in NTSs, *International Journal of Mathematics Trends and Technology (IJMTT)*-Special Issue ICRMIT March (2018).
27. Mary Margaret.A, andTrinita Pricilla.M.,Neutrosophic Vague Generalized Pre-closed Sets in Neutrosophic Vague Topological Spaces,*International Journal of Mathematics And its Applications*,Volume 5, Issue 4-E, 747-759.(2017).
28. Lupianez, Interval neutrosophic sets and topology. Emerald Group publishing limited, vol 38. Nos 3/4, 2009
29. Mukherjee.A,Datta.Mand Smarandache.F, Neutrosophic Interval valued soft topological spaces, Neutrosophic Sets and Systems, Vol 6, 2014.
30. Mondal TK and Samanta.S, Topology of interval – valued Fuzzy sets, Indian Journal Pure appl. Math.30(1): 23-38(1999)

31. Nanthini.T and Pushpalatha.A, Interval valued Neutosophic Topological Space ,Neutrosophic Sets and Systems, Vol. 32, 2020,52-60.
32. Rajesh kannan.T ,Chandrasekar.S,Neutosophic $\omega\alpha$-closed sets in Neutrosophic topological spaces, Journal Of Computer And Mathematical Sciences,vol.9(10),1400-1408 Octobe2018.
33. Rajesh kannan.T , Chandrasekar.S, Neutosophic α-continuous multifunction in Neutrosophic topological spaces, The International Journal of Analytical and Experimental Modal Analysis, Volume XI,IssueIXSeptember 2019,1360-9367
34. Rajesh kannan.T ,Chandrasekar.S, Neutrosophic α-Irresolute Multifunction In Neutrosophic topological spaces, "Neutrosophic Sets and Systems 32, 1 (2020),390-400.https://digitalrepository.unm.edu/ nss_journal/vol32/iss1/25
35. Rajesh kannan.T , Chandrasekar.S,NeutrosophicPRE $-\alpha$, SEMI $-\alpha$ and PRE $-\beta$ irresolute open and closed mappings in Neutrosophic topological spaces,Malaya Journal of Matematik, Vol. 8, No. 4, 1795-1806, 2020
36. Salama.A.A and Alblowi.S.A.., Generalized Neutrosophic Set and Generalized NTSs, *Journal computer Sci. Engineering*, Vol.(ii),No.(7)(2012).
37. Salama.A.A and Alblowi.S.A.,Neutrosophic set and NTS, *ISOR J.mathematics*,Vol.(iii),Issue(4),.pp-31-35,(2012).
38. Shanthi.V.K.,Chandrasekar.S, SafinaBegam.K, Neutrosophic Generalized Semi-closed Sets In NTSs, *International Journal of Research in Advent Technology*, Vol.(ii),6, No.7, , 1739-1743, July (2018)
39. J. Ye, "A multicriteria decision-making method using aggregation operators for simplified neutrosophic sets," Journal of Intelligent and Fuzzy Systems.
40. Zadeh.L.A., "Fuzzy sets", Information and control, Vol.8 (1965), 338 −353

Indian Journal of Natural Sciences *www.tnsroindia.org.in ©IJONS*

Vol.15 / Issue 83 / Apr / 2024 *International Bimonthly (Print) – Open Access* *ISSN: 0976 – 0997*

REVIEW ARTICLE

Nanocarrier Mediated Transdermal Drug Delivery Systems for the Management of Psoriasis : A Review

Virendra Kumar Singh[1], Hiteshkumar A Patel[2], Ramesh Singh[3] and Bharat Mishra[4*]

[1]Associate Professor, Department of Pharmacy, B.N College of Pharmacy, (Affiliated to Dr. A.P.J. Abdul Kalam Technical University (APJAKTU)), Lucknow, Uttar Pradesh, India.
[2]Associate Professor, Department of Pharmacy, *Nootan Pharmacy College,(*Affiliated to Sankalchand Patel University) Gujarat, India.
[3]Professor, Department of Pharmacy, B.N College of Pharmacy,(Affiliated to Dr. A.P.J. Abdul Kalam Technical University (APJAKTU)) Lucknow, Uttar Pradesh, India.
[4]Professor, Department of Pharmacy, *Dr Shakuntala Misra National Rehabilitation University* , Lucknow, Uttar Pradesh, India.

Received: 11 Nov 2023 Revised: 19 Jan 2024 Accepted: 25 Mar 2024

***Address for Correspondence**
Bharat Mishra
Professor,
Department of Pharmacy,
Dr Shakuntala Misra National Rehabilitation University ,
Lucknow, Uttar Pradesh, India.
Email: bharatekansh@gmail.com

ABSTRACT

Psoriasis is an incessant autoimmune skin disease of inflammatory pathophysiology. It is expressed by prolific growth and abnormal differentiation of keratinocytes. The prevalence of psoriasis is in around 2-5% of the world population. The studies dictate that around 35% of people have moderate to severe psoriasis. Several approaches have been explored by researchers, taking in regard different anti-psoriasis drugs, but psoriasis treatment remains a challenge because of its chronic recurring nature and lack of perfect carrier for a safe and effective delivery of anti-psoriatic drugs. Currently nano carriers have gained prevalent purpose for unscathed and effective treatment of psoriasis. Novel nano carriers like liposomes, transferosomes, niosomes, ethosomes, SLN, NLC, microspheres, micelles, nanocapsules, dendrimers etc. have been thoroughly investigated. This review focuses on existing treatment options along with the recent developments in this direction.

Keywords: Psoriasis, Nanocarriers, Anti-psoriatic drugs, Delivery system, Nanoparticle.

INTRODUCTION

Psoriasis is an incessant inflammatory, autoimmune disorder of the dermis and epidermis. The worldwide occurrence of psoriasis is 2-5%[1]. It is usually characterized by thickening of skin; excessive growth of red scaly patches on the skin. It involves series of cellular changes like epidermal hyperplasia including vascular hyperplasia, ectasia and generation of inflammatory cells such as T-lymphocytes, neutrophils etc. around the affected skin.[2, 3] Psoriasis is categorized as chronic plaque, guttate, pustular, and erythrodermic based on the severity of the patient's condition, location of the rashes and extra clinical characteristics.[4]Among these, chronic plaque psoriasis has the highest incidence rate and occurs early before the age of 40 years and it affect to both male and female.[5] The classification of types of psoriasis is shown in Table1.

Pathophysiology of psoriasis

An array of events is followed in the pathogenesis of psoriasis, these are sequenced in Fig.1.The contrariness between normal and psoriatic skin is elaborated in Table 2.

Challenges in psoriasis treatment

The main challenges in curing psoriasis are described here.

(a) Lack of suitable carrier: The main problem is the selection of an expedient carrier with suitable physicochemical properties, which on addition change the absorption pattern and hence modifying the effect of drug. Problems encountered with traditional carriers could be potentially resolved through the use of unique carriers.[11]

(b) Absence of suitable animal model: Another challenge in the optimal drug delivery system selection is the election of a suitable animal model.[12] While many animal models based on immunology and genetics have been developed but none of them accurately reflects the traits of psoriasis without certain limitation.[13, 14]

Various treatment options for psoriasis

Generally, there are three main types of therapy for psoriasis **a)** Topical treatment**b)** Phototherapy c**)** Systemic therapy. Firstly, topical treatments are taken into consideration. When topical therapy is ineffective then phototherapy is suggested.[15] Detailed descriptions of anti-psoriatic drugs with their novel carrier's system for delivery are given in Table 3. Conventionally, topical medication is used for mild psoriasis, but the absorption rate is slow. In advanced stages of psoriasis, systemic therapy is chosen. In case of systemic therapy, dose administered is high, which might show undesired effect. The pharmaceuticals adopted in the treatment of moderate to severe psoriasis have exorbitant cost. The traditional topical medications are economic but due to the chronic recurrent nature, psoriasis remains a challenge to treat traditionally (topical, oral and systemic) as shown in Fig 2. The overuse of highly potent corticosteroids can cause thinning of the skin and other side effects, while coal tar and dithranol are less effective. In systemic therapy drug like methotrexate, cyclosporine, and acitretin produce significant side effects, low visual and cosmetic appeal leading to poor patient compliance.[16] The available conventional formulation for psoriasis treatment encounters problems such as increased dosing frequency, side effects and decreased safety and efficacy. None of these treatments have been proven to be safe and effective. Additionally the traditional formulation have unaesthetic appearance and toxic effects when used for extended period of time.[17, 18]The need of a novel delivery system cropped up. Extensive investigation is being carried out to accomplish a safe and effective treatment of psoriasis via novel carriers.[19] Numerous approaches using novel carriers offered a variety of proslike enhanced encapsulation efficiency, increased biocompatibility, bioavailability, reduction in dose dosing frequency leading to improved patient compliance.[20, 21]

Prospective management of psoriasis

Recently, several attempts were made to utilize the NDDS approach to improve topical drug formulations used in psoriasis. The most widely used drug delivery systems include lipid-based nanoparticles (i.e., nanoemulsion, SLN,

nanocapsules, nano suspensions, liposomes, liquid nanocrystal, lipid drug conjugates) and polymeric based nanocarriers such as polymeric nanoparticles, micelles, polymer drug conjugates as shown in Table 3.[23]

Classification of novel nanocarriers

Numerous adaptable and intelligent nanocarriers have been created as cutting-edge medication delivery systems for dermal use.[37, 38]The nanocarriers mentioned in this review fall in four main classes:

1. **Nanocarriers based polymers**: micelles, polymeric nanoparticles, dendrimers, nanosphere, and nanocapsule.
2. **Nanocarriers based lipids:** liposomes, solid lipid nanoparticles, nanostructured lipid carriers and Lipospheres.

Figure 3 illustrates many types of nanocarriers used to treat psoriasis.

Nanocarriers based on polymers

Various medicinal agents, including synthetic medications, herbal remedies, vitamins, peptides, and other substances, are delivered via polymers. The size range of polymer-based nanocarriers ranges from 10-1000 nm, and they are often constructed from environmentally benign polymers.[40, 41] Due to their simplicity in preparation, ability to distribute medications precisely, and safety-related considerations, polymer-based nano-formulations have become excellent delivery systems. Additionally, when applied topically, they are structurally stable and capable of maintaining it for a longer period of time.[42, 43]

Polymeric micelles

These are self-assembling nano-sized (5–100 nm) colloidal particles with a hydrophobic core and hydrophilic shell, used as pharmaceutical carriers for water insoluble drugs. These carriers High drug loading capacities, less drug degradation, adverse effects, and enhanced bioavailability. Drug-polymer covalent attachment or physical entrapments are both viable methods for achieving drug loading in a micelle.[44] These micelles nanocarriers have applications in delivery of anticancer drug, antifungal agents, gene delivery, and also for the delivery of anti-psoriatic agents.[45] Recently the therapeutic gene for treating psoriasis has also been delivered via polymeric micelles. In this context, Fan et al. created modified specific si-RNA loaded polyethylene glycol, poly L-lysine, poly L-leucine micelles.[46]

Polymeric nanoparticle

Nanoparticles generally vary in size from 10 to 1000 nm. Polymeric nanoparticles are of two types – nanospheres and nano-capsules depending on the arrangement of drug in the polymer system. In nanosphere drug is entrapped or dispersed in the polymer matrix. Polymers used can be either biodegradable or non-biodegradable in nature. Biodegradable polymers are significantly used as potential drug delivery systems in the controlled or site-specific delivery of drugs or bioactive such as DNA, proteins, peptides and genes through various routes of administration.[47]

Dendrimers

A class of well-defined hyper branched polymers known as dendrimers was initially created under the name cascade polymers.[48] A new family of dendrimers described by Tomalia et al. in 1983 called poly-amidoamine dendrimers, sometimes referred to as PAMAM dendrimers which is blend of amines and amides.[49] Dendrimers proffer space for the loading of drug in the central unit or even interact with the functional groups via electrostatic or covalent bonds.The drug is released from the dendrimer by enzymatic degradation or by change in physical environment (pH or temperature change)[50].Dendrimers have a series of advantages such as increased solubilization, controlled drug release and formation of prodrugs, that is why they have great applications in the drug delivery system.Dendrimers are used for distribution of antiviral, NSAIDS, antihypertensive, anticancer and anti-psoriatic drugs etc.[51, 52]

Nanosphere

In this type of polymeric nanoparticle, drug is entrapped or dispersed in the polymer matrix. Polymers used can either be biodegradable or non-biodegradable. Biodegradable polymeric nanoparticles are significantly used as potential drug delivery systems in the controlled or site-specific delivery of drugs or bioactive such as DNA, proteins, peptides and genes.[53]Polymeric nanoparticles deliver the drugs used in various diseases and dermatological disease including psoriasis. Batheja et al., developed nanospheres in a gel formulation and evaluated its permeation potential by using human cadaver skin exhibited enhanced drug permeation from tyrosphere as compared to aqueous nanosphere formulation. [54]

Nanocapsules

Nanocapsules are polymeric nanoparticles in which one or more active core material is surrounded by polymeric matrix (shell).[55]Nanocapsule can provide as nano drug carriers to achieve controlled release as well as proficient drug targeting. Polymeric Nanocapsules are a valuable means for dermal applications. The primary advantages of Nanocapsules include sustained release, increased drug selectivity and effectiveness, improved drug bioavailability and reduced drug toxicity.[56]

Nanocarriers based on lipids

Generally, lipid-based carriers are comprehended from physiological lipids. Therefore, they are considered to be safe and free from toxicity. Lipid-based nanocarriers are useful in many aspects such as controlled drug release, enhanced stability, biodegradability, drug targeting, increased drug load and cost-effectiveness.

Liposomes

Liposomes are phospholipid bi-layered vesicular structures enclosing an aqueous compartment. Liposomes are suitable for carrying both hydrophilic (in aqueous core) and lipophilic drugs (in lipid bilayer) due to its amphiphilic nature.[57] Dermal delivery of drugs through liposomes is favored by its small size, lamellar, elastic and fluid properties.[58] Phospholipids is main component of liposomal systems, are easily integrated with the skin lipids and maintain the desired hydration condition to improve drug penetration and localization in the skin layers.[59] Liposomes are used in topical as well as transdermal drug delivery , they act as penetration enhancer due to diffusion of phospholipid molecules or nonionic surfactants into the lipid covering of the stratum corneum and promote localized higher drug concentrations.[60] Calcipotriol, a vitamin D analogue was successfully delivered in lipopolymer poly(ethylene glycol)-distearoylphosphoethanolamine (PEG-DSPE) liposomes with a significant increase in drug deposition into the stratum corneum.[61] Doppalapudi et al., developed liposomal nanocarriers containing psoralen for safe and effective PUVA therapy of psoriasis with better skin penetration.[62] Wadhwa et al., prepared fusidic acid (FA) loaded liposomal system for proficient management of plaque psoriasis.[63]

Solid lipid nanoparticles

Solid lipid nanoparticles are nanoparticles systems having size ranging from 50 to 1000 nm. They are composed of physiological lipids and surfactants which form SLN on dispersion in water.[64]SLN offers exclusive advantages such as large surface area, high drug loading capacity, minimal skin irritation, protective and extended drug release. It is used in various cosmetic and dermatological preparations. Gambhire et al. (2011) reported the preparation and optimization of dithranol loaded solid lipid nanoparticles.[65]

Nanostructured lipid carriers

Nanostructured Lipid Carriers (NLCs) represent an advanced form of solid lipid nanoparticles (SLNs) with improved properties of drug loading, modifying drug release profile and stability on storage. NLCs are promising drug carriers for topical application because of their improved skin retention properties.[66]Compared with other topical vehicles like creams, tinctures, lotions and emulsions, the NLCs have several advantages such as controlled drug release, negligible skin irritation, protection of active compounds and targeted drug delivery.[67]NLCs are produced by mixing solid lipids (stearic acid, palmitic acid, carnauba wax, cetyl palmitate) with liquid lipids (oleic acid, isopropyl myristate) and form to a lipid matrix with a specific structure. Lin et al. (2010) combined calcipotriol

and methotrexate in nanostructured lipid carriers for topical delivery, and reported efficient delivery of the drugs.[68]

Liposphere

Lipospheres are lipid-based nanoparticulate carrier which is composed of solid lipid core surrounded by a single unit phospholipid layer that may entrap the drug or coat with the drug. The emulsifying agent or stabilizing agent is used to form uniform coating around the core material and to facilitate partitioning of the drug between the lipid and aqueous phases.[69]Lipospheres have been successfully used orally, intravenously and by transdermal route for the treatment of various ailments including psoriasis.

Nanoemulsion

Nanoemulsions are biphasic dispersion having droplet size ranging 5 nm to 100 nm,which may be either water in oil emulsion or oil in water emulsion.[70] The small droplet size can resist the physical destabilization caused by gravitational separation, flocculation and/or coalescence. It also avoids the creaming process because the droplet's Brownian motion is enough to overcome the gravitational separation force. Nanoemulsions can be delivered in several dosage forms like liquids, creams, sprays, gel, aerosols, and can be administered via various routes like topical, oral, intravenous, intranasal, pulmonary and ocular.[71]Khandavilli and Panchagnula (2007) formulated a nanoemulsion (NE) to achieve penetration of paclitaxel into deeper skin layers while minimizing the systemic escape.[72] Bernardi et al. (2011) formulated rice bran oil nanoemulsions and evaluated it for irritation potential and moisturising activity on volunteers with normal and diseased skin types.[73]

Ethosomes

Ethosomes are soft, flexible and noninvasive delivery carriers. It is mainly composed of phospholipids, ethanol and water. The characteristic feature of Ethosomes is its high ethanol concentration which is responsible for disturbing the organization of skin lipid bilayer. Thus, these vesicles based on ethanol easily penetrate the stratum corneum and are reported to be safe for pharmaceutical and cosmetic use.[74]Ethosomes are suitable for topical drug delivery as they remain confined to the upper layer of stratum corneum. They have also been used for dermal, transdermal delivery of numerous drugs for the treatment of several dermal diseases like alopecia, dermatitis and psoriasis.[75]

CONCLUSION

A variety of treatments are already available for psoriasis, still the treatment remains a challenge due to the reoccurring nature of the ailment. In order to safely manage this disease, a new approach has been adopted by introducing nanoparticle-based drug delivery. This might combat with the limitations of the conventional drug therapy and also minimize the dose and it's frequency, thereby improving patient compliance. Nanocarriers such as liposomes, Ethosomes, Lipospheres, SLNs, polymeric nanoparticles, NLCs, nanocapsule, dendrimers, gold nanoparticles, silver nanoparticles, etc. have successfully employed for anti-psoriatic drug delivery. These carriers clearly present themselves as a tool to overcome the challenges associated with topical anti-psoriatic drug therapy.

REFERENCES

1. M. Sala, A. Elaissari, H. Fessi, 'Advances in psoriasis physiopathology and treatments: Up to date of mechanistic insights and perspectives of novel therapies based on innovative skin drug delivery systems (ISDDS), J. Controlled Release 239 (2016) 182–202.
2. Mendonca CO, Burden AD. Current concepts in psoriasis and its treatment. PharmacolTher 2003; 99(2): 133-47.
3. Krueger J, Bowcock A. Psoriasis pathophysiology: Current concepts of pathogenesis. Ann Dermatol 2005; 64(2): 30-6.

4. E.S. Galimova, V.L. Akhmetova, E.K. Khusnutdinova, Molecular genetic basis of susceptibility to psoriasis, Russ. J. Genet. 44 (2008) 513–522.
5. E. Campalani, J.N.W.N. Barker, The clinical genetics of psoriasis, Curr. Genom. 6(2005) 51–60.
6. Bharat Khurana, Daisy Arora & R.K. NarangTopical delivery of nanoemulsion for antipsoriaticdrugs,Journal of Drug Delivery & Therapeutics. 2018; 8(5-s):1-11
7. Naldi L, Colombo P, Benedetti Placchesi E, et al. Study design and preliminary results from the pilot phase of the PraKtis study: selfreported diagnoses of selected skin diseases in a representative sample of the Italian population. Dermatology 2004; 208:38-42.
8. C.E. Griffiths, J.N. Barker, Pathogenesis and clinical features of psoriasis, Lancet (London, England) 370 (2007) 263–271.
9. C.W. Lynde, Y. Poulin, R. Vender, M. Bourcier, S. Khalil, Interleukin 17A: toward a new understanding of psoriasis pathogenesis, J. Am. Acad. Dermatol. 71 (2014)141–150.
10. Panonnummal, Rajitha, R. Jayakumar M. Sabitha. "Comparative anti-psoriatic efficacy studies of clobetasol loaded chitin nanogel and marketed cream." European journal of pharmaceutical sciences 96 (2017): 193-206.
11. O.P.Katare, K. Raza, B. Singh, S. Dogra, Novel drug delivery systems in topical treatment of psoriasis: rigors and vigors, Indian J. Dermatol. Venereol. Leprol. 76 (2010) 612–621.
12. M.P. Schon, Animal models of psoriasis: a critical appraisal, Exp. Dermatol. 17 (2008) 703–712.
13. J. Jean, R. Pouliot, In vivo and in vitro models of psoriasis, in: Daniel Eberli (Ed.), Tissue Engineering, 2010, pp. 359–382.
14. . H. Mizutani, K. Yamanaka, H. Konishi, T. Murakami, Animal models of psoriasis and pustular psoriasis, Arch. Dermatol. Res. 295 (2003) S67–S68.
15. Chaturvedi SP, Kumar V, a review on disease management and drug delivery aspects in psoriasis, Current Trends In Technology And Science, 2012; 1(3):122-125.
16. Preeti K. Suresh et al.,African Journal of Pharmacy and Pharmacology Vol. 7(5), pp. 138-147, 8 February, 2013
17. Rosado C, Silva C, Reis CP, Hydrocortisone-loaded poly(ε- caprolactone) nanoparticles for atopic dermatitis treatment, Pharm. Dev. Technol. 2013; 18:710–718.
18. Lapteva M, Santer V, Mondon K, Patmanidis I, Chiriano G, Scapozza L, Targeted cutaneous delivery of ciclosporin A using micellar nanocarriers and the possible role of inter- cluster regions as molecular transport pathways, J. Controlled Release. 2014; 196:9–18.
19. M. Rahman, S. Akhter, J. Ahmad, M.Z. Ahmad, S. Beg, F.J. Ahmad, Nanomedicinebased drug targeting for psoriasis: potentials and emerging trends in nanoscale pharmacotherapy, Expert Opin. Drug Deliv. 12 (2015) 635–652.
20. M. Rawat, D. Singh, S. Saraf, S. Saraf, Nanocarriers: promising vehicle for bioactive drugs, Biol. Pharm. Bull. 29 (2006) 1790–1798.
21. D. Singh, M. Pradhan, M. Nag, M.R. Singh, Vesicular system: versatile carrier for transdermal delivery of bioactives, Artif. Cells Nanomed. Biotechnol. 43 (2015) 82–290.
22. John Berth-Jones, Common Dermatoses, Medicine, 41:6, (2013) 334-340.
23. El-Darouti M, Hay RB, Psoriasis: highlights on pathogenesis, adjuvant therapy and treatment of resistant and problematic cases (part I), J. Egypt. Women. Dermatol. Soc. 2010; 64–67.
24. J.C. Cather, W. Abramovits, A. Menter, Cyclosporine and tacrolimus in dermatology, Dermatol. Clin. 19 (2001) 119–137.
25. R. Gupta, M. Gupta, S. Mangal, U. Agrawal, S.P. Vyas, Capsaicin-loaded vesicular systems designed for enhancing localized delivery for psoriasis therapy, Artif. Cells Nanomed. Biotechnol. 44 (2016) 825–834.

A. Zeb, O.S. Qureshi, H.S. Kim, J.H. Cha, H.S. Kim, J.K. Kim, Improved skin permeation of methotrexate via nanosized ultradeformable liposomes, Int. J. Nanomed. 11 (2016) 3813–3824.

26. N. Bavarsad, A. Akhgari, S. Seifmanesh, A. Salimi, A. Rezaie, Statistical optimization of tretinoin-loaded penetration-enhancer vesicles (PEV) for topical delivery, Daru 24 (2016) 7.
27. M.S. Alam, M.S. Ali, N. Alam, M.R. Siddiqui, M. Shamim, M.M. Safhi, In vivo study of clobetasol propionate loaded nanoemulsion for topical application in psoriasis and atopic dermatitis, Drug Invent. Today 5 (2013) 8–12.

28. J.R. Madan, P.A. Khude, K. Dua, Development and evaluation of solid lipid nanoparticles of mometasone furoate for topical delivery, Int. J. Pharm. Investig. 4 (2014) 60–64.
29. K. Borowska, S. Wolowiec, A. Rubaj, K. Glowniak, E. Sieniawska, S. Radej, Effect of polyamidoamine dendrimer G3 and G4 on skin permeation of 8-methoxypsoralene in vivo study, Int. J. Pharm. 426 (2012) 280–283.
30. B.M. Bianca, L.Q. Arturo, M. Begon, D. Charro, A.M. Fadda, J. Blanco-Me'ndez, Microemulsions for topical delivery of 8-methoxsalen, J. Control. Release 69 (2000) 209–218
31. R. Arora, S.S. Katiyar, V. Kushwah, S. Jain, Solid lipid nanoparticles and nanostructured lipid carrier-based nanotherapeutics in treatment of psoriasis: a comparative study, Expert Opin. Drug Deliv. 14 (2017) 165–177.
32. M.L. Marchiori, G. Lubini, G. Dalla Nora, R.B. Friedrich, M.C. Fontana, A.F. Ourique, M.O. Bastos, L.A. Rigo, C.B. Silva, S.B. Tedesco, R.C.R. Beck, Hydrogel containing dexamethasone-loaded nanocapsules for cutaneous administration: preparation, characterization, and in vitro drug release study, Drug Dev. Ind. Pharm. 36 (2010) 962–971.
33. N.O. Knudsen, S. Rønholt, R.D. Salte, L. Jorgensen, T. Thormann, L.H. Basse, J. Hansen, S. Frokjaer, C. Foged, Calcipotriol delivery into the skin with PEGylated liposomes, Int. J. Pharm. 345 (2007) 163–171.
34. V. Doktorovova, J. Araujo, M.L. Garcia, E. Rakovsky, E.B. Souto, Formulating fluticasone propionate in novel PEG-containing nanostructured lipid carriers PEG-NLC), Colloids Surf., B. 75 (2010) 538–542.
35. M. Pradhan, D. Singh, M.R. Singh, Fabrication, optimization and characterization of Triamcinolone acetonide loaded nanostructured lipid carriers for topical treatment of psoriasis: application of Box behnken design, in vitro and ex vivo studies, J. Drug Deliv. Sci. Technol. 41 (2017) 325–333.
36. V.P. Torchilin, Structure and design of polymeric surfactant-based drug delivery systems, J. Controlled Release 73 (2001) 137–172.
37. P.I. Siafaka, N. Ustundag Okur, E. Karavas, D.N. Bikiaris, Surface modified multifunctional and stimuli responsive nanoparticle for drug targeting: current status and uses, Int. J. Mol. Sci. 17 (2016).
38. P. Madhulika, et al. "Understanding the prospective of nano-formulations towards the treatment of psoriasis." Biomedicine & Pharmacotherapy 107 (2018): 447-463.
39. T. Ishihara, N. Izumo, M. Higaki, E. Shimada, T. Hagi, L. Mine, et al., Role of zinc in formulation of PLGA/PLA nanoparticles encapsulating betamethasone phosphate and its release profile, J. Controlled Release 105 (2005) 68–76.
40. S. Gupta, R. Bansal, S. Gupta, N. Jindal, A. Jindal, Nanocarriers and nanoparticles for skin care and dermatological treatments, Indian Dermatol. Online J. 4 (2013) 267–272.
41. W. Ulbrich, A. Lamprecht, Targeted drug-delivery approaches by nanoparticulate carriers in the therapy of inflammatory diseases, J. R. Soc. Interface 7 (Suppl 1) (2010) S55–66.
42. H. Lboutounne, V. Faivre, F. Falson, F. Pirot, Characterization of transport of chlorhexidine-loaded nanocapsules through hairless and wistar rat skin, Skin Pharmacol. Physiol. 17 (2004) 176–182.
43. V.P. Torchilin, Structure and design of polymeric surfactant-based drug delivery systems, J. Control. Release 73 (2001) 137–172.
44. G.N. Dhembre, R.S. Moon, R.V. Kshirsagar, A review on polymeric micellar nanocarriers, Int. J. Pharm. Bio. Sci. 2 (2011) 109–116.
45. T. Fan, S. Wang, L. Yu, H. Yi, R. Liu, W. Geng, et al., Treating psoriasis by targeting its susceptibility gene, Rel. Clin. Immunol. 165 (2016) 47–54.
46. G.P. Carino, J.S. Jacob, E. Mathiowitz, Nanosphere based oral insulin delivery, J. Control. Release 65 (2000) 261–269.
47. E. Buhleier, E. Wehner, and F. V¨ogtle, "Cascade-chain like and nonskid-chain-like synthesis of molecular cavity topologies," *Synthesis*, vol. 2, pp. 155–158, 1978.
48. D. A. Tomalia, H. Baker, J. Dewald et al., "A new class of polymers: starburst-dendritic macromolecules," *Polymer Journal*, vol. 17, no. 1, pp. 117–132, 1984.
49. S. Svenson, D.A. Tomalia, Dendrimers in biomedical applications—reflections on the field, Adv. Drug Deliv. Rev. 64 (2012) 102–115.

50. P. Kesharwani, L. Xie, S. Banerjee, G. Mao, S. Padhye, F.H. Sarkar, et al., Hyaluronic acid-conjugated polyamidoamine dendrimers for targeted delivery of 3,4-difluorobenzylidene curcumin to CD44 overexpressing pancreatic cancer cells, Colloids Surf. B Biointerfaces 136 (2015) 413–423.
51. X. Qi, Y. Fan, H. He, Z. Wu, Hyaluronic acid-grafted polyamidoamine dendrimers enable long circulation and active tumor targeting simultaneously, Carbohydr. Polym. 126 (2015) 231–239.
52. G.P. Carino, J.S. Jacob, E. Mathiowitz, Nanosphere based oral insulin delivery, J. Control. Release 65 (2000) 261–269.
53. P. Batheja, L. Sheihet, J. Kohn, A.J. Singer, B. Michniak-Kohn, Topical drug delivery by a polymeric nanosphere gel: formulation optimization and in vitro and in vivo skin distribution studies, J. Controlled Release 149 (2011) 159–167.
54. C.E. Mora-Huertasa, H. Fessi, A. Elaissari, Polymer-based nanocapsules for drug delivery, Int. J. Pharm. 385 (2010) 113–142.
55. P.R. Radhika, T. Sivakumar Sasikanth, Nanocapsules: a new approach in drug delivery, Int. J. Pharm. Sci. Res. 2 (2011) 1426–1429.
56. M.L. Gonzalez-Rodriguez, A.M. Rabasco, Charged liposomes as carriers to enhance the permeation through the skin, Expert Opin. Drug Deliv. 8 (2011) 857–871.
57. D.D. Verma, S. Verma, G. Blume, A. Fahr, Particle size of liposomes influences dermal delivery of substances into skin, Int. J. Pharm. 258 (2003) 141–151.
58. Moghimi SM, Patel HM (1993). Current progress and future prospects of liposomes in dermal drug delivery. J. Microencapsul. 10:155-162.
59. Y. Guan, T. Zuo, M. Chang, F. Zhang, T. Wei, W. Shao, et al., Propranolol hydrochloride- loaded liposomal gel for transdermal delivery: characterization and in vivo evaluation, Int. J. Pharm. 487 (2015) 135–141.
60. Knudsen NO, Ronholt S, Salte RD, Jorgensen L, Thormann T, Basse LH, Hansen J, Frokjaer S, Foqed C (2012). Calcipotriol delivery into the skin with PEGylated liposomes. Eur. J. Pharm. Biopharm. 81:532-539.
61. S. Doppalapudi, A. Jain, D.K. Chopra, W. Khan, Psoralen loaded liposomal nanocarriers for improved skin penetration and efficacy of topical PUVA in psoriasis, Eur. J. Pharm. Sci. 96 (2017) 515–529.
62. S. Wadhwa, B. Singh, G. Sharma, K. Raza, O.P. Katare, Liposomal fusidic acid as a potential delivery system: a new paradigm in the treatment of chronic plaque psoriasis, Drug Deliv. 23 (2016) 1204–1213.
63. R.H. Muller, M. Radtke, S.A. Wissing, Solid lipid nanoparticles (SLN) and nanostructured lipid carriers (NLC) in cosmetic and dermatological preparations, Adv. Drug Deliv. Rev. 54 (Suppl 1) (2002) S131–55.
64. Gambhire MS, Bhalekar MR, Gambhire VM, Statistical optimization of dithranol-loaded solid lipid nanoparticles using factorial design. Brazil. J. Pharm. Sci. 47:503-511.
65. Xin K, Zhao Y, Quan P, Liang F. Development of a topical ointment of betamethasone dipropionate loaded nanostructured lipid carrier. Asian J Pharm 2016; 11(2): 248-54.
66. Korting SM, Gysler A. Topical Glucocorticoids with Improved Benefit/Risk Ratio: do they exist?. J Am Acad Dermatol 1992; 27(1): 87-92.
67. Lin YK, Huang ZR, Zhuo RZ, Fang JY (2010). Combination of calcipotriol and methotrexate in nanostructured lipid carriers for topical delivery. Int. J. Nanomed. 5:117-128.
68. Zhang L, Long C, Qian Y, Liu L. Stabilizer distribution on the surface of solid lipid microparticles and SLM stability: Mesoscale simulation and experiments. J Chem Ind Eng. 2007;58:181–89.
69. Y.S. Nam, J.W. Kim, J. Park, J. Shim, J.S. Lee, S.H. Han, Tocopheryl acetate nanoemulsions stabilized with lipid-polymer hybrid emulsifiers for effective skin delivery, Colloids Surf. B Biointerfaces 94 (2012) 51–57.
70. R.S. Bhanushali, M.M. Gatne, R.V. Gaikwad, A.N. Bajaj, M.A. Morde, Nanoemulsion based intranasal delivery of antimigraine drugs for nose to brain targeting, Indian J. Pharm. Sci. 71 (2009) 707–709.
71. Khandavilli S, Panchagnula R (2007). Nanoemulsions as versatile formulations for paclitaxel delivery: Peroral and dermal delivery studies in rats. J. Investig. Dermatol. 127:154-162.
72. Bernardi DS, Pereira TA, Maciel NR, Bortoloto J, Viera GS, Oliveira GC, Rocha-Filho PA (2011). Formation and stability of oil-in-water nanoemulsions containing rice bran oil: *In vitro* and *in vivo* assessments. J. Nanobiotechnol. 9:44.

73. V. Dubey, D. Mishra, N.K. Jain, T. Dutta, M. Nahar, D.K. Saraf, Transdermal drug delivery of antipsoriatic agent via ethanolic liposomes, J. Control. Release 123 (2007) 148–154.
74. A.M. Fadda, M. Manconi, C. Sinico, C. Caddeo, A.O. Vila, D. Valentia, Penetration enhancer containing vesicles as carriers for dermal delivery of tretinoin, Int. J. Pharm. 412 (2011) 37–46.

Table 1: Categorization of Psoriasis[6, 7]

Types	Image	Signs and Symptoms
Plaque psoriasis		• Most people have plaque psoriasis. • Characteristic Feature: Silvery-white scale affecting elbows, knees, lower back, and scalp. • It is the most prevalent types of psoriasis.
Guttate psoriasis		• Children and the young are more susceptible to guttate psoriasis. • Characteristic Feature: Tiny red scaly patches across the skin.
Pustular psoriasis		• It is rigorous type of psoriasis. • Characteristic Feature: Small bumps show on palms and soles causing discomfort and pain. Puss containing bumps will dry out and produced brown spot on the skin.
Flexural psoriasis		• Characteristic Feature: It occurs in skin folds, armpits, under the breast and between buttocks.[78] • It can also affect the genitals. It is not usually scaly.

Erythrodermic psoriasis		• Most common types of psoriasis occur only in 1-2% of people. • Characteristic Feature:Skin looks like it is burned. Patient feels severe hot or cold and deep burning sensation.

Table 2: Contrast between normal and psoriatic skin10

S. No	Feature	Normal Skin	Psoriatic Skin
1	Blood Vessel	Small	Dilated and torturous
2	Inflammatory cells	Absent	Present
3	Abscess Formation	Absent	Present
4	Epidermis	Thin	Thickened
5	Scaly skin	Absent	Red, White scaly skin

Table 3: Anti- Psoriatic Drugs And their Novel carrier system

S.No	Novel carrier system	Anti- psoriasis drug	Method of preparation
1.	Liposome[2]	Tacrolimus	Self-assembly of the triblock copolymer
2	Liposomes[25]	Capsaicin	Thin film hydration
3	Ethosomes[26]	Methotrexate	Extrusion method
4	Liposomes[27]	Tretinoin	Fusion method
5	Nano emulsion[28]	Clobetasol propionate	Aqueous phase titration method
6	SLN[29]	Mometasone Furoate	Solvent injection method
7	Dendrimers[30]	8-methoxypsoralene	Divergent method
8	Microemulsion[31]	8-Methoxsalen	Hot homogenization
9	Nanostructured lipid carrier[32]	Cyclosporine	Modified hot Homogenization method
10	Polymer based nanocapsules[33]	Dexamethasone	Polymeric layer at interface
11	PEG based liposomes[34]	Calcipotriol	film hydration method
12	NLC[35]	Fluticasone propionate	Modified micro emulsion Method
13	Nanostructured lipid carrier[36]	Triamcinolone acetonide	Modified emulsification ultrasonication

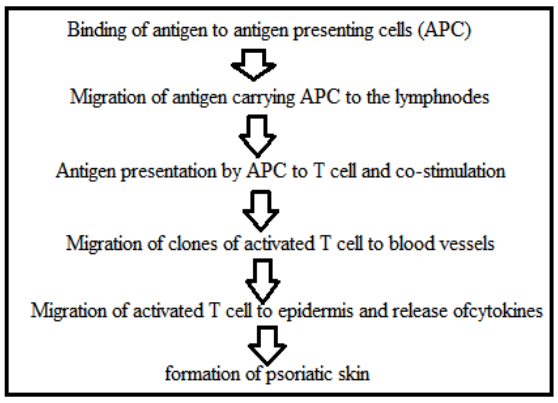

Fig. 1. Pathogenesis of psoriasis.8, 9

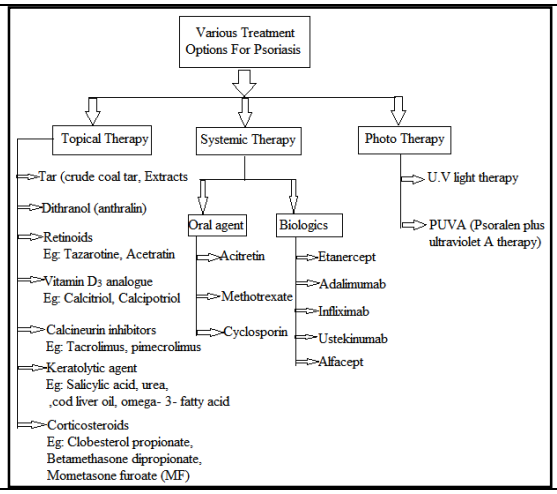

Fig. 2 Medication options for Psoriasis.22

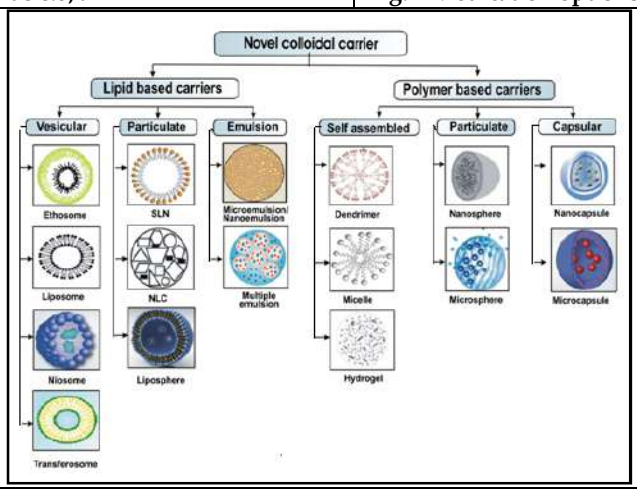

Fig. 3 Variety of nanocarriers used in Anti-psoriatic Drugs 39

Indian Journal of Natural Sciences *www.tnsroindia.org.in ©IJONS*

Vol.15 / Issue 83 / Apr / 2024 *International Bimonthly (Print) – Open Access* *ISSN: 0976 – 0997*

RESEARCH ARTICLE

Authentication and Access using the Multi-Layer Information Security (MLIS) Technology for E-Commerce Applications

Jagan Raj Jayapandiyan[1]* and Anchal Kumari[2]

[1]Software Engineer, British Columbia, Canada, North America.
[2]Research Scholar, Department of Computer Application, Lovely Professional University, Punjab India.

Received: 12 Sep 2023 Revised: 24 Jan 2024 Accepted: 05 Apr 2024

***Address for Correspondence**
Jagan Raj Jayapandiyan
Software Engineer,
British Columbia,
Canada, North America.
Email: jae.jaganraj@gmail.com

ABSTRACT

The Multi-Layered Information Security (MLIS) system introduces a novel approach to authenticating e-commerce applications. Authentication is the process of verifying the identity of a person or entity, and it controls access to systems by comparing user credentials to authorized user databases or data authentication servers. Authentication ensures secure business processes, safe systems, and protect corporate data. To facilitate quick identification of online connections among different users, it is recommended to create a unique identity that matches all online connections. This approach helps the Internet Access Security Service detect compromised physical connections and vulnerable online connections that could be linked to a specific IP address. Multi-layer authentication systems can be useful when there are multiple online connections with a single IP address, and a single user needs to be identified across multiple other IP addresses, which can be accomplished through the Internet Authentication tool. The authentication setup process can be multi-step, depending on the context of the user. The proposed method's strength is to group authentication methods into categories to increase security for each authentication. This approach enables the application to authenticate the user more securely in more than one way than traditional authentication methods and allows authorized users to access the application. Additionally, the MLIS system adds extra security to existing authentication methods, enhancing application security.

Keywords: MLIS, Database, DoS, Cyber Stalking

INTRODUCTION

The purpose of this research paper is to propose a multi-layered information security system that aims to enhance the security of e-commerce applications during authentication. This proposed system is designed to address the vulnerabilities associated with the traditional authentication methods used in most e-commerce applications. The proposed system is made up of three layers: the user layer, service layer, and database layer. The user layer is the

first layer of the system, where users are required to authenticate themselves using their credentials. This layer provides the basic functionality that allows users to securely log into the system. The credentials may include a combination of a username, password, and other biometric factors, depending on the level of security required. The service layer is the second layer of the system, which performs the business logic of the e-commerce application. This layer is responsible for verifying the user's credentials and granting access to the application's features based on the user's permissions. It also ensures that the user data is encrypted and protected during transmission to the database layer.

The database layer is the third layer of the system, where user data and other sensitive information are stored. This layer is responsible for ensuring the integrity and confidentiality of the data stored in the database. It implements various security mechanisms, such as access control and encryption, to prevent unauthorized access to the data. The proposed multi-layered system enhances the security aspect of the application compared to other legacy authentication methods used by today's e-commerce applications. By implementing a multi-layered authentication system, the proposed system can detect and prevent various types of attacks, such as brute force attacks, phishing attacks, and social engineering attacks.

Layers in e-commerce applications

User Layer

In this layer, we have developed a login module that authenticates the user based on his/her username and password. In case the user enters wrong credentials, then he/she gets redirected to the error page. If the user successfully logs in, then the session id is stored in the cookie and sent back to the server. The session id is used to identify the user throughout the application.

Service Layer

This layer contains the business logic of the web application. Here, we have implemented the following methods.

1) Login method : This method checks whether the user's credentials are correct or not.
2) Logout method : This method removes the session id from the cookie and redirects the user to the home page.
3) Register method : This method registers the user if the user does not exist in the database.
4) Update method : This method updates the details of the user if the user exists in the database.
5) Delete method : This method deletes the user if the user already exists in the database.

Database Layer

Here, we have created a table called users in the database. The fields of the table are user_id (primary key), username, password, email, firstname, lastname, address, city, state, zipcode, country, phone, mobile, fax, website, notes, date_created, date_modified. This layer is responsible for storing all the data and all the database operations.

Cyber-attacks in Banking Applications

Attacks on computers can take many different forms. It includes Distributed Denial of Service (DDoS), targeted assaults, SQL injection (SQLi), defacement, and other types of attacks are the most common types of cyber-attacks.

Cyber Stalking

Cyberstalking is the use of the internet or other electronic devices with the intent to track someone. Online bullying and online abuse are both terms that are used interchangeably. In general, following involves persistently annoying or undermining behavior, such as following someone, visiting them at their place of business or residence, persisting in badgering them on the phone, leaving written notes or complaints, or damaging their property. Cyber stalking is an innovatively based "attack" on a single person who has been specifically targeted for that assault out of fury, retaliation, or control.

Hacking

"Hacking" is misconduct, which entails destroying security protocols in order to get unauthorized access to the data stored within them". In this year alone, hacking had increased by 37%. Recently, a case of related hacking with specialized web interfaces and obtaining private locations from city residents' email records was made public.

Saltines are people who try to get unauthorized access to PCs. 'Indirect access' software that has been installed on your computer is frequently used for this. Numerous wafers also try to access assets using sophisticated phrase-cracking software, which checks billions of passwords in an effort to find the one that will allow access to a PC (Stamp, 2011).

Phishing

It is just one of several online frauds that aim to deceive people into handing over their money. Phishing is the practice of sending unsolicited communications to customers of financial institutions asking them to submit their username, passphrase, or other personal information in order to access their account for unexplained reasons. When customers click the links in the email to input their information, they are directed to a phoney replica of the original business's website, keeping them unaware that they have been extorted (Schiller et al., 2007)

Malware

The biggest danger from online criminals is malware (viruses, worms, Trojan horses, and other dangers), which they exploit to break into users' accounts and steal their bank information and other sensitive data. The fast expansion of mobile devices like smartphones and tablet computers encourages the development of harmful software, or malware. Computer scammers have been using malware software for the past few years to commit hundreds of thousands of frauds on online customers in commercial sectors, particularly in online banking, in order to steal substantial sums of money.

Automating online fraud

With the use of Automatic Transfer Systems, computer fraudsters and cybercriminals have now advanced the situation (ATSs). With the help of SpyEye and ZeuS malware variants and WebInject files, which are text files with a lot of JavaScript and HTML codes, a new system for automating online banking fraud has been launched.

Denial of Services (DoS) Attack

Cybercriminals utilize denial-of-service (Dos) attacks to attempt to make network resources unavailable to its users. Due to the seriousness of these attacks, discrete distributed denial-of-service (DDoS) attacks may soon bring down not only a single website but also any intermediate service providers. Because of the significance of these cyberattacks and threats to its business growth, online banking services must take substantial action to increase security and maintain steady business growth.

Authentication types

The process of confirming that someone or something is, in fact, who or what it claims to be is known as authentication. By comparing a user's credentials to those stored in a database of authorised users or on a data authentication server, authentication technology controls access to systems. Authentication ensures safe systems, secure business processes, and secure corporate data. There are several forms of authentication. Users are often assigned a user ID for identification purposes, and authentication takes place when the user enters credentials such a password that exactly matches their user ID. Single-factor authentication is the procedure of needing a user ID and password (SFA). Companies have recently reinforced authentication by requesting more authentication elements, including a special code that is sent to a user through a mobile device when a sign-on attempt is made or a biometric signature, like a thumbprint or face scan. Two-factor authentication is used in this situation (2FA).

One Time Password ***(OTP)***

One-time passwords, or OTPs, are important in many applications today, including e-commerce and banking activities. They are utilized to increase the data communication's security. On the reliability of OTP, several security applications are built. Information security could be seriously threatened by any OTP prediction. A gadget that can produce an OTP using an algorithm and cryptographic keys is provided to the user. By using the same algorithm and keys, an authentication server can validate the password. The OTP can be generated by a variety of software or hardware, including personal digital assistants, mobile phones, and specific hardware tokens. The OTP generator

provides tamper-resistant two-factor authentication using the most secure smart cards available: a PIN to open the OTP generator (something you know), and the OTP smart card itself (something you have). Prior to recently, OTP solutions relied on exclusive, frequently patentable time- or event-based algorithms. Due to the fact that OTP uses a password-based authentication method, it is also susceptible to man-in-the-middle attacks like phishing scams. An attacker can intercept an OTP using a mock-up site and pretend to be the user on the genuine internet web site because there is no mutual authentication between the PC and the internet service provider server. One-time passwords, are created either from a static mathematical formula or from the real time of day and vary on a regular basis. For the generation of OTPs, there are essentially 2 methods:

- Based on a mathematical method
- Based on time-synchronized token

OTPs based on Time-Synchronized Token

Based on the client's password being provided and the authentication server's time synchronization (OTPs are valid only for a short period of time). A security token is a piece of hardware that is used to generate time-synchronized OTPs. A precise clock that is synchronized with the clock on the authentication server is present inside the token. Time is a crucial component of the OTP method for these systems because new OTPs are generated based on the current time rather than, or in addition to, the previous password or a secret.

OTPs based on Mathematical Algorithms

This method uses two different approaches to produce OTPs: one is based on the previous password, and the other is based on a challenge. The order in which OTPs must be used is predetermined and is based on the preceding password technique. The previously used OTPs may be used to create each new OTP.

Captcha Code

The acronym CAPTCHA stands for "Completely Automated Public Turing Test to Tell Computers and People Apart," which refers to an algorithmic programmes for telling computers and humans apart. It can create and assess exams that are simple for people to pass but impossible for computers to do so. Common CAPTCHA is mostly used for human-computer verification and typically consists of symbols, text, photos, and sometimes movies. Numerous harmful attacks against websites, networks, and servers gradually start to appear as the Internet and its connected applications become more widely used. Google is committed to protecting the security of your data. By ensuring that only a person with the correct password may access your account, CAPTCHA protects you from remote digital entry. Computers are able to generate distorted images and process user input, but they are unable to understand or solve problems in the same way as a human would in order to pass the test. Google is one of the many web services that uses CAPTCHA to assist block illegal account entry. Other websites that provide access to private data, such bank or credit card accounts, might also use CAPTCHA.

The effort was intended to help a variety of online activities, including email administrations, online purchasing, web journals, and other online involvement. The client must register for these services by completing an online form. However, since bots mimic human behaviour, they take advantage of these free services. It's a test to keep these robotized bots out of online services. A review led by more than 150 people was conducted to evaluate the coherence speed of CAPTCHA images. The participants in the study came from South Asian countries that do not speak Arabic but can understand the Arabic text. A few tests were conducted to determine the strength of the empowering CAPTCHA.(Bilal Khan et al.)

Permanent Identification Number

PIN codes are implemented independently of smart cards, the PIN code cannot be obtained by hacking a smart card. Instead, each time someone tries to enter, the PIN code is retrieved from a central database. In the event that the central database is unavailable, this PIN code is cached at each building. PIN codes were found to be four-digit integers that cannot begin with a zero, allowing for 9000 possible permutations. Numerous services offered by NI used or interfered with PIN numbers. As demonstrated in the ensuing sections, many services contain weaknesses

that could allow an adversary to obtain and/or modify PIN codes. As a result of this study, NI has fixed several issues. The information required to produce a series of PINs is found in PIN calculators. Additionally, the Internet bank maintains a database where this information is kept. Customers use the calculator to create a new PIN each time they need to access their accounts. They next input the new PIN into the GUI of the online bank, which sends it to the security server of the bank. The server then does a database query to retrieve the information for the specified PIN calculator, calculates the current PIN, and checks to see if it matches the PIN generated by the calculator.

Biometric Identification

Biometric identification is used exclusively for safe ATM transactions. The adoption of a biometric mechanism in such a transaction, such as an iris/retinal scan, hand geometry, or fingerprint scan, can significantly increase overall security. Simply registering their biometric data at a bank branch is all that is required of consumers. Then, customers will only need to enter their biometric password, date of birth, and PIN number to withdraw cash from an ATM. Currently, more than 15 million people utilize 80,000 biometrically enabled ATMs in Japan. In all smart environments, biometric authentication is utilized to the utmost extent possible. The two most common methods for biometric authentication are face and fingerprint recognition. The combination of face recognition and fingerprint recognition can be installed in specific locations where a higher level of security is necessary. Typically, a camera and fingerprint scanner will be used to gather biometric data on the client side, and that data will then be sent to a cloud service provider to perform complicated tasks like face and fingerprint identification. The transmission of facial photos and fingerprints from the client side to a server is a serious problem in these circumstances since an intruder may try to steal that information and utilize it later.

Multi Factor Authentication

Today, digitalization has successfully reached every aspect
of contemporary society. Authentication is a crucial enabler for keeping this procedure secure. It includes a wide range of topics related to a hyperconnected environment, such as communications, access right management, online payments, etc. This study provides insight into how authentication systems have progressed from Single-Factor Authentication (SFA) to Multi-Factor Authentication (MFA), passing through Two-Factor Authentication (2FA). MFA is planned to be used specifically for human-to-everything interactions by facilitating quick, simple, and trustworthy authentication when logging into a service. User authentication is the process of identifying a user based on something they already know, possess, are, or do. It can also be based on a mix of two or more of these characteristics. User authentication techniques are diversifying along with the wide range of dangers in online contexts. A safe authentication mechanism called multi-factor authentication (MFA) calls for multiple authentication methods to be selected from various categories of credentials. Similar to single factor, multi-factor authentication is being used more frequently to confirm users' identities when they access cyber systems and information. MFA provides a more effective and secure method of user authentication by combining two or more methods of authentication.

Push Notifications

In pervasive mobile applications, where invocations happen asynchronously, cloud messaging push notification systems are crucial components. It is crucial that mobile users are alerted promptly of the services that are available. There are four different types of push notifications available, including those from Apple, Blackberry, Google Cloud Messaging, and Microsoft.Push notifications in two factor authentication (MFA) implementation help consumers to secure themselves and prevent cybercriminals, in addition to allowing vendors to send information right to your fingers. It is well known that less is more for the consumer (more convenient, that is). Push notifications give users the impression that they can feel "more" secure with "less" work and time with the simple push of a button.

Password Authentication

Despite widespread hacks and data breaches frequently taking advantage of password-related weaknesses, passwords are still the most popular authentication method employed by Web-based businesses. The strength of passwords is essential to password authentication techniques as multi-user systems quickly develop. Users can

choose secure passwords with the use of password strength meter. However, the current password strength meter are insufficient to offer a good level of protection, forcing users to choose a strong password. The accuracy of rule-based password strength measurement techniques is lacking, because platform-specific password frequencies are different. Some online banking services utilize transaction authentication numbers (TANs) in place of one-time passwords (OTPs) that can only be used once to approve financial transactions. Beyond the conventional single-password authentication, TANs add an additional degree of protection. TANs function as a type of two-factor authentication, adding extra protection (2FA). Without the password, the actual paper or token containing the TANs will be meaningless if it is stolen. On the other hand, if the login information is obtained, no transactions can be completed without a legitimate TAN.

The Web container triggers the authentication mechanism set up for that resource when you attempt to access a protected Web resource. The following authentication techniques are available for selection

1) HTTP based identification
2) Form based identification
3) login authentication
4) Client certificate authentication
5) Mutual authentication
6) Digest authentication
7) The user will not be authorized if one of these techniques is not specified.

Multi-layer Information Security (MLIS)

Multi-layer authentication systems may be useful if, for example, there are multiple online connections with a single IP address and they must resolve the connection of a single user from across multiple other IP addresses. This can be done using the Internet Authentication tool. You can view the security details for an instance of the Microsoft authentication feature, such as the password, a MAC ID, or a private key. The process of setting up authentication can take several steps depending on the context of the specific user. The easiest way to quickly and easily identify an online connection between different users is by creating a unique identity to match all of your online connections to. This can provide the Internet Access Security Service with the ability to detect when a physical connection is compromised and that an online connection is vulnerable because a breach could be linked to a specific IP address.

The user login procedure includes, verification of the user login every time by at least two authentication methods. Also implementing time out for user session and mandate re-login on user session expiry. Example for combines authentication could be Rotating PIN + Password, Password + Bio-metric, Password + OTP, Hardware USB key + Password or Rotating PIN + Password. On the other hand, for the application logs in to a server every time by unique hardware signature. It should also mandate time out values for application session and request re-login on time out expiry. Example for multi layered application login could be MAC based unique machine login along with rotating PIN or SSH login with rotating PIN.

Proposed algorithm for user login

User enters username for login in the application.

1) MLAS select two different authentication methods randomly.
2) One comes from authentication group-1 (Biometric, Password or Hardware key)
3) One comes from authentication group-2 (OTP methods)
4) User responds to the MLAS authentication challenge.
5) If the user's response for both the challenges are same, then security system allows the user and grants access to the application.
6) If the user's response for one of the challenges is invalid, then security system restricts the user and grants access to the application.

CONCLUSION

Advantage of the suggested approach is the greater security it provides for each authentication by grouping the various authentication techniques. The security of the application is multiplied by using this collection of authentication techniques. With the help of this authentication approach, the application is able to rigorously validate the user using a variety of traditional authentication techniques while still granting the authorized user access. MLIS strengthens application security by adding an extra layer of protection to the current user and application authentication techniques.

REFERENCES

1. Ali, L., Ali, F., Surendran, P., & Thomas, B. (2017). The effects of cyber threats on customer's behaviour in e-Banking services. International Journal of E-Education, 7(1), 70–78.
2. Bodkhe, U., Chaklasiya, J., Shah, P., Tanwar, S., & Vora, M. (2020). Markov model for password attack prevention. In Lecture Notes in Networks and Systems (pp. 831–843). Springer Singapore.
3. Carr, M. (Ed.). (2017). Information security: Principles and practices. Larsen and Keller Education.
4. Chowdhury, A. (2016). Recent cyber security attacks and their mitigation approaches-an overview. In International conference on applications and techniques in information security (pp. 54–65). Springer.
5. Grobler, M., Chamikara, M. A. P., Abbott, J., Jeong, J. J., Nepal, S., & Paris, C. (2021). The importance of social identity on password formulations. Personal and Ubiquitous Computing, 25(5), 813–827. https://doi.org/10.1007/s00779-020-01477-1
6. Hasan, M. F., & Al-Ramadan, N. S. (2021). Cyber-attacks and Cyber Security Readiness: Iraqi Private Banks Case. Soc. Sci. Humanit. J, 5(8), 2312–2323.
7. Hole, K. J., Moen, V., & Tjostheim, T. (2006). Case study: online banking security. IEEE Security & Privacy, 4(2), 14–20. https://doi.org/10.1109/msp.2006.36
8. Khan, B., Alghathbar, K., Khan, M. K., Alkelabi, A. M., & Alajaji, A. (2013). Cyber security using arabic CAPTCHA scheme". Int. Arab J. Inf. Technol, 10(1), 76–84.
9. Lee, Y. S., Kim, N. H., Lim, H., Jo, H., & Lee, H. J. (2010). Online banking authentication system using mobile-OTP with QR-code. 5th International Conference on Computer Sciences and Convergence Information Technology.
10. Li, N., Du, Y., & Chen, G. (2013). Survey of cloud messaging push notification service. 2013 International Conference on Information Science and Cloud Computing Companion.
11. Ometov, A., & Bezzateev, S. (2017). Multi-factor authentication: A survey and challenges in V2X applications. 2017 9th International Congress on Ultra Modern Telecommunications and Control Systems and Workshops (ICUMT).
12. Ometov, A., Bezzateev, S., Mäkitalo, N., Andreev, S., Mikkonen, T., & Koucheryavy, Y. (2018). Multi-Factor Authentication: A Survey. Cryptography, 2(1), 1. https://doi.org/10.3390/cryptography2010001
13. Pakojwar, S., & Uke, N. J. (2014). Security in online banking services-A comparative study. International Journal of Innovative Research in Science, Engineering and Technology, 3(10), 16850–16857.
14. Schiller, C., Binkley, J., Harley, D., Evron, G., Bradley, T., Willems, C., & Cross, M. (2007). Botnets: The Killer Web Applications. Elsevier.
15. Shukla, V., Chaturvedi, A., & Srivastava, N. (2019). A new one time password mechanism for client-server applications. Journal of Discrete Mathematical Sciences & Cryptography, 22(8), 1393–1406. https://doi.org/10.1080/09720529.2019.1692447
16. Teule, J. J., Hensel, M. F., Büttner, V., Sørensen, J. V., Melgaard, M., & Olsen, R. L. (2020). Examining the Cyber Security of a Real-World Access Control Implementation. In 2020 International Conference on Cyber Situational Awareness, Data Analytics and Assessment (CyberSA) (pp. 1–3). IEEE.
17. Understanding Login authentication. (n.d.). Oracle.com. Retrieved August 2, 2022, from https://docs.oracle.com/cd/E17802_01/j2ee/j2ee/1.4/docs/tutorial-update2/doc/Security5.html

18. When push comes to breach: Hackers use push notifications to bypass MFA. (n.d.). Acaglobal.com. Retrieved August 2, 2022, from https://www.acaglobal.com/insights/when-push-comes-breach-hackers-use-push-notifications-bypass-mfa
19. Wikipedia contributors. (2022, May 4). Transaction authentication number. Wikipedia, The Free Encyclopedia. https://en.wikipedia.org/w/index.php?title=Transaction_authentication_number&oldid=1086117120
20. Yang, Y. (2018). Understanding of the cyber security and the development of CAPTCHA. Journal of Physics. Conference Series, 1004, 012008. https://doi.org/10.1088/1742-6596/1004/1/012008

Table I. Comparison of legacy and MLIS authentication method

Comparison criteria	Legacy authentication methods	MLIS authentication method (proposed)
Number of authentication modes used on login	One	Two
Group authentication categories available for enhanced security	No	Yes
Hardened security algorithms	No	Yes
Vulnerable to attacks	Yes	No
Addressing user and application login setbacks in one framework	No	Yes

Dr. JAGAN RAJ JAYAPANDIYAN obtained his Ph.D. from Periyar University, located in Salem, India, in 2022. As an accomplished independent researcher, he has established his career as a software engineer, currently working in British Columbia, Canada. With a passion for information security, cyber security, and steganography, he has made significant contributions to these domains through his research endeavors. He is an active member of the Institute of Electrical and Electronics Engineers (IEEE) and the Association of Computer Machineries (ACM). These organizations provide an excellent platform for networking and knowledge sharing among professionals in the field of computer science.

ANCHAL KUMARI is a Ph.D. student currently studying at Lovely Professional University in Jalandhar, India. Her area of research interest is focused on machine learning and artificial intelligence, which are rapidly evolving fields in computer science. Machine learning and artificial intelligence are concerned with the development of algorithms and computer systems that can learn from data and make predictions or decisions without being explicitly programmed.

Indian Journal of Natural Sciences *www.tnsroindia.org.in ©IJONS*

Vol.15 / Issue 83 / Apr / 2024 *International Bimonthly (Print) – Open Access* *ISSN: 0976 – 0997*

RESEARCH ARTICLE

Survival Analysis for Predicting Heart Failure Risk

Sivaranjani P[1]* and Muthukumar M[2]

[1]Research Scholar, Department of Statistics, PSG College of Arts & Science (Affiliated to Bharathiar University) Coimbatore, Tamil Nadu, India.
[2]Assistant Professor, Department of Statistics, PSG College of Arts& Science, (Affiliated to Bharathiar University)Coimbatore, Tamil Nadu, India.

Received: 30 Dec 2023 Revised: 09 Jan 2024 Accepted: 27 Mar 2024

***Address for Correspondence**
Sivaranjani P
Research Scholar,
Department of Statistics,
PSG College of Arts & Science (Affiliated to Bharathiar University)
Coimbatore, Tamil Nadu, India.
Email:ranjani4513@gmail.com

ABSTRACT

Survival analysis, a statistical approach, evaluates the duration until a significant event, like death or failure, transpires within a population. When employed on clinical data concerning heart failure patients, this methodology forecasts the probability of distinct outcomes, such as survival or death, unfolding across time. Such insights prove valuable in guiding treatment choices and enhancing patient well-being. Our study employed a Statistical package to establish a survival function and a Cox proportional hazard model. This enabled the creation of a curve based on heart failure data. Medical professionals can employ our findings to pinpoint areas necessitating attention for augmenting the survival rates of individuals afflicted with heart failure.

Keywords: Heart failure, survival, hazard functions, and Cox proportional

INTRODUCTION

Heart failure is a syndrome with symptoms and signs brought on by a malfunctioning heart and shortens lifespan [1]. In Western nations, heart failure affects 1% to 2% of the adult population and 5 to 10 people per 1000 years, respectively [2], [3]. It is expected that the burden brought on by heart failure will increase soon given the country's rapidly aging population. Therefore, it is crucial to research and examine the variables that affected patients with heart failure of survival times. In medical research, follow-up is a popular method for examining the laws of nature; examples include examining the effectiveness of a drug, the recovery period following surgery, and the lifespan of a medical gadget [4] [5]. The preceding studies have one thing in common: it will take some time to track down the research items. This period is known as the survival time in statistics. The so-called "survival analysis" is the study of

how survival time is distributed and what influences it [6] [7] [8]. Since D.R. Cox first presented this model in 1972, the proportional hazard regression model has become the method that is most frequently employed to predict the connection between covariates and survival or other censored outcomes [9]. In this study, the survival-time data were modelled using the Cox proportional hazards model, and the survival distribution was examined for important influencing factors.

METHODS

Collected information on personal multiple chronic conditions and the length of time the patient has been observed or was observed in the days leading up to their passing. A survival function and a Cox proportional hazard model were used to interpret the results. Serum creatinine and serum sodium were measured in MD/dL. The Cox proportional hazard model was used to test the patient's probability for different parameters. There are statistically significant differences; hence, the study of the probability of survival curves to estimate overall survival time was used for the analysis. The data were analyzed using SPSS software.

Statistical Analysis

The patients with anemia, diabetes, high blood pressure, smoking habits, and gender were entered as covariates. The hypotheses regarding the effects of covariates on time-to-onset for heart failure were analyzed by Cox proportional hazards. The event of interest is anemia: 0 for no anemia, 1 for having anemia, and death treated as 1, death, and 0 for being alive.

Cox Proportional hazard

The Cox proportional hazards model, sometimes referred to as Cox regression, is a semi-parametric method for survival analysis that looks at the correlation between the timing of an event (such as failure or death) and one or more predictor factors. It assumes that the hazard function, or the likelihood that an event will occur at a particular time, is proportional to a baseline hazard function and estimates the coefficients for the predictor variables, which measure their influence on the hazard. The Cox model is frequently employed in engineering, medical research, and other disciplines to assess time-to-event data. The Cox proportional hazards regression model is given as follows: The proportional hazards model assumes that the time to the event and the covariates are related through the following equations

$$h(t) = h_0(t)\,\mathrm{e}^{(b_1X_1+b_2X_2+\ldots+b_pX_p)}$$

where h(t) symbolizes the anticipated hazard at a given time t, and while $h_0(t)$ denotes the fundamental baseline hazard. This baseline hazard signifies the hazard level when all predictors (X_1, X_2, X_P) are set to zero. It's noteworthy that the projected hazard (h(t))—essentially, the likelihood of encountering the event of interest in the imminent moment—is a result of multiplying the baseline hazard ($h_0(t)$) by the exponential function of the linear amalgamation of predictors. Consequently, these predictors impart a multiplicative or proportional influence on the projected hazard.

Hazardratio

The hazard ratio is a measure that quantifies the relative risk or probability of an event occurring at any given time for one group compared to another. It's a key concept in survival analysis, particularly when using techniques like the Cox proportional hazards model. The hazard ratio provides insights into how different factors influence the risk of an event happening over time. In the context of survival analysis, the hazard ratio compares the hazard rates of two groups (often referred to as "treatment" and "control" groups, or "exposed" and "unexposed" groups). It indicates the ratio of the hazard rates for these groups, thus giving an understanding of the impact of a specific factor on the event of interest. The hazard ratio allows researchers to assess how different predictor variables affect the risk over

time. It's a crucial concept in survival analysis for understanding the relative risks associated with various factors and how they influence the timing of events.

RESULTS

The following information summarizes categorical covariates:

According to the aforementioned table, approximately 97.9% of the patients were censored, and the majority of them were male patients (64.9% and 35.1% of the total). 32.1 percent of patients smoke, 67.9 percent of patients do not smoke, 64.9% of patients do not have high blood pressure, 41.8% of patients have diabetes, and 58.2 percent of patients do not have diabetes. 43.1% of patients are anemic, compared to 56.9% who are not. The Cox proportional hazards model accounts for all factors in the survival-time data. The results are displayed in the table below. The Cox proportional hazards model revealed significant effects on patients' survival times for age, high blood pressure, anemia, creatinine phosphokinase, ejection fraction, and serum creatinine. The Exp(B) column presents the hazard ratio, which represents the multiplicative change in the terminal event hazard per unit increase in a predictor. If the hazard ratio is below 1, the regression slope is negative; conversely, if it exceeds 1, the slope is positive [10]. A hazard ratio of 1 denotes an unchanged risk due to the covariate's modification. The succeeding two columns depict the hazard ratio's 95% confidence interval. Age escalated the likelihood of heart failure-related mortality by 4.5 times (HR: 1.047, 95% CI: 1.028-1.067), while serum creatinine augmented the likelihood by 1.366 times (HR: 1.366, 95% CI: 1.191-1.565).

CONCLUSION

Given the global population's aging and the rise in heart failure prevalence that has resulted, the need for developing therapeutic methods to reduce age-related heart failure is critical. As our understanding of the biology of aging and heart failure has advanced in recent years, new avenues for intervention have emerged. The main risk factors for increased mortality among heart failure patients are increasing age, high blood pressure (above the normal range), higher levels of anemia, and lower values for the ejection fraction (EF). Increased serum sodium levels can lower the risk of dying. The presence of diabetes, smoking, or the patient’s gender significantly affects the results.

REFERENCE

1. Mosterd, A. and Hoes, A.W. (2007) Clinical Epidemiology of Heart Failure. Heart, 93,1137-1146. https://doi.org/10.1136/hrt.2003.025270
2. McMurray, J.J., Adamopoulos, S., Anker, S.D., et al. (2012) ESC Guidelines for theDiagnosis and Treatment of Acute and Chronic Heart Failure. European Heart Journal,33, 1787-1146.
3. Cowie, M.R., Wood, D.A., Coats, A.J., et al. (1999) Incidence and Aetiology of HeartFailure: A Population-Based Study. European Heart Journal, 20, 421-428.https://doi.org/10.1053/euhj.1998.1280
4. Bland, J.M. (2000) An Introduction to Medical Statistics. 3rd Edition, Oxford UniversityPress, New York.
5. Kirkwood, B.R. and Sterne, J.C. (2003) Essential Medical Statistics. 2nd Edition,Blackwell Publishers, Malden.
6. Klein, J.P. (2013) Handbook of Survival Analysis. CRC Press, Boca Raton.
7. Lawless, J.F. (2003) Statistical Models and Methods for Lifetime Data. 2nd Edition, JohnWiley and Sons, New York.
8. Kalbfleisch, J.D. and Prentice, R.L. (2002) The Statistical Analysis of Failure Time Data.John Wiley and Sons, New York.https://doi.org/10.1002/9781118032985
9. Cox, D.R. (1972) Regression Models and Lifetables (with Discussion). Journal of theRoyal Statistical Society B, 34, 187-220.
10. Tabachnick, B. G., & Fidell, L. S. (2013). Using Multivariate Statistics (6th ed.).Boston, MA: Pearson.

Table 1:

Covariates	Count	Percentage
Event	96	32.1
Censored	203	97.9
Male	194	64.9
Female	105	35.1
Smoker	96	32.1
Non-Smoker	203	67.9
Hyper tension	105	35.1
Non-Hypertension	194	64.9
Diabetes	125	41.8
Non-Diabetes	174	58.2
Anaemia	129	43.1
Non-Anaemia	170	56.9

Table 2:

Variables in the Equation								
	B	SE	Wald	Df	Sig.	Exp(B)	95% CI for Exp(B)	
							Lower	Upper
Age	.046	.009	24.519	1	.000	1.047	1.028	1.067
Anaemia	-.455	.217	4.407	1	.036	.634	.415	.970
Creatininephosphokinase	.000	.000	4.971	1	.026	1.000	1.000	1.000
Diabetes	-.137	.223	.379	1	.538	.872	.563	1.350
ejection fraction	-.049	.011	21.593	1	.000	.952	.933	.972
High blood pressure	-.472	.216	4.756	1	.029	.624	.408	.953
Platelets	.000	.000	.209	1	.647	1.000	1.000	1.000
Serum creatinine	.312	.070	20.026	1	.000	1.366	1.191	1.565
Serum sodium	-.044	.023	3.652	1	.056	.957	.914	1.001
Sex	.240	.252	.909	1	.340	1.271	.776	2.081
Smoking	-.119	.251	.223	1	.637	.888	.543	1.453

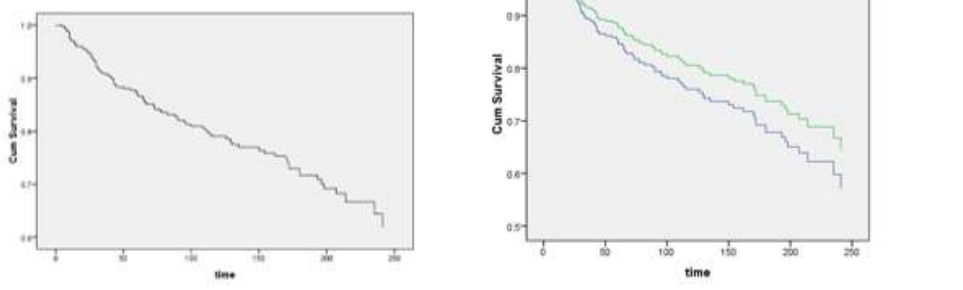

Fig1: a) Survival function at mean of covariates b) Survival curves of male and female

Fig. 1 a): For both men and women, we plot the cumulative survival function while analyzing each covariate at its mean value. The survivor function in the context of this study depicts the probability that a randomly chosen firm will continue to operate over time. b) The survival curve for heart failure patients, assessing the difference between male and female survival.

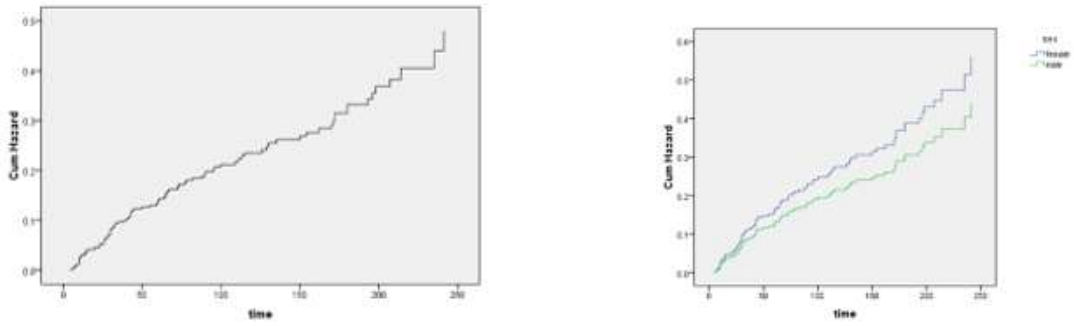

Fig2: a) Hazard function at mean of covariates b) Hazard curves of male and female

Fig. 2a: a) After assessing all factors at their mean values, the cumulative hazard function for both males and females is plotted. This graphical representation effectively illustrates the distribution of risk over time. Generally, this function becomes more informative with time. The hazard function exhibits a peak over time, indicating an escalating risk of occurrence. b) The hazard curve scrutinizes the survival discrepancy between male and female heart failure patients.

Indian Journal of Natural Sciences *www.tnsroindia.org.in ©IJONS*

Vol.15 / Issue 83 / Apr / 2024 *International Bimonthly (Print) – Open Access* *ISSN: 0976 – 0997*

RESEARCH ARTICLE

Laser Micro-Etched Crown and Bridge Restorative Materials: A Simple, Cost-Effective Technique for Personal Identification

Bhupender Yadav[1], Taniya Malhotra[2], Pankaj Ritwal[3]*, Omkar Shetty[4], Jaiveer Yadav[3] and Reshu Madan[5]

[1]Professor and Head, Department of Prosthodontics, Faculty of Dental Sciences, SGT University, Gurgaon, Haryana, India.
[2]PG Student, Department of Prosthodontics, Faculty of Dental Sciences, SGT University, Gurgaon, Haryana, India.
[3]Reader, Department of Prosthodontics, Faculty of Dental Sciences, SGT University, Gurgaon, Haryana, India.
[4]Professor and Dean, Department of Prosthodontics, Faculty of Dental Sciences, SGT University, Gurgaon, Haryana, India.
[5]Professor, Department of Prosthodontics, Faculty of Dental Sciences, SGT University, Gurgaon, Haryana, India.

Received: 19 Oct 2023 Revised: 09 Jan 2024 Accepted: 06 Mar 2024

***Address for Correspondence**
Pankaj Ritwal
Reader,
Department of Prosthodontics,
Faculty of Dental Sciences, SGT University,
Gurgaon, Haryana, India.
Email: pankaj_dental@sgtuniversity.org

ABSTRACT

A forensic dentist plays a significant role in identifying deceased individuals in natural as well as manmade disaster conditions, with specificity in mass casualties linked to aviation disasters. Because of a dearth of an all-encompassing and extensive fingerprint catalog system, dental identification continues to have crucial importance worldwide. The most valuable aids for dental identification are prostheses, restorations, missing, and carious tooth/teeth. The following article aims to discuss the efficacy of laser etching to identify prostheses of three different types during major burns/accidents. All three Laser micro-etched restorations, i.e., all-metal, porcelain fused to metal and zirconia, resisted temperatures up to 1000 degrees for 15 minutes and the etched numbers were easily identifiable. Laser micro etching is an ablative method that is very precise and accurate and can be utilized for marking restorations and can be used for personal identification.

Keywords: Dental identifications, marking/labeling, disaster identification, laser etching, forensic odontology, Engraving

Significance statement

The most common mode of identification is the marking/labeling of a prosthesis, and itis a precise and expeditious method to identify fatalities of anonymous identity. Laser etching can be utilized as a cost-effective marking technique for dental crowns and bridges, which can be helpful in the field of forensics.

INTRODUCTION

The process of recognizing the victims of natural disasters and accidental demise is a highly cumbersome & time-consuming task on the part of the rescuers. Hence, identification done promptly is of paramount significance. Prosthodontists, play a unique role in recognizing the victims with the presence of their natural dentition, records of the carious teeth, teeth restored with various filling materials or with the help of different types of fixed or removable prostheses including partial, or complete dentures along with crowns, bridges and dental implants. All this becomes relatively effortless with the availability of the victim's antemortem records or if the prosthesis is labelled beforehand. There are various treatment options in dentistry, of which replacing missing teeth or restoring endodontically treated teeth with crown and bridge is the most standard treatment carried out by dental practitioners. The incidence of finding a crown or bridge in an individual mouth is quite common nowadays.[1] Recently many aesthetic materials have been introduced in the field of dentistry, such as zirconium which is being used as the substitute to traditional crowns, and bridge restorations such as all-metal or porcelain fused to metal crowns. However, the conventional materials are still in use in clinical practice.[2] Forensic odontology helps in assessing and identifying different type of dental materials employed for restorative purpose exposed to extremes of temperature and can also help in providing vital clues in post mortem investigation if premortem records are available.[3] It can be a real challenge for the investigator to identify burn victims involved in a major fire outbreak. [4] It is hypothesized that high quality data can be retrieved through a systematic approach by examining the restorations and prosthesis in the oral cavity and can aid in identification procedures of victims involved in natural disasters or accidents.

AIM

The aim of the study was to evaluate the efficacy of laser etching technique on different crown and bridge restorative materials cemented on the natural teeth to different temperatures and exposure times and evaluate its importance with regard to its application in forensic identification.

MATERIAL AND METHOD

Three different restorations of varying strengths and heating points were selected, i.e., all-metal, porcelain fused to metal, and zirconia. Laser Engraving was done on the inner walls of all three types of crown and bridges. (Fig 1) 7-10 digits were engraved on the inner walls of the crown. Natural teeth were prepared using an air rotor, and the laser engraved restoration was cemented using permanent luting cement. (Fig 2) The specimens were split into 3 groups. Group 1: natural teeth restored with Ni Cr all-metal crown or bridge, Group 2: Natural teeth restored with porcelain fused to metal crown or bridge, Group 3: Natural teeth restored with zirconia crown or bridge. The blast furnace was heated upto 500 degrees Celsius, and the cemented crown and bridges were incinerated in the furnace for 15 minutes. (Fig 3) After 15 minutes, the crowns were retrieved and observed for any damages. The crowns were decemented from the natural teeth, and the laser etching was analysed under magnification. (Fig 4)And the numbers engraved on the walls of the crown were intact and did not fade away. The same crowns were re-cemented and were incinerated at 1000 degrees for 15 minutes. Again, the crowns were retrieved, and the laser-etched numbers were again analysed. (Fig 5)

RESULTS AND DISCUSSION

1. All metal crowns fabricated from Co-Crrevealed only loss of shine or glaze at 500^0 C with no dislodgement, but subsequently as the temperature was raised to 1000^0 C, the crowns were dislodged from the natural teeth. Laser-etched numbers showed no distortion at the highest temperature. The natural teeth, along with the luting cement, were disintegrated at the highest temperature.
2. Porcelain fused to metal crowns showed no effects at 500^0 C, except for slight debonding, but eventually at 1000°C, they exhibited a changein external form and shape. Laser-etched numbers showed no distortion at the highest temperature.
3. Zirconia crowns did not show any morphological changes even at the highest temperature, and laser-etched numbers showed no distortion and were clearly visible.

The primary scientific indicators for non-visual identification are DNA, fingerprint, and dental comparison. [5,6]But in certain instances, or natural calamities where an individual has been incinerated, the DNA gets denatured, and there may be loss of fingerprint detail. Although natural teeth are extremely durable because of their morphological structure, they can still not resist extreme temperatures, and as a result, the overlying crown and bridges may be the only physical evidence left for identification. crown and bridges are composed of metals such as NiCr, CoCr, Zirconium, etc., which have excellent physical and chemical properties such as high melting and boiling points, high flexural and tensile strength, good corrosion resistance, which make them resistant to physical and thermal assaults. Raymond Richmond and Pretty [7] proposed the basic requirements for an identification system i.e.,it should be easy to implement, should not undermine the restoration, be aesthetically justifiable, and enable reliable identification. The most routinely used methods for marking the restorations/prosthesis are impregnation, engraving, and embossing[8-11] In impregnation techniques chips, barcodes, and other devices are incorporated in the restorations which compromises the aesthetics and also compromises the physical and mechanical properties of the materials. Also, the size of the chips may be a factor if it has to be used for crown and bridge and is virtually impossible to place in these types of restorations. Engraving methods on the external surface of a prosthesis makes it more susceptible to deposition of plaque, colonization of micro-organisms, tarnish and corrosion and subsequently damaging the restoration and infection of the underlying and surrounding soft and hard tissues.

The engraved surface of the prosthesis may also be affected by the usage of dentifrices and antiseptic/mouthwash agents. There are studies in the literature that also suggest that 'embossing' or engraving on the external surface of prosthesis is associated with the occurrence of malignancies that may occur due to constant tissue irritation.[12] Due to the above-mentioned reasons, the laser engraving was done on the cemented/internal surface of the prosthesis and not on the extraoral surface as it will be protected by the luting cement and will be resistant to deposition of plaque. and will not hamper the hygiene and strength of the prosthesis. Recent scientific research reveals a requirement for standardizing the identification methods integrated in restorations and an incursion into the era of digital information storage. Most of the dental associations around the world and forensic odontologists recommends labeling of all dentures. Labelling of prosthesis is controlled by law and legislation in some countries and certain states of the USA.[13] Current methods mentioned in the scientific literature cannot fulfill all the standard requirements for marking of prosthesis, and therefore a unique system of labelling for a particular nation that is universally accepted is needed. Currently in India, as there is no law regarding labeling/marking of the prosthesis, it is neither taught nor practiced in any dental college on a routine basis but the number of individuals wearing some or other type of dental prosthesis is increasing at a rapid pace and there is a need to label prostheses.

In order to address this problem, the authors of the current article suggest linking of marking system with AADHAAR CARD, a citizen's unique identification card in India. Linking of labeling/marking system to a unique ID, AADHAR CARD in India will not only fulfills all standard requirements of labeling but can set an ideal example as the unique id number can give entire information about the person. To support the above statement, various authors such as Baad *et al.*, [14] Mahoorkar and Jain[15] have suggested a national identification number (permanent

account number/Aadhar card number) on dental prostheses as a universal personal identification code. Usually, these identification numbers have 8-10 digits, and laser engraving can easily accommodate the digits in a small area with precision which can be useful in the case of crown and bridge as the available surface for marking is limited.
The technique of laser marking employs various methods such as chemical alteration, carbonization, foaming, melting, and ablation to mark prostheses surface for recognition purposes. Another modification of laser marking is called as laser engraving, which uses laser beam to engrave marks on a surface. The various types of lasers which are employed for engraving purpose are CO2 lasers, fiber lasers and diode lasers.

The method used in the present study for laser marking was flat table engraving in which the laser beam was directed on the prostheses surface to in filtrate till a fixed distance, thereby preventing unavoidable weakening of the restorations. The device used for laser engraving of the various restorations was the Marko fiber Laser instrument which is a non-contact subsurface laser. It engraves an image by removing a portion of the material, layer by layer, to leave a precise dark mark on the surface, which is in the range of a few microns. The device was operated with the help of a computer and software. The letters to be etched on the surface of the prostheses were typed in the software and the laser beam marked it on the surface of the prostheses on activation. One limitation of this device was that high heat was produced during engraving, which may alter the physical properties of the restoration on which engraving is being done. The collimated beam from the laser device generated a high temperature at the contact point, resulting in 'spot evaporation' at a regulated depth of 0.4 mm.20 mA, 70 V, and a frequency of 6 Hz were the conventional recording limits for a metal structure.

The laser utilized in this operation had a wavelength of 1000 nm and a power of 60 W. With a marking speed of 900 mm/s, a marking depth of 0.4 mm, and an accuracy of up to 0.002 mm, a frequency of 6 Hz was used. The power utilized for zirconia was 90 W, with a marking speed of 1000mm/s. Micro-etching, also known as micro-stripping, is the process of selectively exposing the surface layer to reveal the underlying items or selectively removing a portion at a given depth using a laser. Micro-etching is a highly selective removal procedure with a minimum etch value of up to 0.1 microns per laser pulse, according to the definition. This means that the laser etches the material like a fine scalpel, layer by layer, as thin as 0.1 microns. This enables the laser to generate blind holes, blind wells, or channels with more precision.This method is easier to use, less expensive, and saves time in the lab as compared to other prosthetic marking methods. The need for suitable thickness of metal surfaces for etching is one of this process's drawbacks. The availability of a laser engraving machine is another barrier in laser etching. This approach, on the other hand, may be used on any form of prosthesis and is a trustworthy instrument for personal identification.

CONCLUSION

For crown and bridge restorations, laser micro-etching is a precise, cost-effective, and promising marking approach that can provide a permanent mode of personal identification.

ACKNOWLEDGMENT

The authors would like to acknowledge the support received from the ceramic lab of the department of prosthodontics during the course of this study. There is no conflict of interest whatsoever in the present study.

REFERENCES

1. Robinson FG, Rueggeberg FA, Lockwood PE. Thermal stability of direct dental esthetic restorative materials at elevated temperatures. J Forensic Sci. 1998;43:1163–7.

2. ADA Council on scientific affairs. Direct and indirect restorative materials. J Am Dent Assoc. 2003;134:463–72.
3. Harsanyi L. Scanning electron microscopic investigation of thermal damage of the teeth. Acta Morphol Acad Sci Hung. 1975;23:271–81.
4. Bose RS, Mohan B, Lakshminarayanan L. Effects of elevated temperatures on various restorative materials: An in vitro study. Indian J Dent Res. 2005;16:56–60.
5. Merlati G, Savio C, Danesino P, Fassina G, Menghini P. Further Study of restored and unrestored teeth subjected to high temperatures. J Forensic Odontostomatol. 2004;22:17–24.
6. Mazza A, Merlati G, Savio C, Fassina G, Menghini P, Danesino P. Observations on dental structures when placed in contact with acids: Experimental studies to aid identification processes. J Forensic Sci. 2005;50:406–10.
7. Richmond R, Pretty IA. Denture marking – Patient preference of various methods. J Forensic Sci. 2007;52:1338–42.
8. Stevenson RB. Marking dentures for identification. J Prosthet Dent. 1987;58:255.
9. Bernitz H, Blignaut J. An inclusion technique for marking dentures. J Forensic Odontostomatol. 1998;16:14–6.
10. Ling BC, Nambiar P, Low KS, Lee CK. Copper vapour laser ID labelling on metal dentures and restorations. J Forensic Odontostomatol. 2003;21:17–22.
11. Ibrahim WM. Denture microlabeling technique. J Prosthet Dent. 1996;76:104.
12. Datta P, Sood S. The various methods and benefits of denture labelling. J Forensic Dent Sci. 2010;2:53-58
13. Alexander PM. An assessment of attitude to and extent of the ptactice of denture marking in south Australia. Aust Dent J 1998;43:337-41
14. Baad RK, Belgaumi U, Vibhute N, Kadashetti V, Chandrappa PR, Gugwad S. Proposing national identification number on dental prostheses as universal personal identification code –A revolution in forensic odontology. J Forensic Dent Sci. 2015;7:84–9.
15. Mahoorkar S, Jain A. Denture identification using unique identification authority of India barcode. J Forensic Dent Sci. 2013;5:60–3.

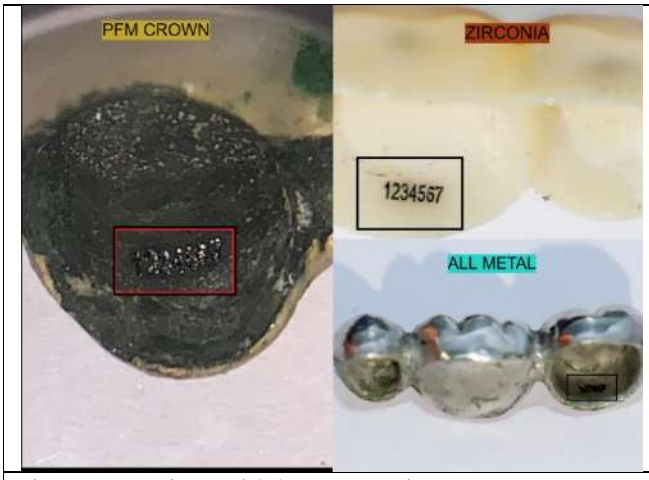

Fig 1: Restorations with laser engraving

Fig 2: Restorations cemented on natural teeth

Fig 3: Restorations at 500 degrees

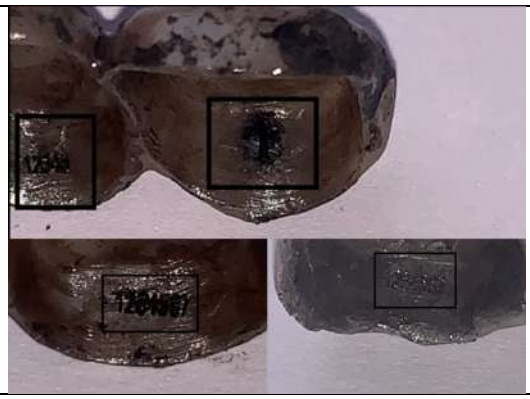

Fig 4: laser etching at 500 degrees

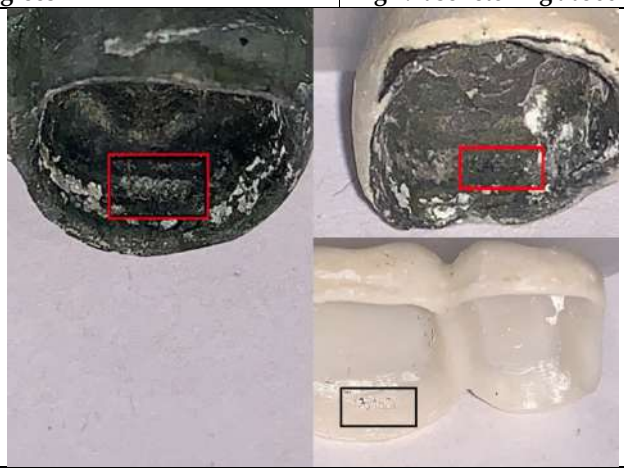

Fig 5: laser etching at 1000 degrees.

Indian Journal of Natural Sciences *www.tnsroindia.org.in ©IJONS*

Vol.15 / Issue 83 / Apr / 2024 *International Bimonthly (Print) – Open Access* *ISSN: 0976 – 0997*

RESEARCH ARTICLE

Phytochemical Screening, *In vitro* Antioxidant, Antidiabetic, Anti-Inflammatory, Anti-Arthritic and Antibacterial Activities in the Leaf Extract of *Kedrostis foetidissima* (Jacq.)cogn.

N.Karthiha[1]* and V.Nivya[2*]

[1]Assistant Professor, Department of Biochemistry, Sri Ramakrishna College of Arts and Science for Women, (Affiliated to Bharathiar University) Coimbatore, Tamil Nadu, India.
[2]Research Scholar, Department of Biochemistry, Sri Ramakrishna College of Arts and Science for Women, (Affiliated to Bharathiar University) Coimbatore, Tamil Nadu, India.

Received: 18 Oct 2023 Revised: 12 Jan 2024 Accepted: 17 Mar 2024

***Address for Correspondence**
N.Karthiha
Assistant Professor,
Department of Biochemistry,
Sri Ramakrishna College of Arts and Science for Women,
(Affiliated to Bharathiar University)
Coimbatore, Tamil Nadu, India.
Email: karthihabio@srcw.ac.in

ABSTRACT

Appakovai (*Kedrostis foetidissima)* of the *Cucurbitaceae* (Pumpkin family). The leaves have a very strong unpleasant smell and the plant can be identified with the red fruits and the smell. The leaf juice is used for treating common cold in children. The paste of the leaves is a good remedy for eczema.The leaf is macerated for 48 hours. The present study was aimed to investigate the phytochemicals and *in vitro* free radical scavenging activity by DPPH and H2O2 method, antidiabetic activity by α amylase inhibition of aqueous extract of *Kedrostis foetidissima,* anti inflammatory activity by albumin denaturation method, anti-arthritic activity by protein denaturation method and antibacterial activities against the microoraganisms *Staphylococcus aureus* and *Escherichia coli.* Phytochemicals,antioxidant,antidiabetic,anti-inflammatory,anti arthritic and antibacterial activities were carried out according to standard methods.It is evaluated for the presence of phytochemicals. Presence of phytoconstituents like alkaloids, flavonoids, saponins,glycosides, carbohydrates, proteins & aminoacids, phenolic components, terpenoids, quinones ,tannins and steroids are tested. The extract was also tested for DPPH and H_2O_2 free radical scavenging activity. The antioxidant activity of aqueous extract was compared with the standard ascorbic acid. The antidiabetic activity of aqueous extract was compared with the standard Metformin. Both the antioxidant and antidiabetic results revealed that the aqueous extract of leaf presented highest concentration of plant extract compared to the standard.

Keywords: *Kedrostis foetidissima, Cucurbitaceae,* Aqueous extract, Phytochemicals, Antioxidant activity, DPPH, H_2O_2, Antidiabetic activity, α amylase inhibition, Anti-inflammatory activity, albumin denaturation, Anti-arthritic activity, protein denaturation, Antibacterial activity, *Staphylococcus aureus* (gram positive), *E.coli* (gram negative).

INTRODUCTION

Medicinal plants are the most important source of life saving drugs and have been widely used for the treatment of diseases in traditional way for several years. An interaction between ancient medicine and biotechnological tools is to be established towards newer drug development. The interface between cell biology, structural chemistry and in vitro assays will be the best way available to obtain valuable leads. The value of plants lies in the potential access to extremely complex molecular structure that would be difficult to synthesize in the laboratory. *Kedrostis foetidissima* has Antimicrobial properties of medicinal plants are being increasingly reported from different parts of the world. Antimicrobials therefore, may have a significant clinical value in treatment of resistant microbial strains.[4] Therefore in the present study *Kedrostis foetidissima* (jacq.) cogn. (Cucurbitaceae) were screened for their antibacterial potential against selected strains.[4]. In the present study, an attempt was made to evaluate the phytochemical, antioxidant,anti-inflammatory, anti-arthritic and anti-bacterial activities in the leaf extract of *Kedrostis foetidissima (Jacq.) Cogn* by using *In vitro* method.

MATERIALS AND METHODS

Collection of Plant
Healthy fresh leaves of *Kedrostis foetidissima* were collected from the region of Kerala district.

Preparation of Extract
The collected leaf parts of plant sample is rinsed with distilled water and dried at room temperature for 7 days. The dried leaves were powdered and stored in air-tight container for further analysis.

Extraction Procedure

Preparation of Ethanol extract
From the powdered sample 4gm of *Kedrostis foetidissima* powder was taken using 70 ml of ethanol. The samples was kept for maceration process for 3 days. The extract was stored in a container and it is used for the entire study.

Preparation of aqueous extract
From the powdered sample taken 30gm of *Kedrostis foetidissima* powder was added with 150 ml of distilled water. Then mixed it well using a glass rod and it is filtered. Then the filtrate was used for phytochemical analysis.

Phytochemical Screening

TEST FOR ALKALOIDS
Hager's Test : A small quantity of extract was treated with Hager's reagent. Yellow precipitate indicates the presence of alkaloids.[3]

TEST FOR CARBOHYDRATES

Benedict's Test : The extract of the powdered leaf was treated with equal volume of Benedict's reagent. A red precipitate was formed indicating the presence of reducing sugar.[6]

TEST FOR FLAVONOIDS

Lead Acetate : To the test solution add a mixture of 10 % lead acetate in few drops added. It gives white precipitate.[2]

TEST FOR PROTEIN & AMINOACIDS

Ninhydrin Test : To the test solution add Ninhydrin solution, boil, violet colour indicates presence of amino acid.[5]

TEST FOR TERPENOIDS

Salkowski Test : Taken 0.5ml of the plant extract added 2ml of chloroform and 3ml of concentrated sulphuric acid along the sides of the test tubes. The appearance of reddish brown colour at the interface indicated the presence of terpenoids.

TEST FOR GLYCOSIDES

Concentrated Sulphuric acid test: To 2ml of the plant extract added 1ml of glacial acetic acid. To that added 1% ferric chloride solution drop by drop and then added concentrated sulphuric acid along the sides of the test tube. The appearance of greenish blue colour indicates the presence of glycosides.[8]

TEST FOR TANNINS

Ferric Chloride : To the 1ml of extract few drops of ferric chloride solution was added. Bluish black colour was produced indicating the presence of tannins.[6]

TEST FOR SAPONINS

Froth Test : With 1ml of extract was vigorously shaken with 5ml of distilled water in a test tube for 30 seconds and was left undisturbed for 20 min, persistent froth indicated presence of saponins.[4]

TEST FOR PHENOLIC COMPOUNDS

Ferric Chloride : To the extract few drops of ferric chloride solution was added. Bluish black colour was produced indicating the presence of tannins.[1]

TEST FOR QUINONES

To 1 ml of plant extract, 1 mL of conc. H_2SO_4 was added formation of red colour indicated the presence of quinones.[3]

TEST FOR STEROIDS

About 0.2 g of extract was taken and 2 ml of acetic acid was added then, the solution was cooled well in ice followed by the addition of concentrated sulphuric acid. Colour development from violet to blue or bluish-green indicated the presence of a steroidal ring.[9]

Preparation of the Bacterial Inoculum

Stock cultures were maintained at 4°C on slopes of nutrient agar. Active culture for experiments were prepared by transferring a loop full of cells from stock cultures to test tubes of 50 ml nutrient broth bacterial cultures were incubated with agitation for 24hours and at 37°C on shaking incubator. Each suspension of test organism was subsequently stroke out on nutrient agar media. Bacterial cultures then incubated at 37°C for 24 hours. A single colony was transferred to nutrient agar media slants were incubated at 37°C for 24 hours. These stock cultures were kept at 4°C. For use in experiments, a loop of each test organism was transferred into 50ml nutrient broth and incubated separately at 37°C for 18-20 hours for bacterial culture.

Agar Well Diffusion Method

The antibacterial activity of extract was determined by Well Diffusion Method. MHA plates were prepared by pouring 20ml of molten media into sterile petri plates. After solidification of media. 20-25ul suspension of bacterial inoculums was swabbed uniformly. The well was prepared by using sterile cork borer made up of stainless steel. Then 20 and 40µl of plant extract was poured into the wells. Chloramphenicol was used as a standard. After that, the plates were incubated at 37°C for 24 hours. Assay was carried into triplicates and control plates were also maintained. Zone of inhibition was measured from the clear zone in mm)

***In vitro* Antioxidant Activity**

DPPH Radical Scavenging Activity

DPPH (2,2-diphenyl-2-picrylhydrazyl) free radical scavenging assay of aqueous leaf extracts of *Kedrostis foetidissima* was determined according to the method by [10] with slight modifications which results in a pale yellow solution .

Procedure

The free radical scavenging activity of the extracts, based on the scavenging activity of the stable 2,2-diphenyl-2-picrylhydrazyl (DPPH) free radical was determined by the method described by Shen *et al*. Plant extract (0.1 mL) was added to 3 mL of a 0.004 % methanol solution of DPPH. The reaction mixture consists of plant extract with the varying concentration (200,400,600,800 and 1000µl) and 5.0ml of DPPH was added and made upto 3.0ml with distilled water. The tubes were shaken well and incubated in the dark at room temperature for 30 minutes. A blue color formed, and the absorbance was measured spectrophotometrically at 517nm. Ascorbic acid was used as a standard for DPPH activity. The ability to scavenge DPPH radical was calculated using the formula

$$\% \text{ of Inhibition} = \frac{\text{Absorbance of control - Absorbance of sample}}{\text{Absorbance of control}} \times 100$$

Hydrogen Peroxide Scavenging Activity

Hydrogen peroxide r adical scavenging assay activity of aqu eous extract of *Kedrostis foetidissima* was determined according to the method by [11] with s l i ght modifications.

Procedure

The reaction mixture consists of plant extract with the concentration (200, 400, 600, 800 and 1000µl) and 1.0ml of Hydrogen peroxide was added The tubes were shaken well and incubated in the dark at room temperature for 10 minutes against a blank solution Absorbance of reaction mixture was measured at 230 nm spectrophotometrically. Ascorbic acid was used as a standard . The ability to Hydrogen peroxide scavenges radical was calculated using the formula

$$\% \text{ of Inhibition} = \frac{\text{Absorbance of control - Absorbance of sample}}{\text{Absorbance of control}} \times 100$$

***In vitro* Antidiabetic activity**

Inhibition of α amylase activity

The determination of α-amylase inhibition was carried out by quantifying the reducing sugar (maltose equivalent) liberated under the assay conditions.[11]

Procedure

To 100µl of (10,20,30,40,50 µg/ml) plant extract.200 µl (1%) starch solution was added and the mixture was incubated at 370c for 20 min. To the reaction mixture 100µl(1% starch solution was added and incubated at 370c for 10 mins. The reaction was stopped by adding 200µl DNSA (1g of 3, 5 di nitro salicylic acid, 30g of sodium potassium tartarate and 20ml of 2N sodium hydroxide was added and made up to a final volume of 100 ml with distilled water) and

kept it in a boiling water bath for 5 minutes. The reaction mixture diluted with 2.2 ml of water and absorbance was read at 540nm. For each concentratrion, blank tubes were prepared by replacing the enzyme solution with 200µl in distilled water. The experiments were repeated thrice using the same protocol.

% of Inhibition = Absorbance of control - Absorbance of sample × 100
Absorbance of control

***In vitro* Anti-inflammatory Activity**

The reaction mixture consists of plant extract with the varying concentration (10,20,30,40 and 50µl) and added 450 µl of BSA Adjusted the pH to 6.3 by using IN HCL. The sample were incubated at 37°C for 20 minutes and heated at 570C for 3minutes. After cooling added 2.5ml of Phosphate solution. Turbidity was measured at 660nm spectrophotometrically. The percentage inhibition of protein denaturation was calculated using formula

% of Inhibition = Absorbance of control - Absorbance of sample × 100
Absorbance of control

***In Vitro* Anti-arthritic Activity**

Prepare the reaction mixture (0.5 mL) by dissolving 0.4 mL of Bovine serum albumin (2 % aqueous solution), 0.05 mL distilled water and 0.05 mL of sample. Incubate the samples at 37 °C for 30 min and then heat at 57 °C for 10 min. After cooling, add 2.5 mL of phosphate-buffered saline (pH 7.4) in each test tube. Measure the turbidity spectrophotometrically at 600 nm. For control, use 0.05 mL distilled water instead of standard/sample.
Calculate the percentage inhibition of protein denaturation as follows:

% of Inhibition = Absorbance of control - Absorbance of sample × 100
Absorbance of control

RESULTS AND DISCUSSION

Table 2: Phytochemical Screening of ethanol and aqueous extract of *Kedrostis foetidissima*
"+++" indicates Strongly Present, "++" indicates Moderately Present, "+" indicates Mildly present, "-" indicates Negative

It is evident from the table 1 of *Kedrostis foetidissima* leaf aqueous extract shows the presence of most of the phytochemicals such as alkaloids, carbohydrate, flavonoids, proteins & aminoacids, terpenoids, tannins, quinones and steroids. Ethanol extract shows the presence of alkaloids, carbohydrate, proteins & aminoacids, terpenoids, phenol, tannins and glycosides.

***In vitro* Antibacterial Activity**

Agar well diffusion method

Plants which are rich in a wide variety of secondary metabolites such as alkaloid and flavonoid have been found In vitro to have antibacterial properties [12]**.** Therefore it is necessary to evaluate the antibacterial effect of the plant extracts. Antibacterial activity of aqueous extract of against *Kedrostis foetidissima* against *Staphylococcus aureus, E.coli* are shown in the figure 2 and 3 respectively.

It is clear from the figure 2 (a) and (b) shows the In vitro antibacterial activity of aqueous extract of *Kedrostis foetidissima* at different concentrations. The figure shows that aqueous extract of *Kedrostis foetidissima* has 7mm,9mm,8mm and 10mm against *Staphylococcus aureus* at the concentration of 25ug,50,75and 100ug respectively. E.coli showed minimum activity of inhibition. *Staphylococcus aureus* is highly efficient than E.coli in the aqueous extract of *Kedrostis foetidissima.*

***In vitro* Antioxidant Activity**

DPPH Radical Scavenging Activity

Free radicals are the unstable molecules that causes damage to the human body. They are mainly reactive oxygen species including highly reactive oxygen containing molecules. Free radicals cause several diseases in humans. Now a days there is an increasing attention in finding antioxidant because they have the ability to inhibit the propagation of free radical reaction and protect the human body from several disorders.[8]

Hydrogen peroxide is an important reactive oxygen species because of its ability to penetrate biological membranes. It is not itself reactive because it may be toxic if it is converted to hydroxyl radicals in the cells.[13] The antioxidant compounds which donates the electrons to hydrogen peroxide and neutralize it into water molecules. Hydrogen peroxide is relatively stable, allowing direct measurement of its concentration in many cases. H_2O; occurs naturally at low concentration levels in air, water, human body, plants, microorganisms etc. It can cross cell membranes and may slowly oxidize a number of compounds. Thus removal of hydrogen peroxide is very important.

It is evident from the figure 4 shows the high antioxidant potential of aqueous extract of *Kedrostis foetidissima* at 600,800,1000 µl/mg concentrations with 91%,95%,98% of inhibition when compared with the standard. This result is in accordance to work of [18] who stated that the extract of *Kedrostis foetidissima* had high Hydrogen Peroxide Scavenging Activity.

***In vitro* Antidiabetic Activity**

Inhibition of α-amylase Activity

The intestinal digestive enzymes alpha- amylase plays a vital role in the carbohydrate digestion. One antidiabetic therapeutic approach reduces the post prandial glucose level in blood by the inhibition of alpha amylase enzyme. These can be an important strategy in management of blood glucose. Alpha- amylase is an enzyme that hydrolyses alpha bonds of alpha lined polysaccharide such as starch to yield high levels of glucose and maltose. Therefore it is quite important to evaluate the alpha- amylase inhibitory activity of extracts. Inhibition of alpha- amylase activity of aqueous extract of *Kedrostis foetidissima* is presented in the Figure 5.

It is evident from the figure 5 shows the high antidiabetic activity of aqueous extract of *Kedrostis foetidissima* at 30,40,150 µl/mg concentrations with 67%,79%,85% of inhibition when compared with the standard.This result is in accordance to work of [19] who stated that the extract of *Kedrostis foetidissima* had high antidiabetic activity.

***In vitro* Anti-inflammatory Activity**

Albumin Denaturation Assay

Albumin denaturation is a process in which the proteins either lose their secondary and tertiary structure due to the external stress or compounds like strong acid or base or concentrated inorganic salt, organic salt. Most of the biological protein lose their function when it is denatured. Denaturation of proteins occurs due to inflammation.[23] Albumin denaturation is a process in which proteins lose their tertiary structure and secondary structure by application of external stress or compound, such as strong acid or base, a concentrated inorganic salt, an organic solvent or heat. Most biological proteins lose their biological function when denatured. Denaturation of proteins is a well-documented cause of inflammation. Anti- inflammatory drugs act by inhibiting the denaturation of protein. Phenylbutazone, salicylic acid, (anti-inflammatory drugs) etc., have shown dose dependent ability to inhibit heat induced protein (albumin) denaturation.Therefore it is necessary to evaluate the effect of the plant extracts in inhibiting heat induced protein. Albumin denaturation assay of aqueous extract of *Kedrostis foetidissima* is presented in the figure 6.

It is evident from the figure 6 shows the high anti-inflammatory activity of aqueous extract of *Kedrostis foetidissima* at 30,40,50 µl/mg concentrations with 34%,44%,54% of inhibition when compared with the standard.This result showed that *Kedrostis foetidissima* had high anti-inflammatory activity.

Antiarthritic Activity

***In vitro* Protein Denaturation Assay**

Protein denaturation is a process in which the proteins either lose their secondary and tertiary structure due to the external stress or compounds like strong acid or base or concentrated inorganic salt, organic salt. Most of the biological protein lose their function when it is denatured. Denaturation of proteins occurs due to inflammation. The leaf extract of antiarthritic activity reported to be useful in the treatment of rheumatoid arthritis activity.

It is evident from the figure 7 shows the high anti-inflammatory activity of aqueous extract of *Kedrostis foetidissima* at 30,40,50 µl/mg concentrations with 31%,39%,53% of inhibition when compared with the standard.The results showed that high antiarthritic activity of *Kedrostis foetidissima.*

SUMMARY AND CONCLUSION

➢ The *Kedrostis foetidissima*(Jacq) cogn were selected for studying the Phytochemicals, Antioxidant, Antidiabetic, Anti-Inflammatory, Antiarthritic and Anti-bacterial activity by using *in-vitro* methods. It was carried out using the Aqueous solvent.

The findings of the current study are summarized as follows:

➢ From the current study, the biochemical test was done for its phytochemical screening in aqueous extract of *Kedrostis foetidissima*(Jacq) cogn. Like alkaloids, carbohydrates, phenol, flavonoids, proteins & aminoacids, terpenoids, quinones, glycosides, tannins, saponins and steroids. From this test we have concluded that most of these chemical tests indicate the presence of secondary metabolites in the selected plant extract. The presence of bioactive components is very important for plant extracts for further analysis.

➢ Aqueous leaf extracts of *Kedrostis foetidissima*(Jacq) cogn were found to contain alkaloids, carbohydrates,flavonoids, proteins & aminoacids, terpenoids is an higher content. Quinones, tannins and steroids were found positive in the leaf extracts.

➢ Antioxidant activity by the DPPH, Hydrogen peroxide radical scavenging assay shows that *Kedrostis foetidissima*(Jacq) cogn leaf extracts shows higher potential with DPPH and H2O2 assay. ➢ *In vitro* Antidiabetic activity by inhibition of α amylase activity on aqueous extract of *Kedrostis foetidissima*(Jacq) cogn leaf. It was observed that the plant extract showed maximum activity against inhibition of α amylase activity.

➢ *In vitro* Anti-Inflammatory activity by albumin denaturation method showed that *Kedrostis foetidissima*(Jacq) cogn aqueous leaf extracts when compared against the standard Aspirin posess greater potential.

➢ *In vitro* Antiarthritic activity by protein denaturation method showed that *Kedrostis foetidissima*(Jacq) cogn aqueous leaf extracts when compared against the standard diclofenac posess greater potential.

➢ The current study has also made attempt to test the *In vitro* antibacterial activity by agar well diffusion method. In this method, the *Staphylococcus aureus* has high efficiency than *E.coli* in aqueous extract of *Kedrostis foetidissima*(Jacq) cogn.

From the above findings it can be concluded that antioxidant, antidiabetic, anti-inflammatory, antiarthritic and antibacterial ativities it may be due to the presence of phytoconstituents in the plants.

FUTURE RECOMMENDATIONS

➢ This study can be carried out in *in vivo* methods to find out antioxidant, antidiabetic, anti inflammatory, antiarthritic and antibacterial activity of *Kedrostis foetidissima*(Jacq) cogn. Leaf extract on animal model.

➢ As the plants for the current study possess greater antiarthritic activity, this might bring some advancements against several bone and joint related disorders like rheumatoid arthritis.

REFERENCES

1. Biljana Bauer Petrovska.(2012).Historical review of medicinal plants usage.*Pharmacognosy 6(11), 1.*
2. Akhileshwar, Kumar .,Srivastava. (2018). Significance of medicinal plants in human lide. *Synthesis of Medicinal Agents from plants, 1-24.*
3. Ansley Hill,RD,LD. (2019). What are tannins in Tea, and do they have benefits?. *Healthline Media.*
4. Bartnik, M & Facey, P.C. (2016). Pharmcognosy Fundamentals, Aplications and Strategies. *Science direct, 101-161.* Bhadra, P.R review paper on the Tulsi plant (Ocimum sanctum). *Indian Journal of Natural Sciences, 10(60),* 20854-20860.
5. Kalaiseziyen Pavithra, Ganapathy Saravanan. (2020). A Review on Phytochemistry, Pharmacological Action, Ethanobotanical Uses and Nutritional Potential of Kedrostis foetidissima (Jacq.) Cogn.*Cardiovascular & Hematological Agents in Medicinal Chemistry (Formerly Current Medicinal Chemistry-Cardiovascular & Hematological Agents) 18 (1), 5-20.*
6. Hassanpour, S., maheriSis, N., & Eshratkhah, B., (2011). Plants and Secondary metabolites (tannins): a Review. [8] Jessie Szalay. (2015). What are flavonoids. *Live science.52524.*
7. Kate Barrington. (2018). What are the benefits of Plant-based Protein ?. *food & Health, Culture & Lifestyle.*
8. Sahira Banu. K., LJIJoARiCS Cathrine. (2015). General techniques involved in phytochemical analysis. *International journal of advanced research in chemical science 2 (4), 25-32.*
9. Jigna Parekh, Sumitra Chanda. (2007). In vitro antimicrobial activity and phytochemical analysis of some Indian edicinal plants. *Turkish journal of biology 31 (1), 53-58.*
10. Nicholas. J., Miller, Julia Sampson, Luis. P., Candeias, Peter. M., Bramley, Catherine. A .,Rice-Evans. (2009). Antioxidant activities of carotenes and xanthophylls. *FEBS letters 384 (3), 240-242.*
11. Sagar. B., Kedare, RP Singh. (2011). Genesis and development of DPPH method of antioxidant assay. *Journal of food science and technology 48, 412-422.*
12. Philip Molyneux. (2004). The use of the stable free radical diphenylpicrylhydrazyl (DPPH) for estimating antioxidant activity. *Songklanakarin J. sci. technol 26 (2), 211-219.*
13. Dal R., Umer J., Syed F., Syed S.S. and Jahan N. (2017). Preliminary Phytochemical Greening, Quantitative Analysis ofAlkaloids, and Antioxidant Activity of Crude Plant Extracts from Ephedra intermedia Indigenous to Balochistan. *The Scientific World Journal.* Volume 2017, Article ID 5873648, 7 pageshttps://doi.org/10.1155/2017/5873648.
14. Chung Yang, S., Chi-Tang Ho, Jinsong Zhang, Xiaochun Wan, Ke Zhang, & Justin Lim. (2018). Antioxidants: Different Meanings in Food Science and Health Science, American Chemical Society, 66(12), 3063-3068. Cohen, M. M. (2014). Tulsi-Ocimum sanctum: A herb for all reasons. *Journal of Ayurveda and integrative medicine, 5(4), 251.*
15. Romanova D., Vachalkova A., Cipak L., Ovesna Z., Rauko P. (2001). Study of antioxidant effect of apigenin, luteolin and quercetin by DNA protective method. *Neoplasma 48 (2), 104-107.*
16. Rashmi Shivanna, Hengameh Parizadeh, Rajkumar H Garampalli. (2015). Screening of lichen extracts for in vitro antidiabetic activity using alpha amylase inhibitory assay. *International Journal Biol Pharm Res 6 (5), 364-367.*
17. Gaofeng Yuan, Mark L., Wahlqvist, Guoqing He, Min Yang, Duo Li. (2012). Natural products and anti-inflammatory activity. *Asia Pacific journal of clinical nutrition 15 (2).*
18. Barry Hallwell. (2015). Antioxidant characterization: methodology and mechanism. *Biochemical pharmacology 49 (10), 1341- 1348.*
19. Mounyr Balouiri, Moulay Sadiki, Saad Koraichi Ibnsouda. (2016). Methods for in vitro evaluating antimicrobial activity: A review. *Journal of pharmaceutical analysis 6 (2), 71-79.*
20. Umme Habiba Hasan. (2018). Antiarthritic efficacy of Clematis orientalis. *Bangladesh Journal of Pharmacology 13 (2), 142-148, 2018.*
21. Ammara Saleem, Mohammad Saleem, Muhammad Furqan Akhtar. (2020). Antioxidant, anti-inflammatory and antiarthritic potential of Moringa oleifera Lam: An ethnomedicinal plant of Moringaceae family. *South African Journal of Botany 128, 246-256.*

Table 1. Scientific Classification

Tamil name	**Appakovai**
	Common name Monkey pepper
English name	**Stinking kedrostis**
Classification	**Benthem & Hooker**
Kingdom	**Plantae**
Class	**Dicotyledons**
Subclass	**Polypetalae**
Series	**calyciflorae**
Order	**Passiflorales**
Family	**Cucurbitaceae**
Genus	**Kedrostis**
Species	***foetidissima***

Table 2: Phytochemical Screening of ethanol and aqueous extract of *Kedrostis foetidissima*

TESTS	ETHANOL	AQUEOUS
Alkaloids (Hager's Reagent)	+	++
Carbohydrate (Benedicts test)	++	+++
Flavonoids (Lead acetate test)	_	+++
Proteins& Aminoacids (Ninhydrin Test)	++	+++
Terpenoids (Salkowski Test)	+	+++
Phenol (Ferric Chloride Test)	+	_
Tannins (Ferric Chloride Test)	+++	+
Saponins (Froth Test)	_	_
Quinones	_	++
Glycosides	+	_
Steroids	-	+

"+++" indicates Strongly Present, "++" indicates Moderately Present, "+" indicates Mildly present, "-" indicates Negative

Tabe 3: Antibacterial activity of aqueous extract

Bacteria	Zone of inhibition (mm)				
	Aqueous extract				
	25(µg/ml)	50(µg/ml)	75(µg/ml)	100(µg/ml)	Standard
Staphylococcus aureus	7mm	9mm	8mm	10mm	9mm
E.coli	2mm	3mm	6mm	7mm	10mm

Figure 1. ***Kedrostis foetidissima*** **(jacq) cogn.**

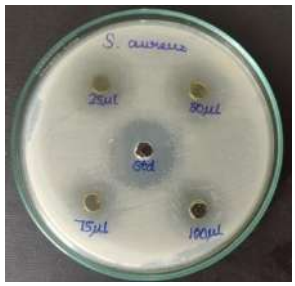

Figure 2: ***Staphylococcus aureus***

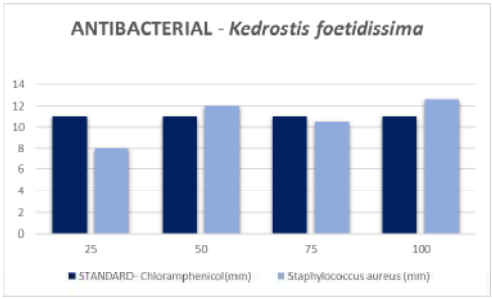

Figure 2 a: ***Staphylococcus aureus***

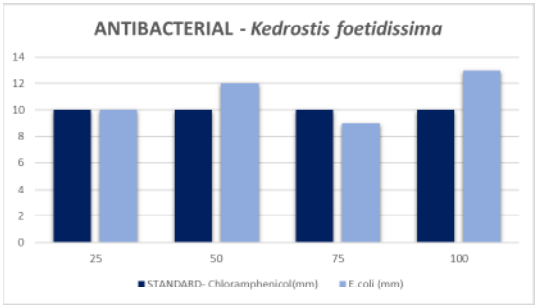

Figure 2 b: ***E.coli***

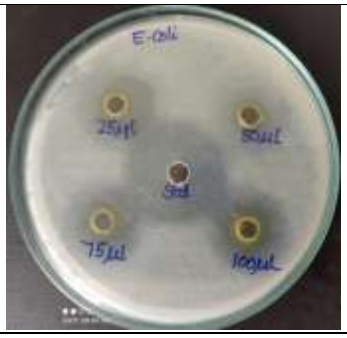

Figure 3: ***E.coli***

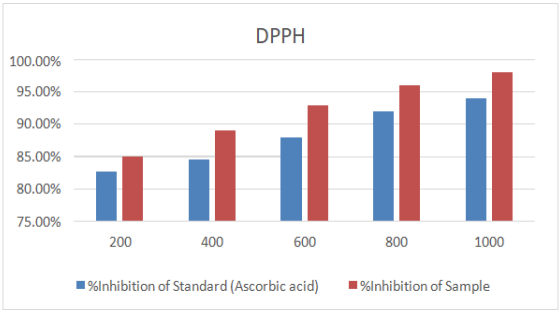

Fig.4.DPPH radical scavenging activity of Aqueous extract of ***Kedrostis***

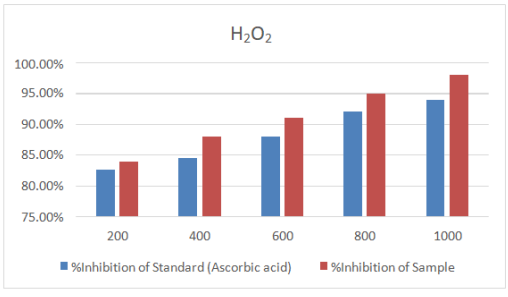

Figure 5. Hydrogen Peroxide Scavenging Activity of aqueous extract of ***Kedrostis foetidissima***

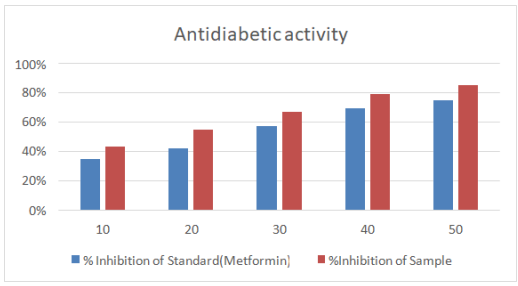

Figure 6. Inhibition of α-amylase Activity of aqueous extract of ***Kedrostis foetidissima***

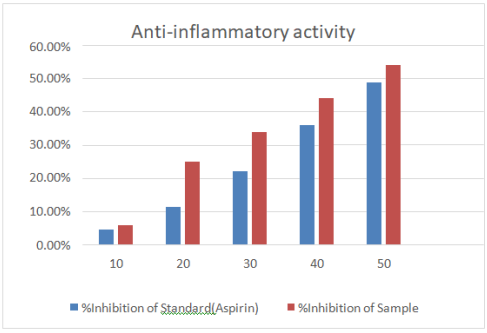

Figure 7. Albumin Denaturation Assay of aqueous extract of *Kedrostis foetidissima*

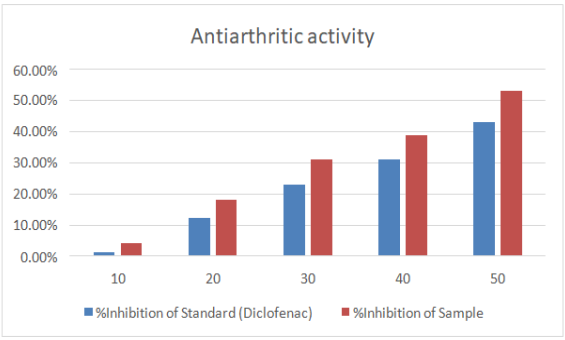

Figure 8. Protein Denaturation Assay of aqueous extract of *Kedrostis foetidissima*

Indian Journal of Natural Sciences *www.tnsroindia.org.in ©IJONS*

Vol.15 / Issue 83 / Apr / 2024 *International Bimonthly (Print) – Open Access* *ISSN: 0976 – 0997*

RESEARCH ARTICLE

The Lattice of Convex Sublattices of $S(B_n \times C_m)$

Aaswin J[1]* and Vethamanickam A[2]

[1]Research Scholar, (Reg. No.19211172092013), Rani Anna Government College for Women, (Affiliated to ManonmaniamSundaranar University), Abishekapatti, Tirunelveli, Tamil Nadu, India
[2]Former Associate Professor, Rani Anna Government College for Women, Tirunelveli, Tamil Nadu, India

Received: 22 Feb 2024 Revised: 06 Mar 2024 Accepted: 20 Mar 2024

***Address for Correspondence**
Aaswin J
Research Scholar,
(Reg. No.19211172092013),
Rani Anna Government College for Women,
(Affiliated to ManonmaniamSundaranar University),
Abishekapatti, Tirunelveli, Tamil Nadu, India.
Email: aaswinj1996@gmail.com

ABSTRACT

In this paper, we prove that the lattice of convex sublattices of $S(B_n \times C_m)$ is an Eulerian lattice under the set inclusion relation which is neither simplicial nor dual simplicial, if $n, m > 1$.

Keywords: Convex sublattice; SimplicialEulerian lattice; Dual simplicial.

INTRODUCTION

The study of lattice of convex sublattices of a lattice was started by K.M.Koh, in the year 1972. He had investigated the internal structure of a lattice L, in relation to $CS(L)$, like so many other authors for various algebraic structures such as groups, Boolean algebras, derived graphs and so on.

A new Eulerian Lattice $S(L) \cong (\overline{B_2} \times \overline{L}) \vee (1,1)$ was formed from a given Eulerian Lattice L by V.K.Santhi in her thesis in the year 1992. Subbarayan. R and Vethamanickam. A have proved that $CS(B_n)$, the lattice of convex sublattices of a Boolean Algebra $B_n$of rank n, with respect to set inclusion relation, is a dual simplicialEulerian Lattice. Subsequently, Sheeba MerlinG and VethamanickamA have proved in their paper that $CS(S(B_n)$ is an Eulerian Lattice under the set inclusion relation which is neither simplicial nor dual simplicial.

A natural question is what would happen if we attempt it for non-Boolean Eulerian lattice. Though for a general non-Boolean Eulerian lattice it may seem to be difficult, we attempt it for the non-Boolean Eulerian lattice $B_n \times C_m$in this paper. we prove here that $S(B_n \times C_m)$is Eulerian which is neither simplicial nor dual simplicial.

In this paper, we are going to look at the structure of $CS(S(B_n \times C_m))$. and prove it to be Eulerian under ′⊆ ′relation.$S(B_1 \times C_4)$is shown in figure.

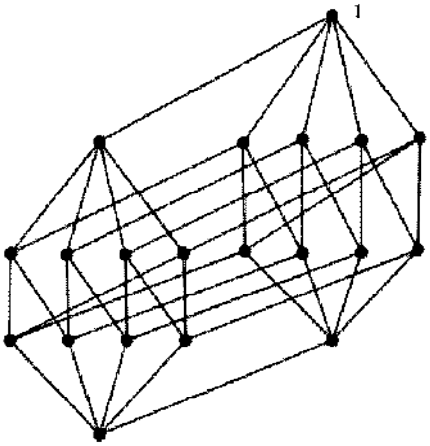

The Eulerian property of the lattice $CS(S(B_n \times C_m))$

Lemma 2.1. For $n \geq 1$, we have$1 + m + \binom{n}{1} + 2 + \binom{n}{2} + \binom{n}{1}m + 2\left[m + \binom{n}{1}\right] + \binom{n}{3} + \binom{n}{2}m + \binom{n}{1}m + 1 + 2\left[\binom{n}{2} + \binom{n}{1}m + m\right] + \binom{n}{4} + \binom{n}{3}m + \binom{n}{2}m + \binom{n}{1} + 2\left[\binom{n}{3} + \binom{n}{2}m + \binom{n}{1}m + \binom{n}{1}\right] + \cdots + \binom{n}{n} + \binom{n}{n-1}m + \binom{n}{n-2}m + \binom{n}{n-3} + 2\left[\binom{n}{n-1} + \binom{n}{n-2}m + \binom{n}{n-3}m + \binom{n}{n-4}\right] + m + \binom{n}{n-1}m + \binom{n}{n-2} + 2\left[2\binom{n}{n} + \binom{n}{n-1}m + \binom{n}{n-2}m + \binom{n}{n-3}\right] + m + \binom{n}{n-1} + 2\left[m + \binom{n}{n-1}m + \binom{n}{n-2}\right] + 2\left[m + \binom{n}{n-1}\right] + 1 = 6.2^n(m+1)$.

Theorem 2.2.$CS(S(B_n \times C_m))$, the lattice of convex sublattices of $S(B_n \times C_m)$ with respect to set inclusion is an Eulerian lattice.

Proof.

We first note that, the number of elements of ranks 0,1,2,…,and $n+3$ in$B_n \times C_m$are respectively, $1, m + \binom{n}{1}, \binom{n}{2} + \binom{n}{1}m + m, \binom{n}{3} + \binom{n}{2}m + \binom{n}{1}m + 1, \binom{n}{4} + \binom{n}{3}m + \binom{n}{2}m + \binom{n}{1}, \ldots, \binom{n}{n} + \binom{n}{n-1}m + \binom{n}{n-2}m + \binom{n}{n-3}, m + \binom{n}{n-1}m + \binom{n}{n-2}, m + \binom{n}{n-1}, and\ 1$.

The number of elements of ranks 0,1,2,…,and $n+4$ in $S(B_n \times C_m)$ are respectively,$1, m + \binom{n}{1} + 2, \binom{n}{2} + \binom{n}{1}m + 2\left[m + \binom{n}{1}\right], \binom{n}{3} + \binom{n}{2}m + \binom{n}{1}m + 1 + 2\left[\binom{n}{2} + \binom{n}{1}m + m\right], \binom{n}{4} + \binom{n}{3}m + \binom{n}{2}m + \binom{n}{1} + 2\left[\binom{n}{3} + \binom{n}{2}m + \binom{n}{1}m + \binom{n}{1}\right], \ldots, \binom{n}{n} + \binom{n}{n-1}m + \binom{n}{n-2}m + \binom{n}{n-3} + 2\left[\binom{n}{n-1} + \binom{n}{n-2}m + \binom{n}{n-3}m + \binom{n}{n-4}\right], m + \binom{n}{n-1}m + \binom{n}{n-2} + 2\left[2\binom{n}{n} + \binom{n}{n-1}m + \binom{n}{n-2}m + \binom{n}{n-3}\right], m + \binom{n}{n-1} + 2\left[m + \binom{n}{n-1}m + \binom{n}{n-2}\right], 2\left[m + \binom{n}{n-1}\right], and\ 1$

It is clear that the rank of $CS(S(B_n \times C_m))$ is $n+5$. We are going to prove that $CS(S(B_n \times C_m))$ is Eulerian.

That is, to prove that the interval $[\phi, S(B_n \times C_m)]$ in $CS(S(B_n \times C_m))$ has the same number of elements of odd and even rank.

Let A_i be the number of elements of rank $i$in $CS(S(B_n \times C_m))$, $i = 1,2,\ldots,n+4$.

We note that when n is even then $r[CS(S(B_n \times C_m))] = n+5$ is odd and if n is odd then $r[CS(S(B_n \times C_m))] = n+5$ is even.Therefore, we prove that $A_1 - A_2 + A_3 - \ldots + A_{n+1} - A_{n+2} + A_{n+3} - A_{n+4} = 0$, if $n$is even.

$A_1 - A_2 + A_3 - \ldots - A_{n+1} + A_{n+2} - A_{n+3} + A_{n+4} = 2$, if n is odd.

Since the elements of rank 1 in $CS(S(B_n \times C_m))$ are just the singleton subsets of $S(B_n \times C_m)$, we have $A_1 = 1 + m + \binom{n}{1} + 2 + \binom{n}{2} + \binom{n}{1}m + 2\left[m + \binom{n}{1}\right] + \binom{n}{3} + \binom{n}{2}m + \binom{n}{1}m + 1 + 2\left[\binom{n}{2} + \binom{n}{1}m + m\right] + \binom{n}{4} + \binom{n}{3}m + \binom{n}{2}m + \binom{n}{1} +$

$2[\binom{n}{3}+\binom{n}{2}m+\binom{n}{1}m+\binom{n}{1}]+\cdots+\binom{n}{n}+\binom{n}{n-1}m+\binom{n}{n-2}m+\binom{n}{n-3}+2[\binom{n}{n-1}+\binom{n}{n-2}m+\binom{n}{n-3}m+\binom{n}{n-4}]+m+\binom{n}{n-1}m+\binom{n}{n-2}+2[2\binom{n}{n}+\binom{n}{n-1}m+\binom{n}{n-2}m+\binom{n}{n-3}]+m+\binom{n}{n-1}+2[m+\binom{n}{n-1}m+\binom{n}{n-2}]+2[m+\binom{n}{n-1}]+1.$
…….(2.1)
To find A_2:

The elements of rank two in the interval $[\phi, S(B_n \times C_m)]$ are the two element chains or edges in $S(B_n \times C_m)$.
We have to determine the total number of two element chains in $S(B_n \times C_m)$,

We observe that,
A_2 = The number of edges (containing 0 + containing an atom+ containing a rank 2 element+…+ containing a rank $n+3$ element at the bottom) in $S(B_n \times C_m)$
Since, there are $m+\binom{n}{1}+2$ atoms in $S(B_n \times C_m)$, the number of edges containing 0 in $S(B_n \times C_m)$is$m+\binom{n}{1}+2$.
Next, we find the number of edges containing an atom at the bottom.
Let x be an atom of $S(B_n \times C_m)$, let x be in the left copy of $S(B_n \times C_m)$,$[x,1] \cong B_n \times C_m$
therefore, the number of edges with x at the bottom is $m+\binom{n}{1}$ There are $m+\binom{n}{1}$ number of edges containing an atom at the bottom in the left copy of $S(B_n \times C_m)$. Similarly, x be in the right copy of $S(B_n \times C_m)$. The number of edges is $m+\binom{n}{1}$. Let x be in the middle copy of $S(B_n \times C_m)$, then it is of the form either $(a,0)$ or $(0,p)$ where a is an atom in B_n and p is an atom in C_m. Therefore,

$[x,1] \cong S(B_{n-1} \times C_m)$, if x is of the form $(a,0)$
$\cong S(B_{n+2})$, if$x$ is of theform $(0,p)$

If $[x,1] \cong S(B_{n-1} \times C_m)$, then the number of edges with x at the bottom is $m+\binom{n-1}{1}+2$. There are $\binom{n}{1}$such x's.Therefore, the total number of such edges is $\binom{n}{1}[m+\binom{n-1}{1}+2]$.
If $[x,1] \cong S(B_{n+2})$, then, the number of edges with x at the bottom is $2+\binom{n+2}{1}$.There are m such x's. Therefore, the total number of edges is $m[2+\binom{n+2}{1}]$. Hence the total number of edges from an atom at the bottom is, $2[m+\binom{n}{1}]+\binom{n}{1}[m+\binom{n-1}{1}+2]+m[2+\binom{n+2}{1}]$

Next, we find the number of edges containing a rank 2 element at the bottom in $S(B_n \times C_m)$.Let x be in the left copy of $S(B_n \times C_m)$. Therefore,

$[x,1] \cong B_{n-1} \times C_m$, if $x=(a,0), a\ is\ an\ atom\ in\ B_n$
$\cong B_{n+2}$, if$x=(0,p), p\ is\ an\ atom\ in\ C_m$

If $[x,1] \cong B_{n-1} \times C_m$, the number of edges with such x at the bottom is $m+\binom{n-1}{1}$. There are $\binom{n}{1}$such x's.Therefore the total number of edges with x at the bottom is $\binom{n}{1}[m+\binom{n-1}{1}]$
If $[x,1] \cong B_{n+2}$,the number of edges from $x$is $\binom{n+2}{1}$, there are m such x's.Therefore, the total number of edges in the left copy is $\binom{n}{1}[m+\binom{n-1}{1}]+m[\binom{n+2}{1}]$. Similarly, the number of edges in the right copy is $\binom{n}{1}[m+\binom{n-1}{1}]+m[\binom{n+2}{1}]$.
Let x be in the middle copy of $S(B_n \times C_m)$, then
$[x,1] \cong S(B_{n-2} \times C_m)$, if x=$(d,0)$
$\cong S(B_{n+1})$, if$x=(a,p)\ or\ (0,t)$

where d is a rank 2 element in B_n, p is a rank 1 element in C_m and t is a rank 2 element in C_m. If $[x,1] \cong S(B_{n-2} \times C_m)$, then the number of edges with such x at the bottom is $\binom{n-2}{1}+m+2$. There are$\binom{n}{2}$ such elements. Therefore, total number of edges is $\binom{n}{2}[\binom{n-2}{1}+m+2]$.If $[x,1] \cong S(B_{n+1})$,the number of edges with such x at the bottom is $\binom{n+1}{1}+2$. There are $m+m\binom{n}{1}$such elements.Therefore, the total number of such edges is $(m+m\binom{n}{1})[\binom{n+1}{1}+2]$. Therefore, the total number of edges in the middle copy is,$\binom{n}{2}[\binom{n-2}{1}+m+2]+(m+m\binom{n}{1})[\binom{n+1}{1}+2]$.

Hence, the total number of edges from a rank 2 element at the bottom is, $2\{\binom{n}{1}[m+\binom{n-1}{1}]+m[\binom{n+2}{1}]\}+\binom{n}{2}[\binom{n-2}{1}+m+2]+(m+m\binom{n}{1})[\binom{n+1}{1}+2]$.

Next, we find the number of edges containing a rank 3 element at the bottom in $S(B_n \times C_m)$. Let x be an element of rank 3 in $S(B_n \times C_m)$. Let x be in the left copy of $S(B_n \times C_m)$, then

$[x,1] \cong B_{n-2} \times C_m$, if $x=(d,0), d \text{ is a rank 2 element in } B_n$

$\cong B_{n+1}$, if$x=(a,p) \text{ or } (0,t)$.

If $[x,1] \cong B_{n-2} \times C_m$, the number of edges with such an x at the bottom is $m+\binom{n-2}{1}$. There are $\binom{n}{2}$ such x's.Therefore, the total number of edges with such an x at the bottom is $\binom{n}{2}[m+\binom{n-2}{1}]$

If $[x,1] \cong B_{n+1}$, Then the number of edges from $x$is $\binom{n+1}{1}$, there are $m+m\binom{n}{1}$ such $x's$. The total number of edges in the left copy is $\binom{n}{2}[m+\binom{n-2}{1}]+\{m+m\binom{n}{1}\}[\binom{n+1}{1}]$. Similarly, the number of edges in right copy is $\binom{n}{2}[m+\binom{n-2}{1}]+\{m+m\binom{n}{1}\}[\binom{n+1}{1}]$.

Let $x$be in the middle copy of $S(B_n \times C_m)$, then

$[x,1] \cong S(B_{n-3} \times C_m)$, if x=$(b,0), b \text{ is a rank 3 element in } B_n$

$\cong S(B_n)$, if$x=(0,1) \text{ or } (a,t) \text{ or } (d,p)$

where a is an atom in B_n, t is a rank 2 element in C_m, p is a rank 1 element in $C_m$and d is a rank 2 element in B_n.

If$[x,1] \cong S(B_{n-3} \times C_m)$, the number of edges with such x at the bottom is $\binom{n-3}{1}+m+2$. There are $\binom{n}{3}$ such elements.Therefore, total number of edges is $\binom{n}{3}[\binom{n-3}{1}+m+2]$.

If $[x,1] \cong S(B_n)$,the number of edges with such x at the bottom is $\binom{n}{1}+2$. There are $m\binom{n}{2}+m\binom{n}{1}+1$ such elements.Therefore, total number of edges is $(m\binom{n}{2}+m\binom{n}{1}+1\binom{n}{1}+2]$.Therefore, the total number of edges in the middle copy is,$\binom{n}{3}[\binom{n-3}{1}+m+2]+(m\binom{n}{2}+m\binom{n}{1}+1\binom{n}{1}+2]$.

Hence, the total number of edges from a rank 3 element at the bottom is, $2\{\binom{n}{2}[m+\binom{n-2}{1}]+\{m+m\binom{n}{1}\}[\binom{n+1}{1}]\}+\binom{n}{3}[\binom{n-3}{1}+m+2]+(m\binom{n}{2}+m\binom{n}{1}+1\binom{n}{1}+2]$.

Proceeding like this we get, the total number of edges from a rank $(n+3)$ element as the bottom is equal to the number of coatoms in $S(B_n \times C_m)$, that is$2[m+\binom{n}{n-1}]$

Therefore, the total number of edges in $S(B_n \times C_m)$is,$A_2=m+\binom{n}{1}+2+2[m+\binom{n}{1}]+\binom{n}{1}[m+\binom{n-1}{1}+2]+m[2+\binom{n+2}{1}]+2\{\binom{n}{1}[m+\binom{n-1}{1}]+m[\binom{n+2}{1}]\}+\binom{n}{2}[\binom{n-2}{1}+m+2]+(m+m\binom{n}{1})[\binom{n+1}{1}+2]+2\{\binom{n}{2}[m+\binom{n-2}{1}]+(m+\binom{n}{1}m)[\binom{n+1}{1}]\}+\binom{n}{3}[\binom{n-3}{1}+m+2]+(1+m\binom{n}{1}+m\binom{n}{2})[\binom{n}{1}+2]+\ldots+2[m+\binom{n}{n-1}]$. ……(2.2)

To find A_3: A rank three element in $CS(S(B_n \times C_m))$ is a sublattice $B_2$of $S(B_n \times C_m)$.

A_3 = Number of B_2's in $CS(S(B_n \times C_m))$ [containing 0 +containing an atom+containing a rank 2 element+…+containing a rank $(n+2)$ element]at the bottom

A sublatticeB_2conatining 0 at the bottom has a rank 2 element at the top.Therefore, the number of B_2's with 0 at the bottom is$\binom{n}{2}+\binom{n}{1}m+m+2[m+\binom{n}{1}]$, since the number of rank 2 elements is $\binom{n}{2}+\binom{n}{1}m+m+2[m+\binom{n}{1}]$. A sublattice B_2containing an atom as the bottom element must have a rank 3 element as the top element.

Let x be an atom in the left copy.$[x,1] \cong S(B_n \times C_m)$, the number of B_2's with 0 at the bottom is $\binom{n}{2}+\binom{n}{1}m+m$. Similarly, Let x be an atom in the right copy, the number of B_2's with 0 at the bottom is $\binom{n}{2}+\binom{n}{1}m+m$. Let x be an atom in the middle copy. As in the previous arguments there are two possibilities.Therefore,

$[x,1] \cong S(B_{n-1} \times C_m)$, if x is of the form $(a,0)$

$\cong S(B_{n+2})$, if$x$ is of theform $(0,p)$

Fix such an element x.If$[x,1] \cong S(B_{n-1} \times C_m)$, the number of B_2's with x at the bottom is $\binom{n-1}{2}+\binom{n-1}{1}m+m+2[m+\binom{n-1}{1}]$. There are $\binom{n}{1}$such x's. Total number of B_2's containing such x is $\binom{n}{1}[\binom{n-1}{2}+\binom{n-1}{1}m+m+2[m+\binom{n-1}{1}]]$.

If $[x,1] \cong S(B_{n+2})$, therefore, the number of B_2's with x at the bottom is $2\binom{n+2}{1}+\binom{n+2}{2}$. There are m such x's.Total number of B_2's containing such an x at the bottom is $m[2\binom{n+2}{1}+\binom{n+2}{2}]$. Hence the total number of B_2's containing an atom at the bottom is,$2\{\binom{n}{2}+\binom{n}{1}m+m\}+\binom{n}{1}[\binom{n-1}{2}+\binom{n-1}{1}m+m+2[m+\binom{n-1}{1}]]+m[2\binom{n+2}{1}+\binom{n+2}{2}]$

Next, we find the number of B_2's containing a rank 2 element at the bottom in $S(B_n \times C_m)$.Let x be in the left copy of $S(B_n \times C_m)$,there are two possibilities.

$[x,1] \cong B_{n-1} \times C_m$, if $x=(a,0), a \text{ is an atom in } B_n$

$\cong B_{n+2}$, if$x = (0,p), p\ is\ an\ atom\ in\ C_m$

If $[x,1] \cong B_{n-1} \times C_m$, the number of B_2's with such x at the bottom is$\binom{n-1}{2} + \binom{n-1}{1}m + m$. There are $\binom{n}{1}$such x's.Therefore the total number of edges with x at the bottom is $\binom{n}{1}\{\binom{n-1}{2} + \binom{n-1}{1}m + m\}$

If $[x,1] \cong B_{n+2}$, The number of B_2's containing a typical x is $\binom{n+2}{2}$, there are m such x's. The total number of B_2's in the left copy is$\binom{n}{1}\{\binom{n-1}{2} + \binom{n-1}{1}m + m\} + m[\binom{n+2}{2}]$. Similarly, the total number of B_2's in the right copy is$\binom{n}{1}\{\binom{n-1}{2} + \binom{n-1}{1}m + m\} + m[\binom{n+2}{2}]$.

Now, let x be in the middle copy of $S(B_n \times C_m)$,$[x,1] \cong S(B_{n-2} \times C_m)$, if x=$(d,0)$
$\cong S(B_{n+1})$, if$x = (a,p)\ or\ (0,t)$

where x isofthe form$(d,o)$where$d$ is a rank 2 element in B_n, p is a rank 1 element in C_m and t is a rank 2 element in C_m. If $[x,1] \cong S(B_{n-2} \times C_m)$, the number of B_2's with such x at the bottom is $\binom{n-2}{2} + \binom{n-2}{1}m + m + 2[m + \binom{n-2}{1}]$. There are $\binom{n}{2}$ such elements.Therefore, total number of B_2's is $\binom{n}{2}\binom{n-2}{2} + \binom{n-2}{1}m + m + 2[m + \binom{n-2}{1}]\}$.

If $[x,1] \cong S(B_{n+1})$,the number of B_2's with such x at the bottom is $2\binom{n+1}{1} + \binom{n+1}{2}$. There are $m + m\binom{n}{1}$such elements.Therefore, total number of B_2's is $(m + m\binom{n}{1})[2\binom{n+1}{1} + \binom{n+1}{2}]$. Then, the total number of B_2's in the middle copy is,$\binom{n}{2}\{\binom{n-2}{2} + \binom{n-2}{1}m + m + 2[m + \binom{n-2}{1}]\} + (m + m\binom{n}{1})[2\binom{n+1}{1} + \binom{n+1}{2}]$.

Hence, the total number of B_2's from a rank 2 element at the bottom is, $2\{\binom{n}{1}\{\binom{n-1}{2} + \binom{n-1}{1}m + m\} + \binom{n}{2}\{\binom{n-2}{2} + \binom{n-2}{1}m + m + 2[m + \binom{n-2}{1}\} + (m + m\binom{n}{1})[2\binom{n+1}{1} + \binom{n+1}{2}]$.

In the same manner we get the total number of B_2'sfrom a rank 3 element at the bottom is$2\binom{n}{2}\left[\binom{n-2}{2} + \binom{n-2}{1}m + m\right] + \left(m + m\binom{n}{1}\right)\left[\binom{n+1}{2}\right] + \binom{n}{3}\binom{n-3}{2} + \binom{n-3}{1}m + m + 2\left[m + \binom{n-3}{1}\right] + \left(m\binom{n}{2} + m\binom{n}{1} + 1\right)\left[2\binom{n}{1} + \binom{n}{2}\right]$.

Proceeding like this we get, the total number of B_2'sfrom a rank $(n+2)$ element as the bottom in $S(B_n \times C_m)$is$m + \binom{n}{n-1} + 2[m + \binom{n}{n-1}m + \binom{n}{n-2}]$.

Therefore, from the total number of B_2's in $S(B_n \times C_m)$ is,$A_3 = \binom{n}{2} + \binom{n}{1}m + m + 2[m + \binom{n}{1}] + 2\{\binom{n}{2} + \binom{n}{1}m + m\} + \binom{n}{1}[\binom{n-1}{2} + \binom{n-1}{1}m + m + 2[m + \binom{n-1}{1}]] + m[2\binom{n+2}{1} + \binom{n+2}{2}] + 2\{\binom{n}{1}\{\binom{n-1}{2} + \binom{n-1}{1}m + m\binom{n+2}{2}\} + \binom{n}{2}\{\binom{n-2}{2} + \binom{n-2}{1}m + m + 2[m + \binom{n-2}{1}]\} + (m + m\binom{n}{1})[2\binom{n+1}{1} + \binom{n+1}{2}] + 2\{\binom{n}{2}[\binom{n-2}{2} + \binom{n-2}{1}m + m] + (m + m\binom{n}{1})[\binom{n+1}{2}]\} + \binom{n}{3}\{\binom{n-3}{2} + \binom{n-3}{1}m + m + 2[m + \binom{n-3}{1}]\} + (m\binom{n}{2} + m\binom{n}{1} + 1)[2\binom{n}{1} + \binom{n}{2}] + \ldots + m\binom{n}{n-1} + 2[m + \binom{n}{n-1}m + \binom{n}{n-2}]$.
…….(2.3)

To find A_4: The number of rank three convex sublattices of $S(B_n \times C_m)$
A_4= Number of rank 3 convex sublattices in $CS(S(B_n \times C_m))$[containing 0 +containing an atom+containing a rank 2 element+ $\cdots$ +containing a rank $(n+1)$ element]at the bottom

By the previous way of proof, we get the total number of rank 3 convex sublattices in $S(B_n \times C_m)$is,$A_4 = \binom{n}{3} + \binom{n}{2}m + \binom{n}{1}m + 1 + 2[\binom{n}{2} + \binom{n}{1}m + m] + 2[\binom{n}{3} + \binom{n}{2}m + \binom{n}{1}m + 1] + \binom{n}{1}[\binom{n-1}{3} + \binom{n-1}{2}m + \binom{n-1}{1}m + 1 + 2[\binom{n-1}{2} + \binom{n-1}{1}m + m]] + m[2\binom{n+2}{2} + \binom{n+2}{3}] + 2\{\binom{n}{1}\{\binom{n-1}{3} + \binom{n-1}{2}m + \binom{n-1}{1}m + 1\} + m[\binom{n+2}{3}]\} + \binom{n}{2}\}\{\binom{n-2}{3} + \binom{n-2}{2}m + \binom{n-2}{1}m + 1 + 2[\binom{n-2}{2} + \binom{n-2}{1}m + m]\} + (m + m\binom{n}{1})[2\binom{n+1}{2} + \binom{n+1}{3}] + 2\{\binom{n}{2}[\binom{n-2}{3} + \binom{n-2}{2}m + \binom{n-2}{1}m + 1] + (m + m\binom{n}{1})[\binom{n+1}{3}]\} + \binom{n}{3}\{\binom{n-3}{3}\} + \binom{n-3}{2}m + \binom{n-3}{1}m + 1 + 2[\binom{n-3}{2} + \binom{n-3}{1}m + m]\} + (m\binom{n}{2} + m\binom{n}{1} + 1)[2\binom{n}{2} + \binom{n}{3}] + \cdots + m + \binom{n}{n-1}m + \binom{n}{n-2} + 2[1 + \binom{n}{n-1}m + \binom{n}{n-2}m + \binom{n}{n-3}]$. …….(2.4)

Proceeding like this,

To find A_{n+1}: The number of rank n convex sublattices of $S(B_n \times C_m)$.
A_{n+1} = Number of rank n convex sublattices in $CS(S(B_n \times C_m))$[containing 0 +containing an atom+containing a rank 2 element+ $\cdots$ +containing a rank 4 element]at the bottom

By the previous way of proof, we get the total number of rank n convex sublattices in $S(B_n \times C_m)$ is,

$$A_{n+1} = 1 + \binom{n}{n-1}m + \binom{n}{n-2}m + \binom{n}{n-3} + 2[\binom{n}{n-1} + \binom{n}{n-2}m + \binom{n}{n-3}m + \binom{n}{n-4}] + 2[1 + \binom{n}{n-1}m + \binom{n}{n-2}m + \binom{n}{n-3}] + \binom{n}{1}[m + \binom{n-1}{n-2}m + \binom{n-1}{n-3} + 2[1 + \binom{n-1}{n-2}m + \binom{n-1}{n-3}m + \binom{n-1}{n-4}]] + m[2\binom{n+2}{n-1} + 2\{\binom{n}{1}\{m + \binom{n-1}{n-2}m + \binom{n-1}{n-3}\} + m[\binom{n+2}{n}]\} + \binom{n}{2}\{m + \binom{n-2}{n-3} + 2[m + \binom{n-2}{n-3}m + \binom{n-2}{n-4}]\} + (m + m\binom{n}{1})[2\binom{n+1}{n-1}] + 2\{\binom{n}{2}[m + \binom{n-2}{n-3}] + (m + m\binom{n}{1})[\binom{n+1}{n}]\} + \binom{n}{3}\{1 + 2[m + \binom{n-3}{n-4}]\} + (m\binom{n}{2} + m\binom{n}{1} + 1)[2\binom{n}{n-1}] + \binom{n}{4} + \binom{n}{3}m + \binom{n}{2}m + \binom{n}{1} + 2[\binom{n}{3} + \binom{n}{2}m + \binom{n}{1}m + 1$. …….(2.5)

To find A_{n+2}= The number of rank $n+1$ convex sublattices of $S(B_n \times C_m)$.
A_{n+2} = Number of rank $n+1$ convex sublattices in $CS(S(B_n \times C_m))$[containing 0 +containing an atom+containing a rank 2 element+containing a rank 3 element]at the bottom

The total number of rank $n+1$ convex sublattices in $S(B_n \times C_m)$is,$A_{n+2} = m + \binom{n}{n-1}m + \binom{n}{n-2}m + 2[1 + \binom{n}{n-1}m + \binom{n}{n-2}m + \binom{n}{n-3}] + 2[m + \binom{n}{n-1}m + \binom{n}{n-2}] + \binom{n}{1}[m + m + \binom{n-1}{n-2} + 2[m + \binom{n-1}{n-2}m + \binom{n-1}{n-3}] + m[2\binom{n+2}{n+1} + \binom{n+2}{n-1}] + 2\{\binom{n}{1}\{m + \binom{n-1}{n-2}\} + m[\binom{n+2}{n+1}]\} + \binom{n}{2}\{m + 1 + 2[m + \binom{n-2}{n-3}]\} + (m + m\binom{n}{1})[2\binom{n+1}{n}] + \binom{n}{3} + \binom{n}{2}m + \binom{n}{1}m + 1 + 2[\binom{n}{2} + \binom{n}{1}m + m]$. ……..(2.6)

The total number of rank $n+2$ convex sublattices in $S(B_n \times C_m)$is,$A_{n+3} = m + \binom{n}{n-1} + 2[m + \binom{n}{n-1}m + \binom{n}{n-2}] + 2[m + \binom{n}{n-1}] + \binom{n}{1}[m + 1 + 2[m + m + \binom{n-1}{n-2}] + m[2\binom{n+1}{n+2}] + \binom{n}{2} + \binom{n}{1}m + m + 2[m + \binom{n}{1}]$ ……(2.7)

And,the total number of rank $n+3$ convex sublattices in $S(B_n \times C_m)$is,$A_{n+3} = 2[m + \binom{n}{n-1}] + m + \binom{n}{1} + 2$

Case (i) When n is odd, $n+5$ is even, that is, rank of $CS(S(B_n \times C_m))$ is even.

$$A_1 - A_2 + A_3 - \cdots - A_{n+1} + A_{n+2} - A_{n+3} + A_{n+4} = 1 + m + \binom{n}{1} + 2 + \binom{n}{2} + \binom{n}{1}m + 2[m + \binom{n}{1}] + \binom{n}{3} + \binom{n}{2}m + \binom{n}{1}m + 1 + 2[\binom{n}{2} + \binom{n}{1}m + m] + \binom{n}{4} + \binom{n}{3}m + \binom{n}{2}m + \binom{n}{1} + 2[\binom{n}{3} + \binom{n}{2}m + \binom{n}{1}m + \binom{n}{1}] + \cdots + \binom{n}{n} + \binom{n}{n-1}m + \binom{n}{n-2}m + \binom{n}{n-3} + 2[\binom{n}{n-1} + \binom{n}{n-2}m + \binom{n}{n-3}m + \binom{n}{n-4}] + m + \binom{n}{n-1}m + \binom{n}{n-2} + 2[2\binom{n}{n} + \binom{n}{n-1}m + \binom{n}{n-2}m + \binom{n}{n-3}] + m + \binom{n}{n-1} + 2[m + \binom{n}{n-1}m + \binom{n}{n-2}] + 2[m + \binom{n}{n-1}] + 1 - m + \binom{n}{1} + 2 + 2[m + \binom{n}{1}] + \binom{n}{1}[m + \binom{n-1}{1} + 2] + m[2 + \binom{n+2}{1}] + 2\{\binom{n}{1}[m + \binom{n-1}{1}] + m[\binom{n+2}{1}]\} + \binom{n}{2}[\binom{n-2}{1} + m + 2] + \left(m + m\binom{n}{1}\right)[\binom{n+1}{1} + 2] + 2\left\{\binom{n}{2}[m + \binom{n-2}{1}] + (m + \binom{n}{1}m)[\binom{n+1}{1}\} + \binom{n}{3}[\binom{n-3}{1} + m + 2] + \left(1 + m\binom{n}{1} + m\binom{n}{2}\right)[\binom{n}{1} + 2] + \ldots + 2[m + \binom{n}{n-1}] + \binom{n}{2} + \binom{n}{1}m + m + 2[m + \binom{n}{1}] + 2\{\binom{n}{2} + \binom{n}{1}m + m\} + \binom{n}{1}\left[\binom{n-1}{2} + \binom{n-1}{1}m + m + 2[m + \binom{n-1}{1}]\right] + m[2\binom{n+2}{1} + \binom{n+2}{2}] + 2\left\{\binom{n}{1}\{\binom{n-1}{2} + \binom{n-1}{1}m + m\binom{n+2}{2}\} + \binom{n}{2}\{\binom{n-2}{2} + \binom{n-2}{1}m + m + 2[m + \binom{n-2}{1}]\} + \left(m + m\binom{n}{1}\right)[2\binom{n+1}{1} + \binom{n+1}{2}] + 2\left\{\binom{n}{2}[\binom{n-2}{2} + \binom{n-2}{1}m + m] + \left(m + m\binom{n}{1}\right)[\binom{n+1}{2}]\right\} + \binom{n}{3}\{\binom{n-3}{2} + \binom{n-3}{1}m + m + 2[m + \binom{n-3}{1}]\} + (m\binom{n}{2} + m\binom{n}{1} + 1)[2\binom{n}{1} + \binom{n}{2}] + \ldots + m\binom{n}{n-1} + 2[m + \binom{n}{n-1}m + \binom{n}{n-2}] - \binom{n}{3} + \binom{n}{2}m + \binom{n}{1}m + 1 + 2[\binom{n}{2} + \binom{n}{1}m + m] + 2[\binom{n}{3} + \binom{n}{2}m + \binom{n}{1}m + 1] + \binom{n}{1}\left[\binom{n-1}{3} + \binom{n-1}{2}m + \binom{n-1}{1}m + 1 + 2[\binom{n-1}{2} + \binom{n-1}{1}m + m]\right] + m[2\binom{n+2}{2} + \binom{n+2}{3}] + 2\{\binom{n}{1}\{\binom{n-1}{3} + \binom{n-1}{2}m + \binom{n-1}{1}m + 1\} + m[\binom{n+2}{3}]\} + \binom{n}{2}\}\{\binom{n-2}{3} + \binom{n-2}{2}m + \binom{n-2}{1}m + 1 + 2[\binom{n-2}{2} + \binom{n-2}{1}m + m]\} + \left(m + m\binom{n}{1}\right)[2\binom{n+1}{2} + \binom{n+1}{3}] + 2\left\{\binom{n}{2}[\binom{n-2}{3} + \binom{n-2}{2}m + \binom{n-2}{1}m + 1] + \left(m + m\binom{n}{1}\right)[\binom{n+1}{3}]\right\} + \binom{n}{3}\{\binom{n-3}{3}\} + \binom{n-3}{2}m + \binom{n-3}{1}m + 1 + 2[\binom{n-3}{2} + \binom{n-3}{1}m + m]\} + (m\binom{n}{2} + m\binom{n}{1} + 1)[2\binom{n}{2} + \binom{n}{3}] + \cdots + m + \binom{n}{n-1}m + \binom{n}{n-2} + 2[1 + \binom{n}{n-1}m + \binom{n}{n-2}m + \binom{n}{n-3}] + \cdots - 1 + \binom{n}{n-1}m + \binom{n}{n-2}m + \binom{n}{n-3} + 2[\binom{n}{n-1} + \binom{n}{n-2}m + \binom{n}{n-3}m + \binom{n}{n-4}] + 2[1 + \binom{n}{n-1}m + \binom{n}{n-2}m + \binom{n}{n-3}] + \binom{n}{1}[m + \binom{n-1}{n-2}m + \binom{n-1}{n-3} + 2[1 + \binom{n-1}{n-2}m + \binom{n-1}{n-3}m + \binom{n-1}{n-4}]] + m[2\binom{n+2}{n-1} + 2\{\binom{n}{1}\{m + \binom{n-1}{n-2}m + \binom{n-1}{n-3}\} + m[\binom{n+2}{n}]\} + \binom{n}{2}\{m + \binom{n-2}{n-3} + 2[m + \binom{n-2}{n-3}m + \binom{n-2}{n-4}]\} + (m + m\binom{n}{1})[2\binom{n+1}{n-1}] + 2\{\binom{n}{2}[m + \binom{n-2}{n-3}] + (m + m\binom{n}{1})[\binom{n+1}{n}]\} + \binom{n}{3}\{1 + 2[m + \binom{n-3}{n-4}]\} + (m\binom{n}{2} + m\binom{n}{1} + 1)[2\binom{n}{n-1}] + \binom{n}{4} + \binom{n}{3}m + \binom{n}{2}m + \binom{n}{1} + 2[\binom{n}{3} + \binom{n}{2}m + \binom{n}{1}m + 1 + m + \binom{n}{n-1}m + \binom{n}{n-2}m + 2[1 + \binom{n}{n-1}m + \binom{n}{n-2}m + \binom{n}{n-3}] + 2[m + \binom{n}{n-1}m + \binom{n}{n-2}] + \binom{n}{1}[m + m + \binom{n-1}{n-2} + 2[m + \binom{n-1}{n-2}m + \binom{n-1}{n-3}] + m[2\binom{n+2}{n+1} + \binom{n+2}{n-1}] + 2\{\binom{n}{1}\{m + \binom{n-1}{n-2}\} + m[\binom{n+2}{n+1}]\} + \binom{n}{2}\{m + 1 + 2[m + \binom{n-2}{n-3}]\} + \left(m + m\binom{n}{1}\right)[2\binom{n+1}{n}] + \binom{n}{3} + \binom{n}{2}m + \binom{n}{1}m + 1 + 2[\binom{n}{2} + \binom{n}{1}m + m] - m + \binom{n}{n-1} + 2[m + \binom{n}{n-1}m + \binom{n}{n-2}] + 2[m + \binom{n}{n-1}] + \binom{n}{1}[m + 1 + 2[m + m + \binom{n-1}{n-2}] + m[2\binom{n+1}{n+2}] + \binom{n}{2} + \binom{n}{1}m + m + 2[m + \binom{n}{1}] + 2[m + \binom{n}{n-1}] + m + \binom{n}{1} + 2 = 0.$$

Case (ii) When n is even, $n+5$ is odd, that is, rank of $CS(S(B_n \times C_m))$is odd.

$$A_1 - A_2 + A_3 - \cdots + A_{n+1} - A_{n+2} + A_{n+3} - A_{n+4} = 2.$$

Hence the interval $[\phi, S(B_n \times C_m)]$ has the same number of elements of odd and even rank.

Though in the above theorem we have proved that $CS(S(B_n \times C_m))$is Eulerian, it is neither simplicial nor dual simplicial.

$CS(S(B_n \times C_m))$is not dual simplicial since, the upper interval $[\{1\}, S(B_n \times C_m)]$in $CS(S(B_n \times C_m))$contains $m + \binom{n}{n-1}$ number of atoms which is greater than $n+5$, the rank of $[\{1\}, S(B_n \times C_m)]$,implying that $[\{1\}, S(B_n \times C_m)]$is not Boolean.

$CS(S(B_n \times C_m))$ is not simplicial since, the lower interval $[\phi, [l_1, 1]]$ where l_1 is the left extreme atom of $S(B_n \times C_m)$ contains $6.2^n(m+1)$number of atoms by Lemma 2.1, which cannot be equal to $n+5$, the rank of $[\phi, [l_1, 1]]$, implying that $[\phi, [l_1, 1]]$ is not Boolean.

CONCLUSION

In this paper, we have proved that $CS[S(B_n \times C_m)]$ is an Eulerian lattice under the set inclusionrelation which is neither simplicial nor dual simplicial, if $n > 1$.

REFERENCES

1. Chen C. K., Koh K. M., *On the lattice of convex sublattices of a finite lattice*, Nanta Math., 5 (1972), 92-95.
2. Gratzer G., *General Lattice Theory*,BirkhauserVerlag, Basel, 1978.
3. Koh K. M., *On the lattice of convex sublattices of a finite lattice*, Nanta Math., 5 (1972), 18-37.
4. Lavanya S., ParameshwaraBhatta S., *A new approach to the lattice of convex sublattices of a lattice, Algebra* Univ., 35 (1996), 63-71.
5. Paffenholz A., *Constructions for Posets, Lattices and Polytopes, Doctoral Dissertation*, School of Mathematics and Natural Sciences, Technical University of Berlin,(2005).
6. RamanaMurty P. V., *On the lattice of convex sublattices of a lattice*, Southeast Asian Bulletin of Mathematics, 26 (2002), 51-55.
7. Rota G. C., *On the foundations of Combinatorial theory I*, Theory of Mobius functions, Z. Wahrschainlichkeitstheorie, 2 (1964), 340-368.
8. Sheeba Merlin and Vethamanickam. A., *On the Lattice of Convex Sublattices of S(Bn) and S(Cn)*, European journal of pure and applied Mathematics., Vol. 10, No. 4, 2017, 916-928.
9. Stanley R.P., *Some aspects of groups acting on finite posets*, J. Combinatoria theory, A. 32 (1982), 131-161.
10. Stanley R.P., *A survey of Eulerianposets, Polytops: abstract, convex and computational*, Kluwer Acad. Publi., Dordrecht, (1994), 301-333.
11. Stanley R.P., *Enumerative Combinatorics*, Woods worth and Brooks, Cole, Vol 1, 1986.
12. Santhi V. K., *Topics in Commutative Algebra, Ph*. D thesis, Madurai Kamaraj University, 1992.
13. Vethamanickam A., *Topics in Universal Algebra*, Ph. D thesis, Madurai Kamaraj University, 1994.
14. Vethamanickam A., Subbarayan R., *Some simple extensions of Eulerian lattices*, Acta Math. Univ., Comenianae, 79(1) (2010), 47-54.
15. Vethamanickam A., Subbarayan R., *On the lattice of convex sublattices*, Elixir Dis.Math., Comenianae, 50 (2012), 10471-10474.

Indian Journal of Natural Sciences *www.tnsroindia.org.in ©IJONS*

Vol.15 / Issue 83 / Apr / 2024 *International Bimonthly (Print) – Open Access* *ISSN: 0976 – 0997*

RESEARCH ARTICLE

Mathematical Modeling of Avian Influenza Transmission Dynamics and its Stability Analysis: A Pandemic Awareness

A. Joshua Cyril Yagan* and D. Jasmine

Department of Mathematics, Bishop Heber College (Autonomous), (Affiliated to Bharathidasan University, Tiruchirappalli), Tamil Nadu, India.

Received: 22 Feb 2024 Revised: 06 Mar 2024 Accepted: 20 Mar 2024

***Address for Correspondence**
A. Joshua Cyril Yagan
Department of Mathematics,
Bishop Heber College (Autonomous),
(Affiliated to Bharathidasan University, Tiruchirappalli),
Tamil Nadu, India.
Email: joshuajcy@gmail.com

ABSTRACT

The widespread transmission of Avian Influenzais seriously threatening both humans and avian populations. As a response, A comprehensive model is constructed which clarifies the dynamics of the virus's transmission while taking into account interactions between avian and human hosts. The model incorporates population dynamics for both species and includes the aspects of transmission from bird to bird, bird to human and human to human. As a precautionary step the model insists vaccinating poultry and practising human safety protocols. By rigorous analysis the stability, boundedness, and the equilibrium points of the model is determined. Additionally, we obtain the expression for the reproduction number (R_0), a pivotal metric for understanding the spread of disease. The stability of the model is analysed through adequate theorems, supplemented by numerical simulations. The article findings highlights the critical importance of preventive measures in mitigating the spread of Avian Influenza. Also, the article emphasizes the urgency of implementing preventive strategies to curb the potential for a widespread pandemic. In conclusion, the proposed model serves as a useful tool for pandemic control, highlighting the need for quick decisions and coordinated actions to combat against Avian Influenza.

Keywords: Mathematical Modeling, Avian Influenza, Jacobian Matrix, Stability Analysis, Sensitivity Index.

INTRODUCTION

The spread of avian influenza must be taken serious as it might develop into a pandemic. It is importantto test case for pandemic preparedness. Also, to explore the use of epidemiological hazard models and sequence-based early viral warning systems to detect and mitigate potential pandemic threats[1]. Further understanding the variation in avian influenza among poultry species and virus subtypes is necessary as there is possible mutations happens in the evolvement of virus [2,3]. It is observed and studied that there is a trace of avian virus strain in the brain of multiple wild species [4], there is more possibility that the domesticated species might be exposed to these wild infected species. So, vaccinating the poultry species might help to control the spread of avian flu. In order to do so, it is necessary that there must be study on vaccination evolvement [5]. Further, the knowledge of mathematical models is in modeling avian influenza is required. The use of compartmental models helps to understand the dynamics of virus spread [6] and use of optimal control strategy [7] enriches the concept of controlling the virus spread. The article focuses on the poultry population and hence the study of how mathematical modeling on poultry farm species [8-10] prevents in development of virus spread. These studies collectively contribute to the understanding of avian influenza dynamics from which the proposed article is furnished providing valuable insights for pandemic preparedness and control strategies.

1. Materials and Methods

2.1 Mathematical Model Formulation:

The aim of the article is to focus on control measures to reduce the spread of avian influenza. So, a comprehensive model is developed considering both the population of avian and human. The proposed model incorporates the idea of vaccinating the poultry and also human to follow control measures. The model is comprised of SIR-SEIR compartments as given as follows.

$$\begin{aligned}
\frac{dS_b(t)}{dt} &= (1-m_1)\Lambda_1 - \beta_b S_b(t) I_b(t) - \mu_1 S_b(t) \\
\frac{dI_b(t)}{dt} &= \beta_b S_b(t) I_b(t) - (\mu_1 + k_1) I_b(t) \\
\frac{dR_b(t)}{dt} &= m_1 \Lambda_b - \mu_1 R_b(t) \\
\frac{dS_h(t)}{dt} &= (1-m_2)\Lambda_h - \beta_h S_h (I_h + E_h) - \beta_{bh} S_h I_b - \mu_2 S_h \\
\frac{dE_h(t)}{dt} &= \beta_h S_h (I_h + E_h) - (\gamma + \delta_1 + \mu_2) E_h \\
\frac{dI_h(t)}{dt} &= \beta_{bh} S_h I_b + \gamma E_h - (\delta_2 + k_2 + \mu_2) I_h \\
\frac{dR_h(t)}{dt} &= m_2 \Lambda_h + \delta_1 E_h + \delta_2 I_h - \mu_2 R_h
\end{aligned} \tag{1}$$

Provided the total avian population is given by $N_b(t) = S_b(t) + I_b(t) + R_b(t)$ and the total human population is given by $N_h(t) = S_h(t) + E_h(t) + I_h(t) + R_h(t)$.

The notations $S_b(t), I_b(t)$ and $R_b(t)$ denotes the susceptible, infected and recovered avian correspondingly, whereas $S_h(t), E_h(t), I_h(t)$ and $R_h(t)$ denotes the susceptible, exposed, infected and recovered human respectively. Here Λ_h, Λ_b are the recruitment rate and μ_2, μ_1 are the mortality rate of human and avian respectively. The rate at which the transmission occurs among avian, avian to human and among human is given by β_b, β_{bh} and β_h respectively. The latency period of the model is denoted as γ. The individual recover without infection depending on their immune power is denoted as δ_1. The infected individual who shows symptoms fall in the infected compartment. Those infected individual might get recover and its rate is given by δ_2 or they may die due to disease and is denoted as k_1 and k_2 respectively. Now, the parameter m_1 gives the vaccination rate of the avian, which is one among our preventive strategy. Similarly, for the human there is no proper available vaccination, so the safety measure has to be followed by the human. Safety measures like avoiding avian contact. If suppose the human is in the situation of being in contact with avian they must use the PPE (Personal Protective Equipment) kit which includes face mask. Later, they must sanitize themselves. Thus, the rate at which human practice control measures is given by m_2. These individuals are considered to move to the recovered compartment directly.

Mathematical Analysis:

The analysis of the proposed begins with some prerequisite lemmas.

Lemma 1. The solution set of the model (1) along with the initial conditions will be non-negative for all time $t > 0$.

Proof.

From model (1), considering the first equation of avian population, we have

$$\frac{dS_b}{dt} = (1-m_1)\Lambda_b - \beta_b S_b I_b - \mu_1 S_b$$

$$\frac{dS_b}{S_b} \geq -(\beta_b I_b + \mu_1)dt$$

Integrating on both sides and simplifying, we get

$$S_b(t) \geq S(0).e^{-(\beta_b I_b + \mu_1)t}$$

As $t \to \infty$, we get

$S_b(t) \geq 0$

Similarly, it can be proved that $I_b(t) \geq 0$, $R_b(t) \geq 0$ and $S_h(t) \geq 0$, $E_h(t) \geq 0$, $I_h(t) \geq 0$ and $R_h(t) \geq 0$.

Lemma 2. Prove that the biological feasible region for the proposed model (1) is

$$\Phi = \left\{ \left(S_b(t), I_b(t), R_b(t), S_h(t), E_b(t), I_b(t), R_b(t)\right) \in \mathbb{R}^7_+ : 0 < N_b(t) \leq \frac{\Lambda_b}{\mu_1}, 0 < N_h(t) \leq \frac{\Lambda_h}{\mu_2} \right\}$$ which is

invariantly positive and is attracted in Φ.

Proof.

We have $N_b(t) = S_b(t) + I_b(t) + R_b(t)$ which implies

$$\frac{dN_b(t)}{dt} = \frac{dS_b(t)}{dt} + \frac{dI_b(t)}{dt} + \frac{dR_b(t)}{dt}$$

$$\leq \Lambda_b - \mu_1 N(t)$$

As $\limsup_{t\to\infty} N_b(t) \leq \frac{\Lambda_b}{\mu_1}$

Similarly, it is possible to prove $\limsup_{t\to\infty} N_h(t) \leq \frac{\Lambda_h}{\mu_2}$.

Hence, solution set is bounded within the region Φ .

Determination of Existence of Equilibrium Points:

In this section, we determine the existence of disease-free equilibrium (DFE) and endemic equilibrium (EE) for both the population. For model (1), the disease-free equilibrium for the avian population is denoted as $\mathcal{E}_b^0$ and is obtained as $\mathcal{E}_b^0 = \left(S_b^0, I_b^0, R_b^0\right) = \left(\frac{(1-m_1)\Lambda_b}{\mu_1}, 0, 0\right)$. Also, the endemic equilibrium of the avian population is denoted and obtained as $\mathcal{E}_b^* = \left(S_b^*, I_b^*, R_b^*\right) = \left(\frac{1}{\beta_b}, \frac{\beta_b(1-m_1)\Lambda_b - \mu_1(\mu_1+k_1)}{\beta_b(\mu_1+k_1)}, \frac{m_1\Lambda_b}{\mu_1}\right)$.

Similarly, the disease-free equilibrium $\left(\mathcal{E}_h^0\right)$ and the endemic equilibrium $\left(\mathcal{E}_h^*\right)$ of the human population is obtained as given below.

$$\mathcal{E}_h^0 = \left(S_h^0, E_h^0, I_h^0, R_h^0\right) = \left(\frac{(1-m_2)\Lambda_h}{\mu_2}, 0, 0, 0\right) \quad \text{and} \quad \mathcal{E}_h^* = \left(S_h^*, E_h^*, I_h^*, R_h^*\right),$$

where

$$S_h^* = \frac{C_2(\gamma+\delta_1+\mu_2)}{\beta_h(C_1+C_2)},\ E_h^* = C_3 I_h^*,\ I_h^* = \frac{\beta_{bh}C_2(\gamma+\delta_1+\mu_2)I_b^*}{\beta_h(C_1+C_2)(\delta_2+k_2+\mu_2-\gamma C_3)} \text{ and } R_h^* = \frac{m_2\Lambda_h}{\mu_2} + \frac{(\delta_1 C_3+\delta_2)}{\mu_2} I_h^*$$

Whereas,

$$C_1 = \beta_{bh}I_b^*(\gamma+\delta_1+\mu_2) + \gamma\left[(1-m_2)\Lambda_h - (\beta_b h I_b^* + \mu_2)\right], \quad C_2 = (\delta_2+k_2+\mu_2)\left[(1-m_2)\Lambda_h - (\beta_{bh})I_b^* + \mu_2\right]$$

and $C_3 = \frac{C_2}{C_1}$

Thus, the equilibria exists for the proposed model and it is determined.

Determination of Basic Reproduction Number:

The basic reproduction number (R_0) is the expected number of individuals directly infected by one infected individual in a population considering all the individuals are susceptible to the infection. The expression of the reproduction number of the proposed model can be obtained by determining the Jacobian matrix of the infective classes namely I_b, E_h, I_h .

$$J(I_b, E_h, I_h) = \begin{pmatrix} \beta_b S_b - (\mu_1+k_1) & 0 & 0 \\ 0 & \beta_h S_h - (\gamma+\delta_1+\mu_2) & \beta_h S_h \\ \beta_{bh} S_h & \gamma & -(\delta_2+k_2+\mu_2) \end{pmatrix}$$

Thus,

$$F = \begin{pmatrix} \beta_b S_b & 0 & 0 \\ 0 & \beta_h S_h & \beta_h S_h \\ \beta_{bh} S_h & 0 & 0 \end{pmatrix} \text{ and } V = \begin{pmatrix} -(\mu_1+k_1) & 0 & 0 \\ 0 & -(\gamma+\delta_1+\mu) & 0 \\ 0 & \gamma & -(\delta_2+k_2+\mu_2) \end{pmatrix}$$

Now,

$$FV^{-1}=\begin{pmatrix} \frac{-\beta_b S_b}{(\mu_1+k_1)} & 0 & 0 \\ 0 & \frac{-\beta_h S_h}{(\gamma+\delta_1+\mu)}\left(1+\frac{\gamma}{(\delta_2+k_2+\mu_2)}\right) & \frac{-\beta_h S_h}{(\delta_2+k_2+\mu_2)} \\ \frac{-\beta_{bh} S_h}{(\mu_1+k_1)} & 0 & 0 \end{pmatrix}$$

The spectral radius of the above matrix yields the basic reproduction number (R_0). Thus the expression of R_0 is obtained as $\rho\left(FV^{-1}\right)=\max\{R_1,R_2\}$,

where $R_1=\frac{\beta_h S_h}{(\gamma+\delta_1+\mu_2)}\left(1+\frac{\gamma}{(\delta_2+k_2+\mu_2)}\right)$ and $R_2=\frac{\beta_b S_b}{(\mu_1+k_1)}$.

Local Stability Analysis of the Equilibrium points:

Theorem 3. The disease-free equilibrium $\mathcal{E}^0=\left(\frac{(1-m_1)\Lambda_b}{\mu_1},0,0,\frac{(1-m_2)\Lambda_h}{\mu_2},0,0,0\right)$ is locally asymptotically stable if $R_0<1$.

Proof.

The Jacobian matrix of the proposed model at the DFE gives,

$$J\left(\mathcal{E}^0\right)=\begin{pmatrix} -\mu_1 & -\beta_b S_b & 0 & 0 & 0 & 0 & 0 \\ 0 & (\mu_1+k_1)(R_2-1) & 0 & 0 & 0 & 0 & 0 \\ 0 & 0 & -\mu_1 & 0 & 0 & 0 & 0 \\ 0 & -\beta_{bh} S_h & 0 & -\mu_2 & -\beta_h S_h & -\beta_h S_h & 0 \\ 0 & 0 & 0 & 0 & j_{55} & \beta_h S_h & 0 \\ 0 & \beta_{bh} S_h & 0 & 0 & \gamma & -(\delta_2+k_2+\mu_2) & 0 \\ 0 & 0 & 0 & 0 & \delta_1 & \delta_2 & -\mu_2 \end{pmatrix}$$

It is clear that $-\mu_1$, $-\mu_2$, $-(\delta_2+k_2+\mu_2)$, $-\mu_1$, j_{22}, $-\mu_2$ and j_{55} are the eigenvalues of $J(\mathcal{E}^0)$.

The above matrix will be stable provided it satisfies the following conditions,

(i) $j_{22}=\beta_b S_b-(\mu_1+k_1)=(\mu_1+k_1)\left(R_2-1\right)<0$ and

(ii) $j_{55}=\beta_h S_h-(\gamma+\delta_1+\mu_2)=(\gamma+\delta_1+\mu_2)\left(\frac{(\delta_2+k_2+\mu_2)}{\delta_2+k_2+\mu_2+\gamma_2}R_1-1\right)<0$

This is possible only if $R_1<1$ and $R_2<1$.

Hence, the DFE is locally asymptotically stable if $R_0<1$.

Theorem 4. The human only endemic equilibrium $\mathcal{E}_h^*=\left(S_b^0,0,0,S_h^*,E_h^*,I_h^*,R_h^*\right)$ is locally asymptotically stable only if $R_1>1$, $R_2<1$.

Proof. The Jacobian matrix of the proposed model at the human only EE gives,

$$J\left(\mathcal{E}^0\right)=\begin{pmatrix} -\mu_1 & -\beta_b S_b^0 & 0 & 0 & 0 & 0 & 0 \\ 0 & \beta_b S_b^0-(\mu_1+k_1) & 0 & 0 & 0 & 0 & 0 \\ 0 & 0 & -\mu_1 & 0 & 0 & 0 & 0 \\ 0 & -\beta_{bh} S_h^* & 0 & -\mu_2 & -\beta_h S_h^* & -\beta_h S_h^* & 0 \\ 0 & 0 & 0 & 0 & j_{55} & \beta_h S_h^* & 0 \\ 0 & \beta_{bh} S_h^* & 0 & 0 & \gamma & -(\delta_2+k_2+\mu_2) & 0 \\ 0 & 0 & 0 & 0 & \delta_1 & \delta_2 & -\mu_2 \end{pmatrix}$$

Clearly, $-\mu_1$, $-\mu_2$, $-(\delta_2+k_2+\mu_2)$, $-\mu_1$, j_{22}, $-\mu_2$ and j_{55} are the eigenvalues of $J(\mathcal{E}^0)$.

The above matrix will be stable only if it satisfies the following conditions,

(i) $j_{22}=\beta_b S_b^0-(\mu_1+k_1)=(\mu_1+k_1)(R_2-1)<0$ and

(ii) $j_{55}=\beta_h S_h^*-(\gamma+\delta_1+\mu_2)<0$

Thus the inequality (i) holds only if $R_2<1$.

Now, inequality (ii) holds as it yields a negative value below

$$\begin{aligned}\beta_h S_h^*-(\gamma+\delta_1+\mu_2) &= \beta_h\left(\frac{(\delta_2+k_2+\mu_2)(\gamma+\delta_1+\mu_2)}{\beta_h(\delta_2+k_2+\mu_2+\gamma)}\right)-(\gamma+\delta_1+\mu_2)\\ &= \frac{(\delta_2+k_2+\mu_2)(\gamma+\delta_1+\mu_2)-(\delta_2+k_2+\mu_2+\gamma)(\gamma+\delta_1+\mu_2)}{(\delta_2+k_2+\mu_2+\gamma)}\\ &= -\frac{\gamma(\gamma+\delta_1+\mu_2)}{(\delta_2+k_2+\mu_2+\gamma)}<0\end{aligned}$$

This occurs only if $R_1>1$.

Hence, the human only EE is locally asymptotically stable only if $R_1>1$ and $R_2<1$.

Global Stability Analysis of the Equilibria:

Theorem 5. The DFE $\mathcal{E}^0$ is globally asymptotically stable in $\Phi:=\left\{\left(S_b(t),I_b(t),R_b(t),S_h(t),E_h(t),I_h(t),R_h(t)\right)\in\mathbb{R}_+^7\right\}$ if $R_0<1$.

Proof.

In Theorem 3, it is proved that the DFE $\mathcal{E}^0$ is locally asymptotically stable only if $R_0<1$. So, it is enough to show that $\mathcal{E}^0$ is globally attractive in the positively invariant and attractive set.

The proof proceeds with the fluctuation lemma by considering the solution set $\left(S_b(t),I_b(t)\right)$ of the avian population subsystem only. It considers only Susceptible and Infected avian populations as these two equations are independent of the Recovered compartment of avian.

The fluctuation lemma states that there exists a sequence $\{t_n\}$ such that $t_n\to\infty$, we have $I(t_n)\to I^\infty$, and $I'(t_n)\to 0$ as $n\to\infty$.

Hence, using the fluctuation lemma, the infected avian becomes $I_b'(t_n) = \beta_b S_b(t_n) I_b(t_n) - (\mu_1 + k_1) I_b(t_n)$ which implies $0 \le \beta_b S_b^{\infty} I_b^{\infty} - (\mu_1 + k_1) I_b^{\infty}$ and hence $0 \le (R_2 - 1) I_b^{\infty}$. Since $R_2 < 1$, we get $I_b^{\infty} = 0$.

Again as $n \to \infty$, the susceptible equation becomes $S_b^{\infty} \le \frac{(1-m_1)\Lambda_b}{\mu_1}$. If $R_2 < 1$, then $\lim_{t\to\infty} S_b(t) = \frac{(1-m_1)\Lambda_b}{\mu_1}$. Thus, for the system of avian population, we have $\lim_{t\to\infty}\left(S_b(t), I_b(t)\right) = \left(\frac{(1-m_1)\Lambda_b}{\mu_1}, 0\right)$ holds for all solutions of the avian system.

Similarly, for the human population it can be proved that $\lim_{t\to\infty}\left(S_h(t), E_h(t), I_h(t)\right) = \left(\frac{(1-m_1)\Lambda_b}{\mu_1}, 0, 0\right)$ if $R_1 < 1$.

Hence, the DFE $\mathcal{E}^0$ is globally asymptotically stable if $R_0 < 1$.

Theorem 6. The EE $\mathcal{E}^*$ is globally asymptotically stable in $\Phi := \left\{\left(S_b(t), I_b(t), R_b(t), S_h(t), E_h(t), I_h(t), R_h(t)\right) \in \mathbb{R}_+^7\right\}$ if $R_0 > 1$.

Proof. Considering a Lyapunov function as follows

$$\mathcal{L} = \frac{1}{2} l_1 \left(S_b - S_b^*\right)^2 + \frac{1}{2} l_2 \left(I_b - I_b^*\right)^2 + \frac{1}{2} l_3 \left(S_h - S_h^*\right)^2 + \frac{1}{2} l_4 \left(E_h - E_h^*\right)^2 + \frac{1}{2} l_5 \left(I_h - I_h^*\right)^2$$

Differentiating with respect to 't', we get

$$\begin{aligned}
\mathcal{L}' &= l_1 \left(S_b - S_b^*\right) S_b' + l_2 \left(I_b - I_b^*\right) I_b' + l_3 \left(S_h - S_h^*\right) S_h' + l_4 \left(E_h - E_h^*\right) E_h' + l_5 \left(I_h - I_h^*\right) I_h' \\
&= -l_1 \left(\beta_b I_b + \mu_1\right)\left(S_b - S_b^*\right)^2 + l_2 \left[\beta_b S_b - (\mu_1 + k_1)\right]\left(I_b - I_b^*\right)^2 - l_3 \left[\beta_h \left(I_b + I_h + E_h\right) + \mu_2\right]\left(S_h - S_h^*\right)^2 \\
&\quad + l_4 \left[\beta_h S_h - (\gamma + \delta_1 + \mu_2)\right]\left(E_h - E_h^*\right)^2 - l_5 \left(\delta_2 + k_2 + \mu_2\right)\left(I_h - I_h^*\right)^2 \\
&\quad - l_1 \beta_b S_b \left(S_b - S_b^*\right)\left(I_b - I_b^*\right) + l_2 \beta_b I_b \left(S_b - S_b^*\right)\left(I_b - I_b^*\right) - l_3 \beta_{bh} S_h \left(S_h - S_h^*\right)\left(I_b - I_b^*\right) \\
&\quad - l_3 \beta_h S_h \left(S_h - S_h^*\right)\left(E_h - E_h^*\right) - l_3 \beta_h S_h \left(S_h - S_h^*\right)\left(I_h - I_h^*\right) \\
&\quad + l_4 \beta_h \left(I_h + E_h\right)\left(S_h - S_h^*\right)\left(E_h - E_h^*\right) + l_4 \beta_h S_h \left(E_h - E_h^*\right)\left(I_h - I_h^*\right) + l_5 \beta_{bh} S_h \left(I_b - I_b^*\right)\left(I_h - I_h^*\right) \\
&\quad + l_5 \beta_{bh} I_b \left(S_h - S_h^*\right)\left(I_h - I_h^*\right) + l_5 \gamma \left(E_h - E_h^*\right)\left(I_h - I_h^*\right)
\end{aligned}$$

It is required to show that $\mathcal{L}'$ is negative.

So, the condition of the global stability of the endemic equilibrium point are determined as

$$a_{12}^2 < \frac{a_{11}a_{22}}{2}, \quad a_{21}^2 < \frac{a_{22}a_{11}}{2}, \quad a_{32}^2 < \frac{a_{33}a_{22}}{5}, \quad a_{34}^2 < \frac{a_{33}a_{44}}{5}, \quad a_{35}^2 < \frac{4a_{33}a_{55}}{25},$$

$$a_{43}^2 < \frac{a_{44}a_{33}}{5}, \quad a_{45}^2 < \frac{a_{44}a_{55}}{5}, \quad a_{52}^2 < \frac{a_{55}a_{22}}{5}, \quad a_{53}^2 < \frac{4a_{55}a_{33}}{25}, \quad a_{54}^2 < \frac{a_{55}a_{44}}{5}.$$

Thus, $\mathcal{L}'$ will be negative only if the foresaid condition holds.

(i) $k_1 \left(\beta_b S_b\right)^2 < \frac{k_2}{2} \mu_1 (\mu_1 + k_1)$

(ii) $k_2(\beta_b I_b)^2 < \frac{k_1}{2}\mu_1(\mu_1 + k_1)$

(iii) $k_3(\beta_{bh} S_h)^2 < \frac{k_2}{5}\mu_2(\mu_1 + k_1)$

(iv) $k_3(\beta_h S_h)^2 < \frac{k_4}{5}\mu_2(\gamma + \delta_1 + \mu_2)$

(v) $k_3(\beta_h S_h)^2 < \frac{4}{25}k_5\mu_2(\delta_2 + k_2 + \mu_2)$

(vi) $k_4\left[\beta_h\left(I_h + E_h\right)\right]^2 < \frac{k_3}{5}\mu_2(\gamma + \delta_1 + \mu_2)$

(vii) $k_4(\beta_h S_h)^2 < \frac{k_2}{5}(\gamma + \delta_1 + \mu_2)(\delta_2 + k_2 + \mu_2)$

(viii) $k_5(\beta_{bh} I_b)^2 < \frac{k_2}{5}(\mu_1 + k_1)(\delta_2 + k_2 + \mu_2)$

(ix) $k_5(\beta_{bh} I_b)^2 < \frac{4}{25}k_3\mu_2(\delta_2 + k_2 + \mu_2)$

$k_5(\delta_2 + k_2 + \mu_2) < \frac{k_4}{5}(\gamma + \delta_1 + \mu_2)$

By considering $k_1 = k_2 = k_4 = 1$, $\mathcal{L}'$ becomes negative. Also, inequality (i) and (vii) holds only if $R_2 > 1$ and $R_1 > 1$. Hence, it is clear that the EE is globally asymptotically stable only if $R_0 > 1$.

RESULTS AND DISCUSSION

In this section, numerical simulations are performed supporting the optimality of the proposed model. Considering the following initial values $S_{h_0} = 99000,\ E_{h_0} = 100,\ I_{h_0} = 100$ and $R_{h_0} = 0$,the dynamics of the human only population in the proposed model is obtained by simulating it in the mathematical software named MATLAB as follows. Figure 1 explicitly shows that the recovery curve inclines enriching the novelty of the proposed model. Also, the exposed and the infected curves are notably declining rapidly showing a better result in reducing the spread of the avian influenza. The susceptibility curve ensures that in future the number of cases will be less in number. Also, the dynamics of the avian population with the initial values $S_{b_0} = 1000,\ \mathrm{I}_{b_0} = 800$ and $R_{b_0} = 10$ is obtained using MATLAB as follows. Clearly, the infected curve of the avian population is reducing after an initial rise. Also, the recovered curve of the avian population is appreciably high. Thus, the spread of avian influenza among the avian will be also controlled. Further, the analysis on reproduction number R_0 is performed by considering the values in Table 2 of [10].Considering the maximum value from R_1 and R_2, we obtained the following result.

Case (a): Reproduction number at the disease-free equilibrium is obtained as $R_0 = 0.001134 < 1$

Case (b): Reproduction number at the endemic equilibrium is obtained as $R_0 \geq 1$

Hence, the numerical simulation sustains the stability of the proposed model.

CONCLUSION

Eventually, the proposed model shows positivity and boundedness. Also, the existence of equilibrium points is determined followed by it the expression for the reproduction number R_0 is obtained by solving the Jacobian matrix of the infected classes of the proposed SIR-SEIR model. Additionally, the stability of the equilibria is determined locally and globally. The local stability is determined by solving the Jacobian matrix of the reduced model. Whereas the global stability is proved with fluctuation lemma and Lyapunov function. The numerical simulation confines to the optimality of the proposed model highlighting the concept of vaccinating the avian and practice of control measures by humans ensures the novelty of the model which helps to control the spread of avian influenza.

REFERENCES

1. Brüssow H. Avian influenza virus cross-infections as test case for pandemic preparedness: From epidemiological hazard models to sequence-based early viral warning systems. Microbial Biotechnology. 2024 Jan 16:e14389. https://doi.org/10.1111/1751-7915.14389
2. Kirkeby C, Boklund A, Larsen LE, Ward MP. Are all avian influenza outbreaks in poultry the same? The predicted impact of poultry species and virus subtype. Zoonoses and Public Health. 2024 Feb 16. https://doi.org/10.1111/zph.13116
3. Altiok E, Taylan F, Yenen OŞ, Demirkeser G, Bozaci M, Önel D, Akcadag B, Iyisan AS, Ciblak M, Bozkaya E, Yuksel S. Mutations in influenza A virus (H5N1) and possible limited spread, Turkey, 2006. https://doi.org/10.3201%2Feid1403.061237
4. Vreman S, Kik M, Germeraad E, Heutink R, Harders F, Spierenburg M, Engelsma M, Rijks J, van den Brand J, Beerens N. Zoonotic Mutation of Highly Pathogenic Avian Influenza H5N1 Virus Identified in the Brain of Multiple Wild Carnivore Species. Pathogens. 2023 Jan 20;12(2):168.https://doi.org/10.3390/pathogens12020168
5. Gomez PL, Robinson JM, Rogalewicz JA. Vaccine manufacturing. Vaccines. 2013:44.https://doi.org/10.1016%2FB978-1-4557-0090-5.00019-7
6. Barua S, Dénes A. Global dynamics of a compartmental model for the spread of Nipah virus. Heliyon. 2023 Sep 1;9(9). https://doi.org/10.1016/j.heliyon.2023.e19682
7. Gourram H, Baroudi M, Labzai A, Belam M. Mathematical modeling and optimal control strategy for the influenza (H5N1). Commun. Math. Biol. Neurosci.. 2023 Oct 23;2023:Article-ID. https://doi.org/10.28919/cmbn/8199
8. Malek A, Hoque A. A Mathematical Model of Avian Influenza for Poultry Farm and its Stability Analysis. Applications and Applied Mathematics: An International Journal (AAM). 2020;15(2):23.https://digitalcommons.pvamu.edu/aam/vol15/iss2/23
9. Inyama SC. Mathematical model for bird flu disease transmission with no bird migration. Global Journal of Mathematical Sciences. 2009;8(2).http://dx.doi.org/10.4314/jonamp.v10i1.40158
10. Chong NS, Tchuenche JM, Smith RJ. A mathematical model of avian influenza with half-saturated incidence. Theory in biosciences. 2014 Mar;133:23-38.https://doi.org/10.1007/s12064-013-0183-6

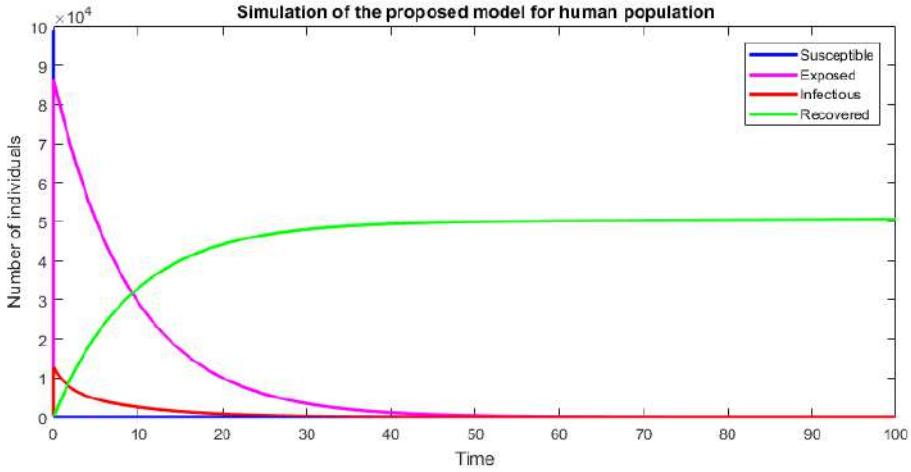

Figure 1: The dynamics of only human population of the SIR-SEIR model

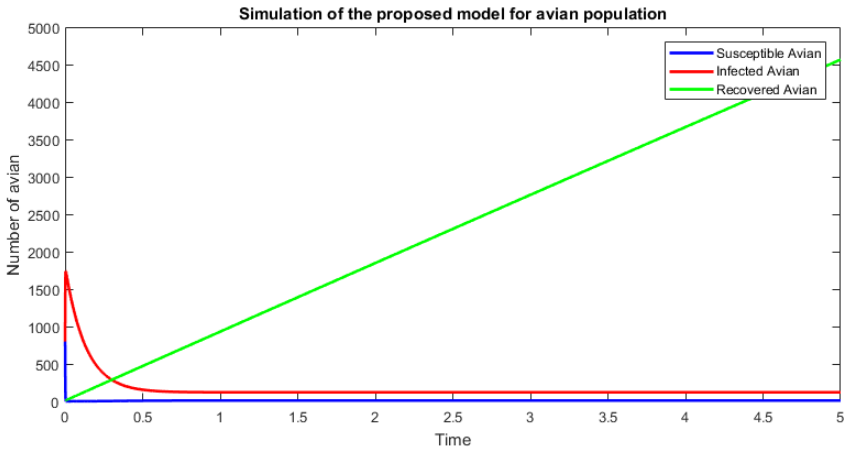

Figure 2: Dynamics of avian population

Indian Journal of Natural Sciences *www.tnsroindia.org.in ©IJONS*

Vol.15 / Issue 83 / Apr / 2024 *International Bimonthly (Print) – Open Access* *ISSN: 0976 – 0997*

RESEARCH ARTICLE

A View on Separation Axioms via Neutrosophic ϒ −Open Sets

C. Reena[1]* and K. S. Yaamini[2]

[1]Assistant Professor, Department of Mathematics, St. Mary's College (Autonomous), Thoothukudi, (Affiliated to Manonmaniam Sundaranar University, Abishekapatti, Tirunelveli) Tamil Nadu, India.
[2]Research Scholar, Reg. No.21212212092002, Department of Mathematics, St. Mary's College (Autonomous), Thoothukudi, (Affiliated to Manonmaniam Sundaranar University, Abishekapatti, Tirunelveli) Tamil Nadu, India.

Received: 30 Dec 2023 Revised: 09 Jan 2024 Accepted: 27 Mar 2024

***Address for Correspondence**
C. Reena
Assistant Professor,
Department of Mathematics,
St. Mary's College (Autonomous),
Thoothukudi, (Affiliated to Manonmaniam Sundaranar University, Abishekapatti, Tirunelveli)
Tamil Nadu, India.
Email: reenastephany@gmail.com

ABSTRACT

This paper presents a novel perspective of separation axioms in neutrosophic topological spaces by means of neutrosophic ϒ −open sets. The concepts of neutrosophic $\Upsilon - T_i$ spaces$(i = 0,1,2)$ are introduced and their characterizations are studied.

Keywords: neutrosophic ϒ −open, neutrosophic $\Upsilon - T_0$ space, neutrosophic $\Upsilon - T_1$ space, neutrosophic $\Upsilon - T_2$ space.

INTRODUCTION

Smarandache9, in 1998 initiated the concept of neutrosophy to study the nature and scope of neutrality which further led to the origination of neutrosophic sets. Salama and Albowi7 introduced neutrosophic topological spaces and other topological concepts have been explored by various researchers.The concept of separation axioms in neutrosophic topological spaces were introduced by Ahu Acikgoz and F. Esenbel1 by employing the notion of quasi-coincidence. Later,Suman Das et.al12 have also defined and established some basic results related to separation axioms in neutrosophictopological spaces. The focus of this paper is to introduce the concept of neutrosophicϒ −separation axioms in neutrosophic topological spaces. We have defined neutrosophic$\Upsilon - T_i$ spaces$(i = 0,1,2)$ and observed the attributes and interrelationship between these spaces. Moreover, the notion of neutrosophicϒ −kernel has also been defined to characterize the spaces.

Preliminaries

Definition 2.1:7Let U be a non-empty fixed set. A **neutrosophic set**L is an object having the form $L = \{< u, \mu_L(u), \sigma_L(u), \gamma_L(u) >: u \in U\}$ where $\mu_L(u), \sigma_L(u)$and $\gamma_L(u)$represent the membership, indeterminacy and non-membership functions respectively of each element $u \in U$.A neutrosophic set $L = \{< u, \mu_L(u), \sigma_L(u), \gamma_L(u) >: u \in U\}$ can be identified to an ordered triple $< \mu_L, \sigma_L, \gamma_L >$ in $]^-0,1^+[$ on U.

Definition 2.2: 7Let U be a non-empty set and $L = \{< u, \mu_L(u), \sigma_L(u), \gamma_L(u) >: u \in U\}, M = \{< u, \mu_M(u), \sigma_M(u), \gamma_M(u) >: u \in U\}$ be neutrosophic sets in U. Then

(i) $L \subseteq M$if$\mu_L(u) \leq \mu_M(u), \sigma_L(u) \leq \sigma_M(u)$ and $\gamma_L(u) \geq \gamma_M(u)$ for all $u \in U$.

(ii)$L \cup M = \{< u,\max\{\mu_L(u), \mu_M(u)\}, \max\{\sigma_L(u), \sigma_M(u)\}, \min\{\gamma_L(u), \gamma_M(u)\}>: u \in U\}$

(iii) $L \cap M = \{< u,\min\{\mu_L(u), \mu_M(u)\}, \min\{\sigma_L(u), \sigma_M(u)\}, \max\{\gamma_L(u), \gamma_M(u)\}>: u \in U\}$

(iv)$L^c = \{< u, \gamma_L(u), 1 - \sigma_L(u), \mu_L(u) >: u \in U\}$

(v) $0_{N_{tr}} = \{< u, 0,0,1 >: u \in U\}and1_{N_{tr}} = \{< u, 1,1,0 >: u \in U\}$

Definition 2.3:7A **neutrosophic topology** on a non-empty set U is a family $\tau_{N_{tr}}$ of neutrosophic sets in U satisfying the following axioms:

(i) $0_{N_{tr}}, 1_{N_{tr}} \in \tau_{N_{tr}}$

(ii)$\cup L_i \in \tau_{N_{tr}} \forall \{L_i : i \in I\} \subseteq \tau_{N_{tr}}$

(iii) $L_1 \cap L_2 \in \tau_{N_{tr}}$for any $L_1, L_2 \in \tau_{N_{tr}}$

The pair $(U, \tau_{N_{tr}})$ is called a neutrosophic topological space. The members of $\tau_{N_{tr}}$ are called neutrosophic open$(N_{tr}O)$ and its complements are called neutrosophic closed$(N_{tr}C)$.

Definition 2.4:1A neutrosophic set $L = \{< u, \mu_L(u), \sigma_L(u), \gamma_L(u) >: u \in U\}$ is called a **neutrosophic point**$(N_{tr}P)$ if for any element $v \in U, \mu_L(v) = a, \sigma_L(v) = b, \gamma_L(v) = c$ for $u = v$ and $\mu_L(v) = 0, \sigma_L(v) = 0, \gamma_L(v) = 1$ for $u \neq v$, where a, b, c are real standard or non-standard subsets of $]^-0,1^+[$. A neutrosophic point is denoted by $u_{a,b,c}$.For the neutrosophic point $u_{a,b,c}$, u will be called its support.

Definition 2.5:1A neutrosophic point $u_{a,b,c}$ is said to be **neutrosophic quasi – coincident** with a neutrosophic set L, denoted by $u_{a,b,c} q L$ if $u_{a,b,c} \notin L^c$. If $u_{a,b,c}$ is not neutrosophic quasi – coincident with L, we denote it by $u_{a,b,c} \hat{q} L$.

Definition 2.6:4A neutrosophic set L of a neutrosophic topological space $(U, \tau_{N_{tr}})$ is said to be **neutrosophicΥ −open**$(N_{tr}\Upsilon O)$ if for every non-empty N_{tr}closed set $F \neq 1_{N_{tr}}, L \subseteq N_{tr}cl\big(N_{tr}int(L \cup F)\big)$. The complement of neutrosophicΥ −open set is neutrosophicΥ −closed. The class of neutrosophic Υ −open sets is denoted by $N_{tr}\Upsilon O\big(U, \tau_{N_{tr}}\big)$.

Theorem 2.7:4Every N_{tr}open set is $N_{tr}\Upsilon$ −open.

Theorem 2.8 :6 Let $(S, \tau^*_{N_{tr}})$ be a neutrosophic subspace of $\big(U, \tau_{N_{tr}}\big)$. Then a neutrosophic set L in S is$N_{tr}\Upsilon$ −closed in $\big(U, \tau_{N_{tr}}\big)$if and only if L is $N_{tr}\Upsilon$ −closed in $\big(S, \tau^*_{N_{tr}}\big)$.

Definition 2.9:5A function $f_{N_{tr}}: (U, \tau_{N_{tr}}) \longrightarrow (V, \rho_{N_{tr}})$ is said to be **neutrosophicΥ −continuous** if $f^{-1}_{N_{tr}}(M)$ is $N_{tr}\Upsilon$ −open in $(U, \tau_{N_{tr}})$ for every N_{tr}open set M in $\big(V, \rho_{N_{tr}}\big)$.

Definition 2.10:5A function $f_{N_{tr}}: (U, \tau_{N_{tr}}) \longrightarrow (V, \rho_{N_{tr}})$ is said to be **neutrosophicΥ −irresolute** if $f^{-1}_{N_{tr}}(M)$ is $N_{tr}\Upsilon$ −open in $(U, \tau_{N_{tr}})$ for every $N_{tr}\Upsilon$ −open set M in $\big(V, \rho_{N_{tr}}\big)$.

Definition 2.11:6A function $f_{N_{tr}}: (U, \tau_{N_{tr}}) \longrightarrow (V, \rho_{N_{tr}})$ is said to be a **neutrosophicΥ −open** if $f_{N_{tr}}(L)$ is $N_{tr}\Upsilon$ −open in $(V, \rho_{N_{tr}})$ for every N_{tr}open set L in $(U, \tau_{N_{tr}})$.

Definition 2.12:12A neutrosophic topological space $(U,\tau_{N_{tr}})$ is said to be a $\boldsymbol{N_{tr}T_0-}$ **space** if for every pair of neutrosophic points $u_{a,b,c}$and $v_{a',b',c'}, u\neq v$ in U, there exists N_{tr}open set L in $(U,\tau_{N_{tr}})$ such that $u_{a,b,c}\in L, v_{a',b',c'}\notin L$ or $u_{a,b,c}\notin L, v_{a',b',c'}\in L$.

Definition 2.13:12A neutrosophic topological space $(U,\tau_{N_{tr}})$ is said to be a $\boldsymbol{N_{tr}T_1-}$ **space** if for every pair of neutrosophic points $u_{a,b,c}$and $v_{a',b',c'}, u\neq v$, there exists N_{tr}open sets L and M in $(U,\tau_{N_{tr}})$ such that $u_{a,b,c}\in L, v_{a',b',c'}\notin L$ and $u_{a,b,c}\notin M, v_{a',b',c'}\in M$.

Definition 2.14:12A neutrosophic topological space $(U,\tau_{N_{tr}})$ is said to be a $\boldsymbol{N_{tr}T_2-}$ **space** or neutrosophichausdorff space if for every pair of neutrosophic points $u_{a,b,c}$and $v_{a',b',c'}, u\neq v$, there exists N_{tr}open sets L and M in $(U,\tau_{N_{tr}})$ such that $u_{a,b,c}\in L, v_{a',b',c'}\in M$ and $L\subseteq M^c$.

Neutrosophic$\boldsymbol{\Upsilon-T_0}$ Spaces

Definition 3.1: A neutrosophic topological space $(U,\tau_{N_{tr}})$ is said to be$N_{tr}\Upsilon-T_0$ if for each pair of$N_{tr}Pu_{a,b,c}$and $v_{a',b',c'}, u\neq v$ in U, there exists$N_{tr}\Upsilon OSL$ in $(U,\tau_{N_{tr}})$ such that $u_{a,b,c}\in L, v_{a',b',c'}\notin L$ or $u_{a,b,c}\notin L, v_{a',b',c'}\in L$.

Example 3.2: Let $U=\{u,v\}$and$\tau_{N_{tr}}=\{0_{N_{tr}},1_{N_{tr}},\mathcal{L}\}$ where

$\mathcal{L}=\{\{<u,a,b,c><v,0,0,1>\}: 0<a\leq 1, 0<b\leq 1, 0\leq c<1\}$is the collection of neutrosophic sets in U. Clearly, $(U,\tau_{N_{tr}})$ is a $N_{tr}\Upsilon-T_0$ space.

Theorem 3.3: Every $N_{tr}T_0$ −space is $N_{tr}\Upsilon-T_0$.

Proof: Let $(U,\tau_{N_{tr}})$ be a $N_{tr}T_0$ −space. Then, for each pair of$N_{tr}Pu_{a,b,c}$and $v_{a',b',c'}, u\neq v$, there exists$N_{tr}OSL$ in $(U,\tau_{N_{tr}})$ such that $u_{a,b,c}\in L, v_{a',b',c'}\notin L$ or $u_{a,b,c}\notin L, v_{a',b',c'}\in L$. By theorem 2.7, $L$is $N_{tr}\Upsilon O$. Hence $(U,\tau_{N_{tr}})$ is $N_{tr}\Upsilon-T_0$.

The following example substantiates that the inverse of the above theorem need not be true.

Example 3.4: Let $U=\{u,v\}$and$\tau_{N_{tr}}=\{0_{N_{tr}},1_{N_{tr}},\mathcal{L}\}$ where

$\mathcal{L}=\{\{<u,a,b,1-a><v,0,0,1>\}: a,b\in(0,0.5]\}$is the collection of neutrosophic sets in U. Clearly, $(U,\tau_{N_{tr}})$ is $N_{tr}\Upsilon-T_0$. Now, for $u_{0.7,0.4,0.3}$and $v_{0.2,0.3,0.7}, u\neq v$ in U,there exists$N_{tr}\Upsilon OS\{<u,0.5,0.5,0.5><v,1,1,0>\}$ containing $v_{0.2,0.3,0.7}$ but not $u_{0.7,0.4,0.3}$. However, there is no $N_{tr}OSL$ such that $u_{0.7,0.4,0.3}\in L, v_{0.2,0.3,0.7}\notin L$ or $u_{0.7,0.4,0.3}\notin L, v_{0.2,0.3,0.7}\in L$. Therefore $(U,\tau_{N_{tr}})$ is not a $N_{tr}T_0$ −space.

Definition 3.5: The neutrosophicΥ −kernel of a neutrosophic set L in $(U,\tau_{N_{tr}})$ is the intersection of all $N_{tr}\Upsilon$ −open supersets of$L$.It is denoted by $N_{tr}\Upsilon ker(L)$.

Theorem 3.6: A neutrosophic topological space $(U,\tau_{N_{tr}})$ is $N_{tr}\Upsilon-T_0$if and only if for every pair $u_{a,b,c}$and $v_{a',b',c'}, u\neq v$ in U, either $u_{a,b,c}\notin N_{tr}\Upsilon ker(v_{a',b',c'})$ or $v_{a',b',c'}\notin N_{tr}\Upsilon ker(u_{a,b,c})$.

Proof: Let U be a $N_{tr}\Upsilon-T_0$ space. Then, for every pair of $N_{tr}Pu_{a,b,c}$and $v_{a',b',c'}, u\neq v$ in U, there exists$N_{tr}\Upsilon OSL$ in U such that $u_{a,b,c}\in L, v_{a',b',c'}\notin L$ or $u_{a,b,c}\notin L, v_{a',b',c'}\in L$. Now, $u_{a,b,c}\in L, v_{a',b',c'}\notin L\Longrightarrow v_{a',b',c'}\notin N_{tr}\Upsilon ker(u_{a,b,c})$ for suppose $v_{a',b',c'}\in N_{tr}\Upsilon ker(u_{a,b,c})$,there exists no $N_{tr}\Upsilon OSL$ in U such that $u_{a,b,c}\in L, v_{a',b',c'}\notin L$ which is a contradiction. Similarly, $u_{a,b,c}\notin L, v_{a',b',c'}\in L\Longrightarrow u_{a,b,c}\notin N_{tr}\Upsilon ker(v_{a',b',c'})$. Conversely, suppose $u_{a,b,c}\notin N_{tr}\Upsilon ker(v_{a',b',c'})$ or $v_{a',b',c'}\notin N_{tr}\Upsilon ker(u_{a,b,c})$ for all $u_{a,b,c}$and $v_{a',b',c'}, u\neq v$ in U. Then, there exists$N_{tr}\Upsilon OSL$ in U such that $u_{a,b,c}\notin L, v_{a',b',c'}\in L$ or $u_{a,b,c}\in L, v_{a',b',c'}\notin L$. Hence U is $N_{tr}\Upsilon-T_0$.

Theorem 3.7: Let $f_{N_{tr}}:(U,\tau_{N_{tr}})\longrightarrow(V,\rho_{N_{tr}})$ be ainjective$N_{tr}\Upsilon$ −continuous function. If $(V,\rho_{N_{tr}})$ is $N_{tr}T_0$, then $(U,\tau_{N_{tr}})$ is $N_{tr}\Upsilon-T_0$.

Proof: Let $u_{1_{a,b,c}}$ and $u_{2_{a,b,c}}, u_1\neq u_2$ be any two $N_{tr}P$in U. Since $f_{N_{tr}}$ is injective, there exists $N_{tr}Pv_{1_{a,b,c}}$ and $v_{2_{a,b,c}}$ in V such that $f_{N_{tr}}(u_{1_{a,b,c}})=v_{1_{a,b,c}}, f_{N_{tr}}(u_{2_{a,b,c}})=v_{2_{a,b,c}}$ and $v_1\neq v_2$. Hence $u_{1_{a,b,c}}=f_{N_{tr}}^{-1}(v_{1_{a,b,c}})$ and $u_{2_{a,b,c}}=f_{N_{tr}}^{-1}(v_{2_{a,b,c}})$. Now, since V is $N_{tr}T_0$, there exists$N_{tr}OSL$ in V such that $v_{1_{a,b,c}}\in L, v_{2_{a,b,c}}\notin L$ or $v_{1_{a,b,c}}\notin L, v_{2_{a,b,c}}\in L$. Again, since $f_{N_{tr}}$ is $N_{tr}\Upsilon$ −continuous, $f_{N_{tr}}^{-1}(L)$ is $N_{tr}\Upsilon O$ in U. Also, $v_{1_{a,b,c}}\in L\Longrightarrow f_{N_{tr}}^{-1}(v_{1_{a,b,c}})\in f_{N_{tr}}^{-1}(L)\Longrightarrow u_{1_{a,b,c}}\in f_{N_{tr}}^{-1}(L)$ and $v_{2_{a,b,c}}\notin L\Longrightarrow$

$u_{2_{a,b,c}} \notin f_{N_{tr}}^{-1}(L)$. Hence, for any two $N_{tr}Pu_{1_{a,b,c}}$ and $u_{2_{a,b,c}}, u_1 \neq u_2$ in U, there exists$N_{tr}\Upsilon OSf_{N_{tr}}^{-1}(L)$ in U such that $u_{1_{a,b,c}} \in f_{N_{tr}}^{-1}(L), u_{2_{a,b,c}} \notin f_{N_{tr}}^{-1}(L)$ or $u_{1_{a,b,c}} \notin f_{N_{tr}}^{-1}(L), u_{2_{a,b,c}} \in f_{N_{tr}}^{-1}(L)$. Therefore, U is $N_{tr}\Upsilon - T_0$.

Theorem 3.8: Let $f_{N_{tr}}: (U, \tau_{N_{tr}}) \longrightarrow (V, \rho_{N_{tr}})$ be a one-one $N_{tr}\Upsilon$ −irresolute function. If $(V, \rho_{N_{tr}})$ is $N_{tr}\Upsilon - T_0$, then $(U, \tau_{N_{tr}})$ is $N_{tr}\Upsilon - T_0$.

Proof: Let $u_{1_{a,b,c}}$ and $u_{2_{a,b,c}}, u_1 \neq u_2$ be any two $N_{tr}P$ in U. Since $f_{N_{tr}}$ is one-one, there exists $N_{tr}Pv_{1_{a,b,c}}$ and $v_{2_{a,b,c}}$ in V such that $f_{N_{tr}}(u_{1_{a,b,c}}) = v_{1_{a,b,c}}, f_{N_{tr}}(u_{2_{a,b,c}}) = v_{2_{a,b,c}}$ and $v_1 \neq v_2$. Hence $u_{1_{a,b,c}} = f_{N_{tr}}^{-1}(v_{1_{a,b,c}})$ and $u_{2_{a,b,c}} = f_{N_{tr}}^{-1}(v_{2_{a,b,c}})$. Now, since V is $N_{tr}\Upsilon - T_0$, there exists$N_{tr}\Upsilon OSL$ in V such that $v_{1_{a,b,c}} \in L, v_{2_{a,b,c}} \notin L$ or $v_{1_{a,b,c}} \notin L, v_{2_{a,b,c}} \in L$. Again, since $f_{N_{tr}}$ is $N_{tr}\Upsilon$ −irresolute, $f_{N_{tr}}^{-1}(L)$ is $N_{tr}\Upsilon O$ in U. Also, $v_{1_{a,b,c}} \in L \Longrightarrow f_{N_{tr}}^{-1}(v_{1_{a,b,c}}) \in f_{N_{tr}}^{-1}(L) \Longrightarrow u_{1_{a,b,c}} \in f_{N_{tr}}^{-1}(L)$ and $v_{2_{a,b,c}} \notin L \Longrightarrow u_{2_{a,b,c}} \notin f_{N_{tr}}^{-1}(L)$. Hence, for any two $N_{tr}Pu_{1_{a,b,c}}$ and $u_{2_{a,b,c}}, u_1 \neq u_2$ in U, there exists$N_{tr}\Upsilon OSf_{N_{tr}}^{-1}(L)$ in U such that $u_{1_{a,b,c}} \in f_{N_{tr}}^{-1}(L), u_{2_{a,b,c}} \notin f_{N_{tr}}^{-1}(L)$ or $u_{1_{a,b,c}} \notin f_{N_{tr}}^{-1}(L), u_{2_{a,b,c}} \in f_{N_{tr}}^{-1}(L)$. Therefore, U is $N_{tr}\Upsilon - T_0$.

Theorem 3.9: Let $f_{N_{tr}}: (U, \tau_{N_{tr}}) \longrightarrow (V, \rho_{N_{tr}})$ be a bijective $N_{tr}\Upsilon$ −open function. If $(U, \tau_{N_{tr}})$ is $N_{tr}T_0$, then $(V, \rho_{N_{tr}})$ is $N_{tr}\Upsilon - T_0$.

Proof: Let $v_{1_{a,b,c}}$ and $v_{2_{a,b,c}}, v_1 \neq v_2$ be any two $N_{tr}P$in V. Since $f_{N_{tr}}$ is bijective, there exists $N_{tr}P\, u_{1_{a,b,c}}$ and $u_{2_{a,b,c}}, u_1 \neq u_2$ in$U$ such that $f_{N_{tr}}(u_{1_{a,b,c}}) = v_{1_{a,b,c}}$ and $f_{N_{tr}}(u_{2_{a,b,c}}) = v_{2_{a,b,c}}$. Now, since U is $N_{tr}T_0$, there exist $N_{tr}OSL$ in U such that $u_{1_{a,b,c}} \in L, u_{2_{a,b,c}} \notin L$ or $u_{1_{a,b,c}} \notin L, u_{2_{a,b,c}} \in L$. Since $f_{N_{tr}}$ is $N_{tr}\Upsilon$ −open, $f_{N_{tr}}(L)$ is $N_{tr}\Upsilon O$ in V. Also, $u_{1_{a,b,c}} \in L \Longrightarrow f_{N_{tr}}(u_{1_{a,b,c}}) \in f_{N_{tr}}(L) \Longrightarrow v_{1_{a,b,c}} \in f_{N_{tr}}(L)$ and $u_{2_{a,b,c}} \notin L \Longrightarrow v_{1_{a,b,c}} \notin f_{N_{tr}}(L)$. Hence, for any two $N_{tr}Pv_{1_{a,b,c}}$ and $v_{2_{a,b,c}}, v_1 \neq v_2$ in V, there exists$N_{tr}\Upsilon OS\, f_{N_{tr}}(L)$ in V such that $v_{1_{a,b,c}} \in f_{N_{tr}}(L), v_{2_{a,b,c}} \notin f_{N_{tr}}(L)$ or $v_{1_{a,b,c}} \notin f_{N_{tr}}(L), v_{2_{a,b,c}} \in f_{N_{tr}}(L)$. Therefore, V is $N_{tr}\Upsilon - T_0$.

Neutrosophic $\Upsilon - T_1$ Spaces

Definition 4.1: A neutrosophic topological space $(U, \tau_{N_{tr}})$ is said to be$N_{tr}\Upsilon - T_1$ if for every pair of $N_{tr}Pu_{a,b,c}$and $v_{a',b',c'}, u \neq v$, there exist $N_{tr}\Upsilon OSL$ and M in $(U, \tau_{N_{tr}})$ such that $u_{a,b,c} \in L, v_{a',b',c'} \notin L$ and $u_{a,b,c} \notin M, v_{a',b',c'} \in M$.

Example 4.2: Let $U = \{u, v\}, \tau_{N_{tr}} = \{0_{N_{tr}}, \mathcal{L}, \mathcal{M}, \mathcal{N}, 1_{N_{tr}}\}$ where

$\mathcal{L} = \{L_i = \{< u, a_i, b_i, c_i >< v, 0,0,1 >\}: 0 < a_i \leq 1, 0 < b_i \leq 1, 0 \leq c_i < 1\}$,

$\mathcal{M} = \{M_i = \{< u, 0,0,1 >< v, a_i', b_i', c_i' >\}: 0 < a_i \leq 1, 0 < b_i \leq 1, 0 \leq c_i < 1\}$and

$\mathcal{N} = \{L_i \cup M_i : L_i \in \mathcal{L}, M_i \in \mathcal{M}\}$are collections of neutrosophic sets in U.

Clearly, $(U, \tau_{N_{tr}})$ is a $N_{tr}\Upsilon - T_1$space.

Theorem 4.3: Every $N_{tr}T_1$ −space is $N_{tr}\Upsilon - T_1$.

Proof: Proof follows from theorem 2.7.

However, the ensuing example reveals that the reverse implication need not hold.

Example 4.4: Let $U = \{u, v\}, \tau_{N_{tr}} = \{0_{N_{tr}}, L_1, L_2, L_3, 1_{N_{tr}}\}$ where $L_1 = \{< u, 0.4,0.3,0.2 >< v, 0.5,0.3,0.3 >\}, L_2 = \{< u, 0.5,0.3,0.2 >< v, 0.4,0.3,0.2 >\}andL_3 = \{< u, 0.5,0.3,0.2 >< v, 0.5,0.3,0.2 >\}$. Clearly, $(U, \tau_{N_{tr}})$is$N_{tr}\Upsilon - T_1$. Now, for $u_{0.5,0.2,0.7}$and $v_{0.2,0.8,0.4}$ in U, there exist$N_{tr}\Upsilon OSL_2$ and $M = \{< u, 0.4,0.7,0.2 >< v, 0.5,0.9,0.2 >\}$ such that $u_{0.5,0.2,0.7} \in L_2 v_{0.2,0.8,0.4} \notin L_2$ and $u_{0.5,0.2,0.7} \notin M, v_{0.2,0.8,0.4} \in M$. However, there is no $N_{tr}OSL$ in U such that $u_{0.5,0.2,0.7} \notin L, v_{0.2,0.8,0.4} \in L$. Hence $(U, \tau_{N_{tr}})$ is not a $N_{tr}T_1$ −space.

Theorem 4.5: Every $N_{tr}\Upsilon - T_1$ space $N_{tr}\Upsilon - T_0$, but not conversely.

Example 4.6: Consider example 3.4 in which the neutrosophic topological space $(U, \tau_{N_{tr}})$is $N_{tr}\Upsilon - T_0$. Now, for any two $N_{tr}Pu_{0.7,0.4,0.3}$and$v_{0.2,0.3,0.7}, u \neq v$ in U, there exists a $N_{tr}\Upsilon OS\{< u, 0.5,0.5,0.5 >< v, 1,1,0 >\}$ containing $v_{0.2,0.3,0.7}$ but not $u_{0.7,0.4,0.3}$. However, there is no $N_{tr}\Upsilon OSL$ such that $u_{0.7,0.4,0.3} \in L$ and $v_{0.2,0.3,0.7} \notin L$. Hence $(U, \tau_{N_{tr}})$ is not $N_{tr}\Upsilon - T_1$.

Theorem 4.7: A neutrosophic topological space$(U, \tau_{N_{tr}})$ is $N_{tr}\Upsilon - T_1$ if and only if for each$N_{tr}Pu_{a,b,c}$ in $U, N_{tr}\Upsilon ker(u_{a,b,c}) = u_{p,q,r}, a \leq p; b \leq q; c \geq r$.

Proof: Let U be a $N_{tr}\Upsilon - T_1$ space and $N_{tr}\Upsilon ker(u_{a,b,c}) \neq u_{p,q,r}, a \leq p; b \leq q; c \geq r$. Then, there exists a $N_{tr}Pv_{a',b',c'}, u \neq v$ such that $v_{a',b',c'} \in N_{tr}\Upsilon ker(u_{a,b,c})$. This ensures that there exists a $N_{tr}\Upsilon OSL$in U such that $u_{a,b,c} \in L$ and$v_{a',b',c'} \in L$ which is a contradiction. Conversely, suppose $N_{tr}\Upsilon ker(u_{a,b,c}) = u_{p,q,r}, a \leq p; b \leq q; c \geq r$ and U is not $N_{tr}\Upsilon - T_1$.

Then, for every $u_{a,b,c}$and $v_{a',b',c'}, u \neq v$, there exists a$N_{tr}\Upsilon OSL$ in U containing $v_{a',b',c'}$ whenever $u_{a,b,c} \in L$. Hence $v_{a',b',c'} \in N_{tr}\Upsilon ker(u_{a,b,c})$ which is a contradiction. Therefore U is a $N_{tr}\Upsilon - T_1$space.

Theorem 4.8: A neutrosophic topological space $(U, \tau_{N_{tr}})$ is $N_{tr}\Upsilon - T_1$ if and only if for every pair $u_{a,b,c}$and $v_{a',b',c'}, u \neq v$ in $U, u_{a,b,c} \notin N_{tr}\Upsilon ker(v_{a',b',c'})$ and $v_{a',b',c'} \notin N_{tr}\Upsilon ker(u_{a,b,c})$.
Proof: Proof is similar to theorem 3.6
Theorem 4.9: A neutrosophic topological space $(U, \tau_{N_{tr}})$ is $N_{tr}\Upsilon - T_1$ iff for every $u_{a,b,c}, v_{a',b',c'}, u \neq v$ in $U, N_{tr}\Upsilon ker(u_{a,b,c}) \cap N_{tr}\Upsilon ker(v_{a',b',c'}) = 0_{N_{tr}}$
Proof: Let U be a $N_{tr}\Upsilon - T_1$ space. Then, by theorem 4.8, for each$u_{a,b,c}$and $v_{a',b',c'}, u \neq v$ in $U, u_{a,b,c} \notin N_{tr}\Upsilon ker(v_{a',b',c'})$ and $v_{a',b',c'} \notin N_{tr}\Upsilon ker(u_{a,b,c})$. Hence $N_{tr}\Upsilon ker(u_{a,b,c}) \cap N_{tr}\Upsilon ker(v_{a',b',c'}) = 0_{N_{tr}}$. Conversely, suppose U is not $N_{tr}\Upsilon - T_1$ Then, for each $u_{a,b,c}$and $v_{a',b',c'}, u \neq v$ in U, either $u_{a,b,c} \in N_{tr}\Upsilon ker(v_{a',b',c'})$ or $v_{a',b',c'} \in N_{tr}\Upsilon ker(u_{a,b,c})$. This implies that $N_{tr}\Upsilon ker(u_{a,b,c}) \cap N_{tr}\Upsilon ker(v_{a',b',c'}) \neq 0_{N_{tr}}$ which is a contradiction. Hence U is a $N_{tr}\Upsilon - T_1$space.

Theorem 4.10: Let $f_{N_{tr}}: (U, \tau_{N_{tr}}) \longrightarrow (V, \rho_{N_{tr}})$ be a function between two neutrosophic topological spaces.
(i) If $f_{N_{tr}}$is $N_{tr}\Upsilon$ −open bijective and $(U, \tau_{N_{tr}})$ is $N_{tr}T_1$, then $(V, \rho_{N_{tr}})$ is $N_{tr}\Upsilon - T_1$.
(ii) If $f_{N_{tr}}$is one-one,$N_{tr}\Upsilon$ −continuous and $(V, \rho_{N_{tr}})$ is $N_{tr}T_1$, then $(U, \tau_{N_{tr}})$ is $N_{tr}\Upsilon - T_1$.
(iii)If $f_{N_{tr}}$is one-one,$N_{tr}\Upsilon$ −irresolute and $(V, \rho_{N_{tr}})$ is $N_{tr}\Upsilon - T_1$, then $(U, \tau_{N_{tr}})$is $N_{tr}\Upsilon - T_1$.
Proof:
(i) Let $v_{1_{a,b,c}}$ and $v_{2_{a,b,c}}, v_1 \neq v_2$ be any two $N_{tr}P$ in V. Since $f_{N_{tr}}$ is bijective, there exists$N_{tr}Pu_{1_{a,b,c}}$ and $u_{2_{a,b,c}}, u_1 \neq u_2$ in$U$ such that $f_{N_{tr}}(u_{1_{a,b,c}}) = v_{1_{a,b,c}}$ and $f_{N_{tr}}(u_{2_{a,b,c}}) = v_{2_{a,b,c}}$. Now, since U is $N_{tr}T_1$, there exist $N_{tr}OSL$ and M in U such that $u_{1_{a,b,c}} \in L, u_{2_{a,b,c}} \notin L$ and $u_{1_{a,b,c}} \notin M, u_{2_{a,b,c}} \in M$. Since $f_{N_{tr}}$ is $N_{tr}\Upsilon$ −open, $f_{N_{tr}}(L)$and $f_{N_{tr}}(M)$ are $N_{tr}\Upsilon O$ in V. Also, $u_{1_{a,b,c}} \in L \Longrightarrow f_{N_{tr}}(u_{1_{a,b,c}}) \in f_{N_{tr}}(L) \Longrightarrow v_{1_{a,b,c}} \in f_{N_{tr}}(L)$ and $u_{2_{a,b,c}} \notin L \Longrightarrow v_{2_{a,b,c}} \notin f_{N_{tr}}(L)$. Similarly, $v_{1_{a,b,c}} \notin f_{N_{tr}}(M)$and $v_{2_{a,b,c}} \in f_{N_{tr}}(M)$. Hence, for any two $N_{tr}Pv_{1_{a,b,c}}$ and $v_{2_{a,b,c}}, v_1 \neq v_2$ in V, there exists $N_{tr}\Upsilon OSf_{N_{tr}}(L)$ in V such that $v_{1_{a,b,c}} \in f_{N_{tr}}(L), v_{2_{a,b,c}} \notin f_{N_{tr}}(L)$ and $v_{1_{a,b,c}} \notin f_{N_{tr}}(M), v_{2_{a,b,c}} \in f_{N_{tr}}(M)$. Therefore, V is $N_{tr}\Upsilon - T_1$.
(ii) Let $u_{1_{a,b,c}}$ and $u_{2_{a,b,c}}, u_1 \neq u_2$ be any two $N_{tr}P$ in U. Since $f_{N_{tr}}$ is one-one, there exists $N_{tr}Pv_{1_{a,b,c}}$ and $v_{2_{a,b,c}}$ in V such that $f_{N_{tr}}(u_{1_{a,b,c}}) = v_{1_{a,b,c}}, f_{N_{tr}}(u_{2_{a,b,c}}) = v_{2_{a,b,c}}$ and $v_1 \neq v_2$. Hence $u_{1_{a,b,c}} = f_{N_{tr}}^{-1}(v_{1_{a,b,c}})$ and $u_{2_{a,b,c}} = f_{N_{tr}}^{-1}(v_{2_{a,b,c}})$. Now, since V is $N_{tr}T_1$, there exist$N_{tr}OSL$ and M in V such that $v_{1_{a,b,c}} \in L, v_{2_{a,b,c}} \notin L$ and $v_{1_{a,b,c}} \notin M, v_{2_{a,b,c}} \in M$. Again, since $f_{N_{tr}}$ is $N_{tr}\Upsilon$ −continuous, $f_{N_{tr}}^{-1}(L)$ and $f_{N_{tr}}^{-1}(M)$ are $N_{tr}\Upsilon O$ in U. Also, $v_{1_{a,b,c}} \in L \Longrightarrow f_{N_{tr}}^{-1}(v_{1_{a,b,c}}) \in f_{N_{tr}}^{-1}(L) \Longrightarrow u_{1_{a,b,c}} \in f_{N_{tr}}^{-1}(L)$ and $v_{2_{a,b,c}} \notin L \Longrightarrow u_{2_{a,b,c}} \notin f_{N_{tr}}^{-1}(L)$. Similarly, $v_{1_{a,b,c}} \notin M \Longrightarrow u_{1_{a,b,c}} \notin f_{N_{tr}}^{-1}(M)$and $v_{2_{a,b,c}} \in M \Longrightarrow u_{2_{a,b,c}} \in f_{N_{tr}}^{-1}(M)$. Hence, for any two $N_{tr}Pu_{1_{a,b,c}}$ and $u_{2_{a,b,c}}, u_1 \neq u_2$ in U, there exist$N_{tr}\Upsilon OSf_{N_{tr}}^{-1}(L)$ and $f_{N_{tr}}^{-1}(M)$ in U such that $u_{1_{a,b,c}} \in f_{N_{tr}}^{-1}(L), u_{2_{a,b,c}} \notin f_{N_{tr}}^{-1}(L)$ and $u_{1_{a,b,c}} \notin f_{N_{tr}}^{-1}(M), u_{2_{a,b,c}} \in f_{N_{tr}}^{-1}(M)$. Therefore, U is $N_{tr}\Upsilon - T_1$.
(iii) Proof is similar to (ii).

Neutrosophic $\Upsilon - T_2$ Spaces
Definition 5.1: A neutrosophic topological space $(U, \tau_{N_{tr}})$ is said to be$N_{tr}\Upsilon - T_2$ or $N_{tr}\Upsilon$ −hausdorff if for every pair of $N_{tr}Pu_{a,b,c}$and $v_{a',b',c'}, u \neq v$, there exist $N_{tr}\Upsilon OSL$ and M in $(U, \tau_{N_{tr}})$ such that $u_{a,b,c} \in L, v_{a',b',c'} \in M$ and $L \cap M = 0_{N_{tr}}$.

Example 5.2: Let $U = \{u, v\}, \tau_{N_{tr}} = \{0_{N_{tr}}, L_1, L_2, 1_{N_{tr}}\}$ where $L_1 = \{< u, 1,1,0 >< v, 0,0,1 >\}$ and $L_2 = \{< u, 0,0,1 >< v, 1,1,0 >\}$.Clearly, $(U, \tau_{N_{tr}})$ is a $N_{tr}\Upsilon - T_2$ space.
Theorem 5.3: Every $N_{tr}\Upsilon - T_2$ space $N_{tr}\Upsilon - T_1$.
Proof: Let $u_{a,b,c}, v_{a',b',c'}, u \neq v$ be any two $N_{tr}P$ in U. Since U is $N_{tr}\Upsilon - T_2$, there exist $N_{tr}\Upsilon OSL$ and M in $(U, \tau_{N_{tr}})$ such that $u_{a,b,c} \in L, v_{a',b',c'} \in M$ and $L \cap M = 0_{N_{tr}}$. Since $u_{a,b,c} \in L$ and $L \cap M = 0_{N_{tr}}, u_{a,b,c} \notin M$. Similarly, $v_{a',b',c'} \notin L$. Hence there exist $N_{tr}\Upsilon OSL$ and M in $(U, \tau_{N_{tr}})$ such that $u_{a,b,c} \in L, v_{a',b',c'} \notin L$ and $u_{a,b,c} \notin M, v_{a',b',c'} \in M$. Therefore U is $N_{tr}\Upsilon - T_1$.
The following example substantiates that the inverse of the above theorem need not be true.

Example 5.4: Consider example 4.4 in which the neutrosophic topological space $(U, \tau_{N_{tr}})$is $N_{tr}\Upsilon - T_1$. Now, for$u_{0.5,0.2,0.7}$and $v_{0.2,0.8,0.4}$ in U, there exist$N_{tr}\Upsilon OSL = \{< u, 0.5,0.3,0.2 >< v, 0.4,0.3,0.2 >\}$ and $M = \{< u, 0.4,0.7,0.2 >< v, 0.5,0.9,0.2 >\}$ such that $u_{0.5,0.2,0.7} \in L v_{0.2,0.8,0.4} \notin L$ and $u_{0.5,0.2,0.7} \notin M, v_{0.2,0.8,0.4} \in M$. However, $L \cap M \neq 0_{N_{tr}}$. Therefore U is not $N_{tr}\Upsilon - T_2$.

Definition 5.5: A neutrosophic topological space $(U, \tau_{N_{tr}})$ is said to be$N_{tr}\Upsilon - qT_2$ or $N_{tr}\Upsilon -$quasi hausdorff if for every pair of $N_{tr}Pu_{a,b,c}$and $v_{a',b',c'}, u \neq v$, there exist$N_{tr}\Upsilon OSL$ and M in $(U, \tau_{N_{tr}})$ such that $u_{a,b,c} \in L, v_{a',b',c'} \in M$ and $L\tilde{q}M$.

Example 5.6: Let $U = \{u, v\}, \tau_{N_{tr}} = \{0_{N_{tr}}, L_1, L_2, L_3, L_4, 1_{N_{tr}}\}$ where $L_1 = \{< u, 0.3,0.8,0.4 >< v, 0,0,1 >\}, L_2 = \{< u, 0,0.9,1 >< v, 0.4,0.2,0.1 >\}, L_3 = \{< u, 0,0.8,1 >< v, 0,0,1 >\}$and $L_4 = \{< u, 0.3,0.9,0.4 >< v, 0.4,0.2,0.1 >\}$.Clearly, $(U, \tau_{N_{tr}})$ is a $N_{tr}\Upsilon - qT_2$ space.

Theorem 5.7: Every $N_{tr}T_2$ −space is $N_{tr}\Upsilon - qT_2$.
Proof: Proof follows from theorem 2.7
However, the ensuing example reveals that the reverse implication need not hold.
Example 5.8: Let $U = \{u, v\}, \tau_{N_{tr}} = \{0_{N_{tr}}, L_1, L_2, L_3, 1_{N_{tr}}\}$ where $L_1 = \{< u, 0.3,0.4,0.1 >< v, 0,0,1 >\}, L_2 = \{< u, 0,0,1 >< v, 0.4,0.2,0.1 >\}, L_3 = \{< u, 0.3,0.4,0.1 >< v, 0.2,0.4,0.1 >\}$. Clearly, $(U, \tau_{N_{tr}})$is $N_{tr}\Upsilon - qT_2$. Now, for $u_{0.4,0.1,0.6}$ and $v_{0.2,0.7,0.3}$ in U, there exists $N_{tr}\Upsilon OSM = \{< u, 0.5,0.4,0.1 >< v, 0,0,1 >\}, N = \{< u, 0,0,1 >< v, 0.4,0.9,0.1 >\}$ such that $u_{0.4,0.1,0.6} \in M, v_{0.2,0.7,0.3} \in N$ and$M\tilde{q}N$.However, there exists no $N_{tr}OSL_i, L_j$ in U such that $u_{0.4,0.1,0.6} \in L_i, v_{0.2,0.7,0.3} \in L_j$ and $L_i\tilde{q}L_j$for some$i, j = 1,2,3$. Hence $(U, \tau_{N_{tr}})$ is not $N_{tr}T_2 -$ space.

Theorem 5.9: A neutrosophic topological space $(U, \tau_{N_{tr}})$ is $N_{tr}\Upsilon - qT_2$ if and only if for every $N_{tr}Pv_{a',b',c'}$ distinct from $u_{a,b,c}$, there exists$N_{tr}\Upsilon OSL$ containing $u_{a,b,c}$ such that $v_{a',b',c'}\hat{q}N_{tr}\Upsilon cl(L)$.
Proof: Let U be a $N_{tr}\Upsilon - qT_2$ space and $u_{a,b,c}, v_{a',b',c'}$be $N_{tr}P$ in U. Since U is $N_{tr}\Upsilon - qT_2$ and $u \neq v$, there exists $N_{tr}\Upsilon OSL$ and M in U such that $u_{a,b,c} \in L, v_{a',b',c'} \in M$ and $L\hat{q}M. L\hat{q}M \Rightarrow L \subseteq M^c \Rightarrow N_{tr}\Upsilon cl(L) \subseteq M^c \Rightarrow M \subseteq (N_{tr}\Upsilon cl(L))^c \Rightarrow v_{a',b',c'} \in (N_{tr}\Upsilon cl(L))^c$. Hence $v_{a',b',c'}\hat{q}N_{tr}\Upsilon cl(L)$. Conversely, suppose for every $N_{tr}Pv_{a',b',c'}$ distinct from $u_{a,b,c}$, there exists $N_{tr}\Upsilon OSL$ such that$u_{a,b,c} \in L$ and$v_{a',b',c'}\hat{q}N_{tr}\Upsilon cl(L)$. Then, for every pair of $N_{tr}Pu_{a,b,c}$ and $v_{a',b',c'}, u \neq v$, there exist $N_{tr}\Upsilon OSL$ and $M = (N_{tr}\Upsilon cl(L))^c$ such that $u_{a,b,c} \in L$, $v_{a',b',c'} \in M$ and $L \subseteq M^c$. Hence U is a $N_{tr}\Upsilon - qT_2$ space.

Theorem 5.10: Let $f_{N_{tr}}: (U, \tau_{N_{tr}}) \rightarrow (V, \rho_{N_{tr}})$ be a function between two neutrosophic topological spaces.
(i)If $f_{N_{tr}}$is $N_{tr}\Upsilon -$open bijective and $(U, \tau_{N_{tr}})$ is $N_{tr}T_2$, then $(V, \rho_{N_{tr}})$ is $N_{tr}\Upsilon - T_2$.
(ii) If $f_{N_{tr}}$is one-one,$N_{tr}\Upsilon -$continuous and $(V, \rho_{N_{tr}})$ is $N_{tr}T_2$, then $(U, \tau_{N_{tr}})$ is $N_{tr}\Upsilon - T_2$.
(iii) If $f_{N_{tr}}$is one-one,$N_{tr}\Upsilon -$irresolute and $(V, \rho_{N_{tr}})$ is $N_{tr}\Upsilon - T_2$,then $(U, \tau_{N_{tr}})$is $N_{tr}\Upsilon - T_2$.

Proof:
(i) Let $v_{1_{a,b,c}}$ and $v_{2_{a,b,c}}, v_1 \neq v_2$ be any two $N_{tr}P$ in V. Since $f_{N_{tr}}$ is bijective, there exists $N_{tr}Pu_{1_{a,b,c}}$ and $u_{2_{a,b,c}}, u_1 \neq u_2$ in$U$ such that $f_{N_{tr}}(u_{1_{a,b,c}}) = v_{1_{a,b,c}}$ and $f_{N_{tr}}(u_{2_{a,b,c}}) = v_{2_{a,b,c}}$. Now, since U is $N_{tr}T_2$, there exist$N_{tr}OSL$ and M in U such that $u_{1_{a,b,c}} \in L, u_{2_{a,b,c}} \in M$ and $L \cap M = 0_{N_{tr}}$. Since $f_{N_{tr}}$ is $N_{tr}\Upsilon -$open, $f_{N_{tr}}(L)$and $f_{N_{tr}}(M)$ are $N_{tr}\Upsilon O$ in V.Also, $u_{1_{a,b,c}} \in L \Rightarrow f_{N_{tr}}(u_{1_{a,b,c}}) \in f_{N_{tr}}(L) \Rightarrow v_{1_{a,b,c}} \in f_{N_{tr}}(L)$ and $u_{2_{a,b,c}} \in M \Rightarrow v_{2_{a,b,c}} \in f_{N_{tr}}(M)$.Hence, for any two $N_{tr}Pv_{1_{a,b,c}}$ and $v_{2_{a,b,c}}, v_1 \neq v_2$ in V, there exist $N_{tr}\Upsilon OSf_{N_{tr}}(L)$and $f_{N_{tr}}(M)$ in V such that $v_{1_{a,b,c}} \in f_{N_{tr}}(L), v_{2_{a,b,c}} \in f_{N_{tr}}(M)$and $f_{N_{tr}}(L) \cap f_{N_{tr}}(M) = 0_{N_{tr}}$. Therefore, V is $N_{tr}\Upsilon - T_2$.
(ii)Let $u_{1_{a,b,c}}$ and $u_{2_{a,b,c}}, u_1 \neq u_2$ be any two $N_{tr}P$ in U. Since $f_{N_{tr}}$ is one-one, there exists $N_{tr}Pv_{1_{a,b,c}}$ and $v_{2_{a,b,c}}$ in V such that $f_{N_{tr}}(u_{1_{a,b,c}}) = v_{1_{a,b,c}}, f_{N_{tr}}(u_{2_{a,b,c}}) = v_{2_{a,b,c}}$ and $v_1 \neq v_2$.Then, $u_{1_{a,b,c}} = f_{N_{tr}}^{-1}(v_{1_{a,b,c}})$ and $u_{2_{a,b,c}} = f_{N_{tr}}^{-1}(v_{2_{a,b,c}})$. Now, since V is $N_{tr}T_2$, there exist$N_{tr}OSL$ and M in V such that $v_{1_{a,b,c}} \in L, v_{2_{a,b,c}} \in M$ and $L \cap M = 0_{N_{tr}}$.Again, since $f_{N_{tr}}$ is $N_{tr}\Upsilon -$continuous, $f_{N_{tr}}^{-1}(L)$ and $f_{N_{tr}}^{-1}(M)$ are $N_{tr}\Upsilon O$ in U. Also, $v_{1_{a,b,c}} \in L \Rightarrow f_{N_{tr}}^{-1}(v_{1_{a,b,c}}) \in f_{N_{tr}}^{-1}(L) \Rightarrow u_{1_{a,b,c}} \in f_{N_{tr}}^{-1}(L)$. Similarly, $v_{2_{a,b,c}} \in M \Rightarrow u_{2_{a,b,c}} \in f_{N_{tr}}^{-1}(M)$. Hence, for any two $N_{tr}Pu_{1_{a,b,c}}$ and $u_{2_{a,b,c}}, u_1 \neq u_2$ in U, there exist

$N_{tr}\Upsilon OSf_{N_{tr}}^{-1}(L)$ and $f_{N_{tr}}^{-1}(M)$ in U such that $u_{1_{a,b,c}} \in f_{N_{tr}}^{-1}(L), u_{2_{a,b,c}} \in f_{N_{tr}}^{-1}(M)$ and $f_{N_{tr}}^{-1}(L) \cap f_{N_{tr}}^{-1}(M) = 0_{N_{tr}}$. Therefore, $U$is $N_{tr}\Upsilon - T_2$.
(iii) Proof is similar to (ii).

Theorem 5.11: Let $(U, \tau_{N_{tr}})$ be a $N_{tr}\Upsilon - T_i$ $(i = 0,1,2)$ space in which the class of all $N_{tr}\Upsilon OS$ is closed under finite intersection. Then every neutrosophic open subspace of $(U, \tau_{N_{tr}})$ is also a $N_{tr}\Upsilon - T_i$ $(i = 0,1,2)$ space.
Proof: We shall prove for $i = 0$.The other cases$(i = 1, 2)$ can be proved in a similar way.
Let $(S, \tau_{N_{tr}}^S)$ be a neutrosophic open subspace of $(U, \tau_{N_{tr}}), u_{a,b,c}$ and $v_{a',b',c'}, u \neq v$ be any two $N_{tr}P$in S. Then $u_{a,b,c}$ and $v_{a',b',c'}, u \neq v$ are $N_{tr}P$ in U. Since U is $N_{tr}\Upsilon - T_0$, there exists$N_{tr}\Upsilon OSL$ in U such that $u_{a,b,c} \in L, v_{a',b',c'} \notin L$ or $u_{a,b,c} \notin L, v_{a',b',c'} \in L$. Now, without loss of generality, let us assume that $u_{a,b,c} \in L, v_{a',b',c'} \notin L$. Then $u_{a,b,c} \in L \cap 1_{N_{tr}}^S$ and$v_{a',b',c'} \notin L \cap 1_{N_{tr}}^S$. By theorem2.7, $1_{N_{tr}}^S$is $N_{tr}\Upsilon O$ in U and by hypothesis, $L \cap 1_{N_{tr}}^S$ is $N_{tr}\Upsilon O$ in U. By theorem2.8, $L \cap 1_{N_{tr}}^S$ is $N_{tr}\Upsilon O$ in S. Hence there exists$N_{tr}\Upsilon OSL \cap 1_{N_{tr}}^S$ in S such that $u_{a,b,c} \in L \cap 1_{N_{tr}}^Sandv_{a',b',c'} \notin L \cap 1_{N_{tr}}^S$. Therefore $(S, \tau_{N_{tr}}^S)$ is $N_{tr}\Upsilon - T_0$.

In general, a neutrosophic set over a non-empty fixed set U is of the form$L = \{< u, \mu_L(u), \sigma_L(u), \gamma_L(u) >: u \in U\}$ where$\mu_L(u), \sigma_L(u), \gamma_L(u) \epsilon\,]^-0,1^+[$. Henceforth, we consider the neutrosophic sets whose values are confined to the standard unit interval. Such a neutrosophic set L is called a neutrosophic point denoted by$u_{a,b,c}$ if for any element $v \in U, \mu_L(v) = a, \sigma_L(v) = b, \gamma_L(v) = c$ for $v = u$ and $\mu_L(v) = 0, \sigma_L(v) = 0, \gamma_L(v) =$ for $v \neq u$, where $0 < a \leq 1, 0 < b \leq 1$ and $0 \leq c \leq 1$. $u_{a,b,c}$ is called a neutrosophic crisp point$(N_{tr}C_p)$ if $= 0, b = 0, c = 1$.CITATION Ray \l 1033 (Ray G. C., 2021)
Theorem 5.12: A neutrosophic topological space $(U, \tau_{N_{tr}})$ is $N_{tr}\Upsilon - T_0$ if and only if for every pair of $N_{tr}C_p u_{1,1,0}$and $v_{1,1,0}, u \neq v$ in $U, u_{1,1,0}\hat{q}\ N_{tr}\Upsilon cl(v_{1,1,0})$ and $v_{1,1,0}\hat{q}\ N_{tr}\Upsilon cl(v_{1,1,0})$.

Proof: Let U be a $N_{tr}\Upsilon - T_0$ space. Suppose both $u_{1,1,0}\hat{q}\ N_{tr}\Upsilon cl(v_{1,1,0})$ and $v_{1,1,0}\hat{q}\ N_{tr}\Upsilon cl(v_{1,1,0})$ are false. Then $u_{1,1,0}\ q\ N_{tr}\Upsilon cl(v_{1,1,0})$ and $v_{1,1,0}\ q\ N_{tr}\Upsilon cl(u_{1,1,0})$. Now, $u_{1,1,0}\ q\ N_{tr}\Upsilon cl(v_{1,1,0}) \Rightarrow u_{1,1,0} \notin (N_{tr}\Upsilon cl(v_{1,1,0}))^c$. This implies $u_{1,1,0} \notin (\cap\{L : L \in N_{tr}\Upsilon C(U, \tau_{N_{tr}})$ and $v_{1,1,0} \in L\})^c \Rightarrow u_{1,1,0} \notin \cup\{L^c : L^c \in N_{tr}\Upsilon O(U, \tau_{N_{tr}})andv_{1,1,0} \notin L^c\}$. Hence there exists no $N_{tr}\Upsilon OSM$ in U such that $u_{1,1,0} \in M$ and $v_{1,1,0} \notin M$. Similarly, $v_{1,1,0}\ q\ N_{tr}\Upsilon cl(u_{1,1,0})$ensures that there exists no $N_{tr}\Upsilon OSM$ in U such that $u_{1,1,0} \notin M$ and $v_{1,1,0} \in M$. This is a contradiction to our hypothesis. Hence $u_{1,1,0}\hat{q}\ N_{tr}\Upsilon cl(v_{1,1,0})$ and $v_{1,1,0}\hat{q}\ N_{tr}\Upsilon cl(v_{1,1,0})$. Conversely, suppose $u_{1,1,0}\hat{q}\ N_{tr}\Upsilon cl(v_{1,1,0})$ and $v_{1,1,0}\hat{q}\ N_{tr}\Upsilon cl(v_{1,1,0})$. Let $u_{a,b,c}$and $v_{a',b',c'}, u \neq v$ be any two $N_{tr}P$in U. Now, $u_{1,1,0}\hat{q}\ N_{tr}\Upsilon cl(v_{1,1,0}) \Rightarrow u_{1,1,0} \in (N_{tr}\Upsilon cl(v_{1,1,0}))^c$. Then $u_{a,b,c} \in (N_{tr}\Upsilon cl(v_{1,1,0}))^c$. and it is obvious that $v_{a',b',c'} \notin (N_{tr}\Upsilon cl(v_{1,1,0}))^c$. Since $N_{tr}\Upsilon cl(v_{1,1,0})$ is $N_{tr}\Upsilon C, (N_{tr}\Upsilon cl(v_{1,1,0}))^c$ is $N_{tr}\Upsilon O$. Hence there exists $N_{tr}\Upsilon OS\ (N_{tr}\Upsilon cl(v_{1,1,0}))^c$ such that $u_{a,b,c} \in (N_{tr}\Upsilon cl(v_{1,1,0}))^c$ and $v_{a',b',c'} \notin (N_{tr}\Upsilon cl(v_{1,1,0}))^c$. Hence U is a $N_{tr}\Upsilon - T_0$ space.
Theorem 5.13: If $(U, \tau_{N_{tr}})$ isa neutrosophic topological space in which every $N_{tr}P$is $N_{tr}\Upsilon C$, then $(U, \tau_{N_{tr}})$ is a $N_{tr}\Upsilon - T_1$ space.
Proof: Let $u_{a,b,c}$and $v_{a',b',c'}, u \neq v$ be any two $N_{tr}P$ in U. Since $u \neq v, u_{a,b,c} \in (v_{1,1,0})^c$. By assumption, $v_{1,1,0}$is $N_{tr}\Upsilon C$. Therefore $(v_{1,1,0})^c$ is $N_{tr}\Upsilon O$ in U and obviously $v_{a',b',c'} \notin (v_{1,1,0})^c$.Hence there exists a $N_{tr}\Upsilon OS(v_{1,1,0})^c$ such that $u_{a,b,c} \in (v_{1,1,0})^c, v_{a',b',c'} \notin (v_{1,1,0})^c$. Similarly, there exists a $N_{tr}\Upsilon OS(u_{1,1,0})^c$ such that $u_{a,b,c} \notin (u_{1,1,0})^c, v_{a',b',c'} \in (v_{1,1,0})^c$. Hence $(U, \tau_{N_{tr}})$ is $N_{tr}\Upsilon - T_1$.
Remark 5.14: In particular, a neutrosophic topological space is $N_{tr}\Upsilon - T_1$ if every $N_{tr}C_p$in the space is $N_{tr}\Upsilon$ −closed.
Theorem 5.15: Let $(U, \tau_{N_{tr}})$ be a $N_{tr}\Upsilon - qT_2$ space if and only if for every $N_{tr}Pu_{a,b,c}$ in $U, \cap\{N_{tr}\Upsilon cl(L): u_{a,b,c} \in L\ and\ L \in N_{tr}\Upsilon O(U, \tau_{N_{tr}})\} = u_{p,q,r}, a \leq p; b \leq q; c \geq r$.
Proof: Let U be a $N_{tr}\Upsilon - qT_2$ space and $u_{a,b,c}, v_{1,1,0}, u \neq v$ be $N_{tr}P$ in U. Then, by theorem 5.9, there exists a $N_{tr}\Upsilon OSL$ containing $u_{a,b,c}$ such that $v_{1,1,0}\hat{q}N_{tr}\Upsilon cl(L)$. This implies$v_{1,1,0} \in (N_{tr}\Upsilon cl(L))^c \Rightarrow v_{1,1,0} \cap N_{tr}\Upsilon cl(L) = 0_{N_{tr}} \Rightarrow v_{a',b',c'} \cap N_{tr}\Upsilon cl(L) = 0_{N_{tr}} \Rightarrow v_{a',b',c'} \notin N_{tr}\Upsilon cl(L)$. Hence for every $N_{tr}Pv_{a',b',c'}$ distinct from $u_{a,b,c}, v_{a',b',c'} \notin \cap\{N_{tr}\Upsilon cl(L): u_{a,b,c} \in L\ and\ L \in N_{tr}\Upsilon O(U, \tau_{N_{tr}})\}$ Obviously, $u_{a,b,c} \in \cap\{N_{tr}\Upsilon cl(L): u_{a,b,c} \in L\ and\ L \in N_{tr}\Upsilon O(U, \tau_{N_{tr}})\}$ since $u_{a,b,c} \in L$. Therefore $\cap\{N_{tr}\Upsilon cl(L): u_{a,b,c} \in L\ and\ L \in N_{tr}\Upsilon O(U, \tau_{N_{tr}})\} = u_{p,q,r}, a \leq p; b \leq q; c \geq r$. The converse part can be proved by retracing the above steps.

Theorem 5.16: Let $(U, \tau_{N_{tr}})$ be a $N_{tr}\Upsilon - T_2$ space in which every $N_{tr}C_p$is $N_{tr}\Upsilon O$. Then the following assertions hold
(i) for every $N_{tr}Pv_{a',b',c'}$ distinct from $u_{a,b,c}$, there exists a $N_{tr}\Upsilon OSL$ containing $u_{a,b,c}$ such that $v_{a',b',c'}\hat{q}N_{tr}\Upsilon cl(L)$.
(ii)$\cap\{N_{tr}\Upsilon cl(L)$: $u_{a,b,c} \in L \; and \; L \in N_{tr}\Upsilon O(U, \tau_{N_{tr}})\} = u_{p,q,r}, a \leq p; b \leq q; c \geq r$,for every $u_{a,b,c}$ in U.

Proof: (i) Since U is $N_{tr}\Upsilon - T_2$ space, for every pair of $N_{tr}Pu_{a,b,c}$, $v_{a',b',c'}, u \neq v$ in U, there exists $N_{tr}\Upsilon OSL$ and $v_{1,1,0}$ such that $u_{a,b,c} \in L, v_{a',b',c'} \in v_{1,1,0}$ and $L \cap v_{1,1,0} = 0_{N_{tr}}$. Since $v_{1,1,0}$ is $N_{tr}\Upsilon O$, ${v_{1,1,0}}^c$ is $N_{tr}\Upsilon C$ and$L \subseteq {v_{1,1,0}}^c$. This implies $N_{tr}\Upsilon cl(L) \subseteq {v_{1,1,0}}^c \Longrightarrow v_{1,1,0} \subseteq (N_{tr}\Upsilon cl(L))^c \Longrightarrow v_{a',b',c'} \in (N_{tr}\Upsilon cl(L))^c$. Hence $v_{a',b',c'}\hat{q}N_{tr}\Upsilon cl(L)$.
(ii) Proof is similar to theorem 5.15.

REFERENCES

1. Acikgoz, A., Esenbel F.,*A Look on Separation Axioms in Neutrosophic Topological Spaces*, AIP Conference Proceedings 2334, 020002, 2021.
2. Ray, G. C., SudeepDey, *Neutrosophic point and its neighbourhood structure*, Neutrosophic sets and Systems, 43, 156-168.
3. Jafari S., Rajesh N., *Neutrosophic Contra-continuous Multi-functions*, New Trends in Neutrosophic Theory and Applications, II, 2017.
4. Reena C., Yaamini, K. S.,*On NeutrosophicΥ −open Sets in Neutrosophic Topological Spaces*, paper presented in the International Conference on Applied Mathematics and Computing(ICAMC 2023).
5. ReenaC., Yaamini, K. S., *A New Notion of Neighbourhood and Continuity in Neutrosophic Topological Spaces*, Neutrosophic Sets and Systems, 60, 2024, 74-87.
6. Reena C., Yaamini, K. S., *On NeutrosophicΥ −homeomorphisms in Neutrosophic Topological Spaces*, Neutrosophic Sets and Systems(communicated).
7. Salama, A. A., Alblowi, S. A., *Neutrosophic Set and Neutrosophic Topological Spaces*, IOSR Jouranal of Mathematics,3(4), 2012.
8. Salama, A. A., Smarandache F.,Kromov V., *Neutrosophic Closed Set and Neutrosophic Continuous Functions*, Neutrosophic Sets and Systems, 4, 2014, 4-8.
9. SmarandacheF., *A Unifying Field in Logics: Neutrosophic Logic, Neutrosophy, Neutrosophic Set, Neutrosophic Probability*, American Research Press, Rehaboth, 1999.
10. SmarandacheF., *Neutrosophy and Neutrosophic Logic , First International Conference on Neutrosophy , Neutrosophic Logic, Set, Probability, and Statistics*, University of New Mexico, Gallup, NM 87301, USA, 2002.
11. SudeepDey, Ray G. C., *Pre-separation Axioms in Neutrosophic Topological Spaces*, International Journal of Neutrosophic Science, 22(2), 2023, 15-28.
12. Suman Das, Rakhal Das, Pramanik S., *Neutrosophic Separation Axioms*, Neutrosophic Sets and Systems, 49, 2022, 103-110.

Indian Journal of Natural Sciences *www.tnsroindia.org.in ©IJONS*

Vol.15 / Issue 83 / Apr / 2024 *International Bimonthly (Print) – Open Access* *ISSN: 0976 – 0997*

RESEARCH ARTICLE

On Alpha Product of Hesitancy Fuzzy Graphs and Intuitionistic Hesitancy Fuzzy Graphs

Sunil M P* and J Suresh Kumar

PG and Research Department of Mathematics, N.S.S. Hindu College, Changanacherry, Kottayam, Kerala, India

Received: 22 Feb 2024 Revised: 06 Mar 2024 Accepted: 20 Mar 2024

***Address for Correspondence**
Sunil M P
PG and Research Department of Mathematics,
N.S.S. Hindu College, Changanacherry,
Kottayam, Kerala, India.
Email: sunilmp.mp@gmail.com

ABSTRACT

We make a study on the Alpha product of a pair of Hesitancy fuzzy graphs (HFG) and Intuitionistic hesitancy fuzzy graphs (IHFG) and validate specific outcomes in relation with this product.

Keywords: HFG, IHFG, strong IHFG, alpha product.

2020 Mathematics Subject Classification: 05C72, 05C76

INTRODUCTION

Euler initiated the development of graph theory. Zadeh [1] introduced fuzzy set concept. Rosenfeld [2] created the idea of fuzzy graphs in 1975. Atanassov [3] introduced intuitionistic fuzzy sets. R.Parvathi [4] developed Intuitionistic fuzzy graph (IFG). The Hesitancy fuzzy graph concept was created by Pathinathan [5]. Intuitionistic hesitancy fuzzy graphs (IHFG) concept was discussed in [6,7]. We define the alpha product (α-product) of two HFGs and IHFGs.The degree to which a vertex is hesitant in a HFG is determined by its membership (MS) and non-membership (NMS) degree. Conversely, in an IHFG, the degree to which a vertex is hesitant is not related to its degree of MS and NMS. We establish that, for two strong HFGs, theirα-productis not necessarily be a strong HFG. But, in the case of strong IHFGs, their α-product is a strong IHFG. If two IHFGs have a strong α-product, then at least one of the IHFG will be strong.

Preliminaries

Definition 2.1. [6] A HFG is $G:(V,E,\sigma,\mu)$, V the set of vertices, $\sigma=(\zeta_1,\chi_1,\psi_1)$, $\mu=(\zeta_2,\chi_2,\psi_2)$ and $\zeta_1,\chi_1,\psi_1:V\rightarrow$ [0,1]indicates MS, NMS, hesitancy degree of $v\in V$,

$\zeta_1(v)+\chi_1(v)+\psi_1(v)=1$ where $\psi_1(v)=1-[\zeta_1(v)+\chi_1(v)]$
$\zeta_2,\chi_2,\psi_2: V\times V\longrightarrow[0,1]$indicates MS, NMS, hesitancy degree of x,
$\zeta_2(x)\le\zeta_1(u)\wedge\zeta_1(v)\chi_2(x)\le\chi_1(u)\vee\chi_1(v)\psi_2(x)\le\psi_1(u)\wedge\psi_1(v)0\le\zeta_2(x)+\chi_2(x)+\psi_2(x)\le 1,\forall\, x=(u,v)\in V\times V$, $\wedge$ and $\vee$ represents minimum and maximum respectively.

Definition 2.2.[6] IHFG isG_α: (V,E,σ,μ), $\sigma=(\zeta_1,\chi_1,\psi_1)$, $\mu=(\zeta_2,\chi_2,\psi_2)$,

$$0\le\zeta_1(v)+\chi_1(v)+\psi_1(v)\le 1$$

$\zeta_2(x)\le\zeta_1(u)\wedge\zeta_1(v)\chi_2(x)\le\chi_1(u)\vee\chi_1(v)\psi_2(x)\le\psi_1(u)\wedge\psi_1(v)0\le\zeta_2(x)+\chi_2(x)+\psi_2(x)\le 1$, for all $x=(u,v)$.
Remark 2.3. [6] A HFG is an IHFG. But, an IHFG does not have to be a HFG. G in figure 1 is a HFG with $\zeta_1(u_i)+\chi_1(u_i)+\psi_1(u_i)=1$, $\forall i$,where $\psi_1(u_i)=1-[\zeta_1(u_i)+\chi_1(u_i)]$. G is also an IHFG. $G_\alpha$is an IHFG since, $0\le\zeta_1(v_i)+\chi_1(v_i)+\psi_1(v_i)\le 1,\forall i$. But, G_α is not a HFG.

Definition 2.4.[6] G or G_α is
ζ-strong if $\zeta_2(x)=\zeta_1(u)\wedge\zeta_1(v)$ (1)χ-strong if $\chi_2(x)=\chi_1(u)\vee\chi_1(v)$(2) ψ-strong if $\psi_2(x)=\psi_1(u)\wedge\psi_1(v)$, (3)
for all $x=(u,v)\in E$. G or G_α is strong if it satisfies (1), (2) and (3).
Example 2.5. Strong HFG G and strong IHFG $G_\alpha$are shown in figure 2.

MAIN RESULTS

Definition 3.1. Let $G_1=(X,E_X,\sigma,\mu)$, $G_2=(Y,E_Y,\sigma',\mu')$ with $\sigma=(\zeta_1,\chi_1,\psi_1)$, $\mu=(\zeta_2,\chi_2,\psi_2)$, $\sigma'=(\zeta_1',\chi_1',\psi_1')$, $\mu'=(\zeta_2',\chi_2',\psi_2')$ be two HFGs. Their α-product is the HFG $G_1\times_\alpha G_2=(X\times Y,\ E,\sigma\times_\alpha\sigma',\ \mu\times_\alpha\mu')$, $E=\cup_{i=1}^{4}E_i$, $E_1=\{w: u_1=u_2, w_2\in E_Y\}$, $E_2=\{w: v_1=v_2, w_1\in E_X\}$, $E_3=\{w: w_1\in E_X, w_2\notin E_Y\}$, $E_4=\{w: w_1\notin E_X, w_2\in E_Y\}$,$w_1=(u_1,u_2)$,$w_2=(v_1,v_2)$, $w=((u_1,v_1),(u_2,v_2))$.Then, for $x=(u,v)$,
$(\zeta_1\times_\alpha\zeta_1')(x)=\zeta_1(u)\wedge\zeta_1'(v)(\chi_1\times_\alpha\chi_1')(x)=\chi_1(u)\vee\chi_1'(v)(\psi_1\times_\alpha\psi_1')(x)=1-[\zeta_1(u)\wedge\zeta_1'(v)+\chi_1(u)\vee\chi_1'(v)]$,

$$(\zeta_2\times_\alpha\zeta_2')(w)=\begin{cases}\zeta_1(u_1)\wedge\zeta_2'(w_2),\text{if } w\in E_1\\ \zeta_1'(v_1)\wedge\zeta_2(w_1),\text{if } w\in E_2\\ \zeta_2(w_1)\wedge\zeta_1'(v_1)\wedge\zeta_1'(v_2),\text{if } w\in E_3\\ \zeta_1(u_1)\wedge\zeta_1(u_2)\wedge\zeta_2'(w_2),\text{if } w\in E_4\end{cases}\quad(4)$$

$$(\chi_2\times_\alpha\chi_2')(w)=\begin{cases}\chi_1(u_1)\vee\chi_2'(w_2),\ \text{if } w\in E_1\\ \chi_1'(v_1)\vee\chi_2(w_1),\ \text{if } w\in E_2\\ \chi_2(w_1)\vee\chi_1'(v_1)\vee\chi_1'(v_2),\text{if } w\in E_3\\ \chi_1(u_1)\vee\chi_1(u_2)\vee\chi_2'(w_2),\text{if } w\in E_4\end{cases}\quad(5)$$

$$(\psi_2\times_\alpha\psi_2')(w)=\begin{cases}\psi_1(u_1)\wedge\psi_2'(w_2),\ \text{if } w\in E_1\\ \psi_1'(v_1)\wedge\psi_2(w_1),\ \text{if } w\in E_2\\ \psi_2(w_1)\wedge\psi_1'(v_1)\wedge\psi_1'(v_2),\text{if } w\in E_3\\ \psi_1(u_1)\wedge\psi_1(u_2)\wedge\psi_2'(w_2),\text{if } w\in E_4\end{cases}\quad(6)$$

Remark 3.2. The α-product $G_1\times_\alpha G_2$of strong HFGs G_1,G_2 may not result in a strong HFG. G_1 and G_2 are two strong HFGs in figure 3 and figure 4 is their α-product $G_1\times_\alpha G_2$.

$$(\zeta_1\times_\alpha\zeta_1')(u_2,v_2)=\zeta_1(u_2)\wedge\zeta_1'(v_2)=0.2\wedge 0.3=0.2$$

$(\chi_1\times_\alpha\chi_1')(u_2,v_2)=\chi_1(u_2)\vee\chi_1'(v_2)=0.4\vee 0.4=0.4(\psi_1\times_\alpha\psi_1')(u_2,v_2)=1-(0.2+0.4)=0.4(\zeta_1\times_\alpha\zeta_1')(u_2,v_1)=0.2(\chi_1\times_\alpha\chi_1')(u_2,v_1)=0.4(\psi_1\times_\alpha\psi_1')(u_2,v_1)=1-(0.2+0.4)=0.4$For the edge $z=((u_2,v_1),(u_2,v_2))$ in figure 4, since $z\in E_1,(\zeta_2\times_\alpha\zeta_2')(z)=\zeta_1(u_2)\wedge\zeta_2'(w_2)=0.2(\chi_2\times_\alpha\chi_2')(z)=\chi_1(u_2)\vee\chi_2'(w_2)=0.4(\psi_2\times_\alpha\psi_2')(z)=\psi_1(u_2)\wedge\psi_2'(w_2)=0.3$. Here, $G_1\times_\alpha G_2$isζ-strong and χ-strong.But, $(\psi_2\times_\alpha\psi_2')(z)\neq(\psi_1\times_\alpha\psi_1')(u_2,v_1)\wedge(\psi_1\times_\alpha\psi_1')(u_2,v_2)$. Thus, the alpha product is not ψ-strong.

Definition 3.3. Let $G_{\alpha_1} = (X, E_X, \sigma, \mu)$, $G_{\alpha_2} = (Y, E_Y, \sigma', \mu')$ with $\sigma = (\zeta_1, \chi_1, \psi_1)$, $\mu = (\zeta_2, \chi_2, \psi_2)$, $\sigma' = (\zeta_1', \chi_1', \psi_1')$, $\mu' = (\zeta_2', \chi_2', \psi_2')$ be two IHFGs. Their α-product is the IHFG $G_{\alpha_1} \times_\alpha G_{\alpha_2} = (X \times Y,\ E, \sigma \times_\alpha \sigma',\ \mu \times_\alpha \mu')$, $E = \cup_{i=1}^{4} E_i$, as defined in 3.1,
$(\zeta_1 \times_\alpha \zeta_1')(x) = \zeta_1(u) \wedge \zeta_1'(v)(\chi_1 \times_\alpha \chi_1')(x) = \chi_1(u) \vee \chi_1'(v)(\psi_1 \times_\alpha \psi_1')(x) = \psi_1(u) \wedge \psi_1'(v)$,
and equations (4), (5) and (6).

Theorem 3.4. If G_{α_1} and G_{α_2} are two strong IHFGs, then $G_{\alpha_1} \times_\alpha G_{\alpha_2}$ is also a strong IHFG.
Proof: For strong IHFGsG_{α_1}, G_{α_2} and$w_1 \in E_X, w_2 \in E_Y$,
$\zeta_2(w_1) = \zeta_1(u_1) \wedge \zeta_1(u_2)$, $\zeta_2'(w_2) = \zeta_1'(v_1) \wedge \zeta_1'(v_2)\chi_2(w_1) = \chi_1(u_1) \vee \chi_1(u_2)$, $\chi_2'(w_2) = \chi_1'(v_1) \vee \chi_1'(v_2)\psi_2(w_1) = \psi_1(u_1) \wedge \psi_1(u_2)$, $\psi_2'(w_2) = \psi_1'(v_1) \wedge \psi_1'(v_2)$
Case(i) When $w \in E_1$
$(\zeta_2 \times_\alpha \zeta_2')(w) = \zeta_1(u_1) \wedge \zeta_2'(w_2) = \zeta_1(u_1) \wedge \zeta_1(u_2) \wedge \zeta_1'(v_1) \wedge \zeta_1'(v_2)$, since $u_1 = u_2$ $= (\zeta_1 \times_\alpha \zeta_1')(u_1, v_1) \wedge (\zeta_1 \times_\alpha \zeta_1')(u_2, v_2)(\chi_2 \times_\alpha \chi_2')(w) = \chi_1(u_1) \vee \chi_2'(w_2) = \chi_1(u_1) \vee \chi_1(u_2) \vee \chi_1'(v_1) \vee \chi_1'(v_2) = (\chi_1 \times_\alpha \chi_1')(u_1, v_1) \vee (\chi_1 \times_\alpha \chi_1')(u_2, v_2)$
$(\psi_2 \times_\alpha \psi_2')(w) = \psi_1(u_1) \wedge \psi_2'(w_2) = \psi_1(u_1) \wedge \psi_1(u_2) \wedge \psi_1'(v_1) \wedge \psi_1'(v_2) = (\psi_1 \times_\alpha \psi_1')(u_1, v_1) \wedge (\psi_1 \times_\alpha \psi_1')(u_2, v_2)$

Case(ii) When $w \in E_2$
$(\zeta_2 \times_\alpha \zeta_2')(w) = \zeta_1'(v_1) \wedge \zeta_2(w_1) = \zeta_1'(v_1) \wedge \zeta_1'(v_2) \wedge \zeta_1(u_1) \wedge \zeta_1(u_2)$, since $v_1 = v_2$ $= (\zeta_1 \times_\alpha \zeta_1')(u_1, v_1) \wedge (\zeta_1 \times_\alpha \zeta_1')(u_2, v_2)$
$(\chi_2 \times_\alpha \chi_2')(w) = \chi_1'(v_1) \vee \chi_2(w_1) = \chi_1'(v_1) \vee \chi_1'(v_2) \vee \chi_1(u_1) \vee \chi_1(u_2) = (\chi_1 \times_\alpha \chi_1')(u_1, v_1) \vee (\chi_1 \times_\alpha \chi_1')(u_2, v_2)$
$(\psi_2 \times_\alpha \psi_2')(w) = \psi_1'(v_1) \wedge \psi_2(w_1) = \psi_1'(v_1) \wedge \psi_1'(v_2) \wedge \psi_1(u_1) \wedge \psi_1(u_2) = (\psi_1 \times_\alpha \psi_1')(u_1, v_1) \wedge (\psi_1 \times_\alpha \psi_1')(u_2, v_2)$

Case(iii) When $w \in E_3$
$(\zeta_2 \times_\alpha \zeta_2')(w) = \zeta_2(w_1) \wedge \zeta_1'(v_1) \wedge \zeta_1'(v_2) = \zeta_1(u_1) \wedge \zeta_1(u_2) \wedge \zeta_1'(v_1) \wedge \zeta_1'(v_2) = (\zeta_1 \times_\alpha \zeta_1')(u_1, v_1) \wedge (\zeta_1 \times_\alpha \zeta_1')(u_2, v_2)$
$(\chi_2 \times_\alpha \chi_2')(w) = \chi_2(w_1) \vee \chi_1'(v_1) \vee \chi_1'(v_2) = \chi_1(u_1) \vee \chi_1(u_2) \vee \chi_1'(v_1) \vee \chi_1'(v_2) = (\chi_1 \times_\alpha \chi_1')(u_1, v_1) \vee (\chi_1 \times_\alpha \chi_1')(u_2, v_2)$
$(\psi_2 \times_\alpha \psi_2')(w) = \psi_2(w_1) \wedge \psi_1'(v_1) \wedge \psi_1'(v_2) = \psi_1(u_1) \wedge \psi_1(u_2) \wedge \psi_1'(v_1) \wedge \psi_1'(v_2) = (\psi_1 \times_\alpha \psi_1')(u_1, v_1) \wedge (\psi_1 \times_\alpha \psi_1')(u_2, v_2)$
Case(iv) When $w \in E_4$. Similar to case (iii). Thus, $G_{\alpha_1} \times_\alpha G_{\alpha_2}$ is a strong IHFG.
Example 3.5. Figure 6 is the α-product $G_{\alpha_1} \times_\alpha G_{\alpha_2}$of strong IHFGs$G_{\alpha_1}$,$G_{\alpha_2}$given in figure5.

Theorem 3.6. If two IHFGs have a strongα-product,then eitherG_{α_1} or G_{α_2}or both will be strong.
Proof: IfG_{α_1}, $G_{\alpha_2}$are not strong, there exists w_1 or w_2 or both with
$\zeta_2(w_1) < \zeta_1(u_1) \wedge \zeta_1(u_2)$, $\zeta_2'(w_2) < \zeta_1'(v_1) \wedge \zeta_1'(v_2)\chi_2(w_1) < \chi_1(u_1) \vee \chi_1(u_2)$, $\chi_2'(w_2) < \chi_1'(v_1) \vee \chi_1'(v_2)\psi_2(w_1) < \psi_1(u_1) \wedge \psi_1(u_2)$, $\psi_2'(w_2) < \psi_1'(v_1) \wedge \psi_1'(v_2)$
Let$w \in E_1$. Then, $(\zeta_2 \times_\alpha \zeta_2')(w) = \zeta_1(u_1) \wedge \zeta_2'(w_2) < \zeta_1(u_1) \wedge \zeta_1(u_2) \wedge \zeta_1'(v_1) \wedge \zeta_1'(v_2)$, since $u_1 = u_2$i.e., $(\zeta_2 \times_\alpha \zeta_2')(w) < (\zeta_1 \times_\alpha \zeta_1')(u_1, v_1) \wedge (\zeta_1 \times_\alpha \zeta_1')(u_2, v_2)$
$(\chi_2 \times_\alpha \chi_2')(w) = \chi_1(u_1) \vee \chi_2'(w_2) < \chi_1(u_1) \vee \chi_1(u_2) \vee \chi_1'(v_1) \vee \chi_1'(v_2)$
i.e., $(\chi_2 \times_\alpha \chi_2')(w) < (\chi_1 \times_\alpha \chi_1')(u_1, v_1) \vee (\chi_1 \times_\alpha \chi_1')(u_2, v_2)$
$(\psi_2 \times_\alpha \psi_2')(w) = \psi_1(u_1) \wedge \psi_2'(w_2) < \psi_1(u_1) \wedge \psi_1(u_2) \wedge \psi_1'(v_1) \wedge \psi_1'(v_2)$
i.e., $(\psi_2 \times_\alpha \psi_2')(w) < (\psi_1 \times_\alpha \psi_1')(u_1, v_1) \wedge (\psi_1 \times_\alpha \psi_1')(u_2, v_2)$
which is a contradiction.

CONCLUSION

We introduced the alpha product of a pair of HFGs and IHFGs and proved that for two strong HFGs, their alpha product need not be strong. But in the case of strong IHFGs, this product is strong. If two IHFGs have a strong alpha product, then at least one of them will be strong. IHFGs are of immense help in making decisions regarding companies' merger problems. LetG_{α_1} and G_{α_2} be two strong networks with vertices representing companies. The market value of individual companies is represented by the MS degree of vertices while edge membership represents the market value of joint venture of the companies. As G_{α_1} and $G_{\alpha_2}$are strong, their alpha product is also strong. Possible strong joint ventures are developed, from which optimal joint venture can be selected by a company, keeping in mind their preferences and needs.

REFERENCES

1. Zadeh L.A, Fuzzy sets, Inform Control, 1965;8: 338–356. DOI: https://doi.org/10.1016/S0019-9958(65)90241-X
2. Rosenfeld A, Fuzzy graphs, In: L. A. Zadeh, K. S. Fu, M. Shimura, Eds., Fuzzy Sets and Their Applications to Cognitive and Decision Process, Academic Press, New York,1975: 77–95.
3. Atanassov K.T, Intuitionistic fuzzy sets, Fuzzy Sets and Systems, 1986; 20: 87–96.
4. DOI: https://doi.org/10.1016/S0165-0114(86)80034-3
5. Parvathi R, Karunambigai M. G, Intuitionistic fuzzy graphs, Computational intelligence, theory and applications, Springer, Berlin, Heidelberg, 2006;139-150. DOI: https://doi.org/10.1007/3-540-34783-6_15
6. Pathinathan T, Arockiaraj J, Rosline J.J, Hesitancy fuzzy graph, Indian Journal of Science and Technology, 2015; 8 (35): 1-5. DOI: 10.17485/ijst/2015/v8i35/86672
7. Sunil M.P, Suresh Kumar J, On beta product of hesitancy fuzzy graphs and intuitionistic hesitancy fuzzy graphs, Korean J. Math. 2023; 31 (4):485-494. DOI: https://doi.org/10.11568/kjm.2023.31.4.485
8. Sunil M.P, Suresh Kumar J, On Intuitionistic Hesitancy Fuzzy Graphs, Mathematics and Statistics, 2024;12 (1): 48 – 54.DOI: 10.13189/ms.2024.120107.

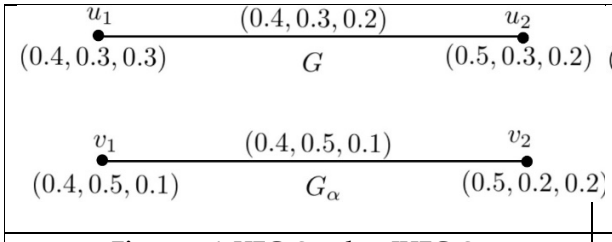

Figure 1. A HFG G and an IHFG G_α

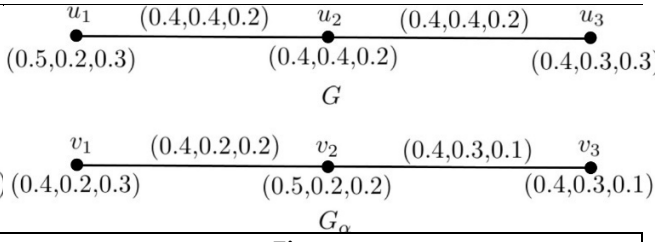

Figure 2

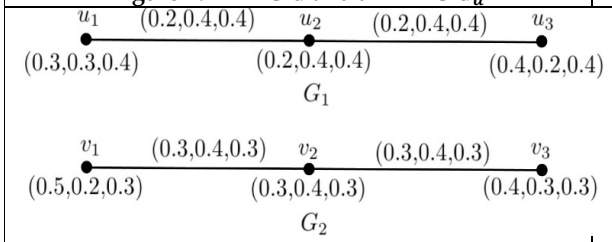

Figure 3.

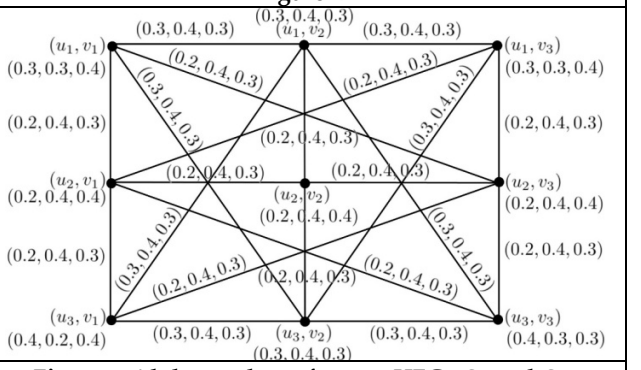

Figure 4. Alpha product of strong HFGs G_1 and G_2

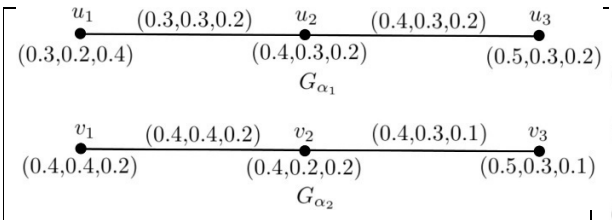

Figure 5

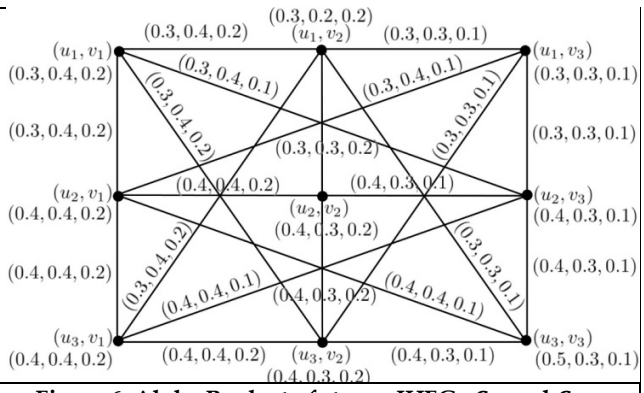

Figure 6. Alpha Product of strong IHFGs G_{α_1} and G_{α_2}

Indian Journal of Natural Sciences *www.tnsroindia.org.in ©IJONS*

Vol.15 / Issue 83 / Apr / 2024 *International Bimonthly (Print) – Open Access* *ISSN: 0976 – 0997*

RESEARCH ARTICLE

Exploring Methodologies and Applications of Data Science Integration in Electrical and Electronics Engineering

[1]Ramya Hyacinth L., [1]William Christopher I., [2]Anitha Juliette A.

[1]Department of Electrical and Electronics Engineering, Loyola-ICAM College of Engineering and Technology, Nungambakkam, Chennai, India
[2]Department of Electronics and Communication Engineering, Loyola-ICAM College of Engineering and Technology, Nungambakkam, Chennai, India

Received: 30 Dec 2023 Revised: 09 Jan 2024 Accepted: 12 Mar 2024

***Address for Correspondence**
Ramya Hyacinth L
Department of Electrical and Electronics Engineering,
Loyola-ICAM College of Engineering and Technology,
Nungambakkam, Chennai, India

ABSTRACT

In recent years, the advancements in data science techniques have helped address the intricacies of Electrical and Electronics Engineering. The rapid expansion of data and the emergence of new intelligent algorithms present a significant opportunity to integrate data science principles and modernize conventional engineering systems. This paper presents an all-inclusive exploration of the integration of data science methodologies in the realm of Electrical and Electronics Engineering. The specific applications of machine learning and artificial intelligence algorithms in diverse areas such as – Power system analysis and optimisation; Renewable energy forecasting and management; Smart grid technologies and applications; Telecommunications network optimisation; Signal processing and analysis; Power Electronics and Control; Electronic design automation are discussed. Furthermore, the transformative potential of the data-driven approaches towards optimisation, increasing efficiency and enhancing predictive maintenance are highlighted. Thus, a comprehensive overview of the potential impacts of data-driven algorithms to address real-world engineering problems concerning Electrical and Electronics Engineering is given.

Keywords: Machine Learning, IoT, Bid Data, Data-Driven Approach and Data Analytics

INTRODUCTION

The application of data science in electrical and electronics engineering acts as a transformative force in reshaping industries and accelerating research [1]. Data science techniques offer innovative solutions to complicated problems and open new opportunities for research and development. The intensification of digital technologies and the

Internet of Things (IoT) have led to an exponential generation of data from various domains of electrical and electronics engineering [2]. This deluge of data provides ample opportunities for engineers to harness sophisticated data analytics, statistical modelling and Machine Learning techniques to unearth meaningful observations from the available inundation of data. Also, the increasing complexity of electrical and electronic systems appeals to analysis, optimisation and control techniques to make informed decisions. Traditional practices often fall short in addressing the intricacies of modern engineering problems [3]. This necessitates a paradigm shift towards the use of data-driven technologies [4]. Applying data-driven approaches, engineers gain deeper insight on the system behaviour [5], predict outcomes [6] [7] and optimise design problems [8] [9] to obtain better accuracy and efficiency [10].

In data science, the convergence of different disciplines such as mathematics, computer science and engineering has fostered interdisciplinary collaboration and cross-pollination of ideas. The impact of data science permeates every facet of modern engineering practice. Numerous studies have demonstrated the efficacy of data science techniques in tackling the challenges across the spectrum of electrical and electronics engineering domains. For instance, in power systems, predictive analytics [11] and optimisation algorithms [12] are being used to enhance grid reliability [13], optimise energy consumption [14] and integrate renewable energy resources [15] effectively. Likewise, within signal processing, ML algorithms have gained recognition for their exceptional performance in areas like speech recognition[16], image classification [17] and anomaly detection [18]. This paper expands on previous research and consolidates perspectives from various studies, case examples, and real-world applications to offer a comprehensive examination of the impact of data science in the field of electrical and electronics engineering. In addition, the key challenges associated with integrating data science and the integration strategies that could be adopted to mitigate these challenges are addressed.

Opportunities for Data Science in Electrical and Electronics Engineering

Power System Analysis and Control

Data science could be applied to various aspects of grid operations, including load forecasting [19], predictive maintenance [20], real-time monitoring [21], adaptive control, optimal operation, fault detection and stability enhancement [22]. Accurate load forecasting helps utilities optimize generation and scheduling resources, leading to cost savings and improved reliability. ML algorithms play a key role in load forecasting due to their ability to analyse historical data and identify patterns to make accurate forecasts. Autoregressive Integrated Moving Average (ARIMA) uses a time-series forecasting method [23] and can handle seasonal patterns. This approach is well-suited for capturing linear dependencies and trends in data. While, it assumes stationarity which may not be applicable for all load data and has limited ability to capture complex non-linear relationships. Load forecasting problems involve high-dimensional data. Hence, Support Vector Regression (SVR) is used as it is robust to outliers. Also, SVR possesses the ability to capture intricate non-linear relationships by employing kernel functions[24]. However, fine-tuning of hyperparameters, including the selection of kernels and regularization parameters, is necessary for this model. Random Forest (RF) applied to load forecasting problems is robust to overfitting and can handle noisy data [25]. They are also effective in capturing the non-linear relationships and interactions between the features. However, RF does not perform well with highly imbalanced datasets and is computationally expensive for large datasets. Having access to historical data for load forecasting enables the utilization of Long Short-Term Memory (LSTM) Networks. LSTM Networks are adept at capturing both short-term and long-term patterns within time series data, rendering them particularly applicable to load forecasting challenges[26]. The ability to handle time series data with irregularities and seasonal peaks is an added advantage. However, careful adjustment of hyperparameters, such as the quantity of layers and hidden units, is necessary. Also, it is vulnerable to vanishing gradient problems in deep architectures. Nevertheless, these algorithms have their limitations and strengths. The selection of the algorithm relies on factors including the nature of load data, computational capabilities, and the unique demands of the forecasting tasks. Predictive maintenance analyses data from various sensors and equipment to predict potential failures and schedule maintenance activities proactively. Just as in load forecasting, ML algorithms such as Random Forest, SVM, and LSTM Networks can be applied to address predictive maintenance challenges. In addition, Recurrent Neural Networks (RNN) has the capability to analyse time series data with irregular patterns and long dependencies. RNN is effective for sequential data analysis and is capable of capturing temporal dependencies [27].

This makes it suitable to solve predictive maintenance challenges. The vulnerability to vanishing gradient problems with long sequences and the requirement to carefully tune hyperparameters (learning rate and batch size) are a few limitations of RNN. Another fundamental analysis performed in the domain of power systems is Optimal Power Flow (OPF). Khaloie *et al.* present works focussed on leveraging machine learning algorithms to solve the transmission-level OPF problem [28]. Real-time monitoring leverages sensors, IoT devices, and data analytics to monitor grid conditions in real-time, enabling early detection of anomalies and proactive intervention[29]. Furthermore, machine learning algorithms enable adaptive control strategies that optimize grid operation in response to changing conditions and dynamic constraints [30]. As advancements in Information and Communication Technologies continue, the traditional grid is evolving into a more intelligent infrastructure commonly referred to as the smart grid.

Smart Grid Technologies and Applications

The fundamental principles of data science, including ML techniques, statistical analysis, and data visualization are used in Advanced Metering Infrastructure (AMI), Grid Monitoring and Control as well as Grid Planning and Optimisation. Data Science coupled with advanced metering infrastructure is revolutionizing energy management and consumption monitoring. Data is continuously collected from advanced meters like Smart meters and Phasor Measurement Unit (PMU) at high rates. Data analytics help utilities optimize billing, demand response programs, and grid operations [31]. Data analytics techniques used in Smart Grids are Descriptive Analytics to understand historical trends in energy consumption [32], Predictive Analytics to forecast future demand and identify potential system issues [33], Anomaly detection & Time series Analysis to analyse meter data and identify recurring patterns, seasonal trends and anomalies [34], Data visualization to present data in visually understandable format that aids in decision-making [35] and Optimisation Algorithms to find the most optimal allocation of resources and relevant factors [36]. Depending on the obtained meter information, Grid operations are monitored and controlled. Grid monitoring and control involves optimising voltage regulation, reactive power control, and fault detection in distribution and transmission systems by analyzing sensor data and historical maintenance records. Reinforcement Learning assists in learning optimal control policies through trial-and-error interactions with the grid and facilitates adaptive and self-learning control strategies [37]. Effective monitoring and control of grid operations facilitates grid planning and optimization.

PV Systems Real-Time Monitoring

A significant volume of photovoltaic (PV) power generation data, along with corresponding weather data, is required to examine the relationship between weather factors and PV power generation, as well as to monitor the operational status of the PV system. The authors [38] suggest using an IoT monitoring cloud platform in conjunction with the PV/T façade system to track the PVT system online and in real time. The authors [39]showcase the setup and operation of a real-time monitoring system for Building Integrated Photovoltaic (BIPV) systems, or photovoltaic self-consumption, employing Internet of Things (IoT) technology. Concentrating on various data processing modules and transmission protocols, the authors [40] examine the emergence of numerous monitoring solutions based on solar PV. The system presented in [41] enables real-time measurements of all characteristics of the PV system, including ambient weather conditions. These measurements are then made available at the remote-control centre, where IoT is used to track the PV power system. In order to optimize the performance of electricity supply generated from solar PV systems, the author[42] suggested creating a framework for monitoring solar PV systems within a Smart Home Micro Grid (SHMG) using Artificial Intelligence (AI) and IoT.This study presents the design and discussion of a real-time monitoring system for photovoltaic parameters, utilizing IoT technology[43]. An off-grid solar system with two subsystems—one for the hardware system and the other for software—that could automatically monitor the system's performance was conceived and developed by the current research [44].

Data-Driven Approach for Wind Power

Precise wind power forecasting is crucial for mitigating the effects of wind power fluctuations on system dispatch planning. With the rapid expansion of data resources and ongoing enhancements in processing capabilities, data-driven AI technology has gained widespread adoption across various industries in recent times. In [45], the authors

offer guidance for designing and implementing several data-driven control strategies on a wind turbine benchmark. Their methods include fuzzy logic, adaptive, self-tuning PID, and model predictive control. Multi-objective optimization technologies in the field of wind power prediction (WPP) were examined [46]. The prediction accuracy of short-term statistical WPP models is evaluated [47] through an overview of performance evaluation techniques. To anticipate wind turbine output, the authors [48] utilised historical turbine data collected through the SCADA system, meteorological reanalysis data, and numerical weather prediction (NWP) data. However, the accuracy of the prediction was impacted by the 0.25° spatial resolution of the NWP data. The AI-based models for wind power prediction are thoroughly reviewed [49] at several temporal and spatial scales, ranging from the level of wind turbines to the regional level. From ultra-short, short, and long-term perspectives, the authors [50] provided a thorough analysis of AI-based wind power forecast models. A review of the deep learning models utilized for WPP, including feature extraction, relationship learning, and data processing, was conducted [51]. A model integratingAquila optimization (AO), squeeze wavelet transform (SWT), isolated forest (IF), and LSTM was proposed [52] for the WPP of new wind turbines.

Signal Processing

In signal processing, feature engineering may include deriving statistical characteristics (e.g., mean, variance, skewness) [53], time-domain features (e.g., entropy, autocorrelation) [54], frequency-domain features (e.g., Fourier transform coefficients) [55], and wavelet transform coefficients [56]. Data science techniques are increasingly being applied to signal processing tasks, leveraging advanced algorithms and methodologies to extract insights and knowledge from signals. Supervised learning techniques like support vector machines (SVMs), decision trees, random forests, and neural networks are employed for both classification and regression assignments[57]. Unsupervised learning techniques like clustering algorithms (e.g., k-means clustering, hierarchical clustering) for signal segmentation and pattern discovery [58]. Semi-supervised learning methods combine labelled and unlabelled data [59] to improve model performance, especially when labelled data is scarce. These data science techniques are instrumental in advancing signal processing capabilities, enabling the derivation of meaningful insights and knowledge from diverse types of signals across various domains such as telecommunications, audio and speech processing, image processing, biomedical engineering, and environmental monitoring.

Electronic Design Automation (EDA) and testing

EDA tools and workflow are optimised using data science techniques. ML algorithms have the capability to analyze historical design data, user interactions, and tool performance metrics to detect bottlenecks, inefficiencies, and areas for enhancement[60]. By understanding patterns in design flows, data scientists can develop predictive models to optimize tool settings, runtime, and resource allocation, leading to faster design iterations and reduced time-to-market [61]. Data science techniques are applied to analyze test data generated during manufacturing tests [62] and system-level testing. Statistical methods, ML algorithms, and data mining techniques are applied to analyse test results, recognize test patterns, and extract actionable insights [63]. By correlating test data with design parameters, process parameters, and field failure data, data scientists can develop predictive models to optimize test strategies, improve fault coverage, and reduce test costs.

Challenges Associated with Integrating Data Science

Incorporating data science into electrical and electronics engineering poses numerous challenges, mainly stemming from the intricate characteristics of both fields and their distinct operational needs. A few major challenges associated with applying data science techniques to electrical and electronic engineering problems are:

Data Collection and Preprocessing

Electrical and electronics engineering produces extensive data from sensors, devices, and systems. Nonetheless, this data often comes with challenges such as noise, incompleteness, or inconsistency, necessitating meticulous preprocessing before analysis. The integration of data science encompasses the creation of resilient techniques for data collection, cleaning, and preprocessing.

Data Fusion and Integration

Electrical and electronic systems frequently entail diverse data from different origins like sensors, control systems, and communication networks. To extract valuable insights by merging these varied data sources, it's essential to employ methods for data fusion and integration. This process may involve resolving challenges related to data compatibility, format conversion, and synchronization

Complexity and Dimensionality

Electrical and electronics systems are often intricate, characterized by nonlinear behaviour, dynamic changes over time, and interlinked components. Achieving precise predictive models through data science necessitates sophisticated modelling methods like machine learning, deep learning, and system identification, which effectively encapsulate the system's complexity. Moreover, the deluge of data generated by advanced meters adds another layer of complexity to the system, requiring efficient handling of big data and accelerated processing speeds.

Interdisciplinary Knowledge

Incorporating data science into electrical and electronics engineering demands interdisciplinary expertise across both fields. Engineers must possess a comprehensive comprehension of the fundamental principles of electrical engineering and the methodologies of data science to adeptly apply data-driven techniques to engineering challenges.

Real-time processing and control

Numerous applications within electrical and electronics engineering necessitate real-time processing and control, spanning fields like power systems, robotics, and control systems. To integrate data science into these domains, it's crucial to devise streamlined algorithms and methodologies for real-time data analysis, decision-making, and control. However, challenges may emerge concerning computational complexity and latency during this integration process.

Cybersecurity and Privacy

Electrical and electronics engineering often deals with sensitive data, such as personal information in smart grid systems or industrial control systems. Integrating data science requires addressing privacy and security concerns related to data collection, storage, and analysis, including ensuring data anonymity, encryption, and access control.

Validation and Verification

Ensuring the reliability, accuracy, and safety of data-driven models and algorithms in electrical and electronics engineering presents a formidable challenge due to the inherent complexity and critical safety concerns of numerous applications. Engineers are tasked with devising stringent validation methodologies to verify the dependability and precision of these solutions.

Domain Specific Challenges

Various disciplines within electrical and electronics engineering, including power systems, signal processing, and telecommunications, pose distinct challenges when it comes to incorporating data science. Engineers must customize data science methodologies to meet the specific demands and limitations of each domain effectively.

Model Interpretability

Improving the interpretability of data science models within electrical and electronics engineering is essential to ensure that the insights derived from these models are clear and useful.

Integrating Strategies

Integrating data science into electrical and electronics engineering involves a strategic approach to address various challenges effectively. Here are a few potential solutions that could address the challenges posed in implementing data science in this field.

Cross-Disciplinary Collaboration

Addressing these challenges necessitates the collaboration of electrical engineers, data scientists, and domain experts. Collaboratively, inventive solutions that integrate the distinct strengths of each discipline to cater to the exacting requirements of electrical and electronics engineering applications could be developed.

Data Infrastructure Development

Invest in building robust data infrastructure to collect, store, and manage engineering data effectively by establishing data pipelines, databases, and data lakes to aggregate data from various sources such as sensors, simulations, and historical records. Deploy scalable computing platforms, cloud services, and high-performance computing clusters to handle large datasets and complex algorithms.

Data Management and Governance

Establish data governance policies and procedures to ensure the quality, security, and privacy of engineering data. Also, implement data management best practices, including data cataloguing, version control, and metadata management.

Agile Implementation

Implementing data science in electrical and electronics engineering using Agile methodologies involves an iterative and incremental approach to development, emphasizing collaboration, flexibility, and continuous improvement.

Model Validation and Verification

Develop validation and verification methodologies to assess the accuracy, reliability, and safety of data-driven models and algorithms. Also, conduct rigorous testing and validation against real-world data to ensure that data science solutions meet engineering requirements and standards.

Emerging trends and future opportunities

The future scope for the application of data science in electrical and electronics engineering is vast and promising. A few key areas where data science is expected to play a significant role in the future of electrical and electronics engineering are listed below. In Smart Grid and Energy Management, ML can optimize energy distribution and consumption by analysing large-scale data from sensors, meters, and power systems. Predictive analytics and ML techniques can improve grid reliability, efficiency, and resilience while enabling renewable energy integration and demand-response programs. Data-driven approaches can enhance predictive maintenance strategies for electrical and electronics assets such as transformers, generators, and transmission lines. By analysing equipment performance data, engineers can predict and prevent failures, optimize maintenance schedules, and extend the lifespan of critical infrastructure. Data science techniques, including optimization algorithms and control theory, can optimize power generation, transmission, and distribution systems. Real-time data analysis and control strategies can improve grid stability, voltage regulation, and load balancing while integrating distributed energy resources and microgrids. IoT devices and sensor networks generate vast amounts of data in electrical and electronic systems. Data science can extract actionable insights from sensor data for condition monitoring, fault detection, and performance optimization across various applications, including industrial automation, building management, and healthcare. Data science techniques are essential for addressing cybersecurity threats and protecting sensitive information in electrical and electronic systems. Intrusion detection, anomaly detection, and encryption algorithms can enhance the security and privacy of data transmission, storage, and processing in interconnected networks and cyber-physical systems.

CONCLUSION

The implementation of data science in the field of electrical and electronics engineering is expanding rapidly to meet the growing demand for interdisciplinary skills and expertise. It offers insights into how data-driven approaches can revolutionize grid operations and pave the way for a more efficient, reliable, and sustainable energy future. Through this comprehensive exploration, the methodologies, applications, challenges and potential impacts of integrating data science in electrical and electronics engineering are presented, thereby paving the way for transformative advancements in the field. From the challenges of data collection and preprocessing to model interpretability, it is evident that integrating data science into electrical and electronics engineering requires a strategic and multifaceted approach. By leveraging advanced data processing techniques, interdisciplinary collaboration, and agile methodologies, engineers can utinise the power of data science to optimize energy systems, improve predictive maintenance, enhance signal processing, and advance autonomous systems, among other applications. Thus, the future of data science in electrical and electronics engineering holds immense potential for addressing complex

challenges, driving innovation, and creating value across various domains. In a nutshell, the integration of data science into electrical and electronics engineering represents a transformative paradigm shift, enabling engineers to leverage data-driven insights to create smarter, more resilient, and more efficient systems for the benefit of society as a whole.

REFERENCES

1. Kayabay, Kerem, Mert Onuralp Gökalp, Ebru Gökalp, P. Erhan Eren, and Altan Koçyiğit. "Data science roadmapping: An architectural framework for facilitating transformation towards a data-driven organisation." *Technological Forecasting and Social Change* 174 (2022): 121264.
2. Acharjya, D. P., M. Kalaiselvi Geetha, and Sugata Sanyal, eds. "Internet of Things: novel advances and envisioned applications." (2017). [Springer Book]
3. Ahmad, Tanveer, Rafal Madonski, Dongdong Zhang, Chao Huang, and Asad Mujeeb. "Data-driven probabilistic machine learning in sustainable smart energy/smart energy systems: Key developments, challenges, and future research opportunities in the context of smart grid paradigm." *Renewable and Sustainable Energy Reviews* 160 (2022): 112128.
4. Bibri, Simon Elias. "Data-driven smart sustainable cities of the future: An evidence synthesis approach to a comprehensive state-of-the-art literature review." *Sustainable Futures* 3 (2021): 100047.
5. Markovsky, Ivan, and Florian Dörfler. "Behavioral systems theory in data-driven analysis, signal processing, and control." *Annual Reviews in Control* 52 (2021): 42-64.
6. Wei, Yixuan, Xingxing Zhang, Yong Shi, Liang Xia, Song Pan, Jinshun Wu, Mengjie Han, and Xiaoyun Zhao. "A review of data-driven approaches for prediction and classification of building energy consumption." *Renewable and Sustainable Energy Reviews* 82 (2018): 1027-1047.
7. Wang, Jidong, Peng Li, Ran Ran, Yanbo Che, and Yue Zhou. "A short-term photovoltaic power prediction model based on the gradient boost decision tree." *Applied Sciences* 8, no. 5 (2018): 689.
8. Cao, Bing, Lawrence A. Adutwum, Anton O. Oliynyk, Erik J. Luber, Brian C. Olsen, Arthur Mar, and Jillian M. Buriak. "How to optimize materials and devices via design of experiments and machine learning: Demonstration using organic photovoltaics." *ACS nano* 12, no. 8 (2018): 7434-7444.
9. Yao, Zhenpeng, Yanwei Lum, Andrew Johnston, Luis Martin Mejia-Mendoza, Xin Zhou, Yonggang Wen, Alán Aspuru-Guzik, Edward H. Sargent, and Zhi Wei Seh. "Machine learning for a sustainable energy future." *Nature Reviews Materials* 8, no. 3 (2023): 202-215.
10. Begum, Shahida, Reshma Banu, Ali Ahamed, and B. D. Parameshachari. "A comparative study on improving the performance of solar power plants through IOT and predictive data analytics." In *2016 International Conference on Electrical, Electronics, Communication, Computer and Optimization Techniques (ICEECCOT)*, pp. 89-91. IEEE, 2016.
11. Queen, Hephzibah Jose, J. Jayakumar, T. J. Deepika, K. Victor Sam Moses Babu, and Surya Prakash Thota. "Machine learning-based predictive techno-economic analysis of power system." *IEEE Access* 9 (2021): 123504-123516.
12. Prasad, Kalapala, J. Samson Isaac, P. Ponsudha, N. Nithya, Santaji Krishna Shinde, S. Raja Gopal, Atul Sarojwal, K. Karthikumar, and Kibrom Menasbo Hadish. "A machine learning-based novel energy optimization algorithm in a photovoltaic solar power system." *International Journal of Photoenergy* 2022 (2022).
13. Dehghanian, Payman, Bei Zhang, Tatjana Dokic, and Mladen Kezunovic. "Predictive risk analytics for weather-resilient operation of electric power systems." *IEEE Transactions on Sustainable Energy* 10, no. 1 (2018): 3-15.
14. Hernandez-Matheus, Alejandro, Markus Löschenbrand, Kjersti Berg, Ida Fuchs, Mònica Aragüés-Peñalba, Eduard Bullich-Massagué, and Andreas Sumper. "A systematic review of machine learning techniques related to local energy communities." *Renewable and Sustainable Energy Reviews* 170 (2022): 112651.
15. S. Wu, C. Wang, and R. Tang, "Optical efficiency and performance optimization of a two-stage secondary reflection hyperbolic solar concentrator using machine learning," Renewable Energy, vol. 188, pp. 437–449, 2022.
16. Vashisht, Vineet, Aditya Kumar Pandey, and Satya Prakash Yadav. "Speech recognition using machine learning." *IEIE Transactions on Smart Processing & Computing* 10, no. 3 (2021): 233-239.

17. Wang, Pin, En Fan, and Peng Wang. "Comparative analysis of image classification algorithms based on traditional machine learning and deep learning." *Pattern Recognition Letters* 141 (2021): 61-67.
18. Ahrens, Lia, Julian Ahrens, and Hans D. Schotten. "A machine-learning phase classification scheme for anomaly detection in signals with periodic characteristics." *EURASIP Journal on Advances in Signal Processing* 2019, no. 1 (2019): 27.
19. Wazirali, Raniyah, Elnaz Yaghoubi, Mohammed Shadi S. Abujazar, Rami Ahmad, and Amir Hossein Vakili. "State-of-the-art review on energy and load forecasting in microgrids using artificial neural networks, machine learning, and deep learning techniques." *Electric power systems research* 225 (2023): 109792.
20. Wang, Qi, Siqi Bu, and Zhengyou He. "Achieving predictive and proactive maintenance for high-speed railway power equipment with LSTM-RNN." *IEEE Transactions on Industrial Informatics* 16, no. 10 (2020): 6509-6517.
21. Dharmapala, Kalana Dulanjith, Athula Rajapakse, Krish Narendra, and Yi Zhang. "Machine learning based real-time monitoring of long-term voltage stability using voltage stability indices." *IEEE Access* 8 (2020): 222544-222555.
22. Chahal, Ayushi, Preeti Gulia, Nasib Singh Gill, and Jyotir Moy Chatterjee. "Performance analysis of an optimized ANN model to predict the stability of smart grid." *Complexity* 2022 (2022): 1-13.
23. Chodakowska, Ewa, Joanicjusz Nazarko, and Łukasz Nazarko. "Arima models in electrical load forecasting and their robustness to noise." *Energies* 14, no. 23 (2021): 7952.
24. Che, JinXing, and JianZhou Wang. "Short-term load forecasting using a kernel-based support vector regression combination model." Applied Energy 132 (2014): 602-609.
25. Dudek, Grzegorz. "A comprehensive study of random forest for short-term load forecasting." *Energies* 15, no. 20 (2022): 7547.
26. Muzaffar, Shahzad, and Afshin Afshari. "Short-term load forecasts using LSTM networks." *Energy Procedia* 158 (2019): 2922-2927.
27. Rivas, Alberto, Jesús M. Fraile, Pablo Chamoso, Alfonso González-Briones, Inés Sittón, and Juan M. Corchado. "A predictive maintenance model using recurrent neural networks." In *14th International Conference on Soft Computing Models in Industrial and Environmental Applications (SOCO 2019) Seville, Spain, May 13–15, 2019, Proceedings 14*, pp. 261-270. Springer International Publishing, 2020.
28. Khaloie, Hooman, Mihaly Dolanyi, Jean-Francois Toubeau, and François Vallée. "Review of Machine Learning Techniques for Optimal Power Flow." *Available at SSRN 4681955* (2024).
29. Ingram, Michael, Anthony Florita, Maurice Martin, Kenny Gruchalla, Xin Fang, Mengmeng Cai, Graham Johnson *et al*. *Situational Awareness of Grid Anomalies (SAGA) for Visual Analytics—Near-Real-Time Cyber-Physical Resiliency Through Machine Learning*. No. NREL/TP-5D00-85187. National Renewable Energy Laboratory (NREL), Golden, CO (United States), 2023.
30. Huang, Qiuhua, Renke Huang, Weituo Hao, Jie Tan, Rui Fan, and Zhenyu Huang. "Adaptive power system emergency control using deep reinforcement learning." *IEEE Transactions on Smart Grid* 11, no. 2 (2019): 1171-1182.
31. Wang, Yi, Qixin Chen, Tao Hong, and Chongqing Kang. "Review of smart meter data analytics: Applications, methodologies, and challenges." *IEEE Transactions on Smart Grid* 10, no. 3 (2018): 3125-3148.
32. Yildiz, Baran, Jose I. Bilbao, Jonathon Dore, and Alistair B. Sproul. "Recent advances in the analysis of residential electricity consumption and applications of smart meter data." *Applied Energy* 208 (2017): 402-427.
33. Syed, Dabeeruddin, Ameema Zainab, Ali Ghrayeb, Shady S. Refaat, Haitham Abu-Rub, and Othmane Bouhali. "Smart grid big data analytics: Survey of technologies, techniques, and applications." *IEEE Access* 9 (2020): 59564-59585.
34. Zhang, Jiuqi Elise, Di Wu, and Benoit Boulet. "Time series anomaly detection for smart grids: A survey." In *2021 IEEE Electrical Power and Energy Conference (EPEC)*, pp. 125-130. IEEE, 2021.
35. Stefan, Maria, Jose G. Lopez, Morten H. Andreasen, and Rasmus L. Olsen. "Visualization techniques for electrical grid smart metering data: A survey." In *2017 IEEE third international conference on big data computing service and applications (bigdataservice)*, pp. 165-171. IEEE, 2017.

36. Longe, Omowunmi Mary, Khmaies Ouahada, Suvendi Rimer, Hendrik C. Ferreira, and A. J. Han Vinck. "Distributed optimization algorithm for demand side management in a grid-connected smart microgrid." *Sustainability* 9, no. 7 (2017): 1088.
37. Zhang, Dongxia, Xiaoqing Han, and Chunyu Deng. "Review on the research and practice of deep learning and reinforcement learning in smart grids." *CSEE Journal of Power and Energy Systems* 4, no. 3 (2018): 362-370.
38. Ruobing Liang, Yifan Guo, Liang Zhao, Yan Gao, "Real-time Monitoring implementation of PV/T façade system based on IoT", Journal of Building Engineering, Vol.41, Article 102451, 2021.
39. Atef Ftirich; Bechir Bouaziz; Faouzi Bacha, "Design and Implementation of Real-Time Monitoring System for Building-integrated Photovoltaic System", IEEE International Conference on Advanced Systems and Emergent Technologies (IC_ASET), Tunisia, 29 April 2023 - 01 May 2023.
40. Shaheer Ansari, Afida Ayob, Molla S. Hossain Lipu, Mohamad Hanif Md Saadand Aini Hussain, "A Review of Monitoring Technologies for Solar PV Systems Using Data Processing Modules and Transmission Protocols: Progress, Challenges and Prospects", Sustainability, Vol.13, Article 8120, 2021.
41. Ghedhan Boubakr, Fengshou Gu, Laith Farhan and Andrew Ball, "Enhancing Virtual Real-Time Monitoring of Photovoltaic Power Systems Based on the Internet of Things", Electronics, Vol.11, Article 2469,2022.
42. Nur Iksan, Purwanto and Heri Sutanto, "Smart Micro Grid Architecture for Realtime Monitoring of Solar Photovoltaic Based on Internet of Things", IOP Conference Series: Earth and Environmental Science, Vol.1203, Article 012042,2023.
43. Asnil Asnil, Krismadinata Krismadinata, Irma Husnaini, Hanif Hazman, Erita Astrid, "Real-Time Monitoring System Using IoT for Photovoltaic Parameters", TEM Journal. Vol.12, Issue 3, pp.1316-1322, August 2023.
44. M Sesa and F Mahmuddin, "Development of Real-Time Monitoring System for an Off-Grid Photovoltaic System", IOP Conference Series: Earth and Environmental Science, Vol.921, Article 012031, 2021.
45. Silvio Simani, Stefano Alvisi and Mauro Venturini, "Data-Driven Control Techniques for Renewable Energy Conversion Systems: Wind Turbine and Hydroelectric Plants", Electronics 2019, Vol.8, Article 237, 2019.
46. Liu, H., Li, Y., Duan, Z., and Chen, C, "A review on multi-objective optimization framework in wind energy forecasting techniques and applications", Energy Conversion and Management, Vol.224, Article113324, Nov.2020.
47. González-Sopeña, J. M., Pakrashi, V., and Ghosh, B. (2021). An overview of performance evaluation metrics for short-term statistical wind power forecasting. Renew. Sustain. Energy Rev. 138, 110515. doi:10.1016/j.rser.2020.110515
48. Sobolewski, R. A., Tchakorom, M., and Couturier. R, "Gradient boosting-based approach for short- and medium-term wind turbine output power prediction. Renewable Energy, Vol.203, pp.142–160, 2023.
49. Yaxin Liu , Yunjing Wang , Qingtian Wang, Kegong Zhang, Weiwei Qiang and Qiuzi Han Wen, "Recent advances in data-driven prediction for wind power", Frontiers in Energy Research, Vol,11, Article 1204343, 2023.
50. Sawant, M., Patil, R., Shikhare, T., Nagle, S., Chavan, S., Negi, S., *et al*, "A selective review on recent advancements in long, short and ultra-short-term wind power prediction", *Energies, Vol.5,*Issue.21, Article 8107, 2022,
51. Wang, Y., Zou, R., Liu, F., Zhang, L., and Liu, Q, "A review of wind speed and wind power forecasting with deep neural networks", Applied Energy, Vol.304, Article 117766, Dec.2021.
52. Li, Z., Luo, X., Liu, M., Cao, X., Du, S., and Sun, H, "Short-term prediction of the power of a new wind turbine based on IAO-LSTM", Energy Reports, Vol.8, pp.9025-9037, Nov 2022.
53. Nandi, Swagata, and Debasis Kundu. Statistical signal processing. Springer Singapore, 2020.
54. Chapeau-Blondeau, François. "Autocorrelation versus entropy-based auto information for measuring dependence in random signal." Physica A: Statistical Mechanics and its Applications 380 (2007): 1-18.
55. Brandwood, David. Fourier transforms in radar and signal processing. Artech House, 2012.
56. Li, Xiang, and Haiyan Yao. "Improved Signal Processing Algorithm Based on Wavelet Transform." Journal of Multimedia 8, no. 3 (2013).
57. Hosseini, Mohammad-Parsa, Amin Hosseini, and Kiarash Ahi. "A review on machine learning for EEG signal processing in bioengineering." IEEE reviews in biomedical engineering 14 (2020): 204-218.

58. Kimes, Patrick K., Yufeng Liu, David Neil Hayes, and James Stephen Marron. "Statistical significance for hierarchical clustering." Biometrics 73, no. 3 (2017): 811-821.
59. Dong, Yihong, Xiaohan Jiang, Lei Cheng, and Qingjiang Shi. "SSRCNN: A semi-supervised learning framework for signal recognition." IEEE Transactions on Cognitive Communications and Networking 7, no. 3 (2021): 780-789.
60. Huang, Guyue, Jingbo Hu, Yifan He, Jialong Liu, Mingyuan Ma, Zhaoyang Shen, Juejian Wu *et al.* "Machine learning for electronic design automation: A survey." ACM Transactions on Design Automation of Electronic Systems (TODAES) 26, no. 5 (2021): 1-46.
61. Ning, Fei, Yuzhe Ma, Haoyu Yang, Bei Yu, Huazhong Yang, and Yu Wang. "Machine Learning for Electronic Design Automation: A Survey." arXiv preprint arXiv:2102.03357 (2021).
62. Dogan, Alican, and Derya Birant. "Machine learning and data mining in manufacturing." Expert Systems with Applications 166 (2021): 114060.
63. Raman, Srikanth Venkat, Pongpachara Limpisathian, Pascal Meinerzhagen, Suriyaprakash Natarajan, and Eric Yang. "Automating design for yield: Silicon learning to predictive models and design optimization." In 2020 IEEE International Test Conference (ITC), pp. 1-10. IEEE, 2020.

Indian Journal of Natural Sciences *www.tnsroindia.org.in ©IJONS*

Vol.15 / Issue 83 / Apr / 2024 *International Bimonthly (Print) – Open Access* *ISSN: 0976 – 0997*

RESEARCH ARTICLE

A pilot study on the use of *Annona squamosa* extract in the application of Wet Wipes

Sujatha Raghu*, Ilakkia Sivaji, Sivapriya.s

SRM Arts and Science College, Kattankulathur, (Affiliated to University of Madras) Chennai, Tamil Nadu, India.

Received: 22 Feb 2024 Revised: 07 Mar 2024 Accepted: 20 Mar 2024

***Address for Correspondence**
Sujatha Raghu
SRM Arts and Science College,
Kattankulathur, (Affiliated to University of Madras)
Chennai, Tamil Nadu, India.
Email: sujatharaghubt@srmasc.ac.in

ABSTRACT

Annona squamosa leaf extract was used for making wet wipes. The leaf extract was obtained by maceration using isopropanol. The leaf extract was subjected to thin-layer chromatography. The various secondary metabolites were resolved using hexane and ethyl acetate as the solvent system. The qualitative test confirmed the presence of alkaloids, saponins, flavonoids and triterpenoids. The antibacterial activity of the crude extract against *Aeromonas caviae* (MTCC7725) was confirmed in Muller Hinton agar. The wet wipes were prepared using bamboo tissue paper. The presence of secondary metabolites was confirmed using scanning electron microscopy and Fourier transform infrared spectroscopy. The patch test was analyzed using a statistical test and it was confirmed that the wet wipes were safe to use.

Keywords: A*nnona squamosa*, secondary metabolites, antibacterial activity patch test, FTIR, and wet wipes

INTRODUCTION

The recent coronavirus pandemic has created awareness among people about the spread of diseases and has made self-hygiene a top priority. Self–hygiene affects a person's physical and mental health. Self-hygiene prevents the spread of infectious diseases .An easy way to combat the spread of germs is to use wet wipes that help sterilize the surface or skin. Although products such as wet wipes are handy and kill most germs quickly, the harsh chemicals used have a long-term impact on the skin. Another major concern is the source and amount of raw materials used to develop these wet wipes. It is also a major environmental pollutant. Some studies have shown that wet wipes can be developed using natural polymers, such as bamboo containing extracts of Aloe Vera. The medicinal properties of aloe vera are well known and play an indispensable role in the cosmetic industry. It is important to explore other

natural products that are skin–friendly. As the demand for wet wipes has drastically increased, it is necessary to develop environmentally benign wet wipes for commercialization. The current study focused on the use of *Annona squamosa* extract to develop wet wipes. *Annona squamosa Linn* (Custard apple) belongs to the Annonaceae family. They are also commonly found in India. Extracts obtained from different parts of the plant have been studied to understand their role in diseases, such as cancer, diabetes, obesity, and liver failure. The various phytochemicals of Annona squamosal can be classified as acetogenins, alkaloids, flavonoids, phenols, saponins, tannins, glycosides, sesquiterpenes, anthocyanins, steroids, diterpenes, terpenoids, quinones, amino acids, and fatty [1,2,3,4] A hand sanitizer has been prepared using the peel and seed extracts of Annona squamosa to develop a hand sanitizer gel[5]. The antimicrobial activity of the gel was tested against both gram-positive and gram-negative bacteria. The raw material used for developing these wet wipes was 100% organic and biodegradable. The extract of Annona squamosal was tested for antibacterial activity and was adsorbed on bamboo tissue paper (Rusabl Company). The extract contained several secondary metabolites, which were screened using thin-layer chromatography and confirmed using qualitative phytochemical tests. Wet wipes were developed using the adsorption method. FTIR analysis was performed to determine whether adsorption had occurred. FTIR analysis showed morphological differences in wet wipes upon adsorption. The adsorbed wet-wipe containing the leaf extracts of *Annona squamosa* was subjected to SEM analysis to study its morphological characteristics. The developed wet wipes were used for patch testing among the 50 volunteers. The wet wipes were found to be skin-friendly. The use of *Annona squamosa* extract in wet wipes can be a better alternative to the harmful chemical substances that are used in commercially available wet wipes. Moreover, these wet wipes are 100% organic; therefore, they are a better alternative than their commercial counterparts.

MATERIALS AND METHODS

Extraction of phytochemicals from the leaves of *Annona squamosa*

The *A. squamosa* leaves were sun-dried and powdered. Coarsely powdered leaves (10 g) were macerated using isopropanol. The contents were covered with aluminum foil and stirred constantly using a magnetic stirrer for 24 h. The extract was obtained by evaporation of the solvent in a microwave oven [6].

Qualitative test analysis and TLC for the confirmation of bioactive compounds

The phytochemicals present in the leaf extracts were analyzed using TLC. 10µl of the leaf extract were loaded onto silica gel G 25 plates. Hexane and ethyl acetate were used at a ratio of 7:3 as developing solvents. The TLC plates were run in triplicate. Spot A was the control without leaf extract. Spot B contained the leaf extract. The extract was tested for carbohydrates, saponins, tannins, flavonoids,alkaloids, betacyanin, and triterpenoidsas suggested by Shaiek et al[7].

Antibacterial activity of the leaf extract

The antibacterial activity of *A. squamosa* extracts was determined using a modified Kirby-Bauer disc diffusion method[8]. Briefly, a loop of *Aeromonas caviae* culture was inoculated in 100 ml of nutrient broth and kept in an incubator for 24 h at 37 °C. One hundred microliters of the grown microbial suspension was spread onto Muller Hinton (MH) agar in petri plates using autoclaved buds. The extract was diluted in 1 ml of isopropanol: distilled water at a ratio (15% to 85%). Three wells with a diameter of 6 mm were punched into the agar and 20 µL of (15%:85%) isopropanol: distilled water were loaded in the negative control and 50 µg, 75 µg of dissolved extract was loaded into two wells. An antibiotic disc (kanamycin) was used as a positive control. The plates were then incubated at 37 °C for 24 h.

Preparation of wet wipes using the leaf extract of Annona Squamosa

Bamboo tissue paper was used for the adsorption of the leaf extract to prepare wet wipes. The extract was dissolved in 85% isopropanol. It was then filtered using Whatman No. 1 filter paper. The filtered extract was mixed with 2 ml

glycerin, 1 ml of rose water, vitamin E oil (2 capsules), and 100µl of jasmine oil. The mixture was then diluted with 50 ml of distilled water. The solution was poured into an air-tight container, and tissue paper was placed for absorption. The preparation was left for three days for complete absorption.

SEM, FTIR and UV analysis of the adsorbed wet wipes

Morphological analysis of the wet wipes was performed using scanning electron microscopy and Fourier-transform infrared spectroscopy. The surface morphology of the wet wipes was characterized using Scanning Electron Microscopy. The instrument was operated at a voltage of 15 kV. The dried adsorbed wipe was mounted on metal grids using carbon tape and sputter coated with gold. An FTIR spectrophotometer (Shimadzu IRTRACER 100) was used to study the adsorbed wet wipes using the ATR mode in the range 4000-400 cm^{-1}. The UV spectra of the leaf extract before and after adsorption were recorded using a SHIMADZU, UV 3600 PLUS instrument.

Patch testing of wet wipes

The extract was used at a ratio of 85:15 in distilled water and isopropanol. It was then filtered using Whatman No. 1 filter paper. The filtered extract was mixed with 2 ml glycerin, 1 ml of rose water, vitamin E oil (2 capsules), and jasmine oil for fragrance (2 drops). The mixture was then diluted with 50 ml of distilled water. The solution was poured into an air-tight container, and tissue paper was placed for absorption. The preparation was left for three days for complete absorption.

Because the components used in the wet wipes were skin-friendly, they were further moved for patch testing. Fifty volunteers were selected, the prepared wipes were tested in the hands of the volunteers, and the result was absorbed after 24 h.

RESULTS AND DISCUSSION

phytochemical extraction

The extracts were then subjected to qualitative analysis. The extract tested positive for Mayer's test, confirming the presence of alkaloids, betacyanin, quinones, flavonoids, terpenoids, and phenols (Table 1). The crude extract obtained by Lakshmi et al. (2013) confirmed the presence of alkaloids in the seeds of *Annona Squamosa*[9 &10].The antibacterial activity of the phytochemical extract showed a zone of inhibition against the gram-negative bacterium *Aeromonas caviae* (MTCC 7725), as shown in Figure 1. The methanolic leaf extract of *Annona Squamosa* was found to have antibacterial activity against *Bacillus subtilis* and *Staphylococcus aureus*[10].

Morphological analysis of the wet wipes using SEM, UV and FTIR

Scanning electron microscopy showed the native bamboo tissue paper and absorbed leaf extract. The bamboo tissue paper absorbed with the leaf extract showed a random arrangement of cellulose fibers. These cellulose fibers are hundreds of micrometers long and 50-100 micrometers in diameter, as shown in figure 2[11]. The absorbed extracts can be seen as knots on the wet wipes. UV-visible spectrophotometry indicated that the leaf extract was absorbed on the cellulose matrix. The UV-visible spectra of the leaf extract showed important peaks at 310,422 and 730. These peaks indicate the presence of phenolic compounds, carotenoids, and chlorophyll[12]. As shown in figure 3, the UV spectra of the extract after absorption decreased to 0.559 a.m. u. at 310 nm and 0.449 a.m. u. at 422 nm, indicating the absorption of phytochemicals. The FTIR spectra of the plain bamboo wipe were compared with those of the adsorbed wet wipe. The plain bamboo tissue paper showed a peak at 3334.92 cm^{-1}. This is assigned to the hydroxyl group stretching in the cellulose microfiber[13]. This peak shifted to 3332.99 cm^{-1} in the adsorbed wet wipe. New peaks can be seen in the adsorbed wet wipe such as 2900.94 cm^{-1} and 1643.33 cm^{-1}. The peak at 2900cm^{-1} indicated the presence of C=O stretching, confirming the presence of alpha/beta-unsaturated aldehydes and ketones. The peak at 1643.33 cm^{-1} shows the presence of an N- O asymmetric stretch for nitro compounds[13,14,15,16]. The shifts in the peak indicate the interaction between the cellulose microfibers and phytochemicals found in the leaf extract of *Annona squamosa*.

Patch test of the wet wipes

Patch tests were performed on 50 volunteers. Fisher's exact test indicated that there was no evidence to indicate that wet wipes containing the leaf extract of *Annona squamosa* caused allergic reactions.

CONCLUSION

The wet wipes developed using *A. squamosa* leaf extract were found to be skin-friendly. It can also circumvent the problem of microplastics released into water bodies using commercially available wet wipes. Operational stability, such as shelf life, must be optimized so that it can be a promising alternative to commercially available wet wipes.

REFERENCES

1. Kumar Manoj Sushil Changan Maharishi Tomar, Uma Prajapati, Vivek Saurabh, Muzaffar Hasan, Minnu Sasi et al. "Custard apple (*Annona squamosa* L.) leaves: Nutritional composition, phytochemical profile, and health-promoting biological activities." *Biomolecules* 11, no. 5 (2021): 614.
2. Hussain, Iqbal, Riaz Ullah, Muhammad Khurram, Nazeem Ullah, A. Baseer, Farhat Ali Khan, M. U. R. Khattak, Mohammad Zahoor, Jehangir Khan, and N. Khan. "Phytochemical analysis of selected medicinal plants." *African Journal of Biotechnology* 10, no. 38 (2011): 7487-7492
3. Santhoshkumar, R., and Neethu S. Kumar. "Phytochemical analysis and antimicrobial activities of Annona squamosa (L) leaf extracts." *Journal of Pharmacognosy and phytochemistry* 5, no. 4 (2016): 128-131.
4. Saha, Rajsekhar. "Pharmacognosy and pharmacology of Annona squamosa." *Int. J. Pharm. Life Sci* 2 (2011): 1183-1189.
5. Safira, Arifia, PrasitaWidayani, Dhiya An-Najaaty, Cinta Atsa Mahesa Rani, Mela Septiani, Yan Arengga Syah Putra, Tridiganita Intan Solikhah, Aswin Rafif Khairullah, and Hartanto Mulyo Raharjo. "A review of an important plants: Annona squamosa leaf." *Pharmacognosy Journal* 14, no. 2 (2022).
6. Thi Hieu Trang, Nguyen, Nguyen Van Lai, and Duong Quoc Khanh. "Agricultural Waste Annona squamosa L. Peel and Seed Extract: Biosynthesis of Hand Sanitizer Gel against Skin Pathogens." (2021).
7. Safira, Arifia, PrasitaWidayani, Dhiya An-Najaaty, Cinta Atsa Mahesa Rani, Mela Septiani, Yan Arengga Syah Putra, Tridiganita Intan Solikhah, Aswin Rafif Khairullah, and Hartanto Mulyo Raharjo. "A review of an important plants: Annona squamosa leaf." *Pharmacognosy Journal* 14, no. 2 (2022).
8. Biemer, James J. "Antimicrobial susceptibility testing by the Kirby-Bauer disc diffusion method." *Annals of Clinical & Laboratory Science* 3, no. 2 (1973): 135-140.
9. Abubakar, Abdullahi R., and Mainul Haque. "Preparation of medicinal plants: Basic extraction and fractionation procedures for experimental purposes." *Journal of pharmacy &bioallied sciences* 12, no. 1 (2020): 1.
10. Shaikh, Junaid R., and M. Patil. "Qualitative tests for preliminary phytochemical screening: An overview." *International Journal of Chemical Studies* 8, no. 2 (2020): 603-608.
11. Ali, Saima, Muhammad Rashid Khan, Irfanullah, Moniba Sajid, and Zartash Zahra. "Phytochemical investigation and antimicrobial appraisal of Parrotiopsisjacquemontiana (Decne) Rehder." *BMC complementary and alternative medicine* 18 (2018): 1-15.
12. Lakshmi, S., and G. S. Dhanya. "Phytochemical analysis of Annona squamosa seed extracts." *International Research Journal of Pharmaceutical and Applied Sciences* 3, no. 4 (2013): 29-31.
13. Al-Nemari, Rawan, Abdulrahman Al-Senaidy, Abdelhabib Semlali, Mohammad Ismael, Ahmed Yacine Badjah-Hadj-Ahmed, and Abir Ben Bacha. "GC-MS profiling and assessment of antioxidant, antibacterial, and anticancer properties of extracts of Annona squamosa L. leaves." *BMC Complementary Medicine and Therapies* 20, no. 1 (2020): 1-1
14. Cao, Cong-Xiao, Jiayin Yuan, Jin-Pei Cheng, and Bao-Hang Han. "Synthesis of porous polymer/tissue paper hybrid membranes for switchable oil/water separation." *Scientific Reports* 7, no. 1 (2017): 3101.

15. Mabasa, X. E., L. M. Mathomu, N. E. Madala, E. M. Musie, and M. T. Sigidi. "Molecular spectroscopic (FTIR and UV-Vis) and hyphenated chromatographic (UHPLC-qTOF-MS) analysis and in vitro bioactivities of the Momordica balsamina leaf extract." *Biochemistry Research International* 2021 (2021).
16. Hospodarova, Viola, Eva Singovszka, and Nadezda Stevulova. "Characterization of cellulosic fibers by FTIR spectroscopy for their further implementation to building materials." *American journal of analytical chemistry* 9, no. 6 (2018): 303-310.
17. Chandran, M., R. Mangaleshwari, K. R. Udhayavani, and Kadarkarai Murugan. "Studies on FTIR analysis of fraction I and II of Annonasquamosa methanol leaf extract." *World journal of pharmacy and pharmaceutical sciences* 5, no. 8 (2016): 1247-1256.
18. Warshaw, Erin M., Kelly A. Aschenbeck, Kathryn A. Zug, Donald V. Belsito, Matthew J. Zirwas, Joseph F. Fowler Jr, James S. Taylor et al. "Wet Wipe Allergens: Retrospective Cross-Sectional Analysis of North American Contact Dermatitis Group Data From 2011 to 2014." *Dermatitis* (2016).

Table 1: Qualitative test for secondary metabolites in *Annona squamosa*

Phytochemical extract	Test	Result
Alkaloids	Mayer's test	+
Saponins	Foam test	+
Flavanoids	Shinoda test	+
Quinones	Sulphuric acid	+
Phenols	Ferric chloride	+

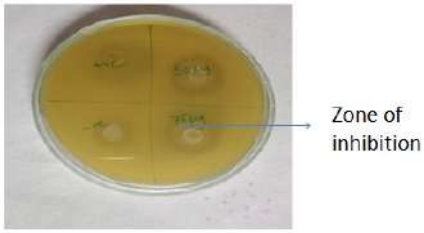

Figure 1: Zone of inhibition is observed for the leaf extract of Annona Squamosa

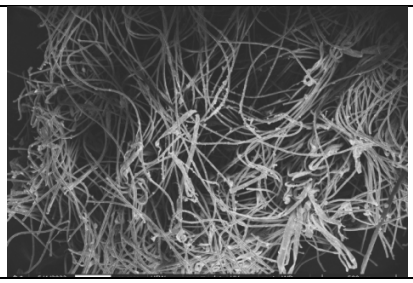

Figure 2:The scanning Electron Microscope shows the presence of absorbed extract on the organic bamboo tissue paper matrix

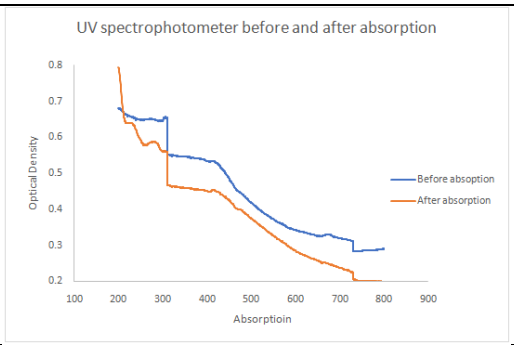

Figure 3: The UV absorption spectra of the various phytochemicals in the leaf extract of AnnonaSquamosa

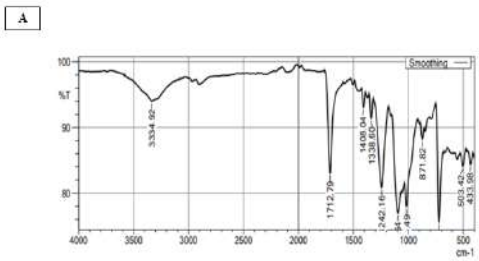

Figure 4: FTIR spectrum of A) plain bamboo tissue

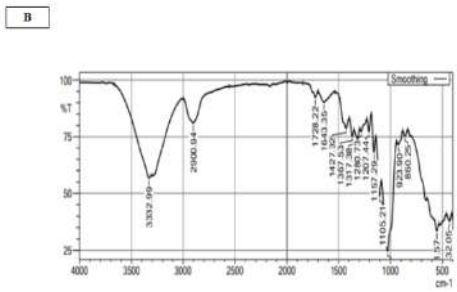

Fig 4: B) leaf extract adsorbed wet wipe of Annona Squamosa

Indian Journal of Natural Sciences *www.tnsroindia.org.in ©IJONS*

Vol.15 / Issue 83 / Apr / 2024 *International Bimonthly (Print) – Open Access* *ISSN: 0976 – 0997*

RESEARCH ARTICLE

Rainfall Forecasting: A Harmonic Analysis Perspective

R. Shanmugapriya[1]*, R. Shenbagavalli[1] and Hemalatha N C[2]

[1]PG Department of Mathematics, St.Francis de Sales College, Bangalore, Karnataka, India.
[2]Department of Mathematics, The Oxford College of Engineering, Bangalore, Karnataka, India.

Received: 29 Jan 2024 Revised: 22 Feb 2024 Accepted: 13 Mar 2024

***Address for Correspondence**
R. Shanmugapriya
PG Department of Mathematics,
St.Francis de Sales College,
Bangalore, Karnataka, India.

ABSTRACT

Estimating the Quantity of monthly a torrential comes brighter agriculture and secures food preserve the water supply for the continued health of our people. To predict rainfall, several types of research have been conducted using Harmonic Analysis of various cities in Tamil Nadu. The primary objective of this investigation is to forecast the monthly variations in rainfall over Tiruvannamalai, Tamil Nadu. Considering the fluctuations in monthly rainfall are periodic, there is an excellent likelihood that they will occur again the next year.

Keywords: Quantity, forecast, rainfall, agriculture, food.

INTRODUCTION

The hydrological cycle focuses heavily on rainfall, and variations in its pattern have a rapid effect on the affordability of water. Hydrologists and managers of water-related assets are becoming increasingly worried regarding how climate change has impacted the timing of precipitation. In India, the monsoon rains are essential to agriculture. Rain-fed agriculture, which sustains 40% of the population of humanity and 60% of the animal population, accounts for 68% of India's total cultivated land [9]. Therefore, extensive research on the detection and measurement of climate change is essential for the long-term viability of agriculture in India. Above all, an in-depth awareness of the forecast pattern in the dynamic environment will encourage enhanced choices and increase communities' capacity to adapt to.

Objective of the study:
This study demonstrates a method using harmonic analysis techniques to predict monthly rainfall amount with the highest amount of accuracy so that it can help the farming community in

i Estimating the type of crop to be grown a few months before each session.
ii Isolating the effects of the monsoon vagaries in crop destructions.

Rainfall Pattern in Tamil Nadu

The rainfall distribution in Tamil Nadu state is of a monsoon type with particular seasons of rainfall and intervening dry periods. The cropping and cultivation have been adjusted to these conditions. The monsoon season and the dry periods in Tamil Nadu are distributed as

- During a cold spell (winter rain) - January to February
- Warm weather duration - March to May
- The monsoon season in the South West - June to September
- Monsoon season in the northeast - October to December

It is known that the trigonometric functions sin x and cos x are otherwise called periodic functions, since their values repeated itself periodically. Hence a combination of the two could better express the behavior of any time series which is periodic. The time series data on the rainfall expresses cyclic variations, every year. Hence it was thought appropriate to use the combination is sin and cos functions otherwise known as the Fourier series expression as an appropriate tool to analyze the rainfall data.[2] The details of rainfall for each one of the months over the 50 years were exhibited in the Fourier analysis. For each monthly data periodic oscillations were observed and hence an equation of the form,

$$y = \frac{a_0}{2} + \sum_{i=1}^{n} (a_i cositz + b_i sinitz)$$

was attempted. In this,

- y is the average monthly rainfall
- t is month from January to December
- ai and bi are the fourier constants
- 'i' is the harmonic number
- n is the end value of the order of the harmonic used

$$z = \frac{360^0}{12} = 30^0$$

The estimated value of the coefficients for Thiruvannamalai are presented below in Table-1

Thus in the case of Thiruvannamalai the absolute deviations for observed and estimated were estimated upto the eighth harmonic and is minimum for the eighth harmonic as seen in Table-2. Results presented in Table reveal that the absolute deviations are minimum only during the months of June, July, October and November in all the harmonics and is maximum during the month of February in all the harmonics[4]. This shows the predictability is higher if it is a rainfall season and in the non-seasonal periods, it is natural that the variability will always be higher and that is being reflected in this analysis[5]. The deviations started increasing from the ninth harmonic onwards and hence the computation of harmonics is stopped at the ninth.

These deviations were tested through chi-square and the estimated chi-square are presented below in Table-3.

The chi-square value also shows that the minimum chi-square is for October followed by July, November and June[7]. For all other months all results showed higher deviations. As explained earlier this might probably be due to the fact that regular rainfall occurred in this station in all the above four months and in the other months there is no consistency of rainfall[6]. This is again ascertained by the minimum coefficients of variation values in the regular rainfall months and the higher coefficient of variability in the non-seasonal months. The mean, standard deviation, coefficient of variation, skewness and kurtosis are presented below in Table-4.

The results presented Table-4 reveals that it is in agreement with the results got through harmonic analysis.
The results so far obtained and those computed for all over state.

1.The closeness to the actual value are the highest in a particular harmonic for each or few similar stations.
2. The absolute deviations are minimum during the south-west and the north-east monsoon periods. i.e., the regular rainfall seasons.
3. Among the rainfall seasons the co-efficients of variation is the least for the highest rainfall seasons.

DISCUSSION AND CONCLUSION

The results so far obtained and those computed for all over state.

1. The closeness to the actual.
2. The absolute deviations.
3. Among.

The Harmonic analysis reveals the proximity between the observed rainfall and expected rainfall during the rainy season as expressed by the co-efficient of variation. It should be noted that the order of the harmonic, which reaches the closeness, indicates the cyclic period of the rainfall. Thus the harmonic analysis of rainfall data shows the period of possibility for drought as well as the year of heavy showers[5].

REFERENCES

1. Durairaj. S, Agriculture price analysis regression and time series approach, Unbublished Ph. D., thesis submitted to Manonmaniyam Sundaranar University(2001).
2. H. Darmon, F. Diamond, and R Taylor. Fermat's last theorem. Current Developments in Mathematics, 1995(1):1-154,1995.
3. C. Frei, D. Loughran, and R. Newton. Number fields with prescribed norms, 2019.
4. Immaculate Mary.M, Senthamarai Kannan.K and Suyambulingam.C(2005): Harmonic analysis and probability distributions-An application to rainfall forecast, Journal of extension and research. Vol.II, Nos. 1 2, 83-85.
5. Todini. E. and Bacco.M(1997): A combined polya process and mixture 1:367-368.
6. Wilby. R.L(2001): Down scaling summer rainfall in the UK from north atlantic ocean temperatures, Hydrology and earth system science, 5:245- 257.
7. Zekai Sen and Ali Geath Eljadid(1999): Rain fall distribution function for Libya and rainfall production, Hydrology and earth system science - Journal des Sciences Hydrologiques, 44(5): 665-680.
8. Bushra Praveen, Swapan Talukdar, Shahfahad, Susanta Mahato, Jayanta Mondal, Pritee Sharma, Aburaza Md. Towfiqul Islam and Atiqur Rah- man, Scientific Reports(2020) 10:10342.
9. Chalechew Muluken Liyew and Haileyesus Amsaya Melese, Machine Learning techniques to predict daily rainfall amount, Journal of Big data8, Article number:153(2021)
10. M.M. Wood. On the probabilties of local behaviors in abelian field exten- sions. Composition Mathematica, 146(01):102-128, Aug 2009.
11. S. Wanga. On Grunwald's theorem. Annals of Mathematics, 51(2):411- 484,1950.

Table 1 - Estimated Fourier Co-efficient for Thiruvannamalai

		b	
a_0	1.316	b_0	-
a_1	1.115	b_1	1.062
a_2	0.028	b_2	-0.985
a_3	-0.927	b_3	0.851
a_4	0.834	b_4	**0.763**
a_5	0.612	b_5	-0.651
a_6	-0.468	b_6	0.532
a_7	0.210	b_7	0.301
a_8	0.126	b_8	-0.214
a_9	-0.058	b_9	0.082

The measured and expected rainfalls are presented in Table-1 for Thiruvannamalai using the estimated harmonic co-efficient[3].

Table 2 - Absolute deviations for the observed and the estimated rainfall by different harmonics Thiruvannamalai

Months	5 HAR	6 HAR	7 HAR	8 HAR	9 HAR
January	10.954	10.367	9.851	9.264	10.417
February	11.372	10.548	9.979	9.351	9.996
March	12.517	12.108	11.643	11.110	11.842
April	11.718	11.534	10.976	10.218	10.859
May	11.226	10.783	10.425	9.674	10.053
June	10.421	10.173	9.679	9.134	9.785
July	9.638	9.258	8.897	8.352	8.742
August	10.338	10.106	9.845	9.173	9.975
September	11.369	10.947	10.710	9.458	10.117
October	9.257	9.082	8.976	8.358	8.969
November	9.596	9.274	9.004	8.485	8.857
December	11.147	10.776	10.143	9.675	10.141

Table 3 - Chi-Square values between the observed and the estimated rainfall for different harmonics Thiruvannamalai

Months	5 HAR	6 HAR	7 HAR	8 HAR	9 HAR
January	12.673	12.402	12.081	11.759	12.252
February	13.215	12.847	12.518	12.132	12.854
March	12.905	11.673	11.529	10.042	10.647
April	12.041	11.662	11.434	10.754	12.312
May	11.684	11.259	10.638	10.286	11.142
June	10.945	10.718	10.537	10.284	10.649
July	9.941	9.637	9.329	9.112	9.453
August	10.354	9.767	9.631	9.979	10.149
September	11.215	10.943	10.758	10.321	10.846
October	9.473	9.165	8.874	8.539	8.869
November	10.751	10.428	10.217	9.964	10.582
December	11.425	11.259	10.485	10.139	10.758

Table 4 - Mean, Standard Deviation, Co-efficient of variation, Skewness and Kurtosis of Thiruvannamalai

Months	Mean	S.D	C.V	Skewness	Kurtosis
January	94.51	87.31	92.38	1.054	1.221
February	111.38	94.78	85.09	1.328	1.164
March	123.51	86.51	70.04	0.953	1.281
April	151.84	100.47	66.17	1.326	1.153
May	173.21	98.95	54.82	1.151	-0.967
June	466.27	173.85	37.29	0.896	0.913
July	513.58	137.15	26.70	0.746	0.817
August	334.21	162.73	48.69	0.884	0.965
September	223.58	187.47	70.88	0.928	1.132
October	976.48	124.58	12.76	0.657	0.842
November	893.52	186.93	20.92	0.853	0.785
December	613.72	221.32	36.06	1.372	1.158

Indian Journal of Natural Sciences www.tnsroindia.org.in ©IJONS

Vol.15 / Issue 83 / Apr / 2024 International Bimonthly (Print) – Open Access ISSN: 0976 – 0997

RESEARCH ARTICLE

MAGDAM ROBLEM WITH NEUTROSOPHIC FUZZY SET

R. Shenbagavalli[1]*, R. Shanmugapriya[1] and M. Rajeswari[2]

[1]PG Department of Mathematics, St. Francis de Sales College, Bangalore, Karnataka, India.
[2]Department of Mathematics, Govt. Arts College, Hosur, Krishnagiri, Tamil Nadu India.

Received: 29 Jan 2024 Revised: 22 Feb 2024 Accepted: 13 Mar 2024

***Address for Correspondence**
R. Shenbagavalli
PG Department of Mathematics,
St. Francis de Sales College,
Bangalore, Karnataka, India.

ABSTRACT

This endeavor investigates Multiple Attribute Group Decision Making (MAGDM) scenarios, where all decision makers' wisdom is provided as fuzzy soft sets and fuzzy soft decision matrices.

Keywords: Attribute, wisdom, matrices, fuzzy

INTRODUCTION

An further extension of fuzzy sets, intuitionistic fuzzy sets, image fuzzy sets, Pythagorean fuzzy sets, spherical fuzzy sets, etc. is the Neutrosophic theory, which has been developed by F. Smarandache in 1998. This reasoning has since been used in other scientific and technical fields.

Assumptions

Roughly speaking, a fuzzy set is a class with fuzzy boundaries. The fuzzy set A in the universe of discourse *S*, *S* = {s1,s2,s3------sn}, is a set of ordered pairs {(*s*1, μQ(*s*1)), (*s*2, μQ(*s*2)), . . . , (*sn*, μQ(*sn*))}, where μQ is the membership function of the fuzzy set *Q*, $\mu Q : S \rightarrow [0, 1]$, and $\mu Q(si)$ indicates the grade of membership of *ui* in *Q*. When the universe of discourse *S* is a finite set, then the fuzzy set *Q* can be represented by Q= μQ(s1)/s1 + μQ(s2)/s2 +... + μQ(sn)/sn is a comparable Q. The evidence for s in S and the evidence against s in S are amalgamated into a single quantity, which does not specify the specific quantities of each, as mentioned by Gau & Buehrer (1994). They also stressed that it contains little data regarding the exactitude of the single number. Thus, ideas of hazy sets was first proposed by Gau & Buehrer (1994). In order to explain the lower bound on μQ, they adopted a truth-membership function (tQ) and a false-membership function (fQ). a little the help of these smaller limits, a subinterval [tQ(si), 1 – fQ(si)] is created on [0, 1], whose dismisses the μQ(si) of fuzzy sets, where tQ(si) < μQ(si) ≤ 1 – fQ(si). Let Q be a vague set, for instance, and suppose the set's truth-membership function is tQ and its false-membership

function is fQ. Given that [tQ(si), 1 – fQ(si)] = [0.5,0.8] then we can see that tQ(si)=0.5 ; 1-fQ(si) = 0.8; fQ(si) = 0.2. It can be interpreted as, the vote for resolution is 5 in favour, 2 against, and 3 abstentions. A multiple attribute group decision making (MAGDM) difficulty seeks to determine a desired solution from a finite set of realistic prospects that have been appraised on a wide range of attributes, both qualitative and quantitative.

PRELIMINARIES OF VAGUE SETS

Definition: 1

"A vague set V is characterized by,

Its true membership function tv(x)

Its false membership function fv(x)

With 0 ≤ tv(x)≤ fv(x)≤ 1"

Definition: 2

"Suppose *S*, {*s*1, *s*2, . . ., *sn*}. Let the vague set *A* of the universe of discourse *S* can be represented by $\sum_{i=1}^{n} \frac{[t(s_i), 1-f(s_i)]}{u_i}$, 0≤(*si*)≤1−*f*(*si*)≤*ni*=11,1≤*i*≤*n*. In other words, the grade of membership of si bounded to a sub interval [*tQ* (*si*), 1 – *fQ* (*si*)] of [0, 1]. Thus, vague sets are a generalization of Fuzzy sets, since the grade of membership $\mu Q(s)$ of *s* in the above definition may be inexact in a vague set."

Definition: 3

"The minimum operation of vague values s and t is defined by

s and t = [minimum (ts ,tt), minimum (1-fs , f t)]

= [minimum (ts ,tt), 1-maximum(1-fs, 1-ft)]"

Definition: 4

"The Maximum operation of vague values s and t is defined by

s or t = [maximum(ts ,tt), maximum(1-fs , f t)]

= [maximum (ts ,tt), 1-maximum(1-fs, 1-ft)]"

Definition: 5

"The complement of vague value *s* is defined by $\bar{s}$=[*ts* ,1−*ts*]

Let *Q*, *P* be two vague sets in the universe of discourse *S*= {*u*1, *u*2, . . . , *un*},

$Q = [t_Q(u_i),\ 1 - f_Q(u_i)]/u_i$ and $P = [t_P(u_i),\ 1 - f_P(u_i)]/u_i$''

Definition: 6

"The intersection of vague sets *Q* and *P* is defined by,

$$Q \cap P = \sum_{i=1}^{n}\{[t_Q(u_i), 1 - f_Q(u_i)] \wedge [t_P(u_i), 1 - f_P(u_i)]\}/u_i$$

The union of vague sets *Q* and *P* is defined by,

$$Q \cup P = \{[t_Q(u_i),\ 1 - f_Q(u_i)] \vee [t_P(u_i),\ 1 - f_P(u_i)]\}/u_i.$$

The complement of vague set *Q* is defined by

$$\bar{Q} = \sum_{i=1}^{n}[f_Q(u_i), 1 - t_Q(u_i)]/u_i$$."

Definition: 7

"For vague value *x* = [*tx*, 1 − *fx*], define the defuzzification function to get the precise value as follows.

$Df_{zz}(x) = t_x/(t_x + f_x)$''.

Proposed model of decision making:

Let $W = \{W1, W2, \ldots, Wn\}$ be a set of alternatives, $G = \{G1, G2, \ldots, Gn\}$ be the set of attributes, $\omega = (\omega 1, \omega 2, \ldots, \omega n)$ is the weighting vector of the attribute Gj, $j = 1, 2, \ldots, n$, where $\omega j \in [0, 1]$, such that $\sum^{n} w_j = 1 = 1$. Let $D = \{D1, D2, \ldots, Dn\}$ be the set of decision makers, $V = (V1, V2, \ldots, Vn)T$ be the weighting vector of the dec ision makers, with $Vk \in [0,1]$, $\sum^{t} v_k = 1$

The developed model of MAGDM is given as follows:

Step 1:

Let $R_i = (r)_{ij}^{(k)} = T_{ij}^{(k)}, I_{ij}^{(k)}, F_{ij}^{(k)}$ be the Neutrosophic fuzzy decision matrix, where $(T)_{ij}^{(k)}$ is the extent to which the alternative A_i meets the characteristic in terms of the truth membership value G_j given by the decision maker D_k, $(I)_{ij}^{(k)}$ is the extent to which the indeterministic membership value that the alternative A_i satisfies the attribute G_j given by the decision maker D_k and $(F)^{(k)}$ is the degree of false membership value for the alternative A_i, where $T^{(k)}$, $I^{(k)}$, $F^{(k)}$ are in $[0, 1]$, $i = 1, 2, \ldots, m, j = 1, 2, \ldots, n, k = 1, 2, \ldots, t$.

Step 2:

Make right $i=1, 2, \ldots, m$, and $j = 1, 2, \ldots, n$

$\mu_{ij}^{(k)} = max\{T_{ij}^{(k)}::k=1,2,3----t\}$

$\gamma_{ij}^{(k)} = min\{I_{ij}^{(k)}::k=1,2,3----t\}$

$\lambda_{ij}^{(k)} = min\{F_{ij}^{(k)}::k=1,2,3----t\}$

Step 3:

Assume weight $w = (0.28, 0.24, 0.20, 0.16, 0.12)$ is determined from standard normal distribution about 5 variables.

Step 4:

Find reduced matrix $R = (Rij) = (Tij\ Iij,\ Fij)$ from the given k decision making matrices as follows:

$$T_{ij} = \sum_{k=1}^{t} T_{ij}^{(k)} \mu_{ij}^{(k)}$$

$$I_{ij} = \sum_{k=1}^{t} I_{ij}^{(k)} \gamma_{ij}^{(k)}$$

$$F_{ij} = \sum_{k=1}^{t} F_{ij}^{(k)} \lambda_{ij}^{(k)}$$

Step 5:

Taking $r = (1, 0, 0)$ as decision row is fixed.

Step 6:

The distance $4d(r,r_i) = \sqrt{(\frac{1}{2}[\prod_{j=1}^{n} T_{ij} + \prod_{j=1}^{n}(1 - I_{ij}) + \prod_{j=1}^{n}(1 - F_{ij})])}$ where i varies from 1 to n.

Step 7: Select the alternative $max_i\, d(r, r_i)$, say s.

Step 8: Identity the best alternative is W_s.

NUMERICAL ILLUSTRATION:

Step 1:

Assume that an investing firm, wanted should allocate a certain amount of money to the best selection out of five options on a panel; *W*1 is a Unlimited enterprise, *W*2 is a Private enterprises, *W*3 is a public enterprise, *W*4 is an associate enterprise & *W*5 is an Holding and Subsidiary enterprises.

The investment company must take a decision according to the four following attributes; *G*1 is the risk analysis, *G*2 is the growth analysis, *G*3 is the political impact analysis and *G*4 is the environmental impact analysis. The decision matrices of vague values $R_k = (\tilde{r}^{(k)})_{5x4}$, k = 1,2,3 are given as,

$R^1 =$

< 0.25, 0.54, 0.8 >	< 0.3, 0.4, 0.9 >	< 0.7, 0.35, 0.5 >	< 0.9, 0.2, 0.8 >
< 0.6, 0.5, 0.5 >	< 0.6, 0.2, 0.3 >	< 0.2.0.4.0.9 >	< 0.6, 0.23, 0.7 >
< 0.3, 0.45, 0.9 >	< 0.7, 0.1, 0.4 >	< 0.6, 0.5, 0.5 >	< 0.4, 0.2, 0.9 >
< 0.45, 0.38, 0.27 >	< 0.37, 0.68, 0.16 >	< 0.6, 0.25, 0.3 >	< 0.1, 0.4, 0.8 >

$R^2 =$

< 0.1, 0.3, 0.7 >	< 0.6, 0.6, 0.5 >	< 0.4, 0.2, 0.1 >	< 0.3, 0.7, 0.6 >
< 0.3, 0.55, 0.37 >	< 0.75, 0.42, 0.1 >	< 0.32, 0.67, 0.56 >	< 0.35, 0.56, 0.72 >
< 0.5, 0.4, 0.32 >	< 0.65, 0.25, 0.32 >	< 0.6, 0.3, 0.1 >	< 0.75, 0.25, 0.55 >
< 0.27, 0.9, 0.81 >	< 0.31, 0.4, 0.6 >	< 0.75, 0.65, 0.55 >	< 0.3, 0.7, 0.9 >

$R^3 =$

< 0.32, 0.47, 0.6 >	< 0.9, 0.1, 0.3 >	< 0.6, 0.4, 0.5 >	< 0.3, 0.5, 0.7 >
< 0.12, 0.32, 0.52 >	< 0.17, 0.81, 0.9 >	< 0.5, 0.3, 0.1 >	< 0.45, 0.65, 0.27 >
< 0.50, 0.6, 0.23 >	< 0.56, 0.52, 0.23 >	< 0.3, 0.6, 0.1 >	< 0.57, 0.52, 0.55 >
< 0.54, 0.83, 0.72 >	< 0.73, 0.86, 0.61 >	< 0.5, 0.52, 0.4 >	< 0.6, 0.4, 0.2 >

$$R^4 = \begin{bmatrix} < 0.7, 0.3, 0.1 > & < 0.5, 0.4, 0.4 > & < 0.2, 0.1, 0.6 > & < 0.7, 0.9, 0.6 > \\ < 0.3, 0.56, 0.73 > & < 0.57, 0.24, 0.1 > & < 0.23, 0.76, 0.65 > & < 0.53, 0.65, 0.27 > \\ < 0.32, 0.32, 0.6 > & < 0.56, 0.52, 0.32 > & < 0.1, 0.3, 0.9 > & < 0.57, 0.52, 0.55 > \\ < 0.72, 0.5, 0.18 > & < 0.13, 0.6, 0.4 > & < 0.55, 0.56, 0.78 > & < 0.7, 0.1, 0.6 > \end{bmatrix}$$

$$R^5 = \begin{bmatrix} < 0.52, 0.45, 0.1 > & < 0.57, 0.37, 0.1 > & < 0.76, 0.65, 0.23 > & < 0.57, 0.52, 0.55 > \\ < 0.3, 0.6, 0.7 > & < 0.7, 0.4, 0.1 > & < 0.3, 0.7, 0.6 > & < 0.5, 0.4, 0.6 > \\ < 0.2, 0.3, 0.2 > & < 0.6, 0.2, 0.5 > & < 0.1, 0.6, 0.65 > & < 0.3, 0.9, 0.7 > \\ < 0.27, 0.5, 0.81 > & < 0.75, 0.25, 0.32 > & < 0.32, 0.67, 0.56 > & < 0.35, 0.56, 0.72 > \end{bmatrix}$$

$W = \{0.28, 0.24, 0.2, 0.16, 0.12\}$

Step 2:

NEW REDUCED MATRIX

$$R = \begin{bmatrix} < 0.0465, 0.0252, 0.0108 > & < 0.1043, 0.0077, 0.0102 > & < 0.0814, 0.0064, 0.0078 > \\ < 0.0418, 0.0318, 0.0395 > & < 0.0836, 0.0162, 0.0063 > & < 0.0306, 0.0323, 0.0116 > \\ < 0.0379, 0.0258, 0.0198 > & < 0.0876, 0.0060, 0.0159 > & < 0.0480, 0.0271, 0.0081 > \\ < 0.0643, 0.0478, 0.0194 > & < 0.0652, 0.0277, 0.0099 > & < 0.0862, 0.0250, 0.0293 > \end{bmatrix}$$

$$\begin{bmatrix} < 0.1016, 0.212, 0.0737 > \\ < 0.0584, 0.0221, 0.0291 > \\ < 0.0800, 0.0179, 0.0733 > \\ < 0.0524, 0.0089, 0.0265 > \end{bmatrix}$$

Step 3:

$d(r, r_1) = 0.9594 = W_1$

$d(r, r_2) = 0.9635 = W_2$

$d(r, r_3) = 0.9518 = W_3$

$d(r, r_4) = 0.9586 = W_4$

Step 4: $W_2 > W_1 > W_4 > W_3$

Step 5: W_2 is best alternative

CONCLUSION

In this MAGDM procedure, hazy, ambiguous numbers are encountered. There are instances when attribute weight information is fully unknown, occasionally known, and occasionally partially known. One assumption about MAGDM issues is that there are a fixed number of possible solutions. Sorting and ranking are the two main steps in solving a MAGDM issue. They may be thought of as alternate approaches of integrating the data in a problem's decision matrix with extra information from the decision maker to arrive at a final ranking or choice among the options. All but the most basic MAGDM approaches require extra information from the decision matrix in addition to the information already present in the matrix in order to determine a final ranking or selection.

REFERENCES

1. Aktas.H., and Cagman. N., Soft sets and soft groups, Inform. Sci. 177 (2007), 2726-2735.
2. Atanassov.K., (1986). Intuitionistic Fuzzy sets. Fuzzy Sets and Systems, 20, 87-96.
3. Atanassov .K., (1994). Operators over interval valued intuitionistic fuzzy sets.
4. Atanassov .K., Gargov .G., (1989). Interval valued intuitionistic fuzzy sets. Fuzzy Sets and Systems, 31, 343-349.
5. Aygunouglu.A., and Aygun,.H., Introductions to fuzzy soft groups, Comput. Math. Appl. 58 (2009), 1279-1286.
6. Bustince.H., Burillo.P., (1995). Correlation of interval-valued intuitionistic fuzzy sets. Fuzzy Sets and Systems, 74, 237-244.
7. Chen.S.M., Tan.J.M., (1994). Handling multi-criteria fuzzy decision-making problems based on vague sets. Fuzzy Sets and Systems, 67, 163-172.
8. Guiwu Wei. (2010). Some arithmetic aggregation operators with intuitionistic trapezoidal fuzzy numbers and their application to group decision making, Journal of Computers, 5 (3), 345-351.
9. Guiwu Wei., Wang H.J., Rui Lin. (2011). Applications of correlation coefficient to interval-valued intuitionistic fuzzy multiple attribute decision-making with incomplete weight information. Knowledge and Information Systems.26, 337-349.
10. Park .D.G., Kwun .Y.C., Park .J.H., Park .I.Y., (2009). Correlation coefficient of Interval-valued intuitionistic fuzzy sets and its application to multiple attribute group decision making problems. Mathematical and Computer Modeling, 50, 1279-129.
11. Shakib.M.D., Fazli.S., (2012). Separating successful and unsuccessful firms using -making methods. International Journal of Information and Decision Sciences, 4(1), 19-47.
12. Hong.D.H., & Choi D.H., (2000). Multicriteria fuzzy decision making problems based on vague set theory, Fuzzy Sets and Systems, 114 , 103-113.
13. Wang.H., C.L, Yoon, K (1981). Multiple Attributes Decision Making Methods and Applications, Springer, Berlin-Heidelberg.
14. Zhang.H.Y., Wang. J.Q., and Chen.X.H., Interval Neutrosophic sets and their application in multicriteria decision making problem, The Scientific world Journal (2014).

Indian Journal of Natural Sciences *www.tnsroindia.org.in ©IJONS*

Vol.15 / Issue 83 / Apr / 2024 *International Bimonthly (Print) – Open Access* *ISSN: 0976 – 0997*

RESEARCH ARTICLE

Demand Forecasting on Pharmacy Sales using Deep Learning Approach

Roopesh Makwana[1]* and Vaishali Gupta[2]

[1]Research Scholar, Department of Computer Science Engineering, IPS Academy Institute of Engineering and Science, Indore, Madhya Pradesh, India
[2]Associate Professor, Department of Computer Science Engineering, IPS Academy Institute of Engineering and Science, Indore, Madhya Pradesh, India.

Received: 08 Dec 2023 Revised: 24 Feb 2024 Accepted: 21 Mar 2024

***Address for Correspondence**
Roopesh Makwana
Research Scholar,
Department of Computer Science Engineering,
IPS Academy Institute of Engineering and Science,
Indore, Madhya Pradesh, India
Email: bhawanalakhani2711@gmail.com

ABSTRACT

Accurate demand forecasting is crucial for efficient inventory management and ensuring customer satisfaction in the pharmacy industry. Traditional forecasting methods often struggle to capture the complex patterns and dynamics inherent in pharmaceutical sales data. In recent years, machine learning techniques have emerged as powerful tools for demand forecasting. This research paper aims to explore the application of machine learning algorithms in forecasting pharmacy sales. Specifically, we employ regression models, decision trees, random forests, and neural networks to predict future sales volumes based on historical data. The dataset used in this study comprises daily sales data, product attributes, and external factors such as seasonality and promotions. Through extensive experimentation and evaluation, we compare the performance of different machine learning models in terms of forecasting accuracy, robustness, and computational efficiency. The results demonstrate the efficacy of machine learning techniques in demand forecasting for pharmacy sales, with the neural network models outperforming other methods, achieving a significantly lower mean absolute error and root mean square error. These findings provide valuable insights for pharmacy retailers and stakeholders to optimize inventory planning, supply chain operations, and customer satisfaction. Furthermore, the research highlights the potential of machine learning as a transformative approach in improving demand forecasting accuracy in the pharmacy industry. Future research may explore advanced deep learning architectures and incorporate additional data sources to enhance the forecasting capabilities and address specific challenges unique to the pharmacy domain.

Keywords: Machine Learning, efficiency, forecasting, regression, deep learning, accuracy

INTRODUCTION

Demand forecasting plays a critical role in the pharmaceutical industry, where accurate predictions of sales volumes are essential for effective inventory management, supply chain optimization, and meeting customer demands. The ability to forecast future sales accurately enables pharmaceutical companies and retailers to optimize their operations, streamline production, reduce costs, and ensure adequate stock availability of medications. However, the dynamic and complex nature of pharmaceutical sales poses challenges for traditional forecasting methods. Pharmaceutical sales are influenced by various factors, including market trends, seasonality, product attributes, promotional activities, and external factors such as disease outbreaks or regulatory changes. These factors introduce significant variability and make it difficult to capture the underlying patterns using conventional forecasting approaches such as time-series analysis or simple regression models. As a result, there is a growing need for advanced forecasting techniques that can handle the intricacies of pharmaceutical sales data and provide more accurate predictions.

In recent years, machine learning has emerged as a powerful tool for demand forecasting in various industries. Leveraging its ability to analyze vast amounts of data and identify complex patterns, machine learning offers the potential to improve the accuracy and reliability of pharmaceutical sales forecasting. Machine learning algorithms can capture nonlinear relationships, identify hidden patterns, and incorporate multiple variables simultaneously, thereby enabling more precise predictions. The objective of this research paper is to explore the application of machine learning techniques in demand forecasting of pharmaceutical sales. We aim to investigate various machine learning algorithms, including regression models, decision trees, random forests, and neural networks, to predict future sales volumes based on historical data. Additionally, we consider the inclusion of relevant factors such as product attributes, promotional activities, and external variables to enhance the forecasting accuracy.

LITERATURE REVIEW

Learning applied to demand prediction, highlighting its benefits, targeted business sectors, and advantages over traditional statistical techniques. Conventional methods used in forecasting grocery store sales often lead to ineffective predictive models, leaving many challenges unresolved. The study emphasizes the importance of training AI models on data to accurately anticipate future events. Sales prediction is a crucial aspect of business intelligence, particularly in cases of data scarcity, missing information, and anomalies. Businesses are urged to explore alternative approaches for improved revenue and preparedness. The findings from a research paper [1] suggest that leveraging Machine Learning approaches, along with a combination of techniques in market forecasting models, can greatly benefit producers and retailers in the fast-moving consumer goods industry. Notably, these approaches result in improved accuracy when predicting demand compared to conventional methods. They offer greater flexibility in handling diverse data factors and the ability to process large volumes of data effectively. Furthermore, the research emphasizes that predicting demand resembles solving a regression problem rather than a mathematical one. As a result, employing regression approaches in sales forecasting leads to enhanced outcomes compared to traditional predictive techniques.

In a different study [2], researchers examined the use of a stacking method to create a regression ensemble comprising individual models. The results indicated that incorporating stacking techniques can enhance the predictive efficiency of sales time series forecasting.Error estimation was conducted using a relative mean absolute error (MAE), calculated as error = MAE/mean (Sales) * 100%. Commonly employed methods for demand estimation include time series forecasting strategies, such as exponential smoothing, Holt Winters model, Box & Jenkins model, regression simulations, and ARIMA. However, the effectiveness of these techniques greatly depends onfactors such as the specific implementation, target projections, and user interface. Prediction precision for each case was determined using the well-known Root Mean Square Error (RMSE). As anticipated, improving forecast accuracy by

reducing the RMSE leads to enhanced outcomes for both consumers and manufacturers [3]. In this study [4], a comprehensive demand forecasting framework is developed, aiming to improve upon traditional methods. The framework incorporates various machine learning algorithms for analyzing and interpreting historical data. Nine different time series techniques, including moving average (MA), exponential smoothing,Holt-Winters, ARIMA strategies, and three Regression Models, as well as SVR and MLFANN, a multilayer feedforward artificial neural network, are combined using a boosting ensemble approach. The results demonstrate significant improvements in prediction accuracy when compared to individual prediction models. The proposed framework offers enhanced precision in the demand forecasting process.

In the study [5], recent advancements in the field of sales forecasting, specifically in the context of fashion and new product forecasting, were outlined. Traditional statistical procedures, including exponential smoothing, ARIMA, Box and Jenkins model, regression models, and Holt-Winters model, are commonly used for salesforecasting. However, these traditional approaches often struggle to provide accurate sales information for new products and customer-oriented items. The study highlights the effectiveness of hybrid forecasting models as a promising solution to address these challenges and improve the accuracy of sales forecasting. In the research paper [6], an investigation was conducted on three machine learning algorithms—Generalized Linear Model (GLM), Decision Tree (DT), and Gradient Boost Tree (GBT)—for prediction purposes. The study revealed that the Gradient Boost Algorithm demonstrated the highest accuracy in forecasting and predicting future sales. With the rise of e-commerce websites and the ability for customers to leave feedback on various products, there is a growing need to analyze and extract valuable information from large volumes of customer reviews. To address this, the study utilized supervised machine learning techniques, specifically Support Vector Machines(SVM) and Naive Bayes, to classify beauty products from Amazon. The results indicated that SVM outperformed Naive Bayes when dealing with larger datasets [7].

Problem Identification

One of the significant hurdles faced by supermarkets is the manager's ability to accurately predict sales patterns and proactively plan stock replenishment and staffing. The key challenges identified include:

- Insufficient accuracy in sales forecasting
- Inadequacy of conventional statistical techniques in handling large datasets
- Subpar performance of predictive models

These challenges necessitate the exploration and implementation of more robust and efficient approaches to improve forecasting accuracy, effectively manage large data volumes, and enhance the performance of predictive models in the supermarket industry.

A. Problem Formulation:

1. Define the objective as forecasting pharmacy sales based on pharmacy sales data.
2. Let X = {(x1, y1), (x2, y2), ..., (xN, yN)} be the dataset, where N is the number of sales per week.
3. In the dataset, xi denotes the input features for the ith sales record, and yi represents the corresponding sales label.

B. Data Preprocessing:

1. Perform data cleaning, including handling missing values, outliers, and inconsistencies.
2. Normalize the input features to ensure they have similar scales.
3. Split the dataset into training, validation, and testing sets.

C. RNN Model Architecture:

1. Design the RNN architecture with long short-term memory (LSTM) units to capture temporal dependencies in the sequential patient data.
2. Define the number of LSTM layers, the number of hidden units in each layer, and the activation functions.

3. Specify the input shape and sequence length for the RNN model.
4. Consider techniques like dropout or recurrent dropout to prevent over fitting.

D. Training the Model:

1. Initialize the model's parameters and hyper parameters.
2. Utilize an optimization algorithm, such as stochastic gradient descent (SGD), Adam, or RMSprop, to train the model.
3. Define an appropriate loss function, such as binary cross-entropy or categorical cross-entropy, to measure the model's performance.
4. Iterate through multiple epochs, adjusting the model's parameters to minimize the loss and improve predictions.
5. Monitor the training process and utilize early stopping if necessary to prevent overfitting.

E. Model Evaluation:

1. Evaluate the trained RNN model on the validation set to assess its performance and tune hyperparameters if needed.
2. Calculate various performance metrics, including accuracy, precision, recall, F1-scoreto measure the model's effectiveness in predicting pharmacy sales.
3. Analyze and interpret the model's predictions to gain insights into important sales factors and their impact.

Training & Testing

We train a recurrent neural network (RNN) with Two layers, including one input layer, one output layer, and Twohidden layers. The output layer utilizes the softmax activation function for multi-class classification. Each layer consists of a variable number of recurrent units. After pre-processing, the input features are represented as a sequence of vectors with a dimension of 139. The number of recurrent units in the input layer matches the input feature dimension, and the number of units in the output layer matches the number of output classes. The RNN processes the sequential input data, capturing temporal dependencies and modeling sequential patterns. The hidden layers allow the network to learn complex representations and extract relevant features from the sequential data.

CONCLUSION

The demand forecasting of pharma sales using RNN (Recurrent Neural Network) and LSTM (Long Short-Term Memory) models achieved an accuracy of 86%. This accuracy indicates that the models were able to predict the sales with a high level of precision.Models are particularly well-suited for time series forecasting tasks like sales prediction. They are capable of capturing sequential dependencies and long-term patterns in the data, allowing them to make accurate predictions based on historical information.Additionally, other evaluation metrics such as confusion matrix can provide further insights into the performance of the models.

FUTURE SCOPE

One potential avenue is model optimization, where hyperparameters and network architecture can be fine-tuned to enhance performance. Additionally, incorporating additional relevant features such as macroeconomic indicators, weather data, or promotional events could provide valuable insights for more accurate predictions. Exploring more granular data, such as hourly or real-time data, may also capture finer fluctuations in sales and lead to more precise forecasts.By addressing these future scopes, businesses can leverage advanced forecasting techniques to optimize their operations, make informed decisions, and stay ahead in the competitive pharmaceutical industry.

REFERENCES

1. M. J. Iqbal, M. I. Geer, and P. A. Dar, "Evaluation of Medicines Forecasting and Quantification Practices in Various Evaluation of Medicines Forecasting and Quantification Practices in Various Public Sector Hospitals Using Indicator Based Assessment Tool," J. Appl. Pharm. Sci., vol. 7, no. 12, pp. 72-76, 2018.
2. P.-A. Cornillon, W. Imam, and E. Matzner-LZber, "Forecasting time series using principal component analysis with respect to instrumental variables Forecasting time series using principal component analysis with respect to instrumental variables," Comput. Stat. Data Anal., vol. 52, no. 7, pp. 1269-1280, 2008.
3. I. A. Gheyas and L. S. Smith, "A Neural Network Approach to Time Series Forecasting," Proc. World Congr. Eng., vol. II, no. 1, pp. 1-5, 2009.
4. G. Lai, W.-C. Chang, Y. Yang, and H. Liu, "Modeling Long- and Short-Term Temporal Patterns with Deep Neural Networks," SIGIR, pp. 1-5, 2018.
5. K. N. Mahajan, "Business Intelligent Smart Sales Prediction Analysis for Pharmaceutical Distribution and Proposed Generic Model," vol. 8, no. 3, pp. 407-412, 2017.
6. Y. Tech, "A Deep Learning Algorithm to Forecast Sales of Pharmaceutical Products," pp. 1-5, 2017.
7. R. Guseo et al., "Pre-launch forecasting of a pharmaceutical drug," Int. J. Pharm. Healthc. Mark., vol. 11, no. 4, pp. 412-438, 2017.
8. A. Papana, D. Folinas, and A. Fotiadis, "Forecasting the consumption and the purchase of a drug," Int. Conf. SUPPLY Chain. Funct., vol. 2, pp. 1-5, 2016.
9. N. K. Zadeh, M. M. Sepehri, and H. Farvaresh, "Intelligent Sales Prediction for Pharmaceutical Distribution Companies: A Data Mining Based Approach," Hindawi Publ. Corp., vol. 2014, pp. 1-10, 2014.
10. T. Pham, T. Tran, and D. Phung, "Predicting healthcare trajectories from medical records: A deep learning approach Predicting healthcare trajectories from medical records: A deep learning approach," pp. 1-5, 2017.
11. E. AL-Shamery and A. AL-haq, "An Optimized Feed Forward Neural Network for Reducing Error Based Stoch Market Prediction," J. Eng. Appl. Sci., vol. 13, no. 5, pp. 4616-4621, 2018.
12. F. Jiang et al., "Artificial intelligence in healthcare: past, present and future," stroke Vasc. Neurol., pp. 1-9, 2017.
13. E. AL-Shamery and A. AL-haq, "Enhancing Prediction of NASDAQ Stock Market Based on Technical Indicators," J. Eng. Appl. Sci., vol. 13, no. 5, pp. 4630-4636, 2018.

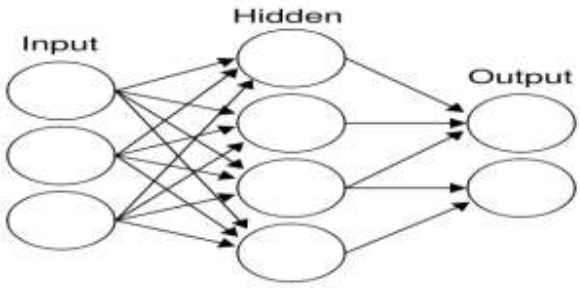

Fig. 1 General Structure of RNN (Guseo, 2017)

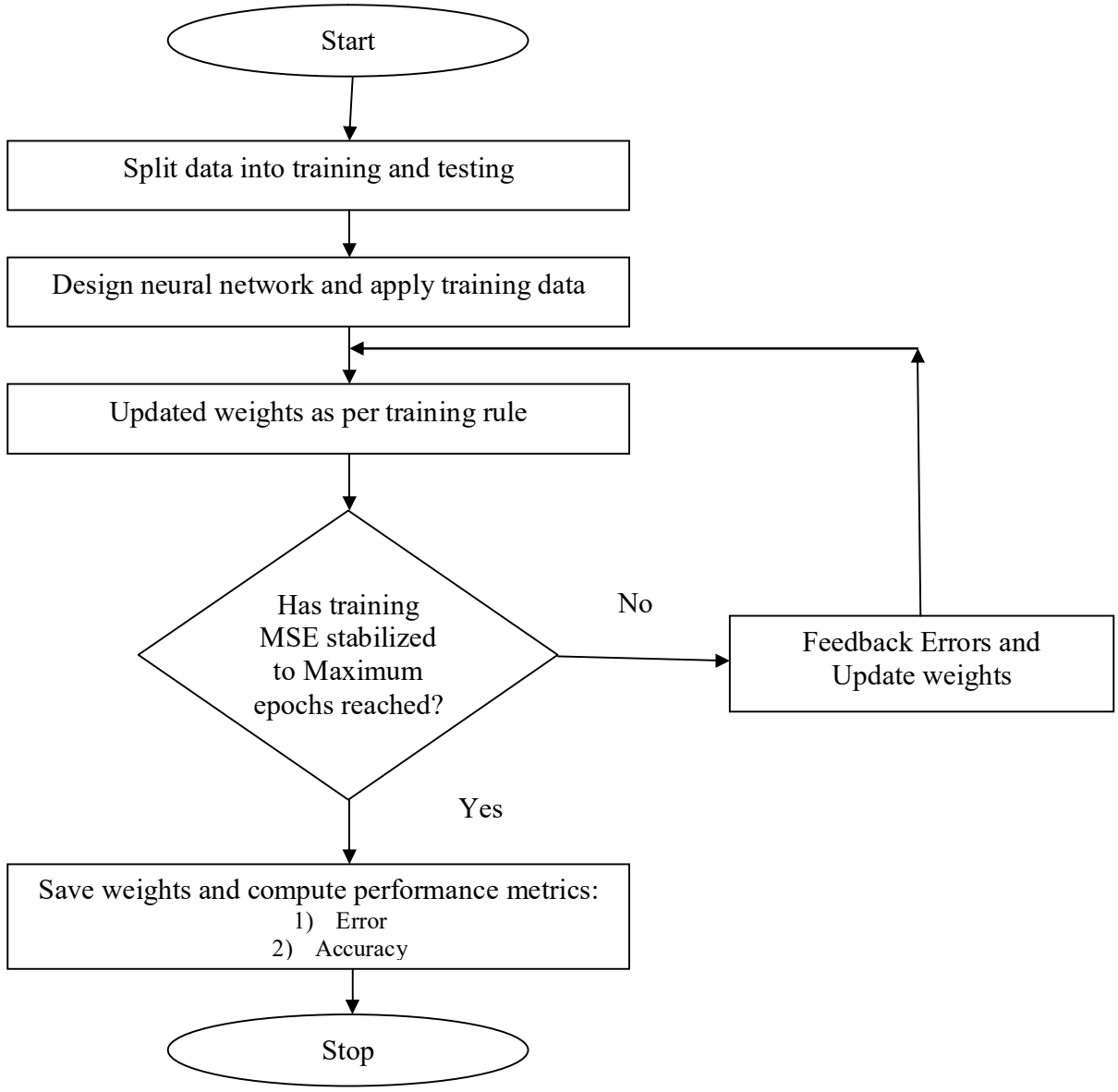

Fig. 2 Flowchart of Proposed System

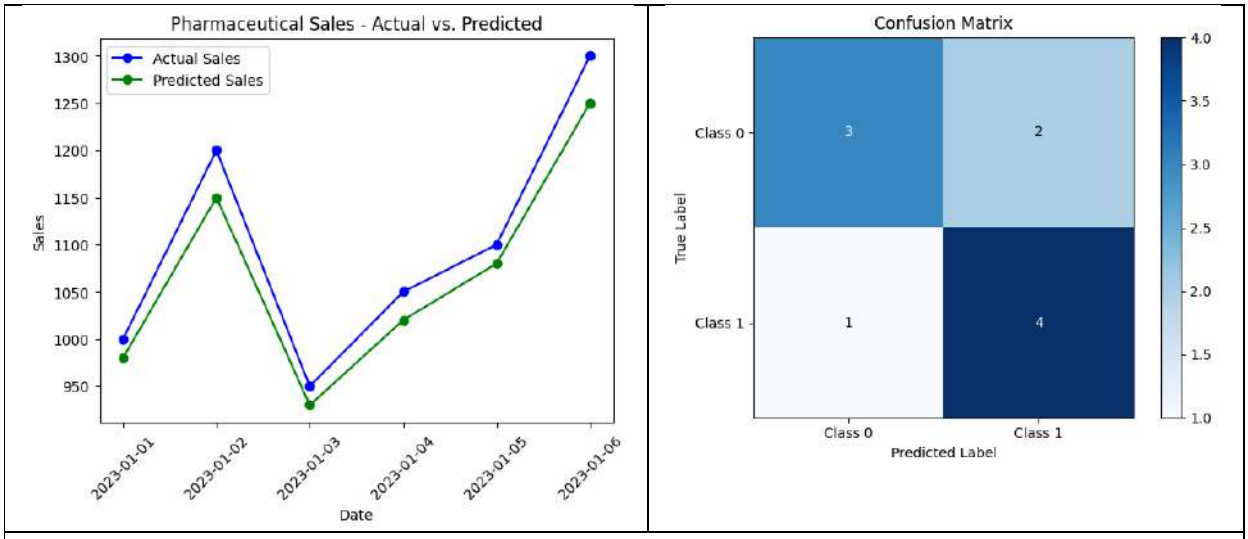

Fig 3. Confusion Matrix of given results

Indian Journal of Natural Sciences *www.tnsroindia.org.in ©IJONS*

Vol.15 / Issue 83 / Apr / 2024 *International Bimonthly (Print) – Open Access* *ISSN: 0976 – 0997*

RESEARCH ARTICLE

Density Functional Theory (DFT) and Time - Dependent DFT Investigations on the Geometric, Optical Properties and Molecular Descriptors of a Varied Array of Ureidopeptidomimetics (UPM)

Y. Pavani[1], S. Aravind[2], M. Yanadirao[3], K. V. Padmavathi[4] and M. Subba Rao[5]*

[1]Assistant Professor, Department of Freshman Enigneering , PVP Siddhartha Institute of Technology (Affiliated to Jawaharlal Nehru Technological University Kakinada) Andhra Pradesh, India.
[2]Assistant Professor, Department Chemistry, University College of Sciences, Osmania University, Hyderabad, Telangana, India.
[3]Lecturer, Department of Chemistry, SKBR Govt. Degree College, Macherla, (Affiliated to *Acharya Nagarjuna University*) Andhra Pradesh, India.
[4]Lecturer, Department of Chemistry, TRR Govt. Degree College,(Affiliated to Acharya Nagarjuna University) Andhra Pradesh, India.
[5]Professor, Department of Chemistry, University College of Sciences, Acharya Nagarjuna University, Andhra Pradesh, India.

Received: 30 Dec 2023 Revised: 09 Jan 2024 Accepted: 27 Mar 2024

***Address for Correspondence**
M. Subba Rao
Professor,
Department of Chemistry,
University College of Sciences,
Acharya Nagarjuna University,
Andhra Pradesh, India.
Email: mannasrao@gmail.com

ABSTRACT

The study uses density functional theory (DFT) with the B3LYP function and the 6-311++G(d,p) basis set for structure optimization. The introduction of electron donor groups at ureido and carboxylate termini decreases the C-O and C-N bond distances in UPM, which is due to their electron-donating nature. The OH-UPM model is found to be the most stable and has lower HOMO energy and ionization values, indicating increased stability and reduced reactivity. The reactivity assessment based on energy gap parameters rates OH-UPM as the most stable among the studied models. Additional parameters (η, S and μ) are measured to evaluate the stability of the connection. Excitation calculations show intense peaks corresponding to n-to-π* or π-to-π* transitions and are influenced by substituent groups. OH and NH_2 phenyl substituent's dominate in π-to-π* transitions, while CH_3 and OCH_3 groups favour both n-to-π* and π-to-π* transitions.

Keywords: Ureidopeptidomimetics, density functional theory, geometric structures, Frontier molecular orbital's (FMOs) and Global chemical reactivity descriptor

INTRODUCTION

In 1922, the first clinical use of bioactive peptides involved administering insulin to a patient suffering from type I diabetes. Since then, researchers looking to create novel therapeutic medications have become interested in bioactive peptides [1]. Sanger's discovery of insulin's amino acid sequence in the early 1950s allowed chemists to investigate peptides as a novel class of compounds. Clinical applications are made of some endogenous bioactive peptides, particularly hormones that circulate in the bloodstream, in their intact forms (e.g., insulin, vasopressin) or their chemically modified forms (e.g., calcitonin analogues, glucagon-like protein 1 analogues) [2]. The majority of bioactive peptides that have been found thus far, however, are not suitable for drug application due to their low cell-membrane permeability, low metabolic stability, lack of oral activity, and rapid excretion [3].Consequently, peptidomimeticsthe structural and functional mimicking of bioactive peptides using non-canonical amino acids or non-peptidic scaffolds has emerged as a proven technique for addressing the pharmacokinetic limitations of peptides[4].Another significant function of peptidomimetics in medicinal chemistry is conformational restriction, which can offer peptides a higher binding potency and target selectivity than they do as parents[5].Even though free rotation about single bonds allows a biologically active compound, like a drug, chemical transmitter, or peptide, to assume a variety of conformations, it binds to the target biomolecule assuming one of these conformers, which is a bioactive conformation. A compound may only have an unstable active conformer if it has a low binding affinity for its target molecule. As a result, the synthesis of lead compound analogues with conformational restrictions frequently produces an enhanced specific binding affinity for the target molecule [6].

Another useful method for examining the bioactive conformation of a chemical is to restrict its conformation. Peptidomimetics have embraced the conformational restriction concept because of its beneficial aspects for drug design [7].Mimicking the secondary structure of the amino acid sequence necessary for interacting with the target is crucial in peptidomimetic design. One of the most thoroughly studied methods for creating peptidomimetics that target peptide–protein and peptide–receptor interactions mimic a typical secondary structure, such as the b-turn, g-turn, a-helix, or b-strand. This is primarily due to the binding site of the bioactive peptides frequently forming this kind of characteristic secondary structure for the target biomolecules to recognize it. Proteolytic enzymes are likely to recognize an extended b-strand conformation of their target peptides, whereas receptors like G-protein coupled receptors (GPCRs) frequently recognize a turn conformation of their endogenous peptide ligands [8-10]. To replicate the secondary structures necessary for particular target binding, several conformations limited scaffolds were created. There have been published thorough and excellent reviews on a variety of peptidomimetic scaffolds [11]. Many experimental and theoretical techniques have been used to study peptidomimetics and its applications in great detail [12,13]. Ureidopeptidomimetics (UPMs) are a type of synthetic peptidomimetics [14] where a ureido group is substituted for a peptide bond. It has been demonstrated that the presence of anureido group improves the probereceptor specificity and metabolic stability for drug binding [15].

UPMs, which are more commonly known as antibiotics, have also been shown to function as HIV-1 protease inhibitors[16, 17]. Different substituents, such as organic groups (carboxylic groups, amines, etc.), have been used to synthesize UPs. From organic (ferrocene units)[18-20] to inorganic (functional groups). These peptidomimetic compounds have the potential to be developed as drugs due to their permeability, metabolic stability, and extended degradation time [21] To be used in therapeutic applications, these mimetics must be understood at the microscopic level, which can be done with the aid of density functional theory (DFT) techniques. Understanding the behavior and function of biomolecules, which span a wide range of biological processes, requires a fundamental understanding of their molecular properties. Determining the intricate connections between molecular structure and biological activity requires the use of molecular descriptors, which are quantitative depictions of structural and physicochemical

features. Robust molecular descriptors are becoming more and more necessary as bimolecular research progresses because they offer important information about the properties that affect biological functions. The structural subtleties of these various biomolecules can be quantified and compared using molecular descriptors, which help predict their interactions, functions, and roles in biological systems. In the age of computational biology, where combining computational techniques with experimental data improves our comprehension of biomolecular structures and functions, the use of molecular descriptors have become especially important [22]. Molecular descriptors facilitate drug discovery and design processes by enabling the creation of predictive models for biological activities through the capture of crucial structural features [23]. Key biopharmaceutical properties that facilitate a drug's passage through various cellular barriers and entry into the body include solubility, stability, permeability, and first-pass effect [24, 25]. Furthermore, the pharmacokinetic properties of the following details [26] guarantee efficient drug delivery to the targeted locations: volume of distribution, biological half-life, and clearance rate. Lipophilicity, or a compound's ability to dissolve in fats, oils, lipids, and nonpolar solvents like hexane or toluene, has long been recognized as being essential to a drug's ability to proceed through the clinical development process [27, 28]. The total of all intermolecular forces acting on a solute and the two phases it partitions between is reflected in this quantity [29]. In general, distribution coefficients (logD) or the Octanol-water partition coefficient logP are used in experiments to express lipophilicity. While log p calculates the ratio of the sum of the concentrations of all forms of the compound (pH-dependent mixture of ionized and unionized forms) in each of the two phases, logP describes the partition equilibrium of an un-ionized solute. One crucial prerequisite for developing new drugs is the precise and effective assessment of lipophilicity.

Rather than using costly experimental logP measurements, the theoretical logP values determined by the quantitative structure-activity relationship (QSAR) models [30] are frequently employed in practice. Since the partition coefficients and the solvated molecules' electronic structures are closely related, quantum chemistry techniques can also be applied to this kind of study. Computational techniques for accurately describing the electronic structure of single, non-interacting relatively large molecules have become widespread, particularly in the last ten years [31].The application of DFT and TD-DFT techniques facilitates a comprehensive and precise investigation of molecular characteristics, providing valuable perspectives that may steer the logical development of innovative compounds with augmented therapeutic potential [32]. The assortment of Ureidopeptidomimetics chosen for this research contributes to the analysis by taking into account variances in chemical structures and functional groups. The electronic characteristics of the compounds under study guided the choice of molecular descriptors for this study. The HOMO-LUMO band gap, softness, chemical hardness, chemical potential, dipole moment, salvation energy, global nucleophilicity, log P, ovality, area volume, polar surface area (PSA), and polarizability were among these descriptors. The lowest unoccupied molecular orbital (LUMO) and the highest occupied molecular orbital (HOMO) were also included. To shed light on the interaction between hydrophobic and hydrophilic forces within the complex molecular landscapes of living organisms, this paper hopes to investigate the application of the logP concept to studied molecules. We can learn more about the structures, operations, and roles that different biomolecules play in cellular processes by analyzing their hydrophobicity profiles, which advances our knowledge of the molecular underpinnings of life. By using cutting-edge computational techniques, this study seeks to illuminate the complex interactions between the structural characteristics, optical attributes, and molecular reactivity descriptors of ureidopeptidomimetics. Predicting the bioavailability and distribution of these molecules in biological systems also depends on determining the octanol/water partition coefficients.

Computational methods

Density functional theory (DFT) is used for structural optimizations of all models. The long-range electron-electron interaction-corrected hybrid B3LYP [33] functional is used with the 6-311++ G(d,p) basis set, which is implemented in the Gaussian 09 package [34]. It is discovered that this functional provides suitable long-range electron-electron correlation interactions [35–37]. This basis set can be regarded as sufficiently large and can yield dependable molecular geometries and reaction enthalpies [38]. Here, the models are chosen so that the carboxylate end (UPM–R2) and ureido end (R1–UPM) are where the substituent groups (R1/R2 =-CH_3,-CH_3O,-OH, and -NH_2) are located (Fig. 1). Based on frequency analysis, the structures are classified as minima or maxima. The structure is confirmed to

be minima by the presence of all real frequencies. Geometries of excited states and their characteristics, such as excitation energies, have been studied using time-dependent density functional theory, or TD-DFT [39]. In this work, the chemical properties of the molecules under investigation in various solvents and the gas phase are examined using the implicit polarizable continuum model (PCM). A popular implicit solvent model in quantum chemistry and Density Functional Theory (DFT) computations is the Polarizable Continuum Model (PCM). It is designed to incorporate the effects of a solvent environment without explicitly representing the solvent molecules. In this research utilize the solvents such as methanol (ε = 32.6), acetonitrile (ε = 37.5),DMSO(ε = 47) and water (ε = 78.5).

RESULTS AND DISCUSSION

Optimized geometric structures

Using the DFT/B3LYP method for the ground state and the TD-DFT/B3LYP method for the excited state, the optimized structures of all UPM models of molecules have been obtained. Figure 2 displays the optimized geometrical structures, while Table 1& 2 contains a list of the parameters. In this work, all models are reported with their energetics analyzed and optimized. The relaxation reveals that, as in natural peptides and unsubstituted UPMs, the conformers with all of their bonds oriented trans to one another have the lowest energy. The substitution at the carboxylate end (C6–O7–C8–R2), on the other hand, follows the same trans orientation as other bonds (87^0), whereas the substitution at the ureido end causes it to be oriented perpendicular to the plane of the peptide backbone, creating a dihedral angle (C3–N2–C1–R1) of about 154^0. Analyzing the structural parameters reveals that, in comparison to the unsubstituted UPM, the substitution of electron donor groups at the ureido and carboxylate ends shortens the C-O and C-N bond distances in PM by 0.004^0^A and 0.0002^0^A, respectively (Tables 1 and 2). This is explained by the electron-donating nature of the substitution. When substituted at the ureido end, all of the substituents demonstrate their capacity to donate electrons. Regardless of the models employed here, the groups substituted at the ureido end function as electron-rich groups.

Frontier molecular orbital's (FMOs)

By examining the HOMO and LUMO, the charge transfer that occurred within the molecule was explained. As FMOs, both orbitals are named. The final charge transfer interaction within the molecule is explained by the HOMO-LUMO energy gap, which is also helpful in determining the electrical transport properties of molecules. Low kinetic stability and high chemical reactivity are characteristics of molecules with small frontier orbital gaps (HOMO-LUMO energy gaps) [40–42]. This is because it is energetically advantageous to add an electron to the high-lying LUMO to remove electrons from the low-lying MOMO. How it interacts with other species is determined by HOMO and LUMO. Using the DFT method with B3LYP functional and 6-311++G (d,p) basis set , the frontier molecular orbitals (FMOs) of the molecules under study have been computed. Figure 3&4 displays the molecular orbital structures in gas phase for R-UPM and UPM-R models. The lowest unoccupied molecular orbital (LUMO) and the highest occupied molecular orbital (HOMO) make up the FMOs. The energy differential between the HOMO and the LUMO is known as the HOMO-LUMO Gap energy. When describing a molecule's chemical reactivity and interactions, the FMOs are crucial parameters. Additionally, it can shed light on the characteristics of the molecules in both gas phase and aqueous solution. The HOMO and LUMO energies, as well as the energy gap (ΔE) between them, are obtained for the gas phase and various solvents shown in Table 3&4 and Figures 5 &6. Based on Table 3&4, it can be inferred that the OH-UPM model exhibits greater stability when compared to other models. This is because the molecule's large energy gap contributes to its higher stability and lower chemical reactivity.

Global chemical reactivity descriptor

The global chemical reactivity descriptors of the molecule, including the ionization potential electron affinity, electro negativity, global softness, global hardness, chemical potential, and electrophilicity index, were ascertained using the FMOs energies (E_{HOMO}, E_{LUMO}) [43, 44]. To interpret and comprehend the stability and reactivity of molecular systems, it is helpful to consider two significant molecular properties: electronegativity and hardness [45].

Molecular descriptors measured with quantum mechanical techniques have been used in many QSAR studies [46]. They calculate molecular volumes that describe form, binding effects, and molecular reactivity. The most well-known quantum chemical descriptors are HOMO and LUMO energy because they are the reaction species that control multiple chemical reactions [47]. HOMO energy is used to quantify the molecular sensitivity to electrophile attacks and is directly correlated with the ionization potential. On the other hand, the LUMO energy explains the molecule's vulnerability to nuclear attack and is directly related to the electron affinity. The energies known as HOMO and LUMO both control radical. Reactions You can also succinctly define hard and soft nucleophiles, electrophiles and molecule stability, and active durability of HOMO and LUMO. The global reactivity descriptors, such as energy gap (Eg), ionizing potential (IP), affinity of electrons (EA), electron-negativity (χ), hardness (n), hardness (S), chemical potentials (μ), electrophilicity index (χ), charge-transfer (ΔNmax), nucleofugality (ΔEn), and electrofugality in gas phased form, are therefore determined using HOMO-LUMO energies.

$$\chi = -\frac{(E_{HOMO} + E_{LUMO})}{2} = \frac{I + A}{2} \quad \text{and} \quad \mu = \frac{(E_{HOMO} + E_{LUMO})}{2} \tag{2}$$

$$\eta = \frac{E_{LUMO} - E_{HOMO}}{2} \tag{3}$$

$$s = \frac{1}{2\eta} \tag{4}$$

$$\omega = \frac{\mu^2}{2\eta} \tag{5}$$

Two new reactivity indices, nucleofugality (ΔEn) and electrofugality (ΔEe) were proposed by Ayers and colleagues [48] to measure the ability of nucleophiles and electrophiles to leave the community. These indices are explained as follows.

$$\Delta E_n = -A + \omega = \frac{(\mu + \eta)^2}{2\eta} \tag{6}$$

$$\Delta E_e = I + \omega = \frac{(\mu - \eta)^2}{2\eta} \tag{7}$$

Table 3 & 4 displays the chemical and global descriptors for the following: ionization potential (IP), durability (S), softness (μ), charge transfer (ΔNmax), electrofugality, electronegative affinity (EA), electronegativity (χ), durability (S), softness (μ), and electrophilicity index (A).

The best electron donor in the models under study is OH-UPM, which also has the lowest ionization value (IP = 6.8265 eV) and lowest HOMO energy (EHOMO = -6.8265 eV) (Table 3 &4). Moreover, comparable trends are evident for the UPM-R2 models. Based on energy gap (ΔE) parameters, the compounds exhibit the highest reactivity, indicating that compound OH-UPM is the most stable among them, with the order being OH-UPM> CH3O-UPM > NH2-UPM > CH3-UPM.

It's crucial to remember that these descriptors give a simplified picture of a molecule's reactivity, even though they contain useful information. Reactivity is a complicated attribute that is influenced by many different things. For a thorough evaluation, it may be necessary to take into account several descriptors and experimental data. The best electron acceptor in the models under study, UPM-OH, has a higher electronegativity value. An atom's propensity to draw electrons into a covalent bond is indicated by higher electronegativity values. When a high electronegativity molecule interacts with other ions or in polar environments, it can become more reactive.

Because the OH-UPM model has a higher chemical potential, there is a greater chance that the system will experience a chemical change, which suggests increased reactivity.

Excited states and absorption spectra

Using the TD/DFT method for the gas phase and the PCM-TD/DFT method for the solvent phase, the excited states of the molecules have been calculated. Table 5 displays the values for the oscillator strength (f), excitation energy (Ex), maximum absorption wavelength (λ_{max}), and significant MO assignments in both the gas and solvent phases for R-UPM model. The result is that the maximum values of the studied molecules (R1–R4) range from 218.00 to 209 nm and 218.00 to 250.00 nm for R-UPM and UPM-R models respectively. The first excited state in the Franck-Condon region corresponds to the change from the highest energy occupied molecular orbital to the lowest energy molecular orbital, based on results from calculations conducted in the gas phase and solvent phase. The first excited state correlates to the transition from HOMO to LUMO, while the second excited state corresponds to the HOMO -> LUMO +1 transition, based on data from solvent phase calculations. Figure 7-10 illustrates how the investigated molecules' absorption spectra in the two environments differ in terms of spectral region pattern. The dominance of the HOMO→LUMO transition has been revealed by comparing the results for the two environments. The electronic structure of the peptide backbone is found to be significantly altered, along with its polarization, when UPMs are substituted with different donor units (CH_3, OCH_3,OH, and NH_2). This led to a shift in the un-substituted UPM's negative charge polarization from the ureido group towards the end where the substituent was located. The calculations of excitation reveal two sharp peaks that correspond to the transitions from n to π^* or π to π^*, where π and n are localized at distinct energy levels based on the substituent groups selected. The OH and NH_2 phenyl substituent's in UPM are predominant in π to π^* transitions, whereas the CH_3 and OCH_3 groups favor both π to π^* and n to π^* transitions. Excitation studies reveal that, except for the OH-UPM model, all of the models exhibit strong peaks that transition from one end to the other of the orbitals.

CONCLUSIONS

This work investigates chemical modifications in UPM mimetics and finds that structural and electronic properties are affected by the substitution of electron donor groups. Similar characteristics are shown by computational analysis of different UPM models, where bond distances are shortened by specific substitutions. The most stable model is the OH-UPM model, which has lower ionization and HOMO energy values. OH-UPM is ranked as the most stable model among the models examined in the reactivity assessment based on energy gap parameters. The results of the excitation calculations show that different transitions are affected by substituent groups. OH and NH_2 are more prominent in the π to π^* transitions, whereas CH_3 and OCH_3 are more favourable in the n to π^* and π to π^* transitions.

REFERENCES

1. Bliss, M.. Rewriting Medical History: Charles Best and the Banting and Best Myth. *J. Hist. Med. Allied Sci.*1993, *48* (3), 253–274.
2. Sanger, F.; Tuppy, H.. The Amino-Acid Sequence in the Phenylalanyl Chain of Insulin. I. the Identification of Lower Peptides from Partial Hydrolysates. *Biochem. J.*1951, *49* (4), 463–481.
3. Fosgerau, K.; Hoffmann, T.. Peptide Therapeutics: Current Status and Future Directions. *Drug Discov. Today*2015, *20* (1), 122–128.
4. Liskamp, R. M. J.; Rijkers, D. T. S.; Kruijtzer, J. A. W.; Kemmink, J. Peptides and Proteins as a Continuing Exciting Source of Inspiration for Peptidomimetics. *Chembiochem*2011, *12* (11), 1626–1653.
5. DeLorbe, J. E.; Clements, J. H.; Teresk, M. G.; Benfield, A. P.; Plake, H. R.; Millspaugh, L. E.; Martin, S. F.. Thermodynamic and Structural Effects of Conformational Constraints in Protein-Ligand Interactions. Entropic Paradoxy Associated with Ligand Preorganization. *J. Am. Chem. Soc.*2009, *131* (46), 16758–16770.

6. *The Practice of Medicinal Chemistry*, 4th ed., Wermuth, C. G., Aldous, D., Raboisson, P., Rognan, D., Eds.; Academic Press, 2015.
7. Watanabe, M.; Hirokawa, T.; Kobayashi, T.; Yoshida, A.; Ito, Y.; Yamada, S.; Orimoto, N.; Yamasaki, Y.; Arisawa, M.; Shuto, S.. Investigation of the Bioactive Conformation of Histamine H3 Receptor Antagonists by the Cyclopropylic Strain-Based Conformational Restriction Strategy. *J. Med. Chem.*2010, *53* (9), 3585–3593
8. Whitby, L. R.; Ando, Y.; Setola, V.; Vogt, P. K.; Roth, B. L.; Boger, D. L.. Design, Synthesis, and Validation of a β-Turn Mimetic Library Targeting Protein-Protein and Peptide-Receptor Interactions. *J. Am. Chem. Soc.*2011, *133* (26), 10184–10194.
9. Ruiz-Gómez, G.; Tyndall, J. D. A.; Pfeiffer, B.; Abbenante, G.; Fairlie, D. P.. Update 1 Of: Over One Hundred Peptide-Activated G Protein-Coupled Receptors Recognize Ligands with Turn Structure. *Chem. Rev.*2010, *110* (4), PR1–P41.
10. Madala, P. K.; Tyndall, J. D. A.; Nall, T.; Fairlie, D. P.. Update 1 Of: Proteases Universally Recognize Beta Strands in Their Active Sites. *Chem. Rev.*2010, *110* (6), PR1–P31.
11. Gillespie, P.; Cicariello, J.; Olson, G. L.. Conformational Analysis of Dipeptide Mimetics. *Biopolymers*1997, *43* (3), 191–217.
12. Gao, J.; Müller, P.; Wang, M.; Eckhardt, S.; Lauz, M.; Fromm, K. M.; Giese, B. Electron Transfer in Peptides: The Influence of Charged Amino Acids. *Angew. Chem. Int. Ed.* 2011, *50* (8), 1926–1930
13. Remacle, F.; Levine, R. D. An Electronic Time Scale in Chemistry. *Proc. Natl. Acad. Sci. U. S. A.*2006, *103* (18), 6793–6798.
14. Holmes, D. L.; Smith, E. M.; Nowick, J. S. Solid-Phase Synthesis of Artificial Beta- Sheets. *J. Am. Chem. Soc.*1997, *119* (33), 7665–7669.
15. Boeijen, A.; Liskamp, R. M. J. Solid-Phase Synthesis of OligoureaPeptidomimetics. *Eur. J. Org. Chem.*1999, 2127–2135.
16. Lam, P. Y. S.; Jadhav, P. K.; Eyermann, C. J.; Hodge, C. N.; Ru, Y.; Bacheler, L. T.; Meek, J. L.; Otto, M. J.; Rayner, M. M.; Wong, Y. N.; Chang, C. H.; Weber, P. C.; Jackson, D. A.; Sharpe, T. R.; Ericksonviitanen, S. Rational Design of Potent, Bioavailable, Nonpeptide Cyclic HIV Protease Inhibitors. *Science*1995, *9*, 13.
17. Beach, J. W. Chemotherapeutic Agents for Human Immunodeficiency Virus Infection: Mechanism of Action, Pharmacokinetics, Metabolism and Adverse Reactions. *Clin. Ther.* 1998, *20* (1), 2–25; discussion l.
18. Sañudo, M.; Marcaccini, S.; Basurto, S.; Torroba, T. Synthesis of 3-Hydroxy-6-oxo 1,2,4 Triazin-1-yl Alaninamides, a New Class of Cyclic DipeptidylUreas. *J. Org. Chem.*2006, *71* (12), 4578–4584.
19. Rincón, A. M.; Prados, P.; de Mendoza, J. A Calix 4 AreneUreidopeptide Dimer Self- Assembled Through Two Superposed Hydrogen Bond Arrays. *J. Am. Chem. Soc.*2001, *123* (15), 3493–3498.
20. Siebler, D.; Förster, C.; Gasi, T.; Heinze, K. Biferrocene Amino Acid, a Ferrocenylogoue of Ferrocene Amino Acid: Synthesis, Cross-Linking, and Redox Chemistry. *Organometallics*2011, *30* (2), 313–327.
21. Pauletti, G. M.; Jeffrey, S.; Siahaan, T. J.; Gangwar, S.; Pauletti, G. M. Improvement of Oral Peptide Bioavailability: Peptidomimetics and Prodrug Strategies. *Adv. Drug Deliv. Rev.*1997, *27* (2–3), 235–256.
22. Tropsha, A. Best Practices for QSAR Model Development, Validation, and Exploitation. *Mol. Inform.*2010, *29* (6–7), 476–488.
23. Gasteiger, J.; Hutchings, M. G.; Steinbeck, C.; Willighagen, E. L. The Evolution of the Beilstein Database: Integration into the Chemical Information Environment. *J. Chem. Inf. Comput. Sci.*2003, *43* (6), 1602–1607.
24. Planey, S. L.; Kumar, R. *J. App. Pharmacokinet. Biop*2013, *1*, 31–36.
25. Arnott, J. A.; Planey, S. L.. The Influence of Lipophilicity in Drug Discovery and Design. *Expert Opin. Drug Discov.*2012, *7* (10), 863–875.
26. Pieńko, T.; Grudzień, M.; Taciak, P. P.; Mazurek, A. P. Cytisine Basicity, Solvation, logP, and logD Theoretical Determination as Tool for Bioavailability Prediction. *J. Mol. Graph. Model.*2016, *63*, 15–21.
27. Lombardo, F.; Shalaeva, M. Y.; Tupper, K. A.; Gao, F.; Abraham, M. H..ElogPoct: A Tool for Lipophilicity Determination in Drug Discovery. *J. Med. Chem.*2000, *43* (15), 2922–2928.

28. Sârbu, C.; Naşcu-Briciu, R. D.; Casoni, D.; Kot-Wasik, A.; Wasik, A.; Namieśnik, J.. Chromatographic Lipophilicity Determination Using Large Volume Injections of the Solvents Non-Miscible with the Mobile Phase. *J. Chromatogr. A*2012, *1266*, 53–60.
29. IUPAC. *Compendium of Chemical Terminology*, 2nd ed.; Blackwell Scientific Publications, 1997.
30. Molinspiration. *Cheminformatics*; Bratislava, Slovakia, 2016.
31. Burke, K.; Wagner, L. O.. DFT in a Nutshell. *Int. J. Quantum Chem.*2013, *113* (2), 96– 101.
32. Kohn, W.; Sham, L. J. Self-Consistent Equations Including Exchange and Correlation Effects. *Phys. Rev.*1965, *140* (4A), A1133–A1138.
33. Yanai, T.; Tew, D. P.; Handy, N. C.. A New Hybrid Exchange–Correlation Functional Using the Coulomb-Attenuating Method (CAM-B3LYP). *Chem. Phys. Lett.*2004, *393* (1–3), 51–57.
34. Frisch, M. J.; Trucks, G. W.; Schlegel, H. B.; Scuseria, G. E.; Robb, M. A.; Cheeseman, J. R.; Scalmani, G.;Barone, V.; Mennucci, B.; Petersson, G. A.; Nakatsuji, H.; Caricato, M.; Li, X.; Hratchian, H. P.; Izmaylov, A. F.; Bloino, J.; Zheng, G.; Sonnenberg, J. L.; Hada, M.; Ehara, M.; Toyota, K.; Fukuda, R.; Hasegawa, J.; Ishida, M.; Nakajima, T.; Honda, Y.; Kitao, O.; Nakai, H.; Vreven, T.; Montgomery, J. A.; Peralta, J. E.; Ogliaro, F.; Bearpark, M.; Heyd, J. J.; Brothers, E.; Kudin, K. N.; Staroverov, V. N.; Kobayashi, R.;Normand, J.; Raghavachari, K.; Rendell, A.; Burant, J. C.; Iyengar, S. S.; Tomasi, J.; Cossi, M.; Rega, N.;Millam, J. M.; Klene, M.; Knox, J. E.; Cross, J. B.; Bakken, V.; Adamo, C.; Jaramillo, J.; Gomperts, R.; Stratmann, R. E.; Yazyev, O.; Austin, A. J.; Cammi, R.; Pomelli, C.; Ochterski, J. W.; Martin, R. L.; Morokuma, K.; Zakrzewski, V. G.; Voth, G. A.; Salvador, P.; Dannenberg, J. J.; Dapprich, S.; Daniels, A. D.; Farkas, O.; Foresman, J. B.; Ortiz, J. V.; Cioslowski, J.; Fox, D. J. A. Gaussian 09 Revision D.01. *Gaussian Inc. Wallingford*2009, *3*.
35. Joy, S.; Sureshbabu, V. V.; Periyasamy, G.. Computational Studies on Structural, Excitation, and Charge-Transfer Properties of Ureidopeptidomimetics. *J. Phys. Chem. B* 2016, *120* (27), 6469–6478.
36. Joy, S.; Sureshbabu, V. V.; Periyasamy, G.. Density Functional Theoretical Studies on Photoswitching and Charge Migration Dynamics of Thio and Selenoureidopeptides. *J. Phys. Org. Chem.*2017, 30 (12), e3693.
37. Joy, S.; Sureshbabu, V. V.; Periyasamy, G.. DFT Studies on the Terminal Dependent Reversible Switching of Selenoxo Peptides Induced by Cationization. *ChemistrySelect* 2017, *2* (15), 4261–4266.
38. Škorňa, P.; Lengyel, J.; Rimarčík, J.; Klein, E.. Investigation of Oxidation Attack Sites in Sterols: Thermodynamics of Hydrogen Atom Transfer. *Comput. Theor. Chem.*2014, *1038*, 26–32.
39. Mignolet, B.; Levine, R. D.; Remacle, F.. Charge Migration in the Bifunctional PENNA Cation Induced and Probed by Ultrafast Ionization: A Dynamical Study. *J. Phys. B: At. Mol. Opt. Phys.*2014, *47* (12), 124011.
40. Nehra, N.; Tittal, R. K.; V.D. Ghule. 3- Triazoles of 8-Hydroxyquinoline and HBT: Synthesis and Studies (DNA Binding, Antimicrobial, Molecular Docking, ADME, and DFT). *A.C.S. Omega*2021, 1,2, *6* (41), 27089–27100.
41. Singh, J. S.; Khan, M. S.; Uddin, S. A DFT Study of Vibrational Spectra of 5- Chlorouracil with Molecular Structure, HOMO–LUMO, MEPs/ESPs and Thermodynamic Properties. *Polym. Bull. (Berl)*2023, *80* (3), 3055–3083.
42. Li, D. D.; Greenfield, M. L. Chemical Compositions of Improved Model Asphalt Systems for Molecular Simulations. *Fuel*2014, *115*, 347–356.
43. Boukabcha, N.; Direm, A.; Drissi, M.; Megrouss, Y.; Khelloul, N.; Dege, N.; Tuna, M.; Chouaih, A. Synthesis, Structural Determination, Hirshfeld Surface Analysis, 3D Energy Frameworks, Electronic and (Static, Dynamic) NLO Properties of o-Nitroacetanilide (o- NAA): A Combined Experimental and Quantum Chemical Study. *Inorg. Chem. Commun.*2021, *133*, 108884.
44. Mollaamin, F.; Monajjemi, M. Molecular Modelling Framework of Metal-Organic Clusters Forconserving Surfaces: Langmuir Sorption Through the TD-DFT/ONIOM Approach. *Mol. Simul.*2023, *49* (4), 365–376.
45. Suresh, C. H.; Remya, G. S.; Anjalikrishna, P. K. Molecular Electrostatic Potential Analysis: A Powerful Tool to Interpret and Predict Chemical Reactivity. *WIREs Comput. Mol. Sci.*2022, *12* (5), e1601.
46. Karelson, M. *Molecular Descriptors in QSAR/QSPR*; John Wiley & Sons, 2000.
47. Zhou, Z. Pan-, R.G. Activation Hardness: New Index for Describing the Orientation of Electrophilic Aromatic Substitution. *J. Am. Chem. Soc.*1990, *772* (15), 5720–5724.

48. Roos, G.; Loverix, S.; Brosens, E., et al. Chem. *Biol. Chem.*2006, *7*, 981.

Table 1. Structural parameters (bond length (A) and bond angles (˚)) of R-UPM model studied at the neutral state using DFT/B3LYP/6-311++G(d,p) basis set.

	ureido end				carboxylate end			
Solvent	r_{C-R}	r_{C-N}	$r_{C=O}$	**N–C–R_1**	$r_{C=O}$	r_{O-C}	r_{C-R2}	r_{O-C-R2}
Un substituted UPM								
GAS	-----	1.45663	1.23089	-----	1.21662	1.44352	-----	-----
METH	-----	1.45716	1.24354	-----	1.21942	1.44899	-----	-----
ACET	-----	1.45716	1.24362	-----	1.21943	1.44901	-----	-----
DMSO	-----	1.45714	1.24380	-----	1.21946	1.44906	-----	-----
WATER	-----	1.45711	1.24404	-----	1.21948	1.44912	-----	-----
CH_3-UPM								
GAS	1.52733	1.46096	1.23111	111.12	1.21665	1.44345	-----	-----
METH	1.52673	1.46272	1.24325	110.86	1.21943	1.44895	-----	-----
ACET	1.52672	1.46273	1.24331	110.86	1.21944	1.44897	-----	-----
DMSO	1.52666	1.46279	1.24347	110.83	1.21947	1.44904	-----	-----
WATER	1.52662	1.46284	1.24368	110.81	1.21951	1.44911	-----	-----
CH_3O-UPM								
GAS	1.41555	1.44716	1.23082	114.27	1.21651	1.44411	-----	-----
METH	1.42222	1.44257	1.24107	114.09	1.21938	1.44936	-----	-----
ACET	1.42225	1.44255	1.24112	114.09	1.21939	1.44938	-----	-----
DMSO	1.42233	1.44251	1.24126	114.08	1.21941	1.44943	-----	-----
WATER	1.42243	1.44245	1.24144	114.08	1.21943	1.44945	-----	-----
OH-UPM								
GAS	1.41462	1.45395	1.23503	114.19	1.21619	1.44432	-----	-----
METH	1.42593	1.44601	1.24379	114.04	1.21925	1.44947	-----	-----
ACET	1.42598	1.44597	1.24383	114.04	1.21926	1.44949	-----	-----
DMSO	1.42611	1.44586	1.24395	114.04	1.21929	1.44953	-----	-----
WATER	1.42628	1.44573	1.24411	114.04	1.21933	1.44959	-----	-----
NH_2-UPM								
GAS	1.46439	1.45342	1.23231	111.74	1.21627	1.44373	-----	-----
METH	1.46843	1.45213	1.24235	112.16	1.21938	1.44916	-----	-----
ACET	1.46846	1.45211	1.24241	112.16	1.21941	1.44918	-----	-----
DMSO	1.46848	1.45214	1.24255	112.17	1.21943	1.44923	-----	-----
WATER	1.46853	1.45214	1.24273	112.18	1.21946	1.44930	-----	-----

Table 2. Structural parameters (bond length (A) and bond angles (˚)) of UPM-Rmodel studied at the neutral state using DFT/B3LYP/6-311++G(d,p) basis set.

	ureido end				**carboxylate end**			
Solvent	r_{C-R}	r_{C-N}	$r_{C=O}$	**N–C–R**	$r_{C=O}$	r_{O-C}	r_{C-R2}	r_{O-C-R2}
Un substituted UPM								
GAS	-----	1.45663	1.23089	-----	1.21662	1.44352	-----	-----
METH	-----	1.45716	1.24354	-----	1.21942	1.44899	-----	-----
ACET	-----	1.45716	1.24362	-----	1.21943	1.44901	-----	-----
DMSO	-----	1.45714	1.24380	-----	1.21946	1.44906	-----	-----
WATER	-----	1.45711	1.24404	-----	1.21948	1.44912	-----	-----
UPM- CH_3								

GAS	-----	1.45667	1.23094	-----	1.21748	1.45583	1.52038	111.18
METH	-----	1.45699	1.24352	-----	1.22009	1.46205	1.51907	111.00
ACET	-----	1.45699	1.24359	-----	1.22010	1.46208	1.51906	111.00
DMSO	-----	1.45699	1.24378	-----	1.22012	1.46215	1.51905	111.00
WATER	-----	1.45698	1.24402	-----	1.22015	1.46224	1.51903	111.00
UPM-OCH_3								
GAS	-----	1.45678	1.23063	-----	1.21297	1.42416	1.39979	107.66
METH	-----	1.45707	1.24311	-----	1.21472	1.42761	1.40306	107.30
ACET	-----	1.45707	1.24318	-----	1.21473	1.42763	1.40308	107.30
DMSO	-----	1.45706	1.24337	-----	1.21475	1.42769	1.40313	107.30
WATER	-----	1.45706	1.24361	-----	1.21478	1.42777	1.40320	107.30
UPM-OH								
GAS	-----	1.45823	1.25708	-----	1.24562	1.49939	1.40371	113.00
METH	-----	1.45969	1.26696	-----	1.24388	1.49907	1.40808	112.33
ACET	-----	1.45970	1.26701	-----	1.24387	1.49906	1.40810	112.33
DMSO	-----	1.45973	1.26714	-----	1.24382	1.49903	1.40816	112.32
WATER	-----	1.45976	1.26732	-----	1.24377	1.49901	1.40823	112.31
UUP-NH_2								
GAS	-----	1.45695	1.23085	-----	1.22090	1.49144	1.41254	115.58
METH	-----	1.45705	1.24366	-----	1.22234	1.49703	1.41380	115.10
ACET	-----	1.45704	1.24373	-----	1.22234	1.49703	1.41382	115.10
DMSO	-----	1.45703	1.24391	-----	1.22235	1.49705	1.41386	115.09
WATER	-----	1.45702	1.24414	-----	1.22236	1.49706	1.41391	115.08

Table 3: Calculated Global chemical reactivity descriptors of the studied molecules in the gas and different solvents

HOMO	LUMO	I	A	x	η	μ	s	ω	ΔN	ΔE_n	ΔE_e	ΔE	phase
UPM													
-6.8646	-0.3957	6.8646	0.3957	3.6302	3.2345	-3.6302	0.3092	2.0371	1.1223	1.6414	8.9017	-6.4689	**Gas**
-6.9027	-0.4242	6.9027	0.4242	3.6635	3.2393	-3.6635	0.3087	2.0716	1.1310	1.6474	8.9743	-6.4785	**Methanol**
-6.9027	-0.4245	6.9027	0.4245	3.6636	3.2391	-3.6636	0.3087	2.0719	1.1311	1.6474	8.9746	-6.4782	***Acetonitrile***
-6.9030	-0.4245	6.9030	0.4245	3.6638	3.2393	-3.6638	0.3087	2.0719	1.1310	1.6474	8.9749	-6.4785	**DMSO**
-6.9027	-0.4248	6.9027	0.4248	3.6638	3.2390	-3.6638	0.3087	2.0721	1.1312	1.6473	8.9748	-6.4779	**water**
CH_3- UPM													
-6.8265	-0.3826	6.8265	0.3826	3.6046	3.2220	-3.6046	0.3104	2.0163	1.1187	1.6337	8.8428	-6.4439	Gas
-6.8856	-0.4226	6.8856	0.4226	3.6541	3.2315	-3.6541	0.3095	2.0660	1.1308	1.6434	8.9516	-6.4630	Methanol
-6.8861	-0.4229	6.8861	0.4229	3.6545	3.2316	-3.6545	0.3094	2.0664	1.1309	1.6435	8.9525	-6.4632	***Acetonitrile***
-6.8869	-0.4231	6.8869	0.4231	3.6550	3.2319	-3.6550	0.3094	2.0667	1.1309	1.6436	8.9536	-6.4638	DMSO
-6.8883	-0.4234	6.8883	0.4234	3.6559	3.2325	-3.6559	0.3094	2.0674	1.1310	1.6440	8.9557	-6.4649	water
CH_3O-U PM													
-7.1144	-0.5056	7.1144	0.5056	3.8100	3.3044	-3.8100	0.3026	2.1965	1.1530	1.6909	9.3109	-6.6088	Gas
-7.1667	-0.4487	7.1667	0.4487	3.8077	3.3590	-3.8077	0.2977	2.1582	1.1336	1.7095	9.3249	-6.7180	Methanol
-7.1669	-0.4484	7.1669	0.4484	3.8077	3.3593	-3.8077	0.2977	2.1580	1.1335	1.7096	9.3249	-6.7185	***Acetonitrile***
-7.1675	-0.4479	7.1675	0.4479	3.8077	3.3598	-3.8077	0.2976	2.1577	1.1333	1.7098	9.3252	-6.7196	DMSO
-7.1920	-0.4471	7.1920	0.4471	3.8196	3.3725	-3.8196	0.2965	2.1630	1.1326	1.7159	9.3550	-6.7449	water
OH- UPM													
-7.2869	-0.5676	7.2869	0.5676	3.9273	3.3597	-3.9273	0.2977	2.2954	1.1689	1.7278	9.5823	-6.7193	Gas

-7.2510	-0.4620	7.2510	0.4620	3.8565	3.3945	-3.8565	0.2946	2.1907	1.1361	1.7287	9.4417	-6.7890	Methanol
-7.2507	-0.4615	7.2507	0.4615	3.8561	3.3946	-3.8561	0.2946	2.1902	1.1360	1.7287	9.4409	-6.7892	***Acetonitrile***
-7.2502	-0.4607	7.2502	0.4607	3.8555	3.3948	-3.8555	0.2946	2.1893	1.1357	1.7286	9.4395	-6.7895	DMSO
-7.2497	-0.4593	7.2497	0.4593	3.8545	3.3952	-3.8545	0.2945	2.1880	1.1353	1.7287	9.4377	-6.7904	water
NH_2- UPM													
-6.8341	-0.4218	6.8341	0.4218	3.6280	3.2062	-3.6280	0.3119	2.0526	1.1316	1.6308	8.8867	-6.4123	Gas
-7.0442	-0.4370	7.0442	0.4370	3.7406	3.3036	-3.7406	0.3027	2.1177	1.1323	1.6807	9.1619	-6.6072	Methanol
-7.0456	-0.4373	7.0456	0.4373	3.7415	3.3042	-3.7415	0.3026	2.1183	1.1323	1.6810	9.1639	-6.6083	***Acetonitrile***
-7.0480	-0.4376	7.0480	0.4376	3.7428	3.3052	-3.7428	0.3026	2.1192	1.1324	1.6816	9.1672	-6.6104	DMSO
-7.0516	-0.4381	7.0516	0.4381	3.7449	3.3068	-3.7449	0.3024	2.1205	1.1325	1.6824	9.1721	-6.6135	water

Table.4: Calculated Global chemical reactivity descriptors of the studied molecules in the gas and different solvents.

HOMO	LUMO	I	A	x	η	μ	s	ω	ΔN	ΔE_n	ΔE_e	ΔE	phase
UPM -CH_3													
-6.8377	-0.3649	6.8377	0.3649	3.6013	3.2364	-3.6013	0.3090	2.0037	1.1127	1.6388	8.8414	-6.4728	Gas
-6.8932	-0.4041	6.8932	0.4041	3.6487	3.2446	-3.6487	0.3082	2.0515	1.1245	1.6474	8.9447	-6.4891	Methanol
-6.8935	-0.4044	6.8935	0.4044	3.6490	3.2446	-3.6490	0.3082	2.0519	1.1246	1.6475	8.9454	-6.4891	*Acetonitrile*
-6.8940	-0.4049	6.8940	0.4049	3.6495	3.2446	-3.6495	0.3082	2.0524	1.1248	1.6475	8.9464	-6.4891	DMSO
-6.8948	-0.4054	6.8948	0.4054	3.6501	3.2447	-3.6501	0.3082	2.0531	1.1249	1.6477	8.9479	-6.4894	water
UPM -CH_3O													
-6.8733	-0.5358	6.8733	0.5358	3.7046	3.1688	-3.7046	0.3156	2.1655	1.1691	1.6297	9.0388	-6.3375	Gas
-6.9305	-0.6430	6.9305	0.6430	3.7868	3.1438	-3.7868	0.3181	2.2806	1.2045	1.6376	9.2111	-6.2875	Methanol
-6.9305	-0.6435	6.9305	0.6435	3.7870	3.1435	-3.7870	0.3181	2.2811	1.2047	1.6376	9.2116	-6.2870	***Acetonitrile***
-6.9310	-0.6452	6.9310	0.6452	3.7881	3.1429	-3.7881	0.3182	2.2829	1.2053	1.6377	9.2139	-6.2858	DMSO
-6.9316	-0.6471	6.9316	0.6471	3.7894	3.1423	-3.7894	0.3182	2.2849	1.2059	1.6378	9.2165	-6.2845	water
UPM -OH													
-6.9827	-0.7886	6.9827	0.7886	3.8857	3.0971	-3.8857	0.3229	2.4375	1.2546	1.6489	9.4202	-6.1941	Gas
-6.5824	-0.7861	6.5824	0.7861	3.6843	2.8982	-3.6843	0.3450	2.3418	1.2712	1.5557	8.9242	-5.7963	Methanol
-6.9335	-0.6977	6.9335	0.6977	3.8156	3.1179	-3.8156	0.3207	2.3347	1.2238	1.6370	9.2682	-6.2358	***Acetonitrile***
-6.9332	-0.6963	6.9332	0.6963	3.8148	3.1185	-3.8148	0.3207	2.3333	1.2233	1.6370	9.2665	-6.2369	DMSO
-6.5830	-0.7823	6.5830	0.7823	3.6827	2.9004	-3.6827	0.3448	2.3380	1.2697	1.5557	8.9210	-5.8007	water
UPM -NH_2													
-6.8728	-0.4825	6.8728	0.4825	3.6777	3.1952	-3.6777	0.3130	2.1165	1.1510	1.6340	8.9893	-6.3903	Gas
-6.8897	-0.4533	6.8897	0.4533	3.6715	3.2182	-3.6715	0.3107	2.0943	1.1409	1.6410	8.9840	-6.4364	Methanol
-6.8897	-0.4533	6.8897	0.4533	3.6715	3.2182	-3.6715	0.3107	2.0943	1.1409	1.6410	8.9840	-6.4364	***Acetonitrile***
-6.8899	-0.4528	6.8899	0.4528	3.6714	3.2186	-3.6714	0.3107	2.0939	1.1407	1.6411	8.9838	-6.4371	DMSO
-6.8902	-0.4523	6.8902	0.4523	3.6713	3.2190	-3.6713	0.3107	2.0936	1.1405	1.6413	8.9838	-6.4379	water

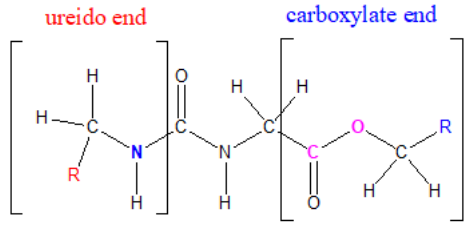

Fig. 1 The various peptidomimetic models that were examined in this work are shown schematically.

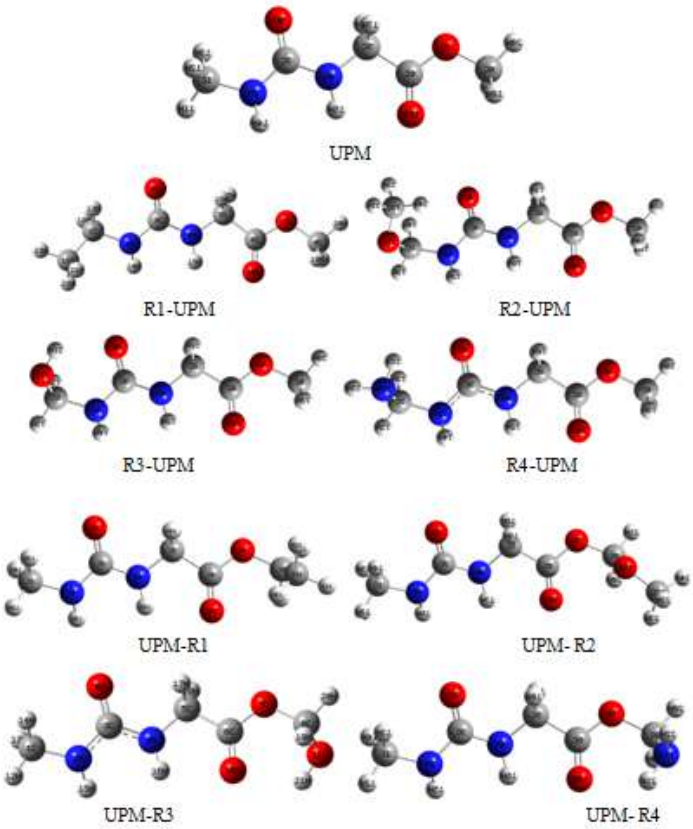

Fig. 2: The Geometry optimized structures for R-UPM and UPM-R models in the gas phase. (R1=-CH_3, R2= OCH_3, R3= -OH, R4=-NH_2)

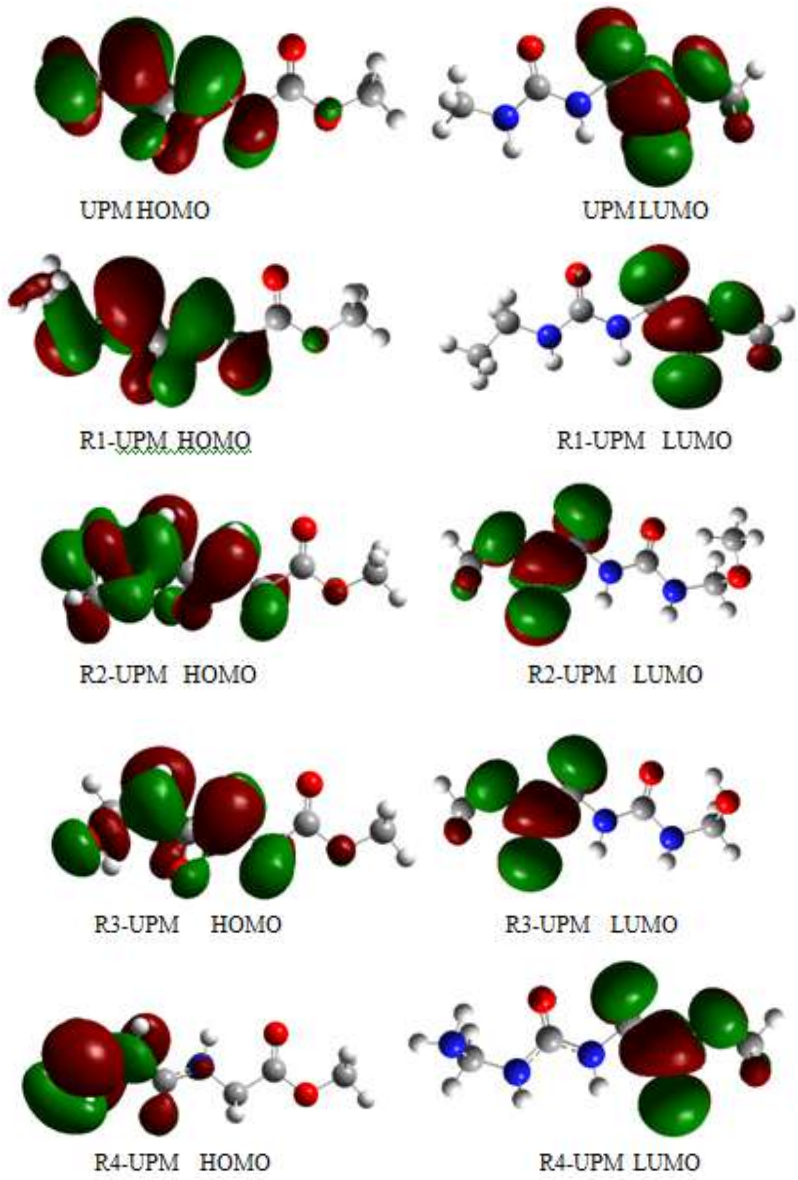

Fig. 3: HOMO and LUMO molecular orbital diagrams of the studied R-UPM model structures using B3LYP/ 6-311++ G(d,p) in the gas phase.

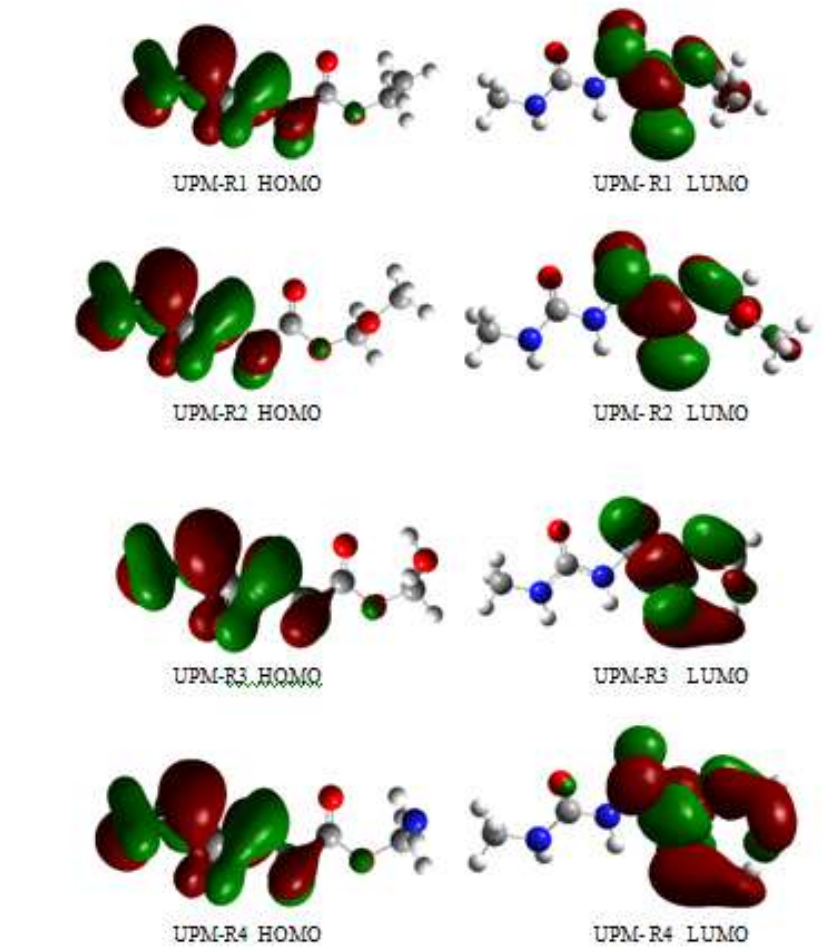

Fig. 4: HOMO and LUMO molecular orbital diagrams of the studied UPM-R model structures using B3LYP/ 6-311++ G(d,p) in the gas phase.

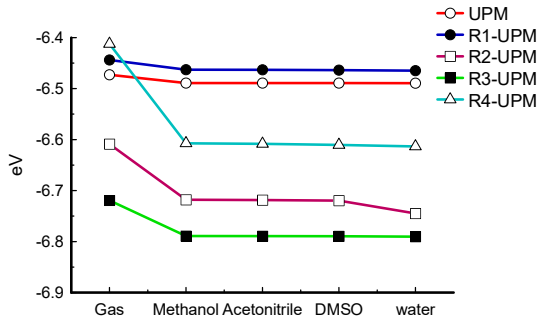

Fig. 5: The energy gap (ΔE) between HOMO and LUMO for studied model R-UPM in the gas and different solvents.

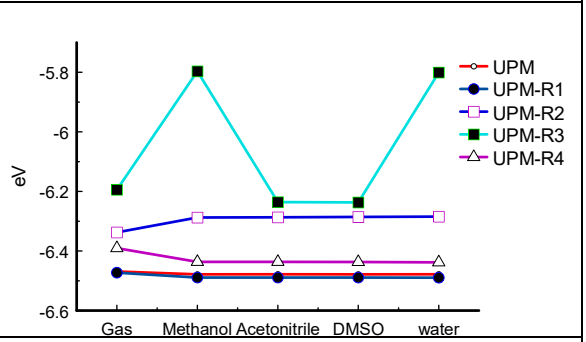

Fig .6: Fig. 5: The energy gap (ΔE) between HOMO and LUMO for studied model UPM-R in the gas and different solvents.

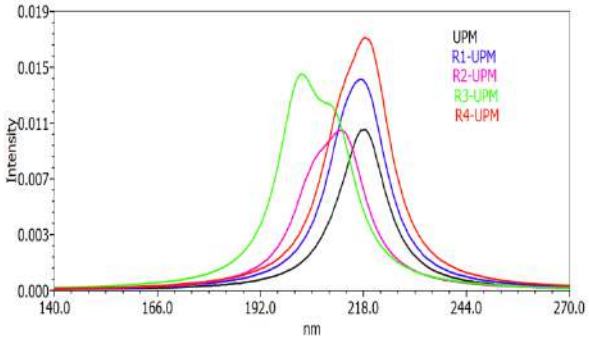

Fig.7: Simulated UV–visible optical absorption spectra of the studied molecules of model R-UPM (R1=-CH_3, R2= OCH_3, R3= -OH, R4=-NH_2) with calculated data at the TD-DFT/B3LYP/6- 311++ G (d,p) level in gas phase.

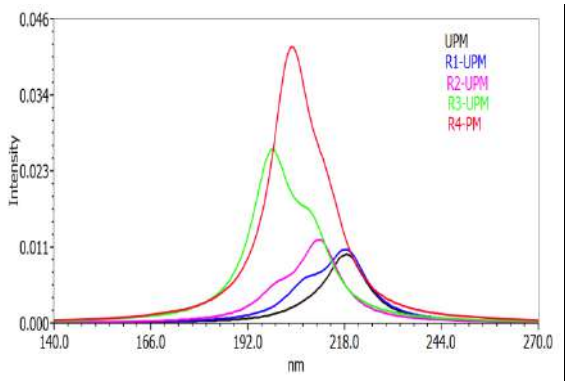

Fig.8: Simulated UV–visible optical absorption spectra of the studied molecules of model R-UPM (R1=-CH_3, R2= OCH_3, R3= -OH, R4=-NH_2) with calculated data at the TD-DFT/B3LYP/6- 311G++ (d,p) level in aqueous solvent.

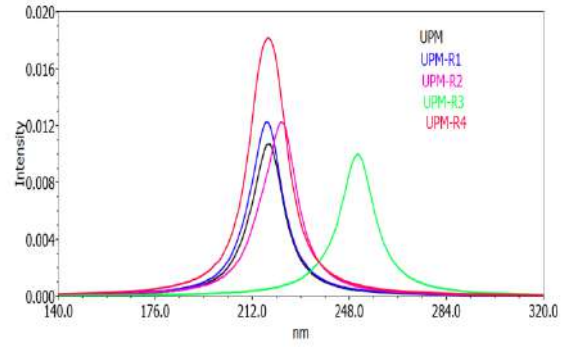

Fig.9: Simulated UV–visible optical absorption spectra of the studied molecules of model UPM-R (R1=-CH_3, R2= OCH_3, R3= -OH, R4=-NH_2) with calculated data at the TD-DFT/B3LYP/6- 311++ G(d,p) level in gas phase.

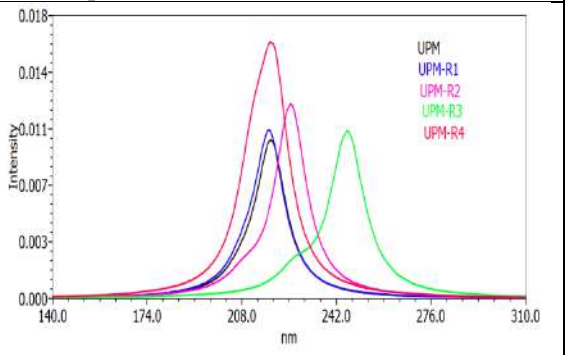

Fig.10: Simulated UV–visible optical absorption spectra of the studied molecules of model UPM-R (R1=-CH_3, R2= OCH_3, R3=-OH, R4=-NH_2) with calculated data at the TD-DFT/B3LYP/6- 311++ G(d,p) level in aqueous solvent.

Indian Journal of Natural Sciences *www.tnsroindia.org.in ©IJONS*

Vol.15 / Issue 83 / Apr / 2024 *International Bimonthly (Print) – Open Access* *ISSN: 0976 – 0997*

RESEARCH ARTICLE

Role and Responsibilities of Teachers for Promoting Environmental Ethics among Students

P.Pachaiyappan[1*], Radhika Vidyasagar[2] and B.Venkatarathanam[3]

[1]Professor, Department of Education, GRT College of Education, Tiruttani (Affiliated to Tamil Nadu Teachers Education University) Tamilnadu, India.
[2]Principal, Department of Education, GRT College of Education, Tiruttani (Affiliated to Tamil Nadu Teachers Education University) Tamilnadu, India.
[3]Assistant Professor, Department of Education, GRT College of Education, Tiruttani (Affiliated to Tamil Nadu Teachers Education University) Tamilnadu, India.

Received: 03 Sep 2023 Revised: 24 Dec 2023 Accepted: 06 Mar 2024

***Address for Correspondence**
P.Pachaiyappan
Professor,
Department of Education,
GRT College of Education,
Tiruttani (Affiliated to Tamil Nadu Teachers Education University)
Tamilnadu, India.
Email: edugreenict@gmail.com

ABSTRACT

Environmental ethics is the philosophical discipline that considers the moral and ethical relationship of human beings to the environment. In other words it considers the ethical basis of environmental protection. This paper provides a concise overview of the role and responsibilities of teachers in fostering environmental ethics among students. In an era marked by escalating environmental challenges, educators emerge as pivotal agents of change. This paper explores the multifaceted responsibilities of teachers in cultivating a sense of environmental ethics among students. It delves into pedagogical approaches, curriculum integration, and the cultivation of eco-conscious attitudes. By examining the educator's role as a catalyst for environmental awareness, this abstract underscores the significance of instilling a deep-seated commitment to sustainable practices and environmental stewardship. The study aims to contribute insights into the effective strategies teachers can employ to nurture environmentally responsible citizens, emphasizing the critical connection between education, ethics, and the well-being of the planet.

Keywords: Environmental Ethics, Types of Environmental Ethics, Role of Teachers in Environmental Ethics, Strategies for Promoting Environmental Ethics, Students, Pedagogical Approaches to Environmental Ethics.

INTRODUCTION

The role and responsibilities of teachers in promoting environmental ethics among students are paramount in shaping the future stewards of our planet. In an era marked by environmental challenges, educators play a pivotal role in instilling a sense of responsibility, awareness, and ethical consciousness in the minds of their students. Teachers are not merely transmitters of knowledge; they are catalysts for positive change. By incorporating environmental ethics into the educational landscape, educators can inspire a generation to appreciate, respect, and safeguard the natural world. This introduction explores the multifaceted responsibilities of teachers, delving into how they can cultivate a deep environmental ethic within their students, fostering a commitment to sustainable practices and a profound sense of responsibility towards the well-being of the Earth. The word Ethics is emerged from the Greek word "ethos" which means "character". The determination of ethics is not possible until we get the knowledge of the right and wrong. According to Webster Dictionary, "Ethics is the science of moral duties or it is the science of ideal human character." Ethics is a system of rules and moral principles guiding conduct. It can be a framework for judging what is good and bad, right and wrong. It guides the reasoning that one makes before acting; understanding the consequences of one's action (also known as moral philosophy). Ethics is a branch of philosophy which addresses questions of morality. Ethics is highly important to science because the scientific inquires merit ethical assessment.

Environmental Ethics

Environmental Ethics is the ethical study of the relationship of human and environment. It is the discipline that studies the moral relationship of human being and also the value and moral status of the natural environment and its Non-human content. Environmental Ethics is a topic of applied ethics which examine the moral basis of environmental responsibility. It focuses on the moral foundation of environment responsibility and how far this responsibility extends. More specifically, it refers to the value that mankind places on protecting, conserving and efficiently using resources that the earth provides. Environmental Ethics emerged as a new sub-discipline of practical philosophy that deals with the ethical problems concerning environmental protection and conservation. It aims at providing ethical justification and moral motivation for the cause of global environmental protection. On the one hand, at the level of ideas, Environmental Ethics challenges the dominant and deep-rooted anthropocentrism of modern mainstreams ethics and extends the object of our duty to future generation and non-human beings as well and on the other hand at the practical level, Environmental Ethics criticizes the materialistic and consumerist attitude of modern capitalism and demands for the healthy and green- lifestyle, that is harmonious with nature.

Environmental ethics is a theoretical discipline that examines all kinds of attitudes and behaviors that people consider important when making decisions about nature, factors that make up nature, or the environment (Karaca, 2007). The environmental ethic evaluates the relationship of people to nature in a moral framework (Ozer & Keleş, 2016) and tries to find the right behavior towards the environment. Environmental ethics allows the individual to appreciate the value of nature (Mahmutoglu, 2009). It is emphasized that environmental ethics is the responsibility of the environment in which the person lived, and that every living thing should behave in a way that considers the vital rights it possesses (Ozer & Keleş, 2016). Approaches about environmental ethics, (Karaca, 2007; Kayaer, 2013; Agbuga, 2016), consciousness (Kılıc & Inal, 2010; Talas & Karatas, 2012), aweraness (cabuk & Karacaoglu, 2003; Şenyurt, Bayık Temel & Ozkahraman, 2011; Dolmacı ve Bulgan, 2013), perception (Blbul, 2013; Gerçek, 2016; Tesfai, Nagothu, Simek & Fucik, 2016) and approach (Saka, Surmeli ve Oztuna, 2009; Ozdemir, 2012) studies are found. Teachers have to remember to their students about responsibilities on environment and they have to get awareness (Ozer & Keles, 2016). In order to make this kind of consciousness, teachers have to become their awareness much more than students (Keles, Uzun & Varnacı Uzun, 2010). Living and non-living goods are semmed as a whole by environmental-centered approach. Also, ethical approaches of humans about environment are distant from human centered approach to living environment centered approach (Kayaer, 2013). Basic principles of environmental problems are human behavious, as results of this awareness of humans about environment become an important issue (Erten, 2004).

The History of Environmental Ethics

The history of environmental ethics can be traced to pivotal moments in the mid-20th century when concerns about the ecological impact of human activities began to gain widespread attention. Rachel Carson's "Silent Spring" (1962) raised awareness about the environmental consequences of pesticide use, setting the stage for the modern environmental movement. Lynn White Jr.'s essay "The Historical Roots of Our Ecologic Crisis" (1967) prompted reflection on the cultural and religious foundations of anthropocentrism. The first Earth Day in 1970 further mobilized public sentiment towards environmental protection. Aldo Leopold's "A Sand County Almanac" (1949) introduced the concept of a "land ethic," emphasizing the ethical relationship between humans and the land. Arne Naess's deep ecology movement and J. Baird Callicott's contributions in the 1970s and 1980s solidified environmental ethics as a distinct field of study. This history reflects a growing recognition of the ethical dimensions of human interactions with the environment, culminating in the formalization and expansion of environmental ethics as a field addressing contemporary global challenges.

Need for Environmental Ethics Education

Environmental ethics education is indispensable in our contemporary world as it equips individuals with the knowledge, values, and ethical frameworks necessary to navigate and address pressing environmental challenges. With the planet facing issues such as climate change, biodiversity loss, and resource depletion, understanding the ethical dimensions of human-nature interactions is critical. Environmental ethics education fosters awareness about the interconnectedness of ecosystems, encouraging responsible resource management and sustainable practices. It empowers individuals to make ethically informed decisions, promoting environmental justice, biodiversity conservation, and climate change mitigation. As technology advances and global interconnectivity increases, the ethical implications of human activities on the environment become more pronounced, making environmental ethics education essential for fostering a sense of individual and collective responsibility towards the well-being of the planet. Ultimately, this education is a cornerstone for cultivating a sustainable and ethical relationship between humanity and the natural world.

Principles of Environmental Ethics

Environmental ethics is a branch of ethics that examines the moral principles and values that should guide human interactions with the natural world. These principles provide a framework for addressing ethical issues related to the environment. While there may be variations in the formulation of these principles, the following are commonly recognized as key principles of environmental ethics:

1. *Respect for the intrinsic value of nature:* Nature should not be treated as a commodity or resource to be exploited and discarded.
2. *Interdependence of species and ecosystems:* Humans depend on nature and natural systems. We must recognize our role in preserving and protecting the environment.
3. *Ecological sustainability:* We must strive to use resources responsibly and with an eye to preserving ecosystems and biodiversity.
4. *Human responsibility:* We are responsible for our own actions and decisions and their consequences for the environment.
5. *Human equity:* We must strive for a just world where the rights and needs of humans, animals, and plants are respected and protected.
6. *Precautionary principle:* We should take precautions against environmental harm, even when scientific evidence is inconclusive.
7. *Right to know:* Individuals have the right to access information about environmental issues.
8. *Right to participate:* Citizens have the right to participate in environmental decision-making processes.

Types of Environmental Ethics

Environmental ethics encompasses various perspectives and approaches that guide individuals and societies in understanding and addressing ethical issues related to the environment. Different types of environmental ethics represent diverse philosophical and ethical frameworks. Here are some major types:

1. ***Anthropocentrism:*** Anthropocentrism places human interests at the center and considers the environment valuable only to the extent that it serves human needs and desires. This perspective sees nature as a resource for human well-being.
2. ***Biocentrism:*** Biocentrism extends intrinsic value beyond humans to all living organisms. It asserts that all living beings have inherent worth and should be considered in ethical decision-making, not just for their utility to humans.
3. ***Ecocentrism:*** Ecocentrism takes a broader view, attributing intrinsic value to entire ecosystems and the biosphere. It emphasizes the interdependence of all living and non-living elements in an ecosystem and advocates for the well-being of the entire ecological community.
4. ***Deep Ecology:*** Deep ecology, developed by Arne Naess and George Sessions, goes beyond traditional environmental ethics by proposing a radical shift in human consciousness. It encourages a reevaluation of human relationships with nature, emphasizing a spiritual or metaphysical connection with the Earth.
5. ***Ecofeminism:*** Ecofeminism explores the connections between the exploitation of nature and the oppression of women. It critiques patriarchal structures and argues for the need to address both environmental and social injustices.
6. ***Environmental Virtue Ethics:*** Environmental virtue ethics focuses on cultivating virtuous character traits in individuals. It emphasizes the development of virtues such as responsibility, humility, and compassion in the context of environmental decision-making.
7. ***Social Ecology:*** Social ecology, developed by Murray Bookchin, integrates ecological principles with social justice concerns. It emphasizes the need to address both environmental issues and social inequalities simultaneously.
8. ***Shallow Ecology:*** Shallow ecology is often used to contrast with deep ecology. It focuses on practical and immediate solutions to environmental problems without necessarily challenging the deeper values and structures of society.
9. ***Conservation Ethics:*** Conservation ethics emphasizes the responsible use and management of natural resources for the benefit of present and future generations. It seeks to balance human needs with the conservation of biodiversity and ecosystems.
10. ***Land Ethic:*** Developed by Aldo Leopold, the land ethic proposes an expansion of ethical consideration to include the land as a whole. It argues for an ethical relationship with the land, recognizing that humans are just one part of a larger ecological community.
11. ***Animal Rights Ethics:*** This perspective extends ethical consideration to individual animals, emphasizing their inherent value and rights. It advocates for the ethical treatment of animals and challenges practices that exploit or harm them.
12. ***Environmental Justice:*** Environmental justice focuses on the fair distribution of environmental benefits and burdens, particularly in relation to marginalized communities. It seeks to address issues of environmental racism and unequal exposure to environmental hazards.

These types of environmental ethics reflect the diversity of thought within the field, providing different lenses through which individuals and societies can approach environmental issues. Often, ethical decisions involve a combination of these perspectives, as environmental challenges are multifaceted and interconnected.

Role of Teachers for Promoting Environmental Ethics among Students

Teachers play a crucial role in promoting environmental ethics among students. Environmental ethics involves fostering a sense of responsibility, awareness, and values towards the environment. Here are some key roles and responsibilities of teachers in this regard:

Educator

Provide students with a comprehensive understanding of environmental issues, including climate change, pollution, deforestation, and biodiversity loss. Incorporate environmental topics into the curriculum across various subjects, illustrating the interconnectedness of environmental issues with other disciplines.

Role Model
Demonstrate environmentally friendly practices in the classroom, such as waste reduction, energy conservation, and sustainable resource use. Share personal experiences and stories related to environmental stewardship to inspire students.

Facilitator of Experiential Learning
Organize field trips, nature walks, and hands-on activities that allow students to directly engage with and appreciate the environment. Encourage outdoor learning experiences to develop a connection between students and the natural world.

Promoter of Critical Thinking
Encourage students to analyze and question environmental issues critically. Foster a sense of environmental responsibility by helping students understand the consequences of individual and collective actions on the environment.

Advocate for Environmental Issues
Guide students in researching and understanding local and global environmental challenges. Encourage students to participate in environmental advocacy, awareness campaigns, or community service projects.

Integration of Ethics and Values
Discuss and explore ethical frameworks related to the environment, emphasizing the importance of responsible decision-making. Help students develop a personal code of environmental ethics based on values such as stewardship, sustainability, and social responsibility.

Promotion of Sustainable Practices
Teach and model sustainable practices, such as recycling, reducing waste, and conserving resources. Integrate discussions on sustainable development and green technologies into the curriculum.

Cultivator of Empathy and Compassion
Encourage students to develop empathy for the natural world and an understanding of how their actions impact ecosystems and other living beings. Foster a sense of responsibility towards future generations and the planet.

Incorporation of Multidisciplinary Perspectives
Integrate perspectives from various disciplines, such as science, social studies, and ethics, to provide a holistic understanding of environmental issues. Collaborate with other teachers to create interdisciplinary projects related to environmental ethics.

Assessment and Feedback
Evaluate students' understanding of environmental issues and ethics through assessments, projects, and discussions. Provide constructive feedback to help students improve their environmental awareness and ethical reasoning. By fulfilling these roles and responsibilities, teachers can contribute significantly to shaping environmentally conscious and ethically responsible citizens.

Approaches to Teaching Environmental Ethics
Teaching environmental ethics can be approached in various ways to engage students, encourage critical thinking, and instill a sense of responsibility towards the environment. Here are several approaches to teaching environmental ethics:

Interdisciplinary Learning
Integrate environmental ethics into various subjects, fostering interdisciplinary connections. Explore the ethical dimensions of environmental issues in science, social studies, literature, and other disciplines, providing a holistic understanding.

Case Studies and Real-World Examples
Use case studies and real-world examples to illustrate ethical dilemmas related to the environment. Analyzing specific cases encourages students to apply ethical principles to practical situations and develop problem-solving skills.

Outdoor Education and Experiential Learning
Take students outdoors for nature walks, field trips, or experiential learning activities. Direct interaction with the environment fosters a personal connection, deepens appreciation, and encourages a sense of responsibility.

Ethical Debates and Discussions
Organize debates and discussions on environmental issues, encouraging students to explore different ethical perspectives. This approach promotes critical thinking, effective communication, and the ability to consider diverse viewpoints.

Guest Speakers and Expert Panels
Invite guest speakers, environmentalists, or experts in environmental ethics to share their experiences and insights. Hearing from professionals in the field can inspire students and provide real-world context to ethical discussions.

Service-Learning Projects
Engage students in service-learning projects related to environmental ethics. This hands-on approach allows students to apply ethical principles in practical situations, fostering a sense of civic responsibility and community engagement.

Technology and Multimedia Tools
Utilize technology and multimedia tools to enhance learning. Incorporate documentaries, online resources, and virtual field trips to expose students to a variety of perspectives and issues in environmental ethics.

Role-Playing and Simulations
Use role-playing activities and simulations to immerse students in ethical scenarios. This approach encourages empathy, helps students understand the complexities of decision-making, and prompts ethical reflection.

Critical Thinking Exercises
Design critical thinking exercises that challenge students to analyze and evaluate ethical issues in environmental contexts. These exercises can include ethical dilemmas, thought experiments, and reflective writing assignments.

Literature and Art
Integrate literature, poetry, and art that explore environmental themes and ethical considerations. Analyzing literary works and artistic expressions can evoke emotional responses and deepen students' understanding of ethical implications.

Project-Based Learning
Implement project-based learning where students work on extended projects that involve research, analysis, and problem-solving. This approach allows students to apply ethical principles to real-world issues and develop practical skills.

Philosophical Inquiry
Introduce students to key environmental philosophers and ethical theories. Explore philosophical inquiries into the relationship between humans and nature, providing a theoretical foundation for ethical discussions.

Reflective Journals and Portfolios
Incorporate reflective journals or portfolios where students document their thoughts, experiences, and insights regarding environmental ethics. This approach encourages self-reflection and allows students to track their personal development in understanding ethical issues.

Cultural Perspectives
Explore cultural perspectives on environmental ethics by examining how different cultures value and interact with nature. This approach fosters cultural awareness and respect for diverse ethical values associated with the environment. By adopting a variety of these approaches, educators can create a dynamic and engaging learning environment that encourages students to think critically, develop ethical reasoning skills, and become responsible stewards of the environment.

CONCLUSION

The role and responsibilities of teachers in promoting environmental ethics among students are of utmost importance in addressing the pressing challenges of our time. This study has underscored the multifaceted nature of the teacher's role, extending beyond conventional academic instruction to encompass the cultivation of ethical values and environmental consciousness. As educators, their influence goes beyond the classroom, shaping the mindset and behaviors of the next generation. Through intentional integration of environmental ethics into the curriculum, fostering experiential learning, and serving as role models of sustainable practices, teachers become instrumental in instilling a deep sense of responsibility and stewardship towards the environment. This paper highlights the interconnectedness of education, ethics, and environmental sustainability, emphasizing the transformative power teachers wield in nurturing environmentally conscious citizens who are poised to contribute positively to the well-being of the planet. As we recognize the urgency of environmental issues, acknowledging and reinforcing the pivotal role of teachers becomes essential for fostering a generation committed to preserving and protecting our shared global environment.

REFERENCES

1. Armstrong, J. S. ve R. G. Botzler. (1993). Environmental Ethics: Divergence and Convergence. New York: Mc Graw-Hill.
2. Carson, R (1962).Silent spring. New York, Fawcett Crest.
3. David, O. K., & Johan, O. (2012). An environmental ethical conceptual framework for research on sustainability and environmental education. *Environmental Education Research*, 19(1), 21-44.
4. Dhawan, S., Rawat, L. and Sharma, V. (2005). Environmental Education in Pre-Service Teacher Education. *Journal of Indian Education*, 31(2), 29-44.
5. Freiman, C. (2006). Environmental virtue ethics. Ethics and the Environment, 11(1), 133-138.
6. Harpreet Kaur (2019). A Study of Environmental Ethics among the Prospective Teachers of Haryana. *International Journal of Research in Engineering, IT and Social Sciences*, 09 (2), 188-194.
7. Khitoliya,R.K.(2008). Environmental Management & Conservation. APH Publishing Corporation, New Delhi.
8. Laal, M. (2009). A Brief History of Environmental ethics and Its Challenges, *Journal of Medical Ethics and History of Medicine*, 2(10), 1-5.
9. Leopold, A. (1949). *A Sand County Almanac*. pp. 203. Oxford University Press, New York.

10. Marie, C.(2017).Environmental Ethics among higher secondary students. *International Journal of Advance Research and Innovative Ideas in Education*. 3 (1): 506- 511.
11. Nagra,V.(2010).Environmental education awareness among school teachers. *The Environmentalist*, 30(2), 153-162.
12. Ozdemir, O. (2012).The Environmentalism of university students: their ethical attitudes toward the environment. *Hacettepe University Journal of Education*, 43, 373-385.
13. Pant, R., and Singh, A.(2017).Environmental ethics among adolescents: A study of gender, region, and community services. *International Journal of Research Culture Society*, 1(10), 135-139.
14. Saxena, A.B. (1996).Education for the environmental concerns: Implication and Practices. Radha Publication, New Delhi.
15. Tesfai, M., Nagothu, U. S., Simek, J., & Fucikc, P. (2016). Perceptions of secondary school students' towards environmental services: a case study from Czechia. *International Journal of Environmental and Science Education*, 11(12), 5533-5553.
16. White, L.T. Jr., (1967). The Historical Roots of Our Ecologic Crisis. Science, 155, pp.1203– 207.

Indian Journal of Natural Sciences *www.tnsroindia.org.in ©IJONS*

Vol.15 / Issue 83 / Apr / 2024 *International Bimonthly (Print) – Open Access* *ISSN: 0976 – 0997*

RESEARCH ARTICLE

Can Physical Impairments Pose a Threat to Eradication of Poverty Owing to Culture of Poverty?

Tamilarasu Sampath[1]*, N R.Suresh Babu[2], Indhirapriyadharshini M[1], Chandramathi Ramaswamy[3] and Sigamani Panneer[4]

[1]Research Scholar, Department of Sociology and Population Studies, Bharathiar University, Coimbatore, Tamil Nadu, India.
[2]Professor, Department of Sociology and Population Studies, Bharathiar University, Coimbatore, Tamil Nadu, India.
[3]Research Scholar, Department of Social Work, Bharathiar University, Coimbatore, Tamil Nadu, India.
[4]Professor, Centre for the Study of Law and Governance, Jawaharlal Nehru University, Delhi, India.

Received: 30 Dec 2023 Revised: 09 Jan 2024 Accepted: 27 Mar 2024

***Address for Correspondence**
Tamilarasu Sampath
Research Scholar,
Department of Sociology and Population Studies,
Bharathiar University,
Coimbatore, Tamil Nadu, India.
Email: tamilarasu.dsps@buc.edu.in.

ABSTRACT

Explanation of the persisting difference in the structure of disability and increasing dependency have long been debated in social sciences in terms of poverty. Despite the removal of formal restrictions, structural constraints on people with locomotor disabilities continue to be important, according to sociological accounts and empirical investigations. Role of poverty in the lives of people with locomotor disabilities (PwLD), How has poverty become a culture for PwLD? and how the culture of poverty is perpetuating among PwLD? An exploratory study was carried among individuals with locomotor impairment, Tamil Nadu on April 2023 with Focus Group Discussion method. Questions on socioeconomic circumstances in relation with life chances; impact of poverty condition on lifestyle transformation; transmission of poverty as a result of disability to next generation were used as prompts to consolidate into the study. PwLD poverty is not simply a matter of monetary or economic factors, but is closely linked to restraints on their opportunities in life. These lacking, financial dependence, such as less opportunities, social rejection, and unaccredited employment. As a result of poor living conditions and social poverty, the state been perpetuating among the PwLD, however, this could be eradicated by effective role of welfare system.

Keywords: locomotor disability, poverty, impediments, social poverty, culture of poverty.

INTRODUCTION

A social model of disability beyond its usual medical explanation, concentrates on the interaction that people with impairments have with their surrounding environment that possess physical, attitudinal, behavioural, communicational and social barriers (People with disability Australia, 2023). This reminds us of a social construction view that looks into the social system of legislations, policies and programmes of the society in fulfilling the needs of the impaired to accommodate them into the social whole than viewing as an individual problem (Dfid, 2009; Haegele & Hodge, 2016).Persons with disabilities (PwD) often experience poverty as a way of life, and adaptation to such poverty worsens the consequence of their disability. UN report (2018) says, people with disabilities face numerous impediment even to participate among their communities around the world and to enjoy complete inclusion. Meanwhile, inadequate education, healthcare, employment, financial deprivation, social support, community participation and social marginalization are caused by disability which further results in lack of life-chances available for them (Philip, 2015; Pinilla-Roncancio, 2015). It is to understand that disability is both the cause and consequence of poverty and the relation of the two results in higher vulnerability and exclusion of the community (Rohwerder, 2015). PwD in a comprehensive way experience numerous tussles;most adverse group one among themare persons with locomotor disability (PwLD) who are facing even more disastrous effects.

Employment opportunities for PwLD are often limited and are accompanied with discrimination, stigma and attitudinal barriers in the workplace which leads to financial deprivation and dependence on social assistance resulting in complete exclusion from the labour market. Consequently, PwLD face long-term financial struggles, further deepening their experience with poverty and social marginalization is a deep concern for them since they experience rejection in social activities. This can lead to loneliness and low self-esteem, compromising their general well-being and sense of belongingness in their communities(Banks et.al, 2017). Studies proved that PwLD often face larger struggles in self-care, mobility and in interpersonal relations which is mainly because of their improper social support and low understanding of society on their serious issue (Mishra et al., 2019). All the above explanations have provided evidences to state that adaptation to poverty and long-term deprivations of life-chances has habituated the culture of poverty among individuals with locomotor disability (Lewis, 1966; Sonpal& Kumar, 2012; Lewis, 2017). Now, the key questions are how has poverty become a culture for PwLD? and how the culture of poverty is perpetuating among PwLD? Majority of the study experts visualized PwLD having less effect due to their physical immobility and has presented fewer challenges than other disabilities. However, as indicated, disability leading to poverty worsens with existential crisis, limiting one's opportunities in life. Despite the fact that, most of the times, financial condition and economic status were taken as measure of poverty (Waldschmidt, 2021; Schiariti, 2020; Banks et al., 2017; Waldschmidt et al., 2017), understanding of the transmission nature of poverty over generations is necessary in order to comprehend the continuing nature of poverty as culture through the lives of PwLd and their progenies (Department for International Development, 2000). By taking these additional considerations into account, the research hopes to shed insight on the complicated dynamics of poverty and disability, particularly among those with locomotor impairments. It emphasizes the importance of comprehensive interventions that address not just the immediate economic issues faced by PwLD, but also the structural and systemic causes that perpetuate poverty within this marginalized population.

MATERIALS AND METHODS

An exploratory study was conducted in April 2022 among individuals with locomotor impairments in Dharmapuri district of Tamil Nadu. The motivation behind this study stemmed from the observation that existing literature mostly focused on general impairments and individual sufferings. This paved way for highlighting the need to investigate the specific experiences of individuals with locomotor disabilities. By doing so, the aim was to gain a

deeper understanding of the challenges they face, the impact on their prospects for a fulfilling life, and the lasting damages caused by these disabilities. To gather data, the study employed a Focus Group Discussion (FGD) approach, utilizing a discussion guide and a skilled moderator. The FGD allowed participants to share their experiences and perspectives on various aspects, including their standard of living, support systems, quality of life, and socio-economic conditions. To ensure concrete and diverse range of viewpoints, purposive sampling was utilized to identify potential participants. Prior to the commencement of the discussion, discrete informed consent was obtained from each participant in a social setting that was accessible to all. The FGD prompts encompassed a range of topics, such as the participants' social standing, socioeconomic circumstances, and their correlation with life chances. Participants were also prompted to discuss the impact of their poverty conditions on lifestyle transformations and the transmission of poverty to the next generation as a result of their disabilities. By exploring these dimensions, the study aimed to consolidate findings that would contribute to its overall objectives. The use of an exploratory study and the FGD method allowed for a rich nuanced exploration of the experiences of individuals with locomotor disabilities in the Dharmapuri district. This approach aimed to capture the multifaceted nature of their challenges and shed light on the ways in which poverty, disability, and social factors interact to shape their lives and opportunities.

RESULTS

Familiarization of data collected in regional language was done through transcription and translation into English. Following this, transcripts were analyzed using an inductive approach based on thematic analysis. The framework for comprehending poverty and disability was identified through codes in a pattern establishing the themes as living conditions, social poverty and culture of poverty. The consolidated themes were initially categorized into sub themes as financial dependence, structural inequality, social consciousness, social restraints and social alienation which defined the above themes. Continuous monitoring and reassessment was done by all the researchers to have concrete conclusions from the transcripts and to establish the pattern and relationship between the themes. Social poverty and Culture of poverty are the key themes evolved in the study which are operationalized as follows. Social poverty for PwLD is that state of being alienated from the mainstream of the society as in lacking the basic capacity to participate in the social occurrences, and to have good-quality, trustworthy and dependable relationships. In the line of thought, culture of poverty is the cyclical nature of poverty that transfer across generations and the adaptations developed to poverty as a way of life. Categorised sub themes jointly and collaboratively contribute to represent both social poverty and culture of poverty which are likely to be constituted through their living conditions. The relation of all the variables is picturised in the following diagram to point out the theoretical assumptions of the study.

FINDINGS AND DISCUSSION

Theme – I: Culture of Poverty

The root of culture of poverty among PwLD begins with present living conditions insisting on the level of *financial dependence* and *structural inequalities* that they face as challenge in their conventional lives (Eide, 2011). PwLD lack financial autonomy and allege to face discrimination on the surface of their financial dependency such as less opportunities, social rejection, and a range of unaccredited profession (Banks et.al, 2017). Their permanent unemployed status irrespective of age, impairment and basic requirements combined with the thought of being essentially dependent for mundane activities, make them feel useless or an unavoidable liability in other's life, apart from gaining low status (Dammeyer& Chapman, 2018; Philip, 2015; Pinilla-Roncancio, 2015). This is well felt through the words

…not respected within my own family as I am not earning anything and the family considers me as a burden to feed … considered waste of money...if I call family member or friend for help, they condemn for asking them things to do for me...

Few doing seasonal and irregular work also face the same situation as of unemployed. Besides, some benefitting out of government positive discrimination, were also seem placed in low level jobs, doing miscellaneous activities which

do not gain social respect neither in the working atmosphere nor in the personal community. Alternatively, a very fundamental financial sourcing has been done through old age pension (OAP) offered by government and through arrangements of special loans. But the former is insufficient to meet the needs of PwLD themselves and the latter even though given for starting entrepreneurial activities like petty shops, milk parlour, telecommunication centres, are not successful due to indifferent attitude of loan providers and general public (Department for International Development, 2000). An adding hindrance is getting a surety for the sanctioning of loan by a government officer, which never happens in case PwLD.

'…no one (not even relatives) is willing to sign surety.
As in case of not payment of the loan the money will be debited from the salary of the government employee who signed for surety'

Over, all these, family of PwLD relies on the pension or money received and earned by the individuals for their survival, making their condition worse and traumatized. As the head in a patriarchal family, income of the head is more prominent for the livelihood of other members, especially for their children. This is the marking point of unresolved dependencies continuing the poverty over generations (Whyte, 2020; Graham et.al, 2013).

"Children of poor PwD are not getting any guidance as such…children of PwD can avail free seats in educational institutions but are not provided…Once born poor has to die poor"

Adding to the difficulty of financial dependency of PwLD, it is to be noted that they face structural inequalities in terms of infrastructural disparities, systemic error, and prolonging discriminatory practices that fosters their process of becoming 'alienated themselves' from comprehensive society(Qiu et.al, 2022; Rohwerder, 2015; Maroto&Pettinicchio, 2014; Barnes, 2012). The structural inequalities as seen by respondents were as in not providing a seat in public transport or standing in a queue or not having disability friendly infrastructure, and commoners failing to recognize and treat with dignity. Again, it continues in getting a disability certificate which is either improperly assessed or received only through bribe as the case may be. This pose a problem as the facilities and benefits received through the certificate is misused or not properly disposed to deserving individuals.

"…use assessment of disability percentage to deny a seat for PwD through bribery…remove the wheels and sell illegally…need to enquire whether a person is able to drive or not…"

Above mentioned pose a threat to the PwLD, by not stopping with them, and leading to the cyclical process moving further to the next generation as their life-chances has been restricted through structural inequalities. Thereby, the dependents on PwLD suffer as well with limited life conditions of PwLD (Schiariti, 2020). Altogether, the combination of socio-economic determinants and structural inequalities enable one into chained causes of poverty, such as social restraints, social alienation, and false consciousness, unfaithful relationship, all of which produce social poverty (Schiariti, 2020; Goshal, 2018; Banks et.al,, 2017).

Theme – II: Social Poverty

Social poverty is commonly identified as lack of adequate, trustworthy, high-quality relationships to fulfil one's socio-emotional and socio-economicprerequisites. Social poverty among PwLD entails social alienation, social restrain and false consciousness of their social participation (Halpern-meekin, 2020; Palmer, 2011). Being physically restricted, in the first place makes the PwLD feel cut off from family, friends, and the wider society and thus contributes to a feeling of social alienation.To worsen the scenario, there are instances in which PwLD face social stigma caused by false consciousness that prevail in the cultural context such as

" .. it is bad omen to face a lame person while going out…, simply put we are called waste of money… in my community I am respected because of my government job…people are concerned only about their situation and not about our difficulties…"

making it even more challenging for PwLD to socialize and be socially accepted. This prompts a sense of shame and lessens the motivation of a PwLD to indulge in establishing, maintaining and strengthening quality relationships, leaving them socio-emotionally stranded or restricted. It can also be strongly stated that all of the focus group members had a general sensation of not being seen, heard, or appreciated in a way or other, or to put in a comprehensive way, a feeling of social non-acceptance, which was a result of their social isolation brought on by

their disability and financial dependency. When probed further, it is understood that the participants have faced social rejection, humiliation and discrimination during their social participation with general public and institutions that are established to aid the PwLD, to the extent that a participant stated,

"…. 99% of the people doesn't have humanity or any concern over PwLD and maybe only the remaining 1% does…"

This demonstrates the sort of distrust that a PwLD has acquired over another individual and society at large, which undermines the basis for interdependence and, consequently, reliable relationships. In this way, the respondents feel discomfort to have a healthy interaction with their communities

"I could not go out among commonpeople as I wouldn't look good… we are discriminated by family, friends and others based on assets / finance / job that we hold. I can handle these expectations because I am holding a secure job. But a person like this man (pointing towards more vulnerable man) what can he do?"

On the other hand, participants expressed a mixed response while discussing their relationship with their immediate family. Some had a supportive family (spouse) and some didn't and due to which their parents left with no option other than to take care of their son / daughter with disability throughout their life. Causation for social poverty also be understood in terms of social restraints along with consciousness in both persons with disability and persons without disability as well. The perception of disability and its impact turn up with self-attitude and others attitude that drives toward less moral support. In general, a common conception on PwLD is that they are lacking in the ability to engage them with skilled work, however, they are not able to do so. This general sense inhibits life chances of PwLD and the same become a restraint to one's productive life. Being physically restrained prone to be alienated from the mainstream society as mentioned previously, also leads to false consciousness among general public. This physical restriction not only gives employment limitation, rather created worse living condition, financial inadequacy, kicks out trustworthy and dependable social relationships(Dfid, n.d; Haegele& Hodge, 2016; Zhang, 2014).

"…I know carpentry work to certain extend and I was searching for a job, no one is ready to hire me because of my impairment… after 4 to 5 years, a man gave me an opportunity with less pay and that too very occasionally…"

The untold truth from respondents' perspective is that as a result of disability, social poverty can never have positive influence of life changing moment, rather it stresses far more complicated life to the respondents. A young man wants to attain a prestigious life, whereas, an elder one desires to cut off this poverty from assimilating to next generation. This is something to be concerned beyond their ability and inability.

"…unlike others who plan for their future (people without disability) and tastes when it happens, we are waiting for death and counting days…"

It is unfortunate that children of economically vulnerable people with disabilities are experiencing additional difficulties while trying to receive moral, monetary, or educational support from their parents. It is true that parents' ability to secure the future of their children can be impacted by financial constraints and a lack of educational options. However, it is important to remember that not all the parents with disabilities or in financially difficult situations are unable to provide support or guidance to their children. Many parents in similar circumstances find alternative ways to support and nurture their children's development, despite the challenges they face. It's essential to recognize the diversity of individual experiences and the resilience of families in overcoming obstacles.

"…Whatever it is, our life has gone due to disability, at least our children's life should be good or smooth in terms of financial, education and sustainable way of life. The only thing we need that, we have to ensure a secured life for our children..."

From the perspective of the respondent Persons with Disabilities who are now engaged in the government or in any other secured permanent position and who have earned an education can lead their children for future education, provide financial support, and financially protect their children in some way. Children of poor persons with impairments, on the other hand, receive no moral, financial, or literacy assistance from their parents.

"…similar to you people, there are many, specifically from MSW, studies on us and published articles but no improvement or change because of it. I doubt if it is not considered or is been left out conditionally..."

Fabrication of poverty on PwLDs is not mere monetary or economic element, but has strong bond with restraints in their life-chances. For instance, unemployment due to false consciousness, financial dependence as a result of poor

living condition, stigmatized practices over differently abled, social rejection, commoners making them feellow by pretending to abnormal, structural violence and so forth are the vulnerabilities causing disabled into prolonged poverty. Do these really create poverty over generations and make them to adapt as a way of life? all of the above are arbitrarily accountable to transgenerational poverty to PwLD(Varenne& McDermott, 2018; Philip, 2015; Hansen, 2014; Sonpal& Kumar, 2012; Lewis, 1996). Thinking from people without disabilities who are illiterate and poor, without securing financial or social security, also face obstacles to develop their family's living conditions. Additionally, this adversely affects future generations as well. Putting these things into disability's perspective, disability itself is yet another forbidding factor to their empowerment. Behind the scenes, commoners and researchers assumes that the persons with locomotor disability have mere mobility impairmentless than other disabilities such as visual impairment, hearing impairment, mentally retarded and on. Throughout, the study responses clearly manifest that culture of poverty among PwLDs occurs, however, this could be eradicated by effective role of welfare system. From the participants point of view, sufficient pension schemes, free education and provision from PWD, effective implementation of schemes such as increasing loan, economic empowerment programmes, and training for skilled works were expected as the beginning steps to eliminate this assimilating poverty over generations.

CONCLUSION

In order to break the cycle of poverty for people with locomotor disabilities (PwLD), it is crucial to address the systemic barriers they encounter and promote inclusive policies that provide equal access to social, economic, and health-related opportunities. The focus should be on lowering poverty, improving accessibility, creating inclusive employment practices, and supporting inclusive education. Additionally, it is essential to raise awareness, confront societal biases, and enable PwLD to actively participate in decision-making processes. These initiatives are essential to building an inclusive society that promotes the rights and welfare of every person, irrespective of disability or socioeconomic status. However, the present study was limited in understanding role of poverty and its consequences on PwLDs, further studies might be carried out on effective role of welfare system to eradicate the culture of poverty on the same.

Conflict of Interest statement

The authors state that they have no conflicts of interest.

Ethical Considerations

The study obtained an ethical clearance certificate. **Ref:**BUHEC/068/2023. Dated **02.05.2023.**

REFERENCES

1. Banks, L. M., Kuper, H., & Polack, S. (2017). Poverty and disability in low-and middle-income countries: A systematic review. *PloSone*, *12*(12). DOI: 10.1371/journal.pone.0189996.
2. Barnes, C. (2012). Re-thinking disability, work and welfare. *Sociology Compass*, 6(6), 472484.DOI: 10.1111/J.1751-9020.2012.00464.X.
3. Dammeyer, J., & Chapman, M. (2018). A national survey on violence and discrimination among people with disabilities.*BMCpublichealth*,18(1),1-9. DOI: http://doi.org/10.1186/s12889-018-5227-0.
4. DFID, D. (2009). department for international Development. *Trading for Peace–An agenda of Reform*.https://rb.gy/pjjpct.
5. Eide, A. H., Loeb, M. E., Nhiwatiwa, S., Munthali, A., Ngulube, T. J., & Van Rooy, G. (2011). Living conditions among people with disabilities in developing countries. *Disability and poverty: A global challenge*, 55-70.DOI:10.1332/policypress/9781847428851.003.0004.

6. Graham, L., Moodley, J., &Selipsky, L. (2013). The disability–poverty nexus and the case for a capabilities approach: evidence from Johannesburg, South Africa. *Disability & Society*, 28(3), 324-337. https://doi.org/10.1080/09687599.2012.710011.
7. Haegele, J. A., & Hodge, S. (2016). Disability discourse: Overview and critiques of the medicaland social models. *Quest*, *68*(2), 193-206. https://doi.org/10.1080/00336297.2016.1143849.
8. Hansen, H., Bourgois, P., & Drucker, E. (2014). Pathologizing poverty: new forms of diagnosis, disability, and structural stigma under welfare reform. *Social Science & Medicine*, 103, 76-83. DOI: 10.1016/j.socscimed.2013.06.033.
9. Lewis, O. (1996). The Culture of Poverty. *Scientific American*. A division of Nature America,Inc. 215 (4). DOI: 10.2307/24931078.
10. Lewis, O. (2017). The culture of poverty. *In Poor Jews* (pp. 9-25). Routledge.
11. Maroto, M., &Pettinicchio, D. (2014). Disability, structural inequality, and work: The influence of occupational segregation on earnings for people with different disabilities. *Research in Social Stratification and Mobility*, 38, 76-92. https://doi.org/10.1016/j.rssm.2014.08.002.
12. Mishra, K., Siddharth, V., Bharadwaj, P., Elhence, A., Jalan, D., Raghav, P., & Mahmood, S.E. (2019). The Prevalence Pattern of Locomotor Disability and its Impact on Mobility, Self-Care, and Interpersonal Skills in Rural Areas of Jodhpur District. Nigerian Medical Journal, 60 (3): 156-160. https://doi.org/10.4103%2Fnmj.NMJ_144_17
13. Palmer, M. (2011). Disability and poverty: A conceptual review. *Journal of Disability Policy Studies*, 21(4), 210-218.https://doi.org/10.1177/1044207310389333
14. People with Disability Australia. (2023). Social model of disability.https://pwd.org.au/resources/models-of-disability/.
15. Philip, N. (2015). Culture and poverty: a case study of a girl with special educational needs from a poor community in S outh I ndia. *Support for Learning*, 30(3), 205-222. https://doi.org/10.1111/1467-9604.12091.
16. Pinilla-Roncancio, M., Mactaggart, I., Kuper, H., Dionicio, C., Naber, J., Murthy, G. V. S., & Polack, S. (2020). Multidimensional poverty and disability: A case control study in India, Cameroon, and Guatemala. *SSM-population health*, 11, 100591. https://doi.org/10.1016/j.ssmph.2020.100591.
17. Qiu, N., Cheng, J., & Zhang, T. (2022). Spatial disparity and structural inequality in disability patterns across Tianjin municipality: A multiple deprivation perspective. *Habitat International*, 130, 102685. https://doi.org/10.1016/j.habitatint.2022.102685.
18. Rohwerder, B. (November, 2015). Disability inclusion: Topic guide GSDRC. *University ofBirmingham:Birmingham, UK*.https://gsdrc.org/wpcontent/uploads/2015/11/DisabilityInclusion.pdf.
19. Schiariti, V. (2020). The human rights of children with disabilities during health emergencies: the challenge of COVID-19. *Dev Med Child Neurol*, 62(6), 661. DOI:10.1111/dmcn.14526.
20. Sonpal, D., & Kumar, A. (2012). 'Whose Reality Counts?': Notes on Disability, Development and Participation. *Indian Anthropologist*, 71-90.https://rb.gy/bundyd.
21. Varenne, H., & McDermott, R. (2018). Disability as a cultural fact. In *Successful Failure* (pp. 131-156). Routledge. eBook ISBN9780429497056.
22. Waldschmidt, A. (2017). Disability Goes Cultural. In Culture-Theory-Disability (pp. 19-28).*transcript Verlag*.https://doi.org/10.1515/9783839425336-003.
23. Waldschmidt, Anne., Berressem, Hanjo., &Ingwersen, Moritz. (2017). *Culture - Theory – Disability: Encounters between Disability Studies and Cultural Studies*. Transcript Verlag. Vol. 10. https://rb.gy/7ii8jk.
24. Whyte, S. R. (2020). In the long run: Ugandans living with disability. *Current Anthropology*, 61(S21), S132-S140.https://www.journals.uchicago.edu/doi/full/10.1086/704925.

25. Zhang, L., Li, W., Liu, B., &Xie, W. (2014). Self-esteem as mediator and moderator of the relationship between stigma perception and social alienation of Chinese adults with disability. *Disability and health journal*, 7(1), 119-123.DOI: 10.1016/j.dhjo.2013.07.004

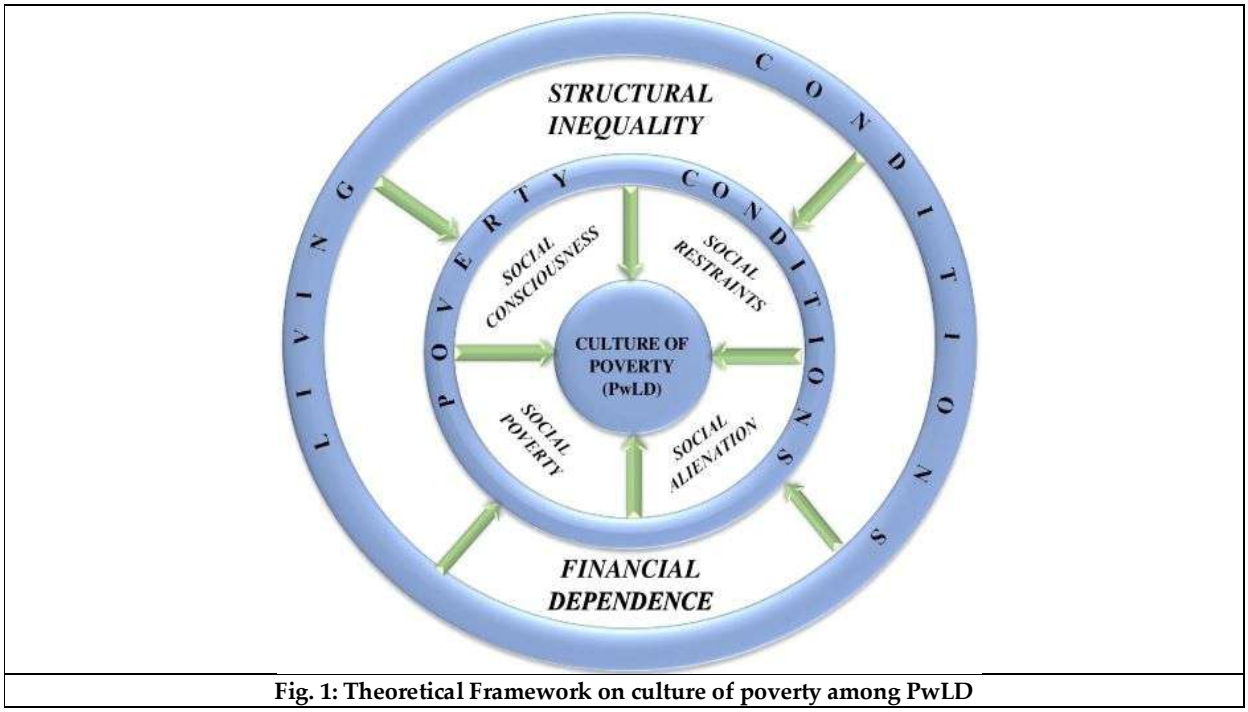

Fig. 1: Theoretical Framework on culture of poverty among PwLD

Indian Journal of Natural Sciences *www.tnsroindia.org.in ©IJONS*

Vol.15 / Issue 83 / Apr / 2024 *International Bimonthly (Print) – Open Access* *ISSN: 0976 – 0997*

RESEARCH ARTICLE

Split Domination Number of Some Generalized Graph's Line Graph

Shaikh Jamir[1,2] and Pranjali Kekre[1]

[1]Department of Mathematics, Medi Caps University, Indore, India
[2]R C Patel Institute of technology, Shirpur , Maharashtra, India

Received: 20 Dec 2023 Revised: 09 Jan 2024 Accepted: 11 Mar 2024

***Address for Correspondence**
Shaikh Jamir
Department of Mathematics,
Medi Caps University,
Indore, India
R C Patel Institute of technology,
Shirpur , Maharashtra, India
Email: jamir.shaikh786@gmail.com

ABSTRACT

The cardinality of the minimal dominating set of the graph, the removal of which causes graph to become disconnected, is commonly referred as the split dominance number. This number describes the minimal dominating set. We investigate the generalized form of Star, Bi Star, Tadpole, Wheel, Banana tree graph's line graph for Split dominance number in order to employ the acquired split dominance number corresponding to edges. This is done in order to take the advantage of split dominance number as per algorithms following in many real word situations where the splitting of network is necessary by removal of the edges.

Keywords: Dominating set, Domination number, Split domination number.

INTRODUCTION

Recent graph theory research in mathematics has focused on the investigation of dominance. The concept of dominance can lead to the development of a number of additional elements. The fundamental dominance problems NP-completeness and tight ties to other NP-completeness problems have increased the quantity of research on the topic. Chess was a difficult for dominance in the 1850s. In an effort to determine the bare minimum of queens necessary to ensure that each square on the chessboard either contains a queen or is under attack by one, C.F.de Jaenisch proposed the concept of dominance in 1862. In the discipline of graph theory, the study of dominance sets has advanced most quickly after 1960. In 1962, Ore and Berge introduced the concept of dominant sets in graphs [3]. In 1962, Ore conducted research on the ideas of dominance set and dominance number. Investigating the ideas of

dominance number and independence number is Cockayne and Hedetniemi [1]. They employed the notation to indicate a graph's dominance number. In 1977[6], Mitchell and Hedetniemi developed the idea of edge domination. Kulli and Janakiram introduced the split domination in graphs [2]. A specific value for split dominance number and many characteristics of the split dominating set have been discovered [7] by T. Chelvam and S. Chellathurai. When we consider the graph of the relationship between domination number and edge domination number, it becomes apparent that Raja Rajmani Iyar and V.R. Kulli defined split edge dominance number of graph [5]. In this study we discuss the split dominance number of line graph of some special graph and justify our results by illustrating various cases.

Elementary Definitions

Line Graph

Graph $G's$ Line graph $L(G)$ is a graph with its vertices as points, which are mapped by the edges of G. If two edges of G have a common vertex, then the two vertices of $L(G)$ that are mapped to those two edges of G are connected [4].

Dominating Set

A dominant set of G is $D \subseteq V$, where V is vertex set of G and each $v_i \in V$ has a proximity to at least one of the vertices of D. The dominance number [2] represents the least cardinality of the dominant set of G, represented by $\gamma(G)$.

Split Dominating Set

The graph's dominating set D is splits dominant if on removal of D the resultant graph $V \setminus D$ is disconnected. Split dominant number $\gamma_s(G)$ is the cardinality of the set with the fewest vertices [2] [7] [8].

Split Domination Number of Some Generalized Graph's Line Graph

Star Graph's Line Graph

A star graph S_n is in fact a complete bipartite graph $K_{(1,n)}$ i.e. it has one internal node and n leaves.

Theorem 3.1.1 The star graph's line graph split domination number is undefined.

Proof: Star graph's line graph i.e. $L(S_n)$ is K_n a complete graph and as $\gamma_s(K_n)$ is not known [2]-[7] [8], so the proof.

Illustration-1

As observed from Figure 1

$\gamma_s(s_n) = \gamma_s(K_{(1,n)}) = 1$, but $\gamma_s(L(S_n)) = \gamma_s(L(K_{(1,n)})) = \gamma_s(K_n)$ not exist.

Bi-Star Graph's Line Graph

Bi-star graphs $B_{(n,n)}$ are created when two copies of star graphs $K_{(1,n)}$ are linked at the root. The Bi-star graph's split domination number is 2.

Theorem 3.2.1 Let $B_{(r,s)}$ be Bi-star graph and $L(B_{(r,s)})$ is line graph of Bi-star graph $B_{(r,s)}$ then

a) $\gamma_s(L(B_{(r,s)})) = 1$

b) $\gamma_s(B_{(r,s)}) > \gamma_s(L(B_{(r,s)}))$

Proof:

a) If G is any Bi-star graph $B_{(r,s)}$, a line graph of bi-star network $L(B_{(r,s)})$ has two complete graphs fused at a vertex; this vertex dominates all other vertices of the line graph, and removal of this vertex disconnects it.
So, $\gamma_s(L(B_{(r,s)})) = 1$ as illustrated for $B_{(4,6)}$ in Figure 2.

b) As $\gamma_s B_{(r,s)} = 2$, we get $\gamma_s(B_{(r,s)}) > \gamma_s(L(B_{(r,s)}))$

Tadpole Graph's Line Graph

Tadpole Graph is represented by the symbol $T(m,n)$ and consists of a cycle graph $C_m (m \geq 3)$ connected to a path graph P_n. $L(T(m,n))$ is line graph of it.

Theorem 3.3.1 Let $T(m,n)$ is Tadpole graph $m \geq 3$ then $\gamma_s(L(T(m,n)))$ is given by

a) $\gamma_s(L(T(3,1))) = 2$

b) $\gamma_s(L(T(3,n))) = 1 + \left\lceil \frac{n-1}{3} \right\rceil, n > 1$

c) $\gamma_s(L(T(m,1))) = 1 + \left\lceil \frac{m-3}{3} \right\rceil, m > 3$

d) $\gamma_s(L(T(m,n))) = \begin{cases} 1 + \left\lceil \frac{m-2}{3} \right\rceil + \left\lceil \frac{n-2}{3} \right\rceil, m \neq 3k \\ 1 + \left\lceil \frac{m-3}{3} \right\rceil + \left\lceil \frac{n-1}{3} \right\rceil, m = 3k \end{cases}$ for $m \geq 4$ and $k \geq 2$

Proof:

a) In the line graph of $T(3,1)$ the set $V = \{1,2,3,4\}$ serves as vertex set and subset $D = \{2,3\}$ serves as the minimal dominant set. As $V \setminus D$ is disconnected graph so this D is split dominating set.
Consequently, $\gamma_s(L(T(3,1))) = 2$, as seen in Figure 3

b) The line graph of $T(3,n)$ is composed of a cycle C_3 that is connected to a path graph of length n by two edges. The split domination set D of $L(T(3,n))$ contains one vertex from C_3, corresponding to the bridge edge, and $\left\lceil \frac{n-1}{3} \right\rceil$ vertex from the connected path graph [4]. $V \setminus D$ is disconnected graph.

So, $\gamma_s(L(T(3,n))) = 1 + \left\lceil \frac{n-1}{3} \right\rceil, n > 1$.

c) The $L(T(m,1))$ is composed of two edges connecting cycle C_m to a vertex corresponding to the $T(m,1)$ bridge. The split domination set D of $L(T(m,1))$ consists of one vertex from C_m; that is connected to the vertex corresponding to the bridge edge and dominates the two neighboring vertices of cycle. The remaining $m-3$ vertices of the cycle are connected by path with split dominance number $\left\lceil \frac{m-3}{3} \right\rceil$. So these $\left\lceil \frac{m-3}{3} \right\rceil$ vertices are also in split domination set D as the induced set $V \setminus D$ is disconnected.

So, $\gamma_s(L(T(m,1))) = 1 + \left\lceil \frac{m-3}{3} \right\rceil, m > 3$.

d) For $m \geq 4$ and $n > 1$, the tadpole graph's line graph's $L(T(m,n))$ consists cycle C_m and path P_n connected by two edges.
To determine the split domination set, we observe that if m is a multiple of three, i.e. $m = 3k, k \geq 2$, then the split domination set consists of a vertex of a cycle C_m that dominates the path's first vertex and two adjacent vertices of

the cycle, including this vertex , there are $m-3$ cycle vertices interconnected by a path and dominated by $\left\lceil \frac{m-3}{3} \right\rceil$ vertices plus $n-1$ path vertices dominated by $\left\lceil \frac{n-1}{3} \right\rceil$ vertices.

In this case, $\gamma_s(L(T(m,n))) = 1 + \left\lceil \frac{m-3}{3} \right\rceil + \left\lceil \frac{n-1}{3} \right\rceil, m = 3k$.

If m is not a multiple of three, the split domination set of $L(T(m,n))$ consists of a vertex corresponding to the bridge edge, that is also the first vertex of the connected path, it dominates two vertices of cycle C_m, and an adjacent vertex of path P_n. As a consequence, in the cycle graph, there are $m-2$ vertices connected by a path and dominated by $\left\lceil \frac{m-2}{3} \right\rceil$ vertices and $n-2$ vertices of path dominated by $\left\lceil \frac{n-2}{3} \right\rceil$ vertices.

In this case $\gamma_s(L(T(m,n))) = 1 + \left\lceil \frac{m-2}{3} \right\rceil + \left\lceil \frac{n-2}{3} \right\rceil, m \neq 3k$.

Thus the case proof follows.

In all the above cases there exist two vertices in $V \setminus D$ not connected by a path. As given in illustration-3 Figure 4, $\gamma_s(L(T(4,4))) = 3$.

Illustration-3

Theorem 3.3.2 $\gamma_s(T(m,n)) \leq \gamma_s(L(T(m,n)))$

Proof: For $n = 1$,

$$\gamma_s(T(m,1)) = \gamma_s(C_m) = \left\lceil \frac{m}{3} \right\rceil$$

For $n > 1$,

$\gamma_s(T(m,n)) = \gamma_s(C_m) + \gamma_s(P_{n-1}) = \left\lceil \frac{m}{3} \right\rceil + \left\lceil \frac{n-1}{3} \right\rceil$ as one vertex of path P_n is dominated by vertex of C_m.

The theorem follows from comparing the above-mentioned results with the various circumstances of Theorem 3.3.1.

Wheel Graph's Line Graph

Any n-vertex Wheel graph has an embedded cycle graph C_{n-1} whose all vertices are connected to one particular vertex. Thus, for n>3, a Wheel Graph of n vertices is represented by W_n is generated by linking all the vertices of a cycle graph C_{n-1} to a particular vertex.

The line graph of Wheel graph $L(W_n)$ contains a complete graph K_{n-1}, with a cycle of $n-1$ vertices, where each vertex of the cycle is connected to two vertices of K_{n-1}.

Theorem 3.4.1 $\gamma_s(L(W_n)) = 4$ **for** $n<6$.

Proof: To find split dominating set of $L(W_n)$ for $n<6$, select two vertices, say v_i and v_j from the outer cycle of line graph of wheel graph, and two vertices in sequence from inner K_{n-1} such that the selected first vertex of K_{n-1} should be in a neighborhood of v_i and the last selected vertex of should be in a neighborhood of v_j. The

remaining vertices are under the dominance of v_i , v_j ,or specified vertices of K_{n-1} . On eliminating this dominated set, the graph becomes disconnected. It is a split dominating set with the fewest possible vertices.

Illustration-4

The line graph of W_4 has $V = \{1,2,3,4,5,6\}$ as vertices set and the subset $D = \{2,3,4,5\}$ is minimal split dominating set.

$\gamma_s(L(W_4)) = 4$. As shown in Figure 5.

The line graph of W_5 has $V = \{1,2,3,4,5,6,7,8\}$ as set of vertices and the subset $D = \{2,3,5,6\}$ is minimal split dominating set. $\gamma_s(L(W_5)) = 4$. As shown in Figure 6.

Theorem 3.4.2 $\gamma_s(L(W_n)) = n - 2$ **for** $n \geq 6$.

Proof: To find split dominating set of $L(W_n)$ for $n \geq 6$, select two vertices, say v_i and v_j , at a distance of three from the outer cycle of line graph of Wheel graph and $n-4$ vertices in sequence from inner graph K_{n-1} , such that the first selected vertex of K_{n-1} should be in a neighbourhood v_i and the last selected vertex of K_{n-1} should be in neighbourhood of v_j . The remaining vertices are in domination of v_i , v_j , or selected vertices of K_{n-1} . On removing this dominated set, we get disconnected graph. It's a split dominated set with minimum number of vertices.

$\gamma_s(L(W_n)) = 2 + n - 4 = n - 2$.

As specified in the following illustration for the line graph of W_7 , and for the line graph of W_{10} Figure 8.

Illustration-5

The line graph of W_7 has $V = \{1,2,...,12\}$ as set of vertices and the subset of vertex set $D = \{1,8,9,10,4\}$ is minimal split dominating set. $\gamma_s(L(W_7)) = 5$ as Shown in Figure 7.

The line graph of W_{10} has $V = \{1,2,...,18\}$ as set of vertices and the subset of vertex set $D = \{2,12,13,14,15,16,17,8\}$ is minimal split dominating set.

$\gamma_s(L(W_{10})) = 10 - 2 = 8$. As Shown in Figure 8.

Banana Tree's Line Graph

An $\beta_{(n,k)}$ -Banana tree, as defined by Chen et al.(1997), is a graph that is produced through linking one leaf of each of 'n' copies of a star graph called S_{k-1} as mentioned in section 3.1, to a single root vertex that is different from all of the stars [9].

Theorem 3.5.1 $\gamma_s(L(\beta_{(n,k)})) = n$ **, where n is number of copies of star graph and k is number of edges in star graph.**

Proof: Trivial as with the $\beta_{(n,k)}$'s line graph, we receive n copies of the complete graph connected to n vertices; corresponding to n branches of a single root vertex, via one vertex of each of the K_{n-1} . These connected vertices of K_{n-1} constitute the dominating set, which is actually a minimal split dominating set, therefore we have $\gamma(L(\beta_{(n,k)})) = \gamma_s(L(\beta_{(n,k)}))$, as seen in the illustration underneath.

Illustration-6

Line graph of Banana tree $\beta_{(2,4)}$ has $V = \{1,2,3,4,5,6,7,8\}$ as set of vertices and subset of vertex set $D = \{3,4\}$ is minimal split dominating set.

$\gamma_s(L(\beta_{(2,4)})) = 2$, as shown in Figure 9.

$\gamma_s(L(\beta_{(3,5)}) = 3$, as shown in Figure 10

Line Graph of $K_2 \times P_n$

Complete graph K_2 and path graph P_n are graphs with vertices set $V(K_2) = \{u_1, u_2\}$ and $V(P_n) = \{v_1, v_2, \cdots, v_n\}$ respectively.

The Cartesian product of K_2 and P_n denoted by $K_2 \times P_n$ is the graph with vertex set $V(K_2 \times P_n) = V(K_2) \times V(P_n) = \{(u_i, v_j) \mid u_i \epsilon V(K_2), v_j \epsilon V(P_n)\}$, edge set $E = \{e\}$ such that 'e' is an edge of $K_2 \times P_n$ if and only if $e = \langle (u_i, v_j), (u_k, v_l) \rangle$

Where either

1. $i = k$ and $v_j v_l \epsilon E(P_n)$
2. $j = l$ and $v_j v_l \epsilon E(K_2)$

Theorem 3.6.1.The split domination number of line graph of $K_2 \times P_n$ is n.

Proof:

Case n=3

In $L(K_2 \times P_3)$ we have two terminal vertices of degree 2 named as u and v, one fused vertex f_1 of degree 4, two vertex in the neighbourhood of u and f_1 named as $u_1 f_1$ and $u_2 f_1$, and two vertex in the neighbourhood of v and f_1 named as $v_1 f_1$ and $v_2 f_1$. In this case, $u_1 f_1$ and $v_1 f_1$ are adjacent, as are $u_2 f_1$ and $v_2 f_1$. These vertices are all of degree 3. Set $D = \{u, f_1, v\}$ is a split dominating set illustrated in Figure 11.

Case $n > 3$

We can see in the line graph of $K_2 \times P_n (n > 3)$ that it has a joint chain of $n-1$ cycles of length 4 and two terminal vertices u and v of degree 2. In this, two consecutive cycles are united by fusing the $n-2$ vertices referred to as $f_1, f_2, \ldots f_{n-2}$; these are intermediate vertices that are not in the neighbourhood of u or v and have degree 4. Two of the remaining vertices of first cycle are in the neighbourhood of u and the first fused vertex f_1 , similarly two vertices of last cycle are in the neighbourhood of v and the last fused vertex f_{n-2}, all these four vertices are of degree 3. The remaining vertices of the line graph are all of degree 4 because they are in the vicinity of two successive fused vertices and are also adjacent to the prior and subsequent vertex. Let D be the set of all fused vertices and terminals of the line graph of $K_2 \times P_n$ highlighted in blue, as illustrated in Figure 12's illustrative example for $K_2 \times P_5$ This set D is a dominant set because, as previously stated, all of the vertices of $V \setminus D$ are in the neighbourhood of either the terminal vertex or either of the fused vertex. There are two vertex in $V \setminus D$ such that any path between these two vertex has at least one vertex of D [2], so it is a split dominating set, and it also satisfies all of the conditions of a minimal split dominating set as stated in Theorem 4 in [2]. As a result, this D is a minimal split dominant set of 'n' vertices. Thus,

$$\gamma_s(K_2 \times P_n) = 2*(\text{terminal vertices}) + (n-2)*(\text{fused vertices}) = n.$$

For Figure 12, $D = \{u, f_1, f_2, f_3, v\}$ and so $\gamma_s(L(K_2 \times P_5)) = 5$.

Illustration-7

Figures 11 and 12 employ blue vertices to represent terminal and fused vertices, which comprise the domination set.

In general, $\gamma_s(L(K_2 \times P_n)) = n$.

CONCLUSIONS

The split domination number for the line graph of Bi-Star, Tadpole, Wheel graph, Banana tree, and Cartesian product of the graph is determined in a generalized manner. Since the graphs we used have many real-world uses in computer networks as well as network research, knowing the split dominance number of their line graph will aid in the search for the graph's most dominant edges.

REFERENCES

1. E.J. Cockayne and Stephen T. Hedetniemi., "Towards a theory of Domination in Graphs, "Networks, vol. 7 , pp. 247-261, 1977.
2. V. Kulli and B. Janakiram, "The split domination number of a graph", Graph Theory Notes of New York, Vol. XXXII, pp. 16-19, 1997.
3. O. Ore, Theory of graphs. American Mathematical Society Colloquium Publications 38,1962.
4. P. Pardalos and Ding-Zhu Du, Ronald L. Graham, Handbook of Combinatorial Optimization. Springer New York, 2013.
5. R. Iyar and V. Kulli, "The Split edge domination number of graph", Journal of Ultra Scientist, vol. 23, pp. 190-194, 2011.
6. S. Mitchell and S. Hedetniemi., "Edge domination in trees", Congr. Number, vol. 19, pp. 489–509,1977
7. T. Chelvam and S. Chellathurai., "A note on split domination number of a graph", Journal of Discrete Mathematical Sciences and Cryptography, vol. 12(2), pp.179-186, 2009.
8. T. Haynes, S. Hedetnimi and P. Slater, Fundamentals of Domination in Graphs. Marcel Dekker, Inc., New York,1998.
9. Weisstein, Eric W, Banana Tree from MathWorld- - A wolfram Web Resource

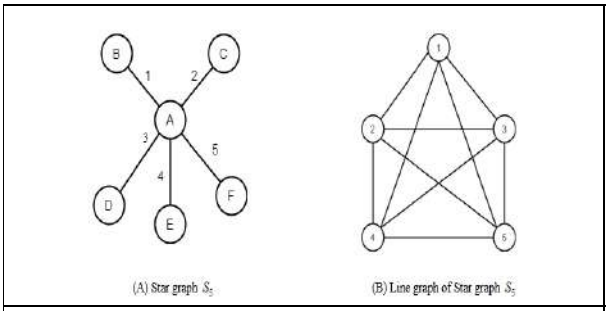

ure 1

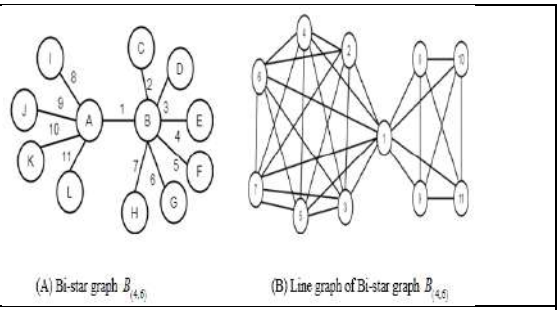

Figure 2

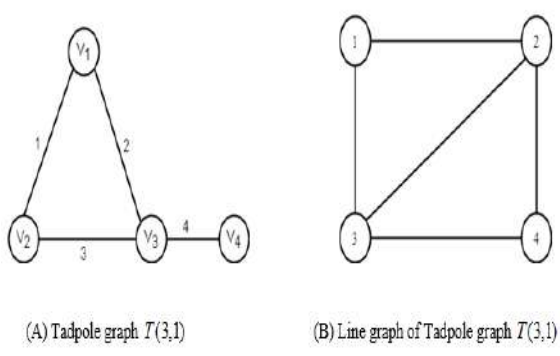

Figure 3

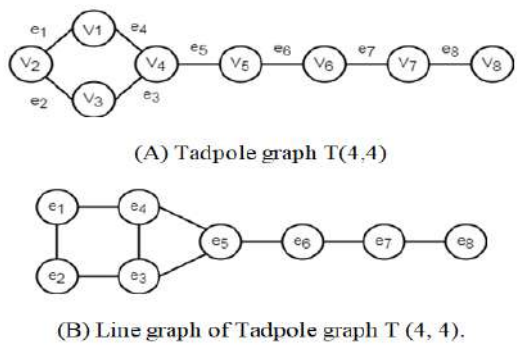

Figure 4

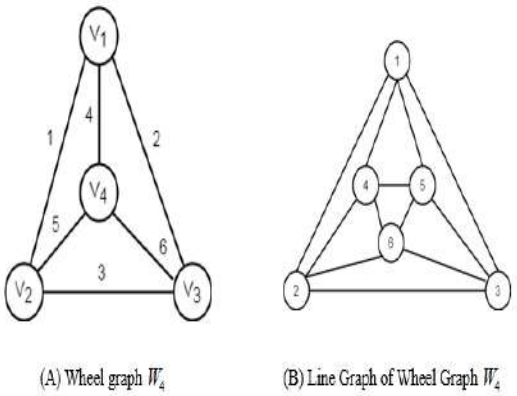

Figure 5

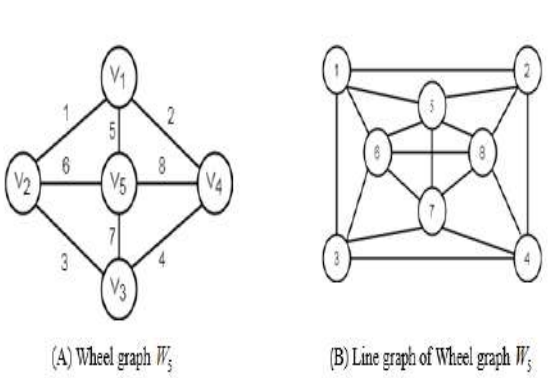

Figure 6

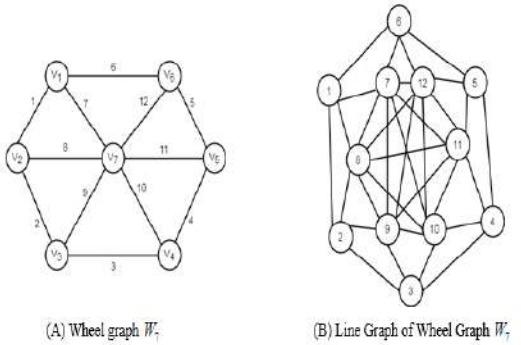

Figure 7

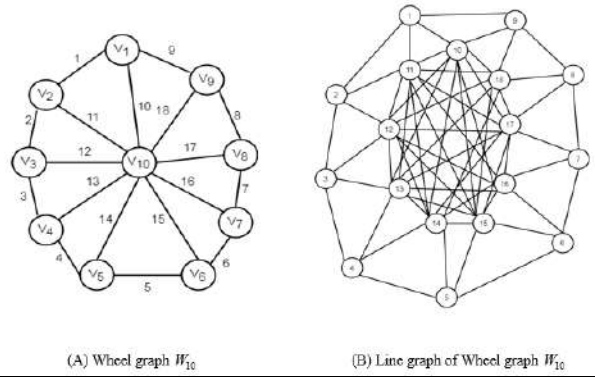

Figure 8

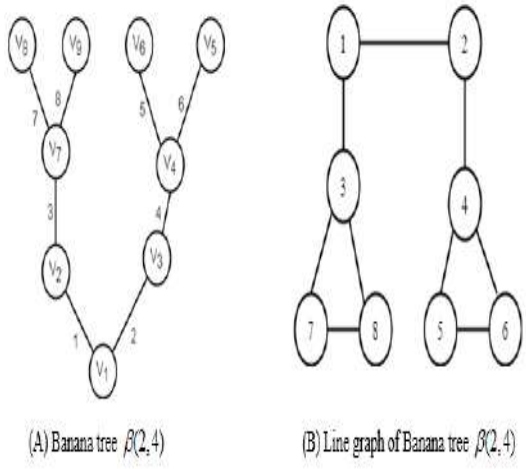

Figure 9

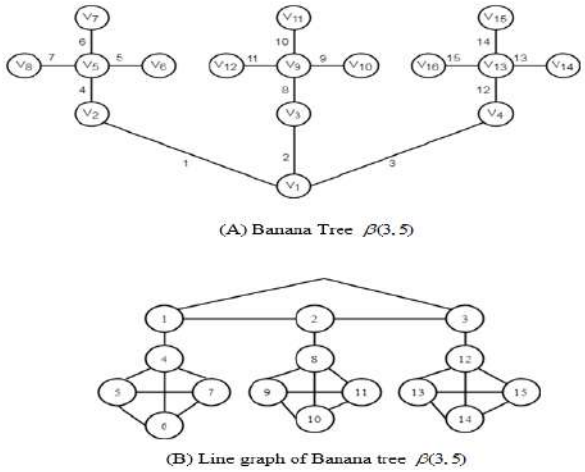

Figure 10

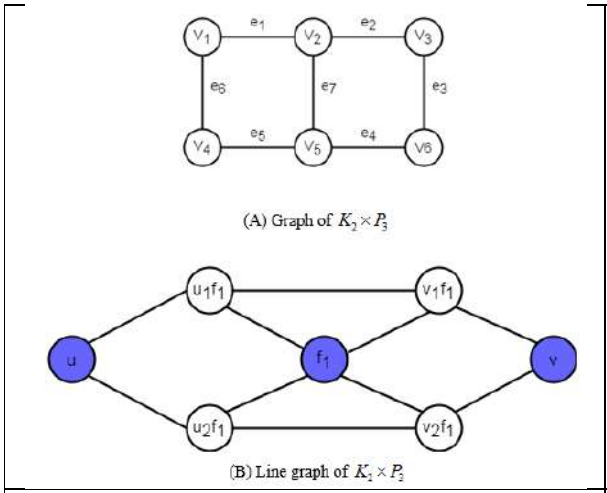

(A) Graph of $K_2 \times P_3$

(B) Line graph of $K_2 \times P_3$

Figure 11

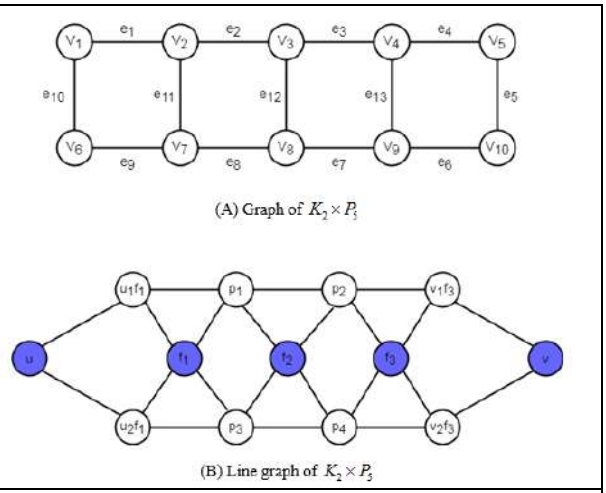

(A) Graph of $K_2 \times P_5$

(B) Line graph of $K_2 \times P_5$

Figure 12

Indian Journal of Natural Sciences *www.tnsroindia.org.in ©IJONS*

Vol.15 / Issue 83 / Apr / 2024 *International Bimonthly (Print) – Open Access* *ISSN: 0976 – 0997*

RESEARCH ARTICLE

Fixed Point Theorems for General Contractive Conditions of Integral Type in Complete*S*-Metric Spaces

Surabhi Bhatt[1]*, Rashmi Tiwari[2] and Kamal Wadhwa[3]

[1]Research Scholar, Department of Mathematics Govt. Narmada College, Narmadapuram, (Affiliated to Barkatuallah University), Bhopal, Madhya Pra
desh, India.
[2]Professor, Department of Mathematics, Govt. M.G.M. College, Itarsi (Affiliated to Barkatuallah University), Bhopal, Madhya Pradesh, India.
[3]Professor, Department of Mathematics Govt. Narmada College, Narmadapuram, (Affiliated to Barkatuallah University), Bhopal, Madhya Pradesh, India.

Received: 11 Nov 2023 Revised: 12 Jan 2024 Accepted: 11 Mar 2024

***Address for Correspondence**
Surabhi Bhatt
Research Scholar, Department of Mathematics,
Govt. Narmada College, Narmadapuram,
(Affiliated to Barkatuallah University), Bhopal,
Madhya Pradesh, India.

ABSTRACT

In this paper we establish fixed point theorems for a self mapping and common fixed point theorems for a pair of self mappings satisfying a general contractive condition of integral type in the setting of complete S-metric space. Our results generalize and essentially improve some fixed point theorems on a complete S-metric space. Specially our results generalize the results of [3] and [6].

Keywords: Integral type mappings, fixed point, complete S-metric space.

INTRODUCTION

The Banach contraction principle is indeed the most celebrated result in metric fixed point theory, which has several applications in many domains. Branciari[2], proved existence of fixed point for a mapping defined on a complete metric space satisfying a general contractive condition of integral type.

Theorem 1.1: [2] Let (X, d) be a complete metric space, $h \in (0,1)$, $f: X \to X$ be a mapping such that, for each $x, y \in X$,
$\int_0^{d(fx,fy)} \varphi(t)dt \leq h \int_0^{d(x,y)} \varphi(t)dt$,

Where $\varphi: R^+ \to R^+$is a Lebesgue integrable function which is summable on each compact subset of R^+, non negative, and such that, for each $\varepsilon > 0$,

$$\int_0^{\varepsilon} \varphi(t)dt > 0.$$

Then$f$ has a unique fixed point $z \in X$, such that for each$x \in X$, $\lim_{n\to\infty} f^n x = z$.

After the study of Branciari[2], a lot of research has been carried out on generalizing contractive conditions of integral type for various contractive conditions on various metric spaces.(see [1,3,5,8]).For instance in [3], authors generalized some mixed type of contractive conditions to the mapping and a pair of mappings satisfying a general contractive condition of integral type.

Very recently, concept of S-metric spaces has been introduced in [11] as a generalization of metric spaces, which has been defined as follows:

Definition 1.2: [11] Let X be a non empty set. An S-metric on X is a function S: $X^3 \to$ [0,∞) that satisfies the following conditions, for each $x, y, z, a \in X$,

1) $S(x, y, z) \geq 0$
2) $S(x, y, z) = 0$ if and only if$x = y = z$
3) $S(x, y, z) \leq S(x, x, a) + S(y, y, a) + S(z, z, a)$.

The pair (X, S) is called an S-metric space.

Example 1.3: [11] Some examples of S-metric spaces are

1. Let $X = R^n$and $\|.\|$a norm on X, then $S(x, y, z) = \|y + z - 2x\| + \|y - z\|$is an S-metric on X.
2. Let $X = R^n$and $\|.\|$ a norm on X, then $S(x, y, z) = \|x - z\| + \|y - z\|$ is an S-metric on X.

Definition 1.4: [11] Let (X, S)be an S-metric space then, a map$f$:$X \to X$is said to be a contraction if there exists a constant $0 \leq \lambda < 1$ such that $S(fx, fx, fy) \leq \lambda S(x, x, y)$, for all $x, y \in X$.

Theorem 1.5: [11] Let (X, S)be a complete S-metric space and f: $X \to X$ be a contraction. Then f has a unique fixed point $u \in X$. Furthermore, for any $x \in X$ we have $\lim_{n\to\infty} f^n(x) = u$ with
$S(f^n x, f^n x, u) \leq 2\frac{\lambda^n}{1-\lambda}(x, x, fx)$.

Many fixed point theorems satisfying different contractive conditions have been proved in the context of S-metric space (see [4],[9-13]).Recently, Ozgur and Tas [6] studied new contractive conditions of integral type on S-metric spaces and proved fixed point theorems for contractive conditions of integral type.

Theorem 1.6:[6] Let (X, S) be a complete$S-$metric space, $h \in (0,1)$and function $T: X \to X$ be a self mapping such that, for each$x, y \in X$,

$$\int_0^{S(Tu,Tu,Tv)} \varphi(t)dt \leq h \int_0^{S(u,u,v)} \varphi(t)dt,$$

where $\varphi: R^+ \to R^+$is a Lebesgue integrable function which is summable on each compact subset of R^+, non negative, and such that, for each $\varepsilon > 0$,

$$\int_0^{\varepsilon} \varphi(t)dt > 0.$$

Then T has a unique fixed point.

Motivated by Ozgur and Tas [6] and some others, we prove some fixed point theorems for general contractive conditions of integral type in the context of S-metric spaces. Also our results extend results of [3] to S- metric spaces. The results presented in this paper generalize and extend several fixed point results in the existing literature.

Fixed Point Results Using Contractive Conditions of Integral Type

At first we recall some basic results about S-metric space. The following lemma and definitions play important role in the paper.

Lemma 2.1 [9] : Let (X,S) be an $S-$metric space. Then we have, $S(x,x,y)=S(y,y,x)$

Definition 2.2 [9]: Let (X,S)be an $S-$metric space and $A\subset X$. Then
1. A sequence $\{x_n\}$ in X converges to x if $S(x_n,x_n,x)\to 0$ as $n\to\infty$, that is for every $\varepsilon>0$ there exists $n_0\in N$ such that for $n\geq n_0, S(x_n,x_n,x)<\varepsilon$. We denote this by $\lim_{n\to\infty}x_n=x$ and we say that x is the limit of $\{x_n\}$ in X.
2. A sequence $\{x_n\}$ in X is said to be cauchy sequence if for each $\varepsilon>0$, there exists $n_0\in N$ such that$S(x_n,x_n,x_m)<\varepsilon$ for each $n,m\geq n_0$.
3. The S-metric space (X,S) is said to be complete if every Cauchy sequence is convergent.

MAIN RESULT

In this section we shall obtain new fixed point theorems under a general contractive condition of integral type on complete S-metric space.

Theorem 2.3 : Let f be a self map of a complete S-metric space (X,S) satisfying the following condition:

$$\int_0^{S(fx,fx,fy)}\varphi(t)dt\leq\alpha\int_0^{S(x,x,fx)+S(y,y,fy)}\varphi(t)dt+\beta\int_0^{S(x,x,y)}\varphi(t)dt$$
$$\gamma\int_0^{\max\{S(x,x,fy),S(y,y,fx)\}}\varphi(t)dt+\delta\int_0^{\frac{S(x,x,fy)+S(y,y,fx)+S(x,x,fx)}{1+S(x,x,fy)S(y,y,fx)S(x,x,fx)}}\varphi(t)dt, \quad (1)$$

for each $x,y\in X$ with nonnegative reals $\alpha,\beta,\gamma,\delta$ such that $2\alpha+\beta+3\gamma+4\delta<1$. where $\varphi:R^+\to R^+$ is a Lebesgue integrable map which is summable on each compact subset of R^+, nonnegative and such that for each $\varepsilon>0$

$\int_0^{\varepsilon}\varphi(t)dt>0.$ (2)

Then f has a unique fixed point such that for each $x\epsilon X$, $\lim_{n\to\infty}f^nx=z$.

Proof: Let $x_0\in X$, and let us define $x_n=fx_{n-1}$. For each integer $n\geq 1$ from (1) we have

$$\int_0^{S(x_n,x_n,x_{n+1})}\varphi(t)dt=\int_0^{S(fx_{n-1},fx_{n-1},fx_n)}\varphi(t)dt$$
$$\leq\alpha\int_0^{S(x_{n-1},x_{n-1},x_n)+S(x_n,x_n,x_{n+1})}\varphi(t)dt+\beta\int_0^{S(x_{n-1},x_{n-1},x_n)}\varphi(t)dt$$
$$\gamma\int_0^{\max\{S(x_{n-1},x_{n-1},x_n),S(x_n,x_n,x_n)\}}\varphi(t)dt$$
$$+\delta\int_0^{\frac{S(x_{n-1},x_{n-1},x_{n+1})+S(x_n,x_n,x_n)+S(x_{n-1},x_{n-1},x_n)}{1+S(x_{n-1},x_{n-1},x_{n+1})S(x_n,x_n,x_n)S(x_{n-1},x_{n-1},x_n)}}\varphi(t)dt$$
$$\leq(\alpha+\beta+2\gamma+3\delta)\int_0^{S(x_{n-1},x_{n-1},x_n)}\varphi(t)dt$$
$$+(\alpha+\gamma+\delta)\int_0^{S(x_n,x_n,x_{n+1})}\varphi(t)dt.$$

which implies,

$$\int_0^{S(x_n,x_n,x_{n+1})}\varphi(t)dt\leq\frac{(\alpha+\beta+2\gamma+3\delta)}{1-\alpha-\gamma-\delta}\int_0^{S(x_{n-1},x_{n-1},x_n)}\varphi(t)dt$$

Or,

$\int_0^{S(x_n,x_n,x_{n+1})}\varphi(t)dt\leq k\int_0^{S(x_{n-1},x_{n-1},x_n)}\varphi(t)dt,$ (3)

where$k=\frac{(\alpha+\beta+2\gamma+3\delta)}{1-\alpha-\gamma-\delta}<1$ (As $2\alpha+\beta+3\gamma+4\delta<1$)

Thus, by routine calculation, we get,

$$\int_0^{S(x_n,x_n,x_{n+1})}\varphi(t)dt\leq k^n\int_0^{S(x_0,x_0,x_1)}\varphi(t)dt.$$

Taking limit as $n\to\infty$ we obtain,

$lim_{n\to\infty}\int_0^{S(x_n,x_n,x_{n+1})}\varphi(t)dt=0.$

which gives by using (2) that,
$lim_{n\to\infty} S(x_n, x_n, x_{n+1}) = 0.$
Now, we will show that $\{x_n\}$is a Cauchy sequence. Suppose that it is not. Then there exists an $\varepsilon > 0$ and subsequences $\{m(p)\}$ and $\{n(p)\}$ such that $m(p) < n(p) < m(p+1)$ with
$S(x_{m(p)}, x_{m(p)}, x_{n(p)}) \geq \varepsilon$, $S(x_{m(p)}, x_{m(p)}, x_{n(p)-1}) < \varepsilon$ (4)
Also,
$S(x_{m(p)-1}, x_{m(p)-1}, x_{n(p)-1}) \leq 2S(x_{m(p)-1}, x_{m(p)-1}, x_{m(p)}) + S(x_{m(p)}, x_{m(p)}, x_{n(p)-1})$
$<2\,S(x_{m(p)-1}, x_{m(p)-1}, x_{n(p)-1}) + \varepsilon.$
Hence,
$\lim_{p\to\infty} \int_0^{S(x_{m(p)-1}, x_{m(p)-1}, x_{n(p)-1})} \varphi(t)dt \leq \int_0^{\varepsilon} \varphi(t)dt.$ (5)
Now using (3), (4) and (5) we get.
$$\int_0^{\varepsilon} \varphi(t)dt \leq \int_0^{S(x_{m(p)}, x_{m(p)}, x_{n(p)})} \varphi(t)dt$$
$$\leq k \int_0^{S(x_{m(p)-1}, x_{m(p)-1}, x_{n(p)}-1)} \varphi(t)dt$$
$$\leq k \int_0^{\varepsilon} \varphi(t)dt.$$
Which is a contradiction, since $k \in (0,1)$. Therefore $\{x_n\}$ is a cauchy sequence and hence convergent. Let us call the limit z.
Again using (1) we get,
$$\int_0^{S(fz, fz, x_{n+1})} \varphi(t)dt = \int_0^{S(fz, fz, fx_n)} \varphi(t)dt$$
$$\leq \alpha \int_0^{S(z,z,fz)+S(x_n,x_n,x_{n+1})} \varphi(t)dt + \beta \int_0^{S(z,z,x_n)} \varphi(t)dt$$
$$\gamma \int_0^{\max\{S(z,z,x_{n+1}), S(x_n,x_n,fz)\}} \varphi(t)dt + \delta \int_0^{\frac{S(z,z,x_{n+1})+S(x_n,x_n,fz)+S(z,z,fz)}{1+S(z,z,x_{n+1})S(x_n,x_n,fz)S(z,z,fz)}} \varphi(t)dt.$$
Taking limit as $n \to \infty$ we get,
$$\int_0^{S(fz, fz, z)} \varphi(t)dt \leq (\alpha + \gamma + 2\delta) \int_0^{S(z,z,fz)} \varphi(t)dt.$$
Which gives,
$\int_0^{S(fz, fz, z)} \varphi(t)dt = 0.$ (As $2\alpha + \beta + 3\gamma + 4\delta < 1$)
Which implies, $S(fz, fz, z) = 0.$
Which gives, $fz = z$.Thus, z is a fixed point of f.
Now, let us suppose that $w(\neq z)$ is another fixed point of f. Then from (1) we have,
$$\int_0^{S(z,z,w)} \varphi(t)dt = \int_0^{S(fz, fz, fw)} \varphi(t)dt$$
$$\leq \alpha \int_0^{S(z,z,fz)+S(w,w,fw)} \varphi(t)dt + \beta \int_0^{S(z,z,w)} \varphi(t)dt$$
$$\gamma \int_0^{\max\{S(z,z,fz), S(w,w,fz)\}} \varphi(t)dt + \delta \int_0^{\frac{S(z,z,w)+S(w,w,z)+S(z,z,fz)}{1+S(z,z,w)S(w,w,z)S(z,z,fz)}} \varphi(t)dt$$
$$\leq (\beta + \gamma + 2\delta) \int_0^{S(z,z,w)} \varphi(t)dt.$$
Since $\beta + \gamma + 2\delta < 1$, this implies that $\int_0^{S(z,z,w)} \varphi(t)dt = 0.$
Which from (2) implies that $S(z, z, w) = 0$ or $z = w$. Thus f has unique fixed point.

Corollary 2.4: Let f be a self map of a complete S-metric space (X, S) satisfying the following condition:
$$\int_0^{S(fx, fx, fy)} \varphi(t)dt \leq \alpha \int_0^{S(x,x,fx)+S(y,y,fy)} \varphi(t)dt + \beta \int_0^{S(x,x,y)} \varphi(t)dt + \gamma \int_0^{\max\{S(x,x,fy), S(y,y,fx)\}} \varphi(t)dt$$

for each $x, y \in X$ with non negative reals α, β, γ such that $2\alpha + \beta + 3\gamma < 1$. where $\varphi: R^+ \to R^+$ is a Lebesgue integrable map which is summable on each compact subset of R^+, nonnegative and such that for each $\varepsilon > 0$, $\int_0^{\varepsilon} \varphi(t)dt > 0$.
Then f has a unique fixed point such that for each $x \in X, \lim_{n\to\infty} f^n x = z$.

Proof: On putting δ=0 in (1) the result follows.

Remark 2.5 :
1. Corollary 2.4 is a special case of theorem with δ=0.
2. Corollary 2.4 extends theorem 2.1[3]to S-metric space.
3. On setting $\varphi(t) = 1$ over R^+, the contractive condition of integral type transforms into a general contractive condition not involving integrals.
4. Theorem 2.3 is a generalization of Theorem 2.4 in [6]on a complete S-metric space. Indeed, if we take $\beta = h$ and $\alpha = \gamma = \delta = 0$ in Theorem 2.3, then we get Theorem 1.6.

Theorem 2.6: Let f be a self map of a complete S-metric space (X, S) satisfying the following condition:

$$\int_0^{S(fx,fxfy)} \varphi(t)dt \le \alpha \int_0^{S(x,x,fx)+S(y,y,fy)} \varphi(t)dt + \beta \int_0^{S(x,x,fy)+S(y,y,fy)} \varphi(t)dt$$
$$\gamma \int_0^{\max\{S(x,x,gy),S(y,y,fx)\}} \varphi(t)dt + \delta \int_0^{S(x,x,y)} \varphi(t)dt,$$

for each $x, y \in X$ with non negative reals $\alpha, \beta, \gamma, \delta$ such that $2\alpha + 3\beta + 3\gamma + \delta < 1$. Where $\varphi: R^+ \to R^+$ is a Lebesgue integrable map which is summable on each compact subset of R^+, nonnegative and such that for each $\varepsilon > 0$, $\int_0^{\varepsilon} \varphi(t)dt > 0$.
Then f has a unique fixed point such that for each $x \in X, \lim_{n\to\infty} f^n x = z$.
Proof: The proof is very similar to the proof of theorem so we omitted it.

Theorem 2.7: Let f and g be two self maps on a complete complete S-metric space (X, S) satisfying the following condition

$$\int_0^{S(fx,fx,gy)} \varphi(t)dt \le \alpha \int_0^{S(x,x,fx)+S(y,y,gy)} \varphi(t)dt + \beta \int_0^{S(x,x,y)} \varphi(t)dt$$
$$+\gamma \int_0^{\max\{S(x,x,gy),S(y,y,fx)\}} \varphi(t)dt + \delta \int_0^{\frac{S(x,x,gy)+S(y,y,fx)+S(x,x,fx)}{1+S(x,x,gy)S(y,y,fx)S(x,x,fx)}} \varphi(t)dt, \quad (6)$$

for each $x, y \in X$ with non negative reals $\alpha, \beta, \gamma, \delta$ such that $2\alpha + \beta + 3\gamma + 4\delta < 1$. Where $\varphi: R^+ \to R^+$ is a Lebesgue integrable map which is summable on each compact subset of R^+, nonnegative and such that for each $\varepsilon > 0$,

$$\int_0^{\varepsilon} \varphi(t)dt > 0 \quad (7)$$

Then f has a unique fixed point such that for each $x \in X, \lim_{n\to\infty} f^n x = z$.
Proof: Let $x_0 \in X$, and let us define $x_{2n+1} = fx_{2n}$ and $x_{2n+2} = gx_{2n+1}$. For each integer $n \ge 1$ from (1) we have

$$\int_0^{S(x_{2n+1},x_{2n+1},x_{2n+2})} \varphi(t)dt = \int_0^{S(fx_{2n},fx_{2n},gx_{2n+1})} \varphi(t)dt$$
$$\le \alpha \int_0^{S(x_{2n},x_{2n},x_{2n+1})+S(x_{2n+1},x_{2n+1},x_{2n+2})} \varphi(t)dt$$
$$+ \beta \int_0^{S(x_{2n},x_{2n},x_{2n+1})} \varphi(t)dt$$
$$\gamma \int_0^{\max\{S(x_{2n},x_{2n},x_{2n+2}),S(x_{2n+1},x_{2n+1},x_{2n+1})\}} \varphi(t)dt$$
$$+ \delta \int_0^{\frac{S(x_{2n},x_{2n},x_{2n+2})+S(x_{2n+1},x_{2n+1},x_{2n+1})+S(x_{2n},x_{2n},x_{2n+1})}{1+S(x_{n-1},x_{n-1},x_{n+1})S(x_{2n+1},x_{2n+1},x_{2n+1})S(x_{2n},x_{2n},x_{2n+1})}} \varphi(t)dt$$
$$\le (\alpha + \beta + 2\gamma + 3\delta) \int_0^{S(x_{2n},x_{2n},x_{2n+1})} \varphi(t)dt$$
$$+(\alpha + \gamma + \delta) \int_0^{S(x_{2n+1},x_{2n+1},x_{2n+2})} \varphi(t)dt.$$

Which implies,

$$\int_0^{S(x_{2n+1},x_{2n+1},x_{2n+2})} \varphi(t)dt \le \frac{(\alpha+\beta+2\gamma+3\delta)}{1-\alpha-\gamma-\delta}\int_0^{S(x_{2n},x_{2n},x_{2n+1})} \varphi(t)dt$$

$$\int_0^{S(x_{2n+1},x_{2n+1},x_{2n+2})} \varphi(t)dt \le k\int_0^{S(x_{2n},x_{2n},x_{2n+1})} \varphi(t)dt,$$

where $k = \frac{(\alpha+\beta+2\gamma+3\delta)}{1-\alpha-\gamma-\delta} < 1$. (As $2\alpha+\beta+3\gamma+4\delta < 1$)

Which in general, gives for all $n = 1,2,\ldots$

$\int_0^{S(x_n,x_n,x_{n+1})} \varphi(t)dt \le k\int_0^{S(x_{n-1},x_{n-1},x_n)} \varphi(t)dt.$ (8)

Thus, by routine calculation, we get,

$$\int_0^{S(x_n,x_n,x_{n+1})} \varphi(t)dt \le k^n \int_0^{S(x_0,x_0,x_1)} \varphi(t)dt$$

Taking limit as $n \to \infty$ we obtain,

$$\lim_{n\to\infty} \int_0^{S(x_n,x_n,x_{n+1})} \varphi(t)dt = 0.$$

Which gives by using (7) that

$\lim_{n\to\infty} S(x_n, x_n, x_{n+1}) = 0.$

Now, we will show that $\{x_n\}$is a Cauchy sequence. Suppose that it is not. Then there exists an $\varepsilon > 0$ and subsequences $\{2m(p)\}$ and $\{2n(p)\}$ such that $p < 2m(p) < 2n(p)$ with

$S(x_{2m(p)}, x_{2m(p)}, x_{2n(p)}) \ge \varepsilon$ and $S(x_{2m(p)}, x_{2m(p)}, x_{2n(p)-2}) < \varepsilon.$ (9)

$S(x_{2m(p)}, x_{2m(p)}, x_{2n(p)}) \le 2S(x_{2m(p)}, x_{2m(p)}, x_{2n(p)-2}) + 2S(x_{2n(p)-2}, x_{2n(p)-2}, x_{2n(p)-1})$

$+ S(x_{2n(p)-1}, x_{2n(p)-1}, x_{2n(p)})$

$< 2\varepsilon + 2S(x_{2n(p)-2}, x_{2n(p)-2}, x_{2n(p)-1})$

$+ S(x_{2n(p)-1}, x_{2n(p)-1}, x_{2n(p)}).$

Thus, $\lim_{p\to\infty} \int_0^{S(x_{2m(p)},x_{2m(p)},x_{2n(p)})} \varphi(t)dt = \int_0^{\varepsilon} \varphi(t)dt.$

Hence,

$$\int_0^{S(x_{2m(p)},x_{2m(p)},x_{2n(p)})} \varphi(t)dt \le k\int_0^{S(x_{2m(p)-1},x_{2m(p)-1},x_{2n(p)-1})} \varphi(t)dt$$

$$\le k[\int_0^{2S(x_{2m(p)-1},\, x_{2m(p)-1},\, x_{2m(p)})} \varphi(t)dt + \int_0^{2S(x_{2m(p)},\, x_{2m(p)},\, x_{2n(p)})} \varphi(t)dt$$

$$+ \int_0^{2S(x_{2n(p)-1},\, x_{2n(p)-1},\, x_{2n(p)})} \varphi(t)dt].$$

Taking limit as $p \to \infty$, we get,

$\int_0^{\varepsilon} \varphi(t)dt \le k\int_0^{\varepsilon} \varphi(t)dt.$

Which is a contradiction, as $k < 1$.

Therefore, $\{x_n\}$ is a Cauchy sequence, hence convergent. Let us call the limit z.

Now, we have from (6),

$$\int_0^{S(fz,fz,x_{2n+2})} \varphi(t)dt = \int_0^{S(fz,fz,gx_{2n+1})} \varphi(t)dt.$$

$$\le \alpha\int_0^{[S(z,z,fz)+S(x_{2n+1},x_{2n+1},x_{2n+2})]} \varphi(t)dt + \beta\int_0^{S(z,z,x_{2n+1})} \varphi(t)dt$$

$$\gamma\int_0^{\max\{S(z,z,x_{2n+2}),S(x_{2n+1},x_{2n+1},fz)\}} \varphi(t)dt$$

$$+\delta\int_0^{\frac{S(z,z,x_{2n+2})+S(x_{2n+1},x_{2n+1},fz)+S(z,z,fz)}{1+S(z,z,x_{2n+2})S(x_{2n+1},x_{2n+1},fz)S(z,z,fz)}} \varphi(t)dt.$$

Taking limit as $n \to \infty$, we get,

$$\int_0^{S(fz,fz,z)} \varphi(t)dt \le (\alpha+\gamma+2\delta)\int_0^{S(z,z,fz)} \varphi(t)dt.$$

Which gives,

$\int_0^{S(z,z,fz)} \varphi(t)dt = 0.$ (As $2\alpha+\beta+3\gamma+4\delta < 1$)

Which gives $S(z,z,fz)=0$ or $fz=z$.
In the similar manner we can show that $gz=z$.Thus, z is a common fixed point of f and g. Now we shall prove that z is a unique common fixed point of f and g. Suppose that it is not. And let $w(\neq z)$ be another common fixed point of f and g.
Then,

$$\int_0^{S(z,z,w)}\varphi(t)dt=\int_0^{S(fz,fz,gw)}\varphi(t)dt$$

$$\int_0^{S(z,z,w)}\varphi(t)dt\le\alpha\int_0^{S(z,z,fz)+S(w,w,gw)}\varphi(t)dt+\beta\int_0^{S(z,z,w)}\varphi(t)dt$$
$$+\gamma\int_0^{\max\{S(z,z,gw),S(w,w,fz)\}}\varphi(t)dt+\delta\int_0^{\frac{S(z,z,gw)+S(w,w,fz)+S(z,z,fz)}{1+S(z,z,gw)S(w,w,fz)S(z,z,fz)}}\varphi(t)dt$$
$$\le(\beta+\gamma+2\delta)\int_0^{S(z,z,w)}\varphi(t)dt.$$

This implies, $\int_0^{S(z,z,w)}\varphi(t)dt=0$.(as $\beta+\gamma+2\delta<1$)
Which implies $S(z,z,w)=0$.
Which gives $w=z$.

Corollary 2.8: Let f and g be two self maps on a complete complete S-metric space (X,S) satisfying the following condition:

$$\int_0^{S(fx,fx,gy)}\varphi(t)dt\le\alpha\int_0^{S(x,x,fx)+S(y,y,gy)}\varphi(t)dt+\beta\int_0^{S(x,x,y)}\varphi(t)dt$$
$$+\gamma\int_0^{\max\{S(x,x,gy),S(y,y,fx)\}}\varphi(t)dt$$

for each $x,y\,\epsilon\,X$ with non negative reals α,β,γ such that $2\alpha+\beta+3\gamma<1$. Where $\varphi:R^+\to R^+$ is a Lebesgue integrable map which is summable on each compact subset of R^+, nonnegative and such that for each $\varepsilon>0$,

$$\int_0^{\varepsilon}\varphi(t)dt>0.$$

Then f has a unique fixed point such that for each $x\epsilon X$, $\lim_{n\to\infty}f^nx=z$.
Proof : On putting δ=0 in (6) the result follows.

Remark 2.9:
1.Corollary 2.8 is a special case of theorem 2.7 with δ=0.
2.On setting $\varphi(t)=1$ over R^+, the contractive condition of integral type transforms into a general contractive condition not involving integrals.

Theorem 2.10: Let f and g be two self maps on a complete complete S-metric space (X,S) satisfying the following condition:

$$\int_0^{S(fx,fx,gy)}\varphi(t)dt\le\alpha\int_0^{S(x,x,fx)+S(y,y,gy)}\varphi(t)dt+\beta\int_0^{S(x,x,gy)+S(y,y,fx)}\varphi(t)dt$$
$$+\gamma\int_0^{\max\{S(x,x,gy),S(y,y,fx)\}}\varphi(t)dt+\delta\int_0^{S(x,x,y)}\varphi(t)dt,$$

for each $x,y\in X$ with non negative reals $\alpha,\beta,\gamma,\delta$ such that $2\alpha+3\beta+3\gamma+\delta<1$. Where $\varphi:R^+\to R^+$ is a Lebesgue integrable map which is summable on each compact subset of R^+, nonnegative and such that for each $\varepsilon>0$,

$$\int_0^{\varepsilon}\varphi(t)dt>0.$$

Then f has a unique fixed point such that for each $x\epsilon X$, $\lim_{n\to\infty}f^nx=z$.
Proof: The proof is very similar to the proof of theorem so we omitted it.

CONCLUSION

In this paper, we proved fixed point theorems for a self mapping and common fixed point theorems for a pair of self mappings satisfying a general contractive condition of integral type in the setting of complete$S$-metric space and

gave some consequences of our main results. The results presented in this paper generalize and improve several results from the existing literature.

REFERENCES

1. Bhardwaj,R.,2012,"Some common fixed point theorem in metric space using integral type mappings", IOSR Journal of Engineering, 2(2), 187-190.
2. Branciari,A.,2002, "A fixed point theorem for mappings satisfying a general contractive condition of integral type", Int. J. Math. Math. Sci., 29(9), 531-536.
3. Dey, D., Ganguly, A. and Saha, M.,2011,"Fixed point theorems for mappings under general contractive condition of integral type", Bull. Math. Anal. Appl. 3(1),27-34.
4. Kyu Kim,J., Sedghi,S., Gholidahneh,A., Mahdi Rezaee, M.,2016,"Fixed point theorems in S-metric spaces", East Asian Math. J. 32(5), 677–684.
5. Kumar,S., Chugh, R. and Kumar,R.,2007,"Fixed point theorem for pair of mappings satisfying a general contractive condition of integral type", Soochow Journal of Mathematics, 33(2), 181-185.
6. Ozgur,N.Y., Tas,N.,2017, "New contractive conditions of integral type on complete *S*- metric spaces", Math Sci 69 (1),39-52.
7. Rahman,M.U., Sarwar,M.,2012, "Fixed point results of Altman integral type mappings in S-metric spaces", Mat. Vesn. 64(3), 258-266.
8. Rhoades, B. E.,2003,"Two fixed point theorems for mappings satisfying a general contractive condition of integral type",International journal of Mathematics and Mathematical Sciences,63,4007-4013.
9. Sedghi, S., Dung, N.V.,2014,"Fixed point theorems on *S*-metric spaces", Mat. Vesn. 66, 113–124.
10. Sedghi, S., Došenović, T., Mahdi Rezaee, M., Radenovic, S.,2016, "Common fixed point theorems for contractive mappings satisfying φ-maps in S-metric spaces",Acta Univ. Sapientiae Math. 8(2), 298311.
11. Sedghi, S., Shobe, N., Aliouche, A.,2012,"A generalization of fixed point theorems in *S*-metric spaces",Mat. Vesn. 64, 258–266.
12. Sedghi, S., Shobe, N., Dosˇenovic´, T., 2015," Fixed point results in *S*-metric spaces",NonlinearFunct. Anal. Appl. 20(1),55–67.
13. Sedghi,S., Shobe,N., Shahraki,M., Došenović,T.,2018,"Common fixed Point of four maps in *S*-Metric Spaces", Math. Sci., 12,137-143.
14. Zamfirescu,T.,1972,"Fixed Point Theorems in metric spaces", Arch. Math.(Basel) 23, 292-298.

Indian Journal of Natural Sciences *www.tnsroindia.org.in ©IJONS*

Vol.15 / Issue 83 / Apr / 2024 *International Bimonthly (Print) – Open Access* *ISSN: 0976 – 0997*

RESEARCH ARTICLE

On $(1,2)^*$-$\ddot{g}$ Continuous Function in Intuitionistic Fuzzy Bitopological Space

S. Mukesh Parkavi[1] and A. Arivu Chelvam[2]

[1]Full-Time Research Scholar, PG & Research Department of Mathematics, Mannar Thirumalai Naicker college (Autonomous), (Affiliated to Madurai Kamaraj University), Madurai, Tamil Nadu, India.
[2]Associate Professor, PG & Research Department of Mathematics, Mannar Thirumalai Naicker college (Autonomous), (Affiliated to Madurai Kamaraj University), Madurai, Tamil Nadu, India.

Received: 30 Dec 2023 Revised: 09 Jan 2024 Accepted: 12 Jan 2024

***Address for Correspondence**
S. Mukesh Parkavi
Full-Time Research Scholar,
PG & Research Department of Mathematics,
Mannar Thirumalai Naicker college (Autonomous),
(Affiliated to Madurai Kamaraj University),
Madurai, Tamil Nadu, India.
Email: mukeshparkavi98@gmail.com

ABSTRACT

The aim of this paper is to introduce a new type of the notions of (1,2)*- ğcontinuous and (1,2)*-ğirresolute functions in intuitionistic fuzzy bitopological spaces and study some their properties in intuitionistic fuzzy bitopological spaces.

Keywords: Intuitionistic fuzzy bitopology, (1,2)*-ğIntuitionistic fuzzy continuous functions,(1,2)*-ğ Intuitionistic fuzzy irresolute functions.

INTRODUCTION

Zadeh [13] was introduced the fuzzy sets and Chang [4] was initiated the fuzzy topology. Kandil [6] introduced the concept of fuzzy bitopological spaces as a natural generalization of Chang's fuzzy topological spaces. Atanassov [3] was introduced the concept of intuitionistic fuzzy sets as a generalization of fuzzy sets. The notion of continuous maps is one of the most important concepts in topological spaces. Intuitionistic fuzzy continuous mappings and intuitionistic fuzzy irresolute mappings were studied by Young Bae Jun and Seok Zun Song [12]. Generalized continuity in intuitionistic fuzzy topological spaces was introduced by Thakur and Rekha Chaturvedi [11]. Using the notation of intuitionistic fuzzy sets Coker [5] introduced the notation of intuitionistic fuzzybitopological spaces.Recently the authors [8] introduced the concept (1,2)*-Intuitionistic fuzzy$\ddot{g}$ closed sets and open sets in bitopological spaces.

In this paper, we introduce the concept of intuitionistic fuzzy bitopological spaces as a generalization of fuzzy bitopological spaces. Next, we introduce the notations of $(1,2)^*$-$\ddot{g}$ continuous functions and $(1,2)^*$-$\ddot{g}$ irresolute functions in intuitionistic fuzzy bitopological spaces and study some their properties in intuitionistic fuzzy bitopological spaces.

Preliminaries

Throughout this paper (X,τ_1,τ_2) and (Y,σ_1,σ_2) or simply X and Y denote the intuitionistic fuzzy bitopological spaces (briefly IFBTS). We recall some basic definitions that are used in the sequel.

Definition 2.1[3]:

Let X be a non-empty set. An intuitionistic fuzzy set (briefly IFS) A in X is an object having the form, A = $\{< X, \mu_A(x), \gamma_A(x) > / x \in X\}$ where the functions $\mu_A : X \to [0,1]$ and γ_A: X → [0,1] denote the degree of membership (i.e., $\mu_A(x)$) and the degree of non-membership (i.e., $\gamma_A(x)$) of each element $x \in X$ to the set A respectively and $0 \leq \mu_A(x) + \gamma_A(x) \leq 1$ for each $x \in X$. The set of all intuitionistic fuzzy sets in X is denote by IFS(X).

Definition 2.2[4]:

Let A and B be IFSs of the form A = $\{< \mu_A(x), \gamma_A(x) > / x \in X\}$ and B = $\{< \mu_B(x), \gamma_B(x) > / x \in X\}$. Then

1. A ⊆ B if and only if $\mu_A(x) \leq \mu_B(x)$ and $\gamma_A(x) \geq \gamma_B(x)$ for all $x \in X$,
2. A = B ⇔ A ⊆ B and B ⊆ A,
3. $A^c = \{<X, \gamma_A(x), \mu_A(x)> / x \in X\}$
4. $A \cap B = \{<X, \mu_A(x) \wedge \mu_B(x), \gamma_A(x) \vee \gamma_B(x)> / x \in X\}$
5. $A \cup B = \{<X, \mu_A(x) \vee \mu_B(x), \gamma_A(x) \wedge \gamma_B(x)> / \in X\}$.

The intuitionistic fuzzy sets 0~ = {<X,0,1> / $x \in X$} and 1~ = {<X,1,0> / $x \in X$} are respectively the empty set and the whole set in X.

Definition 2.3[3]:

An intuitionistic fuzzy topology (briefly IFT) on X is a family τ of IFSs in X satisfying the following axioms.

1. 0~, 1~ ∈ τ
2. $H_1 \cap H_2 \in \tau$ for any $H_1, H_2 \in \tau$
3. $\cup H_i \in \tau$ for any family $\{H_i / i \in J\} \subseteq \tau$.

In this state the pair (X,τ) is called an intuitionistic fuzzy topological space (briefly IFTS) and any IFS in τ is known as an intuitionistic fuzzy open set (briefly IFOS) in X. The complement of an intuitionistic fuzzy open set is called an intuitionistic fuzzy closed set (briefly IFCS) in X.

Definition 2.4[1]:

Let τ_1 and τ_2 be two intuitionistic fuzzy topologies on a non-empty set X. The triple (X,τ_1,τ_2) is called an intuitionistic fuzzy bitopological spaces (briefly IFBTS), every member of $\tau_{1,2}$ is called $\tau_{1,2}$-intuitionistic fuzzy open sets ($\tau_{1,2}$-IFOS) and the complement of $\tau_{1,2}$-IFOS is $\tau_{1,2}$-intuitionistic fuzzy closed sets ($\tau_{1,2}$-IFCS).

Definition 2.5:

An IFS A = $<X,\mu_A,\gamma_A>$ in an IFBTS (X,τ_1,τ_2) is said to be an

- $(1,2)^*$-intuitionistic fuzzy closed set [7] ($(1,2)^*$-IFCS) if A = $\tau_{1,2}$-cl(A).

The complement of $(1,2)^*$-IFCS in an $(1,2)^*$-IFOS.

- $(1,2)^*$-intuitionistic fuzzy regular closed set ($(1,2)^*$-IFRCS) if A = $\tau_{1,2}$-$cl(\tau_{1,2}$-$int(A))$. The complement of $\tau_{1,2}$-IFCS in an $\tau_{1,2}$-IFOS
- $(1,2)^*$-intuitionistic fuzzy generalized closed set [8] ($(1,2)^*$-IFGCS) if $\tau_{1,2}$-cl(A) ⊆ U whenever A ⊆ U and U is an $\tau_{1,2}$-IFOS in X. The complement of an $(1,2)^*$-IFGCS is an $(1,2)^*$-IFGOS.
- $(1,2)^*$-intuitionistic fuzzy $\ddot{g}$ closed set [7] ($(1,2)^*$-IF$\ddot{g}$CS) if $\tau_{1,2}$-cl(A) ⊆ U whenever A ⊆ U and U is an $(1,2)^*$-IFSGOS in X. The complement of the $(1,2)^*$-IF$\ddot{g}$CS is an $(1,2)^*$-IF$\ddot{g}$OS in X.

Definition 2.6: A map f: $(X,\tau_1,\tau_2) \to (Y,\sigma_1,\sigma_2)$ is said to be

- $(1,2)^*$-intuitionistic fuzzy continuous [12] ($(1,2)^*$-IF continuous) if $f^{-1}(V)$ is $\sigma_{1,2}$-IF closed in X for every $\sigma_{1,2}$-IF closed subset V of Y.
- $(1,2)^*$-intuitionistic fuzzy regular continuous ($(1,2)^*$-IFR continuous) if $f^{-1}(V)$ is $(1,2)^*$-IFR closed in X for every $\sigma_{1,2}$- IF closed subset V of Y.
- $(1,2)^*$-intuitionistic fuzzy g-continuous [11] if $f^{-1}(V)$ is $(1,2)^*$-IF g-closed in X for every $\sigma_{1,2}$ -IF closed subset V of Y.

Definition 2.7: A map f: $(X,_{1,2}) \to (Y,\sigma_1,\sigma_2)$ is said to be

- $(1,2)^*$-intuitionistic fuzzy irresolute [12] ($(1,2)^*$-IF irresolute) if $f^{-1}(V)$ is $\sigma_{1,2}$-IFS closed in X for every $\sigma_{1,2}$-IFS closed subset V of Y.
- $(1,2)^*$-intuitionistic fuzzy regular irresolute ($(1,2)^*$-IFR irresolute) if $f^{-1}(V)$ is $(1,2)^*$-IFR closed in X for every $(1,2)^*$-IFR closed subset V of Y.
- $(1,2)^*$-intuitionistic fuzzy g- irresolute [10] if $f^{-1}(V)$ is $(1,2)^*$-IFG closed in X for Every $(1,2)^*$-IFG closed subset V of Y.

$(1,2)^*$-$\ddot{g}$ Intuitionistic Fuzzy Continuous Function

Definition 3.1

A function f: $(X,\tau_1,\tau_2)\to(Y,\sigma_1,\sigma_2)$ is called an $(1,2)^*$-intuitionistic fuzzy *$\ddot{g}$continuous* ($(1,2)^*$-IF$\ddot{g}$ continuous*, in short) iff $f^{-1}(B)$ is an* $(1,2)^*$-IF$\ddot{g}$CS *in $(X,\tau_1,\tau_2)$for every$\sigma_{1,2}$*-IFCS *B in (Y,σ_1,σ_2).*

Example 3.2:

Let X = {a, b} and Y = {u, v}. Let H_1= <x, (0.3,0.4), (0.6,0.5)>, H_2 = <x, (0.1,0.2), (0.6,0.7)> and H_3 = <y, (0.3,0.4), (0.6,0.5)>, H_4 = <y, (0.2,0.1), (0.7,0.6)>. Then τ_1= {0~, H_1,1~}, τ_2 = {0~,H_2,1~} and σ_1 = {0~,H_3,1~},σ_2 = {0~,H_4,1~} are IFBTS on X and Y respectively. Define f: $(X,\tau_1,\tau_2)\to(Y,\sigma_1,\sigma_2)$ by f(a) = u, f(b) = v. Then for $\sigma_{1,2}$-IFCS B = <y,(0.6,0.5), (0.3,0.4) > of (Y,σ_1,σ_2), $f^{-1}(B)$ is an $(1,2)^*$-IF$\ddot{g}$CS *in (X,τ_1,τ_2). Therefore,f is an* $(1,2)^*$-IF$\ddot{g}$continuous function.

Example 3.3

Let X = {a, b} and Y = {u, v}. Let H_1= <x, (0.3,0.4), (0.6,0.5)>, H_2 = <x, (0.1,0.2), (0.6,0.7)> and H_3 = <y, (0.6,0.5), (0.3,0.4)>, H_4 = <y, (0.5,0.5), (0.4,0.5)>. Then τ_1= {0~, H_1,1~},τ_2 = {0~,H_2,1~} and σ_1 = {0~,H_3,1~},σ_2 = {0~,H_4,1~} are IFBTS on X and Y respectively. Define f: $(X,\tau_1,\tau_2)\to(Y,\sigma_1,\sigma_2)$ by f(a) = u, f(b) = v. Then for $\sigma_{1,2}$-IFCS B = <y, (0.3,0.4), (0.6,0.5)> of (Y,σ_1,σ_2), $f^{-1}(B)$ is not an $(1,2)^*$-IF$\ddot{g}$CS *in (X,τ_1,τ_2). Therefore,f is not an* $(1,2)^*$-IF$\ddot{g}$ continuous function.

Theorem 3.4

Every $\tau_{1,2}$-IF continuous function is an $(1,2)^*$-IF$\ddot{g}$ continuous function but not conversely.

Proof:

Let f: $(X,\tau_1,\tau_2)\to(Y,\sigma_1,\sigma_2)$ be an $\tau_{1,2}$-IF continuous function. Let B be an $\sigma_{1,2}$-IFCS in Y. Since f is an $\tau_{1,2}$-IF continuous function, f^{-1}(B) is an $\tau_{1,2}$-IFCS in X. Since every $\tau_{1,2}$-IFCS is an $(1,2)^*$-IF$\ddot{g}$CS,f^{-1}(B) is an $(1,2)^*$-IF$\ddot{g}$CS *in X. Hence f is an* $(1,2)^*$-IF$\ddot{g}$ continuous function.

Example 3.5

Let X = {a, b} and Y = {u, v}. Let H_1= <x, (0.5,0.5), (0.2,0.3)>, H_2 = <x, (0.4,0.5), (0.4,0.3)> andH_3 = <y, (0.5,0.4), (0.3,0.2)>, H_4 = <y, (0.5,0.6), (0.1,0.2)>. Then τ_1= {0~,H_1,1~}, τ_2 = {0~,H_2,1~} and σ_1 = {0~,H_3,1~},σ_2 = {0~,H_4,1~} are IFBTS on X and Y respectively. Define f: $(X,\tau_1,\tau_2)\to(Y,\sigma_1,\sigma_2)$ by f(a) = u, f(b) = v. Then for $\sigma_{1,2}$-IFCS B = <y, (0.1,0.2), (0.5,0.6)> of (Y,σ_1,σ_2), $f^{-1}(B)$ is not an $\tau_{1,2}$-IFCS in (X,τ_1,τ_2). Therefore, f is not an* $(1,2)^*$*-IF continuous function but f is an*$(1,2)^*$-IF$\ddot{g}$ continuous function *in (X,τ_1,τ_2).*

Theorem 3.6

Every $(1,2)^*$-IFR continuous function is an $(1,2)^*$-IF$\ddot{g}$ continuous function but not conversely.

Proof:

Let f: $(X,\tau_1,\tau_2)\to(Y,\sigma_1,\sigma_2)$ be an$(1,2)^*$-IFR continuous function. Let B be an $\sigma_{1,2}$-IFCS in Y. Since f is an $(1,2)^*$-IFR continuous function, $f^{-1}(B)$ is an $(1,2)^*$-IFRCS in X. Since every $(1,2)^*$-IFRCS is an $(1,2)^*$-IF$\ddot{g}$CS,$f^{-1}(B)$ is an $(1,2)^*$-IF$\ddot{g}$CS*in X. Hence f is an* $(1,2)^*$-IF$\ddot{g}$ continuous function.

Example 3.7

Let X = {a, b} and Y = {u, v}. Let H_1= <x, (0.6,0.7), (0.4,0.3)>, H_2 = <x, (0.5,0.6), (0.3,0.3)> and H_3 = <y, (0.7,0.8), (0.2,0.2)>, H_4 = <y, (0.6,0.8), (0.2,0.1)>. Then τ_1= {0~,H_1,1~},τ_2 = {0~,H_2,1~} and σ_1 = {0~,H_3,1~},σ_2 = {0~,H_4,1~} are IFBTS on X and Y respectively. Define f: (X,τ_1,τ_2)→(Y,σ_1,σ_2) by f(a) = u, f(b) = v. Then for $\sigma_{1,2}$-IFCB = <y, (0.2,0.1), (0.7,0.8)> of (Y,σ_1,σ_2), $f^{-1}(B)$ is not an $(1,2)^*$-IFRCS in *(X,τ_1,τ_2). Therefore, f is not an* $(1,2)^*$*-IFR continuous function but f is an* $(1,2)^*$-IF$\ddot{g}$continuous function *in (X,τ_1,τ_2).*

Theorem 3.8

Every $(1,2)^*$-IF$\ddot{g}$ continuous function is an $(1,2)^*$-IFG continuous function, but not conversely.

Proof:

Letf:*(X,τ_1,τ_2)→(Y,σ_1,σ_2) be an* $(1,2)^*$-IF$\ddot{g}$ continuous function. Let B be an $\sigma_{1,2}$-IFCS in Y. Since f is an $(1,2)^*$-IF$\ddot{g}$ continuous function, $f^{-1}(B)$ is an $(1,2)^*$-IF$\ddot{g}$CS in X. Since every $(1,2)^*$-IF$\ddot{g}$CSis an $(1,2)^*$-IFGCS, $f^{-1}(B)$ is an $(1,2)^*$-IFGCS in X. Hence f is an $(1,2)^*$-IFG continuous function.

Example 3.9

Let X = {a, b} and Y = {u, v}. Let H_1= <x, (0.5,0.3), (0.3,0.4)>, H_2 = <x, (0.6,0.4), (0.3,0.3)>and H_3 = <x, (0.8,0.8), (0.2,0.1)>, H_4 = <y, (0.1,0.3), (0.8,0.7)>, H_5 = <y, (0.1,0.2), (0.8,0.8)>. Then τ_1= {0~, H_1,H_2,1~}, τ_2 = {0~,H_3,1~} and σ_1 = {0~,H_4,1~},σ_2 = {0~,H_5,1~} are IFBTS on X and Y respectively. Define f: (X,τ_1,τ_2)→(Y,σ_1,σ_2) by f(a) = u, f(b) = v. Then for $\sigma_{1,2}$-IFCS B = <y, (0.8,0.7), (0.1,0.3)> of (Y,σ_1,σ_2), $f^{-1}(B)$ is not an $(1,2)^*$-IF$\ddot{g}$CSin*(X,τ_1,τ_2). Therefore, f is not an* $(1,2)^*$-IF$\ddot{g}$*continuous function. but f is an* $(1,2)^*$-IFGcontinuous function *in (X,τ_1,τ_2).*

Theorem 3.10

Every $(1,2)^*$-IF$\ddot{g}$ continuous function is an $(1,2)^*$-IFRG continuous function, but not conversely.

Proof:

Letf:*(X,τ_1,τ_2)→(Y,σ_1,σ_2) be an* $(1,2)^*$-IF$\ddot{g}$ continuous function. Let B be an $\sigma_{1,2}$-IFCS in Y. Since f is an $(1,2)^*$-IF$\ddot{g}$ continuous function, $f^{-1}(B)$ is an $(1,2)^*$-IF$\ddot{g}$CS in X. Since every $(1,2)^*$-IF$\ddot{g}$CS is an $(1,2)^*$-IFRGCS, $f^{-1}(B)$ is an $(1,2)^*$-IFRGCS in X. Hence f is an $(1,2)^*$-IFRG continuous function.

Example 3.11

Let X = {a, b} and Y = {u, v}. Let H_1= <x, (0.4,0.3), (0.3,0.4)>, H_2 = <x, (0.6,0.5), (0.3,0.3)> and H_3 = <x, (0.8,0.8), (0.2,0.1)>, H_4 = <y, (0.1,0.3), (0.9,0.7)>, H_5 = <y, (0.1,0.2), (0.9,0.8)>. Then τ_1= {0~,H_1,1~}, τ_2 = {0~,H_2,H_3,1~} and σ_1 = {0~,H_4,1~},σ_2 = {0~,H_5,1~} are IFBTS on X and Y respectively. Define f: (X,τ_1,τ_2)→(Y,σ_1,σ_2) by f(a) = u, f(b) = v. Then for $\sigma_{1,2}$-IFCS B = <y, (0.9,0.7), (0.1,0.3)> of (Y,σ_1,σ_2), $f^{-1}(B)$ is not an $(1,2)^*$-IF$\ddot{g}$CS in*(X,τ_1,τ_2). Therefore, f is not an* $(1,2)^*$-IF$\ddot{g}$*continuous function. but f is an* $(1,2)^*$-IFRG continuous function *in (X,τ_1,τ_2).*

Theorem 3.12

A function f:*(X,τ_1,τ_2)→(Y,σ_1,σ_2) is an* $(1,2)^*$-IF$\ddot{g}$ continuous if and only if the inverse image of every $(1,2)^*$-IFOS in Y is an $(1,2)^*$-IF$\ddot{g}$OS in X.

Proof:

Assuming that f is an $(1,2)^*$-IF$\ddot{g}$ continuous, we prove the required condition on f. Let B be an $(1,2)^*$-IFOS in Y. this implies B^c is an $(1,2)^*$-IFCS in Y. since f is an $(1,2)^*$-IF$\ddot{g}$ continuous, $f^{-1}(B^c)$ is an $(1,2)^*$-IF$\ddot{g}$CS in X. $f^{-1}(B^c) = (f^{-1}(B))^c$ implies $f^{-1}(B)$ is an $(1,2)^*$-IF$\ddot{g}$OS in X. Hence the inverse image of an $(1,2)^*$-IFOS in Y is an $(1,2)^*$-IF$\ddot{g}$OS in X.

Conversely, assuming the given condition on f, we prove that f is $(1,2)^*$-IF$\ddot{g}$ continuous. Let B be an $\sigma_{1,2}$-IFCS in Y. then B^c is an $(1,2)^*$-IFOS in Y. by assumption, $f^{-1}(B^c)$ is an $(1,2)^*$-IF$\ddot{g}$OS in X. since $f^{-1}(B^c) = (f^{-1}(B))^c$, $f^{-1}(A)$ is an$(1,2)^*$-IF$\ddot{g}$CS in X. Hence f is an $(1,2)^*$-IF$\ddot{g}$ continuous.

Remark 3.13

The composition of two $(1,2)^*$-IF$\ddot{g}$ continuous functions need not be an $(1,2)^*$-IF$\ddot{g}$ continuous function.

Example 3.14

Let X = {a, b}, Y = {c, d} and Z = {u, v} Let H_1= <x, (0.3,0.4), (0.6,0.5)>, H_2 = <x, (0.4,0.4), (0.6,0.6)> *and* H_3 = <y, (0,0), (1,1)>, H_4 = <z, (0.7,0.8), (0.3,0.2)>, H_5 = <z, (0.7,0.6), (0.3,0.3)> *Then* τ_1= {0~, H_1,1~},τ_2 = {0~,H_2,1~} *and* σ_1 = {0~,H_3,1~}, σ_2 = {0~,1~} *and* δ_1= {0~, H_4, 1~}, δ_2 = {0~,H_5,1~}*are IFBTS on X, Y and Z respectively. Define f:* $(X,\tau_1,\tau_2)\to(Y,\sigma_1,\sigma_2)$ *by f(a) = c, f(b) = d and define g:*$(Y,\sigma_1,\sigma_2)\to(Z,\delta_1,\delta_2)$ *by g(c) = u, g(d) = v. Then f and g are* $(1,2)^*$-IF$\ddot{g}$continuous functions. consider*an IFS B = <z, (0.3,0.2), (0.7,0.8)>.Then B is an* $\delta_{1,2}$*-IFCS in* (Z,δ_1,δ_2)*. But* $(g\circ f)^{-1}(B)$ *is not an* $(1,2)^*$-IF$\ddot{g}$CS in(X,τ_1,τ_2)*. Hence the composition of two* $(1,2)^*$*-IF*$\ddot{g}$ *continuous functions need not be an* $(1,2)^*$-IF$\ddot{g}$continuous function.

$(1,2)^*$-$\ddot{g}$ Intuitionistic Fuzzy Irresolute Function

Definition 4.1

A function f: $(X,\tau_1,\tau_2)\to(Y,\sigma_1,\sigma_2)$ *is called an* $(1,2)^*$-intuitionistic fuzzy $\ddot{g}$*irresolute (*$(1,2)^*$-IF$\ddot{g}$*irresolute, in short) if* $f^{-1}(B)$ *is an* $(1,2)^*$-IF$\ddot{g}$CS *in* (X,τ_1,τ_2) *for every* $(1,2)^*$-IF$\ddot{g}$CS *B in* (Y,σ_1,σ_2)*.*

Example 4.2

Let X = {a, b} and Y = {u, v}. Let H_1= <x, (0.4,0.6), (0.5,0.3)>, H_2 = <x, (0.5,0.5), (0.4,0.4)> *and* H_3 = <y, (0.5,0.6), (0.4,0.3)>, H_4 = <y, (0.6,0.7), (0.3,0.2)> *and* τ_1 = {0~, H_1,1~}, τ_2 = {0~, H_2,1~} *and* σ_1 = {0~,H_3,1~},σ_2 = { 0~,H_4,1~} *are IFBTS on X and Y respectively. Definef:* $(X,\tau_1,\tau_2)\to(Y,\sigma_1,\sigma_2)$ *by f(a) = u, f(b) = v. Then f is not an* $(1,2)^*$-IF$\ddot{g}$irresolute function.

Theorem 4.3

Let f: $(X,\tau_1,\tau_2)\to(Y,\sigma_1,\sigma_2)$ *be an*$(1,2)^*$-IF$\ddot{g}$*irresolute. Then f is an*$(1,2)^*$-IF$\ddot{g}$ continuous function but not conversely.

Proof:

Let f be an $(1,2)^*$-IF$\ddot{g}$ irresolute function. Let B be any $\sigma_{1,2}$-IFCS in Y. Since every $\sigma_{1,2}$-IFCS is a $(1,2)^*$-IF$\ddot{g}$CS and B is an $(1,2)^*$-IF$\ddot{g}$CS in Y. By hypothesis, $f^{-1}(B)$ *is an*$(1,2)^*$-IF$\ddot{g}$CS*in X. Hence f is an*$(1,2)^*$-IF$\ddot{g}$ continuous function.

Example 4.4

Let X = {a, b} and Y = {u, v}. Let H_1= <x, (0.2,0.4), (0.8,0.6)>, H_2 = <x, (0.3,0.4), (0.7,0.6)> *and* H_3 = <y, (0.7,0.6), (0.3,0.4)>. *Then* τ_1= {0~, H_1,1~}, τ_2 = {0~,H_2,1~} *and* σ_1 = {0~, 1~},σ_2 = {0~,H_3,1~} *are IFBTS on X and Y respectively. Define f:*$(X,\tau_1,\tau_2)\to(Y,\sigma_1,\sigma_2)$ *by f(a) = 1-u, f(b) = 1-v. Then f is an* $(1,2)^*$-IF$\ddot{g}$ continuous function. But f is not an $(1,2)^*$-IF$\ddot{g}$irresolute function. *We have the B = <y, (0.2,0.3), (0.8,0.7)> is an* $(1,2)^*$-IF$\ddot{g}$CS in (Y,σ_1,σ_2)*, but* $f^{-1}(B)$ = <x, (0.8,0.7), (0.2,0.3)>*is not an* $(1,2)^*$-IF$\ddot{g}$CS in (X,τ_1,τ_2)*. Hence f is an* $(1,2)^*$*-IF*$\ddot{g}$ *continuous function but f is not an*$(1,2)^*$-IF$\ddot{g}$ irresolute function.

Theorem 4.5

Let*f:* $(X,\tau_1,\tau_2)\to(Y,\sigma_1,\sigma_2)$ *and g:* $(Y,\sigma_1,\sigma_2)\to(Z,\delta_1,\delta_2)$ *be an* $(1,2)^*$-IF$\ddot{g}$*irresolute function.Then* $g\circ f : (X,\tau_1,\tau_2)\to(Z,\delta_1,\delta_2)$ *is an*$(1,2)^*$-IF$\ddot{g}$ irresolute function.

Proof:

Let B be an $(1,2)^*$-IF$\ddot{g}$CS in Z. then $g^{-1}(B)$ is an $(1,2)^*$-IF$\ddot{g}$CS in Y. Since f is an $(1,2)^*$-IF$\ddot{g}$ irresolute function, $f^{-1}(g^{-1}(B))$ is an $(1,2)^*$-IF$\ddot{g}$CS in X. Hence $g\circ f$ *is an* $(1,2)^*$-IF$\ddot{g}$ irresolute function.

Theorem 4.6

Let *f:* $(X,\tau_1,\tau_2)\to(Y,\sigma_1,\sigma_2)$ *be an*$(1,2)^*$-IF$\ddot{g}$*irresolute function andg:* $(Y,\sigma_1,\sigma_2)\to(Z,\delta_1,\delta_2)$ *be an*$(1,2)^*$-IF$\ddot{g}$*continuous function. Then*$g\circ f$*:* $(X,\tau_1,\tau_2)\to(Z,\delta_1,\delta_2)$ *is an* $(1,2)^*$-IF$\ddot{g}$continuous function.

Proof:

Let B be an $\delta_{1,2}$-IFCS in Z. Since g is an $(1,2)^*$-IF$\ddot{g}$*continuous function,*$g^{-1}(B)$*is an*$(1,2)^*$-IF$\ddot{g}$CS in Y. Since f is an $(1,2)^*$-IF$\ddot{g}$*irresolute function,*$f^{-1}(g^{-1}(B))$ is an $(1,2)^*$-IF$\ddot{g}$CS in X. Hence $g\circ f$ *is an*$(1,2)^*$-IF$\ddot{g}$ continuous function.

REFERENCES

1. Alaa Saleh Abed, Yiezi Kadhum Mahdi Al-talkany, Special Cases of Intuitionistic Fuzzy BitopologicalSpaces, International Journal of Pure and Applied Mathematics, Vol. 119, No. 10, pp. 313 – 330 (2018).

2. Anitha, S., Mohana, K., IFgsr- continuous mapping in Intuitionistic FuzzyTopological Spaces, International Journal of Innovative Research in Technology, Vol.5 (2018), Issue 2.
3. Atanassov, K.T., Intuitionistic Fuzzy Sets, Fuzzy sets and Systems, 20(1986), pp. 87 – 96.
4. Chang, C.L., Fuzzy Topological Spaces, J.Math.Anal.Appl., 24(1986), pp. 81 – 89.
5. Coker, D., An Introduction to Intuitionistic Fuzzy Topological Spaces, Fuzzy Sets and Systems, 88(1997),pp. 81 – 89.
6. Kandil, A., Biproximities and Fuzzy Bitopological Spaces, Vol. 63, pp. 45 – 66 (1989).
7. Mohammed Jassin Tuaimah, Mohammed Jassin Mohammed, On Intuitionistic Fuzzy Ideals BitopologicalSpace, Journal of Advances in Mathematics, Vol.11, No.6, ISSN: 2347 – 1921 (2015).
8. Mukesh Parkavi, S., and Arivu Chelvam, A., On $(1,2)^{*}$-$\ddot{g}$ Closed Sets in Intuitionistic Fuzzy BitopologicalSpace, Indian Journal of Natural Sciences, vol. 13, 2023, pp. 52962– 52968.
9. Ramesh, K., Chithra, S., Shanmugapriya, B., IFπGP Closed Sets in Intuitionistic Fuzzy Topological Spaces, International Research Journal of Advanced Engineering and Science, Vol.2 (2017), pp. 82-86.
10. Rose Mary, S., Malarvizhi, R., Ravi, O., Intuitionistic Fuzzy g''' Continuous Mapping, International Journal of Mathematical and its Applications, Vol. 5 (2017), Issue 3.
11. Thakur, S. S., and Rekha Chaturvedi,Generalized Continuity in Intuitionistic Fuzzy Topological Space, Notes on Intuitionistic Fuzzy Sets, 12, 2006, 38-44.
12. Young Bae Jun, Jung Ok Kang and Seok-Zun Song,Intuitionistic Fuzzy Irresolute and Continuous Mappings, Far East Journal of Mathematical Sciences, 17, 2005, 201-216.
13. Zadeh, L.A., Fuzzy Sets, Information and Control, 8(1965), pp. 338 – 353.

Indian Journal of Natural Sciences *www.tnsroindia.org.in ©IJONS*

Vol.15 / Issue 83 / Apr / 2024 *International Bimonthly (Print) – Open Access* *ISSN: 0976 – 0997*

RESEARCH ARTICLE

Minimization of Complete Awaiting Duration of Tasks in Multi-Stage Flow Shop Scheduling

Deepak Gupta* and Malvika Sharma

Department of Mathematics, Maharishi Markandeshwar Engineering College, Maharishi Markandeshwar (Deemed to be University), Mullana-133207, Ambala, India.

Received: 30 Dec 2023 Revised: 09 Jan 2024 Accepted: 12 Jan 2024

***Address for Correspondence**
Deepak Gupta
Department of Mathematics,
Maharishi Markandeshwar Engineering College,
Maharishi Markandeshwar (Deemed to be University),
Mullana-133207, Ambala, India.

ABSTRACT

The current paper analyses a multi stage flow shop scheduling in order to diminish the complete awaiting duration of all the tasks. The heuristic algorithm has been developed to reduce the complete awaiting duration of all the tasks on m stations. A numerical example is illustrated in support of algorithm to build a profitable platform for the industrialists.

Keywords: Awaiting duration of tasks, flow shop scheduling, processing time.

INTRODUCTION

In day-to-day life, doing any work without managing time is totally wastage of money and time. Proceeding any establishment of system, scheduling of jobs or tasks are very fruitful concept from last decades, in which arranging the number of jobs in a particular order which not only saves the time but also increases efficiency and effectivity of the system by reducing manufacturing costs. Optimization of flow shop scheduling problem in production, manufacturing, establishment, management, computer science etc. is widespread in society for economical purpose as it is very important. Scheduling models work with the resolution to find the most beneficial sequence of tasks to reduce the complete period of doing all the tasks or to optimize some other measure of performance. Johnson S.M. (1954) was the god father of flow shop scheduling problem who gave the algorithm to diminish the duration of work where all tasks are completed on two stations flow shop. Ignall and Schrage (1965) analyzed permutation flow shop problem to decrease the makespan by branch and bound method. Smith and Dudek (1967) developed the structural model for the reduction of complete duration of work for all tasks on multi stations. Maggu P.L. and Dass G. (1977) became famous by giving the tremendous concept of job block for equivalent jobs in flow shop scheduling problems. Yoshida and Hitomi (1979), studied those scheduling problem which have setup time with processing time to

minimize duration of all tasks on two stations. The work on the job block conception was carried by Maggu P.L., G. Dass & Kumar R. (1981),Singh T.P.(1985) by evolving various parameters. Adiri, Bruno, et al. (1989) worked on method of breakdown for individual station. Rajendran(1992) proposed the branch and bound belief with bicriteria for two stage scheduling problem. Narain L. (2003) devised a model to reduce rental price of all the stations for all tasks working on multi stations. Heydari(2003) attempted to study different optimal problem where p number of tasks are executed on two separate job blocks, one in fixed order and another in arbitrary order, in a string.

Gupta and Singh (2005) manifested open shop scheduling for two stations where processing time connected to respective probabilities which includes job block concept. Singh and Gupta (2006), Singla P. et al. (2011),Singh Vijay (2011),Sharma S. and Gupta D.(2011), Shashi B. et al. (2012) studied the scheduling problem to reduce hiring cost using various parameters. Aggarwal S. et al. (2012) put the efforts to study structural model for n tasks on three station to diminish complete duration including strand of separate job-blocks. Sharma S., Gupta D. and Aggarwal S. (2013) developed the method for two stage scheduling including setup time, transportation time and job block to minimize the makespan in Fuzzy environment. Gupta D., Shashi B., Singla P., Sharma S. (2015) investigated the process for three stage scheduling problem for the reduction of hiring cost with various parameters. Then, the production finds some problem that they are getting loss as time is very crucial, and they wanted to deliver the service in short span. Based on the concept, Goyal B. and Gupta D. (2016),(2017),(2018) constructed the structural model for the reduction of complete awaiting duration of tasks using various parameters for two stage scheduling problems. Gupta D., Singla P. and Singh S. (2020) gave technique to solve the problem of all the tasks working on three station whose executing time is associated with probabilities to decrease awaiting duration of tasks. Goyal B. & Kaur S. (2021),(2022) solved fuzzy scheduling for two stage under undetermined environment. For benefit of huge manufacturing units and production, the absolute paper is an extension to diminish the complete awaiting duration of n tasks on m stations.

PRACTICAL SITUATION

Textile industry in India is one of the largest resources contributing to the economy. The growth of this industry in India cannot be ignored as it is climbing the heights of international platforms day by day. As a fashion evolves, we need more production of garments. Let us assume, in a garment industry, there are five stations, a cutting machine, dying machine, stitching machine, pressing machine and packing machine. Suppose, different sizes of shirts are to be processed on these machines and we want to diminish the complete awaiting duration of all jobs or tasks on all machines in order to fasten the production so that orders may be completed on or before due date.

NOTATIONS

h_k : Optimal sequence for the problem
U_{i1} : Processing time of n tasks on first station
U_{i2} : Processing time of n tasks on second station
U_{im} : Processing time of n tasks on last station
Q_i : Processing time of n tasks on fictitious station Q
R_i : Processing time of n tasks on fictitious station R
T_w : Total awaiting duration of all the tasks

PROBLEM FORMULATION

Suppose n tasks be processed on m stations$U_1,U_2,U_3\ldots,U_m$ in the order $U_1\rightarrow U_2\rightarrow U_3\rightarrow\ldots U_m$. Let U_{i1},U_{i2}, ...,U_{im} be the processing time of i^{th} task on stationU_1,U_2, $U_3\ldots$,U_m respectively . The target of this model is to acquire an optimal sequence of tasks to diminish the complete awaiting duration of all the n tasks on m stations.

ASSUMPTIONS

1. The n tasks are executing on m stations.

2. Tasks are independent of each other.
3. The arrangement of operations in a sequence working on all stations are same.
4. No task can switch from one station to another in between without completion of the operation.

ALGORITHM

Step1: Examine the structural relationship:
either min $U_{is} \geq$ max $U_{(s+1)}$,where(s=1,2..., m-2)
or min $U_{i(s+1)} \geq$ max U_{is}, where (s= 2, 3, ...m-1)
If any of these two conditions or both are satisfied then move to step 2.

Step 2: Set up two fictitious stations Q and R with processing times Q_i and R_i as follows:
$Q_i = U_{i1} + U_{i2}..... + U_{i(m-1)}$
$R_i = U_{i2} + U_{i3} +.....+U_{im}$
Thus, problem reduces to two stage flow shop scheduling model as follows in table 2.

Step 3: Check structural condition:
max $Q_i \leq$ min R_i
If condition is satisfied then move to step 4.

Step 4: Calculate $j_i=R_i-Q_i$ and $F_{ie} = (n-e) j_i$ for e=1,2,3 up to (n-1) as per the corresponding table:

Step 5: Line up the tasks in ascending order of j_i.
Let the sequence thus formed be $<b_1, b_2, b_3 .....b_n >$

Step 6: Find min $\{Q_i\}$.
If min $\{Q_i\} = Q_{b1}$ then the sequence attained in step 5 is required sequence. Otherwise,
if min $\{Q_i\} \neq Q_{b1}$ then move to step 7.

Step 7: Calculate complete waiting time $T_w= n Q_{ji} + \sum_{e=1}^{n-1} F_{ie}- \sum_{i=1}^{n} Q_i$ for the following n sequences

$h_1 = <b_1, b_2, b_3 ..... b_{n-1}, b_n>$
$h_2 = <b_2, b_1, b_3 ..... b_{n-1}, b_n>$
$h_3 = <b_3, b_1, b_2 ..... b_{n-1}, b_n>$
.
.
.
$h_{k-1} = <b_{n-1}, b_1, b_2..... b_{n-2}, b_n>$
$h_k= <b_n, b_1, b_2 ..... b_{n-2}, b_{n-1}>$

Step 8: Find minimum of T_w for all the sequences in step 7
The sequence with least complete awaiting duration is the required sequence.

NUMERICAL ILLUSTRATION

Consider five tasks processing on five stations named as Ai, Bi, Ci, Di and Ei , shown in table 4.
The target of this model is to acquire an optimal sequence of tasks to diminish the complete awaiting duration of all the tasks on these five stations.
Solution:

Step1: Check the structural relationship:
Min Ai ≥ max Bi
11 = 11

and Min Bi ≥ max Ci
7 = 7
and Min Ci ≥ max Di
5 = 5
Thus, structural relation exists.

Step2: Then convert 5 machines into two fictitious stations Q and R with processing times Q_i and $R_i$in table 5 as:
$Q_i = A_i + B_i + C_i + D_i$
$R_i = B_i + C_i + D_i + E_i$

Step 3: Check structural condition
max Qi ≤ min Ri= 38

Step 4: Calculate ji=Ri-Qi and Fie = (n-e) jifor e=1,2,3,4 as per the corresponding table 6.

Step 5: Line up the tasks in ascending order of j_i.
Let the sequence thus formed be <3,5,2,1,4>

Step 6: Find min {Q_i}, and check which case does it holds.
Min {Q_i}= 30 and Q_3 = 37, which is not equal.
Then move to step 7.

Step 7: Calculate complete awaiting duration T_w = n Q_{bi} + $\sum_{e=1}^{n-1} F_{ie}$- $\sum_{i=1}^{n} Q_i$ for the following n sequences <3,5,2,1,4><5,3,2,1,4><2,3,5,1,4><1,3,5,2,4><4,3,5,2,1>

- For sequence<3,5,2,1,4>

$b_1 = 3, b_2 = 5, b_3 = 2, b_4 = 1, b_5 = 4$
Therefore, complete awaiting duration T_w = 5×37+4+9+8+5-178 =185+26-178=211-178=33

- For sequence<5,3,2,1,4>

$b_1 = 5, b_2 = 3, b_3 = 2, b_4 = 1, b_5 = 4$
Therefore, complete awaiting duration T_w= 5×38+12+3+8+5-178=190+28-178=218-178=40

- For sequence <2,3,5,1,4>

$b_1 = 2, b_2 = 3, b_3 = 5, b_4 = 1, b_5 = 4$
Therefore, complete awaiting duration Tw = 5×35+16+3+6+5-178 =175+30-178=205-178=27

- For sequence<1,3,5,2,4>

$b_1 = 1, b_2 = 3, b_3 = 5, b_4 = 2, b_5 = 4$
Therefore, complete awaiting duration T_w = 5×38+20+3+6+4-178=190+33-178=223-178=45

- For sequence<4,3,5,2,1>

$b_1 = 4, b_2 = 3, b_3 = 5, b_4 = 2, b_5 = 1$
Therefore, complete awaiting duration T_w = 5×30+40+3+6+4-178 =150+53-178=203-178=25

Step 8: Find minimum of T_w for all the sequences in step 7.
Hence, the sequence <4,3,5,2,1> is the required sequence with least complete awaiting duration.

CONCLUSION

The algorithm is designed to reduce the total waiting time spent on m machines for all the tasks. Reducing the waiting time is a cost-effective solution in cases where the factory or the industry management has a short-term contract with the commercial company to carry out their tasks on time.

REFERENCES

1. Johnsons S. M. (1954), Optimal Two and Three-stage Production Schedules with Setup Times Included, Naval Research Logistics Quarterly, vol 1, pp 61-68.
2. Ignall E. and Schrage L.E.(1965), Application of the Branch and Bound Techniques to Some Flow-Shop Scheduling Problems, Operation Research, vol 13, pp 400-412.
3. Maggu P.L. and Dass G.(1977), Equivalent Jobs for Job Block in Job Sequencing, Operations Research, vol 14(4), pp 277-281.
4. Yoshida &Hitomi(1979), Optimal Two-stage Production Scheduling with Set- up Time Separated, AIIE Transactions, vol 11(3), pp 261-263.
5. Maggu P.L., G. Dass & Kumar R.(1981), On Equivalent-Jobfor Job-blockin nx2 Sequencing Problemwith Transportation-Times, Journal of the Operations Research Society of Japan, vol 24(2),pp 136-146.
6. Singh T.P.(1985), On nx2 Shop Problem involving Job-block, Transportation Times and Break-down Machine Times, PAMS, vol 21, pp 1-2.
7. Adiri I., Bruno J., Frostig E. & Kan R.A.H.G (1989), Single machine flowtime scheduling with a single break-down, Acta Information, vol 26(7), pp 679-696.
8. Rajendran(1992), Two-stage flow-shop scheduling problem with bicriteria, Journal of the Operational Research Society, vol 43(9), pp 871-884.
9. Narain L.(2003), Minimizing total hiring cost of machines in nxm flowshop problem, Journal of decisions and mathematical science, vol. 7(3), pp 1-3.
10. Heydari A. P. D.(2003), On flow-shop scheduling problem with processing of jobs in a string of disjoint job blocks: fixed order jobs and arbitrary order jobs, Journal of the Indian Society of Statistics and Operations, vol 24, pp 1-4.
11. Gupta D. and Singh T.(2005), On job-block open shop scheduling, the processing time associated with probability, Journal of the Indian Society of Statistics and Operations Research, vol 26, pp 91–96.
12. Singh T.P, Gupta Deepak(2006),Minimizing rental cost in two stage shop, the processing time associated withprobabilities including jo ERA Reflections, vol 1(2), pp 107-120.
13. Gupta D., Sharma S., Gulati N. & Singla P. (2011), Optimal two stage flow shop scheduling to minimize the rental cost including job- block criteria, set up times and processing times associated with probabilities, European Journal of Business and Management, vol 3(3), pp 268-286.
14. Singh Vijay(2011), Three machines flow-shop scheduling problems with total rental cost, International referred journal, pp 79-80.
15. Sharma S. and Gupta D.(2011), Minimizing rental cost under specified rental policy in two stage flow-shop, the processing time associated with probabilities including break down interval and job block criteria, European Journal of Business and Management (USA), vol 3(2), pp 85-103.
16. Gupta D., Sharma S. & Shashi B.(2012), Specially Structured Three Stage Flowshop Scheduling to Minimize the Rental Cost, International Journal of Applied Physics and Mathematics, vol 2(3), pp 156-158.
17. Gupta D., Sharma S., Aggarwal S.(2012), Three stage constrainted flow shop scheduling with jobs in a string of disjoint job-block, In Engineering and System (SCES), Students Conference, pp 1-6
18. Gupta D., Sharma S., and Aggarwal S.(2013), Flow shop scheduling on 2-machines with setup time and single transport facility under fuzzy environment, Opsearch, vol 50(1), pp 14-24.
19. Gupta D., Shashi B., Singla P., Sharma S.(2015), 3-stage specially structured flow shop scheduling to minimize the rental cost including transportation time, job weightage and job block criteria, European Journal of Business and Management, vol 7(4), pp 1-6.

20. Goyal B. and Gupta D.(2016), Optimal Scheduling for Total Waiting Time of Jobs in Specially Structured Two Stage Flow Shop Problem Processing Times Associated with Probabilities, Arya Bhatta Journal of Mathematics and Informatics, vol 8(1), pp 45-52.
21. Goyal B. and Gupta D.(2016), Job block concept in two stage specially structured Flow shop scheduling to minimize the total waiting time of jobs, International Journal of Latest Trends in Engineering and Technology, vol 7(3), pp 287-295.
22. Goyal B. and Gupta D(2017), Minimization of total waiting time of jobs in n× 2 specially structured Flow Shop Scheduling with set up time separated from processing time and each associated with probabilities, International Journal of Engineering Research and Application, vol 7(6), pp 27-33.
23. Goyal B. and Gupta D.(2018), Specially structured flow shop scheduling in two stages with concept of job block and transportation time to optimize total waiting time of jobs, Int J Eng Technol, vol 10(5), pp 1273-1284.
24. Gupta D., Singla P. and Singh S.(2020), Optimal three stage specially structured flow-shop scheduling to minimize the total waiting time of jobs, processing time associated with probabilities, Advances in Mathematics: Scientific Journal, vol 9(7), pp 4597-4605.
25. Goyal B. & Kaur S.(2021), Specially structured flow shop scheduling models with processing times as trapezoidal fuzzy numbers to optimize waiting time of jobs, Springer Singapore, vol 2, pp 27-42.
26. Goyal B. & Kaur S.(2022), Flow shop scheduling-especially structured models under fuzzy environment with optimal waiting time of jobs, International Journal of Design Engineering, vol 11(1), pp 47-60.

Table 1

Task	**StationU_1**	**StationU_2**	**StationU_3**	**….**	**….**	**StationU_m**
i	U_{i1}	U_{i2}	U_{i3}	….	….	U_{im}
1	U_{11}	U_{12}	U_{13}	….	….	U_{1m}
2	U_{21}	U_{22}	U_{23}	….	….	U_{2m}
3	U_{31}	U_{32}	U_{33}	….	….	U_{3m}
….	. …	….	….	….	….	….
….	….	….	….	….	….	….
….	….	….	….	….	….	….
n	U_{n1}	U_{n2}	U_{n3}	….	….	U_{nm}

Table 2

Task	**Station Q**	**Station R**
i	Q_i	R_i
1	Q_1	R_1
2	Q_2	R_2
3	Q_3	R_3
…	…	…
n	Q_n	R_n

Table 3

Task	Station Q	Station R		F_{ie} = (n-e) j_i				
i	Q_i	R_i	j_i=R_i-Q_i	e=1	e=2	e=3	…	e=(n-1)
1	Q_1	R_1	j_1	F_{11}	F_{12}	F_{13}	…	$F_{1(n-1)}$
2	Q_2	R_2	j_2	F_{21}	F_{22}	F_{23}	…	$F_{2(n-1)}$
3	Q_3	R_3	j_3	F_{31}	F_{32}	F_{33}	…	$F_{3(n-1)}$
…	…	…	…	…	…	…	…	…
n	Q_n	R_n	j_n	F_{n1}	F_{n2}	F_{n3}	…	$F_{n(n-1)}$

Table 4

Task	Station A	StationB	StationC	StationD	StationE
I	A_i	B_i	C_i	D_i	E_i
1	20	8	6	4	25
2	15	11	7	2	19
3	21	7	5	4	22
4	11	10	6	3	21
5	17	9	7	5	20

Table 5

Task	StationQ	StationR
i	Q_i	R_i
1	38	43
2	35	39
3	37	38
4	30	40
5	38	41

Table 6

Task	Station Q	Station R		$F_{ie} = (n-e)\, j_i$			
i	Q_i	R_i	$j_i=R_i-Q_i$	e=1	e=2	e=3	e=4
1	38	43	5	20	15	10	5
2	35	39	4	16	12	8	4
3	37	38	1	4	3	2	1
4	30	40	10	40	30	20	10
5	38	41	3	12	9	6	3

Indian Journal of Natural Sciences *www.tnsroindia.org.in ©IJONS*

Vol.15 / Issue 83 / Apr / 2024 *International Bimonthly (Print) – Open Access* *ISSN: 0976 – 0997*

RESEARCH ARTICLE

Application-Specific Efficiently Approximated Adders and Multipliers Design and Its Metrics Evaluation

Yogeswari .P[1]*, Ishwarya.S[2] , Kathirvelu.M[3] and Arul.A[1]

[1]Research Scholar, Department of Electronics and Communication Engineering, KPR Institute of Engineering and Technology, Coimbatore, (Affiliated to Anna University, Chennai), Tamil Nadu, India.
[2]PG Student, Department of Electronics and Communication Engineering, KPR Institute of Engineering and Technology, Coimbatore, (Affiliated to Anna University, Chennai), Tamil Nadu, India.
[3]Professor, Department of Electronics and Communication Engineering, Faculty in KPR Institute of Engineering and Technology, (Affiliated to Anna University), Coimbatore, Tamilnadu, India.

Received: 30 Dec 2023 Revised: 09 Jan 2024 Accepted: 27 Mar 2024

***Address for Correspondence**
Yogeswari .P
Research Scholar,
Department of Electronics and Communication Engineering,
KPR Institute of Engineering and Technology,
Coimbatore, (Affiliated to Anna University, Chennai),
Tamil Nadu, India.
Email: palanisamy.yogeswari@gmail.com

ABSTRACT

Adder and multiplier form the core part of VLSI signal and image processing applications. Metric evaluation of these adders helps in the identification of suitable energy-efficientadders for a targeted application. The proposed work focuses on the analysis of various approximate full adders with minimal error values. Various performance metrics such as mean errorand error distance are calculated to analyze its reliability. Further, these adders with minimal error are applied to the Dadda multiplier in the partial product reduction stage and its metrics are also evaluated. For efficient multiplier implementation, these 4:2 compressors are also designed using approximate full adders. The adders and multipliers are designed using Verilog HDL and synthesized using Xilinx ISE. The results show that approximate adders and multipliers produce better results in terms of area, power, and delay compared to exact adders and multipliers.

Keywords: Approximate Adders, Dadda Multiplier, Low Power VLSI, Error analysis

INTRODUCTION

Approximate computing is one of the recent trends for optimizing energy consumption for various data handling and high memory usage-related applications. The applications such as machine learning accelerators, signal & image processing, multimedia, and data processing fall under this category [1] - [3]. The other prime area of research related to these applications is utilizing the feature of its error-tolerant property. This approximation in VLSI-based architecture results in meeting the real-time demand of increasing battery life and various other high throughput requirements. Approximation can be done at various levels like approximating in arithmetic operations and also by using voltage-frequency scaling [4]-[6]. Approximation in arithmetic blocks is commonly used in various applications compared to voltage and frequency scaling designs which mostly operate with physical constraints. The adder and multiplier form the vital part occupying more than 60-70% of various signal, image, and machine learning applications [7]-[8]. So, approximation in this area will drastically reduce the energy consumption. In the literature, various methods are performed for approximation and are also suitably used in error-resilient applications. Some of the higher-order multipliers also used higher-order compressors with and without approximation for partial product minimization [9]-[11]. Some methods also include some error compensation circuits for making the result as close to the actual circuit. Hybrid models for adders are introduced in previous work for achieving power-delay-area trade-offs. Block-based and least significant truncation is also selected for application considering the parameter to be optimized [12] - [14]. An approximate multiplier is a type of digital circuit that performs multiplication operations but with a reduced level of precision compared to a full-precision multiplier. It is typically used in applications where the accuracy requirements are not as strict, but the speed and power consumption are critical factors. There are several ways to implement an approximate multiplier, but one common approach is to use a tree multiplication algorithm, which reduces the number of partial products used in the multiplication process.

Approximate multipliers can reduce the area and complexity of the overall system, which can lower the cost of the hardware implementation whereas normal multiplication is a mathematical operation that calculates the product of two numbers. To perform multiplication, you align the rightmost digits of the two numbers and multiply them together, then move one digit to the left and repeat until all digits have been multiplied. The final result is obtained by adding all the partial products obtained in the previous steps. Compressor methods are techniques used to reduce the number of partial products generated during the multiplication process. These methods are used to optimize the efficiency and speed of the multiplication operation, particularly in high-performance computing applications. Dadda tree algorithms are examples of parallel prefix adder circuits, which are widely used in digital signal processing and other high-performance computing applications to perform efficient and fast arithmetic operations.
The remainder of this paper is structured as follows. Brief surveys of various existing methods are analyzed in Section II. Section III describes various approximate full adders with minimal error and its truth table value is tabulated. Section IV deals with approximate Dadda multiplier designed using various approximate full adders and approximate compressors. The simulation results along with error metric calculations are performed and various parameters like area, power, and delay analysis of multipliers are compared in section V. Section VI concludes the work.

DADDA MULTIPLIER

The Dadda multiplier algorithm can be broken down into three main steps:

1. Partial Product Generation: This step involves generating a set of partial products by shifting one binary number and multiplying it with the corresponding bits of the other binary number. The partial products are generated using a set of multi-level partial product generators that operate in a tree-like structure. The first level of the generator generates the standard partial products, while the subsequent levels generate partial products by adding together the partial products from the previous level.
2. Partial Product Reduction: In this step, the partial products generated in step 1 are reduced using a set of reduction circuits. The reduction circuits add together multiple partial products to form a smaller set of partial products. The reduction process is repeated until only a small set of partial products remains.

3. Final Addition: The final step involves adding together the partial products generated in step 2 using a binary adder. The binary adder produces the final result of the multiplication operation.

Approximation in arithmetic blocks is commonly used in various applications compared to voltage and frequency scaling design which mostly operates with physical constraints. The adder and multiplier form the vital part occupying more than 60-70% of various signal, image, and machine learning applications. So, approximation in this area will drastically reduce the energy consumption. In the literature, various methods are performed for approximation and are also suitably used in error-resilient applications. Some of the higher-order multipliers also used higher-order compressors with and without approximation for partial product minimization [2]. Some methods also include some error compensation circuits for making the result as close to the actual circuit. Hybrid models for adders are introduced in previous work for achieving power-delay-area trade-offs. Block-based and least significant truncation is also selected for application considering the parameter to be optimized. The Dadda multiplier uses a series of multi-level partial product generators that generate the partial products in a tree-like structure. The first level generates the partial products using the standard multiplication technique, while the subsequent levels generate partial products by adding together the partial products from the previous level. It has been widely used in digital circuit design, especially in the design of high-speed arithmetic circuits such as digital signal processors and microprocessors.

APPROXIMATE ADDERS

An approximate adder is a type of digital circuit that is designed to perform addition operations with a lower accuracy than a conventional (exact) adder. Approximate adders are used in applications where high accuracy is not required, but power consumption and/or area are critical design parameters. Some examples of such applications include image processing, audio and video signal processing, and machine learning. The design of an approximate adder involves trading off accuracy for power consumption and/or area. One way to do this is by reducing the number of gates in the adder circuit or by simplifying the logic of the adder. This can be achieved by using approximate logic gates such as threshold logic gates or probabilistic logic gates. Another way to reduce power consumption by using lower-precision arithmetic units, such as truncated or rounded arithmetic units. Table I and II shows the truth table of the exact full adder and eight different approximate full adders. X, Y, and Zin are the input of the full adder with Sum and Carry its corresponding output. The x indicated in red color denotes the error in the truth table due to approximation.

Approximate adder 1 (FA1)

The logic equations of approximate full adder(FA1) are given in Eqs. (1) and (2). The carry is directly taken from X input and the sum uses one AND gate, inverter, and an OR gate. This low complexity design produceserrors for binary inputs three and four.

Sum=(X'+YZin) (1)

Carry=X(2)

Approximate adder 2 (FA2)

The logic equations of the approximate full adder(FA2) are given in Eqs. (3) and (4). As per Table I the carry is error-free as it uses the exact expression as that of the original full adder. The sum produces 2 errors for the binary inputs 3 and 4.

Sum=(X'(Y+Zin) +YZin)(3)

Carry=XY+YZin+XZin(4)

Approximate adder 3 (FA3)

The logic equations of approximate full adder (FA3) are given in Eqs. (5) and (6). It also uses exact carry similar to approximate adder FA2. The sum equation is optimized compared to FA2 and it results in an overall error of 3.

Sum=(X'+Y) Zin (5)

Carry=XY+YZin+XZin(6)

Approximate adder 4 (FA4)

The logic equations of approximate full adder (FA4) are given in Eqs. (7) and (8). The carry is error-free as shown in eq.8 and the sum produces the error for input 0. The overall error for this expression is 1. This approximate adder has minimal error compared to other approximation adders with minimal area overhead.

Sum=X'Y'+Y'Zin+XYZin+X'YZ'in(7)

Carry=XY+YZin+XZin (8)

Approximate adder 5 (FA5)

The logic equations of approximate full adder (FA5) are given in Eqs. (9) and (10). This method also uses exact carry without error and the sum expression results in an overall error of 2. This design also uses a minimal gate for calculating the sum.

Sum=X'+YZin(9)

Carry=XY+YZin+XZin(10)

Approximate adder 6 (FA6)

The logic equations of approximate full adder (FA6) are given inEqs. (11) and (12). The carry is error-free and the sum produces only one overall error resulting in minimum error similar to approximate adder FA4.

Sum=X'(Y'+Z'in) +X'+YZin (11)

Carry=XY+YZin+XZin(12)

Approximate adder 7 (FA7)

The logic expressions of the approximate full adder (FA7) are given in Eqs. (13) and (14). It is slightly modified from the approximate adder FA6. It also uses exact carry along with sum with a minimum of 1 error resulting in an overall error of 1.

Sum=XY+YZ'in+X'Y'Zin+XY'Z'in(13)

Carry=XY+YZin+XZin(14)

Proposed Approximate Full Adder (PAFA)

The logic expressions of the proposed approximate full adder (PAFA) are given in Eqs. (15) and (16). This approximate adder uses exact carry and uses the same carry expression to produce a sum. The sum generation uses a minimal area with one inverter and OR gate producing overall 3 errors.

Sum=~ (Carry|X) (15)

Carry=XY+YZin+XZin(16)

APPROXIMATE MULTIPLIERS

The proposed approximate adders as tabulated in Table I and II results are used for designing the approximate multipliers. Various adders are selected with different error values for analyzing the performance of the multiplier. Multiplier occupies more area and power compared to the adder, thus optimizing the multiplier with minimal area approximate adder results in an overall reduction of area when used in real-time applications. There are various types of multipliers available such as array multiplier, Wallace tree multiplier, booth multiplier, baugh-wooley multiplier, and various other bypassing multipliers. Wallace tree is commonly used for reducing the partial product using a tree structure. The disadvantage of Wallace is that it has an uneven tree structure resulting in an increase in propagation delay. In this work Dadda multiplier architecture is considered which is similar to Wallace but with even architecture with a decrease in critical path delay. Fig. 1 shows the multiplication process of the Dadda multiplier. The approximate multiplier was designed using five different adders with different error probabilities. The approximate adders FA1, FA5, FA6, FA7, and FA8 are considered for designing a multiplier. The approximation is mostly defined asthe least significant position as the error in the most significant part will degrade the application quality. Along with these 5 types of approximate multiplication, the 6 type of multiplication is designed using 4:2 compressors. The 4:2 compressors are a cascaded combination of 2 full adders. The approximate full adder for the

compressor is selected based on application requirements. Fig.2 shows the partial product generation and reduction of the Dadda multiplier using 4:2 compressors. In the total 16 columns of partial product first 8 columns from the LSP use approximate adders and compressors.

RESULTS AND DISCUSSIONS

The approximate adder and multiplier are designed using Verilog HDL and synthesized in Xilinx ISE. The RTL simulation for functional verification is performed using Modelsim software. Fig. 3 shows the simulation result of the approximate Dadda multiplier using the proposed approximate full adder (PAFA). X and Y are the input operands and PRODUCT is the multiplier output. Fig. 4 shows the simulation result of the approximate multiplier MA-C using approximate adders and 4:2 inaccurate compressors. Table III presents the comparison table of various multipliers named MA1, MA2, MA3, MA4, and MA5 which is constructed based on approximate adders FA1, FA5, FA6, FA7, and FA8, respectively. The multiplier MA-C is designed using approximate compressors. The area utilization summary is analyzed by using the total gate count occupied. The table also shows the power and delay values obtained for different multipliers. For the multiplier constructed using only full adders MA1 results in very low area and power. The multiplier MA-C designed using compressors out performs the result of the other multipliers in terms of area and power consumption. Table IV and V shows the comparison result obtained for various adder and multipliers in terms of accuracy and reliability. Error rate, Mean, and Normalized error distance for 8 types of adders and 6 types are multipliers are compared. This gives the view on choosing the type of adder and multiplier for specific applications. This paper analyzed eight types of approximate adders (FA1-FA8) and 6 types of approximate multipliers (MA1-MA5, MA-C). The proposed method is evaluated for its accuracy through its metric analysis which helps in selecting the required blocks for error-tolerant applications. The proposed multiplier based on approximate compressors occupies a very low area and consumes minimum power compared to other existing multipliers. The results show that approximate adders and multipliers produce better results in terms of area, power, and delay compared to exact adders and multipliers. In the future, these adders and multipliers can be applied to image processing applications for real-time analysis. Higher-order approximate compressors such as 5:2 and 6:3 can also be an area of research in the future.

REFERENCES

1. V. Gupta, D. Mohapatra, S.P. Park, A. Raghunathan, K. Roy, IMPACT imprecise adders for low-power approximate computing, in Proc. IEEE/ACM International Symposium on Low-power Electron Design, 2011, pp. 409–414.
2. N. Zhu, W.L. G.oh, K.S. Y.eo, An enhanced low power high-speed adder for error-tolerant application, in Proceedings of the ISIC, 2009, pp. 69–72.
3. N. Zhu, W.L. G.oh, W. Zhang, K.S. Y.eo, Design of low power high-speed truncation error tolerant adders and its application in DSP, in IEEE Transactions on Very Large Scale Integration (VLSI) Systems, 18, 2010, pp. 1225–1229.
4. H.R. Mahdiani, A. Ahmadi, S.M. F.akhraje, C. Lucas, Bio-inspired imprecise computational blocks for efficient VLSI implementation of soft-computing applications, in IEEE Transactions on Circuits and Systems, 57, 2010, pp. 850–862.
5. Arun Sekar R, Kirubalini, Design of arithmetic circuits using an Approximation computing, IEEE International Conference on Advanced Computing and commuting systems, 17-18March 2013.
6. D. Mohapatra, V. Chippa, A. Raghunathan, K. Roy, Design of voltage-scalable meta functions for approximate computing, in Proceedings of DATE, 2011, pp. 1–6.
7. M. Kathirvelu, Design and Implementation of Optimized Area and PDP Multiplier for High-Speed Digital Circuit Applications, International Journal of Recent Technology and Engineering ISSN: 2277-3878, Volume-7, Issue-6S5, April 2019, PP:1081-1085

8. Muralidharan Jayabalan , E. Srinivas Francis H. Shajin, P. Rajesh, On Reducing Test Data Volume for Circular Scan Architecture Using Modified Shuffled Shepherd Optimization, Journal of Electronic Testing (2021) 37:577–592.
9. V. Gupta, D. Mohapatra, A. Raghunathan, K. Roy, Low power digital signal processing using approximate adders, IEEE Trans. Comput.-Aided Des. Integr. Circuits Syst. 32 (2013) 87–97.
10. Arul A,Kathirvelu M, Parimala V,Ganeshkumar D, Design and Implementation of High-Speed Low Power Bi-stable Circuits for Digital Circuits Applications, 2nd IEEE Mysore Sub Section International Conference, Mysuru Con 2022 Mysuru16 October 2022.
11. Kulkarni, P. Gupta, M. Ercegovac, Trading accuracy for power with an under-designed multiplier architecture, in Proceedings of the 24th IEEE International Conference on VLSI Design, 2011, pp. 346–351.
12. K. Bhardwaj, P.S. Mane, J. Henkel, Power and area-efficient approximate Wallace tree multiplier for error-resilient systems, in Proceedings of the 15th International Symposium on Quality Electronic Design, 2014, pp. 263–269.
13. A. Momeni, J. Hari, P. Montuschi, F. Lombardi, Design and analysis of approximate compressors for multiplication, in IEEE Transactions on Computers, 2014, pp. 99–101
14. Aswini Valluri, Sarada Musala and Muralidharan Jayabalan "Designof Area Efficient, Low-Power, and Reliable Transmission Gate-based10T SRAM Cell for Biomedical Application" Journal of Engg.Research Vol.10 No. (1A) pp. 161-174. DOI: 10.36909/jer.10399.

Table I Truth Table for exact full adder and approximate adders (FA1-FA3)

Input			Output							
			FA		FA1		FA2		FA3	
X	Y	Zin	Sum	Carry	Sum	Carry	Sum	Carry	Sum	Carry
0	0	0	0	0	1x	0	0	0	0	0
0	0	1	1	0	1	0	1	0	1	0
0	1	0	1	0	1	0	1	0	0x	0
0	1	1	0	1	1x	0x	1x	1	1x	1
1	0	0	1	0	0x	1x	0x	0	0x	0
1	0	1	0	1	0	1	0	1	0	1
1	1	0	0	1	0	1	0	1	0	1
1	1	1	1	1	1	1	1	1	1	1

Table II Truth Table for exact full adder and approximate adders (FA4-FA8)

Output									
FA4		FA5		FA6		FA7		PAFA	
Sum	Carry	Sum	Carry	Sum	Carry	Sum	Carry	Sum	Carry
1x	0	1x	0	1x	0	0	0	1x	0
1	0	1	0	1	0	1	0	1	0
1	0	1	0	1	0	1	0	1	0
0	1	1x	1	0	1	0	1	0	1
1	0	0x	0	1	0	1	0	0x	0
0	1	0	1	0	1	0	1	0	1
0	1	0	1	0	1	1x	1	0	1
1	1	1	1	1	1	1	1	0x	1

Table III Comparison of area, power, and delay of different multipliers

Multiplier Types	Area(Gate count)	Power(mW)	Delay(ns)
MA1	777	151	23.950
MA2	927	167.18	24.526
MA3	918	175.67	23.929
MA4	929	169.50	24.197
MA5	915	145.94	26.766
MA-C	762	116.67	32.596

Table IV Comparison of the accuracy and metrics for approximate adders.

Existing and Proposed designs	ED	ER	PR	MED	NED
FA1	5	0.625	0.375	0.48	0.06
FA2	2	0.25	0.75	0.24	0.03
FA3	3	0.375	0.625	0.36	0.045
FA4	1	0.125	0.875	0.09	0.011
FA5	3	0.375	0.625	0.36	0.045
FA6	2	0.25	0.75	0.24	0.03
FA7	1	0.125	0.875	0.09	0.011
PAFA	3	0.375	0.625	0.36	0.045

Table V Comparison of the accuracy and metrics for approximate multipliers.

Existing and Proposed designs	ED	ER	PR	MED	NED
MA1	98	4.56	46	5.18	0.754
MA2	87	3.78	54	4.74	0.604
MA3	62	2.521	42	3.97	0.432
MA4	41	1.793	39	2.46	0.213
MA5	87	3.78	54	4.74	0.604
MA-C	91	4.12	50	4.92	0.675

Fig. 1 Multiplication process of Dadda Multiplier

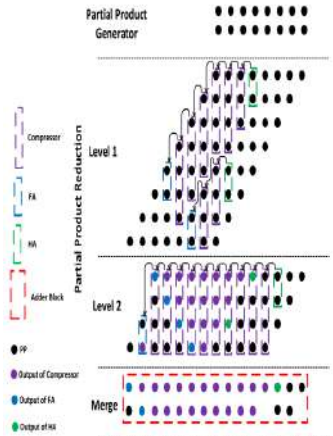

Fig.2 Dadda multiplier design using compressors.

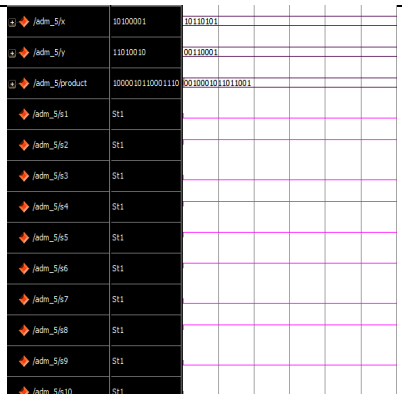

Fig. 3 Simulation result of multiplier using proposed approximate full adder (PAFA)

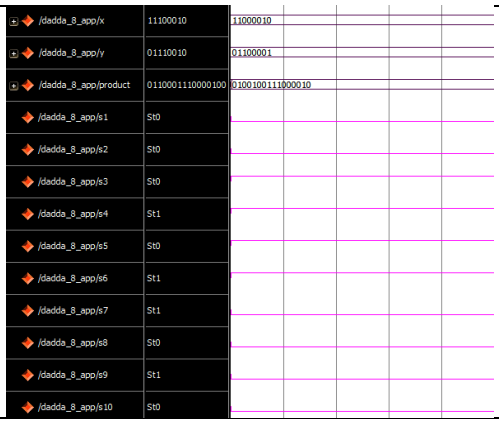

Fig. 4 Simulation result of multiplier using approximate adders and compressors

Indian Journal of Natural Sciences *www.tnsroindia.org.in ©IJONS*

Vol.15 / Issue 83 / Apr / 2024 *International Bimonthly (Print) – Open Access* *ISSN: 0976 – 0997*

RESEARCH ARTICLE

The Impact of Smartphone use on Social Relationships among Young People

Bijoy Das[1], Anupam Chanda[2] and Rituparna Roy[3*]

[1]Assistant Professor, Department of Humanities and Social Sciences, Assam down town University, Guwahati, Assam, India.
[2]Librarian, Bahona College, (Affiliated to Dibrugarh University) Assam, India.
[3]Assistant Professor, Commerce and Management, Assam down town University, Guwahati, Assam, India.

Received: 30 Dec 2023 Revised: 09 Jan 2024 Accepted: 27 Mar 2024

***Address for Correspondence**
Rituparna Roy
Assistant Professor,
Commerce and Management,
Assam down town University,
Guwahati, Assam, India.
Email: rituparna90@gmail.com

ABSTRACT

Apart from making and receiving calls, the mobile phone is being used in a variety of ways. As a result of the widespread use of mobile phone technology, particularly the smartphone and the internet, today's youth are less interested in face-to-face communication with their family and friends. Mobile phone use is no longer just a fad, but a game-changing strategy for accessible communication and corporate growth. It is assisting a million people in various ways. For youth or the younger generation, a mobile phone is necessary. The smartphone, in particular, is capturing the youth's attention to current application developments on their phones. The family, we feel, is the most important institution for our socialisation and growth. However, having access to mobile phones, particularly smartphones, is harming our day-to-day interactions by creating social distance between us. The current study has shed light on a few key features of smartphone use and how it affects social interaction and relationships among young people. Physical engagement is dwindling as the majority of respondents prefer to interact through social media. Furthermore, the study discovered that people who work outside the home make the most phone calls to communicate with their parents, as well as video calls.

Keywords: Smartphone; Social relationship; Youth; Physical interaction.

INTRODUCTION

People can now live better lives thanks to technological advancements. The disadvantage is that those who use high-end mobile phones with infinite applications feel important and never feel inferior in society. However, we cannot ignore the good effects of increased mobile phone use and availability due to social networking. The cell phone, we feel, improves access to straightforward information from a variety of reliable sources. With the use of the internet, we can quickly obtain study materials, books in pdf format, and other software to satisfy our study material needs. The important point is that improving internet access allows people to stay up to date on what's going on in the world. However, we are not fulfilling our full potential and are overly reliant on mobile phones and mobile technologies, which have negative social consequences. Excessive use of mobile phones can have negative consequences for a person's family and social relationships. It creates conditions where family members, such as parents, children, and siblings, have less communication. Apart from making and receiving calls, the mobile phone is being used in a variety of ways. With the availability of many programmes, it is more about texting, songs, films, games, reminders, entertaining videos, and much more. However, just as everything has both positive and negative effects, cell phone use has both beneficial and harmful effects on people and their social lives. Mobile phone use is no longer just a fad, but a game-changing strategy for accessible communication and corporate growth.

It is assisting a million people in various ways. As a result of the widespread use of mobile phones and the internet, today's kids have lost interest in face-to-face communication with their family and friends. Certain value systems, ideas, and customs exist in our culture. There is a distinct social structure and system in place. MacIver's popular notion is that society is a network of relationships. Individuals, groups, and communities all benefit from the importance of human relationships. The family, we feel, is the most important institution for our socialisation and growth. However, having access to mobile phones, particularly smartphones, is harming our day-to-day interactions by creating social distance between us. Social interaction and relationships have an important role in forming and moulding one's behaviour. Poor social connection can have a significant detrimental impact on a young person's general development, including their physical health and behaviours (Umberson and Montez, 2010; cited in Katriina et al., 2017, p.343). Increased alcohol use, drug abuse, and other forms of substance abuse are also on the rise. With the use of technology and various applications in the smartphone, one's behaviour may be diverted into undesirable pursuits. That means they can easily be influenced to engage in delinquent behaviour, such as cybercrime and other forms of crime.

REVIEW OF LITERATURE

Afaliq (2013) suggests that cell phone usage has a substantial negative impact on individuals' lives, particularly among teenagers. Their constant texting and chatting with friends hinder their engagement in face-to-face social interactions, emphasizing the need to understand the influence of mobile phones on the social dynamics of young people.Bhalla's study (2017) further explores the adverse effects of mobile phone usage, including its interference with social activities. This research sheds light on the potential consequences of excessive mobile phone use and raises questions about its long-term effects on interpersonal relationships. Mount (2012) reinforces these findings by emphasizing that mobile phones can affect the lives of young people, leading to health difficulties and strained social connections. This connection between mobile phone use and negative outcomes underscores the importance of raising awareness and implementing measures to mitigate potential health and social issues among youth. Leonard's study (2015) delves into the substantial consequences of mobile phone addiction, as teens use their phones for the majority of their waking hours. This addiction impacts their working hours, productivity, and face-to-face interactions. Leonard's findings highlight the addictive nature of mobile phones and the potential consequences on productivity and interpersonal relationships among young people. Kelley's research (2018) highlights how regular access to mobile phones among youth can have a profound impact on family relationships, potentially disconnecting the bond between parents and children. This emphasizes the need to understand how mobile phones can strain

family relationships and disrupt parent-child connections. Gupta and Kumar (2016) shed light on the implications of youth access to mobile phones, revealing their substantial impact on psycho-social lives, family structure, and communication. Their research underscores the multifaceted influence of mobile phones on various aspects of young people's lives. Lakshmi's study (2016) explores the impact of smartphones on today's society, claiming that they may transform people into obnoxious and non-communicative individuals. The study also delves into the behaviors of today's youth while driving, walking down the street, and in public spaces. Lakshmi's research provides insight into how mobile phones may contribute to negative behaviors and communication patterns in various social contexts.

In conclusion, the existing literature suggests that mobile phones can have a range of negative impacts on people's lives, particularly on teenagers and young adults. These effects encompass disruptions in social interactions, negative consequences on health, and challenges to family relationships. Furthermore, mobile phone addiction can have significant consequences for daily routines and productivity. Understanding the multifaceted implications of mobile phone use is essential to address the challenges it poses in various aspects of individuals' lives. In light of the growing concerns regarding the negative impacts of mobile phone use, this study aims to investigate and understand the specific effects of mobile phone usage on the social, familial, and psychological dimensions of teenagers' lives.

OBJECTIVES

- **To learn about the youth's smartphone usability and purpose;**
- **To learn about the nature of the youths' interactions with their friends and family members.**

METHODOLOGY

The purpose of this study was to conduct a descriptive analysis of data obtained from youth aged 15 to 29 in the Assam metropolis of Guwahati. To obtain the relevant information from the respondents, simple random sampling and structured questionnaires were utilised. A total of 278 respondents have been selected to fulfill the purpose of the study.

Major Findings

About the Socioeconomic Background of the Respondents

According to the findings, the below table no. 1 revealed that the majority of the respondents (62.9%) are between the ages of 20 and 24, indicating that smartphone users are predominantly PG-level students (57.9%). Aside from that, the majority of smartphone users are women, accounting for 69.0 percent of all respondents. It is also discovered that a large number of respondents (76.2 percent) are students, as well as others in business and service. More than 80.0 percent of respondents belong to a nuclear family (62.5 percent) with fewer than five family members and an average of two siblings when it comes to their family and environment.

Uses of Smartphone

As the study is based on smartphone users, it represents all respondents who own a smartphone. the below table no. 2 revealed that 57.9% of respondents have owned a smartphone for 5-10 years, while 25.5 percent have owned a smartphone for less than 5 years. Only 16.5 percent of people have had a smartphone for more than ten years. Although 33.4 percent of smartphone users say they use their phones frequently, nearly half (42.45 percent) say they use them virtually constantly throughout the day. When asked why they use their smartphones, 82.01 percent (multiple responses) said they use them for study, 76.98 percent (multiple responses) said they use them for social media, and 75.9% said they solely use them to receive and make calls as mentioned in the table no. 3. They also use a smartphone to communicate via WhatsApp and other social media platforms, as well as to browse the internet. However, more than three-quarters of respondents say they use their smartphone for social media whenever they

have free time, with the majority of respondents using it for four hours on average per day, while 33.45 percent use it for six hours on average per day, and 15.47 percent use it for more than six hours per day.

Impact of the Use of Smartphones on Social Interaction

The current study also shed light on a few key aspects of smartphone use, including how it affects social interaction and relationships. Hence, table no. 4 represents physical engagement is declining as the majority of respondents prefer to interact via social media, with 94.96 percent using WhatsApp, 83.09 using Facebook, 57.91 percent using Instagram, and 16.83 percent using Telegram (all are multiple responses). This has a significant impact on their personal and social lives, as they prefer communication or engagement through chatting (93.17 percent), voice calls (53.63 percent), and video calling (28.06 percent) (multiple responses). Furthermore, people who stay outside their homes make the most phone calls (90.63 percent) to communicate with their parents, and they also conduct video calls. Furthermore, the majority of respondents (78.06 percent) denied that communication or engagement with parents or siblings via the phone is considerably more effective than actual connection or conversation, claiming that Physical interaction makes it more enjoyable to communicate, counsel, and solve problems. Face-to-face communication is preferable to phone communication because it allows us to express our feelings to our parents or siblings. It has also been observed that when a person spends a day with family, friends, relatives, or siblings, that person performs better.

CONCLUDING DISCUSSIONS

For youth or the younger generation, a mobile phone is necessary. Without a doubt, they are now heavily attached to their phones, which keeps them lonely. When the habit of using phones on a regular basis becomes an obligation, it becomes an addiction (Alavi et al., 2012). Their socialisation has an impact on them in similar ways, as it forces them to experience dissatisfaction and worry, damaging their psychosocial lives. According to a survey (quoted in Lakshmi, 2016; p.270), 77 percent of people believe today's young people's social skills are poorer than they were 20 years ago. There are currently 1.85 billion individuals using Smartphones worldwide, with 2.87 billion projected by 2020(Cha and Seo, 2018). On the other hand, when discussing social relationships, consider the perspective of social interaction. Social interaction is often regarded as a necessary component of social relationships. The smartphone, in particular, is capturing the youth's attention to current application developments on their phones. Young are highly fond of using WhatsApp talk, and video sharing, which is a primary activity of today's TikTok videos; prank videos are drawing a significant section of the youth due to available applications. To summarise, mobile phones, often known as smartphones, are a marvelous invention that mostly benefits our daily life. Simultaneously, we must consider the drawbacks of using it beyond our needs rather than as a requirement. It provides opportunities while also posing problems to our current and future generations. With the developments and quality of technology, it may be argued that smartphones have become more of a fashion statement among today's young than a need. Yes, it is undeniably providing a technologically growing platform for speedier communication. The smartphone is necessary for us, but we must exercise self-control or refrain from using it. If a person is away from home, a smartphone is a good way to communicate. This can be harmful to our lives if we utilise it too often.

Nowadays, most children spend their time on social media or at chill-out parties with pals because other relationships, such as those between parents and children, siblings, and relatives, are eroding day by day. We can better comprehend each relationship when we spend quality time with our parents, relatives, siblings, and friends. Social media is not a bad platform; however, how we use it is up to us; if we use it incorrectly, it will have a negative impact on our life; but, if we use it correctly, it will be a wonderful platform. On the other hand, due to school, work, or other reasons, more individuals are increasingly residing outside of their homes, city, or state. As a result, it is impossible to have physical interactions with friends, family, and relatives in this situation; therefore, the mobile phone is a simple way to contact them. On the other hand, we must limit our usage of mobile phones to a set amount of time so that we can spend time with our loved ones and other well-wishers. As a result, we, as individuals, must cultivate this mindset and work toward more efficient and effective mobile usage.

REFERENCES

1. Abdullah O. Al-Zaghameem, Omar M. Al-Qawabah and Wajedah H. Al-Gmool (2016) " On the Effects of Mobile User Knowledge of Mobile Platform on the Utilization of Mobile Services " Volume (2016), Article ID 526516, Journal of Mobile Technologies, Knowledge and Society, 13 pages, DOI: 10.5171/2016.526516.
2. Afaliq, A. (2013). Smartphone improvements: Positive and negative impact on society.
3. Retrieved from https://sites.psu.edu/alwaleedafaliq/2013/09/19/smartphones-improvements-positive-andnegative-
4. Bhalla, S. (2017). Advantages and disadvantages of mobile. Retrieved from www.myeducorner.com/advantages-disadvantages-of-mobile-essay-speech-article/
5. Gupta, S. and Kumar, N. (2016). Impact of Mobile Phone on Youth: A Psycho-Social Study, *International Journals of Multidisciplinary Research*, *5*(4), 50-56
6. Goswami, V and Singh, D. R. (2016) Impact of mobile phone addiction on adolescent's life: A literature review. *International Journal of Home Science*, *2*(1): 69-74
7. Kelly, J. (2018). The Troubling side effects of smartphones. Retrieved from https://m.medicalxpress.com/news/2018-08-side-effects-smartphones.html
8. Lakshmi, K. R. (2016). Smartphone impact on today's society. *International Journal of Multidisciplinary Research and Development*, 3(5), 269-272
9. Lenord, J. (2015). 16 Seriously damaging side effects of your smartphone addiction. Retrieved From https://www.naturallivingideas.com/16-seriously-damaging-side-effects-of yoursmartphone- addiction/
10. Mount, R. (2012). Advantages and disadvantages of smartphone technology. Retrieved from https://www.mobilecon2012.com/8-advantages-and-disadvantages-of-smartphonetechnology/

Table No: 1 Socio-economic Status of the Respondents

Type of Occupation	**Frequency**	**Percentage (%)**
Student	212	76.26
Business	7	2.52
Job	43	15.46
Unemployed	16	5.76
Total	**278**	**100.00**
Family type	**Frequency**	**Percentage (%)**
Nuclear	223	80.22
Joint	55	19.78
Total	**178**	**100.00**
Number of siblings	**Frequency**	**Percentage (%)**
Less than 2	153	55.04
02 to 05	118	42.45
More than 5	7	2.51
Total	**278**	**100.00**

Table No: 2 Uses of Smartphone

Period of Using Smartphone	**Frequency**	**Percentage (%)**
Less than 5 years	71	25.54
5-10 years	161	57.91
More than 10 years	46	16.55
Total	**278**	**100.00**
Frequency of Uses	**Frequency**	**Percentage (%)**
Often	93	33.45
When necessary	67	24.1
Almost all the time in a day	118	42.45
Total	**278**	**100.00**

Table No.3 Purpose of Using Smartphone

Purpose of Using Smartphone	**Number of respondents**	**Percentage (%)**
Receiving and making calls	211	75.9
Study purpose	228	82.01
Using social media	214	76.98
Browsing internet	178	64.03
Chatting and sharing videos and images	157	56.47

(Multiple responses, N = 278)

Table No.:4 Social Media Platforms using to Interact with Friends and Family Members

Social Media Platforms using to Interact with Friends and Family Members	**Number of respondents**	**Percentage (%)**
Facebook	231	83.09
WhatsApp	264	94.96
Twitter	21	7.55
Telegram	44	16.83
Instagram	161	57.91
Others	37	13.31

(Multiple responses, N = 278)

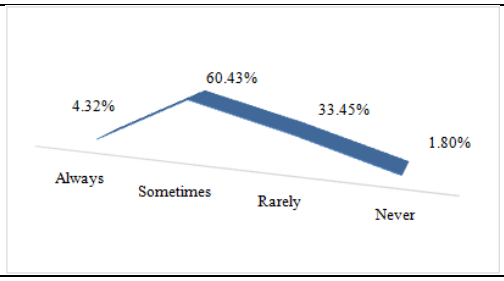

Figure No.: 1 Using a smartphone when you are with your Friends and Family

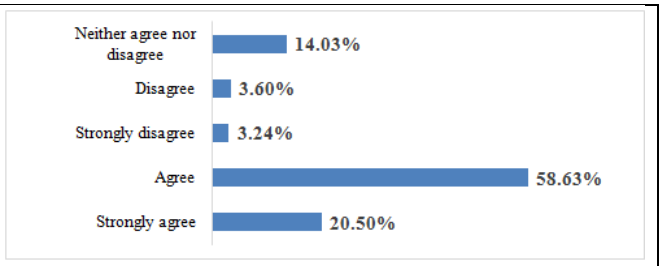

Figure No.: 2 The presence of Technology affects Face to Face Communication Negatively

Indian Journal of Natural Sciences *www.tnsroindia.org.in ©IJONS*

Vol.15 / Issue 83 / Apr / 2024 *International Bimonthly (Print) – Open Access* *ISSN: 0976 – 0997*

RESEARCH ARTICLE

GC-MS Based Phytoconstituents Profiling of Ethanolic Extracts of Leaves, Callus, Root and Stem of *Anisomeles malabarica*

Bhuvaneshwari R[1]* and R. Anandhan[2]

[1]Ph.D. Scholar, Plant Molecular Biology and Biotechnology, Faculty of Agriculture, Department of Genetics and Plant Breeding, Annamalai University, Tamil Nadu, India.
[2]Assistant Professor, Faculty of Agriculture, Department of Genetics and Plant Breeding, Annamalai University, Tamil Nadu, India.

Received: 01 Oct 2023 Revised: 22 Dec 2023 Accepted: 16 Mar 2024

***Address for Correspondence**
Bhuvaneshwari R
Ph.D. Scholar, Plant Molecular Biology and Biotechnology,
Faculty of Agriculture,
Department of Genetics and Plant Breeding,
Annamalai University, Tamil Nadu, India.
Email: bioanandan@gmail.com

ABSTRACT

The present effort was intended to investigate *Anisomeles malabarica* for phytochemical compounds and characterize the chemical constituents of plant using GC-MS. The shade dried leaf, Callus, Root and stem powder of *Anisomeles malabarica* was extracted with Methanol overnight, filtered and concentrated. The GC Clarus 500 (Perkin Elmer) used in the investigation employed a column packed with Elite- 5MS (5%Diphenyl / 95% Dimethyl poly siloxane, 30mm x 0.25mm x0.25µmdf) and the components were separated using Helium (1mL/min) as the carrier gas. The 2 µl sample extract injected into the instrument was detected by the Turbo mass gold detector (Perkin Elmer) with the aid of the Turbomass 5.2 software. The GC-MS analysis provided different peaks determining the presence of various phytochemical for leaf, Callus, Root and stem of *Anisomeles malabarica* . The phytochemical and GC-MS profiling of ethanolic extract ofleaf, Callus, Root and stem of *Anisomeles malabarica* revealed the presence of bioactive compounds with important medicinal properties. Hence, the presence of these phytochemicals could be responsible for the therapeutic effects of the plant.

Keywords: *Anisomeles malabarica* , Methanolic extract, GC-MS analysis, Phytoconstituents.

INTRODUCTION

Plants are used as medicines in various cultures and serve as a source of many potent drugs due to the presence of certain bioactive compounds for pharmaceutical industries Plants contain different phytochemicals, also known as secondary metabolites. Phytochemicals are useful in the treatment of certain disorders by their individual, additive, or synergic actions to improve health [1]. Phytochemicals are vital in pharmaceutical industry for development of new drugs and preparation of therapeutic agents. The development of new drugs starts with identification of active principles from the natural sources [2]. The screening of plant extracts is a new approach to find therapeutically active compounds in various plant species. Phytochemicals such as flavonoids, tannins, saponins, alkaloids, and terpenoids have several biological properties which include antioxidant, anti-inflammatory, anti-diarrhea, anti-ulcer, and anticancer activities, among others [3]; [4] During the last decade, use of traditional medicine has prolonged globally and has gained attractiveness. With the incredible expansion in the use of traditional medicine worldwide, safety and efficiency as well as quality control of herbal medicines and traditional therapies have become important concerns for both health authorities and the public [5].There is still a significant lack of research data in this field. In the absence of pharmacopoeia data on the various plant extracts, it is not possible to isolate or standardize the active contents having the desired effects [6]. Screening of active components from plants has direct to the development of new medicinal drugs which have efficient protection and treatment role against various diseases [7]. The present study is designed to investigate the secondary metabolites of *Anisomeles malabarica* and characterization of compounds using GC-MS analysis to explore the presence of phytoconstituents which could be helpful to treat many diseases and disorders [8] Large number of medicinal plants and their purified constituents has shown beneficial therapeutic potentials. With this situation, this study was aimed to identify the phytoconstituents present in methanolic extract of Anisomeles malabarica using GC-MS analysis.

MATERIALS AND METHODS

Chemicals

All the chemicals and reagents used for the research were of analytical grade.

Collection and Preparation of Plant

The leaf, Callus, Stem, Root of the *Anisomeles malabarica* plant were collected from the natural habitats of Chidambaram, Cuddalore District of Tamilnadu, India. The samples were washed thoroughly in running tap water to remove soil particles and adhered debris and finally washed with sterile distilled water. The leaf, Callus, Stem, Root of the *Anisomeles malabarica* plant were shade dried and ground into fine powder. The powdered materials were stored in air tight polythene bags until use.

Plant sample extraction

Fifty grams of powdered sample was extracted with methanol overnight and filtered through ash less filter paper with sodium sulphate and the extract was concentrated. The extract was analyzed using the Clarus 500 GC-MS (Perkin Elmer). 2 µL of the methanolic extract of *Anisomeles malabarica* was employed for GC-MS analysis.

GC-MS analysis

The Clarus 500 GC (Perkin Elmer) used in this analysis. It employed a fused silica column packed with Elite -5MS (5%Diphenyl / 95% Dimethyl poly siloxane, 30mm x 0.25mm x0.25µm df) and the components were separated using helium as carrier gas at a constant flow of 1 mL/ min. The 2 µL sample extract injected into the instrument. It was detected by the Turbo gold mass detector (Perkin Elmer) with the aid of Turbo mass 5.2 software. During the GC process the oven was maintained at a temperature of 110^0c with 2 min holding. The injector temperature was set at 250^0c. The different parameters involved in the operation of the Clarus 500 MS were also standardized. The Inlet line temperature was 200^0C and source temperature was 200^0C. Mass spectra were taken at 70 eV; a scan interval of 0.5s

and fragments from 45-450 Da. The MS detection was completed in 36 min. The detection employed the NIST ver. 2.0-year 2005 library. Gas chromatography-mass spectroscopy (GC-MS) is a combined analytical technique used to determine and identify compounds present in a plant sample. GC-MS plays an essential role in the phytochemical analysis and chemotaxonomic studies of medicinal plants containing biologically active components.

RESULTS AND DISCUSSION

The results concerning to GC-MS analysis led to the identification of number of compounds from the GC fractions of the ethanolic extract of *Anisomeles malabarica* . These compounds were identified through mass spectrum attached with GC [9]. The active principles with their retention time (RT), molecular formula (MF), molecular weight (MW) and concentration (%) were tabulated in the given tables. The results revealed that the presence of 27 differenent compounds present in the ethanolic extract of *Anisomeles malabarica* leaf, stem, callus and root. From the results, it was clear that, totally, 108more different phyto-constituents were present in the *Anisomeles malabarica* [10].

Gas Chromatography- Mass Spectrometry (GC-MS) is a precious tool for reliable detection of bioactive constituents. This study results were interpreted. By interpreting these compounds, it is found that *Anisomeles malabarica* possesses various therapeutical applications [11]. The present study characterized the chemical profile of *Anisomeles malabarica* using GC-MS. The GC chromatogram shows the relative concentration of various compounds getting eluted as a function of retention time. The heights of the peak point out the relative concentration of the presented components. The mass spectrometer analyzes the compounds eluted at different times to identify the nature and structure of the compounds [12]. The investigation concluded that the stronger extraction capacity of methanol have produced number of active constituents responsible for many biological activities. So these might be utilized for the development of traditional medicines and further investigation needs to elute novel active compounds from the medicinal plants which may be created a new way to treat many incurable diseases including cancer [13]. To separate volatile substances in a mixture, gas chromatography is normally utilized. The biological components of the extracted solvent were examined using a gas chromatography-mass spectrometer (GCMS) [14]. Gas chromatography coupled with mass spectroscopy was performed to analyze and identify the volatile and non-volatile nature of phytochemicals present in the three different extracts such as chloroform, ethyl acetate and methanolAmong this, ethanolic extract possessed more than 24, in that 8 phyto-constituents are considered as major and remaining 16 are considered as minor based on the percentage of peak area. Tridecyl acrylate, Tetratetracontane, Phytol, acetate, Hexadecane, Phytol, Heptadecane,Nonadecane and ethyl palmitate.[8].

Similarly, in other studies reported that the extract revealed the presence of 7 major and 12 minor phytoconstituents such as Tridecyl acrylate 1- Dodecanol, Phytol, acetate, nDecylpropanoate,Perhydrofarnesyl acetone and (E)-phytol [15]. The chloroform extract 4 major and 10 minor phytoconstituents were found such as Hentriacontane (45.29), 2-methyloctacosane (12.35), Tetratetracontane (8.31) and Cholesteryl ethyl ether (7.08). From the results, it was clear that, totally, 57more different phyto-constituents were present in the *Anisomeles malabarica* . All of them were aliphatic and aromatic compound; the mass spectra of the phyto-constituents were matched with those found in the NIST/NBS spectral database. [8]. The GC-MS analysis of different extracts of *Anisomeles malabarica* lead to the identification of 97 phytoconstituents. These compounds were identified through mass spectrometry attached with GC [16]. The mass spectrometer analyzes the compounds eluted at different times to identify the nature and structure of the compounds. Five different extracts possess unique physicochemical characteristics which may be attributed to the compounds naturally present in significant quantities in the leaves of *Anisomeles malabarica* . Phytol was proven to exhibit antioxidant and antinociceptive effects. Phytol, precursor of synthetic vitamin E and vitamin K, was found to be cytotoxic against breast cancer cell lines (MCF7). In addition, squalene possessed antioxidant, chemopreventive, antitumor and hypocholesterolemic activities [17].

CONCLUSION

Several phytochemical evaluations have been carried out in *Anisomeles malabarica* using GC-MS. This analysis showed the existence of various compounds with different chemical structures. The occurrence of various bioactive compounds proves the purpose of *Anisomeles malabarica* for various disorders. However, selection of individual phytochemical constituents may proceed to find an innovative drug. Hence, this type of effort will be supportive for in depth study. Further, extensive research is required to identify and explore bioactive compounds from this plant.

REFERENCES

1. Olivia, N. U., Goodness, U. C., Obinna, O. M. (2021). Phytochemical profiling and GC-MS analysis of aqueous methanol fraction of Hibiscus asper leaves. *Future Journal of Pharmaceutical Sciences 7*, 1-5.
2. Ashraf, M. A. (2020). Phytochemicals as potential anticancer drugs: time to ponder nature's bounty. *BioMed research international* 2020.
3. Ullah, A., Munir, S., Badshah, S. L., Khan, N., Ghani, L., Poulson, B. G., Jaremko, M.(2020).Important flavonoids and their role as a therapeutic agent. *Molecules* 25(22): 5243.
4. Prasathkumar, M., Anisha, S., Dhrisya, C., Becky, R., Sadhasivam, S. (2021). Therapeutic and pharmacological efficacy of selective Indian medicinal plants–a review. *Phytomedicine Plus* 1(2): 100029.
5. Ekor, M. (2014). The growing use of herbal medicines: issues relating to adverse reactions and challenges in monitoring safety. *Frontiers in pharmacology* 4: 177.
6. Amudha, M., Rani, S. (2014). Assessing the bioactive constituents of Cadabafruticosa (L.) Druce through GC-MS. *Int. J. Pharm6*, 383-385.
7. Zhang, L., Song, J., Kong, L., Yuan, T., Li, W., Zhang, W. Du, G. (2020). The strategies and techniques of drug discovery from natural products. *Pharmacology & Therapeutics*, 216: 107686.
8. Supriya K. A.,LaliGrowther. (2021). Screening of phytochemicals, gc-ms based phytoconstituents profiling and antibacterial efficiency of leaves extracts of Anisomeles malabarica . International journal of pharmaceutical sciences and research., Vol. 12(5): 2902-2912.
9. Krishna, S., Chandrasekaran, S., Dhanasekar, D.,Perumal, A. (2019). GCMS analysis, antioxidant and antibacterial activities of ethanol extract of *Anisomeles malabarica* (L.) R. Br. ex. Sims leaves. *Asian J. Pharm. Pharmacol*, 5: 180-187.
10. Mohanraj, R., Someshwar, N., Pankaj, J. (2012). Bioactivity studies on Anisomeles malabarica (AM) R. Br. *Journal of Biotechnology and Biotherapeutics* 2(9): 1-8.
11. Nasrin, S., Islam, M. N., Tayab, M. A., Nasrin, M. S., Siddique, M. A. B., Emran, T. B.,Reza, A. A. (2022). Chemical profiles and pharmacological insights of *Anisomelesindica*Kuntze: An experimental chemico-biological interaction. *Biomedicine & Pharmacotherapy*, 149: 112842.
12. Lawal, B., Shittu, O. K., AbdulRasheed-Adeleke, T., Ossai, P. C., Ibrahim, A. M. (2015). GC-MS determination of bioactive constituents of giant African Snail (*Archachatinamaginata*) Haemolymph.
13. Gnanashree, G., Sirajudeen, P. M. (2018). Determination of bioactive compounds in ethanolicextract of *Carallumaindica* using GC-MS technique. *Journal of Pharmacognosy and Phytochemistry 7*(6): 1675-1677.
14. Falaki, F. (2019). Sample preparation techniques for gas chromatography. In *Gas Chromatography-Derivatization, Sample Preparation, Application*. IntechOpen.
15. Doan, V. T., Pham, V. T., Le, C. H. D., Luu, T. T. N., Dam, T. U., Le, H. K. H., Ngo, T. T. D. (2023). Two new halogenated sesquiterpene lactones from Palisada intermedia. *Natural Product Research*, 1-6.
16. Kaviyarasi N. S., Priyadarshini G.,Divya Ravichandran. 2023. Phytochemical exploration of Anisomeles malabarica r. Br. Leaves by solvent extraction and gc-ms. International Journal of Pharmaceutical Sciences and Research. 2023; Vol. 14(9): 4440-4450.
17. Casuga, F. P., Castillo, A. L., Corpuz, M. J. A. T. (2016). GC–MS analysis of bioactive compounds present in different extracts of an endemic plant Broussonetialuzonica (Blanco)(Moraceae) leaves. *Asian Pacific Journal of Tropical Biomedicine 6*(11): 957-96

Table: 1 Compounds identified in the ethanolic extract of *Anisomeles malabarica* leaf

Peak	Retention Time	Area	Area%	Height	Height%	A/H	Name
1	8.905	154750	0.56	54093	1.14	2.86	Phenol,3,5-bis(1,1-dimethylethyl)-
2	10.024	178353	0.65	53911	1.14	3.31	DiethylPhthalate
3	10.975	88365	0.32	38671	0.82	2.29	Heptadecane
4	11.117	94514	0.34	30620	0.65	3.09	Tetradecane, 2,6,10-trimethyl-(CAS)2,6,10-T
5	12.582	295524	1.07	122082	2.58	2.42	NEOPHYTADIENE
6	12.687	137681	0.50	44587	0.94	3.09	2-Pentadecanone,6,10,14-trimethyl-
7	12.792	173952	0.63	23043	0.49	7.55	2-(2',4',4',6',6',8',8'-Heptamethyltetrasiloxan-2'
8	13.109	459794	1.67	109987	2.32	4.18	1,2-Benzenedicarboxylic acid,diundecylester
9	13.524	323736	1.17	104963	2.22	3.08	Hexadecanoicacid,methylester(CAS)Methy
10	13.840	260576	0.95	86125	1.82	3.03	EICOSAMETHYLCYCLODECASILOXAN
11	13.974	3628299	13.16	754147	15.92	4.81	l-(+)-Ascorbic acid 2,6-dihexadecanoate
12	14.119	807408	2.93	198051	4.18	4.08	Dibutyl phthalate
13	14.308	667957	2.42	38280	0.81	17.45	1-Isopropylidene-3-methyl-3-vinylcyclobutane
14	14.550	305578	1.11	99408	2.10	3.07	Pentadecanal-
15	14.975	169895	0.62	17751	0.37	9.57	Docosanoicacid(CAS)Behenicacid
16	15.175	187915	0.68	26166	0.55	7.18	1-Eicosanol(CAS)n-Eicosanol
17	15.339	701843	2.55	187260	3.95	3.75	TETRACOSAMETHYLCYCLODODECASI
18	15.510	1144658	4.15	190804	4.03	6.00	Menthol
19	15.577	545805	1.98	151891	3.21	3.59	Heptadecanoicacid,16-methyl-,methylester
20	15.767	1362574	4.94	157961	3.33	8.63	2,8,9-Trioxa-5-aza-1-silabicyclo[3.3.3]undeca
21	15.865	3311785	12.01	329248	6.95	10.06	9-Octadecenoic acid(Z)-(CAS)Oleicacid
22	16.046	2627819	9.53	367144	7.75	7.16	Octadecanoicacid
23	16.325	1153412	4.18	97734	2.06	11.80	[1R*,2R*]-1-acetyl-1,2-dihydroxycyclohex-3-
24	16.505	1305875	4.74	138330	2.92	9.44	1,3-Benzenedicarboxylicacid,bis(2-ethylhexy
25	16.976	301379	1.09	105008	2.22	2.87	Cyclononasiloxane,octadecamethyl-
26	18.758	3974457	14.42	615541	12.99	6.46	cycloheptan,4-methylen-1-methy
27	18.950	259702	0.94	76090	1.61	3.41	ethyl1-hexyl-4-hydroxy-2(1h)-ox

Table: 2 Compounds identified in the ethanolic extract of *Anisomeles malabarica* Callus

Peak	Retention Time	Area	Area%	Height	Height %	A/H	Name
1	8.899	270652	0.84	111117	1.64	2.44	PHENOL,2,4-BIS(1,1-DIMETHYLETHYL)
2	10.017	182571	0.57	57815	0.85	3.16	DiethylPhthalate
3	11.108	329576	1.02	87543	1.29	3.76	TETRADECANE
4	12.100	227344	0.71	47649	0.70	4.77	Nonane,5-(2-methylpropyl)-
5	12.215	193178	0.60	64733	0.96	2.98	SILIKONFETTSE30(GREVELS)
6	12.672	295836	0.92	47617	0.70	6.21	2-Pentadecanone,6,10,14-trimethyl-
7	13.096	450367	1.40	128846	1.90	3.50	1,2-Benzenedicarboxylic acid,diisodecyl

							ester
8	13.519	965553	3.00	327494	4.84	2.95	HEXADECANOICACID,METHYLESTER
9	13.753	254942	0.79	102939	1.52	2.48	7,9-Di-tert-butyl-1-oxaspiro(4,5)deca-6,9-dien
10	13.832	383180	1.19	110571	1.63	3.47	1H-PURIN-6-AMINE, [(2-FLUOROPHENY
11	13.965	8029670	24.95	1798220	26.58	4.47	l-(+)-Ascorbic acid 2,6-dihexadecanoate
12	14.108	1076836	3.35	269516	3.98	4.00	Dibutyl phthalate
13	14.233	249366	0.77	82419	1.22	3.03	Eicosane
14	14.983	350138	1.09	52565	0.78	6.66	l-(+)-Ascorbicacid 2,6-dihexadecanoate
15	15.180	218949	0.68	71990	1.06	3.04	1-Octadecanol
16	15.334	1053645	3.27	238066	3.52	4.43	CYCLODODECASILOXANE,TETRACOS
17	15.400	268751	0.84	86380	1.28	3.11	9,12,15-Octadecatrienoicacid,methylester,(Z
18	15.570	788878	2.45	144760	2.14	5.45	Methylstearate
19	15.758	823773	2.56	299728	4.43	2.75	1-ALLYL-2,8,9-TRIOXA-5-AZA-1-SILABIC
20	15.832	3035185	9.43	410683	6.07	7.39	Octadec-9-enoic acid
21	16.038	3545137	11.02	568106	8.40	6.24	Octadecanoicacid
22	16.317	936983	2.91	122795	1.81	7.63	Tetracosane
23	16.443	493839	1.53	134298	1.98	3.68	9-Octadecynoicacid,methylester
24	17.032	1372793	4.27	195532	2.89	7.02	5-Hexenoicacid,(9-decen-2-yl) ester
25	19.066	384722	1.20	113584	1.68	3.39	Cyclodecasiloxane,eicosamethyl-
26	19.353	336933	1.05	77762	1.15	4.33	SILIKONFETTSE30 (GREVELS)
27	20.116	393752	1.22	45023	0.67	8.75	1,2-Benzenedicarboxylicacid,dinonylester

Table: 3 Compounds identified in the ethanolic extract of *Anisomeles malabarica* Root:

Peak	R.Time	Area	Area%	Height	Height%	A/H	Name
1	5.316	41721	0.34	12353	0.57	3.38	1-PROPYNE
2	6.830	36579	0.30	19062	0.88	1.92	6-OXA-1-AZABICYCLO[3.1.0]HEXANE,5
3	6.925	44522	0.36	12236	0.56	3.64	CYCLOPROPANECARBONYLCHLORIDE
4	7.102	34490	0.28	24515	1.13	1.41	ALLYLFLUOROFORMATE
5	7.201	35592	0.29	21366	0.98	1.67	BORANE,TRIETHYL-
6	8.912	123424	1.00	32013	1.47	3.86	Pentanoicacid,5-hydroxy-,2,4-di-t-butylphen
7	9.514	98168	0.80	22529	1.04	4.36	8,9,9,10,10,11-HEXAFLUORO-4,4-DIMETH
8	9.713	45698	0.37	22734	1.05	2.01	Cyclohexanone,2-propyl-
9	9.817	45058	0.37	13016	0.60	3.46	1,2,2-TRIMETHYLCYCLOPROPYLAMINE
10	10.035	211429	1.72	55500	2.55	3.81	DiethylPhthalate
11	10.217	66088	0.54	16155	0.74	4.09	Argon
12	10.667	36309	0.29	11841	0.55	3.07	1-PROPYNE
13	10.750	61320	0.50	12721	0.59	4.82	Propyne
14	10.977	33868	0.27	24242	1.12	1.40	2-(3-BUTOXY-2-HYDROXYPROPYL) MAL
15	12.346	2918222	23.69	211486	9.74	13.80	2-[5-(2-Methyl-benzooxazol-7-yl)-1H-pyrazol
16	12.508	770009	6.25	142385	6.55	5.41	1(2H)-NAPHTHALENONE,2-(3,3-DIMETH
17	12.617	586592	4.76	105530	4.86	5.56	3-(3-OXO-3H-BENZO[F]CHROMEN-2-YL)
18	12.717	330432	2.68	56622	2.61	5.84	BORANE,TRIETHYL-

19	13.119	155938	1.27	55078	2.54	2.83	Phthalicacid,butylundecylester
20	13.536	375505	3.05	108146	4.98	3.47	Hexadecanoicacid, methylester
21	13.772	49835	0.40	31730	1.46	1.57	7,9-Di-tert-butyl-1-oxaspiro(4,5)deca-6,9-dien
22	13.858	53464	0.43	25384	1.17	2.11	2,2,4,4,6,6,8,8,10,10,12,12,14,14,16,16,18,18
23	13.987	1633141	13.26	361270	16.63	4.52	l-(+)-Ascorbicacid 2,6-dihexadecanoate
24	14.131	410465	3.33	117546	5.41	3.49	Dibutyl phthalate
25	15.359	411208	3.34	96857	4.46	4.25	9-OCTADECENOICACID(Z)-,METHYLE
26	15.592	471246	3.83	76000	3.50	6.20	Heptadecanoicacid,16-methyl-,methylester
27	15.856	1341854	10.89	174786	8.05	7.68	Octadec-9-enoic acid

Table: 4 Compounds identified in the ethanolic extract of *Anisomeles malabarica* stem

Peak	R.Time	Area	Area%	Height	Height%	A/H	Name
1	9.698	299208	0.16	28402	0.13	10.53	9,9-Dimethoxybicyclo[3.3.1]nona-2,4-dione
2	11.858	419127	0.22	58083	0.26	7.22	Tetradecanoicacid(CAS)Myristicacid
3	12.570	407855	0.22	166690	0.74	2.45	NEOPHYTADIENE
4	13.520	522293	0.28	156946	0.69	3.33	Pentadecanoicacid,14-methyl-,methylester
5	13.835	258152	0.14	95072	0.42	2.72	Octasiloxane,1,1,3,3,5,5,7,7,9,9,11,11,13,13,
6	13.964	20258532	10.85	4079474	18.04	4.97	n-Hexadecanoicacid
7	14.108	3930216	2.11	709455	3.14	5.54	Dibutyl phthalate
8	14.342	424248	0.23	119369	0.53	3.55	(t-Butyl-dimethylsilyl)[2-methyl-2-(4-methyl-p
9	14.392	323177	0.17	81476	0.36	3.97	.alpha.-d-Glucofuranose,1,2-O-(2,2,2-trichlor
10	14.983	188099	0.10	31730	0.14	5.93	l-(+)-Ascorbicacid 2,6-dihexadecanoate
11	15.167	247192	0.13	51040	0.23	4.84	n-Pentadecanol
12	15.333	2072618	1.11	465671	2.06	4.45	9-Octadecenoicacid(Z)-,methylester(CAS)
13	15.818	96460723	51.68	9892897	43.75	9.75	9-Octadecenoicacid,1,2,3-propanetriylester,
14	16.026	48017751	25.72	4580894	20.26	10.48	Octadecanoicacid
15	16.783	1365120	0.73	199950	0.88	6.83	Octatriacontylpentafluoropropionate
16	16.875	971128	0.52	169610	0.75	5.73	Bicyclo[10.1.0]tridec-1-ene
17	16.960	1031315	0.55	235317	1.04	4.38	Cyclononasiloxane,octadecamethyl-
18	17.092	1077363	0.58	157380	0.70	6.85	Palmitoylchloride
19	17.752	388774	0.21	110971	0.49	3.50	Hexadecanoicacid,1-(hydroxymethyl)-1,2-eth
20	18.744	2168001	1.16	256785	1.14	8.44	Cycloheptane,4-methylene-1-methyl-2-(2-met
21	19.052	779221	0.42	146376	0.65	5.32	EICOSAMETHYLCYCLODECASILOXAN
22	19.338	1005820	0.54	99499	0.44	10.11	Cyclononasiloxane,octadecamethyl-
23	19.501	344520	0.18	60494	0.27	5.70	Tridecanedial
24	19.966	925143	0.50	152906	0.68	6.05	Oleoylchloride
25	20.100	203033	0.11	46801	0.21	4.34	Heptasiloxane,hexadecamethyl-
26	20.398	208863	0.11	45734	0.20	4.57	Octadecanoicacid,2,3-dihydroxypropylester
27	20.850	268625	0.14	57361	0.25	4.68	1,3,5-Trisilacyclohexane(CAS)Cyclocarbosil

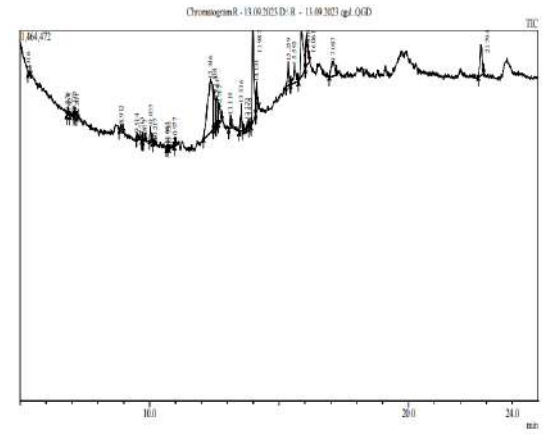

Fig. 1: GC MS chromatogram of the ethanolic extract of *Anisomeles malabarica* leaf

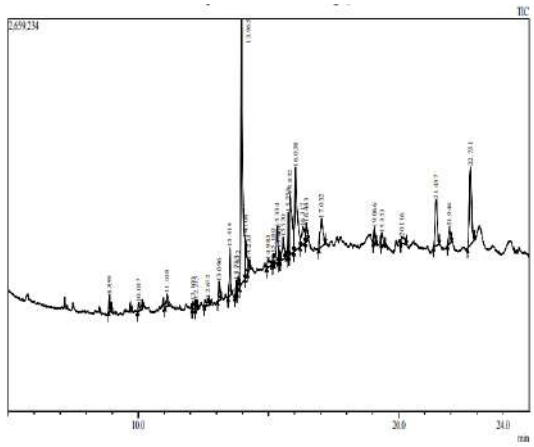

Fig. 2: GC MS chromatogram of the ethanolic extract of *Anisomeles malabarica* Callus

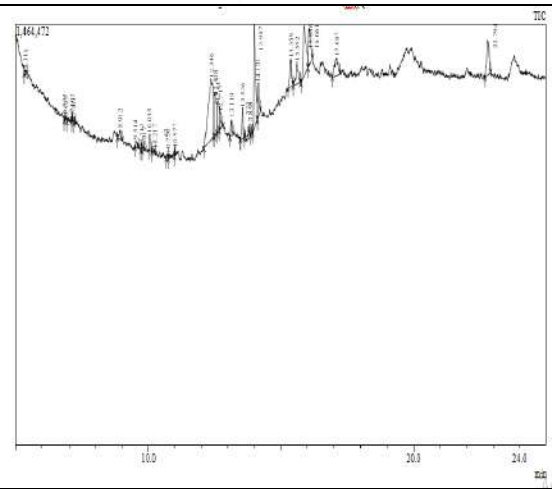

Fig. 3: GC MS chromatogram of the ethanolic extract of *Anisomeles malabarica* Root

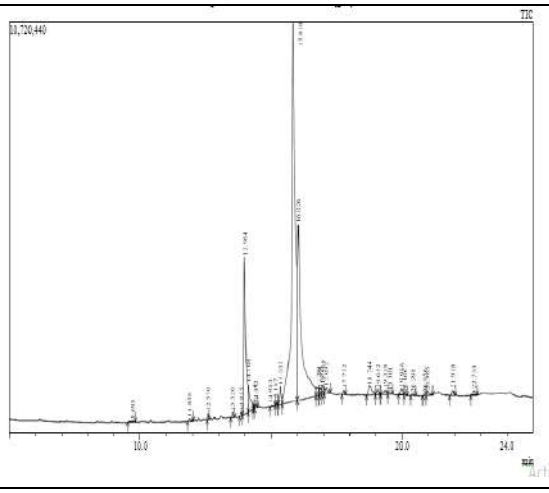

Fig. 4: GC MS chromatogram of the ethanolic extract of *Anisomeles malabarica* Stem

Indian Journal of Natural Sciences *www.tnsroindia.org.in ©IJONS*

Vol.15 / Issue 83 / Apr / 2024 *International Bimonthly (Print) – Open Access* *ISSN: 0976 – 0997*

REVIEW ARTICLE

A Review of Technologies and Challenges Over Wind Power in the Context of Renewable Energy Sources

Ayyappan.P[1*], Abirami P[2], Kiruthika A V[3] and Rajeswari B[4]

[1]Associate Professor, Department of Botany, Government Arts College, Melur, (Affiliated to Madurai Kamaraj University) Madurai, Tamil Nadu, India.
[2]Assistant Professor, Department of Botany, Seethalakshmiachi College for Women,Pallathur, (Affiliated to Alagappa University, Karaikudi) Sivagangai, Tamil Nadu, India.
[3]Assistant Professor, Department of Physics, Seethalakshmiachi College for Women, Pallathur (Affiliated to Alagappa University, Karaikudi) Sivagangai, Tamil Nadu, India.
[4]Associate Professor, Department of Science and Humanities, Kurinji College of Engineering and Technology, Manapparai, Tiruchirappalli (Affiliated to Anna University, Chennai) Tamil Nadu, India.

Received: 30 Dec 2023 Revised: 09 Jan 2024 Accepted: 27 Mar 2024

***Address for Correspondence**
Ayyappan.P
Associate Professor,
Department of Botany,
Government Arts College, Melur,
(Affiliated to Madurai Kamaraj University)
Madurai, Tamil Nadu, India.
Email: ayyappanbotany73@gmail.com

ABSTRACT

In recent decades, wind energy has gained prominence in power grids. This is extremely important in a setting where energy consumption requirements are rising and there is an environmental crisis. This is serious, and it is visible as a result of the global warming phenomenon. The general framework of wind innovation and practical implementations are looked in this review article. Wind energy is the largest source of sustainable energy while comparing to hydroelectricity. Since wind has been used for centuries, the modern wind energy industry began during the oil crisis in the 1970s. However, it is inconsistent. The majority of wind turbines are now built on land, though some are built at sea, frequently in wind farms. Because wind energy is intermittent, it must be supplemented by other power sources. Wind energy can be beneficial in general. However, it has not yet achieved full matrix equality with fossil life forms.

Key words: wind, energy, turbines, power, challenges

INTRODUCTION

Wind energy has grown in popularity in power grids around the world in recent decades. This existence is critical in an environment where energy consumption needs are increasing, as well as an environmental crisis that, at best, can be classified as serious and can be observed through a process known as global warming(Singh *et al.,* 2013). The scientific community appears to be in broad agreement that greenhouse gas emissions are to blame for the current recession, reinforcing the belief that humanity should devote all available resources to the generation of electricity from sources other than fossil fuels (Solarin & Bello, 2022).The rise of renewable energy sources, particularly wind energy, is definitely appropriate. Since the turn of the century, there has been a significant increase in the development on wind energy converters and associated technologies. The research and investigation of wind energy is a hugely popular field of study(Waheeb *et al.,* 2023). There are numerous research sub-domains in this area, including wind energy conversion systems, wind power modelling, energy efficiency and storage, energy economics, wind forecasts, and wind energy's effects on the environment(Porté-Agel *et al.,* 2020).

Finding environmentally friendly energy sources, such as wind energy, is critical due to rising energy demand and the depletion of nonrenewable energy sources. In order to remain competitive in the energy market, wind turbines designers and manufacturers seek the best solutions to meet goals such as minimizing investment, reducing blade size, and increasing annual production(Boretti & Castelletto, 2020). This will eventually result in lower energy costs and higher profits. Although the majority of research studies focused on lowering the cost of wind energy, many also focused on improving the performance of wind turbines while taking multiple disciplinary goals into account(Soulouknga *et al.,* 2020). However, optimizing the shape of wind turbines does not always imply lowering energy costs. Kumar *et al.,*(2018)investigated wind flows, turbines, and wind power grid placement and concluded that economic indicators, regional laws, environmental concerns, and the presence of nearby flows all influence the best wind farm design.Kumar *et al.,*(2019) concluded that computer-aided structural analysis can find better and more cost-effective solutions for the complex engineering system subject to varying and irregular loads in wind turbine design in the context of wind turbine design, installation challenges, and process optimization. An important regarding wind energy technologies are discussed in this article in terms of their turbines, power and challenges. This will lead to a better understanding of wind energy and its potential to meet projected energy needs.

WIND ENERGY

Wind energy is a modified form of sunlight-based energy that is produced in the core of an object by the atomic interaction between hydrogen (H) and helium (He).The H-He dissolving process creates flow of heat and electromagnetic waves which propagate in every direction from the sun to space(Sawant *et al.,* 2021). Even though the Earth only receives a small portion of solar radiation, it provides the majority of the planet's energy requirements.A significant source of modern dynamism and a major player in the global dynamism market is wind energy.The specialized growth and rapid organization of wind energy are perceived as best-in-class energy innovations, as is the absence of a practical upper limit for the amount of wind that can be coordinated into the electrical system.The total amount of sun-directed energy that the Earth receives has been estimated to be around $1.8*10^{11}$ MW. Simply 2% of this solar energy is converted to wind energy, and about 35% of wind energy scatters within 1,000 meters of the Earth's surface (Bonanno *et al.,* 2023). Therefore, the amount of available breeze energy that can be converted into other forms of energy is about $1.26*10^{9}$ MW. Given that this estimate corresponds to a 20-fold increase in global energy consumption, wind energy has the potential to fundamentally meet the world's daily energy requirements(Kumar *et al.,* 2022). When compared to common energy sources, wind energy has many favorable conditions and advantages. As an endless and free source of everyday life, it is widely available and abundant throughout the world. Furthermore, increased wind energy use would contribute to a decrease in demand for nonrenewable energy sources, which may run out sooner or later this century depending on how they are currently used. Wind energy is significantly less expensive per kWh than solar energy (Grimsrud *et al.,* 2023). As a result, it is expected that breeze energy, the most encouraging source of energy, will play a critical role in the global energy supply in the 21stcentury.

WIND TURBINES

Wind turbines develop energy by using the moderately powerful wind to operate a generator. Wind is a pure and sustainable fuel source that never runs out because it is perpetually refilled by the sun's energy. This also does not generate any emissions. In some ways, wind turbines are an improvement over old windmills, but they now occasionally have three blades that rotate around a flat shape at the top of a steel tower. One of the most common and fashionable turbine designs could be a metal pinnacle with a rotor that has three sharp edges, as seen in Figure 1 (Kumar*et al.,* 2018).

The majority wind turbines start producing power at wind speeds of 3 to 4 m/s, reach their ostensible peak power at 15 m/s, and stop producing power altogether at 25 m/s or higher(Wang *et al.,* 2022). Three common types of rotating wind turbines used today are found in their region(Solarin & Bello, 2022):

1. Speed twist turbine with Induction Generator,
2. Variable speed turbine with Induction Generator
3. Variable speed turbine with Synchronous Generator

WIND SPEED

One of the most important fundamental characteristics in the production of electrified energy is wind speed. A few factors that are equivalent to geographic and climatic conditions control the variation in wind speed at every moment and in every house.Due to the possibility that wind speed could be a variable parameter, estimated wind speed information frequently uses related scientific techniques. Incorrect waves frequently delineate the varying tempos of daily standard breeze speeds. Another example is the curved pattern seen in diurnal variations of hourly breeze speed esteem, which are common figured qualities that support data between 1970 and 1984 in Dhahran, Asia(Lee & Xydis, 2023). The most velocity occurs at around 3oclock, demonstrating that the daytime wind speed increased as the day went on.This is important to take note of a significant variation in the average annual breeze speed over the 20-year period, and the more significant portion of the base qualities range from below 7.8 to very nearly 9.2 m/s. The semi-permanent learning of the breeze obtained from the condensed perception framework managed by the mechanical meteorological observatories. The results show that the mean annual breeze speed changes at the same locations (Rozante *et al.,* 2017).

CHALLENGES

The probability of a successful breeze energy structure entry is decreased by variations in network recurrence and voltage that complicate powerhouse operations. The amount of energy produced by wind farms could not be successfully transmitted all the way to clients, resulting in life being wasted. This is due to the constraints of a network framework. Further, high borrowing costs in Asian nations create a barrier to the expansion of the wind energy sector. The project financing strategy used for the majority of wind power comes with a 70:30 debt to equity ratio and high interest rates that result in a large debt under the challenging political and economic circumstances of the Asian nation(McKenna *et al.,* 2022).Innovation in wind rotating motors has come about as a result of ongoing improvements in turbine design, turning motor performance, and overall rotating motor efficiency. Turbine technology has undergone numerous ages of development and change, focusing on cutting-edge technologies, generators, and coordinate drive systems, pitch and yaw management systems, etc.

CONCLUSIONS

The evidence suggests that using wind energy as a long-term solution to global energy issues could be a viable option. However, the property's condition is evaluated. As a result, while the resource is currently useful enough to support many business developments, it has the potential to become infinite if vast technological opportunities are realized. Wind energy has proven to be not only environmentally but also socially beneficial in terms of supporting the wind industry while reducing price competition. A new certificate market is taking over all of the benefits, and

many governments have heard that wind businesses are prepared to require up to the opened business. Furthermore, in relation to the small market, an established set of values should be confirmed. From a societal point of view, the fact that the wind industry supports local development encourages its property. In addition, its proven genuine impact on the population at large may help to impair the general public's personality traits. Finally, it is essential to advocate for additional research into potential environmental analyses. When considering a replacement power plant or reconsidering an existing one, it is prudent to first review the findings of studies related to ecological impact analysis.

REFRENCES

1. Bonanno, R., Viterbo, F., & Maurizio, R. G. (2023). Climate change impacts on wind power generation for the Italian peninsula. *Regional Environmental Change*, *23*(1). https://doi.org/10.1007/s10113-022-02007-w
2. Boretti, A., &Castelletto, S. (2020). Trends in performance factors of wind energy facilities. *SN Applied Sciences*, *2*(10). https://doi.org/10.1007/s42452-020-03526-z
3. Grimsrud, K., Hagem, C., Haaskjold, K., Lindhjem, H., &Nowell, M. (2023). Spatial Trade-Offs in National Land-Based Wind Power Production in Times of Biodiversity and Climate Crises. *Environmental and Resource Economics*. https://doi.org/10.1007/s10640-023-00764-8
4. Kumar, A., Khan, M. Z. U., & Pandey, B. (2018). Wind Energy: A Review Paper. *Gyancity Journal of Engineering and Technology*, *4*(2), 29–37. https://doi.org/10.21058/gjet.2018.42004
5. Kumar, A., Pal, D., Kar, S. K., Mishra, S. K., & Bansal, R. (2022). An overview of wind energy development and policy initiatives in India. *Clean Technologies and Environmental Policy*, *24*(5), 1337–1358. https://doi.org/10.1007/s10098-021-02248-z
6. Kumar, A., Sadhu, P. K., & Singh, J. (2019). A technological review of wind power generation. *IOP Conference Series: Materials Science and Engineering*, *691*(1). https://doi.org/10.1088/1757-899X/691/1/012017
7. Lee, J., & Xydis, G. (2023). Floating offshore wind projects development in South Korea without government subsidies. *Clean Technologies and Environmental Policy*. https://doi.org/10.1007/s10098-023-02564-6
8. McKenna, R., Pfenninger, S., Heinrichs, H., Schmidt, J., Staffell, I., Bauer, C., Gruber, K., Hahmann, A. N., Jansen, M., Klingler, M., Landwehr, N., Larsén, X. G., Lilliestam, J., Pickering, B., Robinius, M., Tröndle, T., Turkovska, O., Wehrle, S., Weinand, J. M., &Wohland, J. (2022). High-resolution large-scale onshore wind energy assessments: A review of potential definitions, methodologies and future research needs. *Renewable Energy*, *182*, 659–684. https://doi.org/10.1016/j.renene.2021.10.027
9. Porté-Agel, F., Bastankhah, M., &Shamsoddin, S. (2020). Wind-Turbine and Wind-Farm Flows: A Review. *Boundary-Layer Meteorology*, *174*(1), 1–59. https://doi.org/10.1007/s10546-019-00473-0
10. Rozante, J. R., Rozante, V., Alvim, D. S., Manzi, A. O., Chiquetto, J. B., D'Amelio, M. T. S., & Moreira, D. S. (2017). Variations of carbon monoxide concentrations in the Megacity of São Paulo from 2000 to 2015 in different time Scales. *Atmosphere*, *8*(5). https://doi.org/10.3390/atmos8050081
11. Sawant, M., Thakare, S., Rao, A. P., Feijóo-Lorenzo, A. E., &Bokde, N. D. (2021). A review on state-of-the-art reviews in wind-turbine-and wind-farm-related topics. *Energies*, *14*(8). https://doi.org/10.3390/en14082041
12. Singh, M., Muljadi, E., Gevorgian, V., &Santoso, S. (2013). Wind Power Generation. *Green Energy and Technology*, *59*, 111–149. https://doi.org/10.1007/978-1-4471-5104-3
13. Solarin, S. A., & Bello, M. O. (2022). Wind energy and sustainable electricity generation: evidence from Germany. *Environment, Development and Sustainability*, *24*(7), 9185–9198. https://doi.org/10.1007/s10668-021-01818-x
14. Soulouknga, M. H., Oyedepo, S. O., Doka, S. Y., &Kofane, T. C. (2020). Evaluation of the cost of producing wind-generated electricity in Chad. *International Journal of Energy and Environmental Engineering*, *11*(2), 275–287. https://doi.org/10.1007/s40095-019-00335-y
15. Waheeb, S. A., Al-Samarai, R. A., Alias, M. F. A., & Al-Douri, Y. (2023). Investigation of wind energy speed and power, and its impact of sustainability: Saudi Arabia a model. *Journal of Umm Al-Qura University for Engineering and Architecture*, *14*(2), 142–149. https://doi.org/10.1007/s43995-023-00019-z

16. Wang, Y., Chao, Q., Zhao, L., & Chang, R. (2022). Assessment of wind and photovoltaic power potential in China. *Carbon Neutrality*, *1*(1). https://doi.org/10.1007/s43979-022-00020-w

Figure 1 Wind Turbine

Indian Journal of Natural Sciences *www.tnsroindia.org.in ©IJONS*

Vol.15 / Issue 83 / Apr / 2024 *International Bimonthly (Print) – Open Access* *ISSN: 0976 – 0997*

RESEARCH ARTICLE

Synthesis and Biological Evaluation of Some Novel 1, 3, 5-Triaryl-2-Pyrazolines Derivatives

J. Subbarao[1]*, S. Ravi Chandra[2] and Venkata Rao[1]

[1]Professor, Department of Pharmaceutical Chemistry, Chebrolu Hanumaiah Institute of Pharmaceutical Sciences, (Affiliated to Acharya Nagarjuna University), Andhra Pradesh, India.
[2]Associate Professor, Department of Pharmaceutical Chemistry, Chebrolu Hanumaiah Institute of Pharmaceutical Sciences, (Affiliated to Acharya Nagarjuna University), Andhra Pradesh, India.

Received: 16 Feb 2024 Revised: 09 Mar 2024 Accepted: 27 Mar 2024

***Address for Correspondence**
J. Subbarao
Professor,
Department of Pharmaceutical Chemistry,
Chebrolu Hanumaiah Institute of Pharmaceutical Sciences,
(Affiliated to Acharya Nagarjuna University),
Andhra Pradesh, India.
Email: subbapharmaco@gmail.com

ABSTRACT

In the current study, 3, 4-dichloroacetophenone yields the appropriate chalcones when it condenses with various aromatic aldehydes in aqueous ethanolic solution. By reacting with phenyl hydrazine, these chalcones create 1, 3, and 5-triaryl-2-pyrazoline derivatives. All of the produced compounds were evaluated using elemental analysis, IR, and NMR spectral data. The synthetic materials were examined for a range of biological functions. The substance 2o, which has a 2''-thienyl ring at the scaffold's fifth position, exhibits strong antifungal activity with a MIC of 2 g/mL. At MIC 1.6 g/mL, the compound 2f and 2h with position-5 moieties of 2,4,6-difluorophenyl and 4,6-trifluorophenyl demonstrated good antitubercular action.

Keywords: Condensation, Phenyl hydrazine, Pyrazoline, Antifungal and cytotoxicity.

INTRODUCTION

Pyrazoline (1) has the molecular formula $C_3H_6N_2$ and 1,2-diazole is the formal name for pyrazole.They possess two nitrogen atoms, are aromatic, and share characteristics with both pyridine and pyrrole. The easiest way to describe the structure of pyrazole is with a resonance structure or set of resonance structures [1] (figure 1). These compounds were created by condensing phenylhydrazine [2] with substituted or unsubstituted, -unsaturated carbonyl compounds or Mannich bases. The three slightly reduced versions of the pyrazole structure, 1-pyrazoline (2), 2-pyrazoline (3), and 3-pyrazoline (4), each having a different position for the double bond, are in equilibrium with one

another. Despite the fact that all three types have been synthesised, the most stable form is the 2-pyrazoline because it possesses the monoimino character [3]. The biological effects of numerous pyrazoline derivatives have been the subject of extensive research throughout the years. The history of pyrazoline demonstrates how many chemists were drawn to study it as a biologically active chemical. It has been a fascinating area of pharmaceutical chemistry to research the biological evaluation of pyrazoline derivatives. The literature reportedly said that several substituted2-pyrazoline derivatives possess tremendous biological activities such as antimicrobial [4-8], anti-inflammatory and analgesic [9-11], antidepressant [12-13], antitubercular [14-15], antiamoebic [16-17], anticonvulsant [18-20], antidiabetic [21-23], antitumor [24-27], anti-proliferative [28-29], antioxidant [30-32], antimalaria [33-34], MAO inhibitors [35], anti-nociceptive activity [36-37] and anti-hepatic activity [38]. The focus of this review is on recent research on the synthesis and diverse pharmacological functions connected to pyrazoline derivatives.

EXPERIMENTAL

Chemistry

The reagents utilized in the synthesis were all bought from commercial sources. A nearby supply of Phenylhydrazine hydrochloride was used. S.D. Fine Chem. Ltd., a Mumbai, India-based Company, was in which some of the solvents were acquired. Utilizing silica gel-G for TLC monitoring, the reactions were examined with a UV lamp. All melting points were calculated in open capillary tubes and conveyed in °C and were uncorrected. The results for the ^{1}H NMR and [13] C NMR spectra of the compounds, which were recorded using TMS as an internal standard on an Avance 400 MHz NMR spectrophotometer, are expressed in ppm. A Carlo Erba 1108 elemental analyzer was used to conduct the elemental analyses. The results of the C, H, and N elemental analyses were within ±0.4% of the calculated values.

Step-1: Synthesis ofchalcone derivatives (2a-o)

A mixture of 3, 4-dichlororacetophenone (0.001mol)and substituted aromatic benzaldehyde (1a-o) (0.001mol) was stirred in ethanol (7.5 ml) and then few drops of alcoholic KOH solution (50%,7.5ml) was added drop wisetoit. The mixture was stirred for 24 hours and it was acidified with 1:1 HCl and H_2O which resulted in the formation of precipitation. Then it was filtered under vacuum and the solidwas washed with water, purified by recrystallization using ethanol as solvent.

Step-2: Synthesis of 1, 3, 5-Triaryl-2-Pyrazolines derivatives (3a-o)

1-(3,4-dichlorophenyl)-3-(p-tolyl)prop-2-en-1-one (2a) (0.005 mol) and phenylhydrazine hydrochloride (0.005 mol) were dissolved in glacial acetic acid (20 ml). After that, the mixture was refluxed for 7 hours, during which time the solvent totally evaporated. This produced a solid product that was then crystallized from chloroform and then further purified using column chromatography with ethyl acetate/hexane. To create the compounds 3a-o, phenyl hydrazine hydrochloride was used to treat all of the chalcone derivatives (2a-o). The synthesized compounds were verified by elemental (table 1) and spectral studies (table 2) and the outcomes were also quite near to the calculated values.

Biological evaluation

One of the significant groups of heterocyclic compounds are pyrazolineshave a wide range of biological functions. They have nitric oxide synthase (NOS) inhibitors, cannabinoid CB1 receptor antagonists, anti-microbial, anti-amoebic, anti-inflammatory, anticancer, antidepressant, and steroidal properties. Based on the aforementioned bioactivities, the antifungal, antitubercular, and cytotoxic activities of all synthesized pyrazolines were assessed using accepted procedures.

Antifungal activity

The antifungal activity of the pyrazolines was performed by serial tube dilution method [39] employing fluconazole as a standard drug. The outcomes of the exercise are shown in table 3.

Antitubercular activity

The antitubercular activity of the pyrazolines was completed by MABA [40,41] assay employing pyrazinamide as standard drug. The results of the activity are shown in table 4.

Anticancer activity

The anticancer activity of the pyrazolines was executed by MTT [42] assay employing methotrexate as a standard drug. The results of the out comeare displayed in table 5.

RESULTS AND DISCUSSION

Chemistry

All the synthesized 2-pyrazoline derivatives exhibited characteristic absorption bands in the IR spectra (cm^{-1}) in between 1520-1650 (C=N of pyrazoline), 1060-1160 (C-N) and at other regions of the spectrum depending upon the specific substituents present in each compound.The ^{1}H NMR spectra**(Table 2)** of the 2-pyrazolines shown characteristic resonance signalat δ 3.00-3.20 (H_A), 3.60-3.90 (H_B) and 5.00-5.50 (H_x) as a doublet of doublets (dd) with J_{AB}=16.98 Hz, J_{AX}=7.50 Hz, and J_{BX}=9.35 Hzrespectively. The ^{13}C NMR spectra of the chalcone **5a** exhibited the characteristic peaks for the carbons of the pyrimidinering at δ152.50 (C-3), 66.54 (C-4), apart from the peaks corresponding to the other carbons.The mass spectra obtained by positive mode ionization method revealed the $[M+H]^{+}$ions, whereas the spectra obtained by the EI method revealed the molecular ion.

Biological evaluation

(i) Antifungal activity

Results of the antifungal activity of the compounds were nearly equipotent against both the fungal species *Aspergillus niger* and *Candida tropicalis*. However, compound 3o containing 2"-thienyl ring present at the 5th position of the pyrazoline scaffold was the most potent with MIC 2µg/mL.The compounds 3h and 3m containing 4″-trifluorophenyl and 2″-furyl scaffolds were next in activity against both *Aspergillus niger* and *Candida tropicalis*with MIC 4 µg/mL. Most of the other compounds were also active against both thefungal strainsat MIC 8 and 16µg/mL respectively.

(ii) Anti-tubercularactivity

All of the compounds showed significant antitubercular activity against the *M. tuberculosis* H37Rv strain, according to the results of the antitubercular activity of novel pyrazolines 3a–3o, and some compounds were even shown to be more effective than the typical pyrazinamide.The compound 3f and 3h containing 2″,4″-difluorophenyl and 4″-trifluorophenyl moieties at position-5 showed excellent activity at MIC 1.6 µg/mL. The compounds,3g and 3o exhibited activity at MIC 3.12 µg/mL which was equal to the potency of pyrazinamide. All the other compounds were somewhat potent with MIC values ranging between 25-100µg/mL.

(iii) Cytotoxicactivity

Using the MTT assay, the named compounds (3a–3o) were tested for their in-vitro cytotoxic activity against the prostate cancer cell line DU-145. At a MIC of 12 g/mL, some pyrazolines, 2"-thienylring at position 5 of the pyrazoline scaffold was **3o**demonstrated appreciable activity. The next most potent molecule was **3n**, which included 2"-pyrrolyl and had a MIC of 30 g/mL. At MICs lower than 100 g/mL, the majority of the other substances likewise displayed cytotoxic action.

CONCLUSION

One of the significant classes of heterocyclic compounds with a wide range of biological activity is pyrazolines. All of the synthesized pyrazolines were tested using standard procedures for their antifungal, antitubercular, and cytotoxic properties based on the literature. Based on the data above, a research of the relationship between structure and

activity found that the antifungal, antitubercular, and cytotoxic activities required the presence of the 2"-thienyl, 4"-trifluorophenyl, 2"-furyl, and 2"-pyrrolyl moieties. The activity of pyrazolines may be improved by further modifying the rings by adding various electron-withdrawing or releasing groups.

ACKNOWLEDGMENT

The authors are thankful to M/S LAILA IMPEX Industries Ltd., Vijayawada, India for providing IR, NMR and elemental analysis data. The authors are also thankful to the management CHIPS, for their constant support throughout this work.

CONFLICT OF INTEREST

There is no conflict of interest

REFERENCES

1. Grimmett, R., in Comprehensive organic chemistry, Ed.Barton, PergamonPress, Oxford, 1979;iv, P.357.
2. Sammour, A. E. A., Tetrahedron.1967;20, 1067.
3. Loudon, J. D., E.H. Rodd, ed., In: "Chemistry of Carbon Compounds".Elsevier Publishing Company New York.,1957;, IV.
4. Tanwar, N., Rana, D., Kaur, R., Singh, R. and Singh, K. Synthesis and characterization of pyrazoline derivatives. *Journal of Integrated Science and Technology*, 2015, 3(2), 39-41.
5. Faiq H. S. Hussein, Farouq E. Hawaiz, Hashim J. Azeez.Synthesis and characterization of some new pyrazoline derivatives derived From 2, 4-Dihydroxybenzaldehyde.*International Journal of Chemical and Environmental Engineering*, 2013, 4(6), 373-377.
6. Desai, P.R. and Desai, S.D. Studies on synthesis of biologically active pyrazoline derivatives. *International research journal of chemistry*, 2014, 7(4), 81.
7. Shah SH, Shukla JR and Patel PS. Synthesis and bio-evaluation of some new phenyl pyrazoline derivatives from p-chloro benzaldehyde moiety. Chem. & Chemical. Sci., 2014, 4(1), 1-7.
8. Naik K, Prasad ARG, Spoorthy YN, and Ravindranath LRKR. Design, synthesis, characterization and antimicrobial evaluation of new pyrazoline-5-ones. *J App Pharm.*, 2013, 4(1), 720-730.
9. A. Rozas I, Kelly B, Kaushik P, Kaushik D. Synthesis, Biological evaluation and Evaluation of Pyrazoline Analogues of Vanillin. *J. Pharm. Sci. Drug Res.*, 2014, 6(2), 128-131.
10. Jadhav SY, Shirame SP, Kulkarni SD, Patil SB, Pasale SK, and Bhosale RB. PEG mediated Synthesis and pharmacological evaluation of some fluoro substituted pyrazoline derivatives as anti-inflammatory and analgesic agents. *Bioorg. Med. Chem. Lett.*, 2013, 23, 2575–2578.
11. Aggarwal R and Bansal. Molecular modeling study of 5-trifluoromethyl-D_2-pyrazoline and isomeric 5/3-trifluoromethylpyrazole derivatives as anti-inflammatory agents. *Eur J Med Chem.* 2013, **70**, 350-357.
12. Rao AS, Saalim M, Bhupesu KV and Prasad K. Anticonvulsant and antidepressant activity studies of synthesized some new 1,3,5-trisubstituted-2-pyrazolines. Int*JPharmTech Res.*, 2014, **6**(3), 1113-1123.
13. Mathew B, Suresh J, and Anbazhagan S. Synthesis, preclinical evaluation and antidepressant activity of 5-substituted phenyl-3-(thiophen-2-yl)-4, 5-dihydro-1h-pyrazole-1-carbothioamides. *EXCLI journal*, 2014, **13**, 437-445.
14. Hipparagi SM and Bhanushali MD. Synthesis and evaluation of the antitubercular activity of some novel 2-pyrazoline derivatives. *Journal of the Scientific Society*, 2013, 40(2), 80-83.
15. Taj T, Kamble RR, Gireesh TM, Hunnur RK, and Margankop SB. One-pot synthesis of pyrazolinederivatizedcarbazoles as anti-tubercular, anticancer agents, their DNA cleavage and antioxidant activities. *Eur J Med Chem.*, 2011, 46, 4366-4373.
16. Hayat F, Salahuddin A, Umar S and Azam A. Synthesis, characterization, antiamoebic activity and cytotoxicity of novel series of pyrazoline derivatives bearing quinoline tail. *Eur J of Med Chem.*, 2010, 45, 4669-4675.

17. Wani MY, Bhat AR, Azam A, Lee DH, Choi I and Athar F. Synthesis and in vitro evaluation of novel tetrazole embedded 1,3,5-trisubstituted pyrazoline derivatives as Entamoebahistolytica growth inhibitors. *Eur J of Med Chem*., 2012, 54, 845-854.
18. Rao BM, Ramesh S, Bardalai D, Rahman H, and Shaik HA. Synthesis, characterization, and evaluation of the antiepileptic activity of four new 2-pyrazoline derivatives compounds. *Sch. J. App. Med. Sci.,* 2013, 1(1), 20-27.
19. Siddiqui AA, Rahman MA, Shaharyar M, and Mishra R. Synthesis And Anticonvulsant Activity Of Some Substituted 3,5-Diphenyl-2- Pyrazoline-1-Carboxamide Derivatives. *CSJ*, 2010, 1-10.
20. Enein MNA, Azzouny AAE, Attia MI, Maklad YA, Kamilia M. Amin KM, Rehim MA, and Behairy MFE. Design and synthesis of novel stiripentol analogs as potential anticonvulsants. *Eur J Med Chem.,* 2012, 47, 360-369.
21. Shelke SN and Mhaske GR, Bonifácio VDB, Gawande MB. Green synthesis and anti-infective activities of fluorinated pyrazoline derivatives. *Bioorg. Med. Chem. Lett.*, 2012, 22, 5727–5730.
22. Ovaisa S, Pushpalatha H, Reddy GB, Rathore P, Bashira R, Yaseena S, Dheyaaa A, Yaseena R, Prakash O, Akthar M, Samima M, and Javeda K. Synthesis and biological evaluation of some new pyrazoline substituted benzenesulfonylurea/thiourea derivatives as anti-hyperglycemic agents and aldose reductase inhibitors. *Eur J Med Chem*., 2014, 80, 209-217.
23. Emayavaramban M, Santhi N, Gopi C, Manivannan C and Raguraman Synthesis, Characterization and Anti-diabetic activity of 1,3,5-triaryl-2-pyrazolines in acetic acid solution under Ultrasound Irradiation. *International Letters of Chemistry, Physics, and Astronomy*., 2013, 9(2), 172-185.
24. Amin KM, Eissa AAM, Seri SMA, Awadallah FM, and Hassan GS. Synthesis and biological evaluation of novel coumarin-pyrazoline hybrids endowed with phenylsulfonyl moiety as antitumor agents. *Eur J Med Chem.,* 2013, 60, 187-198.
25. Zhu SL, Wua Y, Liu CJ, Wei CY, Tao JC, and Liu HM. Design and stereoselective synthesis of novel isosteviol-fused pyrazolines and pyrazoles as potential anticancer agents. *Eur J Med Chem*., 2013, 65, 70-82.
26. Fan NJ, Tang JJ, Li H, Li XJ, Luo B, and Gao JM. Synthesis and cytotoxic activity of some novel steroidal C-17 pyrazolinyl derivatives. *Eur J Med Chem*., 2013, 69, 182-190.
27. Khalil NA, Eman M. Ahmed EM, and Nassan HBE. Synthesis, characterization, and biological evaluation of certain 1,3-thiazolone derivatives bearing pyrazoline moiety as potential anti-breast cancer agents. *Med Chem Res*., 2013, 22, 1021–1027.
28. Rathore P, Yaseen S, Ovais S, Bashir R, Yaseen R, Hameed AD, Samim M, Gupta R, Hussain F and Javed K. Synthesis and evaluation of some new pyrazoline substituted benzenesulfonylureas as potential antiproliferative agents. *Bioorg. Med. Chem. Lett*., 2014, 24, 1685–1691.
29. Awadallah FM, Piazza GA, Gary BD, Keeton AB, and Canzoneri JC. Synthesis of some dihydropyrimidine-based compounds bearing pyrazoline moiety and evaluation of their antiproliferative activity. *Eur J Med Chem*., 2013, 70, 273-279.
30. Kumar A, Varadaraj BG and Singla RK. Synthesis and evaluation of the antioxidant activity of novel3,5-disubstituted-2-pyrazolines. *Bulletin of Faculty of Pharmacy, Cairo University*.,2013, 51, 167–173.
31. Kumar A, Rout S, Sahoo DK and Kumar BVVR. Synthesis and biological evaluation of new 4-Bromo-3, 5-diaryl-1-phenyl-2-pyrazoline derivatives as antioxidant and anti-inflammatory agents. *J. Res. Dev. Pharm. L. Sci.*,2013, 2(2), 349-354.
32. C. Jagadish, NeerajSoni, and AmitaVerma. Design, Synthesis, and In Vitro Antioxidant Activity of 1, 3, 5-Trisubstituted-2-pyrazolines Derivatives. *Journal of Chemistry*., 2013, 2013, 1-6.
33. Insuasty B, Montoya A, Becerra D, Quiroga J, Abonia R, Robledo S, Vélez ID, Upegui Y Nogueras M and Cobo J. Synthesis of novel analogs of 2-pyrazoline obtained from [(7-chloroquinolin-4-yl) amino]chalcones and hydrazine as potential antitumor and antimalarial agents. *Eur J Med Chem*., 2013, 67, 252-262.
34. Acharya BN, Saraswat D, Tiwari M, Shrivastava AK, Ghorpade R, Bapna S and Kaushik MP. Synthesis and antimalarial evaluation of 1, 3, 5-trisubstituted pyrazolines. *Eur J Med Chem*., 2010, 45, 430–438.
35. Daniela Secci, Simone Carradori, Adriana Bolasco, BrunaBizzarri, Melissa D'Ascenzio, Elias Maccioni, Discovery and Optimization of Pyrazoline Derivatives As Promising Monoamine Oxidase Inhibitors, *Current Topics in Medicinal Chemistry*,2012, 12(20),2240-2257.

36. Kaplancikli ZA, Zitouni GT, Ozdemir A and Can OD, Chevallet P. Synthesis and antinociceptive activities of some pyrazoline derivatives. *Eur J Med Chem.*, 2009, 44, 2606–2610.
37. Milano J, Oliveira SM, Rossato MF, Sauzem PD, Machado P, Beck P, Zanatta N, Martins MAP, Mello CF, Rubin MA, Ferreira J, and Bonacorso HG. Antinociceptive effect of novel trihalomethyl substituted pyrazoline methyl esters in formalin and hot-plate tests in mice. *Eur Journal of Pharmacol.*, 2008, 581, 86–96.
38. Khalilullah H, Khan S, Ahsan MJ and Ahmed B. Synthesis and antihepatotoxic activity of 5-(2,3-dihydro-1,4-benzodioxane-6-yl)-3-substituted-phenyl-4,5-dihydro-1H-pyrazole derivatives. *Bioorg. Med. Chem. Lett.*, 2011, 21, 7251–7254.
39. Hollander, J.N.D., *J. Clin.Lab.Anal.*, 1996, 10, 42.
40. Watts, J.L., and Lindeman, C.J. 2006. Chapter 3: Antimicrobial Susceptibility Testing of Bacteria of Veterinary Origin. Antimicrobial Resistance in Bacteria of Animal Origin, FM Aarestrup, *ed. ASM Press*, Washington DC, USA.
41. Waisbren, C., Carr, and Dunette.J. *Am. J. Clin. Pathol.*, 1951, 21, 884-887.
42. Wilson, A.P., in Cytotoxicity and viability assays: In JRW Masters, "Animal Cell Culture", 3rd ed., *Oxford University*, Oxford, 2000,1, 175.

Table 1: Physical characterization and elemental analysis of synthesized compounds (3a-o)

S.No	R	Mol. formula	Mol. Mass	M.P.(°C)	Yield (%)	Elemental analysis					
						% Calculated			% Found		
						C	H	N	C	H	N
3a		$C_{22}H_{18}Cl_2N_2$	381.30	168	55	69.30	4.76	7.35	69.05	4.52	7.05
3b		$C_{21}H_{15}Cl_2FN_2$	385.26	195	70	65.47	3.92	7.27	65.05	3.54	7.01
3c		$C_{21}H_{15}Cl_2FN_2$	385.26	149	61	65.47	3.92	7.27	65.05	3.54	7.01
3d		$C_{21}H_{15}Cl_3N_2$	401.72	261	75	62.79	3.76	6.97	62.15	3.65	6.41
3e		$C_{21}H_{15}Cl_3N_2$	401.72	133	72	62.79	3.76	6.97	62.15	3.65	6.41
3f		$C_{21}H_{14}Cl_2F_3N_2$	403.25	291	81	62.55	3.50	6.95	62.33	3.12	6.55
3g		$C_{21}H_{14}Cl_4N_2$	436.16	302	85	57.83	3.24	6.42	57.38	3.08	6.10
3h		$C_{22}H_{15}Cl_2F_3N_2$	435.27	125	66	60.71	3.47	6.44	60.35	3.12	6.05
3i	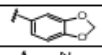	$C_{22}H_{16}Cl_2N_2O_2$	411.28	212	49	64.25	3.92	6.81	64.27	3.78	6.45
3j		$C_{20}H_{15}Cl_2N_3$	368.26	191	55	65.23	4.11	11.41	65.06	3.95	11.24
3k		$C_{20}H_{15}Cl_2N_3$	368.26	184	53	65.23	4.11	11.41	65.06	3.95	11.24
3l		$C_{20}H_{15}Cl_2N_3$	368.26	214	61	65.23	4.11	11.41	65.06	3.95	11.24
3m		$C_{19}H_{14}Cl_2N_2O$	357.23	200	58	63.88	3.95	7.84	63.25	3.29	7.45
3n		$C_{19}H_{15}Cl_2N_3$	356.25	171	48	64.06	4.24	11.80	65.82	4.01	11.21
3o		$C_{19}H_{14}Cl_2N_2S$	373.30	212	41	61.13	3.78	7.50	61.01	3.45	7.12

Table 2: Spectral Data of titled Compounds (3a-o)

S.No	FT-IR, Position of absorption b and (cm^{-1})	^{1}HNMR, Chemical shift (δ) in ppm
3a	1592 (C=N), 1120 (C-N), 1586 (C=C quadrant of Ar), 830 (C-Cl)	3.28 (1H, d, H_A), 3.72 (1H, d, H_B), 5.45 (1H, d, H_x), 2.34 (3H, s, Ar-CH_3), 6.75-7.91 (12H, Ar-H)
3b	1644 (C=N), 1099 (C-N), 1582 (C=C quadrant of Ar), 835 (C-Cl), 922 (C-F)	3.29 (1H, d, H_A), 3.75 (1H, d, H_B), 5.33 (1H, d, H_x), 6.65-7.65 (12H, Ar-H)
3c	1599 (C=N), 1105 (C-N), 1578 (C=C quadrant of Ar), 825 (C-Cl), 925 (C-F)	3.26 (1H, d, H_A), 3.72 (1H, d, H_B), 5.46 (1H, d, H_x), 6.66-7.55 (12H, Ar-H)
3d	1549 (C=N), 1091 (C-N), 1582 (C=C quadrant of Ar), 838 (C-Cl), 846 (C-Cl)	3.28 (1H, d, H_A), 3.77 (1H, d, H_B), 5.49 (1H, d, H_x), 6.56-7.39 (12H, Ar-H)
3e	1552 (C=O), 1591 (C=C quadrant of Ar), 832 (C-Cl), 838 (C-Cl)	3.24 (1H, d, H_A), 3.71 (1H, d, H_B), 5.42 (1H, d, H_x), 6.69-7.42 (12H, Ar-H)
3f	1526 (C=N), 1086 (C-N), 1588 (C=C quadrant of Ar), 831 (C-Cl), 921 (C-F)	3.25 (1H, d, H_A), 3.73 (1H, d, H_B), 5.49 (1H, d, H_x), 6.87-7.69 (11H, Ar-H)
3g	1544 (C=N), 1081 (C-N), 1578 (C=C quadrant of Ar), 821 (C-Cl), 829 (C-Cl)	3.26 (1H, d, H_A), 3.81 (1H, d, H_B), 5.52 (1H, d, H_x), 6.82-7.77 (11H, Ar-H)
3h	1641 (C=N), 1152 (C-N), 1568 (C=C quadrant of Ar), 818 (C-Cl), 926 (C-F)	3.28 (1H, d, H_A), 3.76 (1H, d, H_B), 5.50 (1H, d, H_x), 6.61-7.81 (12H, Ar-H)
3i	1595 (C=N), 1097 (C-N), 1576 (C=C quadrant of Ar), 1236 (O-CH_2-O), 845 (C-Cl)	6.25 (2H,s,-O-CH_2O-), 3.18 (1H, d, H_A), 3.82 (1H, d, H_B), 5.28 (1H, d, H_x), 6.74-7.49 (11H, Ar-H)
3j	1645 (C=N), 1082 (C-N), 1591 (C=N), 1559 (C=C quadrant of Ar), 1325 (C-N)	3.17 (1H, d, H_A), 3.84 (1H, d, H_B), 5.29 (1H, d, H_x), 6.39-7.89 (12H, Ar-H)
3k	1634 (C=N) 1099 (C-N), 1591 (C=N), 1568 (C=C quadrant of Ar), 1344 (C-N), 819 (C-Cl)	3.04 (1H, d, H_A), 3.90 (1H, d, H_B), 5.59 (1H, d, H_x), 6.69-7.59 (12H, Ar-H)
3l	1641 (C=N), 1086 (C-N), 1577 (C=N), 1559 (C=C quadrant of Ar), 1335 (C-N), 832 (C-Cl)	3.17 (1H, d, H_A), 3.87 (1H, d, H_B), 5.27 (1H, d, H_x), 6.79-7.44 (12H, Ar-H)
3m	1612 (C=N), 1091 (C-N), 1555 (C=C quadrant of Ar), 835 (C-Cl)	3.14 (1H, d, H_A), 3.85 (1H, d, H_B), 5.34 (1H, d, Hx), 6.44-7.79 (11H, Ar-H)
3n	1643 (C=N), 1087 (C-N), 1564 (C=C quadrant of Ar), 1584 (C=N), 3240 (N-H), 1371 (C-N), 828 (C-Cl)	3.14 (1H, d, H_A), 3.84 (1H, d, H_B), 5.56 (1H, s, -NH), 5.24 (1H, d, Hx), 6.49-7.59 (11H, Ar-H)
3o	1646 (C=N), 1145 (C-N), 1549 (C=C quadrant of Ar), 633 (C-S), 826 (C-Cl)	3.49 (1H, d, H_A), 3.77 (1H, d, H_B), 5.19 (1H, d, Hx), 6.44-7.59 (11H, Ar-H)

Table 3: Results of the antifungal activity of compounds (3a-3o)

S.No	Compound	R	*An*	*Ct*
1	3a	4"-methylphenyl	16	16
2	3b	4"-fluorophenyl	8	16
3	3c	2"-fluorophenyl	8	16
4	3d	4"-chlorophenyl	8	16
5	3e	2"-chlorophenyl	8	16
6	3f	2",4"-fluorophenyl	8	8

7	3g	2",4"-dichlorophenyl	8	16
8	3h	4"-trifluorophenyl	4	4
9	3i	3",4"-methylenedioxyphenyl	8	8
10	3j	2"-pyridinyl	8	8
11	3k	3"-pyridinyl	8	8
12	3l	4"-pyridinyl	8	8
13	3m	2"-furfuryl	4	4
14	3n	2"-pyrrolyl	16	16
15	3o	2"-thienyl	2	2
16	Fluconazole		≤1	≤1

Table 4: Results of the antitubercular activity of pyrazolines (3a-3o)

S.No	Compound	R	MIC values (µg/mL) of *M. tuberculosis* $H_{37}Rv$
1	3a	4"-methylphenyl	100
2	3b	4"-fluorophenyl	12.5
3	3c	2"-fluorophenyl	12.5
4	3d	4"-chlorophenyl	12.5
5	3e	2"-chlorophenyl	6.25
6	3f	2",4"-fluorophenyl	1.6
7	3g	2",4"-dichlorophenyl	3.12
8	3h	4"-trifluorophenyl	1.6
9	3i	3",4"-methylenedioxyphenyl	25
10	3j	2"-pyridinyl	25
11	3k	3"-pyridinyl	25
12	3l	4"-pyridinyl	25
13	3m	2"-furfuryl	6.25
14	3n	2"-pyrrolyl	25
15	3o	2"-thienyl	3.12
16	Pyrazinamide		3.12

Table 5: Results of the cytotoxic activity of compounds (3a-3o)

S.No	Compound	R	DU-145
1	3a	4"-methylphenyl	134 ± 2
2	3b	4"-fluorophenyl	46 ± 2
3	3c	2"-fluorophenyl	126 ± 2
4	3d	4"-chlorophenyl	60 ± 2
5	3e	2"-chlorophenyl	54 ± 2
6	3f	2",4"-fluorophenyl	106 ± 2
7	3g	2",4"-dichlorophenyl	90 ± 2
8	3h	4"-trifluorophenyl	112 ± 1
9	3i	3",4"-methylenedioxyphenyl	54 ± 2
10	3j	2"-pyridinyl	100 ± 2
11	3k	3"-pyridinyl	78 ± 2
12	3l	4"-pyridinyl	64 ± 2

13	3m	2"-furfuryl	58 ± 2
14	3n	2"-pyrrolyl	30 ± 2
15	3o	2"-thienyl	12 ± 1
16	Methotrexate		5 ± 1

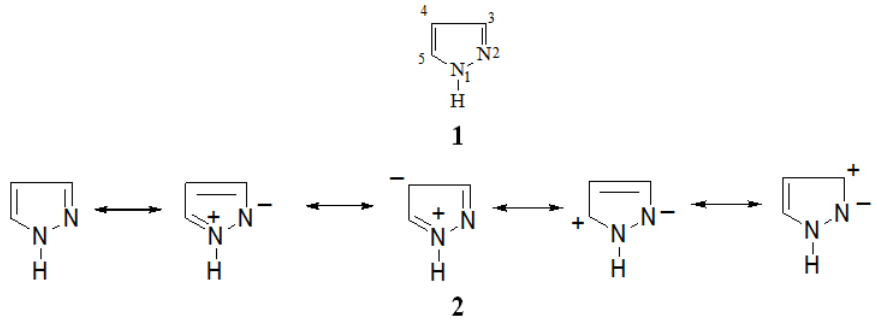

Figure 1: Structure of pyrazole (1) and resonance structures of pyrazole (2)

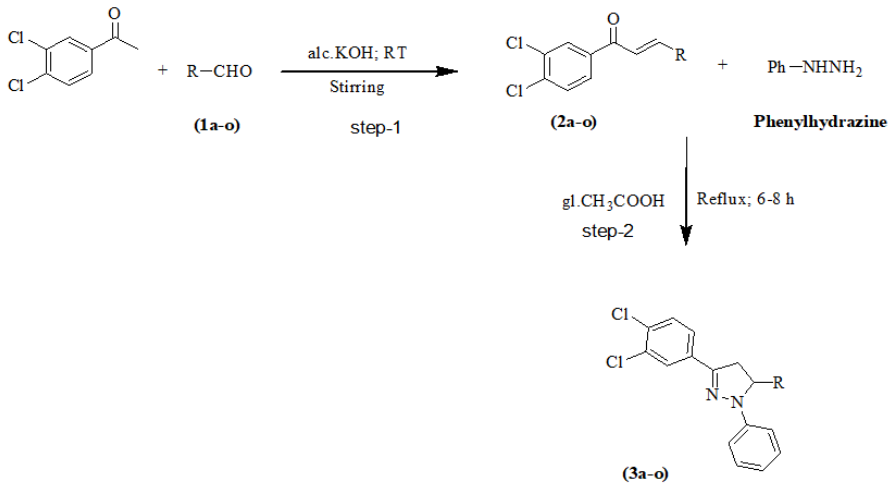

Scheme 1: Protocol for the synthesis of pyrazoline derivatives from chalcones of 3, 4-dichloroacetophenone

Indian Journal of Natural Sciences *www.tnsroindia.org.in ©IJONS*

Vol.15 / Issue 83 / Apr / 2024 *International Bimonthly (Print) – Open Access* *ISSN: 0976 – 0997*

RESEARCH ARTICLE

A Markovian Queue with Second Optional Working Vacation

K.Santhi[1]* and T.Senthamizhselvi[2]

[1]Assistant Professor, Department of Mathematics, PS PT MGR Govt. Arts and Science College, Sirkali, (Affiliated to Annamalai University) Tamil Nadu, India.
[2]Assistant Professor, Department of Mathematics, Aries Arts and Science College for Women, Vadalur (Affiliated to Annamalai University) Tamil Nadu, India.

Received: 08 July 2023 Revised: 30 Dec 2023 Accepted: 27 Mar 2024

***Address for Correspondence**
K.Santhi
Assistant Professor,
Department of Mathematics,
PS PT MGR Govt. Arts and Science College, Sirkali,
(Affiliated to Annamalai University)
Tamil Nadu, India.
Email:santhimano3169@gmail.com

ABSTRACT

In this paper, we analyze an M/M/1 queue with second optional working vacation. To obtain the necessary and sufficient condition for the system to be stable, we use the matrix-Geometric method. We derive stationary probability distribution. We calculate some performance measures. Some numerical examples are illustrated to show the model's stability.

Keywords: M/M/1 queue, Second optional Working Vacation, Matrix-analytic Method, Rate matrix,

INTRODUCTION

Wallace [11] investigated the Quasi Birth-Death process (QBD) in queueing theory using a Markov chain with a tridiagonal generator. Numerical techniques can be used to analyze congestion situations when it is impossible to achieve an explicit solution for queueing problems. The Matrix Geometric technique is ideal for this type of work. Neuts [5], and Latouche and Ramaswami [1] proposed the matrix geometric solution to the QBD process. The queueing system with server vacation is noteworthy, and can be referred in Tian and Zhang [10]. Servi and Finn [9] created a modern vacation policy, termed as Working Vacation (WV), where the server delivers a lesser rate of service than during the engaged period. Wu and Takagi [13] worked on an M/G/1/ with multiple working vacation. Wen-yuan liu [9] analyzed the stochastic decompositions in an M/M/1/ queue with working vacation. The M/M/1/WV queue and WV interruptions was analyzed by Li and Tian [2]. Naishuo Tian [3] considered M/M/1/SWV queue. Qingqing Ye and Liwei Liu [5] discussed the analysis of the M/M/1 Queue with two vacation policies. Santhi [8] analysed a queue with second optional service and multiple working vacation. Pazhani Bala Murugan and Santhi

[7] discussed a queue with working vacation queue. Manoharan and Sankara Sasi [ ] analysed a Queue with Optional Vacation. The outline of this paper is as follows. We present the model in section 2 and find the infinitesimal generator. The stability condition and Rate matrix(R) is computed in section 3. In section 4, we use a matrix-analytic technique to derive the stationary probability distribution. In section 5, we calculate performance measures and section 6 has a firmness of the model by presenting some numerical calculations. In section 7 we present the conclusion.

We consider an M/M/1 queue with second optional working vacation with the parameter λ. The customer's inter-arrival times are exponentially distributed. The service is exponentially distributed with parameter μb and at the time of the regular busy period. The service is exponentially distributed with parameter and μv at the time of the working vacation and second optional working vacation. When the system becomes empty the server will take up WV. When the server switched over to working vacation, he will undergo the task of first regular working vacation. When the system becomes empty, he may opt for second optional vacation with probability pθ1 or he may join the busy period with probability qθ1. If he opt for second optional working vacation, then at the end of this task he will join busy period with completion rate θ2. Inter-arrival times, service periods, and vacation periods are all independent of each other. Let $Q(t)$ be the number of customers in the system at time t, and let $H(t)$ be the state server at the time t. There are three possible states of the server is as follows.

$$H(t) = \begin{cases} 1 - \text{if the server is in first regular working vacation ,} \\ 2 - \text{if the server is in second optional working vacation,} \\ 3 - \text{if the server is busy in normal service period,} \end{cases}$$

Then $\{(Q(t), H(t)); t \geq 0\}$ is a Markov process with state space,
$\Omega = \{(j, 0) \cup (n, j): n \geq 0, j = 1, 2, 3\}$

The states infinitesimal generator can be described by employing *lexicographical sequence* as follows

$$Q = \begin{bmatrix} B_{00} & A & & & & & \\ C_{00} & B & A & & & & \\ & C & B & A & & & \\ & & \ddots & \ddots & \ddots & & \\ & & & C & B & A & \\ & & & & C & B & A \end{bmatrix}$$

Where

$$B = \begin{bmatrix} -(\lambda + \mu_v + q\theta_1 + p\theta_1) & p\theta_1 & q\theta_1 \\ 0 & -(\lambda + \mu_v + \theta_2) & \theta_2 \\ 0 & 0 & -(\lambda + \mu_b) \end{bmatrix}$$

$$A = \begin{bmatrix} \lambda & 0 & 0 \\ 0 & \lambda & 0 \\ 0 & 0 & \lambda \end{bmatrix} \quad C = \begin{bmatrix} \mu_v & 0 & 0 \\ 0 & \mu_v & 0 \\ 0 & 0 & \mu_b \end{bmatrix}$$

$$B_{00} = \begin{bmatrix} -(\lambda + q\theta_1 + p\theta_1) & p\theta_1 & q\theta_1 \\ 0 & -(\lambda + \theta_2) & \theta_2 \\ 0 & 0 & -(\lambda) \end{bmatrix} \quad C_{00} = \begin{bmatrix} \mu_v & 0 & 0 \\ 0 & \mu_v & 0 \\ \mu_b & 0 & 0 \end{bmatrix}$$

THE MODEL'S STABILITY CONDITION AND R

Theorem 1: The *QBD* process $\{(Q(t), H(t)); t \geq 0\}$ is positive recurrent if and only if $\rho < 1$.

Proof: Consider

$$D = B + A + C = \begin{bmatrix} -(q\theta_1 + p\theta_1) & p\theta_1 & q\theta_1 \\ 0 & -\theta_2 & \theta_2 \\ 0 & 0 & 0 \end{bmatrix}$$

In [1], theorem 7.3.1 offers requirement for positive *recurrence* of the QBD process, because matrix *A* is reducible. After permutation of rows and columns it states that the *QBD is* positive recurrent if and only if

$$\pi \begin{bmatrix} \mu_v & 0 \\ 0 & \mu_b \end{bmatrix} e > \pi \begin{bmatrix} \lambda & 0 \\ 0 & \lambda \end{bmatrix} e$$

Here all the elements of the column vector e=1 and π is the unique solution of the system $\begin{bmatrix} -\theta_2 & \theta_2 \\ 0 & 0 \end{bmatrix} = 0$, $\pi e = 1$. Therefore, the *QBD* process is positive recurrent if and only $\rho < 1$ after some algebraic manipulations.

Theorem 2 : If $\rho < 1$, the matrix quadratic equation $R^2C + RB + A = 0$ has the minimal non-negative solution $R = \begin{bmatrix} r_{11} & r_{12} & r_{13} \\ 0 & r_{22} & r_{23} \\ 0 & 0 & r_{33} \end{bmatrix}$ where

$$r_{11} = \frac{(\lambda+\mu_v+q\theta_1+p\theta_1)-\sqrt{(\lambda+\mu_v+q\theta_1+p\theta_1)^2-4\mu_v\lambda}}{2\mu_v} \qquad r_{12} = \frac{r_1 p\theta_1}{\lambda+\mu_v+\theta_2 \ -\mu_v(r_1+r_2)}$$

$$r_{13} = \frac{\mu_b r_3 r_4 + r_1 q\theta_1 + \theta_2 r_3}{(\lambda+\mu_b)-\mu_b(r_1+\rho)} \qquad r_{22} = \frac{(\lambda+\mu_v+\theta_2)-\sqrt{(\lambda+\mu_v+\theta_2)^2-4\mu_v\lambda}}{2\mu_v}$$

$$r_{23} = \frac{r_2\theta_2}{\lambda+\mu_b-(\mu_b r_2+\rho)} \qquad r_{33} = \frac{(\lambda+\mu_b)-\sqrt{(\lambda+\mu_b)^2-4\mu_b\lambda}}{2\mu_{bv}}$$

Proof:

We consider R = $\begin{bmatrix} R_{11} & R_{12} & R_{13} \\ 0 & R_{22} & R_{23} \\ 0 & 0 & R_{33} \end{bmatrix}$

From the matrices C, B, A substituting R into $R^2C + RB + A = 0$, we get

$$r_{11}^2\mu_v - r_{11}(\lambda + \mu_v + q\theta_1 + p\theta_1) + \lambda = 0$$

$$(r_{11}r_{12} + r_{12}r_{22})\mu_v + [r_{11}p\theta_1 - r_{12}(\lambda + \mu_v + \theta_2)] = 0$$

$$[r_{11}r_{13} + r_{12}r_{23} + r_{13}r_{33}]\mu_b + [r_{11}q\theta_1 + \theta_2 r_{12} - r_{12}(\lambda + \mu_b)] = 0$$

$$\mu_v - r_{22}(\lambda + \mu_v + \theta_2) + \lambda = 0$$

$$[r_{22}r_{23} + r_{23}r_{33}]\mu_b + \theta_2 r_{22} - r_{23}(\lambda + \mu_b) = 0$$

$$r_{33}^2\mu_b - r_{33}(\lambda + \mu_b) + \lambda = 0$$

From the above set of equations with some computations, we get *R*11, *R*12, *R*13, *R*22, *R*23 and *R*33

THE MODEL'S STATIONARY PROBABILITY DISTRIBUTION

If $\rho < 1$, assign (Q, H) be the stationary probability distribution of the process {(Q(t), H(t)); t ≥ 0}. Represent, $\pi n = (\pi n0, \pi n1, \pi n2)$, n ≥ 0;

$\pi nj = \Pr\{Q = n, H = j\} = \lim t \to \infty \Pr\{Q(t) = n, H(t) = j\}$, (n, j) ∈ Ω.

Theorem 3: If $\rho < 1$, the stationary probability distribution of (Q, H) is indicated by

$$\pi_{n0} = r_1^n \pi_{10} \qquad n \geq 1$$

$$\pi_{n1} = r_3 \sum_{j=0}^{n-1} r_1^{n-1-j} r_2^j \pi_{10} + r_2^n \frac{\mu_v r_3 + p\theta_1}{\lambda - r_2\mu_v + \theta_2} \pi_{10} \qquad n \geq 1$$

$$\pi_{n2} = \left[r_5 \sum_{j=1}^{k} r_1^{k-j} \rho^{j-1} + r_3 r_4 \sum_{n=2}^{k} \rho^{n-2} + \sum_{j=1}^{k-n+1} r_1^{k-n+1-j} r_2^{j-1} \right] \pi_{10}$$

$$+ r_4 \sum_{j=0}^{n-1} r_2^{n-1-j} \rho^j \frac{\mu_v r_3 + p\theta_1}{\lambda - r_2\mu_v + \theta_2} \pi_{10} + \frac{\rho^n (\lambda - r_2\mu_v + \theta_2)\, q\theta_1 + \theta_2 p\theta_1 + \theta_2\, r_3\mu_v}{\lambda(\lambda - r_2\mu_v + \theta_2)} \pi_{10} \qquad n \geq 1$$

and $\pi_{20} = \frac{\mu_v r_3 + p\theta_1}{\lambda - r_2\mu_v + \theta_2} \pi_{10}$

$\pi_{30} = \frac{(\lambda - r_2\mu_v + \theta_2)\, q\theta_1 + \theta_2 p\theta_1 + \theta_2\, r_3\mu_v}{\lambda(\lambda - r_2\mu_v + \theta_2)} \pi_{10}$. The normalization condition can finally be used to determine π_{00}.

Proof: Using the technique from [12], we have

$$\pi_n = (\pi_{10}, \pi_{20}, \pi_{30}) = \pi_0 R^n = (\pi_{10}, \pi_{20}, \pi_{30},)\, R^n,\ m \geq N.$$

For $m \geq N$,

$$R^n = \begin{bmatrix} r_1^n & r_3 \sum_{j=0}^{n-1} r_1^{n-1-j} r_2^j & r_5 \sum_{j=1}^{k} r_1^{k-j} \rho^{j-1} + r_3 r_4 \sum_{n=2}^{k} \rho^{n-2} + \sum_{j=1}^{k-n+1} r_1^{k-n+1-j} r_2^{j-1} \\ 0 & r_2^n & r_4 \sum_{j=0}^{n-1} r_2^{n-1-j} \rho^j \\ 0 & 0 & \rho^n \end{bmatrix}$$

Substituting R^n into the above equation, we get the required equations. However, π_0 satisfies the equation $\pi_0(B_{00} + RC_{00}) = 0$, where $B_{00} + RC_{00} =$

$$\begin{bmatrix} -(\lambda + q\theta_1 + p\theta_1) + r_1\mu_v + r_5\mu_b & p\theta_1 + r_3\mu_v & q\theta_1 \\ r_4\mu_b & -(\lambda + \theta_2) + r_2\mu_v & \theta_2 \\ \rho\mu_b & 0 & -\lambda \end{bmatrix}$$

The following equations are computed from $B_{00} + RC_{00}$

$$[-(\lambda + q\theta_1 + p\theta_1) + r_1\mu_v + r_5\mu_b]\pi_{10} + r_4\mu_b\pi_{20} + \rho\mu_b\pi_{30} = 0$$

$$(p\theta_1 + r_3\mu_v)\pi_{10} + [-(\lambda + \theta_2) + r_2\mu_v]\pi_{20} = 0$$

$$q\theta_1\pi_{10} + \theta_2\pi_{20} - \lambda\pi_{30} = 0$$

Using normalizing condition, we get

$$\pi_{10} = \left[\frac{r_1}{(1 - r_1)} + \frac{r_2}{(1 - r_2)} \cdot \frac{(p\theta_1 + r_3\mu_v)}{\lambda + \theta_2 - r_2\mu_v} + \frac{r_2 r_3}{(1 - r_2)(1 - r_1)} + \frac{r_5}{(1 - r_1)(1 - \rho)} + \frac{r_4 r_3}{(1 - r_1)(1 - r_2)(1 - \rho)} + \frac{r_4\rho}{(1 - r_2)(1 - \rho)} \cdot \frac{(p\theta_1 + r_3\mu_v)}{\lambda + \theta_2 - r_2\mu_v} + \frac{\rho}{(1 - \rho)} \frac{(\lambda - r_2\mu_v + \theta_2)\, q\theta_1 + \theta_2 p\theta_1 + \theta_2\, r_3\mu_v}{\lambda(\lambda + \theta_2 - r_2\mu_v)} \right]^{-1}$$

The probabilities of the server in various state are respectively as follows.

$P_1 = \Pr\{J = 0\} = \Pr\{$ The server is in a first regular working vacation period $\}$

$$= \sum_{n=0}^{\infty} \pi_{n0} = \frac{r_1}{(1 - r_1)} \pi_{10}$$

$P_2 = \Pr\{J = 1\} = \Pr\{$ The server is in a second optional working vacation $\}$

$$= \sum_{n=0}^{\infty} \pi_{n1} = \left[\frac{r_2}{(1 - r_2)} \cdot \frac{(p\theta_1 + r_3\mu_v)}{\lambda + \theta_2 - r_2\mu_v} + \frac{r_2 r_3}{(1 - r_2)(1 - r_1)} \right] \pi_{10}$$

$P_3 = \Pr\{J = 2\} = \Pr\{$ The server is in normal busy period $\}$

$$= \sum_{n=0}^{\infty} \pi_{n2} = \left[\frac{r_5}{(1 - r_1)(1 - \rho)} + \frac{r_4 r_3}{(1 - r_1)(1 - r_2)(1 - \rho)} + \frac{r_4\rho}{(1 - r_2)(1 - \rho)} \cdot \frac{(p\theta_1 + r_3\mu_v)}{\lambda + \theta_2 - r_2\mu_v} + \frac{\rho}{(1 - \rho)} \frac{(\lambda - r_2\mu_v + \theta_2)\, q\theta_1 + \theta_2 p\theta_1 + \theta_2\, r_3\mu_v}{\lambda(\lambda + \theta_2 - r_2\mu_v)} \right]$$

THE MODEL'S PERFORMANCE MEASURES

The prob. that the server is busy is Pb = Pr {J = 2}= P3

The prob. that the server is free is Pf = Pr{J = 0} + Pr {J = 1} = P1 + P2=1-Pb

Assume that L denotes the number of customers in the system, subsequently

$$E[L] = \sum_{n=0}^{\infty} n(\pi_{n0} + \pi_{n1} + \pi_{n2})$$

$$= \frac{r_1(1-r_1)^2(1-\rho)^2 + r_2r_3(1-\rho)^2 + r_5(1-r_2)^2 + r_3r_4}{(1-r_1)^2(1-r_2)^2(1-\rho)^2}$$

$$+ \frac{r_2(1-\rho)^2 + r_4\rho}{(1-r_2)^2(1-\rho)^2} \frac{(p\theta_1 + r_3\mu_v)}{\lambda + \theta_2 - r_2\mu_v}$$

$$+ \frac{\rho}{(1-\rho)^2} \frac{(\lambda - r_2\mu_v + \theta_2)\, q\theta_1 + \theta_2 p\theta_1 + \theta_2\, r_3\mu_v}{\lambda(\lambda + \theta_2 - r_2\mu_v)}$$

NUMERICAL RESULTS

By fixing the values of μv = 4.0, μb = 3.0, p = 0.3, q = 0.7, and extending the values of λ from 1.0 to 2.0 incremented with 0.2 and extending the values $\theta 1$ from 1.0 to 3.0 insteps of 1.0 subject to the stability condition the values of $E[L]$ are calculated and tabulated in Table 1 and the corresponding line graphs are drawn in the Figure 1. From the graph it is inferred that as λ increases $E[L]$ also increases as expected.

By fixing the values of μv = 4.0, μb = 3.0, p = 0.3, q = 0.7, and extending the values of λ from 1.0 to 2.0 incremented with 0.2 and extending the values $\theta 2$ from 1.0 to insteps of 1.0 subject to the stability condition the values of $E[L]$ are calculated and tabulated in Table 2 and the corresponding line graphs are drawn in the Figure 2. From the graph it is inferred that as λ increases $E[L]$ also incerases as expected.

CONCLUSION

In this paper, we analyzed an M/M/1 queue with second optional working vacation. Using matrix-analytic technique, we obtained the necessary and sufficient condition for the system to be stable. We derived the stationary probability distribution. We calculated some performance measures. Some numerical examples are illustrated to show the model's stability

REFERENCES

1. Latouche, G. and Ramaswami. V. Introduction to matrix analytic methods in stochastic modeling, ASA-SIAM Series on Applied Probability, USA, (1999).
2. Li. J. and Tian. N The M/M/1 queue with working vacations and vacation interrupt tions, J. Syst. Sci. Syst. Eng., Vol.16, (2007), 121-127.
3. Manoharan. P and Sankara Sasi. K (April 2021) "Analysis a Multi type Service of a Non-Markovian Queue with Breakdown, Delay Time and Optional Vacation." Advances and Applications in Mathematical Sciences. Volume 20, Number 06, pp.975-1001. (Web of Sciences)
4. Naishuo Tian, The M/M/1 queue with single working vacation, International journal of Information and Management sciences, Vol. 19, No. 14, (2008), 621-634.
5. Neuts. M. F., Matrix - Geometric solutions in Stochastic models, Johns Hopkins University Press, Baltimore, (1981).

6. Pazhani Bala Murugan. S and Santhi. K (2017) An M/G/1 retrail queue with Single Working Vacation, Applications and Applied Mathematics: An International Journal (AAM) Volume 12, Number 1, Jan 2017, pp1-22
7. Qingqing Ye and Liwei Liu, The analysis of the M/M/1 queue with two vacation policies, International journal of computer mathematics, Vol. 1, No. 20, (2015).
8. Santhi. K (April 2021) An M/G/1 retrial queue with second optional service and multiple working vacation" Advances and Applications in Mathematical Sciences" Volume 20, Issue 6, pp 1129-1146
9. Servi. L., and Finn. S. M/M/1 queue with working vacations (M/M/1/WV), perform. Eval, Vol.50, (2002), 41-52
10. Tian. N., and Zhang. Z. Vacation queueing models-theory and applications, Springer- Verlag, New York,(2006).
11. Wallace. P, The solution of birth and death processes arising from multiple access computer systems, Ph. D. diss. Systems Engineering Laboratory, University of Michigan. Tech. rept. 07742- 6 T,(1969).
12. Wen - yuan Liu, Stochastic decompositions in the M/M/1 queue with working vacations, Operation Research Letters, Vol. 35, (2007), 595-600.
13. Wu. D., and Takagi. H. M/G/1 queue with multiple working vacations, Perform. Eval, Vol. 63, (2006), 654-681.

Table 1: *E*[*L*] with turnover of λ

λ	θ_1=1.0	θ_1=2.0	θ_1=3.0
1.0	1.563599	2.260233	2.929680
1.2	2.064979	2.922325	3.732999
1.4	2.752335	3.836363	4.842713
1.6	3.736138	5.151189	6.439113
1.8	5.228634	7.149471	8.863168
2.0	7.683077	10.426259	12.828804

Table 2: *E*[*L*] with turnover of λ

λ	θ_2=0.5	θ_2=1.5	θ_2=2.5
1.0	1.563599	1.465869	1.409210
1.2	2.064979	1.923841	1.846644
1.4	2.752335	2.558525	2.459527
1.6	3.736138	3.485043	3.367127
1.8	5.228634	4.931312	4.807285
2.0	7.683077	7.395848	7.302814

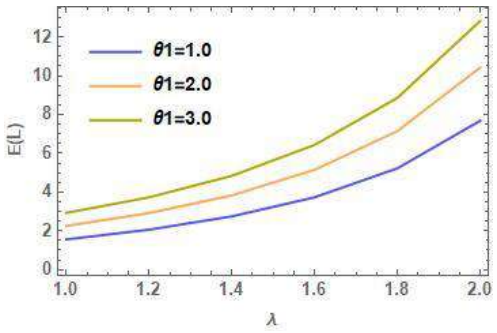

Figure 1 : *E*[*L*] with turnover of λ By

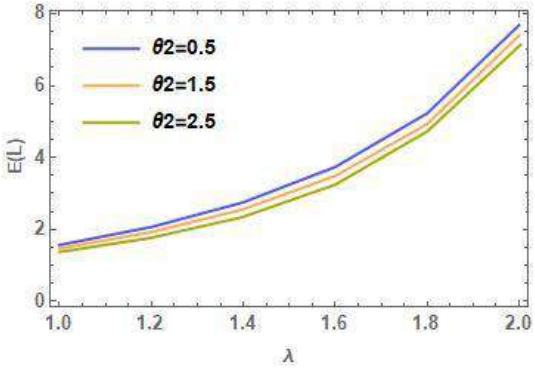

Figure 2 : E[L] with turnover of λ

Indian Journal of Natural Sciences *www.tnsroindia.org.in ©IJONS*

Vol.15 / Issue 83 / Apr / 2024 *International Bimonthly (Print) – Open Access* *ISSN: 0976 – 0997*

RESEARCH ARTICLE

A Study of *In- vitro* Regeneration of Traditional Medicinal Rice, Njavara (Navara)

S.V.Bakiya Lakshmi* and R. Kalaivani

Assistant Professor, Department of Biotechnology, Bon Secours College for Women, Villar, Thanjavur, (Affiliated to Bharathidasan University, Tiruchirappalli), Tamil Nadu, India.

Received: 12 May 2023 Revised: 24 Jan 2024 Accepted: 05 Apr 2024

***Address for Correspondence**
S.V.Bakiya Lakshmi
Assistant Professor,
Department of Biotechnology,
Bon Secours College for Women, Villar, Thanjavur,
(Affiliated to Bharathidasan University, Tiruchirappalli),
Tamil Nadu, India.
Email: bakiyalakshmi.sv@gmail.com

ABSTRACT

The study is intended to optimize suitable methods for high frequency callus induction and regeneration system in the medicinal rice variety Navara under in vitro conditions.MS media supplemented with 2.4mg/l of 2, 4, - D produced the maximum amount of greenish colour callus. The combination of BAP and KN in the ratio of 0.1mg/L and 1.6mg/L offered a best shoot regeneration and multiplication than the other concentration. The well-developed hairy roots were observed in MS medium supplemented with 1.2mg/l of NAA which attained maximum length of root. Hence, the study revealed that the addition of NAA plays a vital role in the formation of roots of paddy Navara. The seed required low concentrations of KN and NAA for regeneration than other paddy varieties and also low concentration of growth hormone produced high regeneration. This is an initial study for in vitro regeneration of Navara on MS media. Further studies will be carried out for creating variations and transformation study in Navara.

Keywords: Medicinal Rice, Navara, *in - vitro* regeneration, 2,4-Dichlorophenoxyacetic acid , 6-Benzylaminopurine, Kinetin, Indole Acetic Acid.

INTRODUCTION

Rice is the staple food of many countries so, with the growing demand it is very important to ensure the constant availability of more rice at less cost. Lifestyle-related diseases are rampant among the world's urban population due to rapid urbanization and lifestyle change. All around the world, there is a great attention towards alternative

holistic therapies. "Food as medicine" is the key emphasis in food industries across the globe. The biological property of the food is attributed by its nutritional richness, mineral (micro and macro) content, vitamins, bio active compounds and also its functional, antioxidant and other physiologically active therapeutic properties (Valko *et al.,*2007*).Navara* is one of such important Indian medicinal rice variety, grown in Southern India and is used mainly for Ayurvedic treatments (Deepa *et al.,*2008; Simi and Abraham, 2008). It is considered as gold among the paddy varieties. It is believed to be a progenitor of Asiatic rice with an unadulterated gene pool. It is presently used in limited Ayurvedic preparations / treatments. It is bestowed with many medicinal properties and the medicinal quality of this rice is preserved by milled rice (Deepa *et al.,*2008).

However, conventional propagation methods have several disadvantages such as the unavailability of large-scale true-to-type planting materials and vulnerability to environmental changes. Thus using biotechnological approaches the regeneration methods can be enhanced along with the variability. Every plant cell considered to be totipotent. The plant has a potential to readily regenerate from the cultured tissue has been considered as a powerful tool for crop improvement and the simplest form of genetic engineering (Larkin and Scowcroft 1981).*In vitro* culture of rice was started with the excised roots and immature embryos using nutrient media supplemented with various concentrations of phytohormones (Fujiwara and Ojima 1995; Amemiya *et al.,*1956). Rice was the first cereal to regenerate into whole plant by *in vitro* regeneration (Vasil 1982 and Vasil 1983). Among 66 rice varieties *japonica* varieties showed high callus yield and regeneration ability while *indica*rice havevery poor response towards*in vitro* culture (Abe and Futsuhara 1986).The frequency of plant regeneration from callus in *indica* rice improved with cytokinins with thidiazuron (Tian *et al.,*1994).Addition of tryptophan to different combinations of auxins and cytokinins in MS media increased the embryogenic callus Massod Swat- II rice variety (Ihsan *et al.,* 2005). The low concentration of dextrose exhibited the maximum shoot and root growth. Maltose showed the moderate growth response of shoot and root length of Basmati rice(Ruby *et al.,* 2007).The maximum percentage of shoot regeneration was recorded at MS media supplemented with 4.0 mg/L of KN+1.0 mg/L NAA and 2.0 mg/L BA for both varieties of aromatic rice. BRRI Dhan 50 (Bangla Moti) and BRRI Dhan 34 (Khaskhani) (Ashrafuzzaman *et al.,*2012).Likewise the *in vitro* performance of high yielding varieties of Govind, Jaya, Pusa Basmati-1,BRRI dhan28, BRRI dhan29, BRRI dhan47, Binadhan-7, Khitish, IR 64, IR 36, IR 72, PNR 546, Swarna, Taraori Basmati and Gobindabhog were successfully regenerated using MS medium with various concentration of 2,4-D, IAA, BAP and KN (Verma *et al.,*2012; Anita *et al.,* 2012; Alam *et al.,* 2012). The optimized regeneration for six aromatic immature embryo rice namely, Chinigura, Kalijira, Radhuni Pagal, Modhumala, Kataribog and Mohonbhog by the combination of BAP and IBA (Zahida *et al.,*2014)

Despite its distinctness among traditional rice strains as a medicinal plant, it is only in recent times *Navara*has become the focus of research.. The medicinal value of *Navara* is being recognized increasingly which can be understood from the fact that recently a website on *Navara* has been launched by the agriculturists, scientists and producers. Thus, there is a need to improve the existing germplasm of *Navara* by introducing variability into plants that could be utilized for crop improvement which further also depends on their regeneration capacity. There was no regeneration system has been reported earlier in *Navara*. Therefore, the study intended to optimized suitable method for high frequency callus induction and regeneration system in medicinal rice variety *Navara* under *invitro* conditions.

MATERIALS AND METHODS

Collection of Plant material

Seeds of *Navara* variety were collected from organic farmland at Musiri Salem Dt, Tamil Nadu. Itis a pigmented variety, having a black seed coat and dehusked seed are red in colour (Fig 1). The paddy was authenticated by Dr. S. John Brito, The Director of Herbarium, St Josph College, Trichy with Accession Number is SVB001 (Fig 1).

***In vitro* regeneration of *Navara* seed**

The dehusked seeds were washed under running tap water for 30 minutes and with Teepol or soap solution for 5 minutes. After rinsing with sterile distilled water, they were surface sterilized in 0.1% (w/v) $HgCl_2$ for 10 minutes and again rinsed thoroughly with sterile disteilled water. The rice grains were then transferred on control MS (Murashige, Skoog, 1962) basal medium containing various concentration of 2,4-dichlorophenoxy acetic acid (2,4-D), Kinetin (KN), 6-Benzylaminopurine (BAP)and Naphthaleneacetic acid (NAA).

Callus Induction medium

MS medium supplemented with 3% sucrose, 0.8% agar, different concentrations of 2,4-dichlorophenoxy acetic acid from 0.8 – 4 mg/L with an intervals of 0.8 mg/L. Seeds were tested with triplicate experiments with 24 h dark period was maintained.

Regeneration medium

The greenish colour healthy embryogenic callus was selected and placed on regeneration medium containing KN, BAP and NAA. 16 h photo period and 8 h dark period was maintained for regeneration of calli. The efficiency was calculated as:

Regeneration efficiency (%) = Total No. of regenerated plants / Total No. of callus – induced seeds × 100.

RESULTS

Effect of 2, 4, -Don callus induction

The callus initiation was observed after 9 days of incubation of the cultured seeds in the callus induction medium (Table 1 and Fig. 3). The callus induction was observed after five weeks of inoculation. It was noticed that MS media supplemented with 0.8, 1.6, 2.4, 3.2 and 4.mg/l of 2, 4, -D produced appreciable amount of callus. The lowest concentration (0.8mg/l) of 2, 4, -D produced 42% of callus which had 47±3mg of weight with white colour appearance of induced calli. The maximum number of callus was produced by 2.4mg/l of 2, 4, - D which formed intense greenish colour callus with 521±23 mg weight. The effects of using only 2, 4, D during callus induction is more efficient than using 2,4-D in combination with other growth regulators. It was observed that the plant regeneration ability of plated calli depends on the callus inducing media.

Effect of KN, BAP and NAA for Shoot and Root Generation

The effect of BAP and KN on shoot multiplication in selected rice variety was calculated and the results were showed in Table 2 & 3and Fig. 3,4&5 respectively. The maximum shoots were obtained in MS media supplemented with 1mg/l of BAP and various concentration of KN like 0.4, 0.8, 1.2, 1.6 and 2.0mg/l. Shoots were protracted and showed dark green in colour. It revealed that the length of shoots increased engaged by BAP and KN concentration with the maximum shoot length was 6.6cm followed by 5.7 cm respectively. Therefore, the combination of BAP and KN in the ratio of 0.1mg/L and 1.6mg/L offered a best shoot regeneration and multiplication. The current study showed that the roots were well developed in MS medium supplemented with 1.2mg/l of NAA which attained 3.7cm length.. Hence, the study revealed that the addition NAA plays a vital role for the formation of root of paddy *Navara.* The present study showed that best combination for regeneration is MS with 2mg/l KN and 1.2mg/l of NAA which furnished regenrants with an average height of 6.6cm after37 day of incubation. The highest percentage of shoot generation efficiency of *Navara* was 86.7%.

DISCUSSION

Tissue culture generates a wide range of variation, which is resulted with supplementation of 2,4-D for callus induction (Rasheed *et al.,* 2005). 60-100 per cent of the cultured seeds formed callus by concentrations of 2,4-D and

also they proved 2.4 mg/l 2,4-D to be the most favorable for callus induction and callus proliferation (Pandey *et al.*,1994; Shankhdhar *et al.*,2002; Tam and Lang, 2003; Naqvi *et al.*,2005. Jaseela *et al.*,2009). The same result was reported by Azrla and Bhalla of getting callus from Australian variety of rice in MS medium supplemented with 2.0mg/l of 2,4,D. The present study also revealed that 2.4mg/l of 2, 4, D was effective for highest number of callus induction by increase in the rate of cell division and this attributes to the increased amount of callus.

Likewise, Ritu mahajan *et al.,(2013*) Sharma *et al.,* (2012) observed better response of callus proliferation and shoot bud regeneration on MS medium supplemented with 2.0 mg IBA and 1.0 mg NAA in immature embryos of three *indica* rice varieties (Heera, Pankaj & Basmati-370 . Liu *et al.* (2002) also investigated with young embryos of grain-straw-dual-use rice 201 and found that 0.05 mg NAA with 2 mg BA L-1 was the most suitable differentiation medium for immature grain-straw-dual-use rice embryos. Ritu*et al.,2013* revealed that the optimum concentration of 2,4-D was2.0mg/l, effective for callus induction. Best combination of plant growth regulators that resulted in plantlet regeneration from callus was 2 mg/l 2,4-D , 0.5 mg/l KN and 2 mg/l NAA in both the Ranbir basmati and Basmati 37 leading to 84.67% and 83.33% shoots respectively. In this swot up the paddy required low concentration of KN and NAA for regeneration than other varieties and also low concentration of growth hormone produced 86.7% of regeneration. This is an initial study for *in vitro* regeneration of *Navara* grows on MS media. The further study will be carried out for creating variation in *Navara*.

REFERENCES

1. Abe and Futsuhara Y (1986) Genotypic variability for callus formation and plant regeneration in rice (Oryza sativa L.). TheorAppl Genet. 72: 3-10.
2. Alam M. J, Imran M, Hassan L, Rubel M. H and Shamsuddoha M (2012). In VitroRegeneration of High Yielding Indica Rice (Oryza sativa L.) Varieties. J. Environ. Sci. & Natural Resources, 5(1): 173 – 177.
3. Amemiya A Akemne H Toriyama K (1956) Bull. Natl. Inst. Agric. Sci. D6, 1. 9. Armstrong C Green C (1985) Planta. 164, 207.
4. Anita Roy,. Aich, S.S, Mukherjee S (2012). Differential Reponses to Indirect Organogenesis in Rice Cultivars. International Journal of Scientific and Research Publications, Volume 2, Issue 9, 1-5.
5. Ashrafuzzaman. M, Golam Gaus Mohiuddin Chowdhury, Raihan F and Shamsul Prodhan. H, (2012). Research Journal of Biology, Vol. 02, Issue 03, pp. 98-103.
6. Burnet G. & Ibrahim R.K. 1973 Tissue culture of Citrus peel and its potential for flavonoid synthesis. Z. Planzenphysiol. 69, 152-162.
7. Deepa G, Singh V, Naidu KA (2008). Nutrient composition and physiochemical properties of Indian medicinal rice - Njavara. Food Chem;106:165–171.
8. Fujiwara, A. and Ojima, K. (1955). Physiological studied on plant root (Part 1). Influent of some environment condition on growth of isolated root and rice and wheat. Journal of Soil Science, Manuse Japan, 28, 9 – 12.
9. Gautam VK, Mutal A, Nanda K, Gupta SC (1983) Plant Sci Lett 29: 25–32.
10. Gilbert Schelater (1922) .The Dravidian element in Indian culture , Madras press.34.
11. Ihsan Ilahi, Shazia Bano, Musarrat Jabeen and Fazal Rahim (2005).Micropropagation of rice (Oryza sativa l. Cv swat-ii) through somatic embryogenesis. Pak. J. Bot., 37(2): 237- 242,
12. Jaseela, F., V.R. Sumitha and G.M. Nair. 2009. Somatic embryogenesis and plantlet regeneration in an agronomically important wild rice species Oryza nivara. Asian J. Biotechnol. 1(2): 74-78.
13. Liu, F., M. Xu, X.F. Wang and J.G. Zheng, 2002. A preliminary study on establishing high regeneration frequency system of grain straw dual use rice 201, an indica rice. J. Fujian Agri. For. Uni., 31: 146–9
14. Majumdar GP, Banerji SC (1960) Krsi-Parasara. He Asiatic Society, Calcutta, West Bengal.
15. Murashige T, Skoog F. (1962). A revised medium for rapid growth and bioassays with tobacco tissue cultures. Physiologia Plantarum 15: 473- 479.
16. Naqvi, S.M., S.Razia and H.Rashid. (2005). Tissue culture studies in Oryza sativa L. cvs. Basmati 385 and Super Basmati. Pak. J.Bot., 37(4): 823-828.

17. Pandey, S.K., B. Ramesh and P.K. Gupta. 1994. Study on effect of genotypes and culture medium on callus formation and plant regeneration in rice (Oryza sativa L.). Indian J. Genet., 54(3): 293-299.
18. Pankar, S. N., and Gowda M.K. (1976). On the origin of rice in India. Science and Culture. 42:547-550.
19. Rasheed, S, T. Fatima, T. Husnain, K. Bashirand S. Riazuddin. 2005. RAPD characterization of somaclonal variation in indica basmati rice. Pak. J. Bot. 37(2): 249-262.
20. Revel, E.D., Le Rizen Asie D and Su D. Est: (1988) Atlas du Vocabulatre de la Plante. Paris Chinese Academy of Agriculture and Sciences.
21. Ritu Mahajan, Lubna Aslam and Hejazy Kousar (2013). Effect of Growth Regulators on In Vitro Cultures Of Two Basmati Rice Genotypes: Ranbir Basmati And Basmati 370. IJPCBS, 3(4), 1131-1138.
22. Ruby Thapa, Dipesh Dhakal, Dhurva Prasad Gauchan. 2007. Effect of different sugars on shoot induction in cv. Basmati. Kathmandu University Journal of Science, Engineering and Technology . Vol.I, No.III. 1-4.
23. Shankhdhar, D., S.C. Shankhdhar and R.C. Pant. 2002. Development of somatic embryos in rice. Indian J. Plant Physiol., 7(3): 211-214.
24. Sharma P, Jha AB, Dubey RS, Pessarakli M (2012) Reactive oxygen species, oxidative damage, and antioxidative defence mechanism in plants under stressful conditions. Journal of Botany, Vol 2012, 1-26.
25. Simi CK, Abraham TE (2008). Physicochemical rheological and thermal properties of Njavara rice (Oryza sativa) starch. J Agric Food Chem. ; 56:12105–12113.
26. Tam, D.M. and N.T.Lang. (2003). In vitro selection for salt tolerance in rice. Omonrice,11: 68-73.
27. Tian Wenzhong, Iam Rance, Elunialai Sivamani, Claud auquet and Roger N. Beachy,1994. Frequency in vitro indica rice.Chinese Journal of GeneticsVolume 21.
28. Valko M, Leibfritz D, Moncol J, Cronin MTD, Mazur M, Telser J, (2007). Free radicals and antioxidants in normal physiological functions and human disease. The International Journal of Biochemistry & Cell Biology, 39,44-84.
29. Vasil VL and Vasil IK (1982) Characterization of an embryogenic cell suspension culture derived from cultured inflorescence of Pennisetum americanum (Pearl millet). Amer. J. Bot 69:1441-49.
30. Vasil VL, and Vasil IK (1983) Plant regeneration from protoplasts of Napier grass (Pennisetumpurpureum Schum) Z Plonzenphysiol. Ill :233-39.
31. Verma Dipti, Joshi Rohit, Shukla Alok and Kumar Pramod (2011) Protocol for in vitrosomatic embryogenesis and regeneration of rice (Oryza sativa L.). Indian Journalof Experimental Biology. 49; 958-963.
32. Zahida Yesmin Roly, Md. Mahmudul Islam, Md. Pallob Ebna Shaekh, Md. Saiful Islam Arman, Shah Md. Shahik, Dipesh Das, Md. Mujjammil E Haamem, Md. Khalekuzzaman(2014). In Vitro callus induction and regeneration potentiality of Aromatic rice (Oryza sativa l.) Cultivars in differential growth Regulators. Int. J. Appl. Sci. Biotechnol, Vol 2(2): 160-167.

Table 1 – Effect of 2,4, -D on Callus Induction of *Navara* Rice using MS Media

Conc. (mg/l)	Percentage of Callus formation Frequency	Weight of the callus (mg)	Colour of the callus
0.8	42	47±3	White
1.6	62	134±13	Pale yellow
2.4	87	521±23	Intense green
3.2	81	405±19	Light green
4.0	77	301±13	Light green

Table 2. Effect of KN and BAP for Shoot Generation using MS Media

Concentarion (mg/l)	Percentage of Regeneration	Length of Shoot (cm)
0.1 + 0.4	46.7	3.8 ± 0.1
0.1 + 0.8	66.7	4.3 ± 0.4
0.1 + 1.2	80	5.7 ± 0.2
0.1 + 1.6	86.7	6.6± 0.1
0.1 + 2.0	73.3	4.8± 0.1

Table 3: Effect of NAA for Root Generation

Conc. mg/l	Length of Shoot (cm)	Type of Root
0.4	1.6 ± 0.1	Thread like root
0.8	2.2 ± 0.4	Small thread like root with less root hair
1.2	3.7 ± 0.2	Long well developed root with root hairs
2.0	2.8± 0.1	Small thread like root with less root hair
2.4	3.2± 0.1	Small thread like root with less root hair

***Fig: 1. Navara* Paddy and Rice**

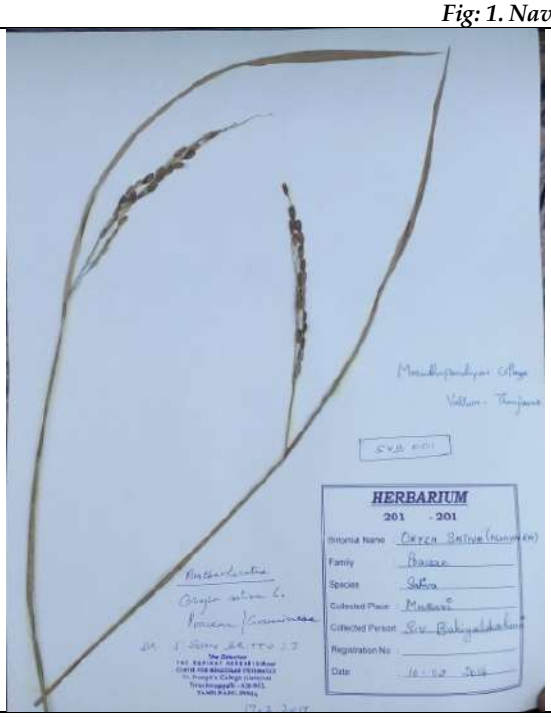

Fig. 2 Herbarium of *Navara* Paddy

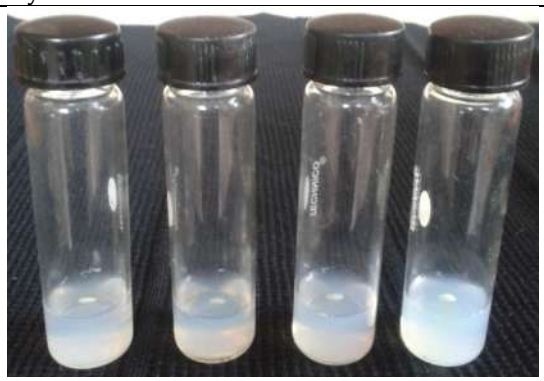

Callus induction test

Fig. 3: *In Vitro* Regeneration of *Navara* on MS Media

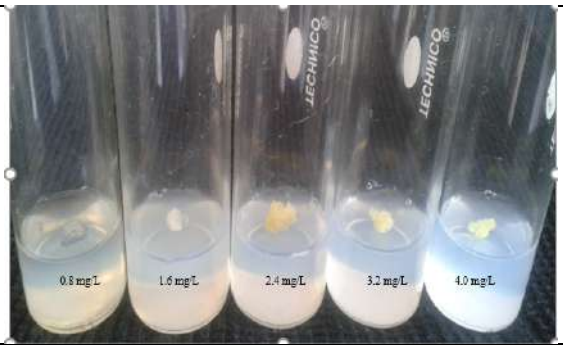

Fig. 4 Callus induction on MS medium supplemented with different concentrations of 2,4-D

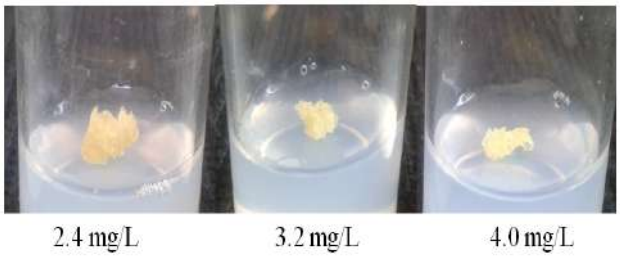

Appreciable values result for callus formation appears in green colour

Fig. 5. 35th Day ofcallus induction on MS callus induction medium supplemented with different concentrations of 2,4-D

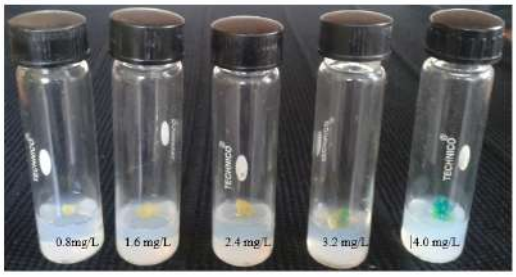

Tested different concentrations of naphthalene acetic acid on MS regeneration medium

Fig .6 Regeneration of *Navara in* MS medium

Fig .7. 2.0 mg/ L Kinetin and 1.2 mg/ L naphthaleneacetic acid shows consistent green color appearance on the 9th day and appreciable regeneration of rice with a height of 6.6 cm length at 37th day

Indian Journal of Natural Sciences *www.tnsroindia.org.in ©IJONS*

Vol.15 / Issue 83 / Apr / 2024 *International Bimonthly (Print) – Open Access* *ISSN: 0976 – 0997*

RESEARCH ARTICLE

Passive Heat Withdrawal from a Concrete Roof: An Eco-Friendly Approach of Space Cooling

S.V.Prayagi[1], Prasad.A.Hatwalne[2]*, A.P.Kedar[1], Prashant D. Kamble[2] and Vikrant Pradip Katekar[3]

[1]Professor, Department of Mechanical Engineering, **Yeshwantrao Chavan College of Engineering** (Affiliated to **Rashtrasant Tukadoji Maharaj Nagpur University**) Nagpur, Maharashtra, India.

[2]Assistant Professor, Department of Mechanical Engineering, **Yeshwantrao Chavan College of Engineering** (Affiliated to **Rashtrasant Tukadoji Maharaj Nagpur University**) Nagpur, Maharashtra, India.

[3]Ph.D Scholar, IIT Bombay, Maharashtra, India.

Received: 30 Dec 2023 Revised: 09 Jan 2024 Accepted: 27 Mar 2024

***Address for Correspondence**
Prasad.A.Hatwalne
Assistant Professor,
Department of Mechanical Engineering,
Yeshwantrao Chavan College of Engineering
(Affiliated to **Rashtrasant Tukadoji Maharaj Nagpur University**)
Nagpur, Maharashtra, India.
Email: hatwalneprasad1@gmail.com

ABSTRACT

The present research introduces an environment-friendly technique for passive heat removal from a building's reinforced concrete roof to maintain it at lower temperatures. The arrangement consists of a reinforced cement concrete roof with several reinforced steel bars and building a parapetby vertically extending the reinforced steel bars and installing an open-ended water piping system with several pipes. From the experimental investigation, it has been revealed that passive heat removal from the concrete roof results in a 5 to 10°C reduction in its temperature, with the sensible heat removal rate ranging from 800 W/m2 per hr to 850 W/m2 per hr; consequently, lowering the space cooling load by 15%.

Keywords: Air conditioning, Building passive cooling, Cement concrete roof slab, Cooling load, Thermal radiation,

INTRODUCTION

Some of the most expensive energy bills in any house are space heating, cooling, and water heating[1].A cool roof is designed to reflect more sunlight than a standard roof, absorbing less solar energy[2]. It reduces the structure's temperature in the same way as wearing light-coloured clothes keeps us cool on a hot day[3]. During the summer season in tropical countries, the heat obtained by the concrete slab is around 832.2 W/m2 per hr after accounting for different losses, and the heat gained by the reinforced metal rods or bars in the slab is almost the same. As a result, conventional roofs may achieve 65°C or more on a hot summer day. A reflective roof might keep more than 28°C cooler under the same circumstances[4]. Lowering heat movement from the top into the inhabited area may save energy and expenditure in buildings with air conditioning. It increases comfort and safety in buildings without air conditioning[5]. Most cool roofs have a high thermal emittance by emitting thermal infrared radiation[6]. Heating and cooling account for a considerable portion of the energy expenditures for the ordinary home or business facility. In hot climates, the roof of a structure, the most exposed surface to solar radiation, may play an essential role in building sustainability by absorbing substantial thermal energy[7]. Many passive solutions, such as reflecting roof systems, green roof systems, and thermal insulation systems, have been used to limit heat gains into the structure.

LITERATURE REVIEW

Reflective roof systems in tropical areas significantly minimize maximum solarheat intake by reflecting solar radiation by around 90% during hot months[8]. Many materials have been suggested for use in solar heat radiation shielding. US20140248467A1 reveals solar heat- reflecting roofing granules an their US64 23129B1 discloses the use of ceramic-containing coatings and additives[10]; US6933007B2 discloses the use of reclaimed porcelain[11]. However, reflecting roof materials have limited utility and lose their reflectivity with time. Highly reflective roofs may cause eye discomfort and glare, making them unsuitable for regions along flight routes. As a result, the geography of the site and building codes restrict its implementation in certain circumstances. A lightweight, pre-seeded, fully-contained, multi-layered modular green roof system that supports plant life and allows rainfall to flow through onto building roofs is described in patent application US20100126066A1[12].Yang He et al.,[13]determined the thermal and energy performance variations between two distinct roof types in Shanghai's climate. First, a field experiment was carried out in the Shanghai region. Cool roofs and common roofs were all measured in the summer and winter. The findings revealed that the cool roof had an average cooling impact of 3.30C on the outer roof deck surface compared to the conventional roof. During the summer, the green roof had a cooling effect of 2.90C. The green roof was useful in the cold. The authors also mentioned that insulation might increase the outside surface temperature of the roof deck by an average of 3.3 degrees Celsius. Nutkiewicz et al., [14]presented an energy modelling framework to study how building design choices affect the onset of heat stress and energy-intensive cooling demand. Authors demonstrated that residents in tropically situated informal settlements are the most sensitive to year-round heat stress. Up to 98 percent of yearly heat stress exposure may be reduced by upgrading the building envelope, which minimises yearly heat stress exposure by up to 91 percent.

Rawat and Singh[15]highlighted cool roof thermal performance with various kinds of surface coatings in various climatic zones for buildings, along with extra advantages, limits, and suggestions for further study work. Their findings may assist engineers, researchers, residents, and architects understand the advantages of cool roofs in reducing energy consumption demand in dwellings in a sustainable, cost-effective, and energy-efficient manner. Authors mentioned that the average energy-saving impact of the roof ranges from 15% to 35.7% in various climatic zones (Temperate, Tropical, Composite, Hot, and Warm-Humid). In addition, cool roof technology may reduce average roof surface temperature by up to 4.7 degrees Celsius. Yazdaniand Baneshi[16]found that, for hot and humid climates, green roofs with regular watering systems are the optimum roof approach, reducing yearly thermal loads of the reference building with the standard concrete roof by 17.8–171.4 kWh/m2 (21.3–66.0percent), depending on thermal mass and insulation levels. Dynamic cool roof outperforms both dry and wet green roofs in hot summer-cold winter cities, potentially reducing yearly energy consumption by 11.8–66.7 kWh/m2 (22.4–

35.4 percent).The WRF-Chem model,in conjunction with a single-layer urban canopy model, is used by Zhong et al., [17] to simulate three heat wave and high ozone pollution occurrences in Shanghai, China. Sensitivity tests on green roofs and cool roofs are conducted, and the findings reveal that both green roofs and cool roofs can successfully decrease urban heat islands. Their cooling efficiencies are comparable even if their cooling processes are different. Chen et al.,[18] integrated radiative sky cooling materials into buildings as part of a super-cool roof approach to deploy passive cooling technology. Authors conducted comprehensive assessments on techno- economic and environmental performance of super-cool roof applications in China by combining model development, experimental validation, and numerical modelling. A unique radiative sky cooling- based super-cool roof model was created by authors in which the entire spectrum selectivity of radiative cooling materials was integrated, and the model was experimentally verified with root mean square errors of less than 4.69 percent, demonstrating its accuracy. Broadbent et al., [19] discovered that installing cool roofs uniformly, rather than targeted, provides an average 0.66°C temperature reduction in the highest heat sensitivity area and a 0.39°C temperature reduction in the lowest heat sensitivity area. Targeting cool roof implementation results in 0.45°C cooling in the most sensitive areas versus 0.22°C cooling in the least sensitive areas, indicating that needs-based targeted cool roofs in high sensitivity areas provide more relief than cool roofs targeted in low sensitivity areas, thus providing more cooling where it is most needed. Through Weather Research and Forecasting (WRF) model simulations, Baik et al., investigated the impacts of cool-roofs on temperature and wind conditions in Seoul, South Korea during the 2018 heat wave[20]. They found that cool roofs reduced the 20C temperature, 10-m wind speed, surface sensible and latent heat fluxes, and planetary boundary layer height during the day. They also reported that the cool roof- induced drop in near surface temperature diminishes with rising heat wave severity. Despite the many benefits of green roofs, the fundamental restriction of these systems the expense of installation since the underlying structure must be upgraded to withstand the additional weight. Thermal insulation solutions assist in reducing energy use and expenses while maintaining the required degree of comfort for building occupants. US7818922B2 describes a thermal insulation system for a building that includes several spaced-apart support components filled with insulator foam[21]. CA2419318A1 describes an improved method and equipment for insulating a building roof that employs a stiff thermal insulating panel positioned between roof rafters[22].Sinsel et al., [23]used the microclimate model to perform sensitivity research on super cool roofing materials' effects on outdoor air temperature compared to regular cool roofs and green roofs.

Authors revealed hat super cool roofs offered 0.1 to 0.15 K greater cooling than cool roofs and green roofs, with an averaged street-level air temperature cooling of roughly 0.85 K in periods of intense solar radiation. The results also revealed that super cool roofs might reduce pedestrian- level air temperatures by up to 2.4 K in certain places. However, geographical research revealed that colder air from the roof prevents street canyons from exchange invertical air. Finally, the street-level cooling effectiveness of all three roof types is anticipated to decline non-linearly with increasing building height by about 0.003 K per metre and to halt at around 100 m. Vinod Kumar et al., [24]evaluated the benefits of a polystyrene foam-aluminum radiation reflector double skin system for usage as a passive cool roof in a desert environment such as Oman, as well as the impact of air ventilation as a thermal barrier between the double skin layers. The experiment was conducted in three phases for air ventilation between polystyrene- aluminum radiation reflector layers 0, 20, and 40 cm. Field testing indicated that a considerable reduction in indoor and roof slab temperatures was found for polystyrene-aluminum radiation reflector passive cool rooms as compared to a standard bare roof. Experiment results showed that, when compare to a traditional roof, the room air temperature of a double skin polystyrene aluminum radiation reflector was reduced by 2.420C (6.7 percent), 3.690C (10.4 percent), and 4.70C (12.8 percent) for 0, 0.2 m, and 0.4 m air ventilation between the polystyrene foam an aluminum reflector, Celsius (16.8 percent), 8.1 degrees Celsius (24.5 percent), and 11.11 degrees Celsius (31.9 percent), respectively. The interior air and roof surface temperature of the passive cool roof decreased as the air ventilation increased from 0 to 0.4 m. Saw et al., [25] evaluated the thermal performances of the closed-loop pulsing heat pipe roof system and compared it to the design of the bare metal roof system. The testing findings indicated that the cool roof system with heat pipe technology could decrease the attic temperature from 34 degrees Celsius to 29.6 degrees Celsius, a 13 percent drop in temperature compared to the bare metal roof design. According

to the findings, the heat pipe cool roof system is a potential solution for attic retrofitting interventions to increase thermal comfort in the structure.

Motivation Behind the Research

None of the patents and research articles mentioned above allows installations that have been established before the construction of a reinforced concrete cement roof slab, parapet enclosure, or any piping or ductwork. As a result, there has long been a perceived need in the art to give a cost-effective and straightforward enhancement in design via the use of passive measures of thermal insulation in buildings. Hence it is necessary to minimise the limitations mentioned above by using a simple change in roof design for cost-efficient for ordinary households. The main objective of the present research is to provide a method for passive heat removal from a building's reinforced cement concrete roof slab. The current research deals with the passive heat removal from a building's reinforced cement concrete roof slab for more significant energy savings by constructing a roof slab from several reinforced steel bars, constructing a parapet enclosure by extending the reinforced steel bars from the roof slab, installing an open-ended piping system with several pipes that include pipe for cold water inlet and pipe for hot water outlet, and welding the bars to the pipes**.**

RESEARCH OBJECTIVES

The objectives of the present research work are as follows:

a. The primary object of the present invention is to provide a method for passive heat removal from reinforcement cement concrete roof slab of a building.
b. To estimate energy saving and reduction in the cooling load of the space.
c. To investigate the additional advantages of the proposed structure.

Projected energy-efficient structure

Following Figure. 1 depicts a perspective view of the present investigation's reinforced cement concrete roof slab components. constructing a reinforced cement concrete roof slab from several reinforced steel bars, extending the reinforced steel bars from the reinforced cement concrete roof slab, installing an open-ended piping system A reinforced concrete roof slab forms a heat exposed building roof surface. Reinforced steel bars were placed to make a mesh in the inner concrete section using standard techniques and cement concrete construction components to produce a heat exposed surface of a building roof. The reinforced steel bars were extended uprightly, resulting in a plurality of vertically extended reinforced steel bars with different pre-determined elevations, and constructed a parapet enclosure of the building roof by placing cement concrete building elements. The height of the strengthened steel bars in the parapet enclosure will provide consistent water flo from the piping system after the thermosyphon effect. An open-ended piping system Has several horizontally extending pipes for cold water intake and hot water output. The open-ended pipe system is at least 150 mm distant from and parallel to the parapet wall. All pipes are installed and attached to the vertically extended reinforced steel bars on the inner side of the concrete parapet enclosure. Welding is used to fastening all of the pipe work to the vertically extended reinforced steel bars in an airtight seal .Because of the thermosyphon effect, the slope assures hot water circulation and removes the need for external energy sources such as electricity for water movement. Passive thermal energy absorption occurs through conduction from the reinforced cement concrete roof slab to the reinforced steel bars and from the vertically extended reinforced steel bars to the cold-water inlet pipe, and from the pipe to the cold water flowing inside the pipe. This increases the temperature of the water, causing it to rise due to the thermosyphon effect, and this occurs without the usage of any external energy source. The hot water is then removed and collected in a how water tank for later home-usage. Another procedure is adding cold water and removing hot water until thermal equilibrium is reached. This also contributes to lowering the internal temperature of the structure during hot weather. The cold water is supplied from an overhead tank through the open-ended piping system. The hot water collection from the circulation and storage in a hot water tank for later use, home or industrial.

EXPERIMENTAL INVESTIGATION

The following experimental steps demonstrate how the different features of the present structure work:

a) The experiment was conducted in Nagpur (Maharashtra), a tropical area of India, throughout March, April, and May.
b) A roof slab was built from a series of reinforced steel bars (10 mm) extended vertically to form a parapet enclosure to which a plumbing system was attached.
c) The roof slab had a 1000 mm × 1000 mm size and a thickness of 100 mm.
d) The piping system was built of galvanised iron pipes (GI-pipe) with a diameter of 15 mm, which were welded to vertically extended reinforced steel bars.
e) The plumbing system was set back parallel to the parapet wall by 150 mm.
f) The piping system was designed with a slope to the pipes, with the cold-water input end at 150 mm and the hot water exit at a higher elevation point of 250 mm from the slab.
g) Considering different losses, the heat gained by the concrete slab was roughly 832.2 W/m2per hr.
h) The temperature of the slab was measured to be about 72°C. The water temperature in the pipe system raised from an initial temperature of approximately 30°C to a final temperature of about 65°C, resulting in a 35°C increase in water temperature.
i) The temperature of the reinforced concrete cement slab was reduced by around 8°C, and a heat removal rate of approximately 830 W/m2 per hr was recorded,
j) It decreases the cooling demand by 15-20%.
k) The hot water collected was then utilized for residential and industrial uses.

CONCLUSION

The present investigation deals with a passive heat removal approach from a building's reinforced concrete roof provide a way for cooling a building's roof and the structure's interior temperature. From the experimental investigation, the following conclusions are drawn: Using the proposed system, the reinforced concrete slab's temperature has been reduced by 5°C to 10°C with a heat removal rate of 800 W/m2 per hr to 850 W/m2 per hr the electrical demand for cooling is reduced by 15% to 20%. The reinforced concrete slab's temperature was reduced by 5°C to 10°C. Cooling load is reduced by 10% to 20%, hence living in comfortable circumstances. Longer energy duration with a positive attitude Reasonably priced The system is simple to construct and use. There is no need for maintenance, and there is no energy waste. Water is not wasted, which is good for the environment. Hot water would be used for secondary purposes, such as washing, cleaning, and bathing. For use in industry, hot water can be used for manufacturing.

Declaration

The authors have declared no conflicts of interest. All co-authors have read and approved the article, and there are no financial conflicts to disclose

REFERENCES

1. V.P. Katekar and S.S. Deshmukh, Energy- Drinking Water-Health Nexus in Developing Countries., in Energy and Environmental Security in Developing Countries. Advanced Sciences and Technologies for Security Applications., Asif M., ed., Springer, Cham., 2021, .
2. M. Kolokotroni, E. Shittu, T. Santos, L. Ramowski, A. Mollard, K. Rowe et al., Cool roofs: High tech low cost solution for energy efficiency and thermal comfort in low rise low income houses in high solar radiation countries, Energy Build. 176 (2018), pp. 58–70.

3. L. Hes, K. Bal and M. Boguslawska- Baczek, Why black clothes can provide better thermal comfort in hot climate than white clothes, Fiber Soc. Spring 2014 Tech. Conf. Fibers Prog. (2014), pp. 1–2.
4. W. Miller, G. Crompton and J. Bell, Analysis of cool roof coatings for residential demand side management in tropical Australia, Energies 8 (2015), pp. 5303–5318.
5. J. Yang, D. llamathy Mohan Kumar, A. Pyrgou, A. Chong, M. Santamouris, D. Kolokotsa et al.,
6. Green and cool roofs' urban heat island mitigation potential in tropical climate, Sol. Energy 173 (2018), pp. 597–609.
7. H. Akbari and R. Levinson, Evolution of cool-roof standards in the US, Adv. Build. Energy Res. Vol. 3 2 (2012), pp. 1–32.
8. C. Murguia, D. Valles, Y.H. Park and S. Kuravi, Effect of high aged albedo cool roofs on commercial buildings energy savings in U.S.A. climates, Int. J. Renew. Energy Res. 9 (2019), pp. 65–72.
9. F. Salamanca, M. Georgescu, A. Mahalov, M. Moustaoui and A. Martilli, Citywide Impacts of Cool Roof and Rooftop Solar Photovoltaic Deployment on Near-Surface Air Temperature and Cooling Energy Demand, Boundary-Layer Meteorol. 161 (2016), pp. 203–221.
10. J. Sarazyn, Solar heat reflective roofing granules, solar heat reflective shingles and process for producing the same, US 2014/0248467 A1 1 (2014), pp. 33.
11. R.T. Fitzgibbons, Coating and additivies containing ceramic material, US 6,423,129 B1 1 (2002), pp. 22.
12. F.A. Fensel, J. Palladino and M.A. Rus,Method of forming an improved roofing material, US 6,933,007 B2 1 (2009), pp.14.
13. D. DeVos, Modular green roof system, US 2010/0126066A1 1 (2010), pp. 12.
14. Y. He, H. Yu, A. Ozaki and N. Dong,Thermal and energy performance of green roof and cool roof: A comparison study in Shanghai area, J. Clean. Prod. 267 (2020),pp. 122205.
15. A. Nutkiewicz, A. Mastrucci, N.D. Rao and R.K. Jain, Cool roofs can mitigate cooling energy demand for informal settlement dwellers, Renew. Sustain. Energy Rev. 159 (2022), pp. 112183.
16. M. Rawat and R.N. Singh, A study on the comparative review of cool roof thermal performance in various regions, Energy Built Environ. 3 (2022), pp. 327–347.
17. H. Yazdani and M. Baneshi, Building energy comparison for dynamic cool roofs and green roofs under various climates, Sol. Energy 230 (2021), pp. 764–778.
18. T. Zhong, N. Zhang and M. Lv, A numerical study of the urban green roof and cool roof strategies' effects on boundary layer meteorology and ozone air quality in a megacity, Atmos. Environ. 264 (2021), .
19. J. Chen, L. Lu, Q. Gong, W.Y. Lau and K.H. Cheung, Techno-economic and environmental performance assessment of radiative sky cooling-based super-cool roof applications in China, Energy Convers. Manag. 245 (2021), pp. 114621.
20. A.M. Broadbent, J. Declet-Barreto, E.S. Krayenhoff, S.L. Harlan and M. Georgescu, Targeted implementation of cool roofs for equitable urban adaptation to extreme heat, Sci. Total Environ. 811 (2021), pp. 151326.
21. J.J. Baik, H. Lim, B.S. Han and H.G. Jin, Cool-roof effects on thermal and wind environments during heat waves: A case modeling study in Seoul, South Korea, Urban Clim. 41 (2022), pp. 101044.
22. B. Ellis, Thermal insulation for a building, US 7,818,922 B2 2 (2010), pp. 2.
23. T.N. Corwin, Process and appratus for insulating building roof, CA2419318A1 2(2003), pp. 32.
24. T. Sinsel, H. Simon, A.M. Broadbent, M. Bruse and J. Heusinger, Modeling the outdoor cooling impact of highly radiative "super cool" materials applied on roofs, Urban Clim. 38 (2021), pp. 100898.
25. V.V. Kumar, N. Raut and N. Akeel, Double skin polystyrene- aluminium radiation reflector roofs in arid environments for passive cooling - A case study in Sohar, Sultanate of Oman, Case Stud.Therm. Eng. 28 (2021), pp. 101655.
26. L.H. Saw, M.C. Yew, M.K. Yew, W.T. Chong, H.M. Poon, W.S. Liew et al., Development of the closed loop pulsating heat pipe cool roof system for residential buildings, Case Stud. Therm. Eng. 28 (2021), pp. 101487.

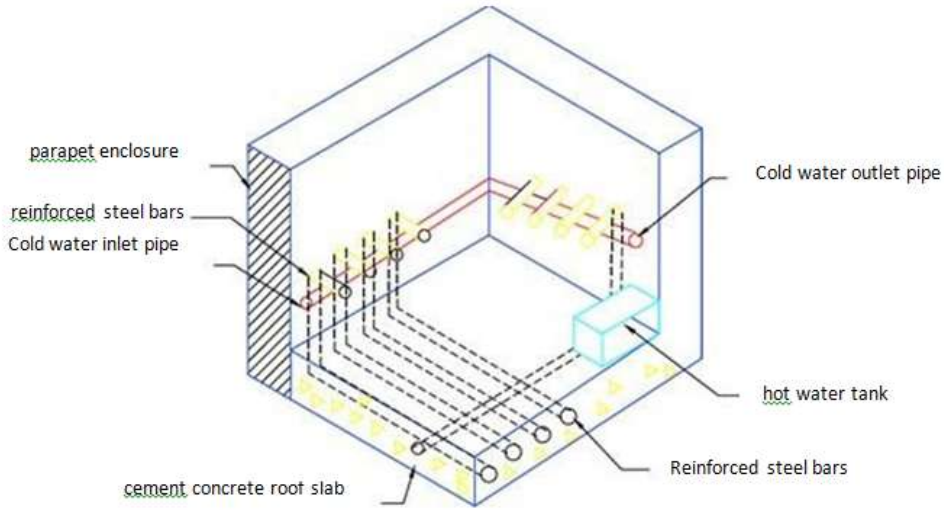

Figure1:Proposed Energy efficient structure

Indian Journal of Natural Sciences *www.tnsroindia.org.in ©IJONS*

Vol.15 / Issue 83 / Apr / 2024 *International Bimonthly (Print) – Open Access* *ISSN: 0976 – 0997*

RESEARCH ARTICLE

A Hydrogeo Chemical Approach to Study the Seasonal Variation of Groundwater Samples of Hunsur Taluk, Mysuru, Karnataka, India

Noushin Afshan[1]*, D.Nagaraju[2], Pradeep Raju .N[3] and Sudeep .S.R.[3]

[1]Research Scholar, Department of Environmental Science, University of Mysore, Mysore, Karnataka, India.
[2]Professor, Department of Earth Science, University of Mysore, Mysore, Karnataka, India
[3]Research Scholar, Department of Earth Science, University of Mysore, Mysore, Karnataka, India.

Received: 30 Dec 2023 Revised: 09 Jan 2024 Accepted: 05 Mar 2024

***Address for Correspondence**
Noushin Afshan
Research Scholar,
Department of Environmental Science,
University of Mysore,
Mysore, Karnataka, India.
Email: noushinshariff7@gmail.com

ABSTRACT

A larger section of the Indian population uses groundwater for its domestic and irrigation needs. In the present study, 30 groundwater samples from different locations of Hunsur taluk of Mysore district in Karnataka, India, were analysed for quality assessment. Handpump samples were collected from three seasons that were categorized namely as"pre-monsoon, "during monsoon" and "post-monsoon seasons of 2019 and comparative studies were undertaken to analyze their basic physico-chemical composition and hydrogeo-chemistry for suitability for drinking and irrigation. Hydro-geochemical facies was performed using different graphical representation techniques such as Piper, Gibbs and Schoellers diagrams that characterized the different geochemical marks in groundwater samples on the basis of their ion, water type and the interaction of water with the underlying rock and the role of the process of evaporation and condensation that affect the overall quality of water. Principal component analysis was used as a statistical extraction tool to study the relationship of various confounding variables that add to the variance in seasonal outputs. Holistically our study firstly highlight the merit of using graphical illustrative hydrogeo-chemical facies as a technique to analyse the chemical nature of the groundwater in the area and help assess the environmental impact of anthropogenic activities on the surrounding environment. Such analysis pave the way for management strategies for water resources, environmental assessment, and making informed decisions about the use and protection of groundwater resources.

Keywords: Hydro-geochemical facies; Hunsur taluk; Piper, Gibbs and Schoellers diagram, Principal Component Analysis; Groundwater.

INTRODUCTION

The Indian aquifers have seen a stark decline in their water levels(Gosain et al., 2011; Saha & Ray, 2019).This could be attributed to the advancing demand for anthropogenic activities of agriculture, cooking and the need for drinking water. Besides, not only have these activities increased the demand for groundwater supply, they also put it at risk of contamination from other activities of domestic, industrial and agricultural practices(Singh et al., 2020,). India being an agricultural nation, it is imperative to thoroughly study the quality of these groundwater resources as they directly impact the health of millions of people dependent on it(Sarath Prasanth et al., 2012; Singh et al., 2018) The groundwater resources that fall in the Indian state of Karnataka generally fall under the crystalline rock zone and are subjected to umpteen seasonal hydro geological weathering processes of rock-water interactions, evaporations and condensation(Afshan et al., 2022; Ramakrishnaiah et al., 2009). The quality of water portability that is usually evaluated on the balance between the cation and anion composition of ground water is often altered with the seasonal variations of anthropogenic activities such as agricultural use of pesticides, industrial runoffs and sewage discharges(Prokop & Walanus, 2015; Sharma et al., 2017). Therefore, understanding the aquifers systems in terms of their geochemistrywill help in management of groundwater resources/aquifers for their sustainability. Since groundwater contributes towards global water-resource, protecting it from subsurface pollution is warranted(Panghal & Bhateria, 2021). Hydro-geochemical facies is used in hydrogeology to classify and describe different chemical compositions or characteristics of groundwater, rocks, and sediments within a hydrogeological system(Chai et al., 2020). It provides a way to categorize groundwater based on its chemical composition. It helps inunderstanding the water chemistry in terms of theratioand concentrations of Ca^{2+}/Mg^{2+}/SO_4/NO_3/Cl^-ions, trace elements, and isotopic ratiosand their interaction and dependence on each other(Ahmad et al., 2020).These parameters can be used to distinguish between different sources of groundwater and to assess water quality.

It further helps in identifying the origin and source of groundwater and can provide insights into changes in water quality(S. Gour et al., 2023). They play a significant role in assessing the environmental impact of activities like mining, industrial processes, and land use changes. By analysing changes in groundwater chemistry and associating them with specific facies, it is possible to determine the impact on the surrounding environment(Kumar et al., 2022). Anthropogenic activities can offset the natural balances in the hydro geochemical properties of water and add to sub-surface pollution(Balogun et al., 2022). Effective management of groundwater resources, that provide for both cattle and man helps inunderstanding the natural, geologically controlled baseline chemistry of the water beds. This is especially important if the impacts of contaminants on groundwater are to be clearly ascertained(Saroli et al., 2019). The present study was carried outin Hunsur taluk of Mysore district of Karnataka, India. 30 hand pumps groundwater samples were collected during 3 predominant seasons as pre-monsoon, during-monsoon and post-monsoon ofthe year of 2019 to identify groundwater areas that were suitable for pumping which would help in catering to the domestic and agricultural needs of the local population. All water samples were analysed for their hydro-geochemicalfacies usingdifferent graphical representation techniquessuch as Piper diagram(Ferhati et al., 2023), Gibbs plot(Sulaiman et al., 2023)&Schoellersdiagram(Gomaa et al., 2023) that characterize different geochemical marks in ground water samples on their ion types, the water type, the interaction of water with the underlying rock, the role of the process of evaporation and condensation that affect the overall quality of water(Igibah & Tanko, 2019; Zhi et al., 2021). Furthermore principal component analysis was used as a statistical extraction tool to study the relationshipof various confounding variables that add to the variance inseasonal outputs(Gupta & Maiti, 2023). Holistically our study on the on the 30 hand pump samples from Hunsur taluk, firstly highlight the merit of using graphical illustrative hydrogeo-chemical facies as a technique to analyse the chemical nature of the ground water in the area and help assess the environmental impact of anthropogenic activities on the surrounding environment. Such analysis pave the way for management strategies for water

resources, environmental assessment, and making informed decisions about the use and protection of groundwater resources.

Study Location and Climate

Hunsur taluk, falls in latitudes 12^0 05′ 00″ - 12^0 26′ 00″ and longitudes 76^0 05′ 00″ - 76^0 32′ 00, with an area encompassing of 897 $km^2$with estimated rainfall of 873 mm(Afshan et al., 2022). It comes under Mysuru district of Karnataka bordered by Piriyapatna taluk north-east, Kodagudistrict on the south-east, Krishnarajanagara taluk north, Mysore taluk on the west, with Heggadadevankote on the southern end(Fig.1a). The area is covered with hilly terrain and contains red-shallowgravelly soils. The lithology of Hunsur taluk could be classified as having predominantly Migmatites and Granodiorite Gneiss, followed by Charnockite, Amphibolitic Metapelitic Schist and lastly Alluvium types(Fig.1b). Major source of occupation in the Hunsur area is agricultural, with a limited supply of water, thus warranting investigation of ground water resources for human and cattle consumption(Afshan et al., 2022)

MATERIALS AND METHODS

The primary objective of the study was to evaluate the hydrogeo-chemical facies of the ground water and identify suitable areas that could be used for pumping groundwater for drinking and agricultural purposes. 30 hand pumps groundwater samples were collected with simple random sampling techniquein1000 ml polyethylene bottles with lids and either refrigerated at 4° C or immediately analysed as per the requirement. Physical constituents of water and hydrogeo-chemical facies were analysed following standard procedures set by WHO (2004) and BIS (2012) guidelines.

Physico-chemicalanalysis

Physical & chemical parameters

pH (using potentiometry, using digital pH meter), color, odor through visual inspection electrical conductivity (EC) was done using potentiometry (through conductivity meter); total hardness was calculated (using EDTA titrimetric) and total dissolved solids (TDS) (using filtration), chloride (argentometry); calcium, magnesium sodium, potassium sulphate and nitrate were evaluated using (flame emission/flame photometry). All these assays were conducted using standardized published protocols(Lal et al., 2023; Pandey et al., 2023).

Evaluation of hydrogeo-chemical facies of ground water

To comprehend the hydro geochemical attributes of ground water, different plots were utilized specifically, Piper, Gibbs and Schoeller plot. These plots represent the graphical relationship characterizing different geochemical marks in ground water samples. The Grapher 12.0 was used to prepare the Piper diagram while Gibbs plot was prepared by Aquachem software. The facies represent zones with definite cation and anion concentrations and it depicts the diagnostic chemical character of water in various parts of the system.

Piper diagram

Piper trilinear diagram analysis was done using protocols from previous published literature(Abdessamed et al., 2023; Chaudhary et al., 2023; Dimple et al., 2023; Ismail, Snousy, Alexakis, Abdelhalim, et al., 2023). Briefly natural waters have an equilibrium between distribution of anions and cations with the "alkaline earth" cations being mostly calcium and magnesium. Likewise the predominant anionsfall either as "weak acid" bicarbonate or "strong acids" such as sulphate and chloride.

Gibbs plot

Gibbs plot analysis was done following protocols from (Ismail, Snousy, Alexakis, Gamvroula, et al., 2023; Liu et al., 2023; Selvaganapathi et al., 2023). Briefly Gibb's plots helps in delineating factors that govern the geochemistry of water holistically. These plots use the concept of interaction of water chemistry with the chemistry of the underlying

rock type, and the influence that rock-water interactions can have on the chemical components of water. Other interactions that are also explored are the influence of the process of chemistry of precipitated water dominance and the rate of water evaporation dominance that could alter the water chemistry altogether. This is plotted as a graph of total dissolved solids/TDSagainstNa +K/ (Na+Ca+K) ion concentrations. Taken together the Gibb's diagram assists in elucidating the nature of the groundwater chemistry of a particular area.

The Schoeller Diagram

Briefly, Schoeller diagram, is a semi-algorithmic plot where exchanges in ionic constituents'in water and rock are studied. There are two formats of this interaction that can take place. One in which the cations like Na^+/K^+in the water bodies get exchanged with the Mg^{2+}/Ca^{2+} in the rock which is the direct affect. When the exchange is between Mg^{2+}/Ca^{2+} in the water with the Na^+/K^+in therock, it is called indirect affect. Similar scenarios of exchange of anions as HCO_3^-&Cl^-, are also studied. This type of analysis helps in estimation of absolute concentration of ions in the sample along with the ratios between various ionic constituents as seen in previous published literature (Nayak et al., 2023; A. Patel et al., 2023; P. S. Patel et al., 2023; Tajbakhshian, 2023).

Principle Component Analysis

Principle component analysis was done following procedures from previous published literature(Garba et al., 2023; Mohammed et al., 2023; Solano S et al., 2023). PCA data is reflected in terms of the decreasing order of variance in the sample and thus help explain the factors that contribute to the highest variability in the analysis. In other words, PCA study delineate the main confounding factors that influence major variability on the data set.

Statistics

Samples from 30 hand pumps were reported as minimum, maximum and average values. The Grapher 12.0 was used to prepare the Piper diagram while Gibbs plot was prepared by Aquachem software. The facies represent zones with definite cation and anion concentrations and it depicts the diagnostic chemical character of water in various parts of the system.

RESULTS

Physical & Chemical parameters

An analysis of the physico-chemical data for the three seasons of pre-monsoon, during monsoon and post-monsoon is shown in **Tab. 1** bearing in mind the limits set by BIS and WHO standards. "During monsoon" season showed higher mean values for all parameters analysed as compared to pre and post monsoon seasons. The mean values for EC (µS/s), TDS (mg/L), TH (mg/L), and major cations like Ca^{2+} (mg/L) and Mg^{2+} (mg/L) were beyond the limits of both BIS and WHO standards for all the three seasons analysed. However all major anions like HCO_3^-, Cl^-, NO_3^-, and SO_4^{2-}were within the prescribed standard limits. Comparing within the three seasons in question EC, TDS and TH were maximum in the "during monsoon season" as compared to the rest. The distribution of cations and anions is maximum again for the "during monsoon season" as compared to the other two pre and post monsoon seasons. Cationic distribution for all three seasons is in the order of Ca^{2+}>Mg^{2+}> Na^+> K^+. Likewise anionic distribution for $HCO_3^-$and $Cl^-$was higher for "during monsoon" as compared to the pre and post monsoon season. NO_3^- and $SO4^{2-}$ values were within the prescribed standard limits for all three seasons.

Piper trilinear diagram

The piper plot as shown in **Fig 2** for the studied area during the "pre-monsoon" reveals that majority of the samples have Ca^{2+} ion, as the dominating cation, whereas few of the samples falls in the no dominant cation zone. On the contrary, all the samples have HCO_3^- and CO_3^{2-} ions as the dominating anion. Overall the groundwater of the studied area is magnesium bicarbonate type of water. The hydrochemistry of the groundwater for "during the monsoon" has shifted from the dominant Ca^{2+} ion zone to the no dominant zone, few even shifted to the magnesium dominant zone. However the dominating anion remains the same i.e. HCO_3^- and CO_3^{2-} ions, except for the sample from the

location Hirikyathanahali, Maragowdanahalli and Kattemalalvadi, which shows Cl^- ion as the dominating anion. Overall the water type remains unchanged except for the above mentioned three locations. The change in the hydrochemistry could be attributed to the infiltration of the rain water, which might have resulted in the dilution as well as dissolution of some ions into the groundwater. During the "post-monsoon" the Piper diagram shows that overall dominance of Ca^{2+} cation in the water samples. Some of the samples fall in the Mg^{2+} dominance region, indicating the presence of significant amounts of Mg^{2+} in the water. However, the dominance of Ca^{2+} cation is more prominent. For "during monsoon season", one location (Dhallalu) shows dominance of Na^+ cation with HCO_3^- as the dominant anion. This indicates a shift in the water chemistry of this location as compared to the other locations. The dominance of Na^+ cation suggests that the water may be influenced by the dissolution of sodium-bearing minerals, such as halite or soda ash. The dominance of HCO_3^- anion indicates that the water may have undergone carbonate mineral dissolution or may be influenced by anthropogenic sources such as sewage or industrial discharges.

Gibbs plot

It is evident from the Gibbs diagram **Fig. 3**that all the samples fall within the rock-water dominance zone for both cations and anions during all three seasons (pre-monsoon, during monsoon and post-monsoon), this indicates that the water chemistry is largely influenced by the mineral composition of the rocks in the area. In this case, the fact that all samples fall within the rock-water dominance zone for both cations and anions suggests that rock weathering is the dominant process controlling water chemistry in the study area. This could be due to the type of rock present in the area, which may be highly weather able and able to release large amounts of ions into the water. Other factors, such as climate, vegetation, and land use, may also play a role in determining water chemistry, but the dominance of the rock-water process suggests that rock weathering is the most important factor. Due to long time rock water interaction, percolations and flow through the rocky lithology has resulted in high solute concentration which is significantly controlling the water quality of the area.

The Schoeller plot

The Schoeller plot as shown in **Fig. 4** is a useful tool to understand the dominant cations and anions in a hydrological system. Based on the Schoeller plot for different seasons, it can be inferred that the water chemistry of the study area is dominated by Ca^{2+} cation and HCO_3^- and Cl^- anions during all the three seasons. The presence of these ions in high concentrations may be attributed to the geology of the region and the weathering of rocks containing calcium and carbonate minerals. However, there is a variation in the chemical composition of water in the Dhallalu location during the post-monsoon season, where Na^+ becomes the dominating cation. This variation may be due to several reasons, such as the geological characteristics of the area, anthropogenic activities, or changes in the hydrological regime. The source of Na^+ may be from the dissolution of minerals such as halite, which is a common rock salt mineral. It is also possible that the water has undergone ion exchange with the soil or rock matrix or due to anthropogenic activities such as agricultural practices that may contribute to the presence of Na+ ions in the water.

Principle Component Analysis

The Principle Component Analysis shown in **Fig. 5& Fig. 6**calculates eigen values, percentage of variance, and cumulative percentage for each principle component obtained from a principal component analysis (PCA). Eigen values of each principle component represent the amount of variance explained by each component. The larger the eigen value, the more variance is explained by that component. During the "pre monsoon season", the first principle component explained 35.89 % of the total variance, second 47.66%. The first three components explained more than 57.37 % of the variance which is also evident from the scree plot of **Fig. 5a**. Therefore, focusing on these three components to capture most of the important information in the data, **Fig. 6a** shows the biplot graph for the pre-monsoon season which represents both the variables (vectors) and the cases (points) distribution. The first five principal components account for more than 76% of the total variance in the dataset. The first component (PC1) which accounts for 35.89 % of the total variance has positive loading for NO_3^-, SiO_2, SO_4^{2-}, $NO3^-$, K^+, Na^+, Ca^{2+}, Cl^-, TDS and EC while total hardness, Mg^{2+}, Fe, HCO_3^- and CO_3^{2-} have negative loading. The second PCA component (PC2) accounts for 11.77 % of the total variance and has positive loadings for pH, Ba and PO_4^{3-}. For the "during monsoon season the first few principal components explain a significant amount of the total variance. In particular, the first six

components explain more than 64% of the variance which is also evident from the scree plot of **Fig. 5b**. Similarly for the "during monsoon season" from the biplot graph in **Fig.6b** it can be seen that the first six components explain more than 64% of the variance. The first component (PC1) which accounts for 14.83 % of the total variance has positive loading for Cl^-, Total Hardness, Mg^{2+}, TDS, NO_3^-, EC, SO_4^{2-}, NO_3^-, BOD, Na^+ and PO_4^{3-} while pH, HCO_3^-, CO_3^{2-}, SiO_2, K^+ and Ca^{2+}have negative loading. The second component (PC 2) which accounts for 12.42 % of the total variance has positive loading for F^-, Fe and COD while it shows negative loading for Ba. **Fig. 5c &6c**show the scree plot and the biplot graph for "post-monsoon season". The first five principal components account for more than 76% of the total variance in the dataset. The first component (PC1) which accounts for 32.41 % of the total variance has positive loading for HCO_3^-,CO_3^{2-},Mg^{2+},Ca^{2+},Fe and total hardness while SO_4^{2-},NO_3^-,K^+,Na^+,F^-,TDS and EC have negative loading. The second PCA component (PC2) accounts for 17.01 % of the total variance and has positive loadings for pH only. Based on the eigen values and the percentage of variance explained by each principal component, it appears that the pre-monsoon, during monsoon, and post-monsoon seasons have different patterns in the chemical parameters being measured.

DISCUSSION

30 groundwater samples from different locations of Hunsur taluk of Mysore district in Karnataka, India, were analysed for issues of water potability. Hand pump samples were collected from three seasons that were categorized namely as "pre-monsoon, "during monsoon" and "post-monsoon season of 2019 and comparative studies were undertaken to analyse their basic physico-chemical structure and hydrogeo-chemistry for suitability for human use and consumption. Physico-chemical analysis was done for EC (µS/s), TDS (mg/L), TH (mg/L); major cations like Ca^{2+} (mg/L) and Mg^{2+} (mg/L) and major anions like HCO_3^-, Cl^-, NO_3^-, and SO_4^2.Hydro-geochemical facies were carried out using Piper diagram, Gibbs illustration& Schoellers plot along with multivariant statistical application as Principal component analysis. All results were derived with comparisons made to the WHO (2004) and BIS (2012) guidelines. In reference to the analysis made for physico-chemical parameters, it was seen that pH values for all the three seasons were within the BIS (2012) (6.5–8.5) and the WHO (2004) standards (7-8.5). The EC values in our study averaged from 1570 µs/cm (pre-monsoon), 1650 µs/cm (during monsoon) to 1580 µs/cm during (post monsoon) seasons and showed that the major EC values were slightly above the permissible limits by BIS(1400 µS/cm), still falling in the acceptable range of 800-3000 µs/cm set by WHO. Total hardness (TH) of water generally is influenced to a greater extent by the concentration of cations like Ca^{2+} and Mg^{2+} ions. In our study, the TH values for all three seasons are slightly above the BIS (100-600 mg/L) and WHO (100 -500 mg/L) values (pre-monsoon: 677 mg/L; during monsoon; 760 mg/L; post-monsoon: 644 mg/L), corroborating with the slightly raised values of both Ca^{2+}(pre-monsoon: 148 mg/L; during monsoon; 162 mg/L; post-monsoon: 121 mg/L), and Mg^{2+}(pre-monsoon: 71 mg/L; during monsoon; 75 mg/L; post-monsoon: 68 mg/L), ions. Although the values of Ca^{2+} and Mg^{2+} ions are raised they are within theWHO (75-200 mg/L) and BIS permissibility range (75-100 mg/L) for Ca^{2+}concentration. For Mg^{2+} these values were again a bit higher to the acceptable but within the permissible limits of WHO (50 to 150 mg/L) and BIS values (30-100 mg/L) range.

Concentrations of TDS in handpump samples were higher to the acceptable limits (500 mg/L), but they were in the permissible range set by WHO and BIS from 1500-2000 mg/L. Na^+ ion concentrations (pre-monsoon: 64 mg/L; during monsoon; 65 mg/L; post-monsoon: 65 mg/L), K^+ were within range WHO and BIS of (100 and 10 mg/L for Na^+ and K^+). Similarly, HCO_3^-&Cl- concentrations were also in range of 250 mg/L. Of late authors like(Hanumanta D. L. et al., 2023)have also investigated the suitability of borewell groundwater for irrigation purposes in Hiriyur Taluk, Chitradurga District. in Karnatakaalong with (Sadashivaiah et al., 2008), who studied the hydrochemical analysis and evaluation of groundwater quality in Tumkur Taluk, again from Karnataka, India. On analysis of data from the experiments on hydrogeo-chemical facies of the groundwater samples, the Piper diagram showed that all the samples were in Ca^{2+}- $Mg^{2+}HCO_3^-$ facies belongs to temporary hardness and alkaline earth elements (Ca^{2+}& Mg^{2+}) exceeded the alkali elements (Na^+ & K^+) where Ca^{2+}& Mg^{2+}were the leading cations in the study area. Furthermore, it was found that the concentration of weak acids (CO_3^{2-}& HCO_3^-), during all the three seasons, was

higher than the strong acids (SO_4^{2-} and Cl^-).Many authors have exploited the fruitfulness of employing Piper diagramin their data analysis. (Hasan et al., 2023), used it to study groundwater in coastal area at Patuakhali District, Bangladesh. (Gyanendra & Alam, 2023), studied the groundwater resources of Manipur Valley, India. (Rahman et al., 2023), applied it to study the groundwater from the south-western parts of Bangladesh. Likewise (Chaudhary et al., 2023) further used the same application in his study of the groundwater assessment from Manipur, India. (Dimple et al., 2023) studied the groundwater quality of hard rock aquifer region of two Rajasthan districts, namely Rajasamand and Udaipur using the Piper plot analysis. (Ismail, Snousy, Alexakis, Abdelhalim, et al., 2023), employed the technique for analysing the groundwater suitability for drinking and irrigation purposes in North Assiut Province, Egypt, along with (Abdessamed et al., 2023)who studied the same in the watershed of Ain Sefra (south west Algeria).

Likewise analysis of the Gibb's plot further reiterated that the dominant processes that was controlling water chemistry in the Hunsur taluk was dominated by the phenomenon of rock-water interactionas compared to the other phases of precipitation- dominance or evaporation dominance. The lithology of Hunsur taluk that bears predominant Migmatites and Granodiorite Gneiss, followed by Charnockite, Amphibolitic Metapelitic Schist and lastly Alluvium type rocks showed dominant interactions with the ground water aquifers. Thus it could be concluded that the ground water interaction between these rocks governedthe water chemistry of Hunsur taluk through the process of weathering and leaching processes.Gibb's plot references can be seen in studies from authors like (Selvaganapathi et al., 2023)who evaluatedthe fluoride content in groundwaters of Palacode and Pennagaram taluk, Dharmapuri district, Tamil Nadu, India and(De et al., 2023), who investigated the fluoride content in groundwater with respect to hydro-geochemical characteristics from Baruipur block of West Bengal, India. Similarly (Izeze et al., 2023)used the Gibbs plotfor analysis of groundwater quality from Ughelli South, Southern Nigeria, (Li et al., 2023)investigated the influence of fluoride sources in desert groundwater from Cherchen River Basin, northwestern China, (Ismail, Snousy, Alexakis, Gamvroula, et al., 2023)assessedits usefulness in analysis of the groundwater quality in West El Minia District, Egypt and (Liu et al., 2023)evaluated it in the quality ofgroundwater from Tailan River Basin, Xinjiang, China.

Similarly the Schoeller plot for different seasons, conferred that the water chemistry was dominated by Ca^{2+} cation and HCO_3^- and Cl^- anions during all the three seasons which could be from weathering of rocks containing calcium and carbonate minerals.(Nayak et al., 2023), (A. Patel et al., 2023), (P. S. Patel et al., 2023), (Tajbakhshian, 2023), and(Manu et al., 2023), have utilized the Schoeller plot in their ground and surface water quality analysis studies.
Overall analysis through Principle Component Analysis suggested that the chemical parameters measured exhibited different patterns during the three seasons, and were- more highly correlated during the pre-monsoon and post-monsoon seasons as compared to the during monsoon season.Many authors have exploited the usefulness of the application PCA in studying ground and surface water quality. (Garba et al., 2023), in their study highlighted the variation in ground water quality was because of the anthrogenic action and geogenic processes. (Mohammed et al., 2023) further studied on similar objectives in the tropical Savanna waters. (Solano S et al., 2023)studied geochemical groundwater composition in the Central Pacific of Costa Rica using PCA approach along with (El-Rawy et al., 2023) who used the PCA multivariant approach to study the groundwater quality analysis in Jazan, Saudi Arabia

CONCLUSION

Conclusively analysis of the 30 groundwater samples from different locations of Hunsur taluk of Mysore district in Karnataka, India, highlight that the water chemistry of the area is Ca^{2+}- Mg^{2+}-HCO_3^- type having temporary hardness Ca^{2+}& Mg^{2+} ionic concentrations exceeded Na^+ & K^+. Furthermore, it was found that the concentration of CO_3^{2-}& HCO_3^- during all the three seasons was higher than SO_4^{2-} and Cl^- dominated by the phenomenon of rock-water interaction as compared to the other phases of precipitation dominance or evaporation dominance. Physico-chemical analysis further highlight the need for treatment of water before they can be used for human consumption.

Funding

Miss. Noushin Afshan, would like to acknowledge funding support from Department of Minorities, GOK. DOM, Karnataka, India(Grant no.DOM/FELLOWSHIP/CR-032019-20. Dated: 11-10-2019).

Competing interest

The authors report no conflict of interest.

REFERENCES

1. Abdessamed, D., Jodar-Abellan, A., Ghoneim, S. S. M., Almaliki, A., Hussein, E. E., & Pardo, M. Á. (2023). Groundwater quality assessment for sustainable human consumption in arid areas based on GIS and water quality index in the watershed of Ain Sefra (SW of Algeria). *Environmental Earth Sciences*, *82*(21), 510. https://doi.org/10.1007/s12665-023-11183-9
2. Afshan, N., Nagaraju, D., Bhanuprakash, H. M., & Deep, P. G. (2022). Seasonal analysis of groundwater samples to identify water quality index and comparative statistical analysis of Hunsur Taluk, Mysuru, Karnataka, India. *SN Applied Sciences*, *4*(8), 210. https://doi.org/10.1007/s42452-022-05102-z
3. Ahmad, A. Y., Al-Ghouti, M. A., Khraisheh, M., & Zouari, N. (2020). Hydrogeochemical characterization and quality evaluation of groundwater suitability for domestic and agricultural uses in the state of Qatar. *Groundwater for Sustainable Development*, *11*, 100467. https://doi.org/10.1016/j.gsd.2020.100467
4. Balogun, M. A., Anumah, A. O., Adegoke, K. A., & Maxakato, N. W. (2022). Environmental health impacts and controlling measures of anthropogenic activities on groundwater quality in Southwestern Nigeria. *Environmental Monitoring and Assessment*, *194*(5), 384. https://doi.org/10.1007/s10661-022-09805-z
5. Chai, Y., Xiao, C., Li, M., & Liang, X. (2020). Hydrogeochemical Characteristics and Groundwater Quality Evaluation Based on Multivariate Statistical Analysis. *Water*, *12*(10), 2792. https://doi.org/10.3390/w12102792
6. Chaudhary, R., Gaur, N., & Yadav, M. (2023). *Groundwater Quality Assessment of Manipur, India, and Worldwide Bibliometric Analysis of Research Progress on Groundwater Quality* [Preprint]. Environmental and Earth Sciences. https://doi.org/10.20944/preprints202309.0944.v1
7. De, A., Das, A., Joardar, M., Mridha, D., Majumdar, A., Das, J., & Roychowdhury, T. (2023). Investigating spatial distribution of fluoride in groundwater with respect to hydro-geochemical characteristics and associated probabilistic health risk in Baruipur block of West Bengal, India. *Science of The Total Environment*, *886*, 163877. https://doi.org/10.1016/j.scitotenv.2023.163877
8. Dimple, Singh, P. K., Kothari, M., Yadav, K. K., & Bhakar, S. R. (2023). Groundwater quality analysis using different water quality indices in the hard rock aquifer region in semi-arid environment. *Water Supply*, *23*(7), 2727–2744. https://doi.org/10.2166/ws.2023.150
9. El-Rawy, M., Fathi, H., Abdalla, F., Alshehri, F., & Eldeeb, H. (2023). An Integrated Principal Component and Hierarchical Cluster Analysis Approach for Groundwater Quality Assessment in Jazan, Saudi Arabia. *Water*, *15*(8), 1466. https://doi.org/10.3390/w15081466
10. Ferhati, A., Kettab, R. M., Belazreg, N. E. H., Khodja, H. D., Djerbouai, S., & Hasbaia, M. (2023). Hydrochemical analysis of groundwater quality in central Hodna Basin, Algeria: A case study. *International Journal of Hydrology Science and Technology*, *15*(1), 22. https://doi.org/10.1504/IJHST.2023.127889
11. Garba, A., Idris, A. M., & Gambo, J. (2023). Groundwater Quality Assessment Using Principal Component and Cluster Analysis. In M. Sherif, V. P. Singh, A. Sefelnasr, & M. Abrar (Eds.), *Water Resources Management and Sustainability* (Vol. 121, pp. 335–346). Springer Nature Switzerland. https://doi.org/10.1007/978-3-031-24506-0_22
12. Gomaa, H. E., Alotibi, A. A., Charni, M., & Gomaa, F. A. (2023). Integrating GIS, Statistical, Hydrogeochemical Modeling and Graphical Approaches for Hydrogeochemical Evaluation of Ad-Dawadmi Ground Water, Saudi Arabia: Status and Implications of Evaporation and Rock–Water Interactions. *Sustainability*, *15*(6), 4863. https://doi.org/10.3390/su15064863
13. Gosain, A. K., Rao, S., & Arora, A. (2011). Climate change impact assessment of water resources of India. *Current Science*, *101*(3), 356–371. JSTOR.

14. Gupta, S., & Maiti, S. (2023). Comparison between self-organizing map and principal component analysis for water quality assessment and hydro-geochemical characterization in dyke intruded complex geological settings. *Water and Environment Journal*, *37*(3), 512–526. https://doi.org/10.1111/wej.12855
15. Gyanendra, Y., & Alam, W. (2023). Geospatial assessment and hydrogeochemical characterization of groundwater resources of Manipur Valley, India. *Environmental Monitoring and Assessment*, *195*(9), 1037. https://doi.org/10.1007/s10661-023-11584-0
16. Hanumanta D. L., Ashok L. B., & Umesh H. R. (2023). Assesment of Borewell Irrigation Water Quality in Hiriyur Taluk Chitradurga District, Karnataka, India. *International Journal of Plant & Soil Science*, *35*(21), 1129–1141. https://doi.org/10.9734/ijpss/2023/v35i214085
17. Hasan, I., Reza, S., Siddique, A. B., Akbor, A., Hasan, M., Nahar, A., & Islam, I. (2023). Assessment of groundwater vulnerability for seawater intrusion using DRASTIC model in coastal area at Patuakhali District, Bangladesh. *Environmental Science and Pollution Research*, *30*(50), 109021–109040. https://doi.org/10.1007/s11356-023-29988-3
18. Igibah, C. E., & Tanko, J. A. (2019). Assessment of urban groundwater quality using Piper trilinear and multivariate techniques: A case study in the Abuja, North-central, Nigeria. *Environmental Systems Research*, *8*(1), 14. https://doi.org/10.1186/s40068-019-0140-6
19. Ismail, E., Snousy, M. G., Alexakis, D. E., Abdelhalim, A., Ahmed, M. S., & Elsayed, E. (2023). Diagnosis of Groundwater Quality in North Assiut Province, Egypt, for Drinking and Irrigation Uses by Applying Multivariate Statistics and Hydrochemical Methods. *Water*, *15*(15), 2812. https://doi.org/10.3390/w15152812
20. Ismail, E., Snousy, M. G., Alexakis, D. E., Gamvroula, D. E., Howard, G., El Sayed, E., Ahmed, M. S., Ali, A., & Abdelhalim, A. (2023). Multivariate Statistical Analysis and Geospatial Mapping for Assessing Groundwater Quality in West El Minia District, Egypt. *Water*, *15*(16), 2909. https://doi.org/10.3390/w15162909
21. Izeze, E. O., Imasuen, O. I., Badmus, G. O., & Gbadebo, A. M. (2023). Hydrogeochemical analysis and groundwater quality assessment of Ughelli South, Southern Nigeria. *Environmental Monitoring and Assessment*, *195*(8), 983. https://doi.org/10.1007/s10661-023-11580-4
22. Kumar, Gvsrp., Rao, Ks., Yadav, A., Kumar, Ml., & Dora, Hs. (2022). Multivariate statistical analysis approach to assess groundwater quality in two selected mandals of Vizianagaram district, Andhra Pradesh, India. *Journal of the Indian Chemical Society*, *99*(5), 100338. https://doi.org/10.1016/j.jics.2021.100338
23. Lal, B., Sengar, S. S., Singh, R., Jhariya, M. K., & Raj, A. (2023). Hydrogeochemistry and groundwater quality assessment in Ambagarh Chowki, Chhattisgarh, India. *Environmental Monitoring and Assessment*, *195*(1), 43. https://doi.org/10.1007/s10661-022-10650-3
24. Li, J., Zhou, Y., Zhou, J., Sun, Y., Zeng, Y., & Ding, Q. (2023). Hydrogeochemical evidence for fluoride sources and enrichment in desert groundwater: A case study of Cherchen River Basin, northwestern China. *Journal of Contaminant Hydrology*, *259*, 104270. https://doi.org/10.1016/j.jconhyd.2023.104270
25. Liu, L., Lu, Y., Yin, L., Yang, Z., Bian, J., & Cui, L. (2023). Chemical Characteristics-Based Evolution of Groundwater in Tailan River Basin, Xinjiang, China. *Water*, *15*(22), 3917. https://doi.org/10.3390/w15223917
26. Manu, E., De Lucia, M., & Kühn, M. (2023). Hydrochemical Characterization of Surface Water and Groundwater in the Crystalline Basement Aquifer System in the Pra Basin (Ghana). *Water*, *15*(7), 1325. https://doi.org/10.3390/w15071325
27. Mohammed, A. U., Aris, A. Z., Ramli, M. F., Isa, N. M., Arabi, A. S., & Jabbo, J. N. (2023). Groundwater pollutants characterization by geochemometric technique and geochemical modeling in tropical savanna watershed. *Environmental Geochemistry and Health*. https://doi.org/10.1007/s10653-022-01468-6
28. Nayak, P., Mohanty, A. K., Samal, P., Khaoash, S., & Mishra, P. (2023). Groundwater Quality, Hydrogeochemical Characteristics, and Potential Health Risk Assessment in the Bhubaneswar City of Eastern India. *Water, Air, & Soil Pollution*, *234*(9), 609. https://doi.org/10.1007/s11270-023-06614-z
29. Pandey, S., Mohapatra, G., & Arora, R. (2023). Groundwater quality, human health risks and major driving factors in arid and semi-arid regions of Rajasthan, India. *Journal of Cleaner Production*, *427*, 139149. https://doi.org/10.1016/j.jclepro.2023.139149

30. Panghal, V., & Bhateria, R. (2021). A multivariate statistical approach for monitoring of groundwater quality: A case study of Beri block, Haryana, India. *Environmental Geochemistry and Health*, *43*(7), 2615–2629. https://doi.org/10.1007/s10653-020-00654-8
31. Patel, A., Rai, S. P., Akpataku, K. V., Puthiyottil, N., Singh, A. K., Pant, N., Singh, R., Rai, P., & Noble, J. (2023). Hydrogeochemical characterization of groundwater in the shallow aquifer system of Middle Ganga Basin, India. *Groundwater for Sustainable Development*, *21*, 100934. https://doi.org/10.1016/j.gsd.2023.100934
32. Patel, P. S., Pandya, D. M., & Shah, M. (2023). A holistic review on the assessment of groundwater quality using multivariate statistical techniques. *Environmental Science and Pollution Research*, *30*(36), 85046–85070. https://doi.org/10.1007/s11356-023-27605-x
33. Prokop, P., & Walanus, A. (2015). Variation in the orographic extreme rain events over the Meghalaya Hills in northeast India in the two halves of the twentieth century. *Theoretical and Applied Climatology*, *121*(1–2), 389–399. https://doi.org/10.1007/s00704-014-1224-x
34. Rahman, M. M., Mahmud, A., Amin, Md. A., Hossain, Md. S., Bai, L., Shaibur, M. R., Rahman, Md. A., & Khan, A. S. (2023). Hydrogeochemical facies analysis of groundwater at parts of south-western Bangladesh: A case study. *Arabian Journal of Geosciences*, *16*(12), 644. https://doi.org/10.1007/s12517-023-11731-4
35. Ramakrishnaiah, C. R., Sadashivaiah, C., & Ranganna, G. (2009). Assessment of Water Quality Index for the Groundwater in Tumkur Taluk, Karnataka State, India. *E-Journal of Chemistry*, *6*(2), 523–530. https://doi.org/10.1155/2009/757424
36. S. Gour, Channamma., Kariyajjanavar, P., K. Channabasappa, K. C., S. L, A. Kumar., C. C, Vidyasagar., & M. Lingadevaru, M. L. (2023). Hydrogeo-Chemical Processess and Evaluation of Groundwater Quality for Drinking and Irrigation Purposes in Afzalpur Taluk, Karnataka, India. *Current Agriculture Research Journal*, *10*(3), 230–246. https://doi.org/10.12944/CARJ.10.3.07
37. Sadashivaiah, C., Ramakrishnaiah, C., & Ranganna, G. (2008). Hydrochemical Analysis and Evaluation of Groundwater Quality in Tumkur Taluk, Karnataka State, India. *International Journal of Environmental Research and Public Health*, *5*(3), 158–164. https://doi.org/10.3390/ijerph5030158
38. Saha, D., & Ray, R. K. (2019). Groundwater Resources of India: Potential, Challenges and Management. In P. K. Sikdar (Ed.), *Groundwater Development and Management* (pp. 19–42). Springer International Publishing. https://doi.org/10.1007/978-3-319-75115-3_2
39. Sarath Prasanth, S. V., Magesh, N. S., Jitheshlal, K. V., Chandrasekar, N., & Gangadhar, K. (2012). Evaluation of groundwater quality and its suitability for drinking and agricultural use in the coastal stretch of Alappuzha District, Kerala, India. *Applied Water Science*, *2*(3), 165–175. https://doi.org/10.1007/s13201-012-0042-5
40. Saroli, M., Lancia, M., & Petitta, M. (2019). The geology and hydrogeology of the Cassino plain (central Apennines, Italy): Redefining the regional groundwater balance. *Hydrogeology Journal*, *27*(5), 1563–1579. https://doi.org/10.1007/s10040-019-01953-w
41. Selvaganapathi, R., Sivaprakasam, V., Sathyanarayanan, B., Balamurugan, P., Das, S., & Sathiyamoorthy, G. (2023). Evaluating hydrogeochemical controls and noncarcinogenic health risk assessment of fluoride concentration in groundwater of Palacode and Pennagaram taluk, Dharmapuri district, Tamil Nadu, India. *Environmental Monitoring and Assessment*, *195*(12), 1472. https://doi.org/10.1007/s10661-023-12082-z
42. Sharma, D. A., Rishi, M. S., & Keesari, T. (2017). Evaluation of groundwater quality and suitability for irrigation and drinking purposes in southwest Punjab, India using hydrochemical approach. *Applied Water Science*, *7*(6), 3137–3150. https://doi.org/10.1007/s13201-016-0456-6
43. Singh, S., Ghosh, N. C., Gurjar, S., Krishan, G., Kumar, S., & Berwal, P. (2018). Index-based assessment of suitability of water quality for irrigation purpose under Indian conditions. *Environmental Monitoring and Assessment*, *190*(1), 29. https://doi.org/10.1007/s10661-017-6407-3
44. Singh, S., Tanvir Hassan, S. M., Hassan, M., & Bharti, N. (2020). Urbanisation and water insecurity in the Hindu Kush Himalaya: Insights from Bangladesh, India, Nepal and Pakistan. *Water Policy*, *22*(S1), 9–32. https://doi.org/10.2166/wp.2019.215
45. Solano S, C., Vargas-Azofeifa, I., Castillo-Muñoz, R., & Huapaya R.P, S. (2023). Multivariate data analysis applied to groundwater geochemical characterization, Central Pacific, Costa Rica. *Applied Geochemistry*, *151*, 105599. https://doi.org/10.1016/j.apgeochem.2023.105599

46. Sulaiman, M. A., Zafar, M. M., Prabhakar, R., Kumar, R., Sinha, R. K., & Kumari, A. (2023). A multivariate statistical approach to evaluate the hydro-geochemistry of groundwater quality in the middle Ganga river basin, Patna, India. *Acta Geophysica*. https://doi.org/10.1007/s11600-023-01071-y
47. Tajbakhshian, M. (2023). Hydrogeochemical evolution and water quality assessment of surface and groundwater resources: Case study, Shirin Darreh dam basin (NE Iran). *Arabian Journal of Geosciences*, *16*(10), 544. https://doi.org/10.1007/s12517-023-11641-5
48. Zhi, C., Cao, W., Zhang, Z., Li, Z., & Ren, Y. (2021). Hydrogeochemical Characteristics and Processes of Shallow Groundwater in the Yellow River Delta, China. *Water*, *13*(4), 534. https://doi.org/10.3390/w13040534

Table 1: Summary of physico-chemical parameters of the ground water sample taken during the "pre, during and post monsoon season" from Hunsur taluk 2019.

Parameter	Prescribed limits		Pre-monsoon		Mean	During monsoon		Mean	Post-monsoon		Mean
	BIS	WHO	Range			Range			Range		
			Min.	Max		Min	Max		Min	Max.	
pH	8.5	8.5	6.6	8.4	7.7	7	8.3	7.2	6.1	8.2	7
EC (µS/s)	1400		676	3070	1570	283	2878	1650	283	2878	1580
TDS (mg/L)	500	500	339	1577	793	570	1905	1096	181	1789	906
TH (mg/L)	500	500	220	1299	677	324	1209	760	209	1124	644
Major Cations (mg/L)											
Ca^{2+}	75	75	41	784	148	78.5	209	162	27.2	272	121
Mg^{2+}	30	50	20.2	142	70.7	51.4	160	75	24.9	122	67.8
Na^{+}	100	100	21.3	83.8	63.7	32.7	80.8	65.2	19.2	81.6	67.4
K^{+}	10	10	1.2	68.2	10.0	3.9	29	10.2	1	25.9	7.3
Major Anions (mg/L)											
HCO_3^-	300	600	197	972	435	133	909	401	64.8	483	318

Cl^-	250	200	42.1	459	179	38.2	358	161	23.4	285	149
NO_3^-	45	50	5.5	22.6	19.3	9.8	31.8	23.4	8.5	29.4	22.2
SO_4^{2-}	200	200	6.5	68.4	35.4	5.5	108	51.2	4.7	105	54.8

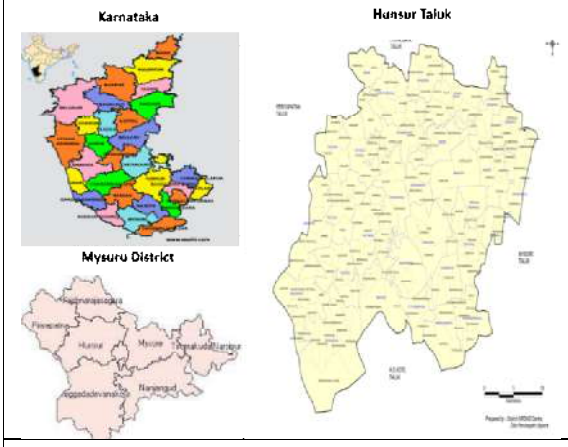

Fig. 1a: Study location Hunsur taluk, Mysuru district, Karnataka, India

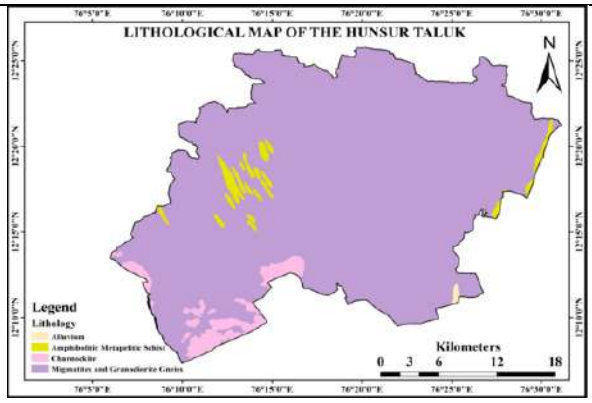

Fig. 1b: lithology: Hunsur taluk, Mysuru district, Karnataka, India(https://doi.org/10.1007/s42452-022-05102-z)

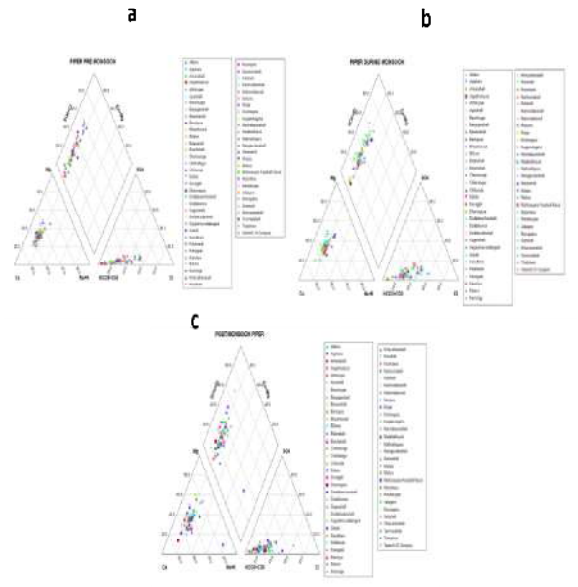

Fig. 2: Piper classification illustrating the chemical composition of ground water of Hunsur taluk. a: Pre monsoon b: during monsoon c: post monsoon.

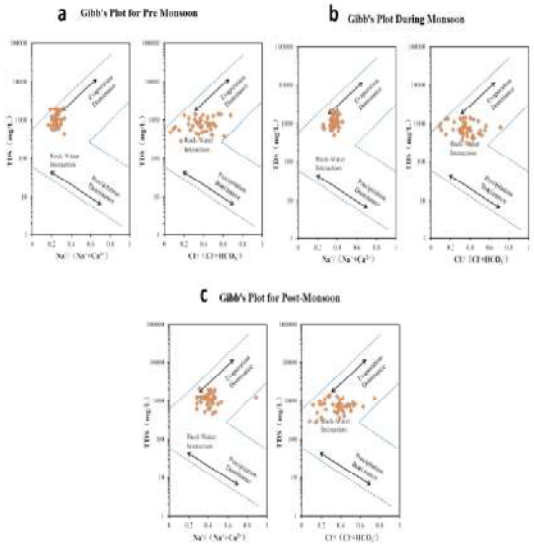

Fig. 3: Gibb's plot delineating the mechanism controlling water chemistry of ground water of Hunsur taluk. a: Pre monsoon b: during monsoon c: post monsoon.

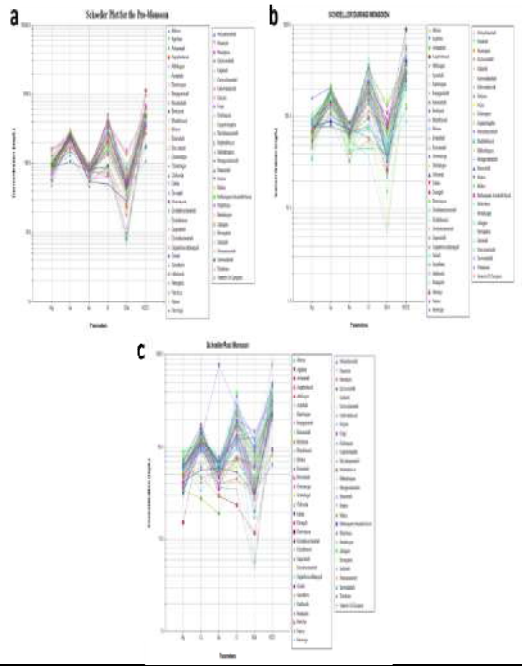

Fig. 4:Schoellers plot of water chemistry of ground water of Hunsur taluk. a: Pre monsoon b: during monsoon c: post monsoon.

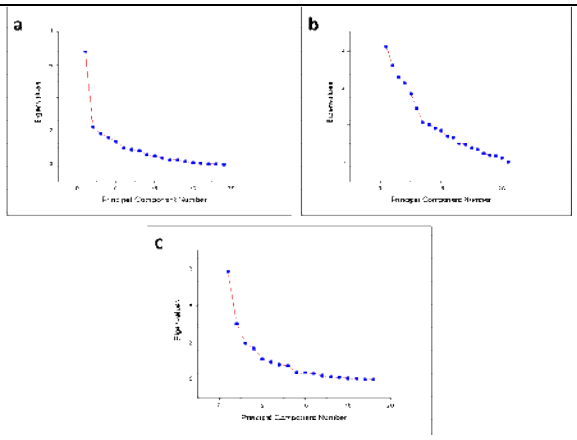

Fig. 5:Scree plots for the ground water samples from Hunsur taluk. a: Pre monsoon b: during monsoon c: post monsoon.

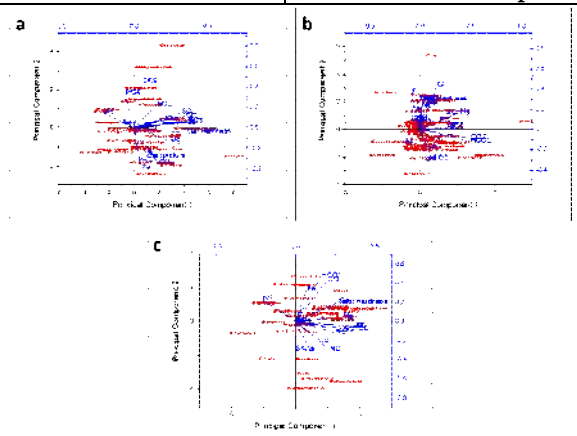

Fig. 6:Biplot for the ground water samples from Hunsur taluk. a: Pre monsoon b: during monsoon c: post monsoon.